C346r(04)
V-51

VERY HIGH MULTIPLICITY PHYSICS

Proceedings of the Sixth International Workshop

C346r(04)
V-51

Joint Institute for Nuclear Research

Экз.чит.зала

VERY HIGH MULTIPLICITY PHYSICS

Sixth International Workshop

Dubna, April 16–17, 2005

Proceedings of the Workshop

1147944

Объединенный институт
ядерных исследований
БИБЛИОТЕКА

Dubna • 2007

УДК 539.12.01(063)
ББК [22.382 + 22.317]я431
V51

The contributions are reproduced directly from the originals presented by the Organizing Committee.

V51 **Very** High Multiplicity Physics: Proceedings of the Sixth International Workshop (Dubna, April 16–17, 2005). — Dubna: JINR, 2007. — 513 p.

ISBN 5-9530-0151-7

The Proceedings collect the selected reports given at the Sixth International Workshop on Very High Multiplicity Physics. These include results of original investigations dedicated to the very high multiplicity processes, correlator analysis, polarization effects, pion gas condensation, Compton scattering, etc. The greater part of the materials is dedicated to the various technical aspects of the «Thermalization» experiment and discussion of the preliminary results obtained.

Физика очень больших множественностей: Труды VI Международного рабочего совещания (Дубна, 16–17 апреля 2005 г.). — Дубна: ОИЯИ, 2007. — 513 с.

ISBN 5-9530-0151-7

В сборнике публикуются доклады, представленные на VI Международном совещании по физике очень больших множественностей. Он включает оригинальные результаты исследования процессов с очень большой множественностью, корреляторного анализа, поляризационных эффектов, конденсации пионного газа, комптоновского рассеяния и др. Большая часть материалов посвящена различным техническим аспектам эксперимента «Термализация» и обсуждению полученных предварительных результатов.

УДК 539.12.01(063)
ББК [22.382 + 22.317]я431

ISBN 5-9530-0151-7

© Joint Institute for Nuclear Research, 2007

CONTENTS

Status of Very High Multiplicity Physics

A.Sissakian
JINR

VHM region: structure of phase space

Why the VHM?

Multiplicity distribution

VHM theory

"THERMALIZATION"

Conclusions

VHM region: structure of the phase space

- "Regge" (BFKL, ...)

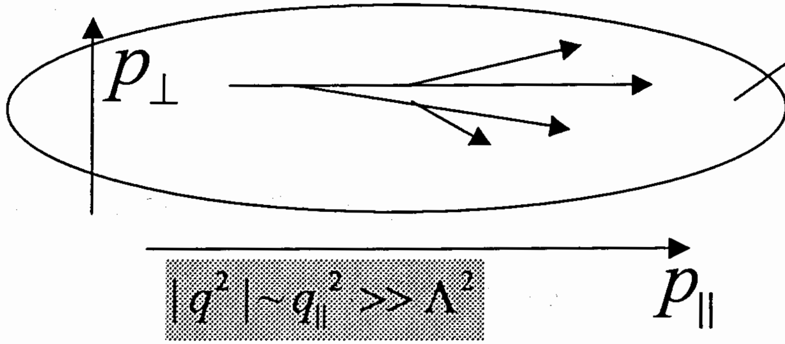

$|K_3|/|K_2|^{3/2} \sim 1/n$

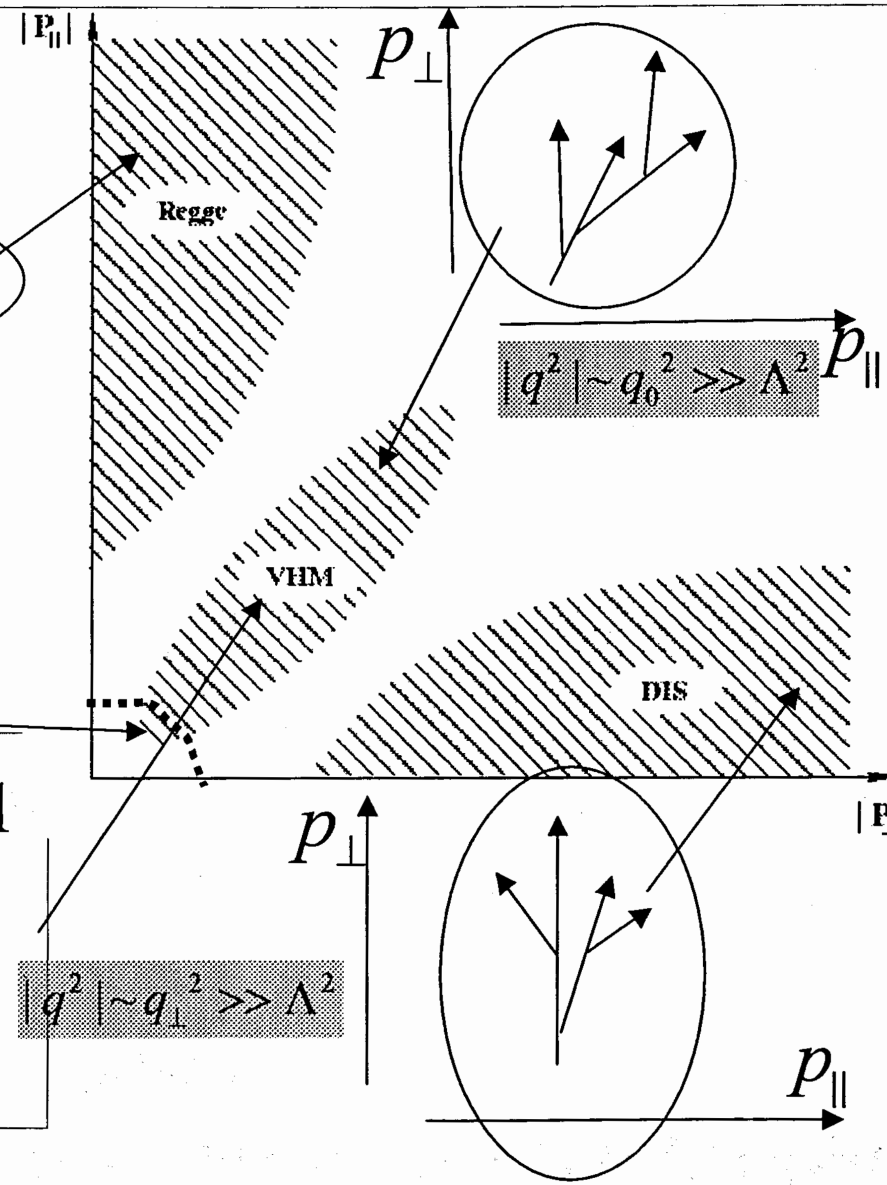

- "VHM" – low-x: $|K_3|/|K_2|^{3/2} \ll 1$
- L.Gribov et al.; L.Lipatov;
- J.Manjavidze & A.Sissakian;
- L.MacLerran, D.Kharzeev

- "DIS" (DGLAP;...)

Why is VHM?

•**The model of Fermi-Landau**

$$\bar{n}_{FL}(s) \sim \sqrt{s} >> \bar{n}_{phys}(s) \sim \ln s$$

threshold multiplicity

•**What will happen if**

$$n \to n_{\max} \sim \sqrt{s}$$

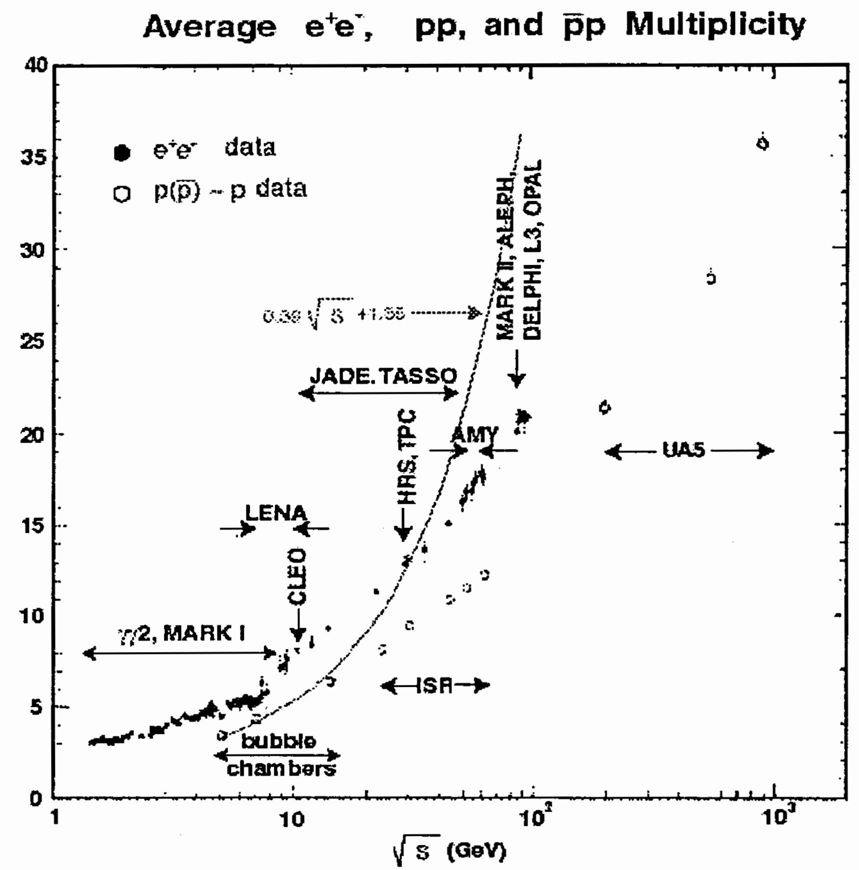

•**Statement: the preventing thermalization constrains must be switched off if**

$$n \to n_{\max}$$

Multiplicity distribution

•Manjavidze & Sissakian

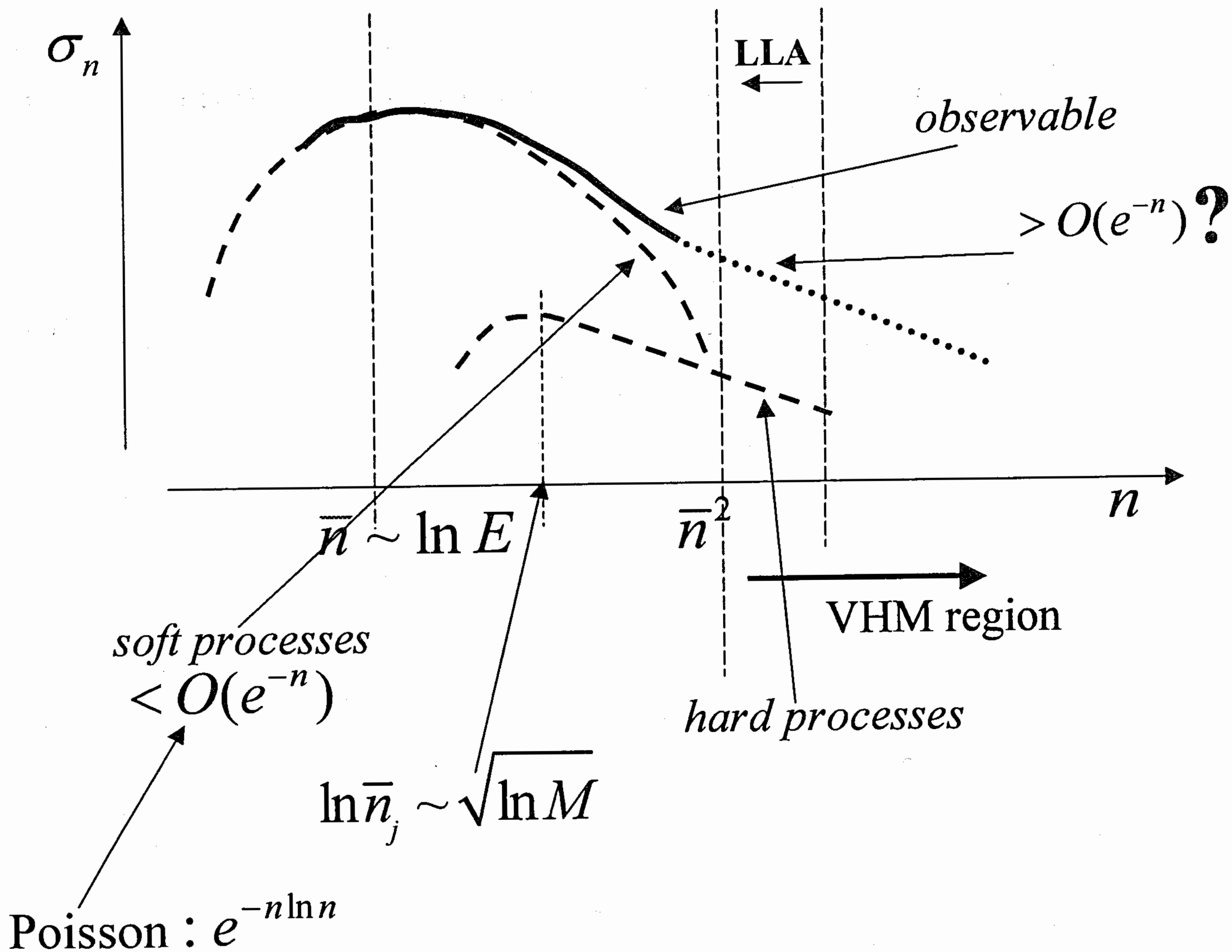

VHM theory

•**Sissakian, Manjavidze (90,...)**

$\rightarrow$ *no LLA approximation* $:|\vec{k}_i| \rightarrow 0,\ |k_\perp| \sim |k_\parallel|$

$\rightarrow$ *no Regge theory* $: n > \bar{n}^2(s)$

$$\rightarrow \left.\begin{array}{l} Regge: \quad \sigma_n < O(e^{-n}) \\ QCD\ jet: \sigma_n = O(e^{-n}) \end{array}\right\} \Leftarrow VHM\ process\ is\ hard\ (\alpha_s << 1)$$

$\rightarrow$ *VHM QCD*: $q^2 >> \Lambda^2, q_0^{\ 2} >> (q_\perp^{\ 2}, q_\parallel^{\ 2})$

$$\rightarrow thermalization: \frac{|K_3(n,s)|}{|K_2(n,s)|^{3/2}} << 1$$

9

"THERMALIZATION"

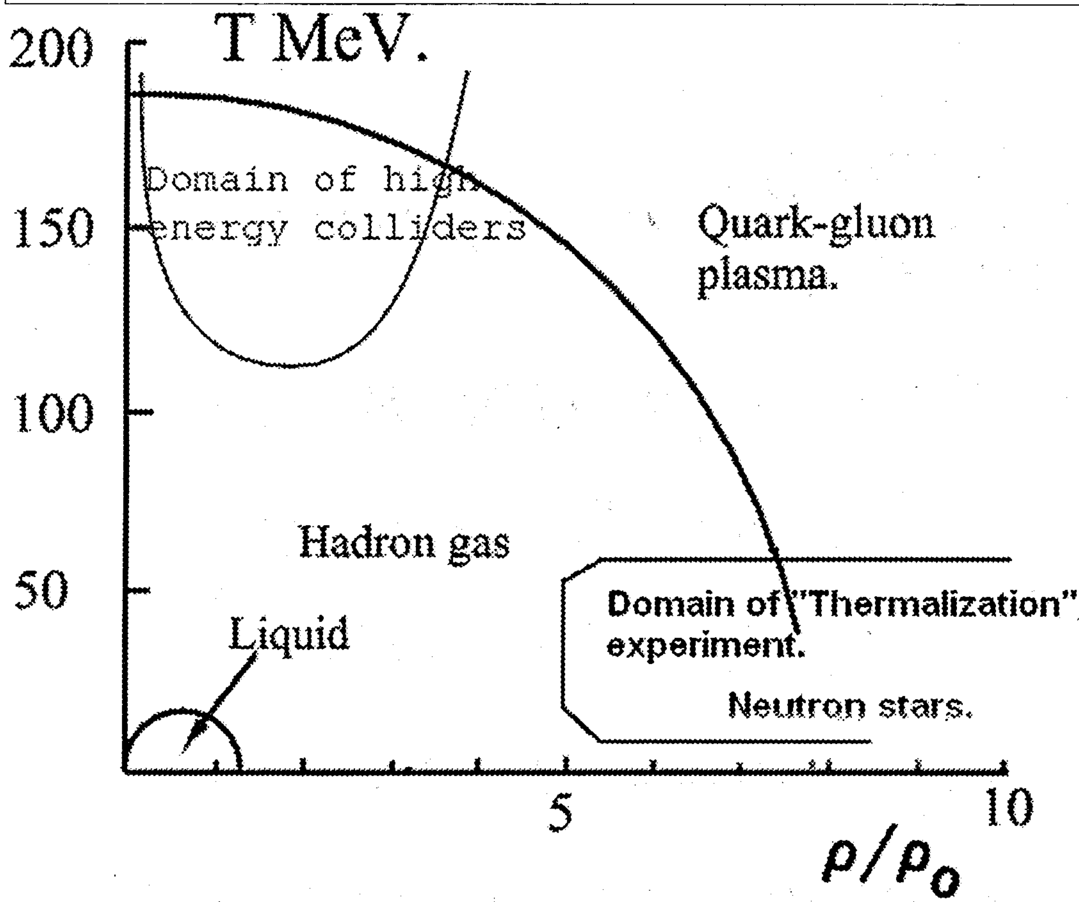

V.Nikitin et al. (2004)

- Production of **thermalized** state
- **Cold** and **dense equilibrium** state is favorable for QG plasma production
- **Multiparticle** Bose-Einstein correlations

Coll. "Thermalization"

JINR(Dubna), MSU(Moscow), IHEP(Prorvino), TSU(Tbilisi)

P.Ermolov, J.Manjavidze, V.Nikitin, A.Sissakian, et. al.

Conclusions

- The VHM kinematics region is outside of LLA abilities

- Ordinary ("Regge", pQCD in LLA,...) theoretical models can not predict even the tendency to equilibrium

- The S-matrix interpretation of thermodynamics permits to show that the thermalization must occur, at least, in a deep asymptotics over multiplicity.

- The test of pQCD frames in VHM region is a necessary task

- Future: VHM experiment!!!

Possible mechanism of condensation of the slow pion gas

E. Kuraev, E. Kokoulina

Joint Institute for Nuclear Research,
Dubna, Moscow Region, 141980, Russia

Abstract

Final state interaction by means of gluon or photon exchanges provide some attraction or repultion forces between hadrons. Some similarity with the percolation process is discussed.

At heavy ions collisions the set of slow pions probably is created (G.E. Soljakin (private communication), PNPI, San-Petersburg, 2004. Winter school). This media has within the colliding point the size of several fermi (center of mass of colliding beams is implied).

One possible mechanism of creation of this set of pions (if it have vacuum quantum numbers 0^{++}) and zero total 3-dimentional momentum-"exitation of the physical vacuum" [1].

According this model part of energy revield in process is accepted by physical vacuum and results creation of current quark-gluon plasma,which,spreading and cooling transforms to the set of slow pions when the temperature becomes in the region of deconfinement phase transition T_D. The estimates of Bose-condensation temperature [2] (the temperature where chemical potential equal to zero) $T_B = 3.31\hat{h}^2(N/V)^{2/3}/(g^{2/3}m_\pi)$ for typical values of pion number $N = 10^2$ and size of pion set size $V \sim (10fm)^3$, leads to value close to deconfinement one $T_D \approx T_B = 140MeV$. At further spreading and decreasing the temperature $T < T_B$ a pion condensate appears with the number of "stopped" pions $N_{\epsilon=\epsilon_0} = N[1-(T/T_B)^{3/2}]$ and the pressure independent from the volume. Here we mean the pions belonging to the condensate ("stopped") really have some average velocity, which can be expressed in terms of kinetic energy K of the set of N slow pions: $v_0 = (2K/(Nm_\pi c^2))^{1/2} << c$.

Amplitude of pion-pion interaction rapidly decrease with increasing of the magnitude of transfer momentum. The reason-formfactor suppression. This fact can be formulated as a fast termalization in the transversal direction.

As for many photons (gluons) exchange contribution to the amplitude-it can be parametrized in terms of wave function-solution of the Bethe-Salpieter equation or the corresponding Schrodinger equation $\psi(r,v)$. It results in factor

$$|\psi(0,v)|^2 = \frac{x}{1-e^{-x}} \approx 1 + \frac{x}{2}, \qquad x = \frac{\pi\alpha}{v}, \tag{1}$$

with $v = |v_1 - v_2|$-is the relative velocity of pions. This is known result of Quantum Electrodynamics (QED) valid for pions of opposite charges, α is QED coupling. The mean distance between pions in pionium atom is $300fm$-is too large. Much more short distances provided by gluon exchange when one can use the QCD coupling α_s. Relative velocities can vary from the atomic velocities αc up to average velocity v_0.

Schematically the interaction amplitude can be presented as a sum of two terms $A_{ij} = a + b/v_{ij}$, one of which a collect the scattering channels contribution, contribution of the repultion forces (white vertex); another b/v collect the attraction forces action (black vertex).

The dynamics of the set of N interacting pions can be expressed in terms of these two types of vertices. Namely one can restrict by consideration of only pairing interactions of white vertex (W) type and the black vertex (B) type. After B -type the particles "stopped" become a part of condensate and ruled out from further dynamics. Other type of interaction, W results in scattering and taking of both the scattered particles patr in dynamics.

This process, being considered backward in time have a resemblance with percolation process, widely studied in many applications of solid state physics [3].

One can obtain (very roughly) the relative pairs velocities distribution

$$P(v) \sim \sum_{pairs(ij)} \frac{1}{(N_{pairs})!} \int_{v}^{v_0} \Pi_{i \neq j} A_{ij} dv_{ij} \sim (\frac{v_0}{v})^{\gamma}, \tag{2}$$

with γ-in principle calculable positive quantity of order of unity, proportional to the coupling constant and to the internal symmetry group factors.

When the concentration of the W-type vertices w becomes less than the critical value w_c the probability of the pion condensate creation can be expressed in form

$$\frac{dW}{dw} \sim (1 - \frac{w}{w_c})^{\eta} \tag{3}$$

In this way we can arrange (pure qualitative) the formula for the ratio of pions in the "stopped" kinematics to the total number of pions as a function of temperature:

$$\frac{N_{\epsilon=\epsilon_0}}{N} = (1 - (\frac{T}{T_B})^{\gamma})^{\eta}, 0 < T < T_B \tag{4}$$

Let us consider now the expected experimental consequences of pionic condensation phenomen. Really, it can manifest itself as a sharp narrow peak in dilepton or photon spectra, mentioned above. This peak will be only smoothed due to general motion of the condensate with the average velocity v_0.

References

1. M.K. Volkov, E.A. Kuraev and E.S. Kokoulina, hep-ph/0402163; Letters to Echaja, v.1 p 16-23 (2004).
2. L.Landau,E.Lifshits, Statistical Physics, Nauka, 1964.
3. A.L. Efros "Physics and geometry of disorder", Kvant, 19, 1982.

Joint Institute for Nuclear Research

Search for the mixed phase of strongly interacting matter at the JINR Nuclotron

A.N.Sissakian, A.S.Sorin, M.K.Suleymanov

VERY HIGH MULTIPLICITY PHYSICS
The Sixth International Workshop, Dubna, April 16-17 2005

Phases of strongly interacting matter

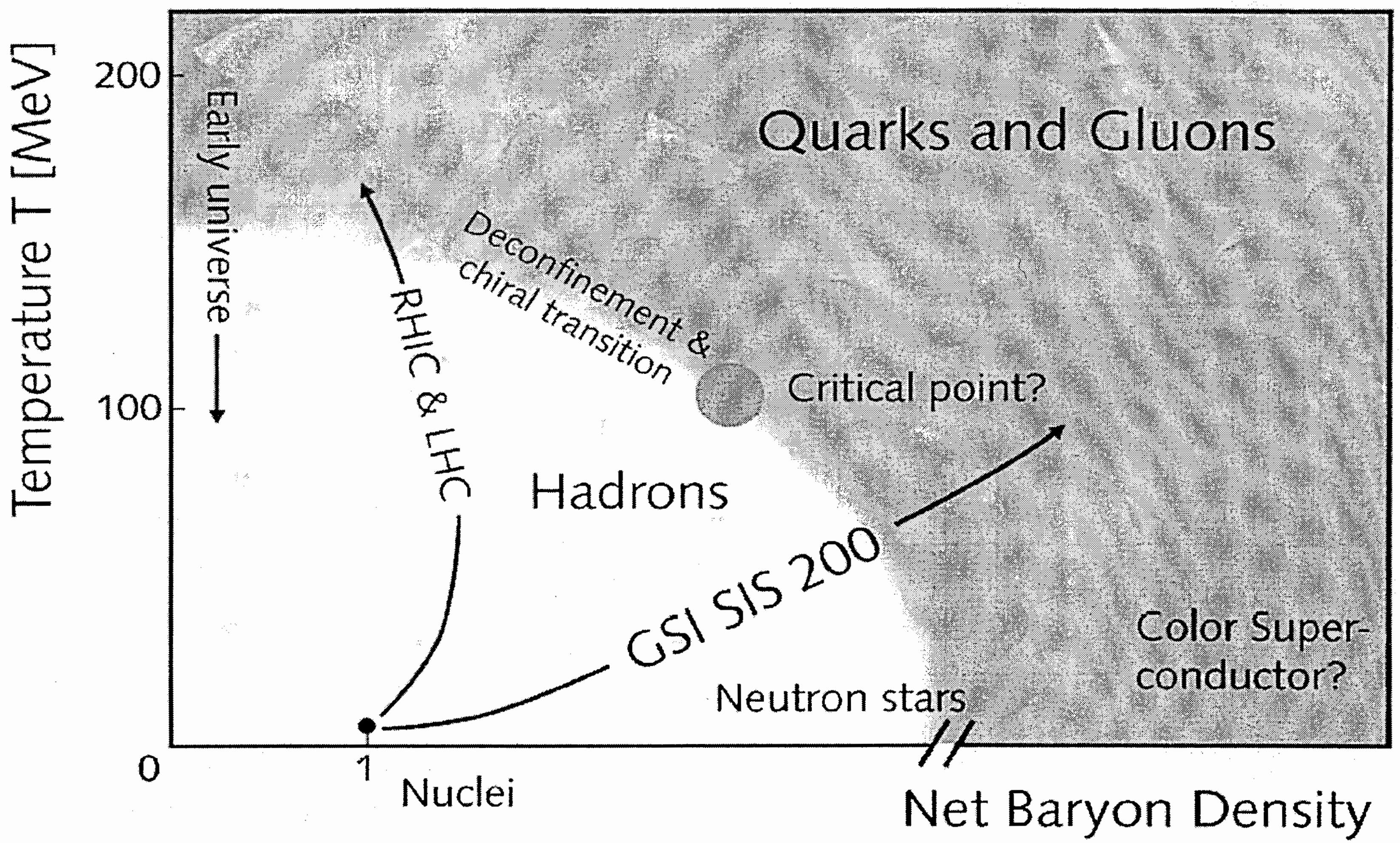

15

Simulations of Heavy-Ion Collisions:
Relativistic 3-fluid hydrodynamic model for the energy range: a few to 200 *A GeV*.
Y.Ivanov, V.Russkikh, V.Toneev

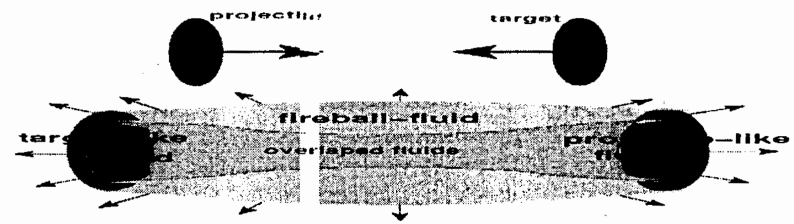

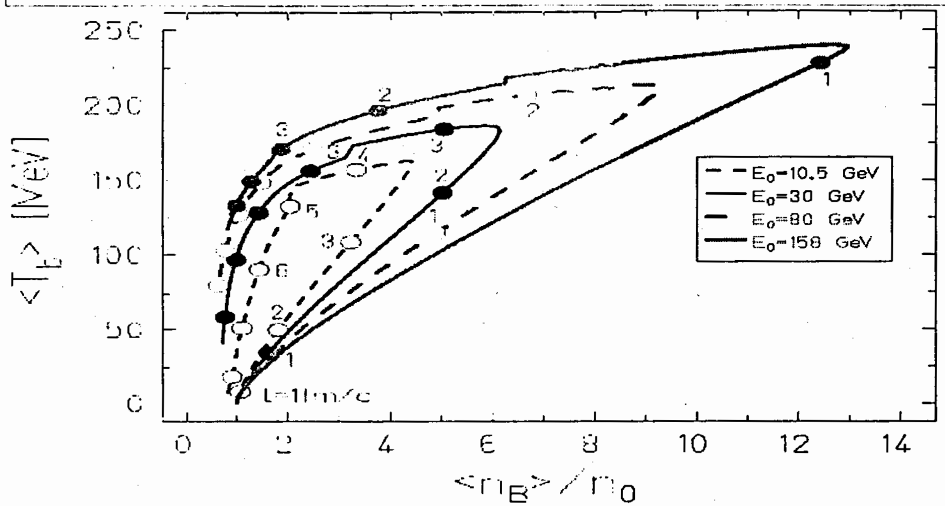

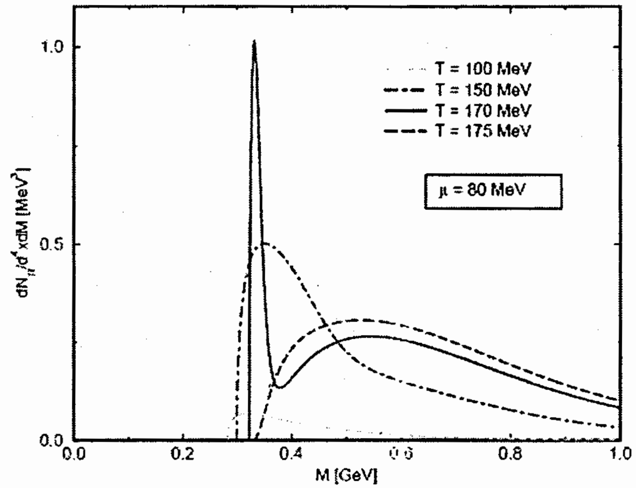

$\pi\pi \to \gamma\gamma$

M.Volkov, E.Kuraev, D.Blaschke, G.R¨opke, S.Schmidt, PLB(1998)

<u>**Proposal for FAIR GSI:**</u> consider the anomalous peak in the two-photon spectrum as a signal of the mixed phase formation and, therefore, a tool to identify the critical point in the QCD phase diagram. **D.Blaschke, A.Sissakian, A.Sorin, M.Suleymanov** (On physical programme at FAIR, 5[th]Workshop on the scientific cooperation between German research centres and JINR, Dubna, 17-19 January 2005, http://cv.jinr.ru/BMBF_05/index.html).

$\sigma \to \pi\pi$ $\sigma \to \gamma\gamma$
$\Gamma_\sigma = 600 - 1000 MeV$
$M_\sigma = 400 - 1200 MeV$

The number of anomalous two-photon events in the narrow invariant mass region M_2gamma ~ M_sigma(mu_c, T_c) can be considered as a "clock" for the duration of the mixed phase.

<u>**Problems of SPS and RHIC: huge background from neutral pion decays complicates identification of this signal. Privilege of FAIR: higher densities entail lower critical temperatures → lower background!**</u>

What about the JINR Nuclotron?

147914

Nuclotron: E ~ 5 GeV/nucleon, heavy nuclei A ~ 200

With light quarks

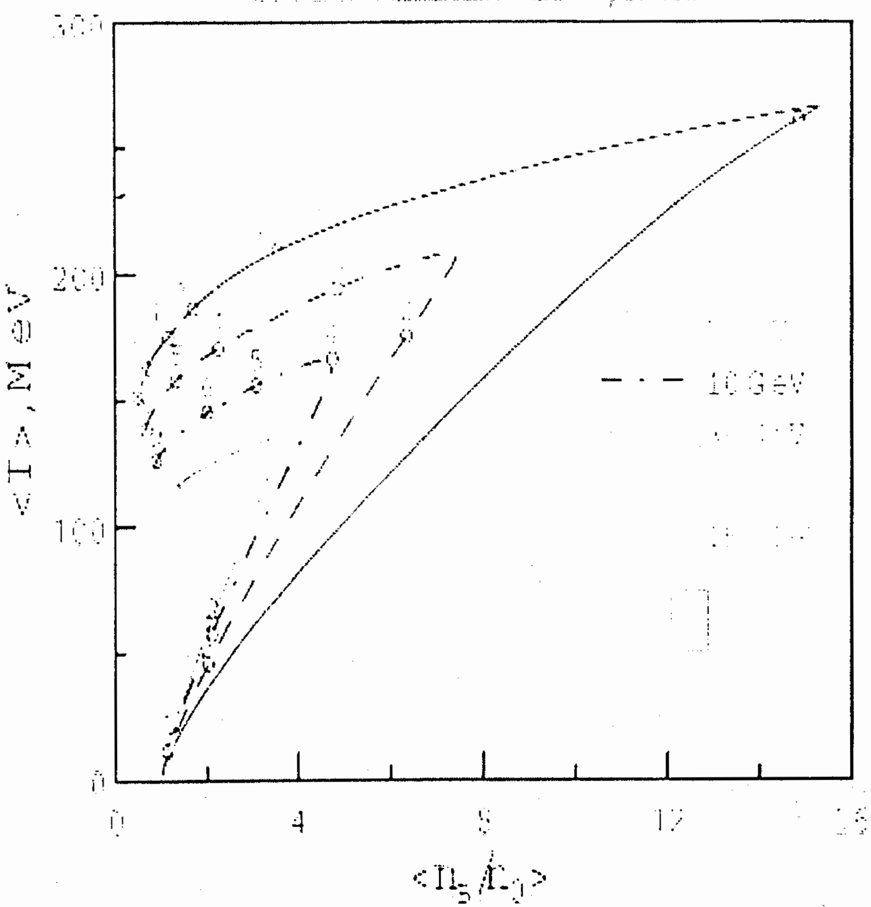

With heavy quarks

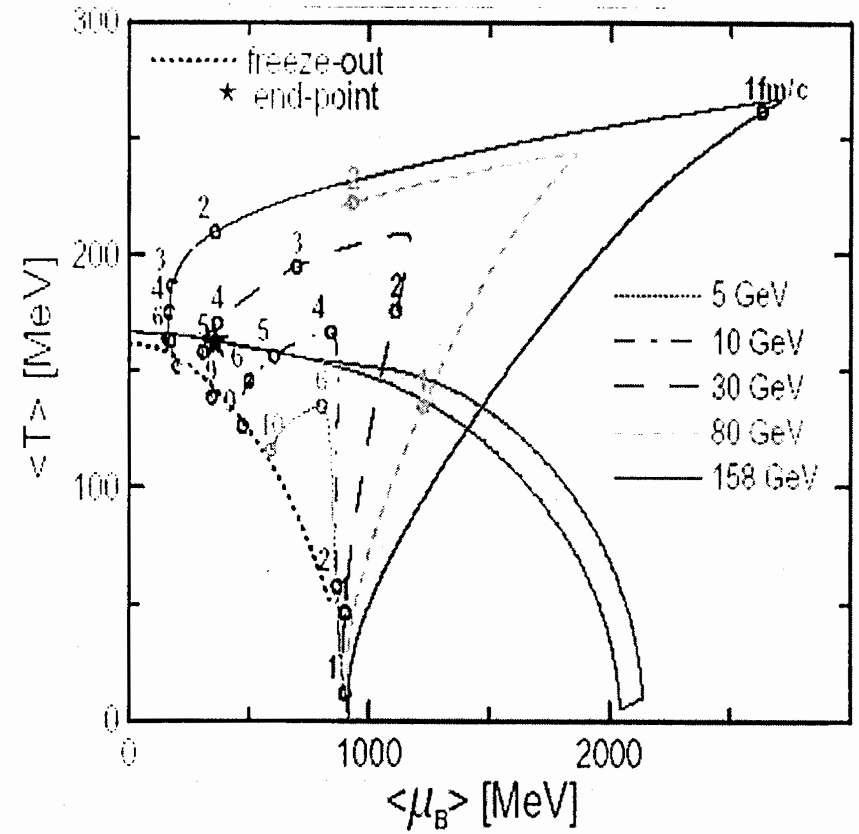

V.Toneev, Talk at the CBM Collaboration Meeting March 9-12, 2005, GSI,Darmstadt, http://www.gsi.de/documents/DOC-2005-Mar-871.pdf

Y.Ivanov,V.Russkikh,V.Toneev, Relativistic Heavy-Ion Collisions within 3-Fluid Hydrodynamics: Hadronic Scenario, nucl-th/0503088 (March 31 2005)

Объединенный институт ядерных исследований БИБЛИОТЕКА

Search for the mixed phase of strongly interacting matter at the JINR Nuclotron

Perspective theoretical and experimental researches

1. Investigation of properties of hadrons in hot and/or dense baryon matter (a change of their masses and widths is expected, first of all of the σ-meson as the partner of pions in the chiral multiplet, which characterizes a degree of chiral symmetry violation and can serve as a "signal" of its restoration as well as the mixed phase formation).

2. Analysis of a role of multiparticle hadron interactions, perfection of available and development of new space-time models of collision of heavy nuclei at high energies as well as "signals" of formation of new phases during the evolution.

3. Analysis of the dependence on energy and centrality of the multiplicity of pions, strange particles, and their ratio, as well as K-meson spectra with respect to transverse momentum (nonmonotonic dependences are expected, which can be due to a manifestation of the mixed phase formation).

4. Analysis of dileptons and slow pion production in collisions of heavy nuclei (their enhancement in comparison with hadron-hadron interactions is expected).

5. Analysis of the behaviour of angular correlations and flows of secondary particles (their abnormal behaviour in comparison with hadron-hadron interactions is expected).

6. Analysis of fluctuations of the multiplicity of secondary particles (their nonmonotonic dependences on energy can give information on the area of the phase transition and, moreover, the matter phase diagram).

7. Analysis of characteristics of nuclear fragments depending on the centrality (abnormal change of the behaviour in comparison with peripheral collisions is expected).

8. Energy and atomic number scanning for all characteristics of central collisions of heavy nuclei (this might allow one to obtain information on the equation of state of strongly interacting matter in the transition area).

3. Analysis of the dependence on energy and centrality of the multiplicity of pions, strange particles, and their ratio, as well as K-meson spectra with respect to transverse momentum (nonmonotonic dependences are expected, which can be due to a manifestation of the MP formation).

NA49 Collaboration SPS **Strangeness production**

C.Alt, et al, System-size dependence of strangeness production in nucleus-nucleus collisions at $\sqrt{s_{NN}}$=17.3 GeV , Phys.Rev.Lett. 94 (2005) 052301

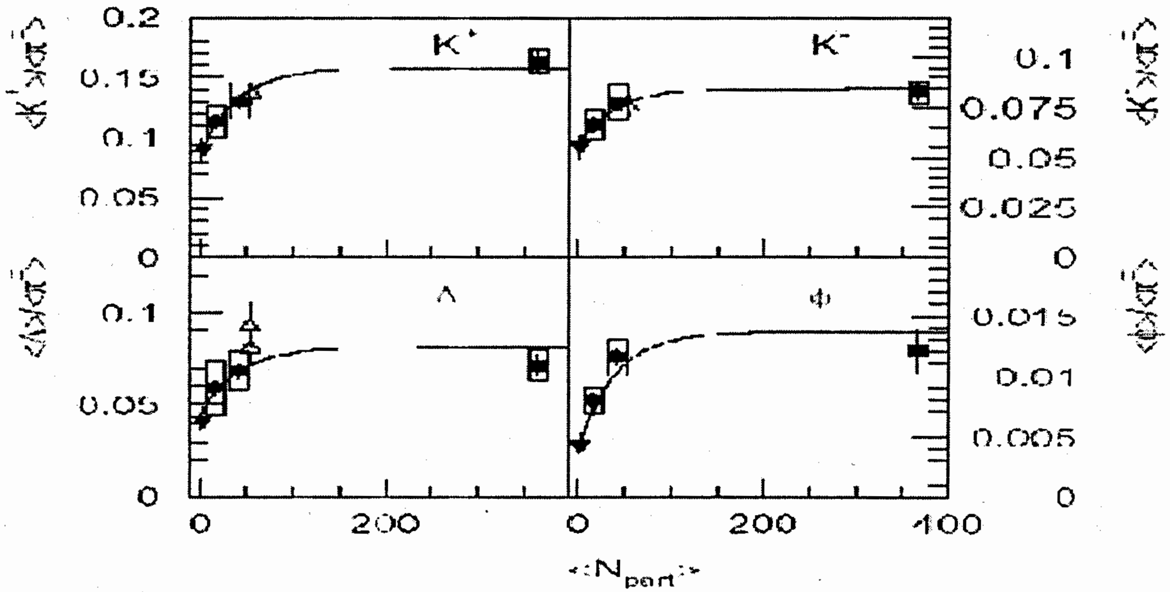

Experimental ratios of $\langle K^+\rangle$,$\langle K^-\rangle$,φ, and Λ to $\langle\pi^\pm\rangle$ plotted as a function of system size (▼ p+p, C+C and Si+Si, ● S+S, ■ Pb+Pb).Statistical errors are shown as error bars,systematic errors if available as rectangular boxes.The curves are shown to guide the eye and represent a functional form a - b exp($-\langle N_{part}\rangle$ /40). At $\langle N_{part}\rangle$=60 they rise to about 80%of the difference of the ratios between N_{part} =2 and 400.

Phenix Collaboration

RHIC

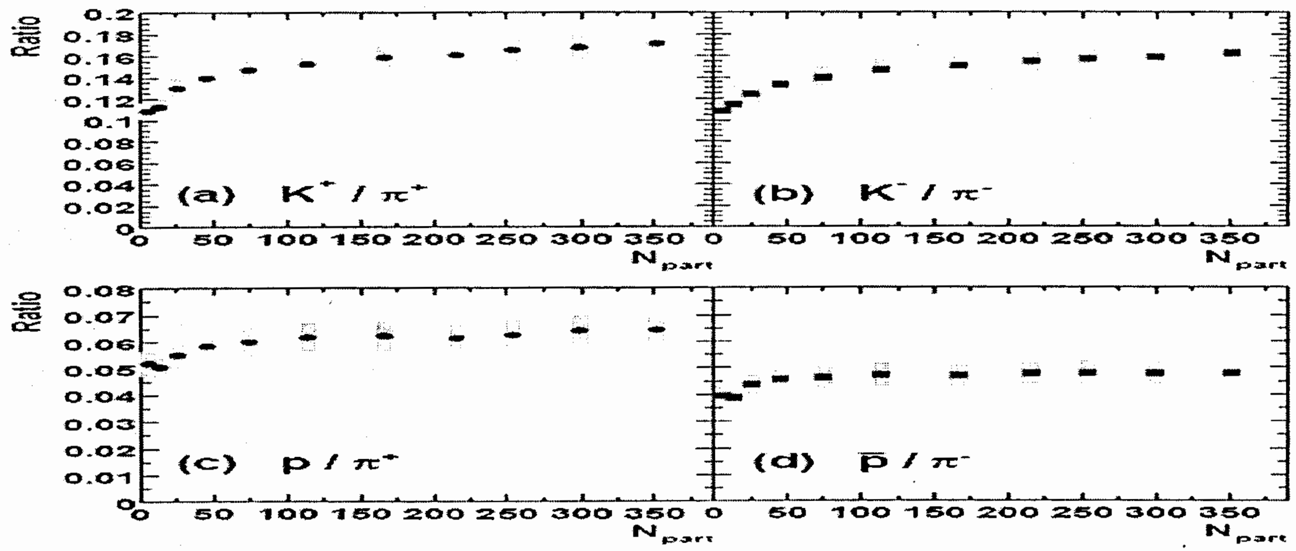

Centrality dependence of particle production ratios for
(a)K+/π+,
(b) K−/π−,
(c) p/π+, and
(d) antip/π−
in Au+Au collisions at $\sqrt{s_{NN}}$ = 200 GeV
[S. S. Adler, et al., Phys. Rev. Lett. 91 (2003) 182301.].

4. Analysis of dileptons and slow pion production in collisions of heavy nuclei (their enhancement in comparison with hadron-hadron interactions is expected).

Mixed Phase is a state of the compressed nuclear matter.

The π -meson condensate

А. Б. Мигдал, 1971, ЖЭТФ, 61, p. 2210;
1972, ЖЕТФ, 34 p. 1184;
1972, ЖЭТФ, 63, p. 1933;
1973, ЖЭТФ, 1973, 36, p. 1052;
R.F. Sawyer, Phys.Rev.Lett., 1972, 29, p. 382 ;
D. J. Scalapino, Phys.Rev.Lett., 1972, 386;
R. F. Sawyer And D. J. Scalapino, Phys.Rev.D, 1972, 7, p. 953.

The minimum baryon density for the pion condensation is expected to be

$$\rho_c \cong (2\text{-}3)\ \rho^0$$

(*T.Takatsuka and R.Tamagaki*, Prog. Theor. Phys 77 (1987), 362).

TAPS Colloboration - *R. Averbeck et al.* Z.Phys.A, 1997, 359, 65;
A.Marin et al., Phys.Lett.B, 1977, 409, 77;
A.R.Wolf et al., Phys. Rev. Lett., 1998, 80, 5281;
A. R. Wolf, geb. Gabler: Doktorarbeit, Gieben 1997.

Invariant inclusive specrtum of the $\pi 0$- and η-mesons produced in Au + Au reactions at 0,8 A GeV (left — noncentral collisions, right - central collisions).

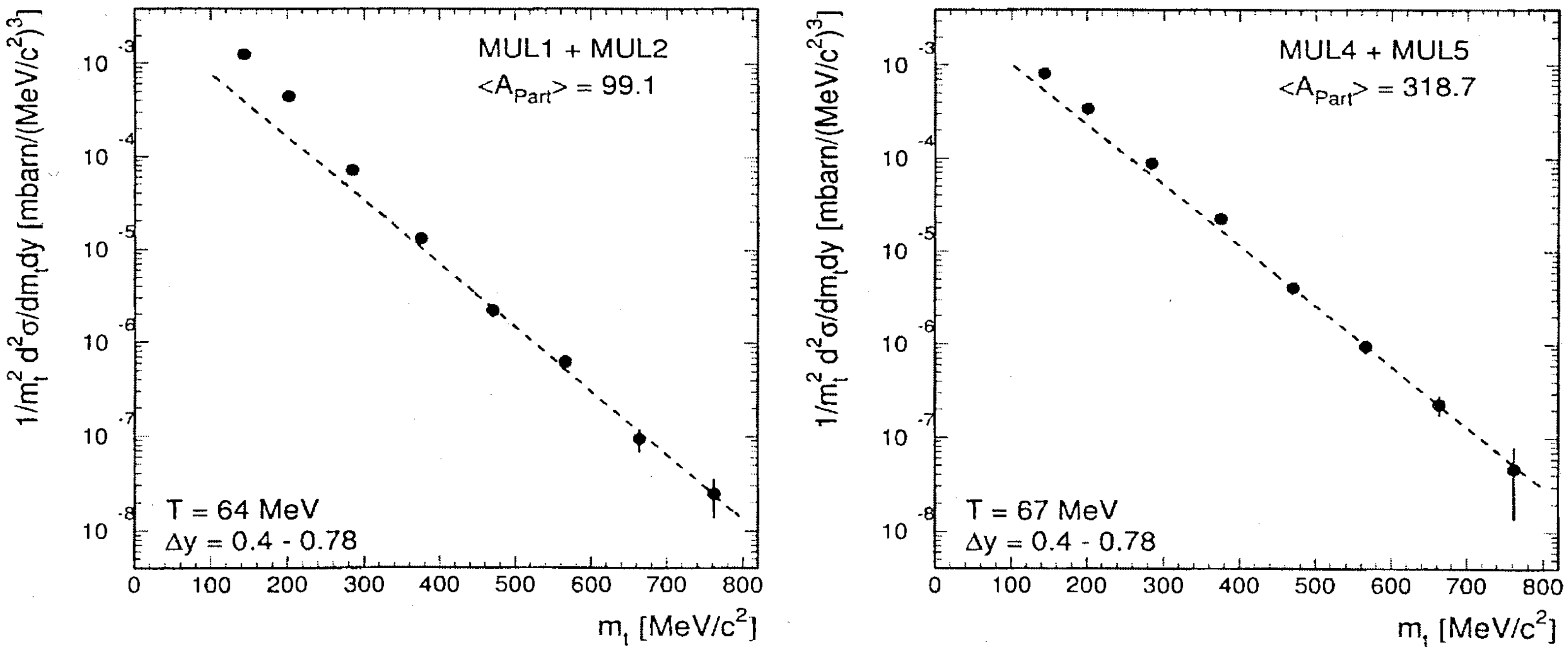

1) Two values of the temperature for π^0 –meson - T≅50 and 70 MeV;
2) dependence of the centrality.

CERN SPS Colloboration: D.Adamova´ et al., Enhanced Production of Low-Mass Electron-Positron Pairs in 40 AGeV Pb-Au Collisions at the CERES/NA45 experiment, nucl-ex/0209024.

Measurements of low-mass electron-positron pairs in Pb-Au collisions at the SPS beam energy of 40 AGeV. The pair yield integrated over the range of invariant masses 0.2<m ≤.1 GeV/c^2 is enhanced over the expectation from neutral meson decays by a factor of 5.9±1.5(stat.) ± 1.2(syst. data) ± 1.8(syst. meson decays), somewhat larger than previously observed at the higher energy of 158 AGeV. It may be linked to chiral symmetry restoration and support the notion that the in-medium modifications of the ρ are more driven by baryon density than by temperature.

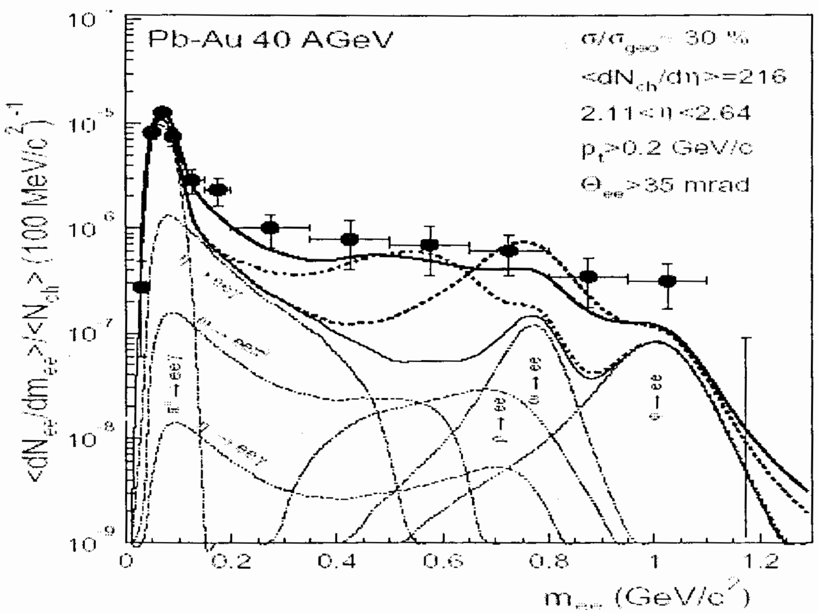

Inclusive e^+e^- mass spectrum, compared to the hadron decay cocktail (thin solid; individual contributions thin dotted) and to theoretical model calculations based on $\pi^+\pi^-$ annihilation with an unmodified ρ (thick dashed), an in-medium dropping mass ρ (thick dashed-dotted) and an in-medium spread ρ width (thick solid). The model calculations contain the cocktail, but without the ρ to avoid double counting. The low-mass tail of the cocktail ρ is due to the inclusion of a $\pi^+\pi^-$phase space correction. The (weaker) tails of the ω and φ are caused by electron bremsstrahlung.

5. Analysis of the behaviour of angular correlations and flows of secondary particles (their abnormal behaviour in comparison with hadron-hadron interactions is expected).

$$dN/d\phi \propto [1+2v_1\cos(\phi)+2v_2\cos(2\phi)]$$

BNL E895 Collaboration has studied the proton elliptic flow as a function of impact-parameter **b**, for two transverse momentum cuts in 2 - 6 *AGeV* *Au* + *Au* collisions (*AGS*).

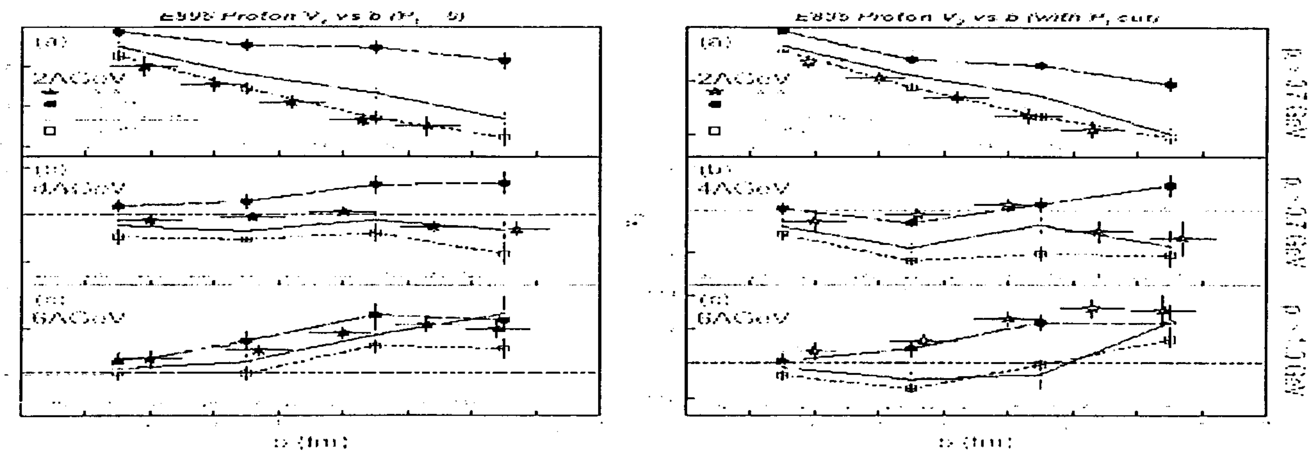

P. Chung et al. Differential Elliptic Flow in 2 - 6 AGeV Au + Au Collisions: A New Constraint for the Nuclear Equation of State, nucl- ex/ 0112002.

The elliptic flow shows an essentially linear dependence on b (for 1.5 < b < 8 fm) with a negative slope at 2 AGeV, a positive slope at 6 AGeV and a near zero slope at 4 AGeV. These dependencies serve as an important constraint for discriminating between various EOS for high density nuclear matter, and they provide important insights on the interplay between collision geometry and the expansion dynamics.

The angular distributions of protons with the momentum less than 1.0 GeV/c in the events of $\pi^{-12}C$ -interactions at the momentum 40 GeV/c with the total disintegration of nuclei [A.I.Anoshin et al.Yad.Fiz.33:164(1981)]. The anomalous peak is seen in this distribution. The behavior of angular distributions of protons emitted in $\pi^{-12}C$ -interactions at momentum 5 GeV/c [O.B.Abdinov et al. Preprint JINR,1-80-859,Dubna (1980)] has also an anomalous peak.

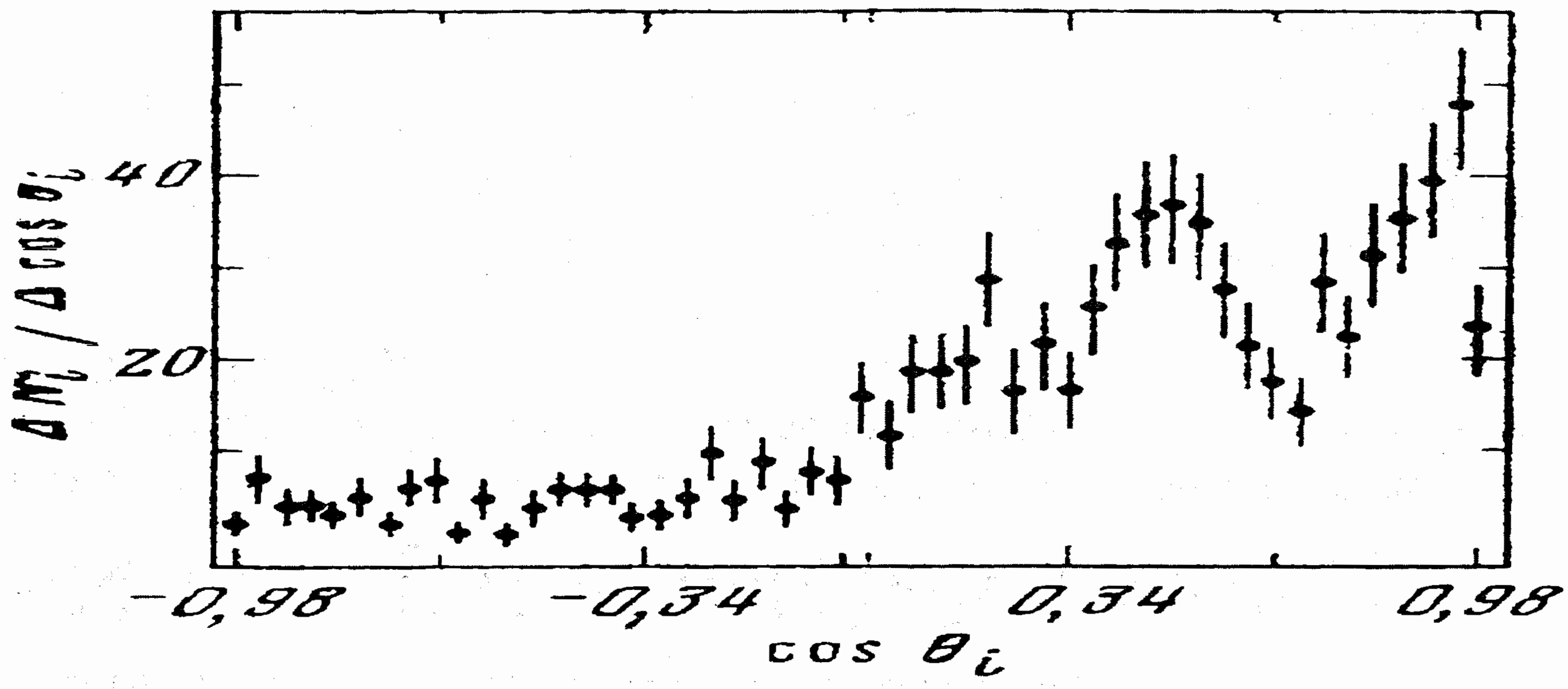

The angular distributions of protons emitted in $\pi^{-12}C$ -interactions at momentum 40 GeV/c.

Centrality experiments

Studying a dependence of characteristics of nuclear-nuclear interactions on the centrality is an important experimental way of obtaining information on phases of strongly interacting matter formed during the collision evolution. It is expected that new structures - changes in the behaviour, will show up in these characteristics due to phase transitions.

Search for the mixed phase of strongly interacting matter

Experimental results give an evidence of existence of sharp regime changes in event characteristics as a function of the collision centrality.

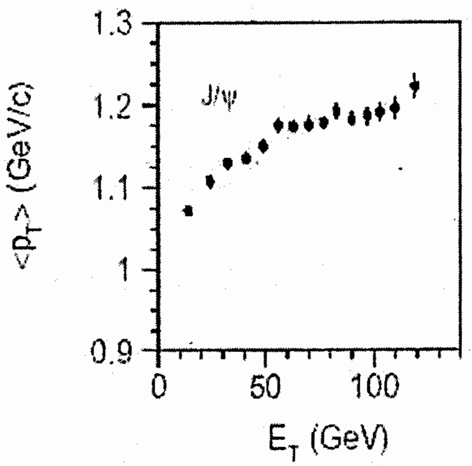

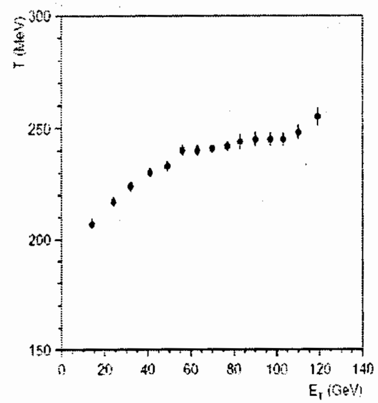

The behaviour changes at $E_T \approx$ 40-50 GeV

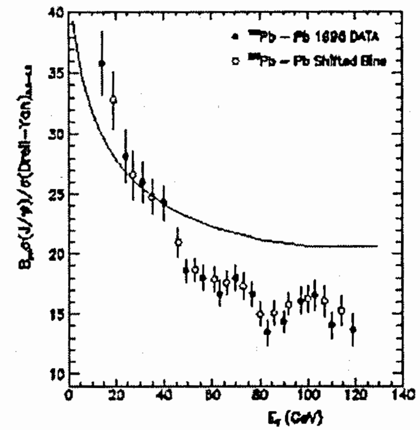

$<P_t>$ of J/Ψ and inverse slope (T) of J/Ψ transverse mass distributions in Pb-Pb interactions at 158 GeV/nucl. as a function of centrality (E_T) (NA38, NA50).

The cross section of J/Ψ production in Pb-Pb interactions at 158 GeV/nucl. as a function of centrality (E_T) (NA38, NA50) normalaized to the cross section of Drell-Yan pairs.

Possible explanation: the regime changes is a manifestation of the Mixed Phase (MP) formation (A.N. Sissakian, A.S. Sorin, M.K. Suleymanov, G.M. Zinovjev).

The experimental information on conditions of MP formation is important to fix the onset stage of the quark deconfiment for its future identification.

Search for MP: anomalous peak in the angular distribution of protons and anomalous angular correlation of secondary particles production and anomaly in the small energy π^0- or (π^+, π^-)-meson (lepton) pairs production, simultaneously, as a function of the centrality.

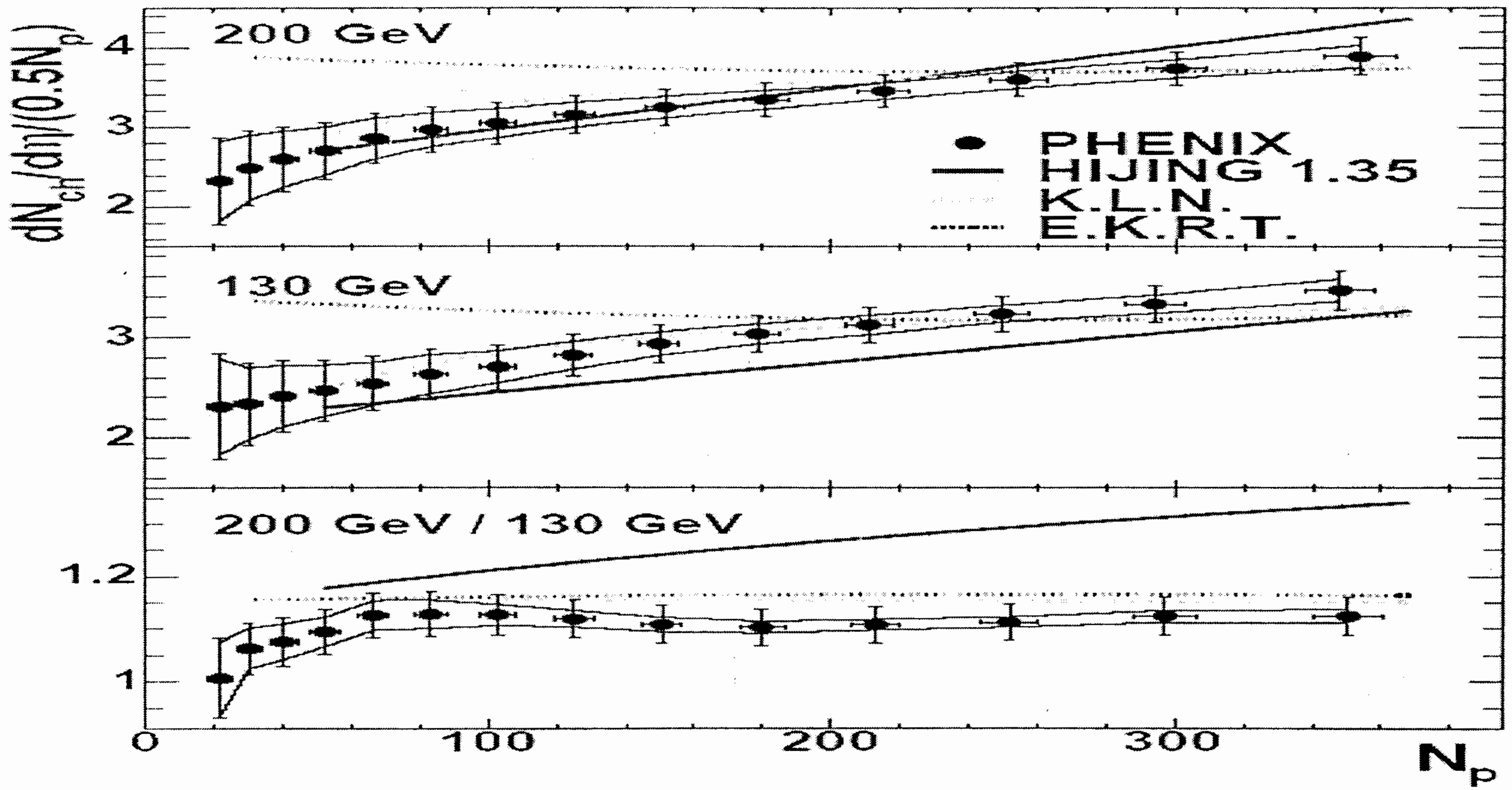

Multiplicity per participant nucleon pair, as a function of the centrality, for $\sqrt{s_{NN}}$ =130 GeV and 200 GeV Au+Au collisions as measured in PHENIX (A. Bazilevsky, Nucl. Phys. A715 (2003) 486).

Preliminary Collaboration

BLTP JINR:
D. Blaschke, E.Kuraev, A.Radzhabov, *A.Sissakian, A.Sorin,* V.Skokov, V.Toneev, M.Volkov, V.Yudichev, ...

LIT JINR:
Yu.Kalinovsky, ...

VBLHE JINR:
K.Abramyan, N.Amelin, B.Batyunya, A.Kovalenko, V.Krasnov, A.Malakhov, M.Suleymanov, A.Vodopianov, ...

DLNP JINR:
V.Karnaukhov, ...

ITEP (Moscow):
S.Molodtsov, ...

INR RAS (Moscow):
A.Kurepin, ...

BITP NAS (Kiev, Ukraine):
V.Begun, M.Gorenstein, S.Konchakovsky, V.Trubnikov, G.Zinovjev, ...

Collaboration, suggestions, and remarks are welcome!

L. Jenkovszky

Deeply Virtual Compton Scattering & Generalized Parton Distributions

Deeply Virtual Compton Scattering (DVCS)

$$\gamma^* N \;\to\; \gamma_{(M\ ,\, l^+ l^-)} N \quad (eN \;\to\; e\,\gamma N\,)$$

&

Generalized Parton Distributions (GPD)

(holography, tomography, phemtophotography)

(Classical) photography and the "phase problem"

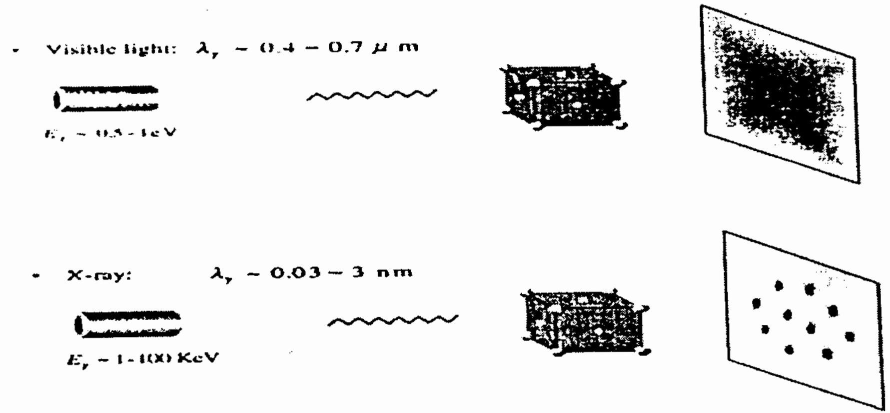

Кило…(гр.) Κιλιόσ = тыс.

мега…(гр.) μεγάσ = большой

гига…(гр.) γίγάσ = гигантский

тера…(гр) τέράσ = чудовище

$10^{\pm n}$

0 3 6 9 12 15

милли…(лат.) Mille – тысяча

микро…(гр.) μικροσ - малый

нано…(гр.) υάυοσ = карлик

пико…(исп.) (малый)

фемто…(дат.) femto = пятнадцать

- Form factor
- Parton density
- Generalized parton distribution at η=0

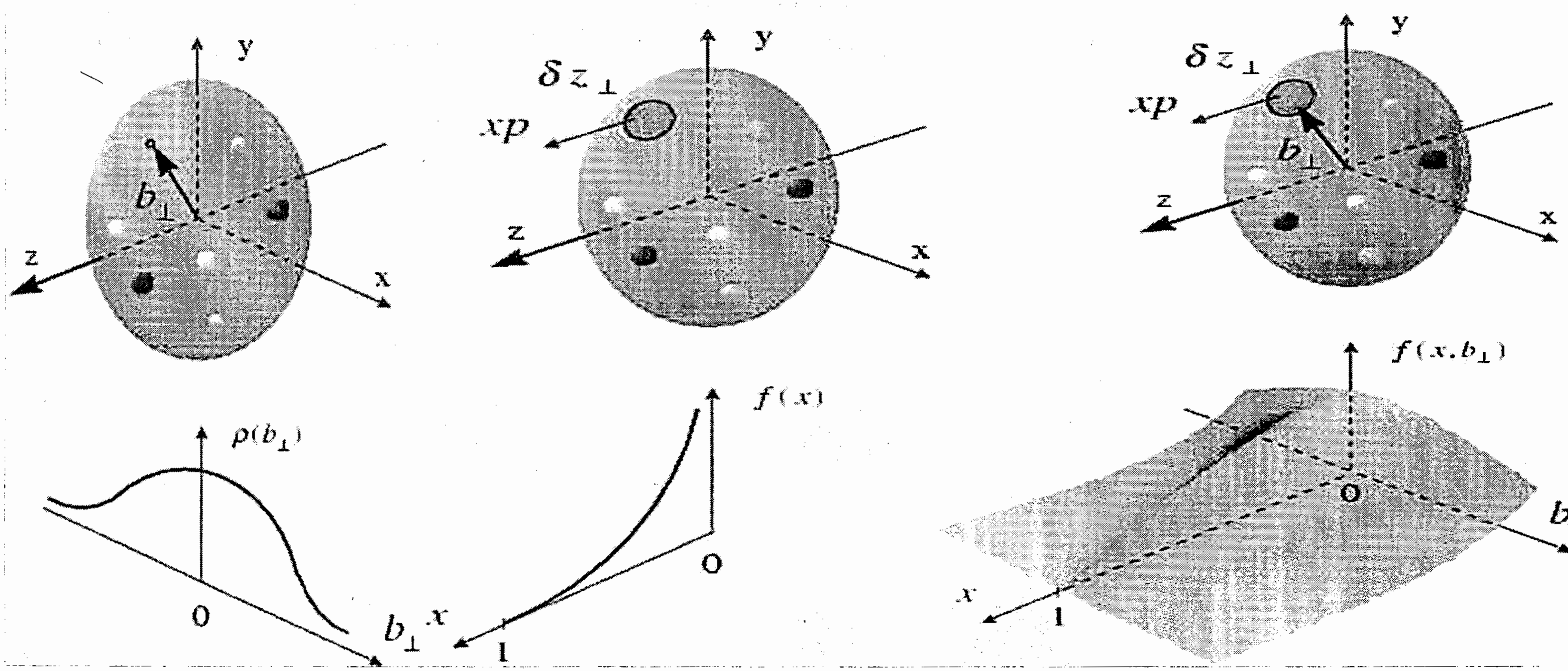

Longitudinal and transverse dimensions

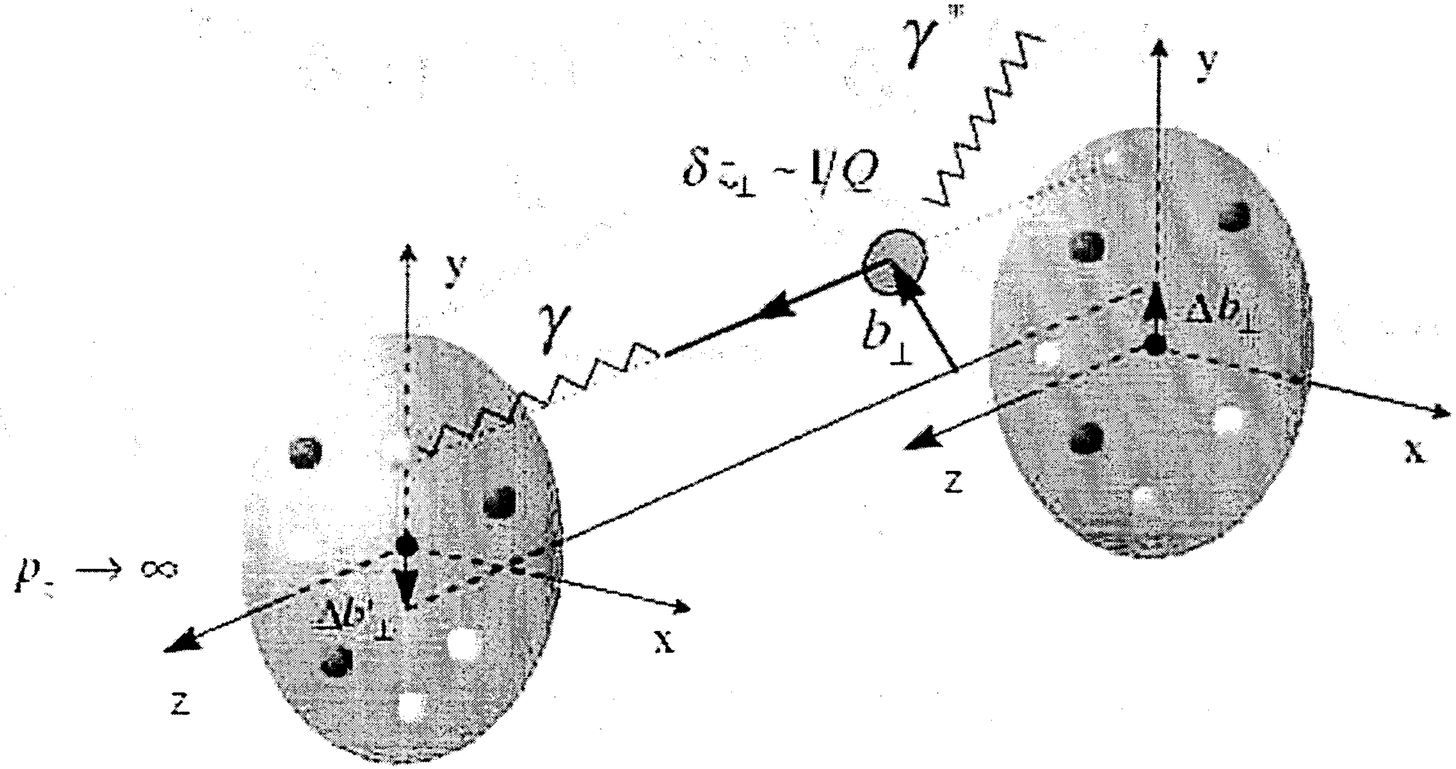

DIS (and ordinary parton distributions)

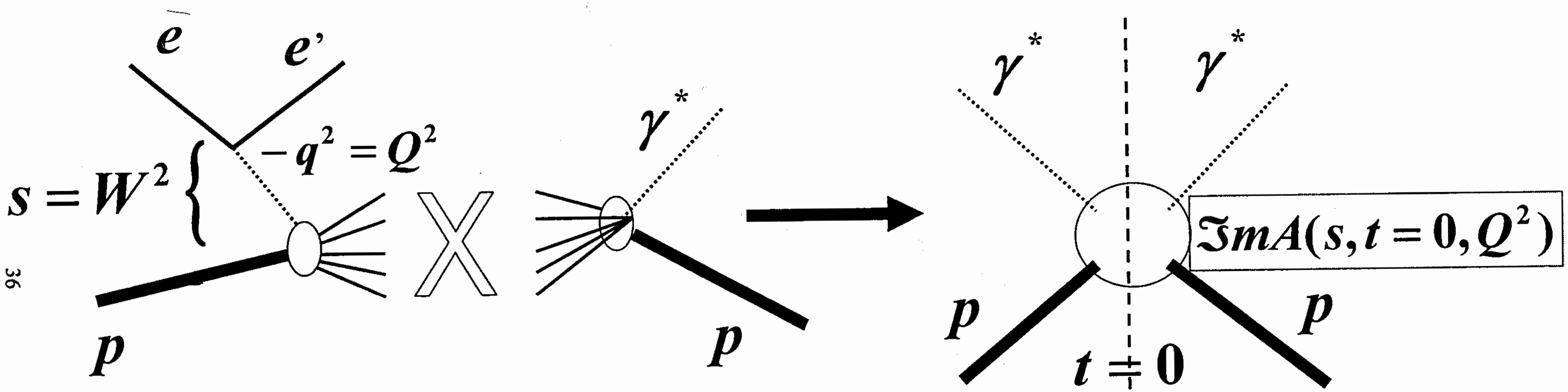

$$x = \frac{Q^2}{2pq} \qquad s = \frac{Q^2(1-x)}{x} + M^2 \approx \frac{Q^2}{x}, x \ll 1$$

The proton is smashed (completely destroyed)

Perturbative Quantum Chromodynamics (DGLAP Evolution)

$$F_2\left(x,Q^2\right)=x\sum_i\{e_i^2(q_i(x,Q^2)+\overline{q_i}(x,Q^2))+\alpha_s\left(Q^2\right)[C_i[x,\alpha_s\left(Q^2\right)]\otimes(q_i(x,Q^2)+$$

$$\overline{q_i}(x,Q^2))+[C_g\ [x,\alpha_s\left(Q^2\right)]\otimes g]\},$$

$$f(f)\otimes g(x)\equiv\int_x^1\frac{dy}{y}f\left(\frac{x}{y}\right)g(y),\ C_i=1+O(\alpha_s)C_s=O(\alpha_s).$$

Nonperturbative ("phenomenological") inputs

$$x(q_i(x,Q^2)=f(Q^2)x^{-\alpha(0)-1}(1-x)^{n(Q^2)}$$

3 "valence quarks"
+
"sea" of gluons and short lived $q\bar{q}$ pairs

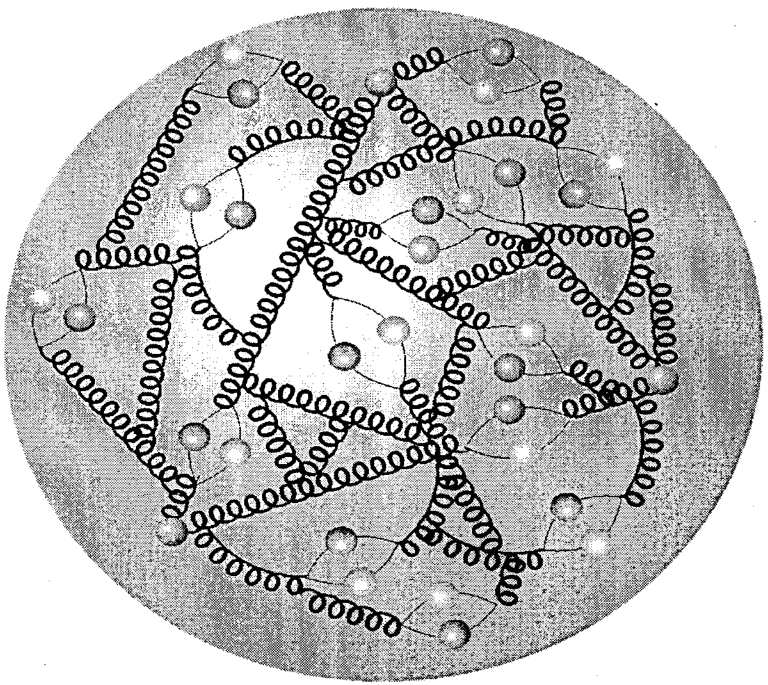

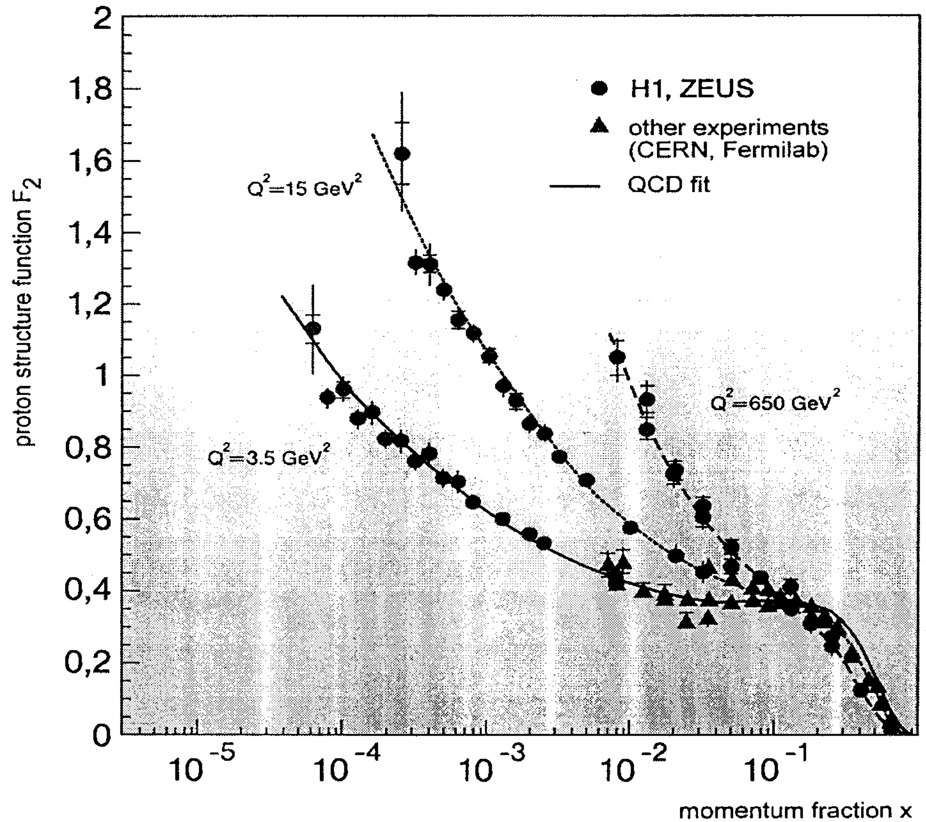

Holography

Dénes Gábor, 1948; Born in 1900 (Budapest),
Nobel Prize in 1971, Died in 1979 (London)

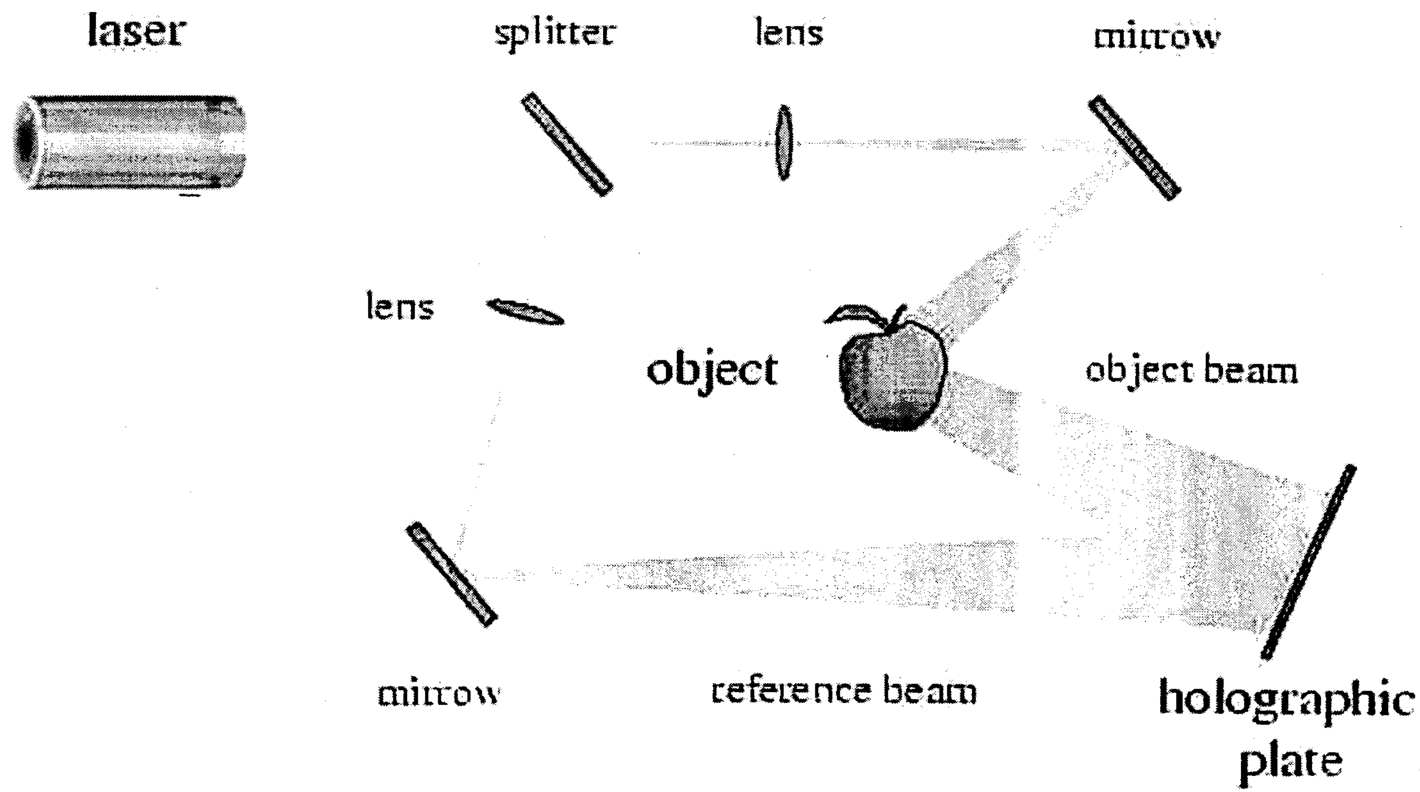

Nuclear holography

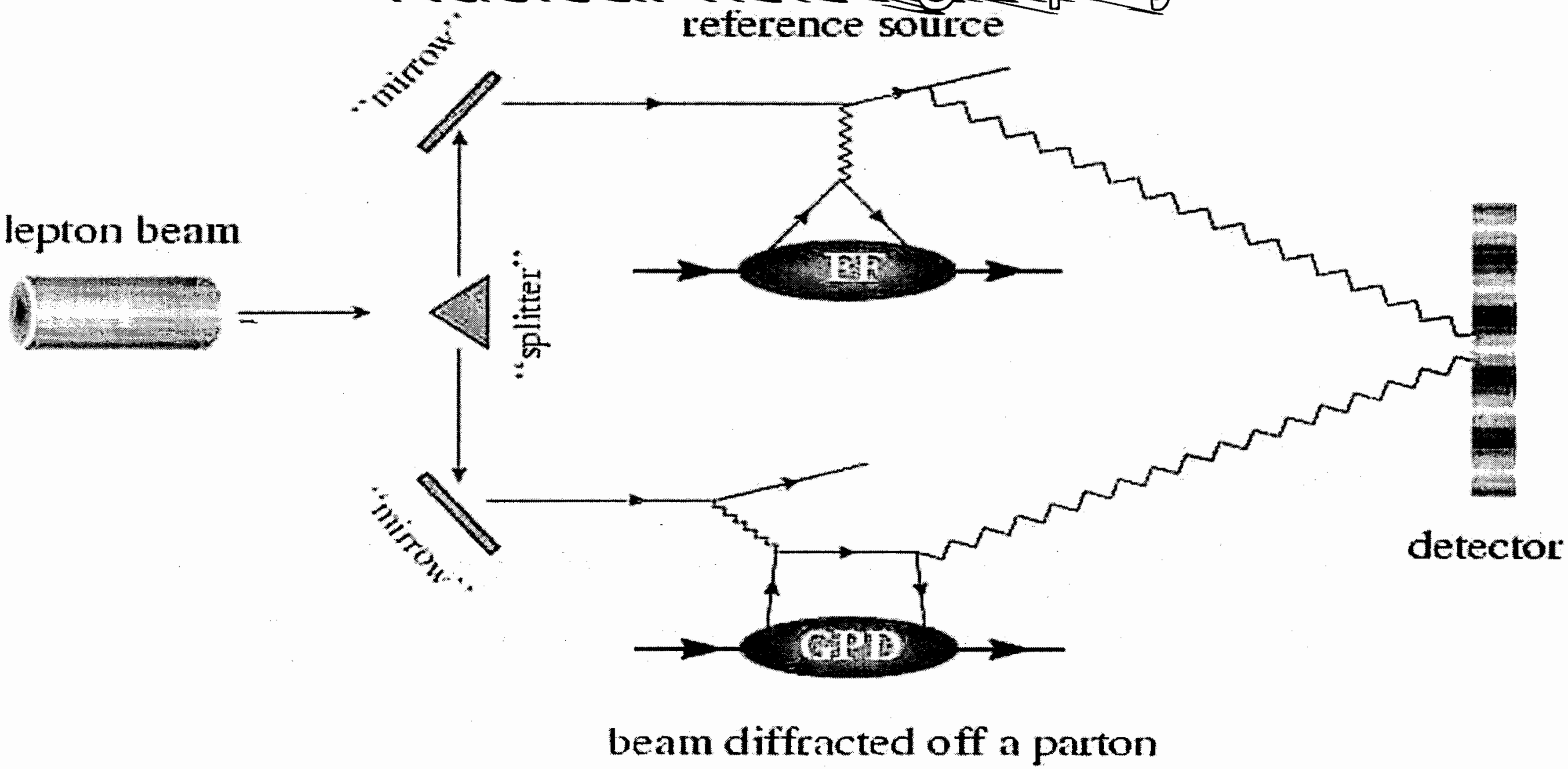

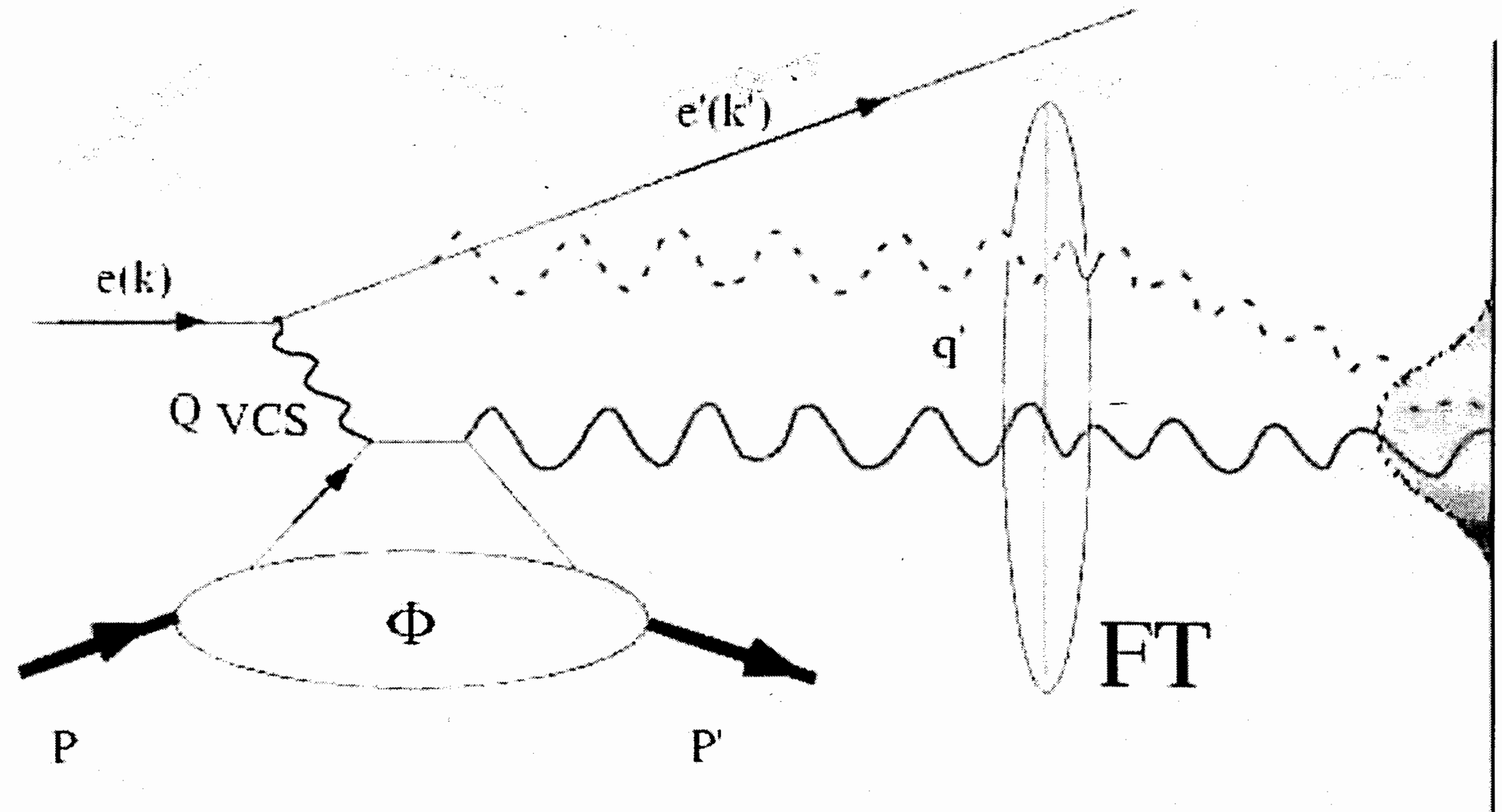
e(k)
e'(k')
Q VCS
q'
Φ
FT
P
P'

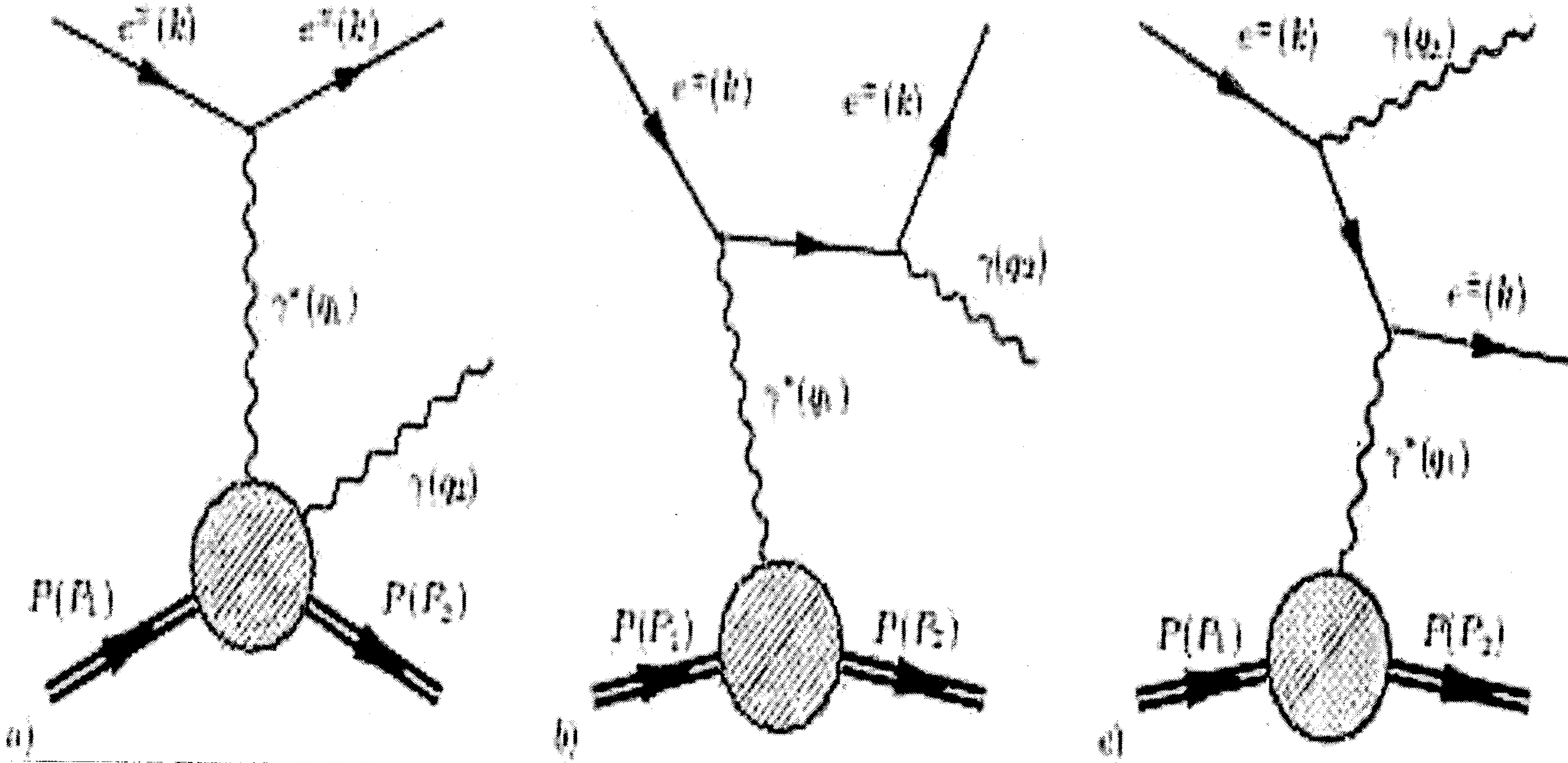
$e^{\pm}(k)$
$e^{\pm}(k')$
$\gamma^{*}(q_1)$
$\gamma(q_2)$
$P(P_1)$
$P(P_2)$
a)
b)
c)

Light-cone formalism

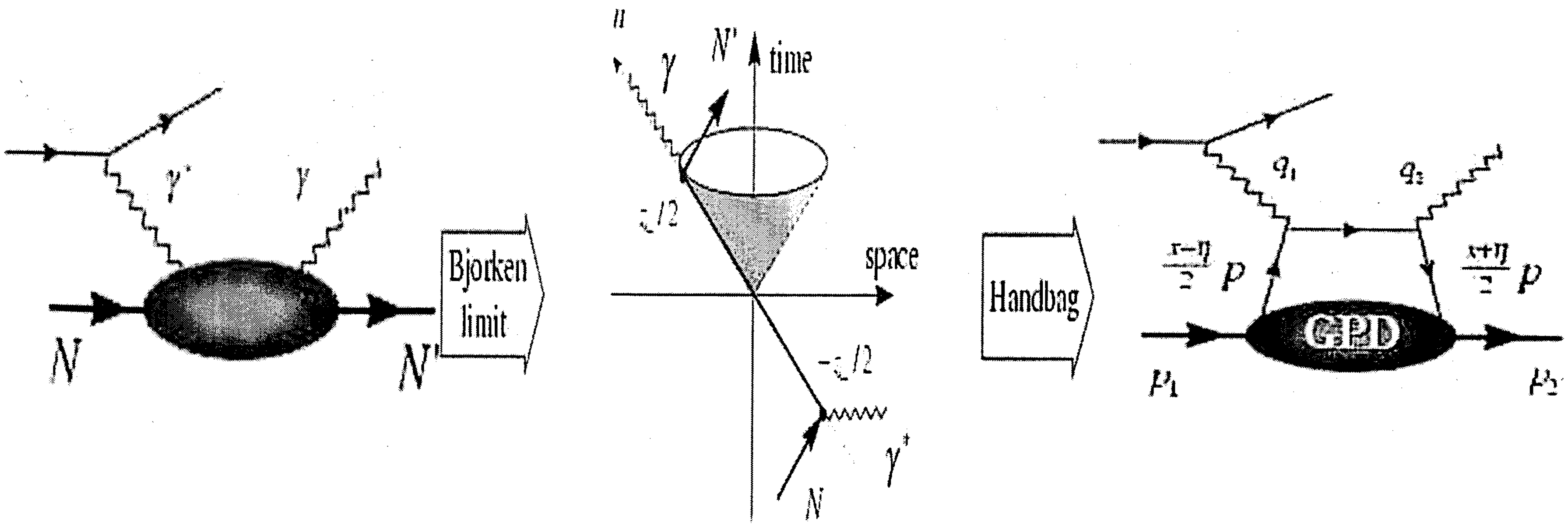

DVCS kinematics

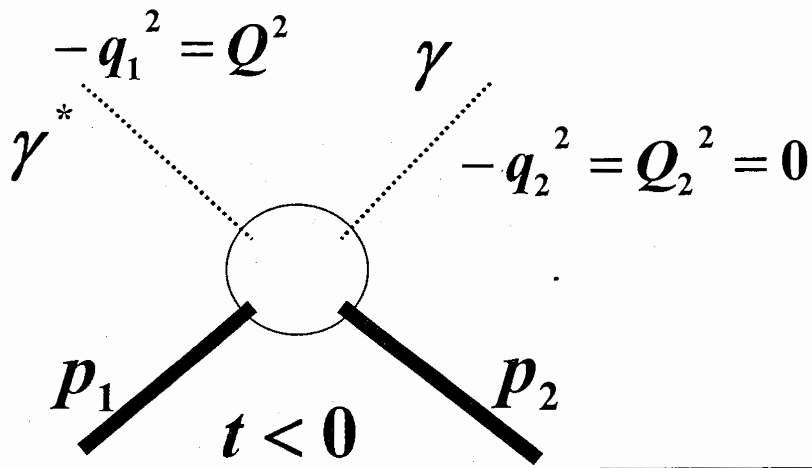

$$P = p_1 + p_2,\, q = (q_1 + q_2)/2$$

$$\Delta = p_2 - p_1, \quad t = \Delta^2$$

$$x_B = \frac{-q_1^{\,2}}{2p_1q_1} = \frac{Q^2}{2p_1q_1}$$

$$\xi = \frac{-q^2}{2Pq} = x_B \frac{1 + \dfrac{\Delta^2}{2Q^2}}{2 - x_B + x_B \dfrac{\Delta^2}{Q^2}}$$

$$\eta = \frac{\Delta q}{Pq} = -\xi \left(1 + \frac{\Delta^2}{2Q^2}\right)^{-1}$$

The basic object of the theory

$$A(s,t,Q^2) \to A(s,t,Q^2=m^2) \text{ (on mass shell)}$$

$$A(s,t,Q^2) \to \Im m A(s,t=0,Q^2) \sim F_2 \qquad \text{DIS}$$

Reconstruction of the DVCS amplitude from DIS

$$F_2 \sim \Im m A(\gamma^* p \to \gamma^* p)\big|_{t=0} \to \Im m A(\gamma^* p \to \gamma p)\big|_{t=0}$$

$$\to A(\gamma^* p \to \gamma p)\big|_{t=0} \to A(\gamma^* p \to \gamma p)$$

or

$$\Im m A(\gamma^* p \to \gamma^* p)\big|_{t=0} \sim F_2(x_B,Q^2) = x_B q(x_B,Q^2)$$

$$q(x_B,Q^2) \to q(\xi,\eta,t,x_B,Q^2) \longrightarrow$$

$$\longrightarrow \xi q(\xi,\eta,t,x_B,Q^2) \stackrel{?}{=} GPD(\xi,\eta,t,x_B,Q^2)$$

[redacted]

Spin

$$q(x) = \frac{1}{2}\Im m\left[F_1(x,Q^2) + F_3(x,Q^2)\right]_{t=0}$$

$$\Delta q(x) = \frac{1}{2}\Im m\left[F_3(x,Q^2) - F_1(x,Q^2)\right]_{t=0}$$

$$\delta q(x) = \frac{1}{2}\Im m F_2(x,Q^2)\Big|_{t=0}$$

J. Bjorken, in Particle Physics, NY 1972, and SLAC-PUB-7096,1996;
R.L. Jaffe and X. Ji, PRL 67 (1991) 552;
J. Soffer, PRL 74 (1995) 1292;
S.M. Troshin and N.E. Tyurin, PR D63 (2001)

$F_i(x,Q^2)$ - helicity scattering amplitudes for q-h scattering

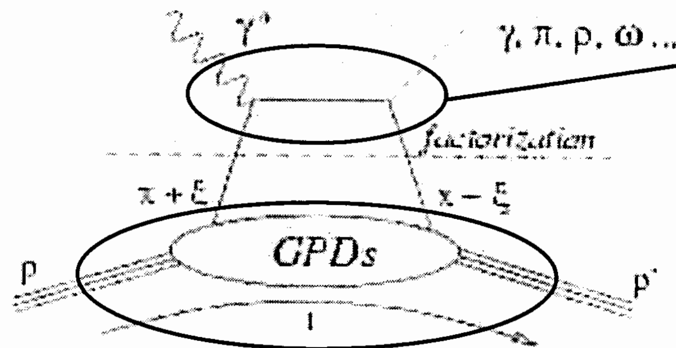

pQCD

$$F_2(x, Q^2) \sim xq(x, Q^2)$$

non-perturbative region

See, however:

S. Brodsky et al., hep-ph/0104291, PR 2002

S. Brodsky et al., hep-ph/0009254, NP 2001

GPDs cannot be measured directly, instead they appear as convolution integrals, difficult to be inverted !

$$A(\xi,\eta,t) \sim \int_{-1}^{1} dx \frac{GPD(x,\eta,t)}{x-\xi+i\varepsilon}$$

"Handbag"

We need clues from phenomenological models - Regge behaviour, t-factorization etc.

$$\sigma_{tot} \sim \Im m A, \qquad \frac{d\sigma}{dt} \sim |A|^2$$

$$A(\xi,\eta,t,x_B,Q^2) \sim \int_{-1}^{1} dx \frac{GPD(x,\eta,t,x_B,Q^2)}{x-\xi+i\varepsilon}$$

If we are interested only in $\Im m A \sim \sigma_{tot} \longrightarrow$

[redacted]

49 $t = 0, Q^2 \to 0, x_B \to 0,$

$$\xi = -\eta = \frac{x_B}{2} \longrightarrow$$

$$\Im m A_{DVCS}(x_B/2, -x_B/2, t=0, x_B, Q^2) =$$

$$\Im m A_{DIS}(x_B, Q^2) \sim F_2(x_B, Q^2) \sim \left(\frac{1}{x_B}\right)^{\alpha_t(0)-1}$$

Various limits

DVCS $\quad t = 0$

$$\eta = -\xi, \; \xi = \frac{x_B}{2 - x_B}$$

50

We can return to symmetric $\gamma p \to \gamma p$ only for $Q^2 \to 0$

$$Q^2 \to 0, x_B \to 0, \xi = x_B / 2$$

$$A_{DIS}(s, t = 0, x_B \to 0, Q^2 \to 0) = A_{DVCS}(s, t = 0, \xi = x_B / 2 \to 0, Q^2 \to 0)$$

General, symmetric

$$\boxed{Q_2^{\,2} = Q^2, \eta = 0}$$

But we may have $t = -\Delta_\perp^2 \neq 0$

Generatization of $A_{DIS}(x_B, Q^2, t)$ **to** $t \neq 0$

V.K. Magas, hep-ph/0404255;
L.L. Jenkovszky, V.K. Magas and E. Predazzi, EPJ A12 (2001) 361;
R. Fiore et al., EPJ A15 (2002) 505

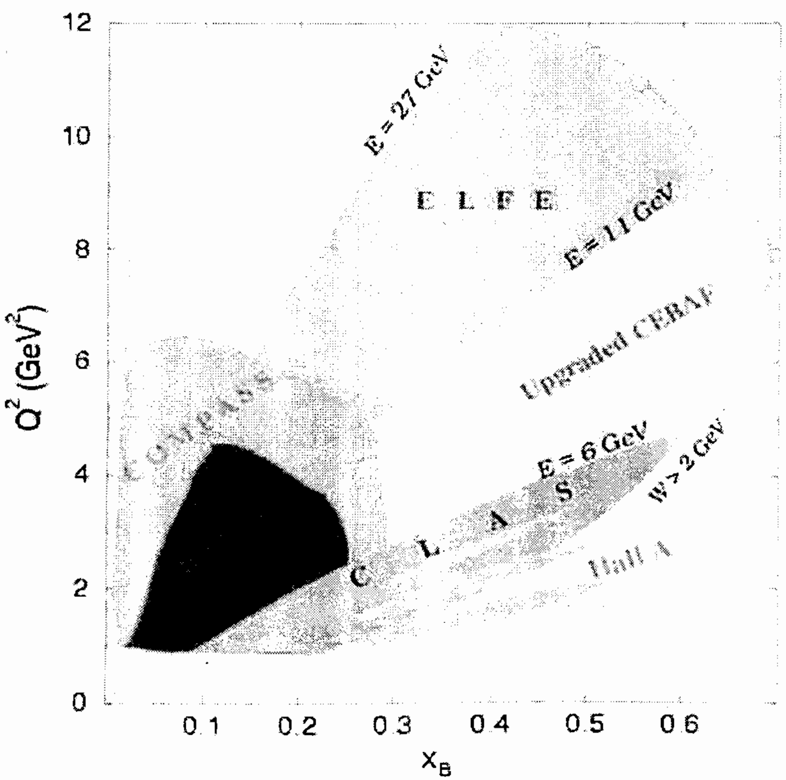

HERMES, E=27 GeV, low luminosity

JLab, E=4-6 GeV

Upgrated CEBAF/Jlab, E=12 GeV

COMPAS, E=200 GeV

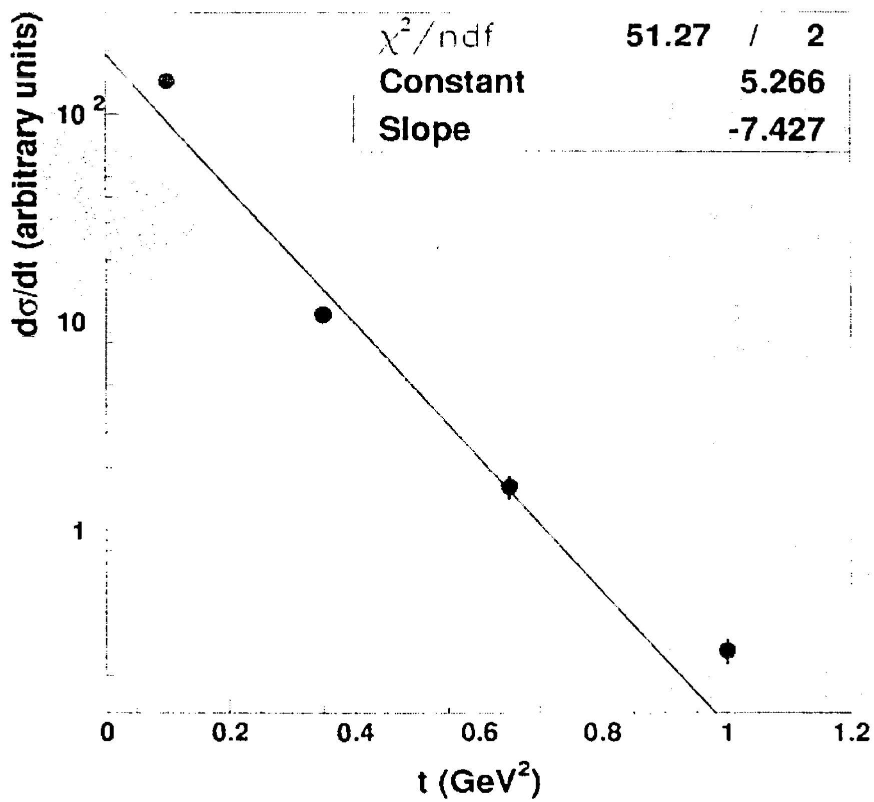

t SLOPE FOR 1999-2000

Fitting a function

$$\frac{d\sigma}{dt} = C \cdot \exp\left(-Slope \cdot t\right),$$

we find for $Q^2 = 9.6\ \mathrm{GeV}^2$:

$$Slope = 7.4 \pm 1.1\ \mathrm{GeV}^{-2}.$$

Note

- χ^2 minimisation method used for the fit,
- poor quality of the fit (large χ^2),
- no systematic error is quoted yet.

t SLOPE AS A FUNCTION OF Q^2

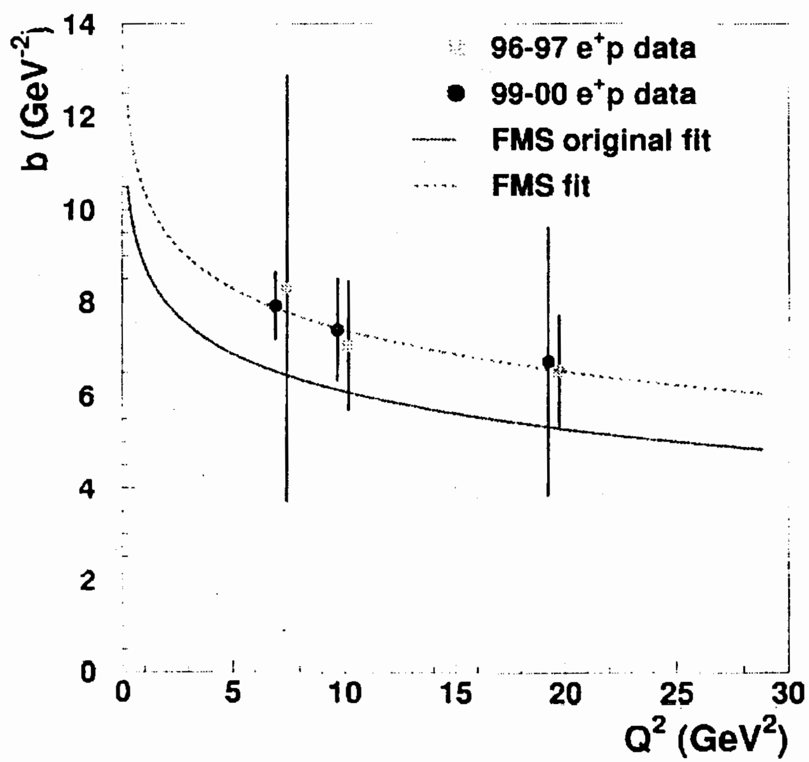

Analysis performed in two bins of Q^2:

$5 < Q^2 < 11 \text{ GeV}^2$ for $\langle Q^2 \rangle = 7.0$

$11 < Q^2 < 100 \text{ GeV}^2$ for $\langle Q^2 \rangle = 19.0$

Results compared with the Freund, Mc Dermott and Strikman fit (solid line):

$$Slope = b(Q^2) = b_0(1 - C \ln \frac{Q^2}{2}),$$

with $b_0 = 8 \, \text{GeV}^{-2}$ and $C = 0.15$.

Also a new fit to the 99-00 data has been performed (dashed line). The new values are:

$b_0 = 9.5 \, \text{GeV}^{-2}$ and $C = 0.14$.

There is an evidence that the t slope decreases with Q^2.

$$A^{\gamma p \to V p} \propto f\left(Q_1^2, Q_2^2\right) e^{R^2\left(s, m^2\right) t}$$

$$R^2 = B = b_2\left(m_p^2\right) + b_1\left(Q_1^2, Q_2^2\right) + \alpha' \ln s$$

$$\widetilde{Q}^2 = Q_1^2 + M_V^2 \, (?)$$

$$1)\text{"}Symmetries\text{"}: B^{\gamma^*\left((Q^2 \approx 9.6) \to \gamma_{real}\right)} = B^{\gamma_{real} \to J/\psi} \, ?$$

$$2)\text{"} B^{\gamma_{real}} \text{"} \approx \text{"} B^{\rho} \, ?$$

$$3) B \propto Q^{-2}, but\, B_{pp} \approx \frac{5}{4} B_{\pi p}.$$

$$A\left(s, t, Q_1^2, Q_2^2\right) = iG(t, Q_1^2, Q_2^2)\left(-\frac{is}{s_0}\right)^{\alpha(t)-1}, \quad G(t, Q_1^2, Q_2^2) = G(Q_1^2, Q_2^2) e^{b(Q_1^2, Q_2^2) t},$$

$$G(Q_1^2, Q_2^2) = \frac{g_0}{\left(\frac{Q_1^2}{Q_0^2} + \frac{Q_2^2}{Q_0^2}\right)^{n_1}}, \quad G(Q_1^2, Q_2^2) = \frac{g_0}{\left(\frac{Q_1^2}{Q_0^2} + \frac{Q_2^2}{Q_0^2}\right)^{n_1}},$$

$$\alpha(t) = \alpha_0 + \alpha' t \Rightarrow \alpha_0 + \alpha_1 - \sqrt{4m_\pi^2 - t}; \; \alpha_i \Rightarrow \alpha_i(Q\text{^}2);$$

$$Adjustable\ parameters: g_0,\ b_0,\ b_1,\ n_1,\ n_2, Q_0^2;\ \ fixed: \alpha_0 \approx 1.1,\ \alpha' \approx 0.2,\ s_0 = 1,\ Q_0^2 = 0,\ M^2.$$

$$A\left(s, t, Q_1^2, Q_2^2\right) \Rightarrow A\left(\xi, \zeta, x_{Bj}, t\right)$$

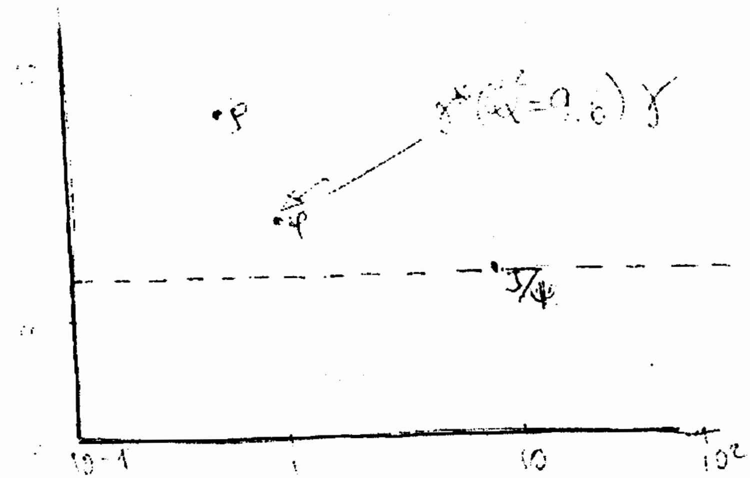

Process	Value of slope b, GeV^{-2}	W, GeV	$\|t\|, GeV^2$	Exp.	Ref.
$\gamma p \to \rho p$	$10.31 \pm 0.77(stat.) \pm 0.52(sys.)$	25-70	0.073-0.45	H1	[69]
	$10.9 \pm 0.3(stat.)^{+1.0}_{-0.5}(sys.)$	50-100	0.-0.5	ZEUS	[68]
	$6.0 \pm 0.3(stat.)^{+0.6}_{-0.3}(sys.) \pm 0.4(mod.)$	85-105	0.4-1.2	ZEUS	[76]
$\gamma p \to \rho Y$	$5.8 \pm 0.3(stat.) \pm 0.5(sys.)$	50-100	0.025-0.5	ZEUS	[68]
	$2.4 \pm 0.2(stat.)^{+0.2}_{-0.1}(sys.) \pm 0.3(mod.)$	85-105	0.4-1.2	ZEUS	[76]
$\gamma p \to \phi p$	$7.3 \pm 1.0(stat.) \pm 0.8(syst.)$	60-80	0.1-0.5	ZEUS	[293]
	$6.3 \pm 0.7(stat.) \pm 0.6(sys.) \pm 0.3(mod.)$	85-105	0.4-1.2	ZEUS	[76]
$\gamma p \to \phi Y$	$2.1 \pm 0.5(stat.) \pm 0.3(sys.) \pm 0.4(mod.)$	85-105	0.4-1.2	ZEUS	[76]
$\gamma p \to J/\psi p$	$4.73 \pm 0.25(stat.)^{+0.30}_{-0.39}(sys.)$	40-150	0-1.2	H1	[70]
	$4.99 \pm 0.13(stat.)^{\pm 0.45}(sys.)$	40-150	0.07-0.9	H1	[73]
	$4.15 \pm 0.05(stat.)^{+0.30}_{-0.18}(sys)$	20-290	0-1.2	ZEUS	[71]
	$4.0 \pm 1.2(stat.)^{+0.7}_{-1.1}(sys)^{+0.4}_{-0.6}(mod.)$	85-105	0.4-1.2	ZEUS	[76]
$\gamma p \to J/\psi Y$	$0.7 \pm 0.4(stat.) \pm 0.2(sys.)^{+0.5}_{-0.3}(mod.)$	85-105	0.4-1.2	ZEUS	[76]
	$1.07 \pm 0.03(stat.) \pm 0.11(sys.)$	40-150	0.15-3	H1	[73]
$\gamma p \to \Psi(2S) p$	$4.69 \pm 0.57(stat.) \pm 0.46$	40-150	0.07-0.9	H1	[73]
$\gamma p \to \Psi(2S) Y$	$0.59 \pm 0.13(stat.) \pm 0.12(sys.)$	40-150	0.15-3	H1	[73]

Table 4: *Recent HERA measurements of the b slope for PHP elastic and proton-dissociative vector-meson production.*

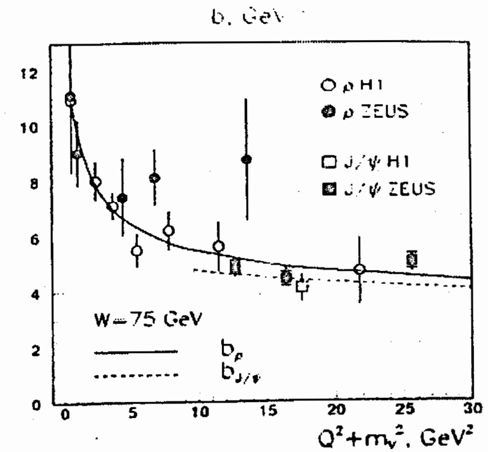

Figure 61: *The diffraction slope b of elastic production of the ρ (H1: [16], ZEUS: [68, 81]) and J/ψ (H1: [89], ZEUS: [90]) mesons as a function of $Q^2 + M_V^2$. The predictions of from the k_t-factorization approach [54, 55] are shown.*

8.3 Shrinkage of the diffraction cone and the Pomeron trajectory

8.3.1 The W-dependence in photoproduction

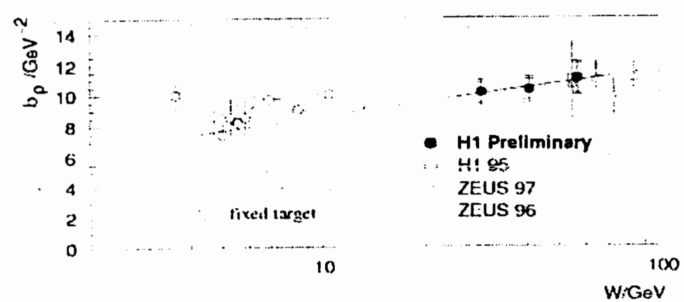

Figure 62: *The diffraction slope b_ρ as a function of W for ρ photoproduction [69]. The continuous line shows the result of the fit of the form (37) to the recent H1 measurement, other HERA and fixed target measurements are shown for comparison; the extrapolation of the fit to the low W region is indicated by the dashed*

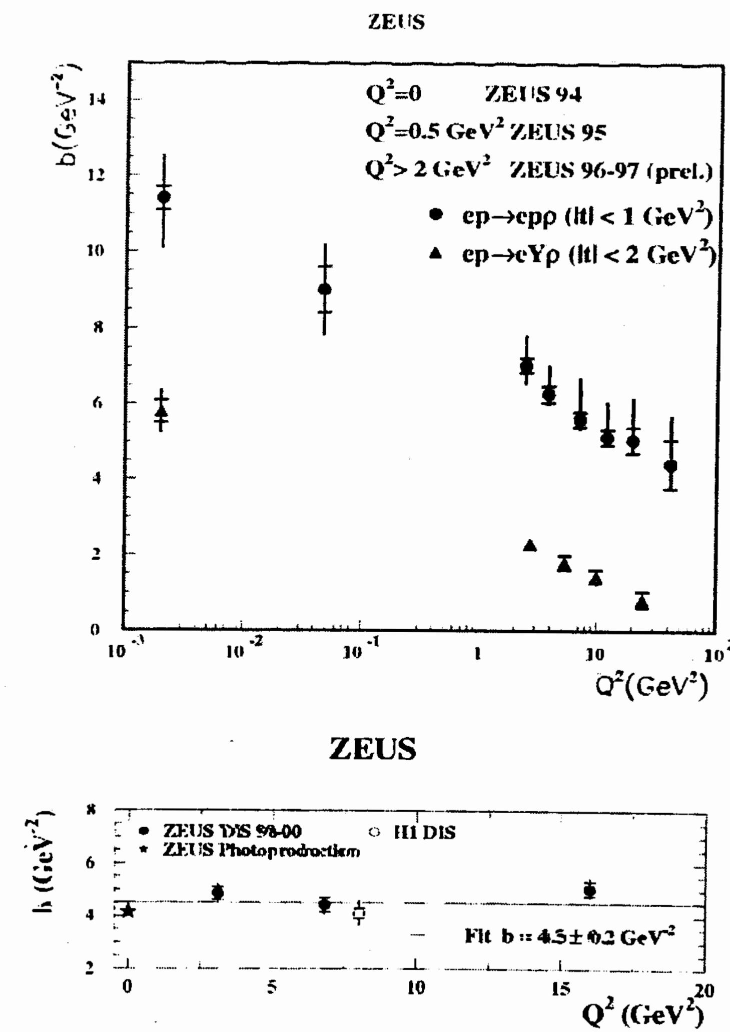

Figure 60: *The preliminary ZEUS data on diffraction slope b for elastic and proton-dissociative production of the ρ (upper box, [84]) and (bottom box) recent ZEUS [90] and H1 [89] data for elastic production of the J/ψ mesons as a function of Q^2.*

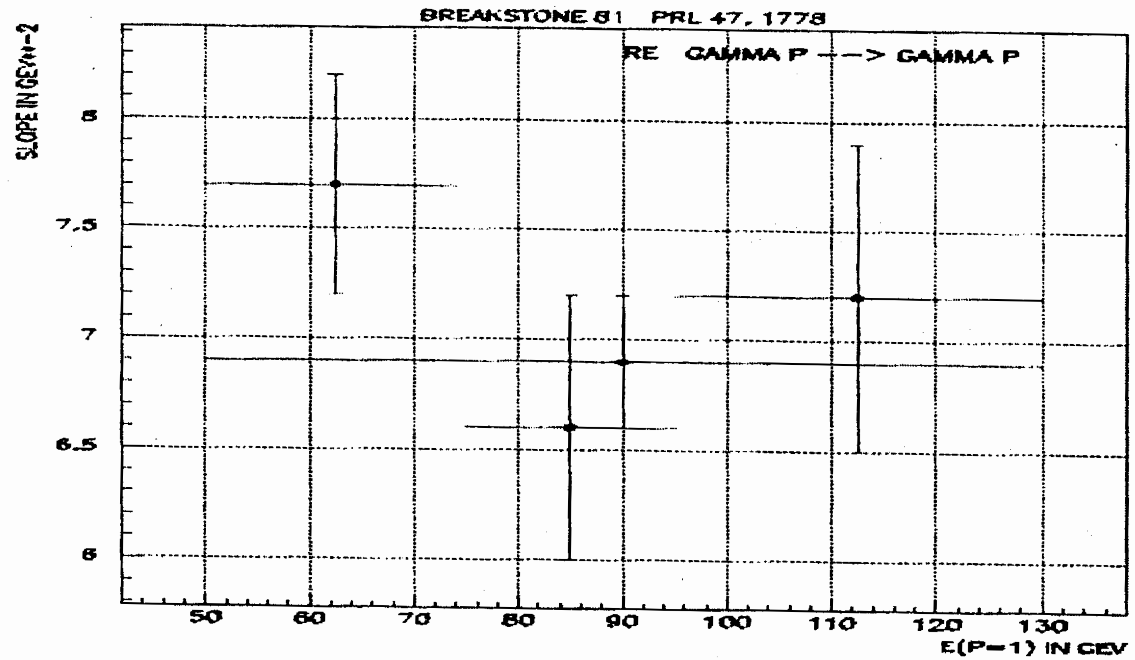

Breakstone PRL 47 (1981) 1778

E_γ = 50 - 130 GeV

W = 10 - 14

A phemtophotography of the nucleon

$$H\left(x,t)\right) = x^{-0.08}(1-x)^4 e^{-10t(1-x)}$$

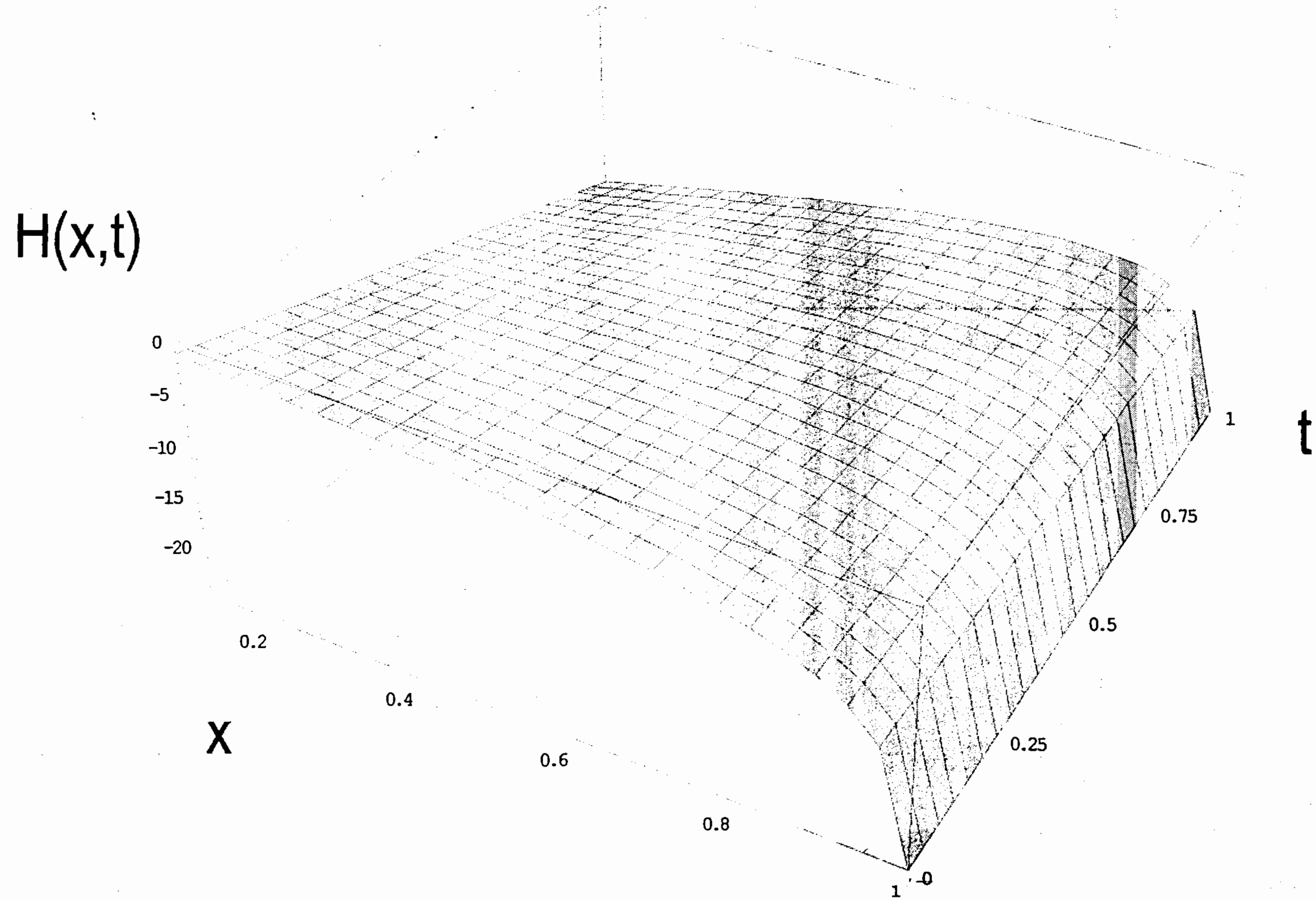

The basic object of the theory $A(s,t,Q^2)$

Two-dimensionally dual picture of the strong interactions

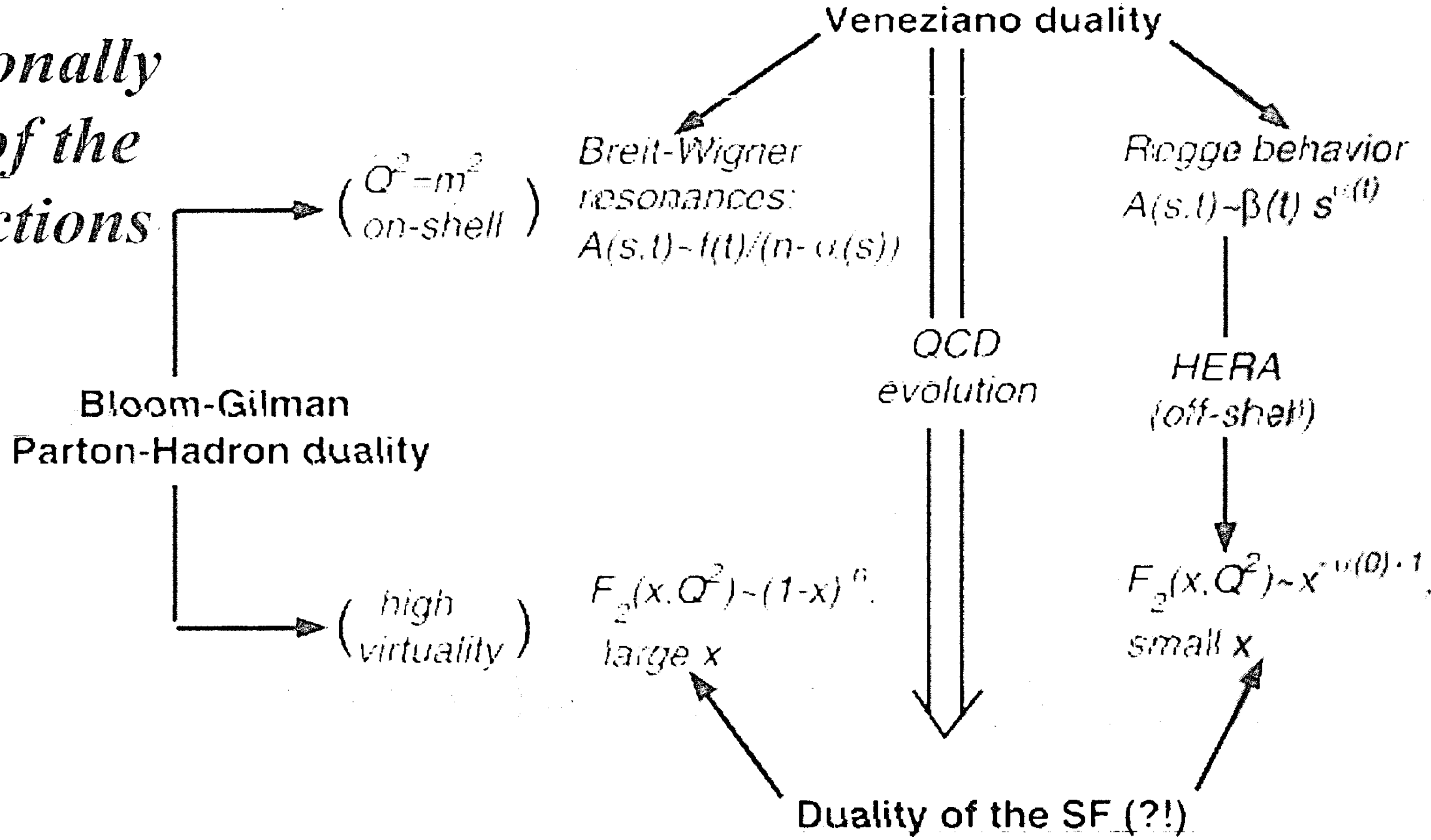

$$\boxed{D(s,t)=\int_0^1 dz\left(\frac{z}{g}\right)^{-\alpha_s(s')-1}\left(\frac{1-z}{g}\right)^{-\alpha_t(t'')-1},}\quad s'=s(1-z),\, t''=tz,\, g>1$$

$$s\to\infty,\, t=const$$

$$D(s,t)\sim g^{1-\alpha\left(\frac{\alpha_t(t)}{\alpha_s'(0)\ln g}\right)}\left(\frac{s\alpha_s'(0)g\ln g}{\alpha_t(t)}\right)^{\alpha_t(t)-1}$$

$$D(s,t)=\sum_n g^{n+\alpha_t(t)}\frac{C_n(t)}{n-\alpha_s(s)},\quad C_n(t)=\frac{1}{n!}\frac{d^n}{dz^n}\left[\left(\frac{1-z}{g}\right)^{-\alpha_t(t')-1}\right]$$

Introducing Q-dependence in the S-matrix (dual models)

L.L. Jenkovszky, V.K. Magas and E. Predazzi, EPJ A12 (2001) 361;
R. Fiore et al., EPJ A15 (2002) 505 ➡ $+g \to g(Q^2)$

V.K. Magas, hep-ph/0404255 ➡

$$D(s,t,Q^2) = \int_0^1 dz \left(\frac{z}{g}\right)^{-\alpha_s(s')-\beta(Q^{2''})-1} \left(\frac{1-z}{g}\right)^{-\alpha_t(t'')-\beta(Q^{2'})-1}$$

R. Fiore, L. Jenkovszky, V. Magas, E. Predazzi:

$$D(s,t,Q_1^{\,2},Q_2^{\,2}) = \int_0^1 dz \left(\frac{z}{g(Q_1^{\,2})} \right)^{-\alpha_s(s')-1} \left(\frac{1-z}{g(Q_2^{\,2})} \right)^{-\alpha_t(t'')-1}$$

Regge asymptotic for DVCS ($Q_2^{\,2} = 0$)

$$D(s,t,Q^2,0) \approx iG(t,Q^2)\left(-i\frac{s}{s_0} \right)^{\alpha_t(t)-1}, \quad G(t,Q^2) = \frac{G_0}{Q^2 + Q_0^{\,2}} e^{b(t,Q^2)},$$

$$b(t,Q^2) = \left(b_0 + \frac{b_1}{1 + Q^2 / Q_0^{\,2}} \right) t$$

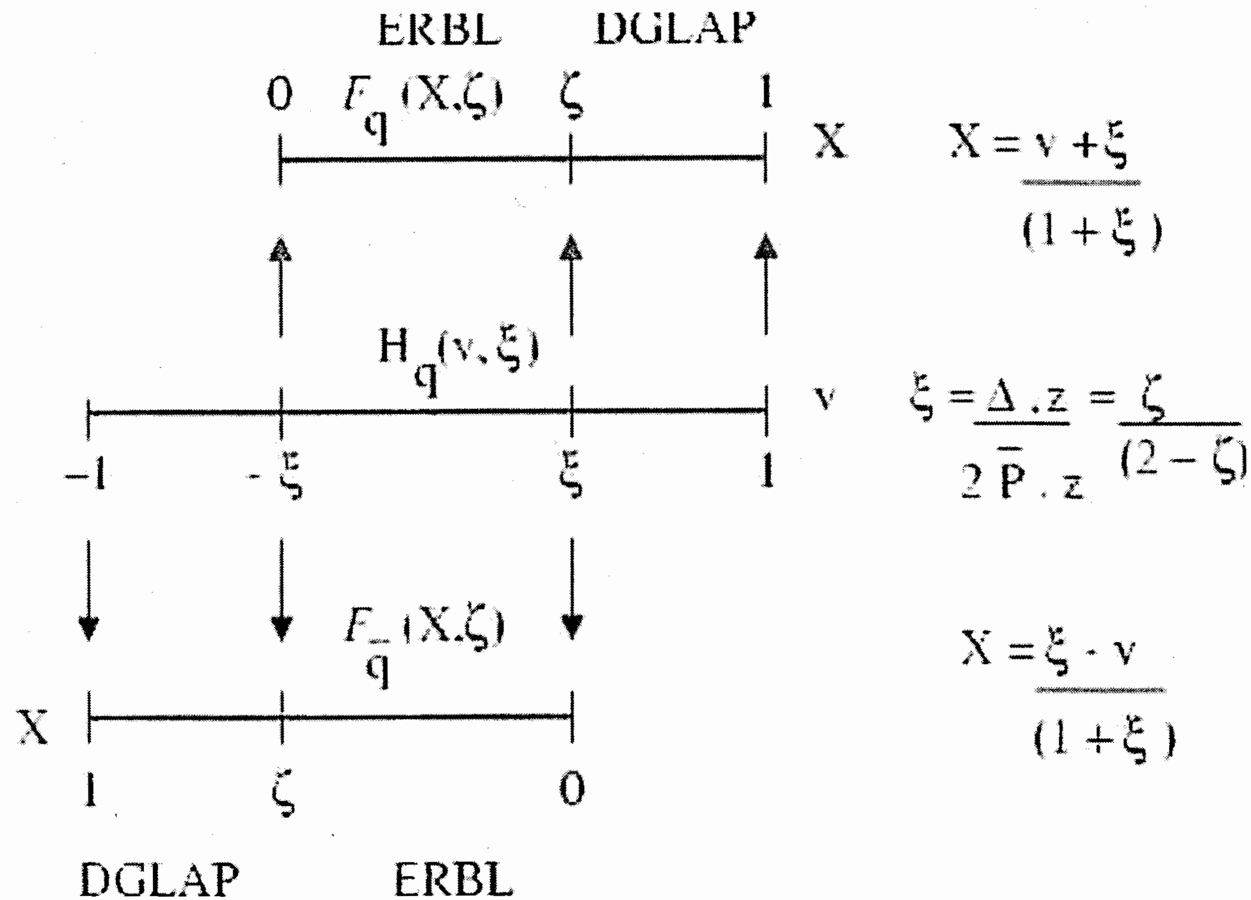
ERBL DGLAP
0 $F_q(X,\zeta)$ ζ 1
X
$X = \frac{v+\xi}{(1+\xi)}$
$H_q(v,\xi)$
v
$\xi = \frac{\Delta . z}{2\bar{P} . z} = \frac{\zeta}{(2-\zeta)}$
−1 -ξ ξ 1
$F_{\bar{q}}(X,\zeta)$
$X = \frac{\xi - v}{(1+\xi)}$
X
1 ζ 0
DGLAP ERBL

We have suggested a boostrap procedure for the construction of GPDs to solve the integral equation with a iteration procedure in which the lowest order approximation for GPD is the (ut)-term of a dual amplitude for quark-hadron scattering.

A particular model, based on the off-mass-shell continuation of a Regge-type amplitude, is constructed to fit high-energy DVCS measured by ZEUS.

S. Mavrodiev

Some phenomenology of multiplicity particles production

Average e+e⁻, pp; and ep Multiplicity (Data from http://home.cern.ch/b/biebel/www/RPP02)

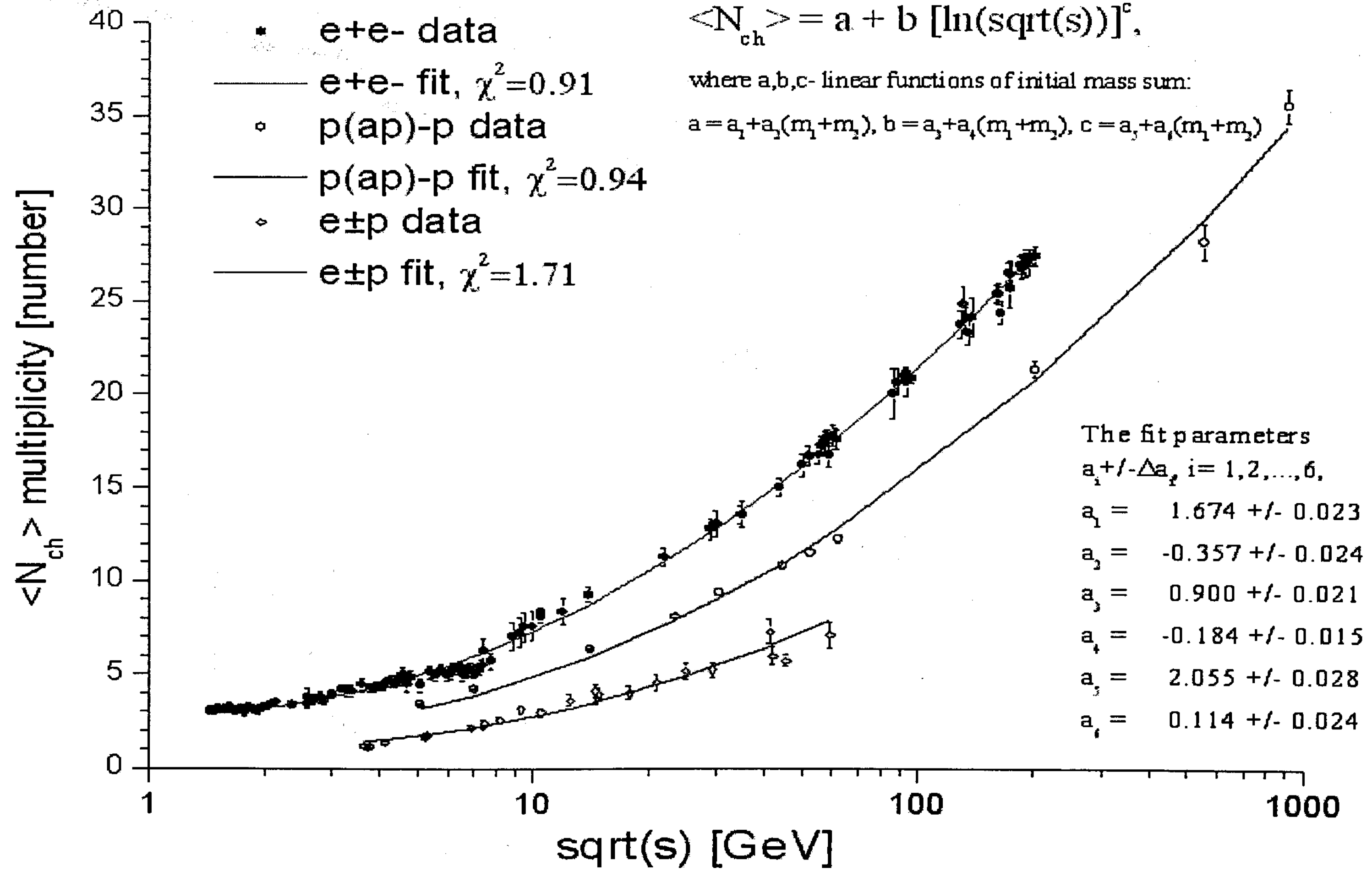

Average e+e⁻, pp; and ep Multiplicity (Data from http://home.cern.ch/b/biebel/www/RPP02)

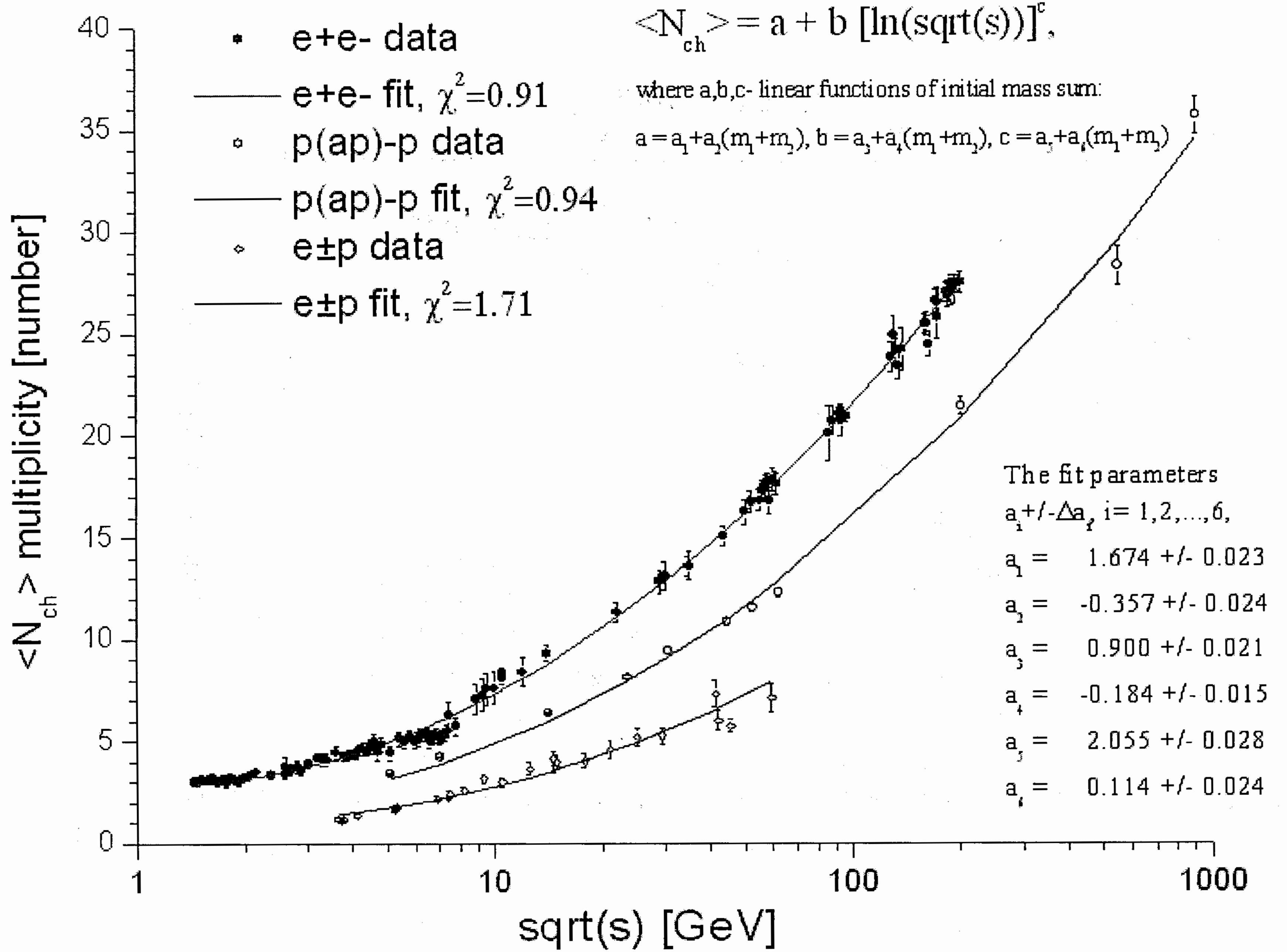

Average e+e-; pp; and pp Multiplicity (Data from http://home.cern.ch/b/biebel/www/RPP02)

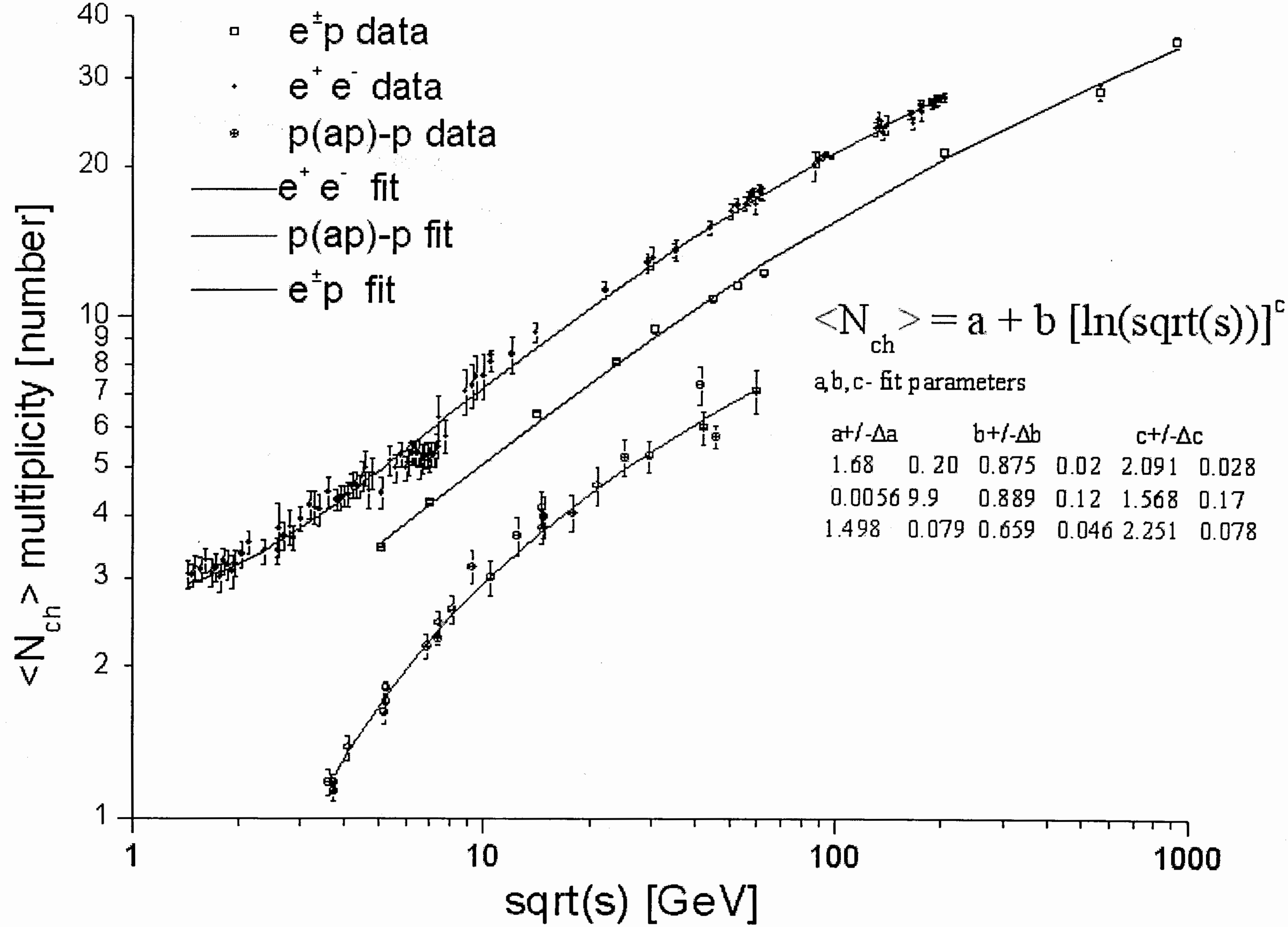

Average e+e⁻, pp; and ep Multiplicity (Data from http://home.cern.ch/b/biebel/www/RPP02)

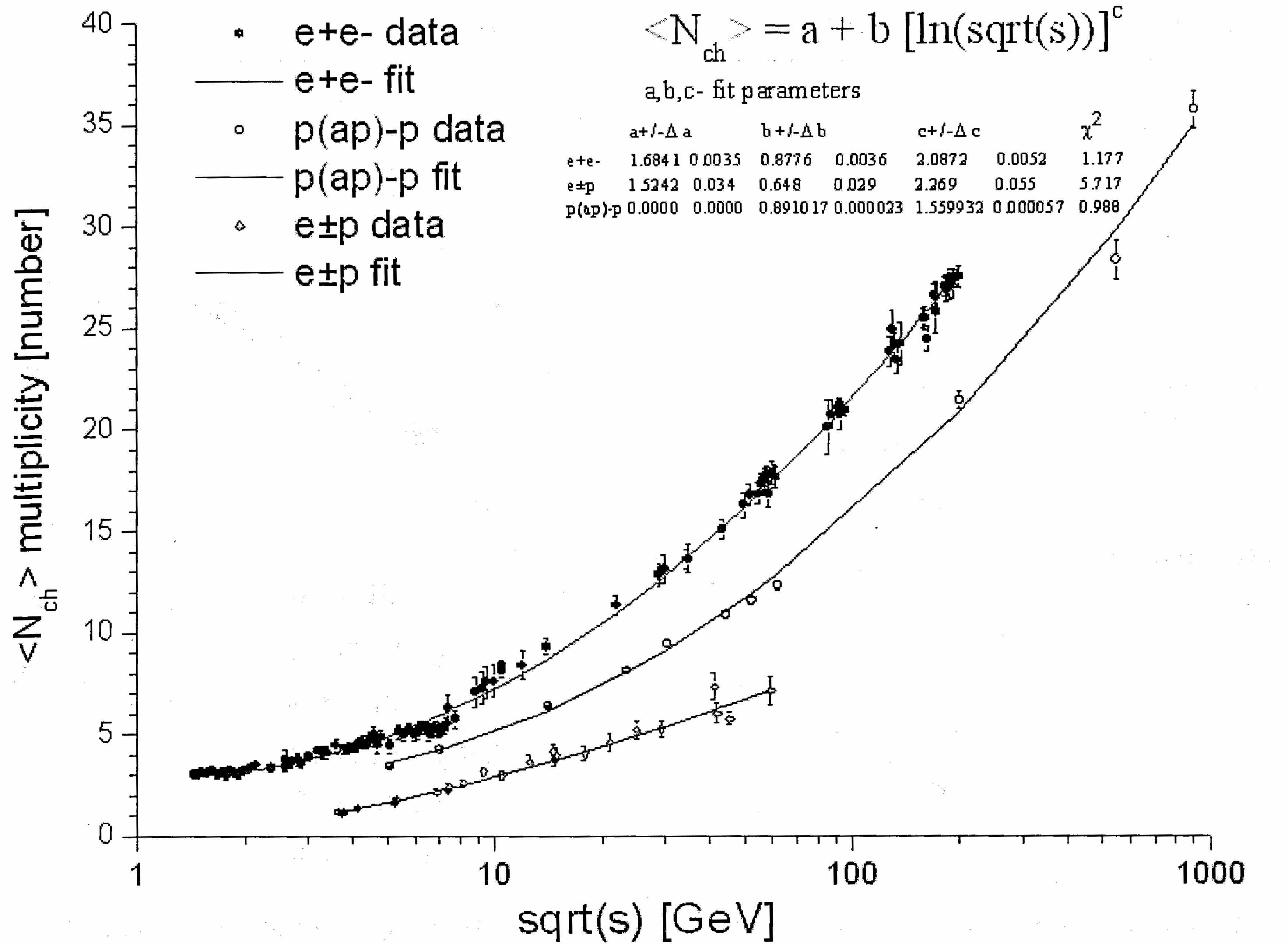

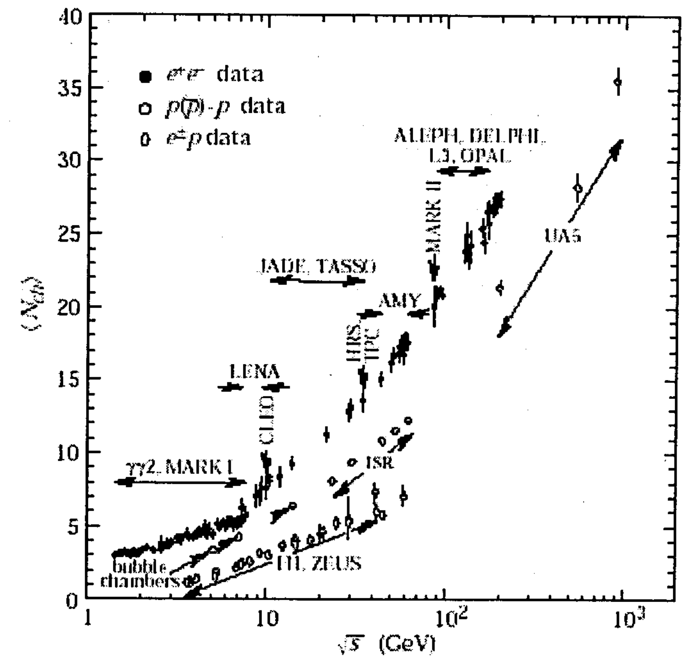

e^+e^- data
$p(\bar{p})$-p data
$e^{\pm}p$ data
γγ2, MARK I
LENA
CLEO
JADE, TASSO
HRS
TPC
AMY
MARK II
ALEPH, DELPHI,
L3, OPAL
UA5
ISR
H1, ZEUS
bubble
chambers
$\langle N_{ch} \rangle$
$\sqrt{s}$ (GeV)

Conclusive Experimental Evidence for Hadron Deconfinement in $\bar{p}-p$ Collisions at 1.8 TeV

L. Gutay
FNAL, E-735 Collaboration
(Purdue, Duke, FNAL, Iowa, Notre Dame, Wisconsin)

Abstract

We have measured deconfined volumes, $4.4 < V < 13.0$ fm^3, produced by a one dimensional (1D) expansion. These volumes are directly proportional to the charged particle pseudorapidity densities $6.75 < dn_c/d\eta < 20.2$. The hadronization temperature is $T = 179.5 \pm 5$ (syst) MeV. Using Bjorken's 1D model, the hadronization energy density is $\varepsilon_F = 1.10 \pm 0.26$ (stat) GeV/fm^3 corresponding to an excitation of 24.8±6.2 (stat) quark-gluon degrees of freedom. [1]

Experiment E-735 was located in the $C\emptyset$ Interaction region of the Fermi National Accelerator Laboratory (FNAL).

The detector was a particle physics version of Plank's heated black box-spectrometer concept. The $\bar{p}-p$ interaction point, corresponding to the heated black box, was surrounded by a cylindrical drift chamber which in turn was covered by a single layer hodoscope including endcaps. The acceptances for charged particle multiplicity n_c and pseudo rapidity η ranges were:

Multiplicity range: $10 < n_c < 200$

Pseudorapitity range: $-3.25 < \eta < 3.25$

A side arm magnetic spectrometer-time of flight system mass identified and momentum analyzed only those particles, which passed through this spectrometer. The acceptances of the transverse momentum p_t, pseudo rapidity η and azimuthal angle ϕ are given below:

Momentum range: $0.1 < p_t < 1.5$ GeV/c

Spectrometer coverage: $-0.37 < \eta < 1.00, \Delta\phi \sim 20^0$

where $\Delta\phi$ is the azimuthal angle around the beam direction.

The expected Hagedorn-Van Hove-Weisskopf deconfinement signatures are that both the energy density $\varepsilon \propto dn/d\eta$ and the temperature T as function $S = dn/d\eta$ exhibit the classical rise-flat-rise variation. Contrary to this expectation we found experimentally an initial rise and subsequent constancy of both ε and T. Ultimately we had realized that Bjorken's expansion phase had to be incorporated into the HVW picture. Once $dn/d\eta$ reaches a critical value and deconfined hadronic matter is formed, it has to expand and cool to reach the universal *constant values for T and ε* before deconfined hadron matter reconfines. Thus, the *expansion length z must become proportional to the rapidity density:* $z \propto \frac{dn_c}{d\eta}$

Temperature Determination

The negative particle p_t spectrum is used to measure the temperature: T. The slope parameter (b^{-1}) i.e. "Temperature" T is obtained from a fit of the invariant cross-section d^2n_c/dyd^2p_t to the function:

$$\text{A} \exp(-bp_t) \text{ for } 0.15 \leq p_t \leq 0.45 \text{ GeV/c}.$$

The T value is constant to $\pm 1\%$ for the rapidity density interval $6.75 < dN_c/d\eta < 20.2$

$$T = 179.5 \pm 5(\text{syst})$$

Determination of the 1D Expansion Length z and expansion Volume V at Hadronization Time

Using Hanbury Brown-Twiss (HBT) pion correlation measurement we determined R_G, the Gaussian radius parallel to the colliding $\bar{p}-p$ beam. The clear linear increase of R_G with $dn_c/d\eta$ is shown on Fig. 1, which we parameterize as

$$R_G = m(dn_c/d\eta)$$

where the slope m is: m=0.0730 ±0.011. The effect of the 1D expansion on the HBT analysis introduces a correction factor ℓ_R. Thus the length of the quark-gluon tube at freeze out is:

$$z = \ell_R m(dn_c/d\eta)$$

Thus the cylindrical volume of the pion source at hadronization is:

$$V = \pi r^2 \times 2\ell_R m(dn_c/d\eta)$$

After substituting the constants

$$\ell_R = 1.56, m = 0.073 \pm 0.011$$

we arrive for the value of V as function of rapidity density:

$$V = (0.645 \pm 0.130)(dn_c/d\eta) fm^3$$

For the rapidity density interval: $6.75 < dn_c/d\eta < 20.2$
we obtain the volume interval:

$$4.4 \pm 0.9 < V < 13.0 \pm 2.6 fm^3$$

We assume that for $dn_c/d\eta > 6.75$ the system is initially above the deconfinement transition and then expands to the final volume V.

Pion Density n_π at Hadronization (After Expansion)

Using Bjorken's 1D boost invariant equation we estimate the number of pions/fm^3

$$n_\pi = \frac{(3/2)(dn_c/d\eta)}{A2\tau}$$

A is the Transverse Area πr^2 and τ is the Proper Time at freeze out. The collision occurs at longitudinal coordinate $z = 0$ and time $t = 0$. The corresponding initial proper time is τ_0. At any t later time $\tau = (t^2 - z^2)^{1/2}$. For a relativistic massless ideal gas above the phase transition the maximum expansion velocity, responsible for most of the longitudinal expansion, is likely to be the sound velocity $\nu_s^2 = 1/3$. Since the expansion time t in terms of the cylinder length z and the expansion velocity ν_s is:

$$t = z/\nu_s$$

Substituting this expression into τ we obtain

$$\tau = (3z^2 - z^2)^{1/2} = \sqrt{2}z$$

The proper time τ_f at hadronization becomes: $\tau_f = \sqrt{2}\ell_R m dn_c/d\eta$
Thus the pion density, pions/fm^3:

$$n_\pi = \frac{(3/2)(dn_c/d\eta)}{\pi r^2\sqrt{2}\ell_R m(dn_c/d\eta)} = \frac{(3/2)(1/\sqrt{2})}{\pi r^2 2\ell_R m}$$

becomes independent of $dn_c/d\eta$. After inserting the experimental values for r, ℓ_R and m we obtain the final result: $n_\pi = 1.64 \pm 0.33(\mathrm{stat})$ pions/fm^3.

Hadronization Energy Density, ε_f

$$\varepsilon_f = \frac{\Sigma_h F_h(m_h)(1/\sqrt{2})}{\pi r^2 2\ell_R m}$$

where F_h is a hadron abundance factor for $\pi, K, \phi, p, n, \Lambda^0, \Xi$ etc. and m_h denotes the relevant hadron mass:

$$(m_h)_\perp = (m_h^2 + p_t^2)^{1/2}$$

is the average transverse mass of hadron h
Using $r = 0.95$ fm, $\ell_R = 1.56, h = 0.073$, we obtain for ε_f:

$$\varepsilon_f = 1.10 \pm 0.26(\text{stat})\ \text{GeV/fm}^3$$

Number of Degrees of Freedom G(T)

¿From quantum statistic the average number of pions in volume V, at temperature T with number of Degrees of Freedom (DoF) G(T) is:

$$n_c = V\frac{G(T)1.202(kT)^3}{\pi^2\hbar^3c^3}$$

For a quark-gluon plasma:

$$G(T) = G_g(T) + G_{\bar{q}}(T) + G_q(T) = 16 + (21/2)(f)$$

where f are the number of quark flavors. In our case we work with $f = 2$. Further we assume that pion emission from the source can be determined by the number of constituents in the source at hadronization: that one pion is a quark-antiquark pair and that two gluons are required to produce two pions $n_\pi = n_g + (n_q + n_{\bar{q}})/2$

$$n_\pi = (1 + 2 \times 21/64)G_g \times 16.1T^3(GeV)$$

where G_g is the effective number of gluon number DoF.
$G(T) = n_g + n_q + n_{\bar{q}} = (1 + 21/16)G_g = 23.5 \pm 6DoF$

G(T) from ε_f and T

After the isentropic expansion, the energy E in the volume V at a temperature T is also constant E= (3/4) S(T)× T

$$E = V\frac{G(T)\pi^2k^4}{30\hbar^3c^3}T^4 \Rightarrow G(T) = 24.8 \pm 6.2(\text{stat})DoF$$

Again nearly 8 times the number of DoF = 3 of a pion gas

CONCLUSIONS

- We have measured the deconfined hadronic volumes produced by a one dimensional isentropic expansion.
- The freeze out number of pions/fm^3 is $n_\pi = 1.64 \pm 0.33$.

- The hadronization temperature is $T = 179 \pm 5$MeV.
- The freeze out energy density is $\varepsilon_f = 1.10 \pm 0.26$GeV/fm^3.
- The number of DoF in the source is 23.5±6 and 24.8±6.2. They are in general agreement with those expected for QGP.
- *The measured constant T, n_π, ε_f, values and the linear dependence of z on $dn_c/d\eta$ all characterize the quark-gluon to hadron thermal phase transition.*

References

[1] T. Alexopoulos *et al.*, Phys. Lett. B **528**, 43 (2002) [arXiv:hep-ex/0201030].

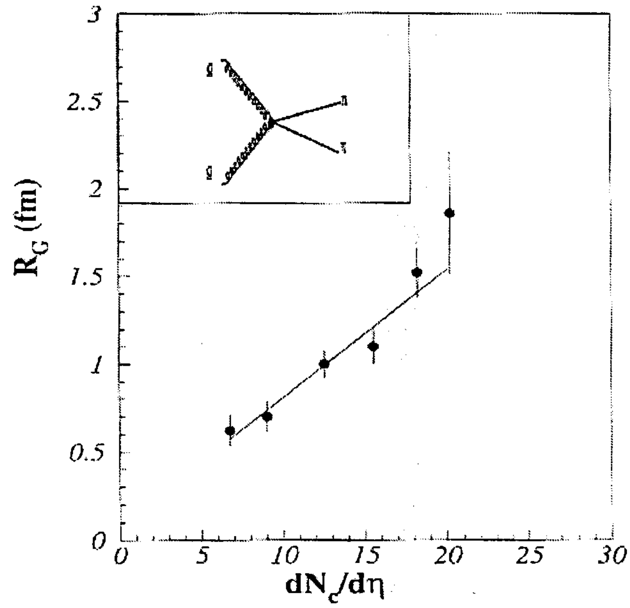

Figure 1: Dependence of the Gaussian radius R_G on $(dn_c/d\eta)$. The gluon diagram indicates that two gluons are required to form two pions.

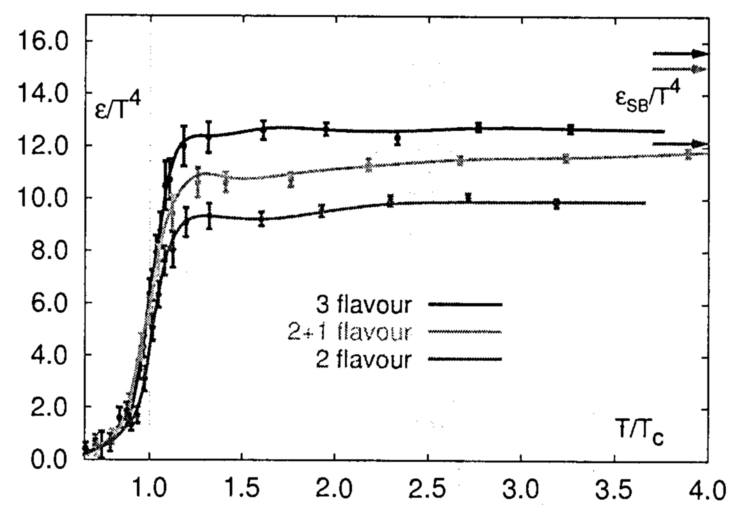

Figure 2: The temperature T_c is the critical temperature and ϵ_{SB}/T^4 is the Stefan-Blotzmann limit.

V.Nikitin

Status of "Thermalization" project on SVD-2

Status of ”Thermalization” project on SVD-2

Рождение частиц в pp-взаимодействии
с высокой множественностью при энергии протонов 70 ГэВ.

Проект "Термализация“

Multiparticle production process in pp-interaction with high multiplicity at Ep=70 GeV.

Project “Thermalization”.

Collaboration
GSTU(Gomel, Belarus), JINR(Dubna), MSU(Moscow),
IHEP(Prorvino), TSU(Tbilisi)

The main goals of the project.

General task. Investigation of collective phenomena in the process $pp \rightarrow n_\pi \pi + 2N$, $n_\pi = 20 \div 35$.

At reaction threshold $n_\pi \rightarrow n_{thresh} = 69$ all particle momenta in c.m.s. vanish $p_\pi \rightarrow 0$. A number of collective effects may show up in cold gas or condensate due to multiboson interference.

- Formation of high density thermalized hadronic system. Transition to pion condensate or cold QGP.
- Increase of partial cross section $\sigma(n)$ is expected, comparing with commonly accepted extrapolation.
- The non-QCD jets formation consisting of identical particles – multiboson interference.
- Fluctuation of charged $n(\pi^+, \pi^-)$ and neutral $n(\pi^0)$ components (centaurs or anticentaurus).
- Enhanced rate of direct photons.
- Search for new phenomena: multipion bound state, events with ring topology, pentaquarks.

Phase diagram of hadronic matter

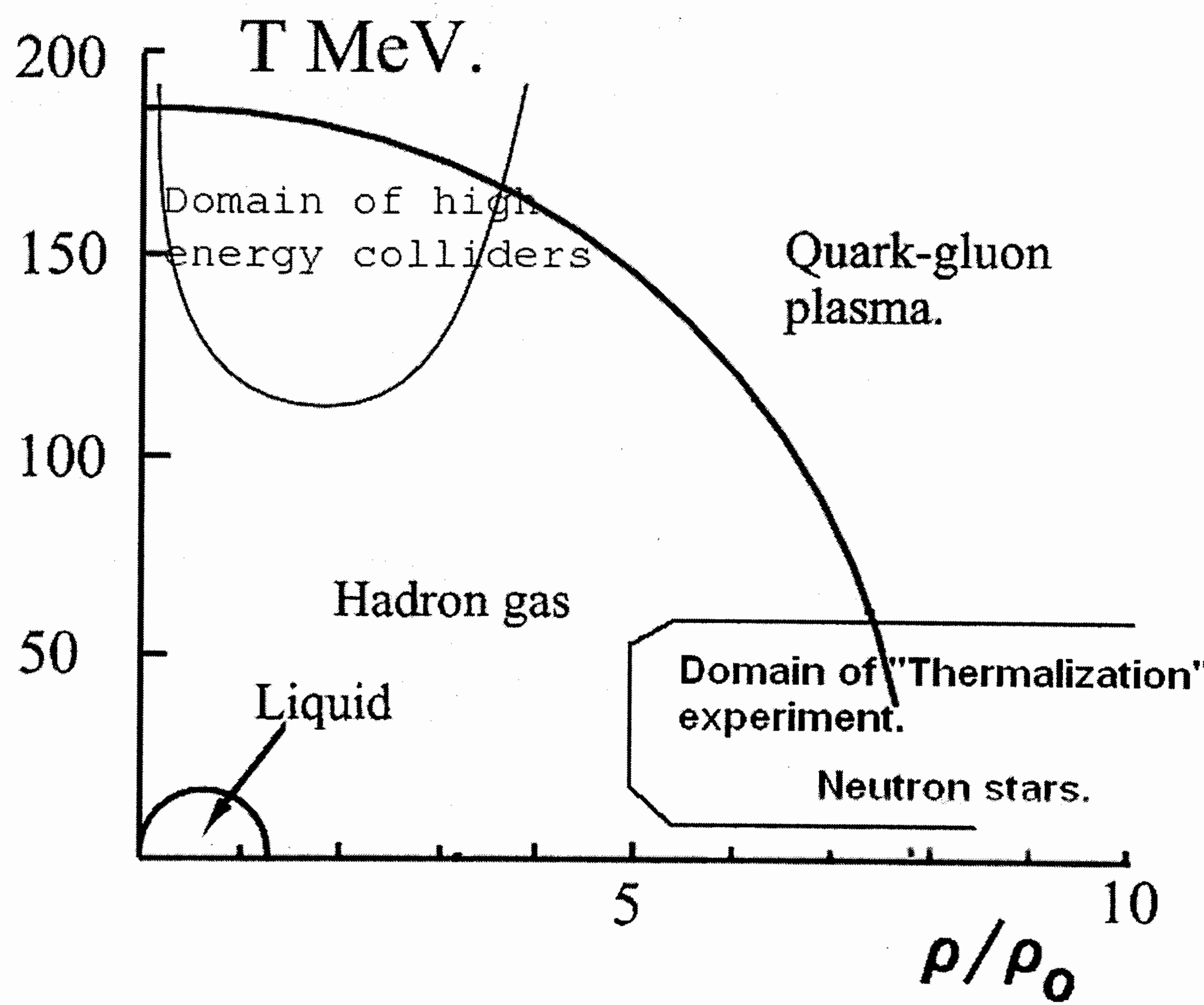

Inelasticity coefficient or rate of energy dissipation

RHIC: AA interaction at Ecm =200 x A =80 TeV.

Central fireball energy density ε =5 GeV/fm**3.

Central fireball volume $V = \frac{4}{3} \pi R^3$

Inelasticity coefficient $K_{inel} = \frac{\varepsilon V}{E_{cm}} = 0.03$

The same estimation for pp interaction at Ecm=11.6 GeV and particles multiplicity 40:

$$K_{inel} = 0.7 - 1$$

Multiplicity distribution in pp interaction at 70 GeV.

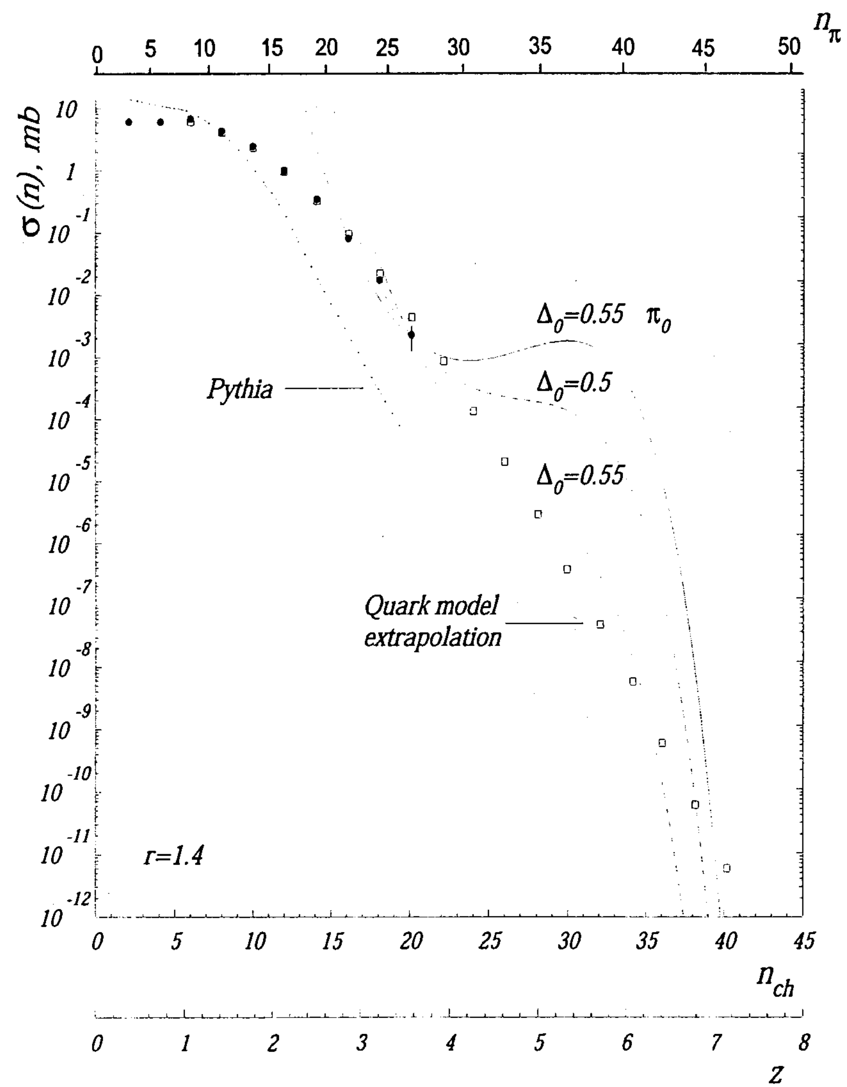

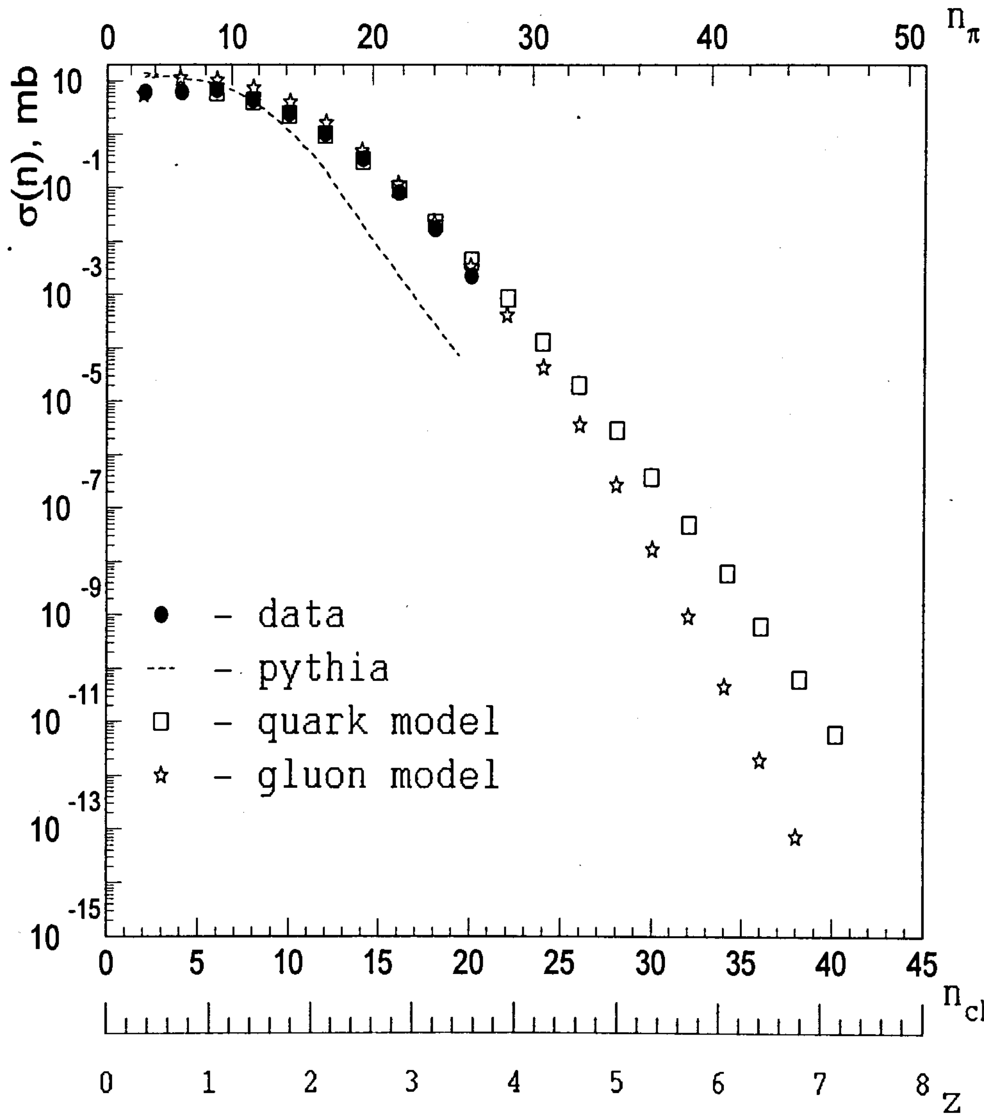

Mean momentum in c.m.s.

$$E_{kin} = (\sqrt{s} - 2m_N - n_\pi \cdot m_\pi)/(n_\pi + n_N) \qquad \frac{dN}{dE} = c\frac{\sqrt{E}}{\exp(E/T) - 1}$$

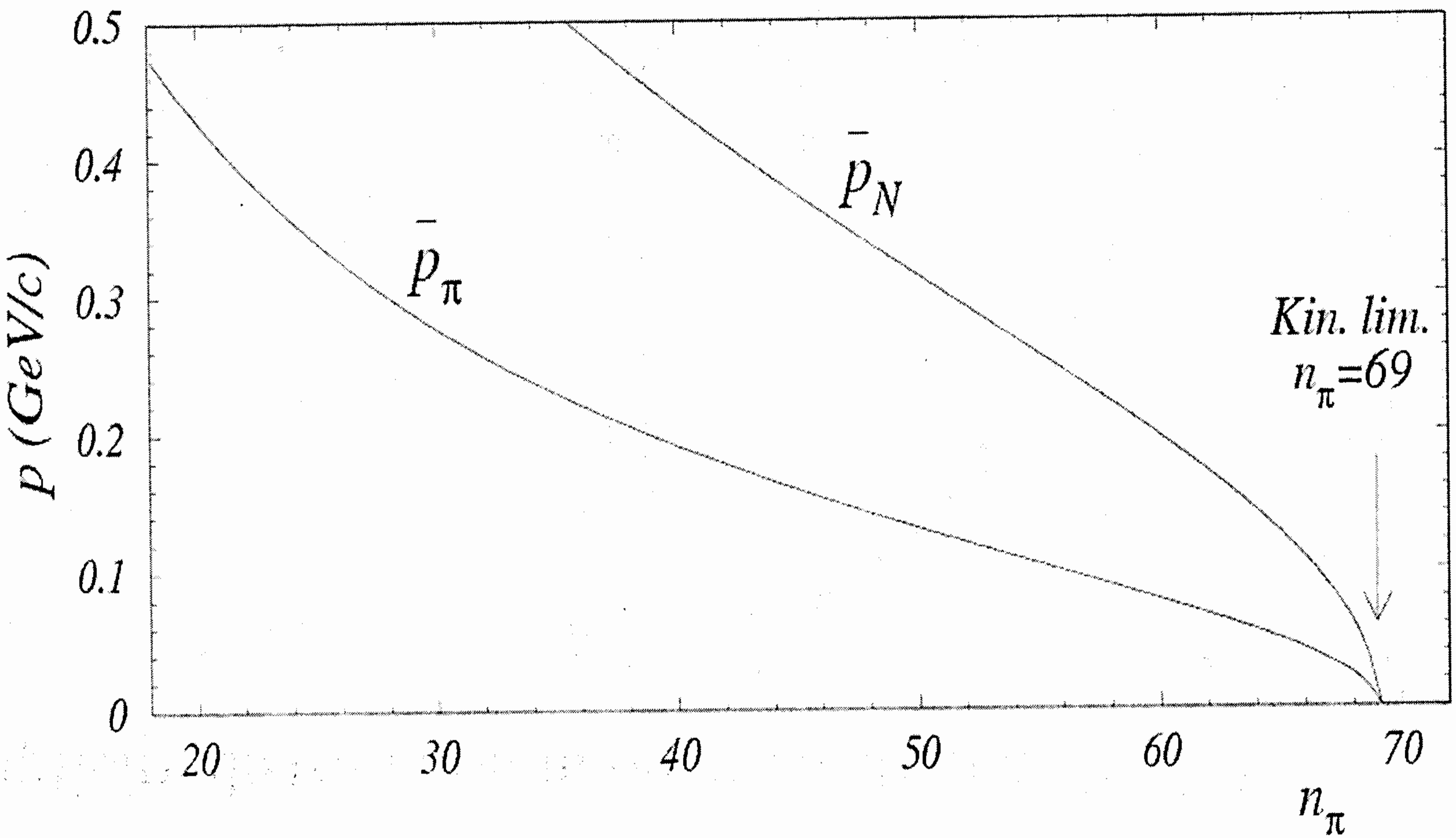

Comparison
of longitudinal p_z and transverse p_x momenta behavior in c.m.s.

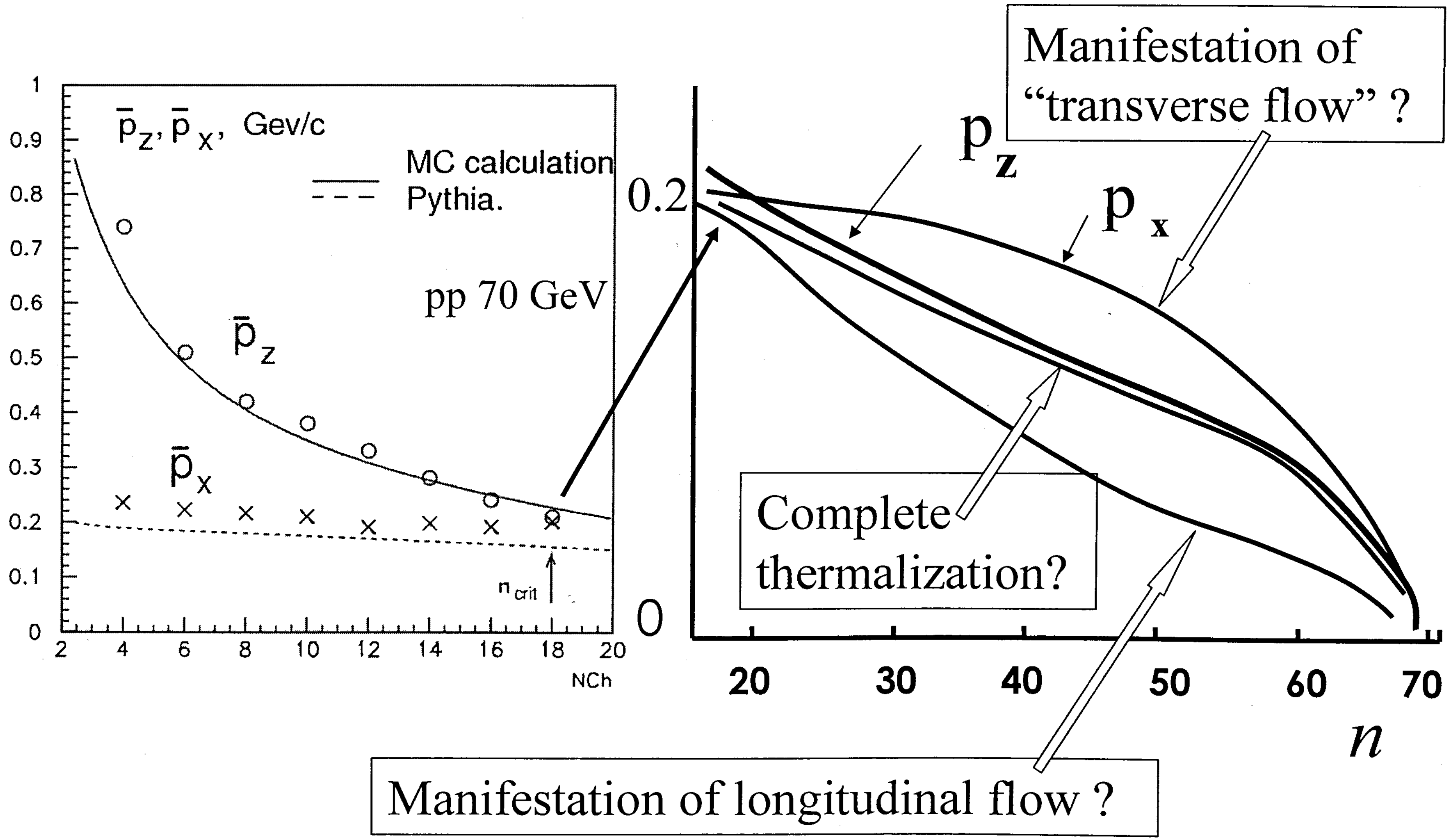

Low energy direct photons.

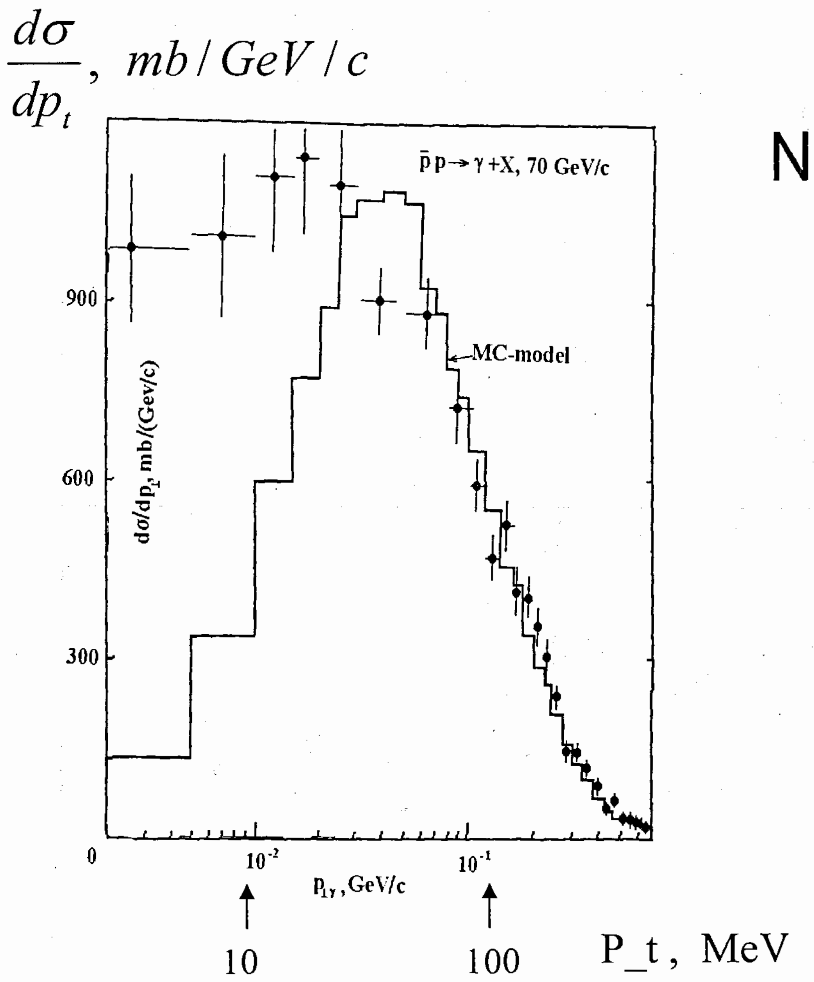

Anti-p + p = γ + X,   70 GeV

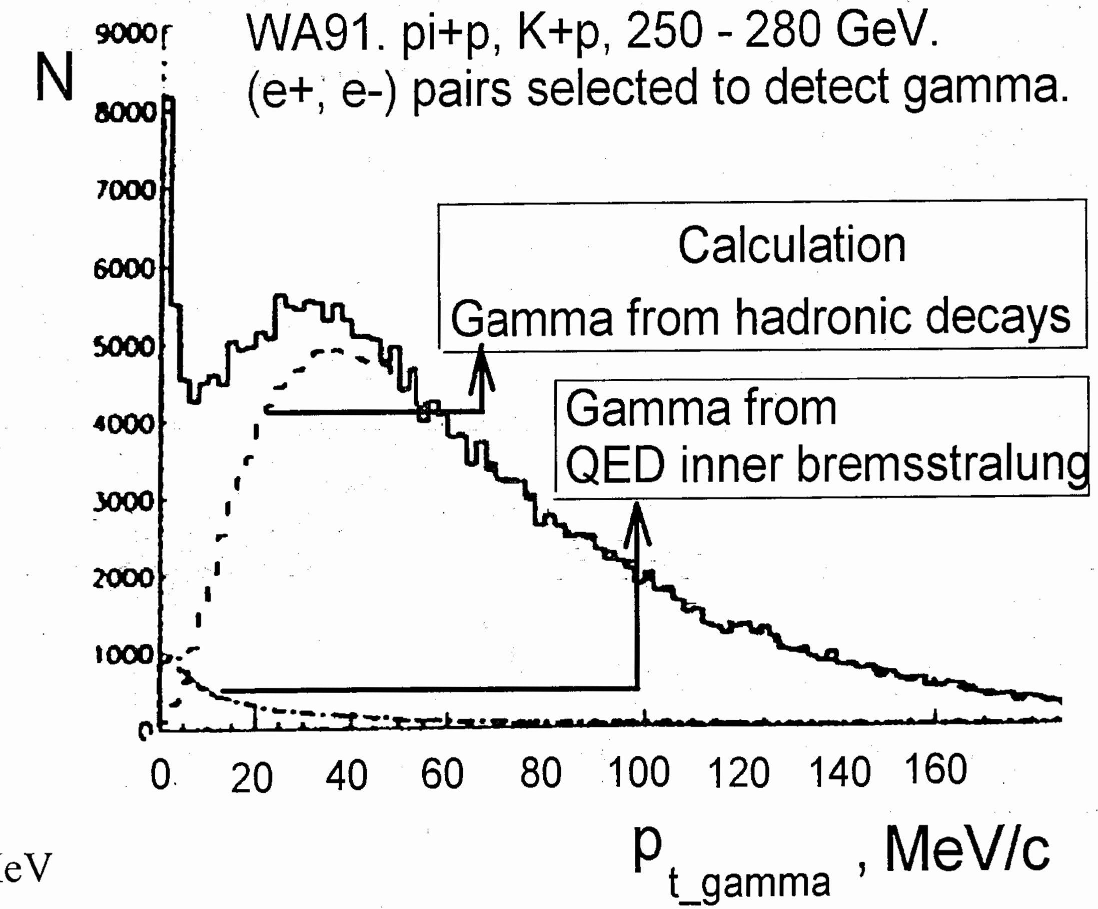

Tentative mechanisms of anomalous low energy photon generation.

- Quasistable cold spot in hadron gas or QGP (P.Lichard, L.Van Hove, E.Shuryak).

- Relic emission of fireball

(M.Volkov, E.Kokoulina, E.Kuraev).

- Formation of multipion bound state.

Results in 2003, 2004.

- Software package for data processing is developed
- Simulation of SVD is in progress
- Trigger concept is worked out
- Monte Carlo generator of the thermalized hadron system and phenomenological studies is in progress
- Liquid hydrogen target is designed and its manufacturing is in progress
- Drift tubes tracking system is developed and is under construction
- Two technical runs were conducted at U-70 accelerator

Lay-out of the SVD setup at U - 70.

- **Scheme of the SVD installation at U - 70.**
- C1, C2 -beam scintillation and Si-hodoscope;
- C3, C4 - target station and vertex Si-detector;
- 1, 2, 3-the drift tubes track system;
- 4 - magnetic spectrometer proportional chambers;
- 5- threshold Cherenkov counter;
- 6 - scintillation hodoscope;
- 7 - electromagnetic calorimeter.}

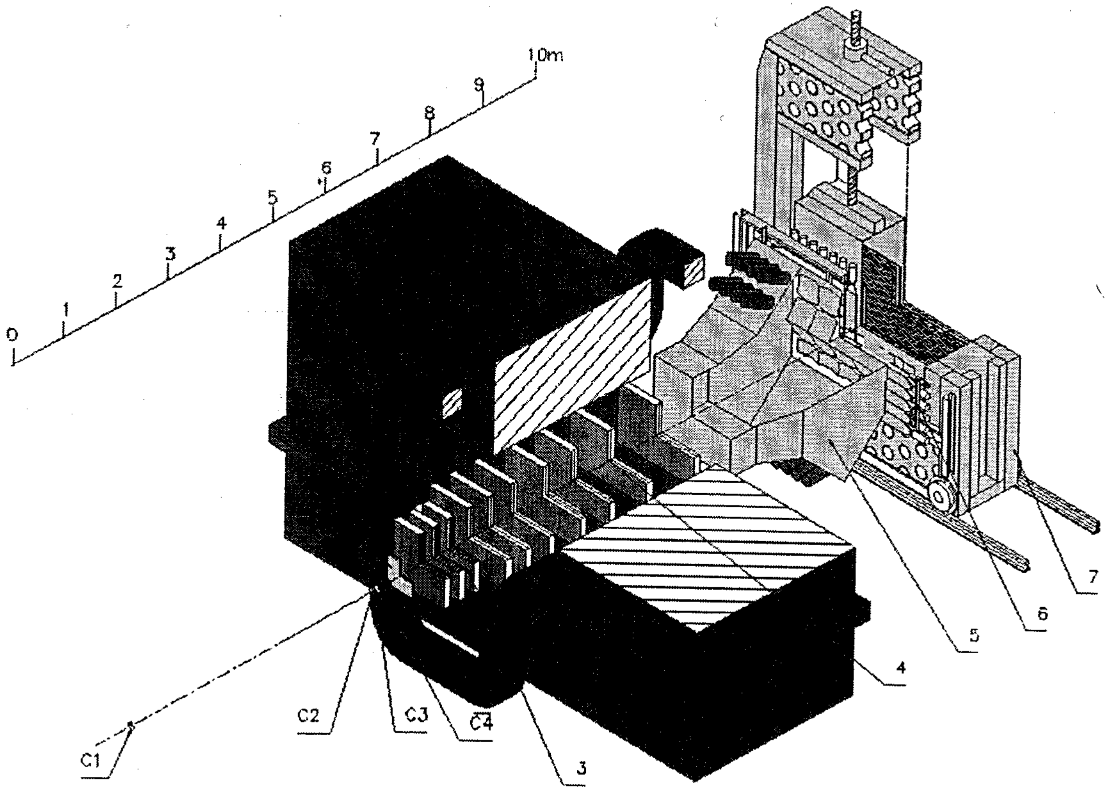

Setup components

- Silicon vertex detector (6 beam planes and 10 tracker planes,
- 10 000 ch.).
- Drift tubes trekker (9 planes, 2300 channels).
- Magnetic spectrometer (18 proportional chambers).
- Liquid hydrogen target (∅ 25 mm, l= 70 mm).
- Threshold Cherenkov detector (32 PMT).
- Electromagnetic calorimeter (1540 channels).
- Trigger system for registration of rare events with high multiplicity.
- Extracted proton beam E = 70 GeV of U70 accelerator, IHEP.
- Beam intensity ~. $10^7 s^{-1}$
- Assuming partial cross section σ (n_π=30)=0.2 mcb expected counting rate is 100 events per hour.

Modernization of SVD setup.

- Design and create trigger system for registration of rare events with high multiplicity.
- Renew and repair silicon vertex detector electronics.
- Repair magnetic spectrometer proportional chambers.
- Design and create drift tubes tracker.
- Design and create Liquid hydrogen target.
- Renew and repair electromagnetic calorimeter electronics.

Silicon micro strip vertex detector. An exsample of foil targets imaging.

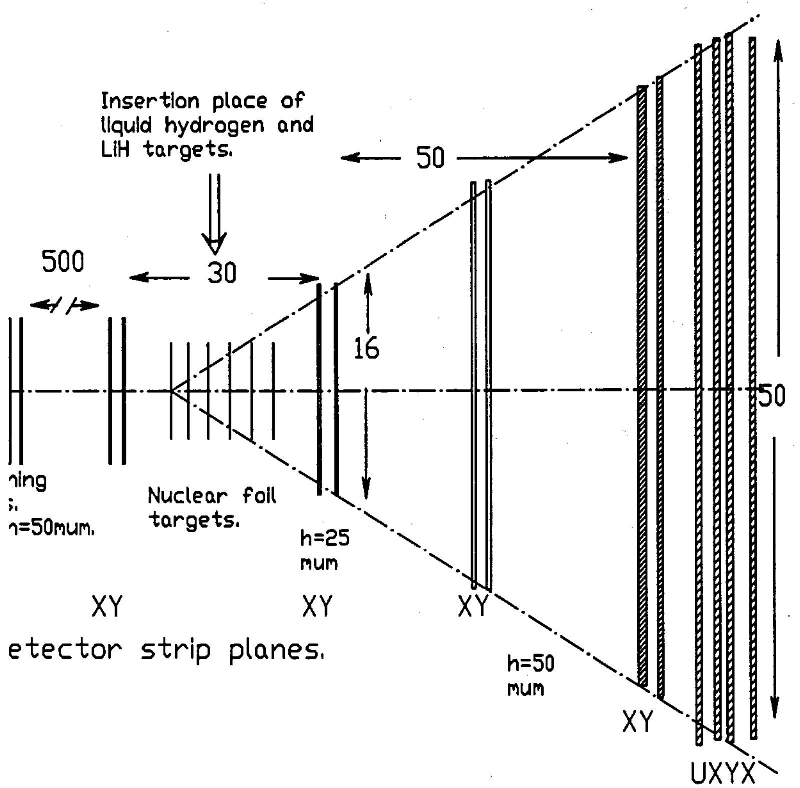

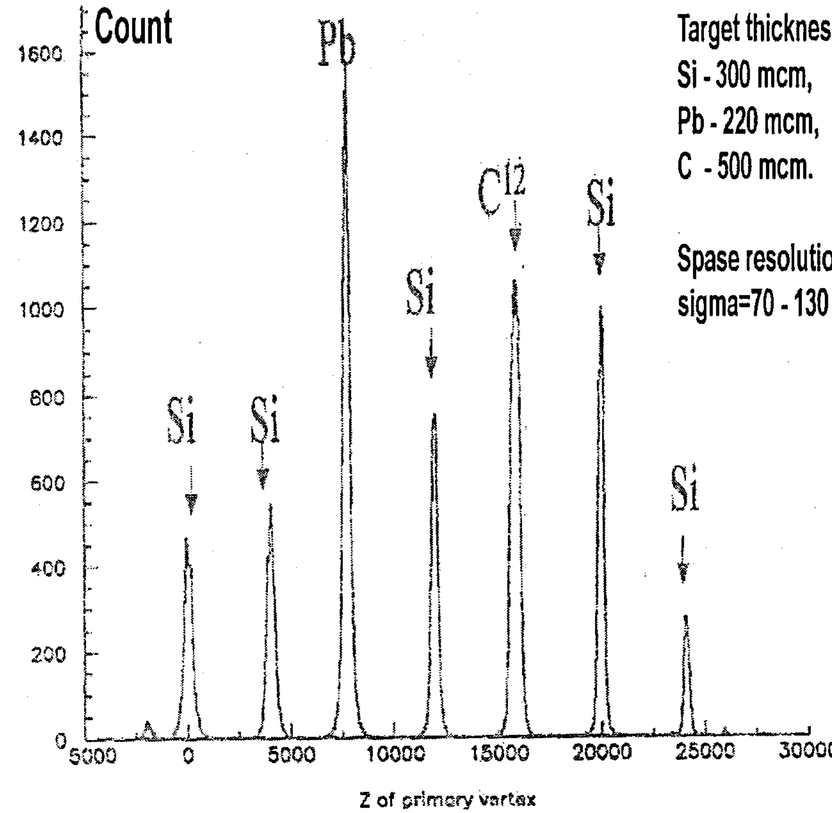

Target thickness:
Si - 300 mcm,
Pb - 220 mcm,
C - 500 mcm.

Spase resolution
sigma=70 - 130 mcm.

Box of vertex detector.

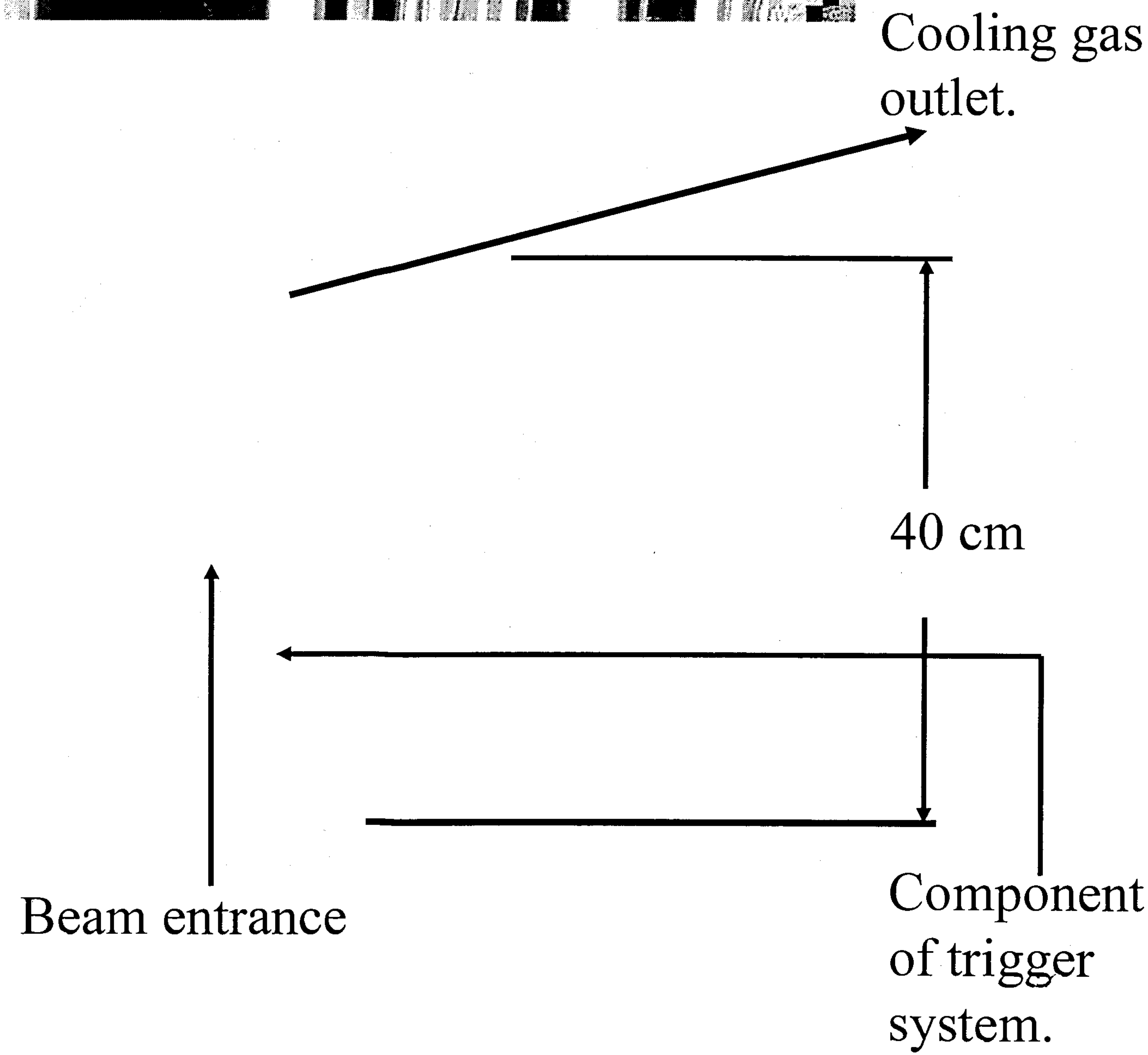

Silicon micro strip vertex detector.
An exsample of pC interaction event.

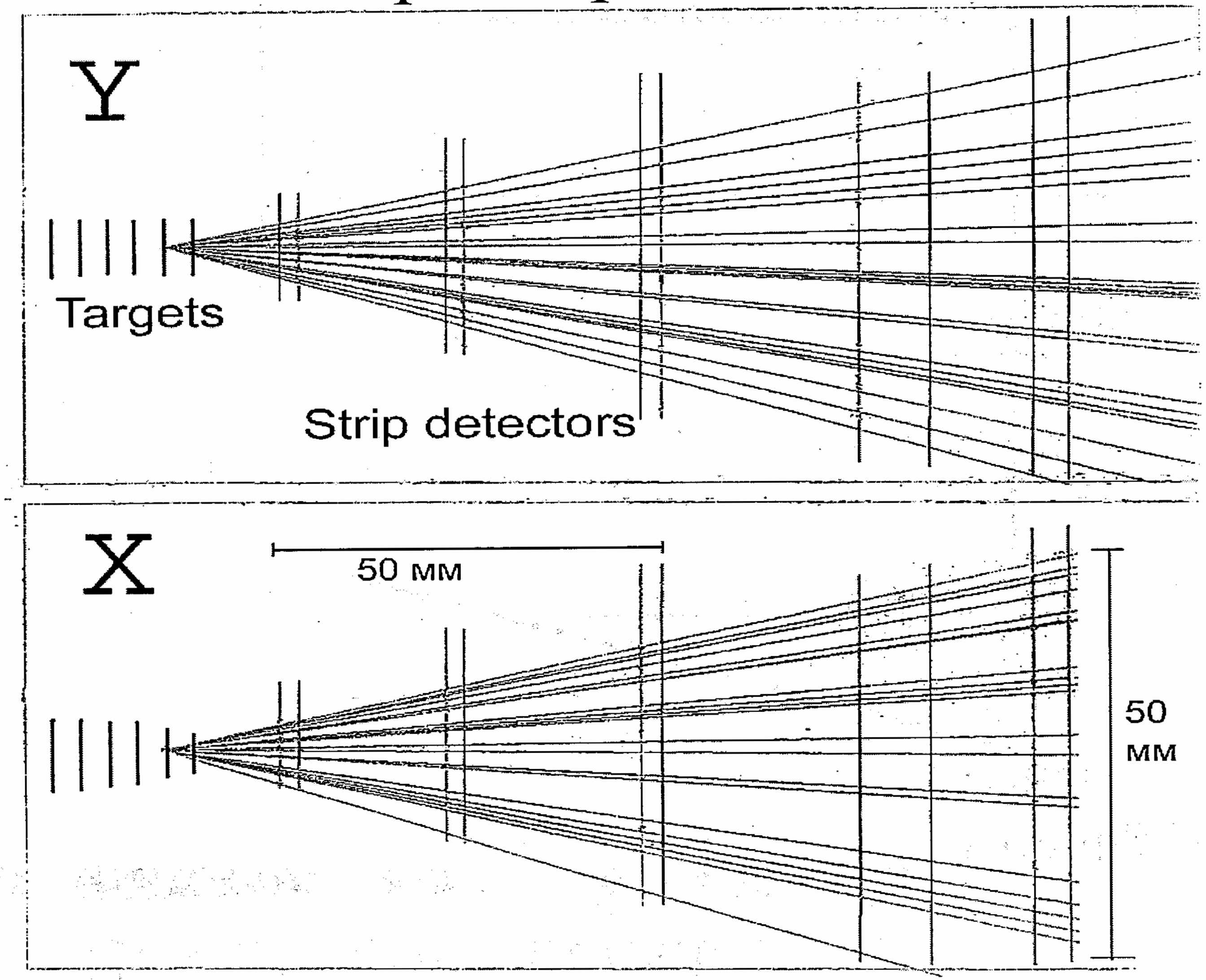

An event of pSi interaction with 30 tracks as it seen in vertex detector

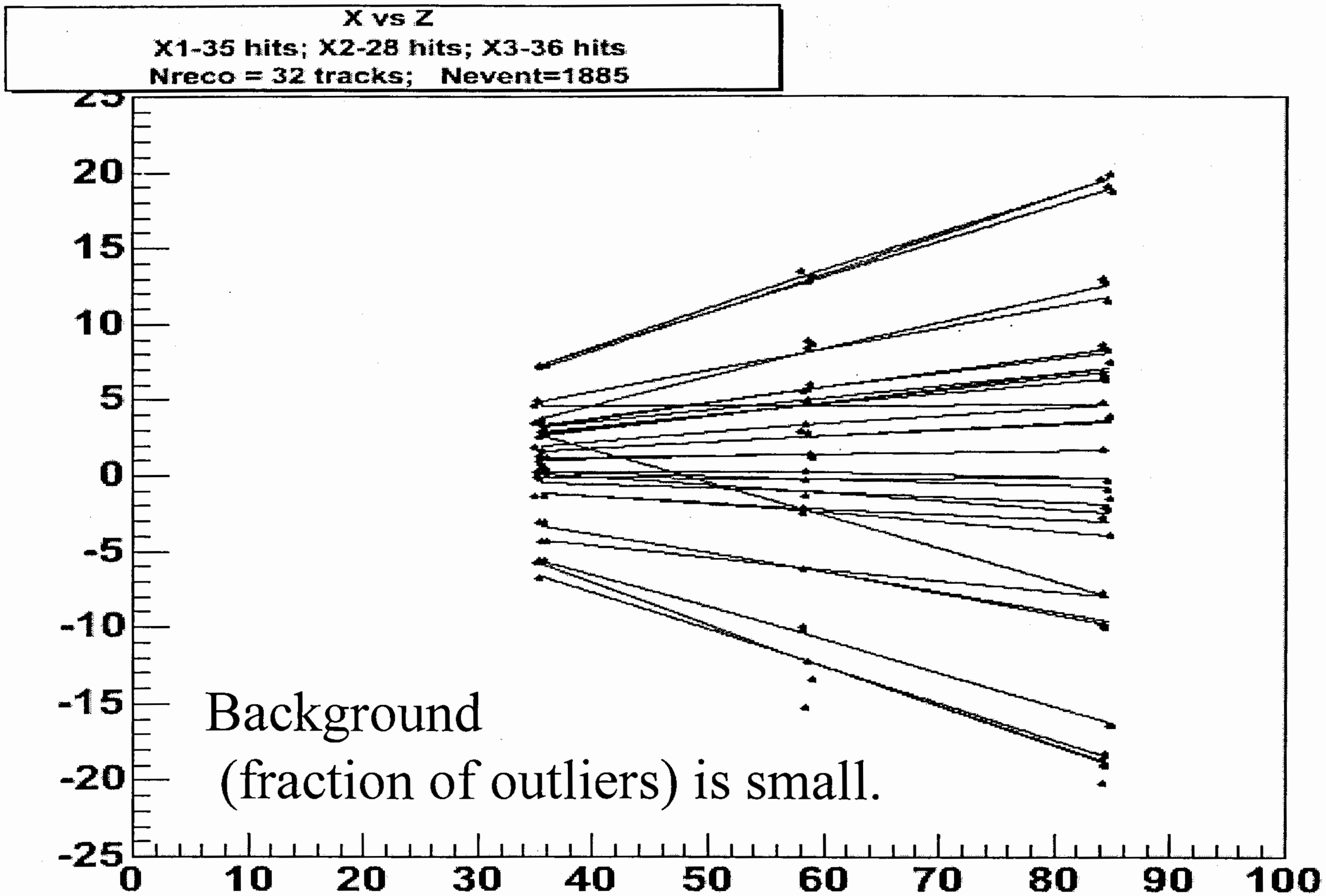

Shape of primary proton beam 70 GeV.

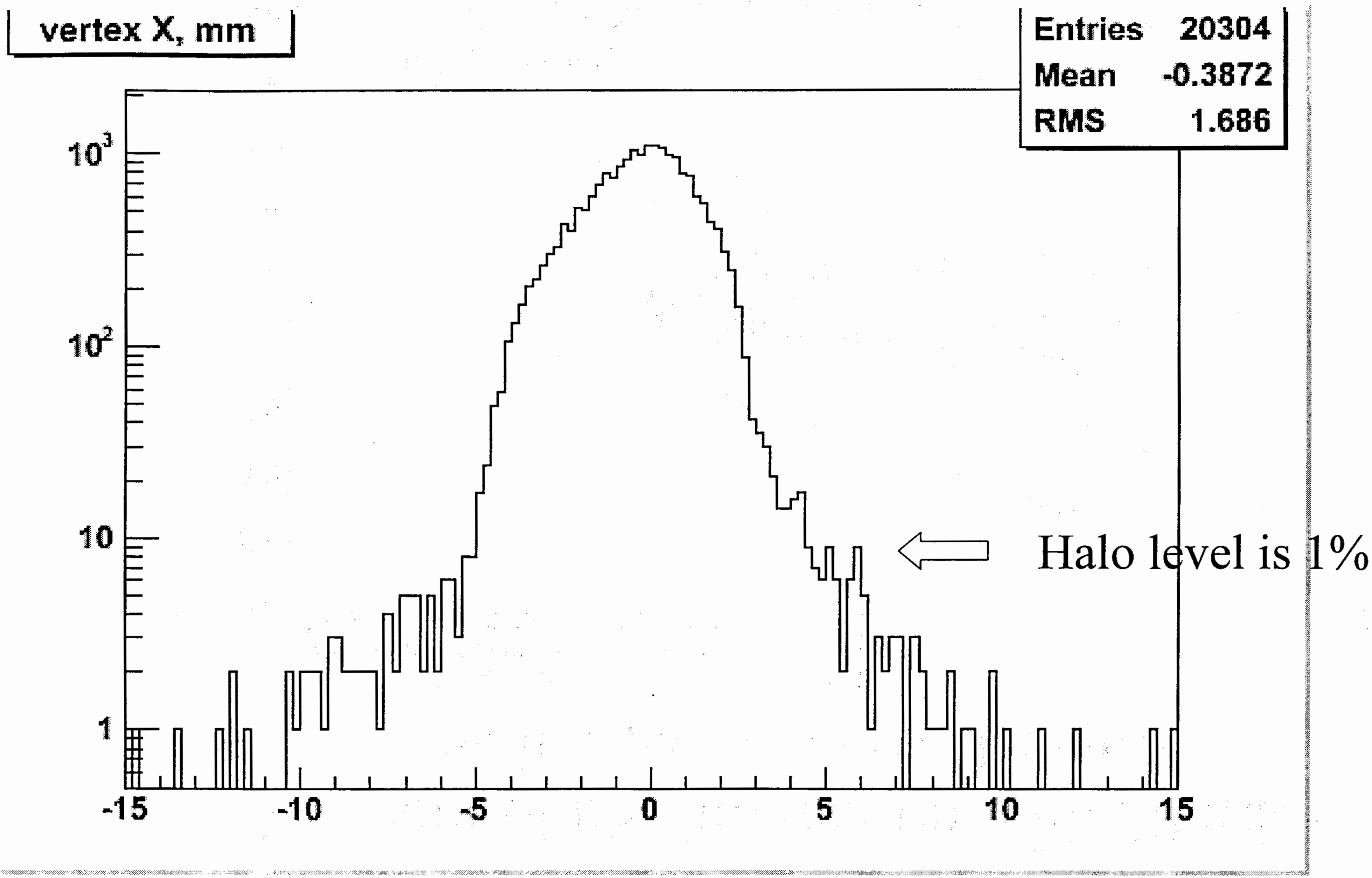

High multiplicity trigger concept

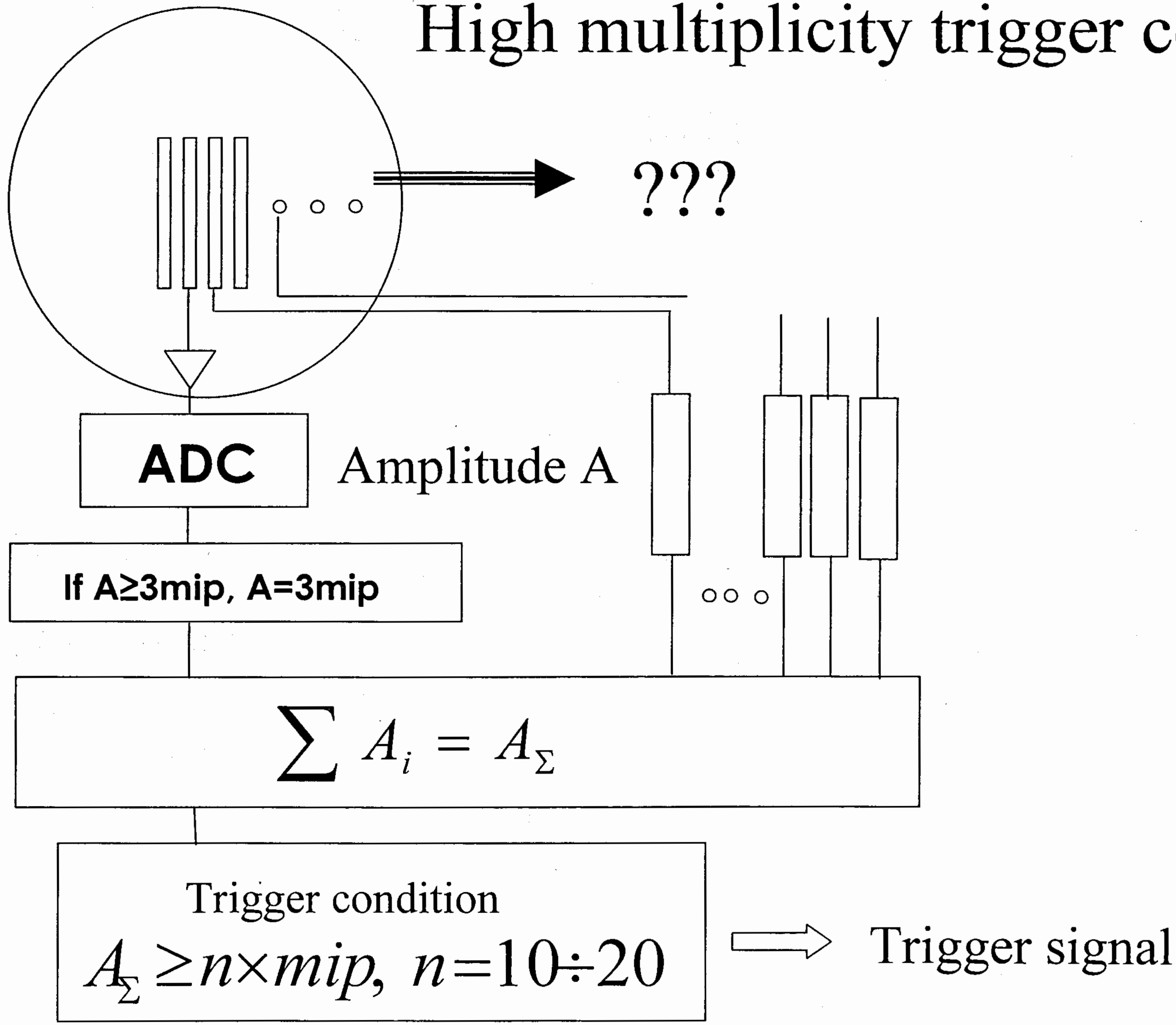

Scintillation hodoscope for trigger system.

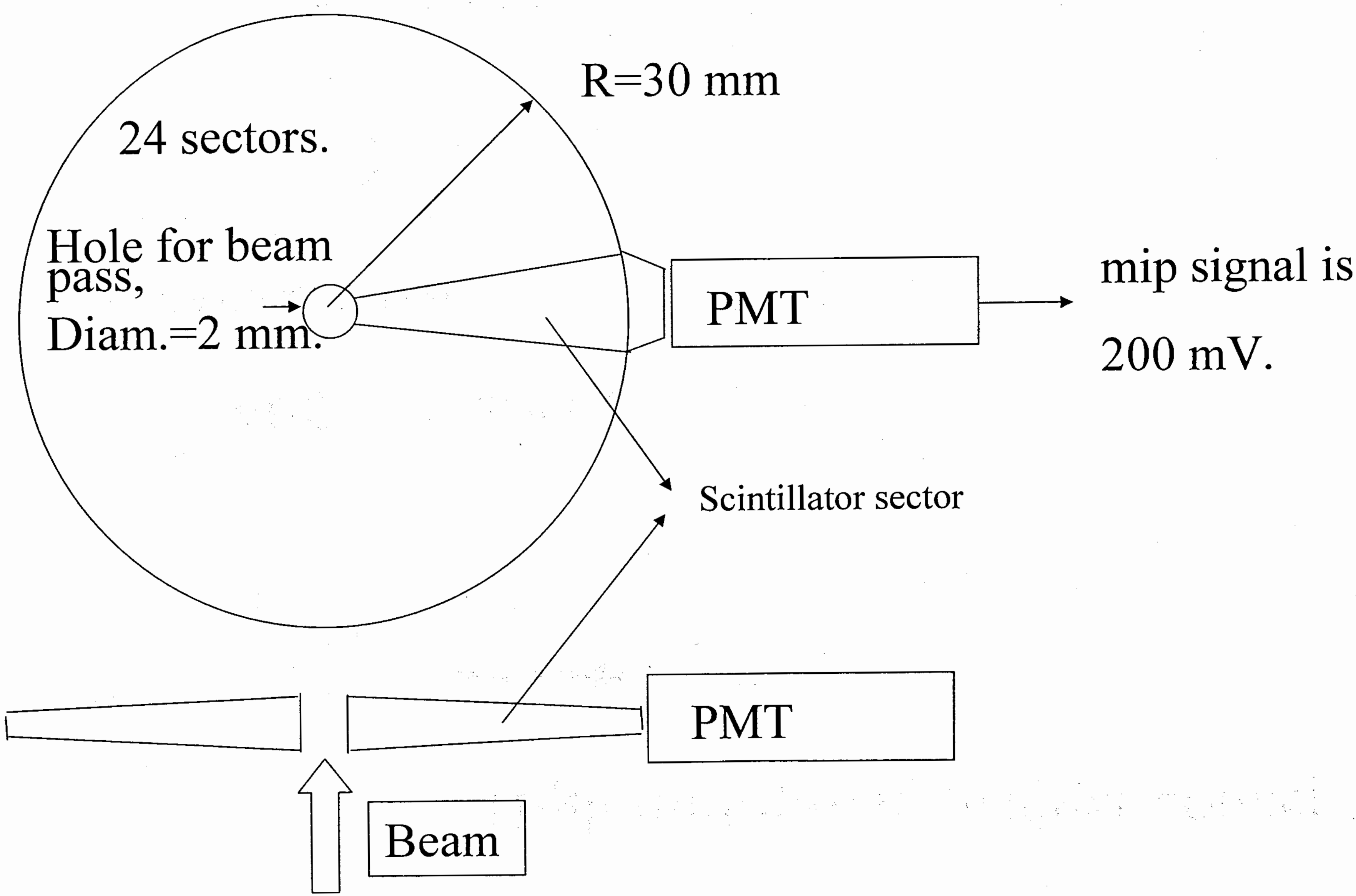

Light collection from one trigger scintillator

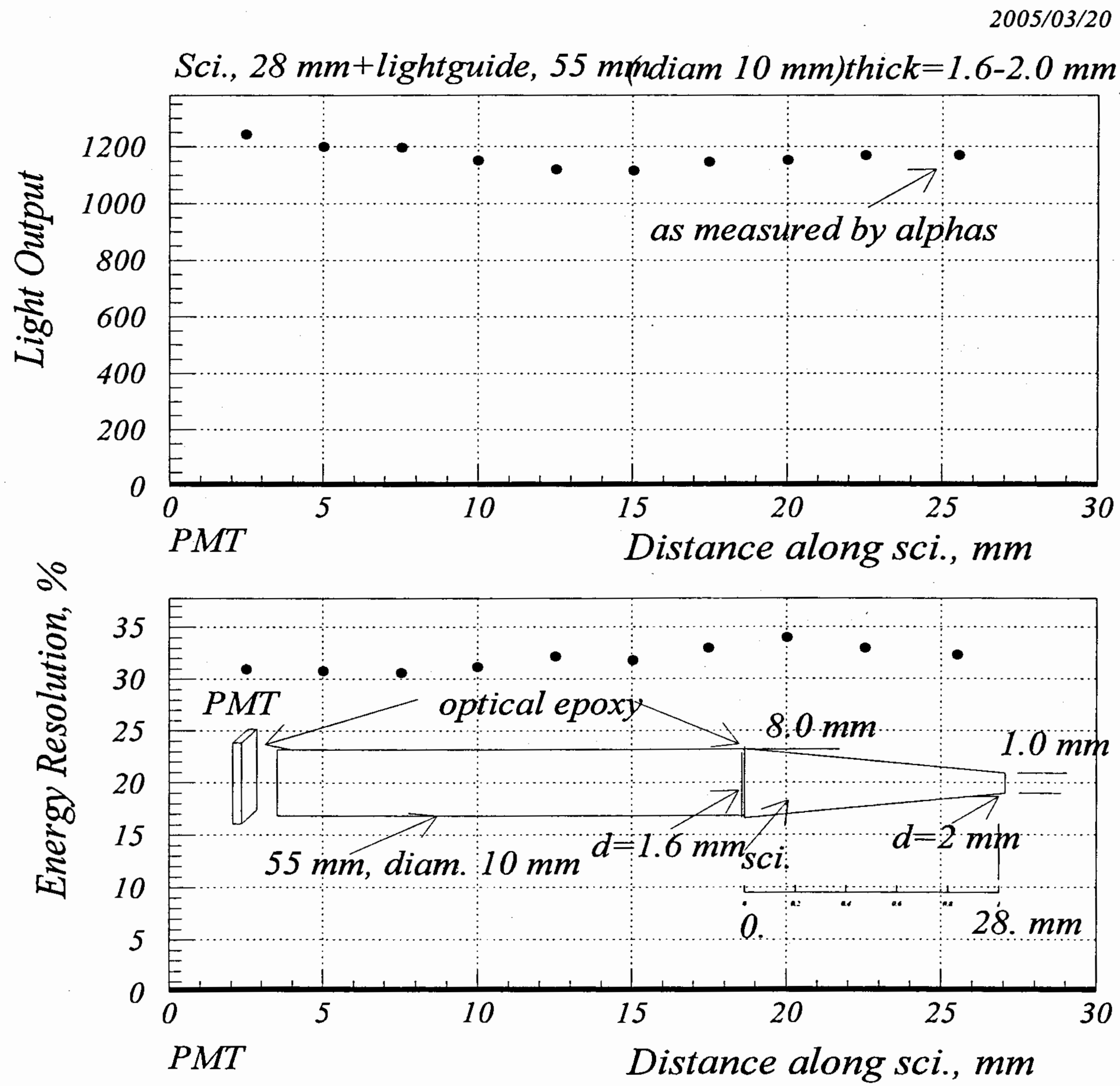

Liquid hydrogen target schematic.

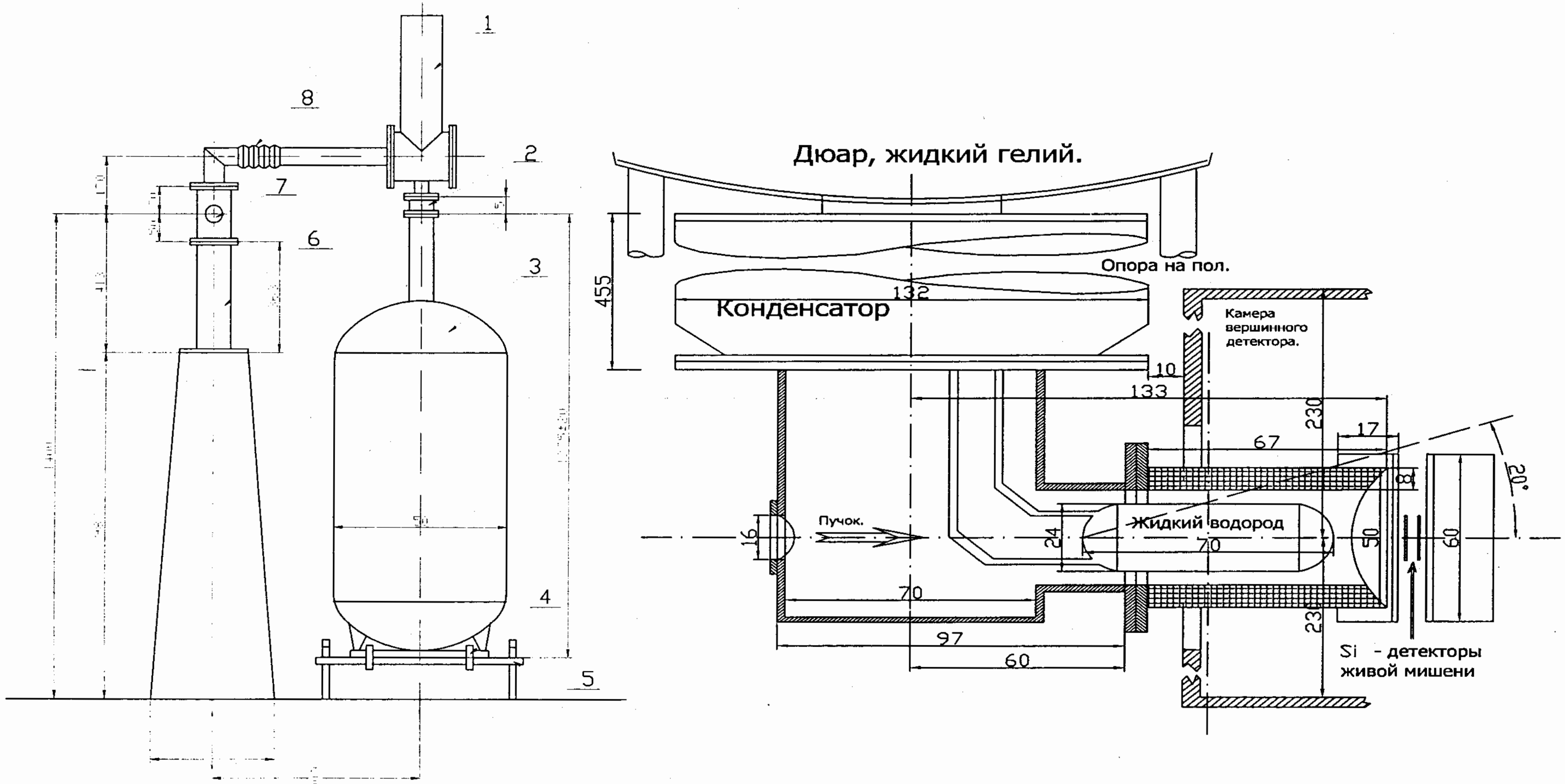

1.Конденсатор H2. 2. Ввод указателя уровня. 3. Дюар He 100 л. 4, 5. Узел крепления и юстировки положения дюара. 6. Система юстировки мишени. 7. H2-мишень. 8. Сильфон.

Пучок перпендикулярен к плоскости чертежа.

Liquid hydrogen target.

Liquid hydrogen target.

Drift tubes tracker is being designed and fabricated in PPL.
Typical plane dimension is 70 x 70 cm. Total number of channels is 2400

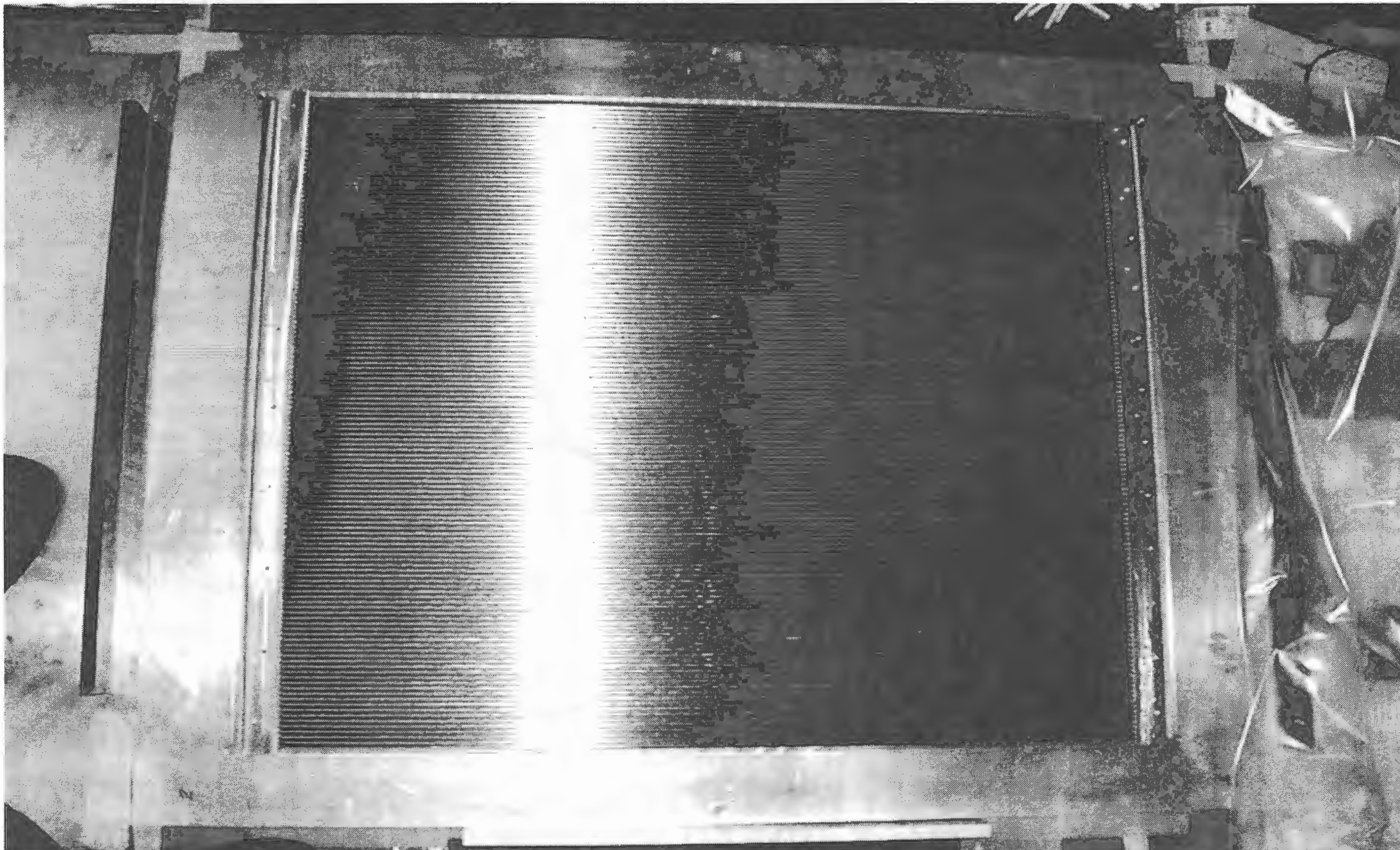

Straw tubes data analysis of run 20.12.04

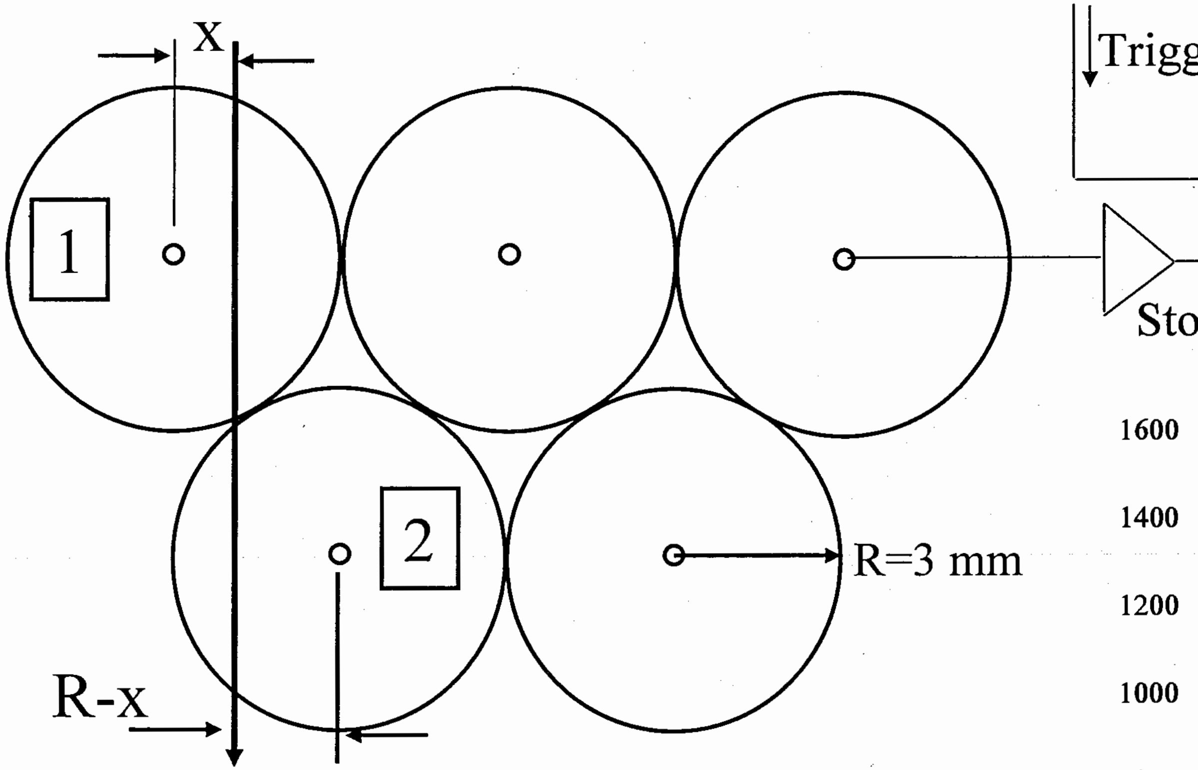

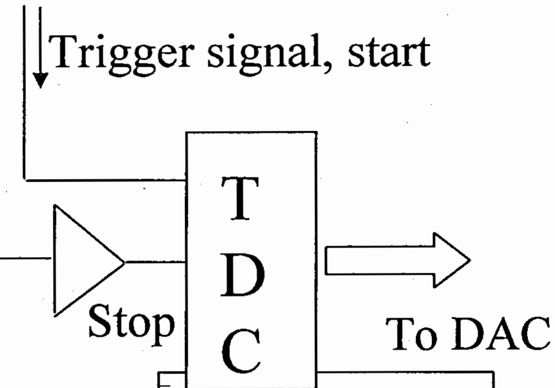

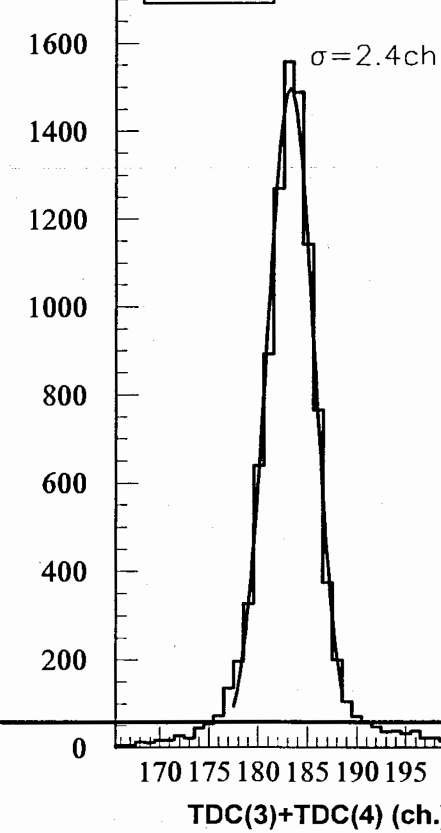

$$t_1 = t_0 + \frac{x}{v}, \quad t_2 = t_0 + \frac{r-x}{v}.$$

$$t_1 + t_2 = 2t_0 + \frac{r}{v} = const\,(x), \qquad t_1 - t_2 = 2\frac{x}{v} - \frac{r}{v}$$

Results: Efficiency: 99%, time resolution 3.7 ns.
Space resolution 210 mcm.

План-график работ первого этапа проекта «Адронизация» - модернизация установки СВД-3.

Наименование работ.	2003 год	2004 год	2005 год
Модификация вершинного детектора и электроники.			
Разработка и изготовление электроники γ детектора.			
Разработка и изготовление мишеней LiH LiD.			
Разработка и изготовление жидководородной мишени.			
Создание системы триггера событий большой множественности.			
Разработка и изготовление дрейфовых трубок на 2100 каналов регистрации для дополнительного трекера.			
Модификация пропорциональных камер для большой интенсивности пучка $I \approx 10^7$.			
Разработка матобеспечения реального времени и пакетной обработки данных.			
Проведение сеансов на У-70.*)			
Обработка данных и публикация результатов.			

*) Сеансы работы на У-70 имеют продолжительность 10÷30 суток. В 2004 – 2005 гг планируются 2 методических сеанса по 30 смен и сеанс набора статистики 120 смен.

Распределение расходов ОИЯИ по годам.

Year	2003	2004	2005	Total
Contrib. $K	52	40	29.5	121.5

Вклад НИИЯФ МГУ в 2003 – 2005 гг - 129 $K.
Вклад ИФВЭ (Протвино) в 2003 – 2005 гг - 26.7 $K

Required extension of work

Budget request.

35 k$ for 2005.

40 k$ per year in 2006 – 2008.

Plan for 2005 -2006.

- Data analysis and publication preparations
- Hardware and software modernization
- Data taking at the accelerator runs
- Technical runs at nuclotron
- The theoretical study of dynamics of hh and hA interactions at 70 GeV in QCD and phenomenological models

Published papers

1. Analysis of multiparticle dynamics in e+e- annihilation into hadrons by two stage model E.S. Kokoulina (Gomel State Tech. U.). 2002. 340-343,World Scientific,2003. Proceeding of the XXXII International Symposium Multiparticle Dynamics. Alushta, Creame, Ukraine, 7-13 Sept. 2002.
2. Multiparticle production process in pp-interaction with high multiplicity at E_p=70 GeV. Nikitin V.A., 36-th PNPI winter school on nuclear and particle physics, St. Petersburg, Repino, Febr. 2002.
3. Description of pp interactions with very high multiplicity at 70 GeV/c. E. Kokoulina. 23-rd International Symposium on Multiparticle Dynamics (ISMD 2003), Cracow, Poland, 5-11 Sep 2003. Acta Phys.Polon.B35:295-302,2004, e-Print Archive: hep-ph/0401223, hep-ph/0209334.
4. Excitement of physical vacuum. M.K. Volkov, E.S. Kokoulina, E.A.Kuraev. Ukr. Jour. of Physics. 48 (2003) 1252.
5. The description of pp-interactions with very high multiplicity at 70 GeV/c by Two Stage Gluon Model. E. Kokoulina (Gomel Tech. U.), V. Nikitin (JINR, Dubna). International School-Seminar The Actual Problems of Microworld Physics, Gomel, Belarus, 2003, Dubna, v. 1 p. 221-236, (2004) hep-ph/0308139.
6. P.F.Ermolov et al. Proton –proton interaction with high multiplicity … (proposal). Nucl.Phys. (Rus.) 67, #1 (2004).
7. A.Aleev at al. Observation of narrow baryon resonance decaying into pK in pA interactions at 70 GeV…Prep. NPI MSU 2004-4/743, hep-ex/0401024.
8. I.D.Manjavidze, A.N.Sissakian. "Where are the thermalized states seen?" Report at Int.conf. Pekin, 2004.
9. I.D.Manjavidze "Thermodynamics for multiple production processes ", Bogolyubov conf., Dubna, 2004.
10. A.Aleev at al. Proton –proton interaction with high multiplicity … (Full text of experiment proposal). To be published as JINR preprint and hep-ex (archive) publication.
11. E.S.Kokoulina. "Description of pp interactions with very high multiplicity at 70 GeV/c". Presented at 23rd International Symposium on Multiparticle production (ISMD) 2003) Cracow, Poland, Acta Phys.Polon. B35(2004)295. hep-ph/0401223.
12. M.K.Volkov,E.S.Kokoulina, E.A.Kuraev. «Exitation of physical vacuum» To be published in Particles and nucleus, Letters, v.1, nom 5 (122), p. 16 – 23 (2004), hep-ph/0402163.
13. On the status of very high multiplicity physics. A.N.Sissakian. Yad. Fis., vol. 67, #1, p. 3, 2004.
14. On thermodynamical description of inelastic hadron collisions. J.Manjavidze. Yad. Fis., vol. 67, #1, p. 13, 2004.
15. On themalization of inelastic processes. J.Manjavidze, A.N.Sissakian. Yad. Fis., vol. 67, #1, p. 23, 2004.
16. The description of multiparticle production in the high multiplicity region by Two Stage Model. E.S. Kokoulina Зимн.школа ПИЯФ, Репино, 2004.
17. Analysis multiparticle production in two stage gluon model at high multiplicity. E.S. Kokoulina , XVII ISHEPP, 27.09.-2.10. 2004 International serminar of high energy particle problems.
18. Multiparticle production process in pp-interaction with high multiplicity at Ep=70 Gev. Nikitin V.A. et al., International conferences "Hadron Structure-2004". Smolenice castle, Slovakiya, 30.09-3.09.2004
19. Исследование множественного рождения в модели глюонной доминантности" E.S. Kokoulina , Nikitin V.A., (ЛФЧ ОИЯИ, 12.11.04 BLTP JINR.
20. Analysis of charged particle emission sources and coalescence in AA collisions. V.A.Avdeichikov et al., Nucl.Phys.A736:22-38,2004 nucl-ex/0401033.
21. Energy calibration of CsI scintillators in pulse-shape identification technique. V.A.Avdeichikov et al., tobe published in NIM.

Conclusion.

•Modernization of the most systems of the SVD-2 setup is in progress.

•Trigger concept is worked out

•Software package for high multiplicity events processing is developed.

•Liquid hydrogen target is designed and manufactured.

•Drift tubes tracking system is developed and is under construction.

•Two technical runs were conducted at U-70 accelerator. Two more runs are planed in 2005 – one at Nuclotron and one at U-70.

•Extention of the theme is requested for 2006 – 2008.

Budget request: 40 k$ per year.

The recent news from SVD-2: pentaquarq search.

Search for pentaquark θ+, 2004.

Number of events:

peak – 52, background 78

Demonstration of setup capability.

Effective mass spectrum of ($\pi\pi$), (πp) and (Kp) systems:

$M(K) = 497.6$ MeV, $\sigma = 4.4$ MeV;

$M(\Lambda) = 1115.0$ MeV, $\sigma = 1.6$ MeV

$M(\theta+) = 1526.0 \pm 3.1$ MeV, $\sigma = 10.2$ MeV

Search for pentaquark θ+, 2005.
K_0 found in vertex detector.

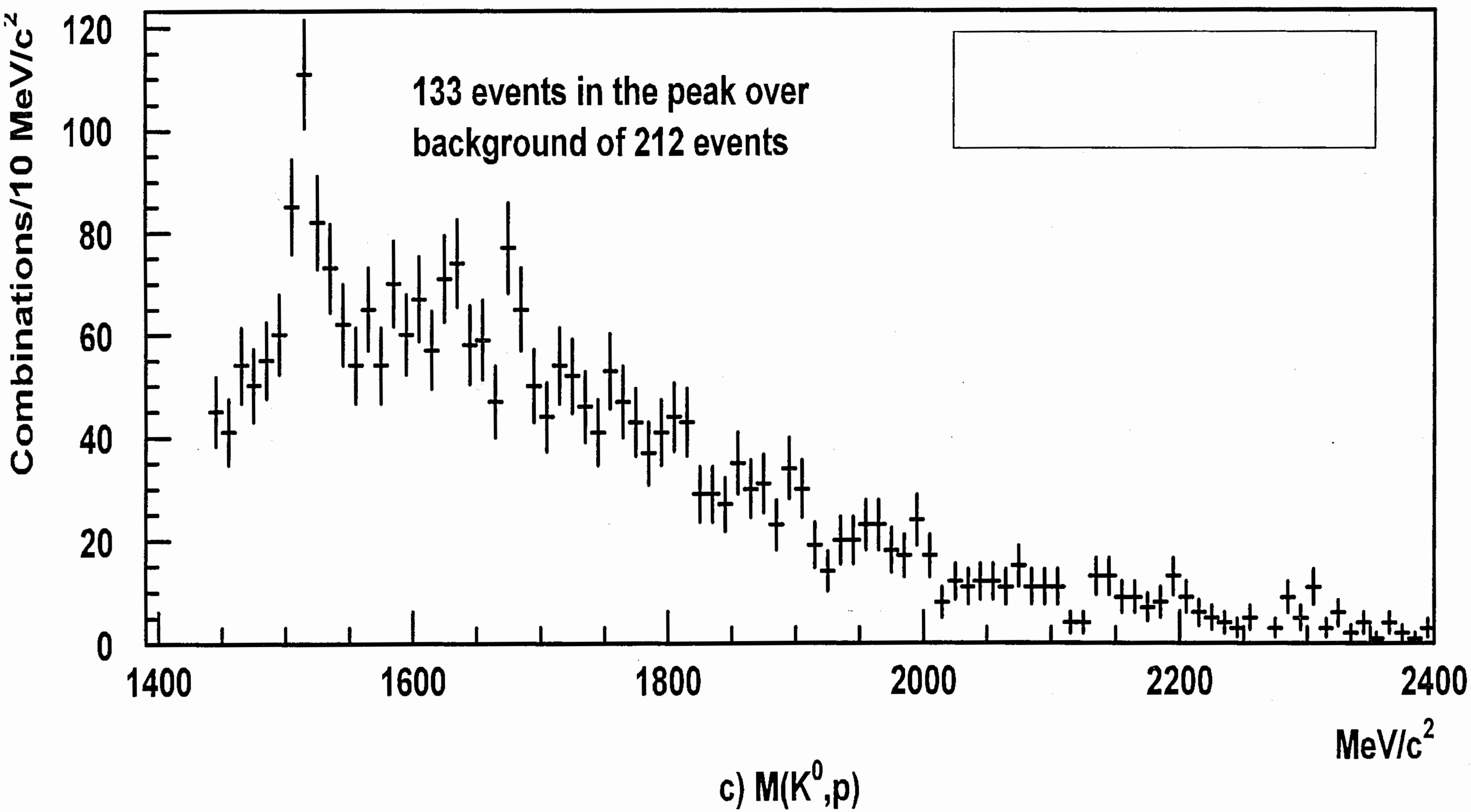

Search for pentaquark θ+, 2005.
K_0 found in magnetic spectrometr.

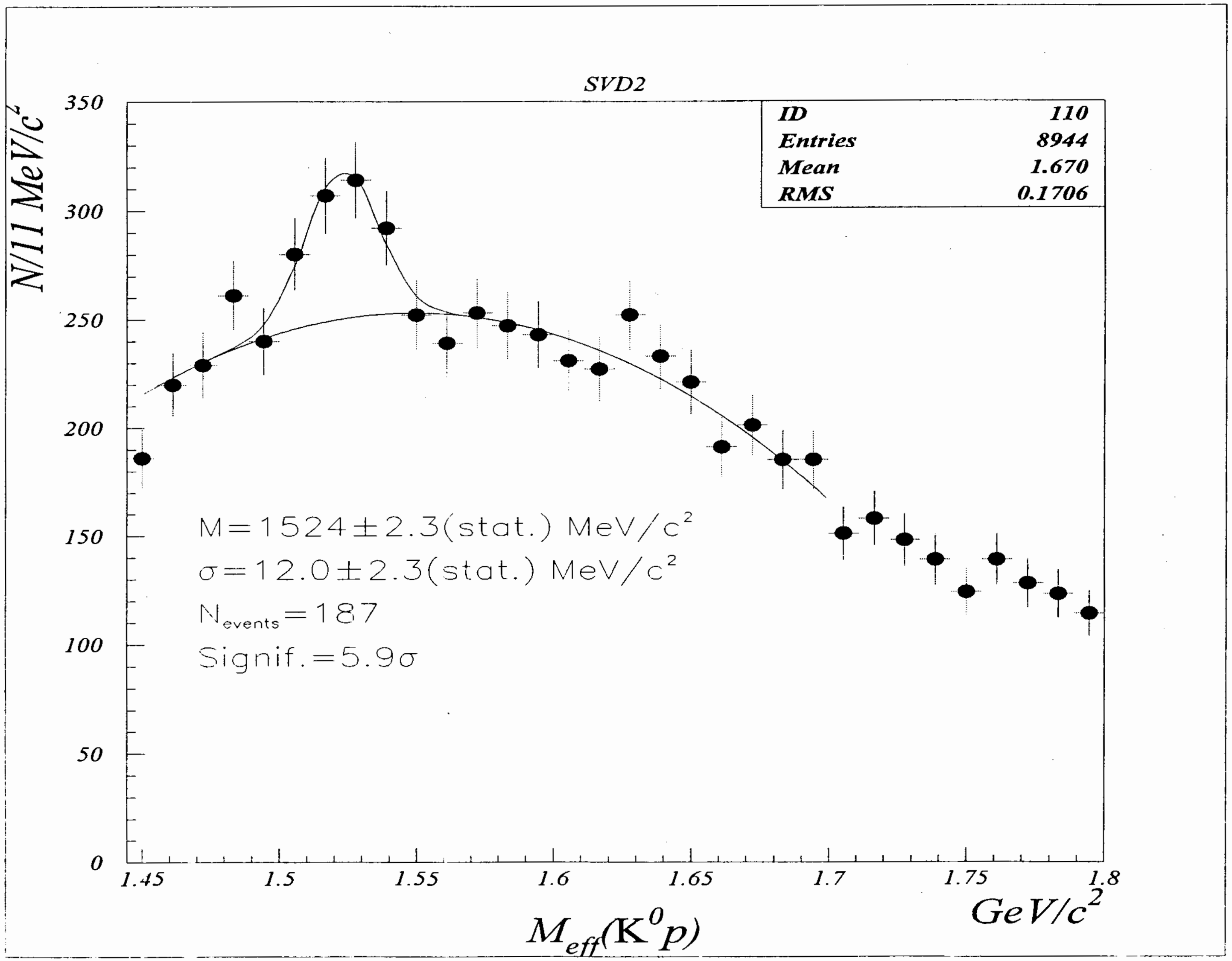

The end.

Thank you.

Conclusion.

The goal of the proposed experiment "Hadronization" is to investigate the collective behavior of particles in the process of multiple hadron production in pp and pA interaction. Near the threshold of reaction all particles get small relative momenta. As a consequence of multiboson interference a number of collective effects may show up.

The processes of the deep energy dissipation at hadron interaction and the thermalization of the formed system are far from full understanding. The further experimental and theoretical studies in this direction are called to throw light on fundamental grounds of the particle physics: confinement mechanism, nature of the vacuum, the equation of state of hadronic matter etc.

Conclusion

The physics objectives of the experiment are as follows.

1. Search for new phenomena.

a) Drastic variation of the multiplicity distribution is expected comparing with the behavior obtained by means of conventional extrapolations. The BEC may manifest itself by formation of narrow jets of identical particles or "cold spots" in the fireball of the secondary particles. The other notions for this effect are pion laser, classical boson field, boson condensate.

b)The measurement of the multiparticle correlation function. Search for identical particles jets.

c) Search for large variation of charged and neutral particles multiplicity. This may also manifest the classical pionic field production or onset of chiral condensate.

Conclusion

The systematic and precision study of known phenomena.

a) Study of anomalous low energy photons.
b) The study of stochastic intermittency is an instrument for phase transition search.
c) Search of events with regular intermittency, so called ring events. This effect is referred as a gluonic Cherenkov radiation. If it exists, it will be a genuine probe of the hadronic matter properties.
d) Simultaneous analysis of the differential cross section and BE correlation functions makes it possible to disentangle the hadronic system size, temperature and expansion rate. All parameters are measured as function of particle multiplicity.

Budget request.

35 k$ for 2005. 40 k$ per year in 2006 – 2008.

Conclusion

Experimental setup.

The experiment is being carried out at 70 GeV extracted proton beam of IHEP U70 accelerator.

The apparatus design is essentially based on the fact that at high multiplicity all the secondary particles have good forward collimation. In spite of the modest setup size (and cost) it is expected that at least 70% of all particles drop into the apparatus aperture and will be detected.

The apparatus includes a liquid hydrogen target, a micro strip silicon vertex detector, Threshold Cherenkov counter, magnetic spectrometer and electromagnetic calorimeter.

The two level trigger system is designed to select the rare events with high charged and neutral multiplicity.

The counting rate of the events with total multiplicity 35 is expected to be 10 events per hour. If scenario of BEC is realized then counting rate will be essentially higher.

The modernization of the setup is in progress.

University of Athens - Physics Department

Section of Nuclear and Particle Physics

Kinematics of Top Decays in the Dilepton and the Lepton + Jets channels: Probing the Top Mass

Nikos Giokaris

OUTLINE

- Introduction
- Top Quark Production and Decay
- Physics Motivation
- Sensitivity to the Top Mass at TEVATRON and LHC
- Results from PYTHIA/HERWIG simulation study
- Conclusions and Future Work

Introduction on top quark

- Top quark was predicted by the SM as the $I_3=+1/2$ member of a weak SU(2) isodoublet that also contains the b quark
- It was discovered by both CDF end DØ at the Fermilab Tevatron in 1995

Top Production and Decay

At high energy $p\bar{p}$ collisions at Tevatron and for M_{top}>100 GeV/c^2 $q\bar{q}$ fusion to a gluon is the main production mechanism.

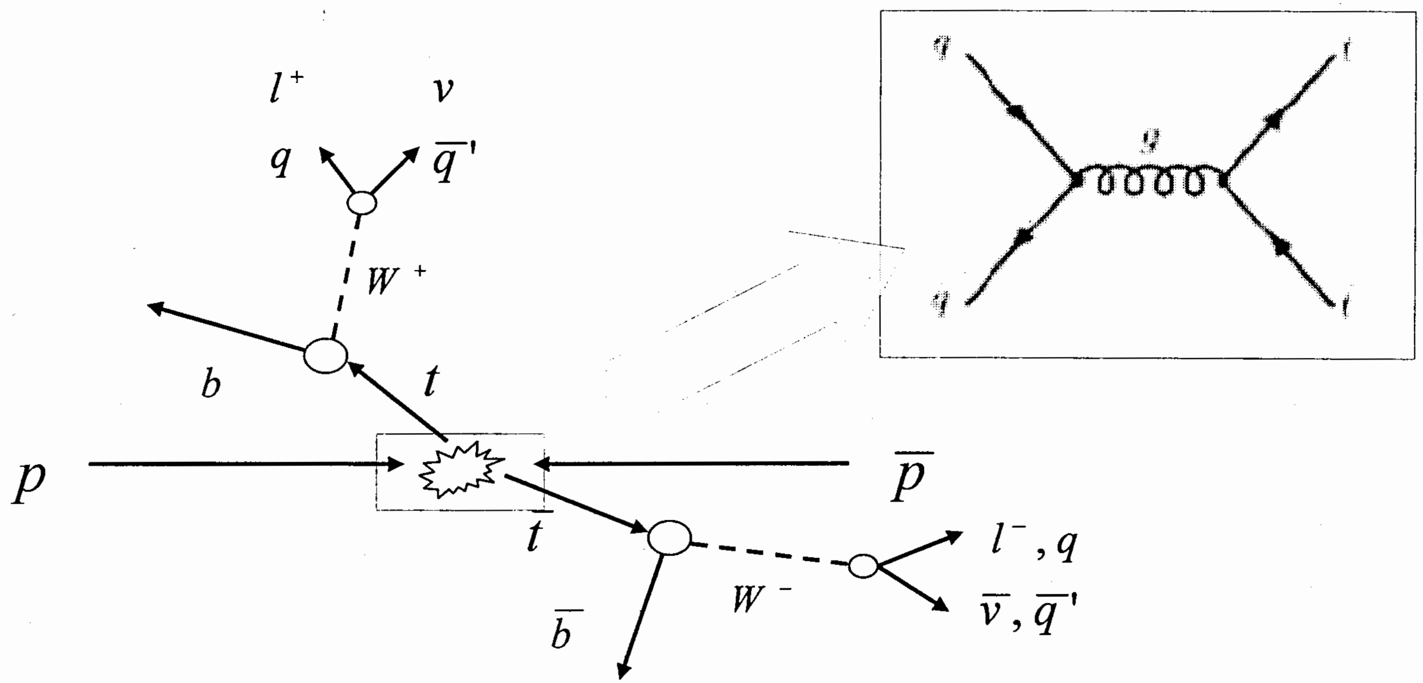

Decay Modes

$W_1 \rightarrow \bar{l}, \nu$ Dilepton

$W_2 \rightarrow l, \bar{\nu}$ BR=11.2%

$W_1 \rightarrow l, \nu$ Lepton + jets

$W_2 \rightarrow q'\bar{q}$ BR=44.4%

$W_1 \rightarrow q', \bar{q}$ All Hadronic

$W_2 \rightarrow q', \bar{q}$ BR=44.4%

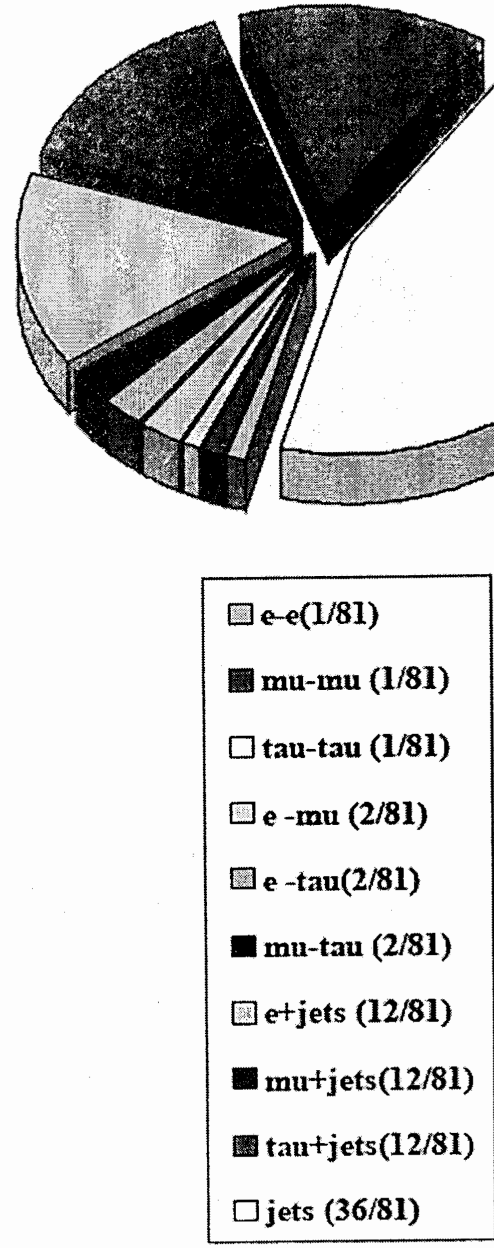

What about the Dilepton Signal?

$t \rightarrow W^+ b$

$b \rightarrow \text{jet}$

$W^+ \rightarrow l^+ \nu_l$

$\bar{t} \rightarrow W^- \bar{b}$

$\bar{b} \rightarrow \text{jet}$

$W^- \rightarrow l^- \bar{\nu}$

Expect to observe:

- two leptons with high P_T
- large missing E_T from the two ν's
- two or more jets

Why study the $t\bar{t}$ to Dilepton channel

- another measurement of the top quark mass with smallest systematic error
  - ➢ better 'localization' of SM Higgs mass
- it can provide many checks on the SM

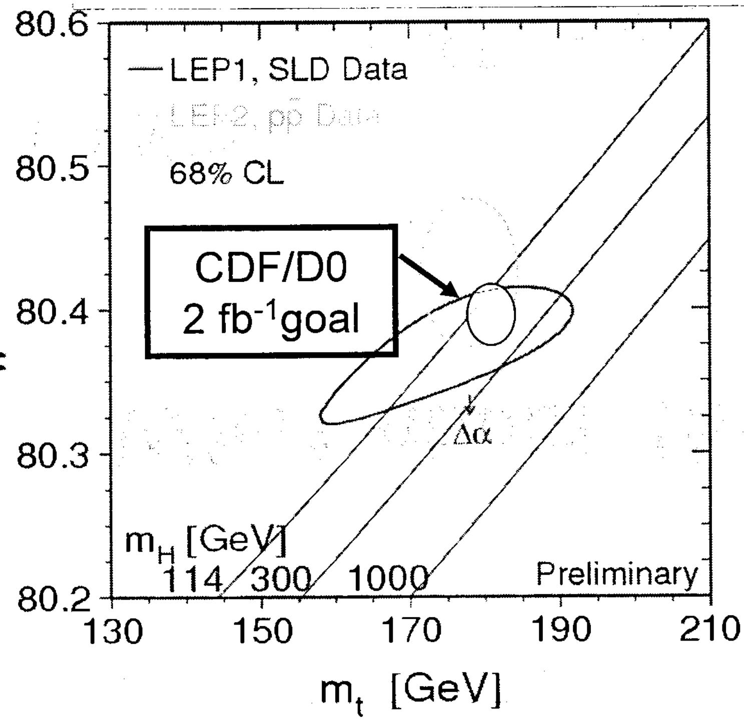

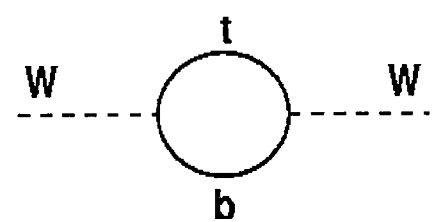

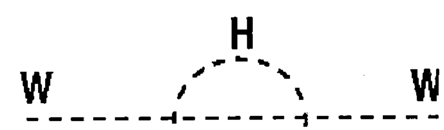

The Top Mass

New World Average (2004) (including RunI results)

$Mt = 178.0 \pm 4.3$ (± 2.7st± 3.3sys) GeV/c^2

hep-ex/0404010

CDF Run II :

$$M_t = 173.5^{+3.7}_{-3.6}(\mathrm{stat}+\mathrm{jets}) \pm 1.7(\mathrm{syst})\ \mathrm{GeV}/c^2$$

Moderate (CDF RUN II) or very high (LHC) statistics of top production are expected soon

The statistical error will decrease

The systematic error will dominate

The Top Mass

Mt = 178.0 ± 4.3 GeV (±2.7st±3.3sys)

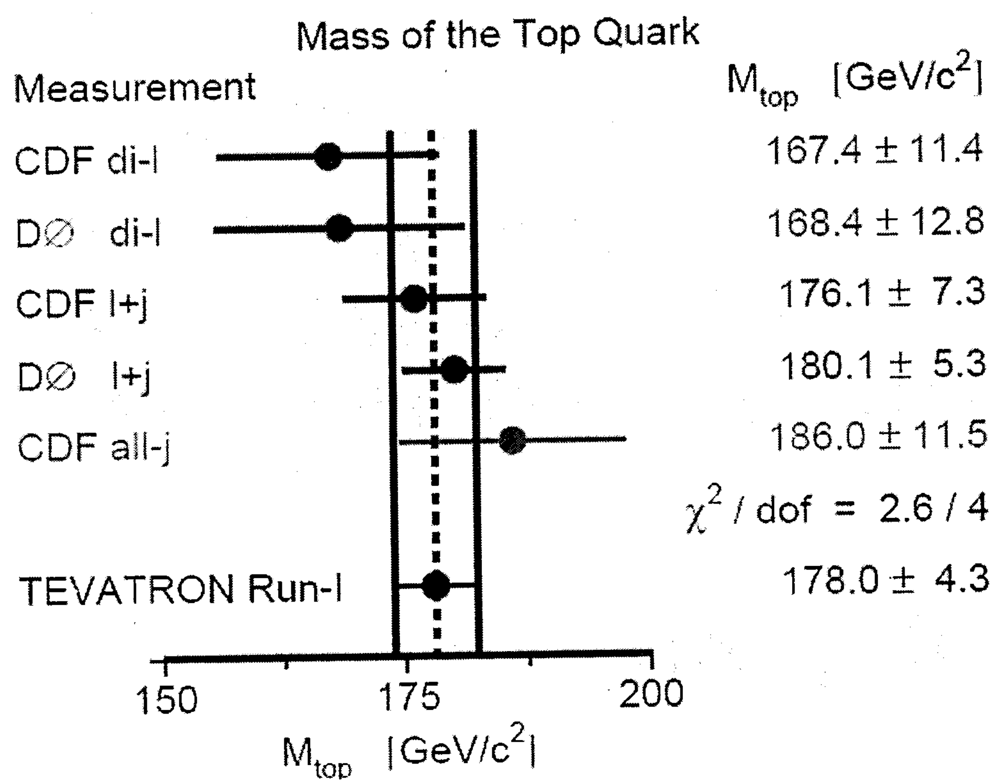

Stat: 2.7 GeV/c^2

Syst: 3.3 GeV/c^2

- 2.6 GeV/c^2 JES
- 1.6 GeV/c^2 signal
- 0.88 GeV/c^2 background
- 0.83 GeV/c^2 UN/MI
- 0.35 GeV/c^2 fit
- 0.12 MC

Relative weight in top mass average

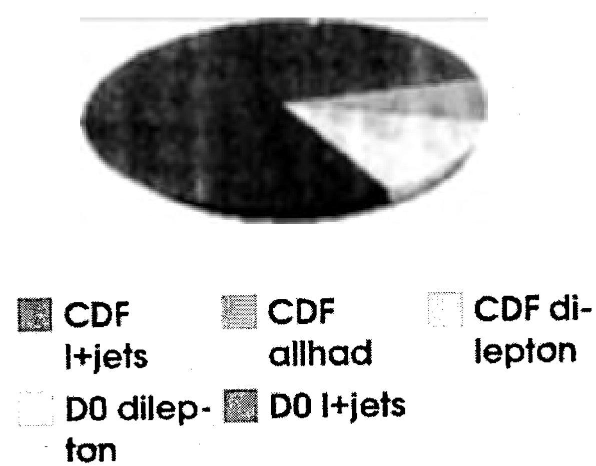

Sensitivity to the Top Mass

PROBLEM →The main source of the systematic error is the jet energy scale.

PROPOSAL →Use a variable(s) that does not depend on the jet energy.

EXAMINE → LEPTON $E_T(P_T)$ sensitivity to the top mass in the $t\bar{t}->\mathrm{Dilepton}$ & $t\bar{t}->\mathrm{lepton}+\mathrm{jets}$ decay channels where leptons are electrons or muons

Analysis Outline

- Generation of $t\bar{t}$ events for several top masses (130 -230 GeV/c^2) for:
  - CDF energy, 2 TeV (HERWIG)
  - LHC energy, 14 TeV (Pythia)
- Selection of dilepton events, in parton level, where leptons are electrons or muons

  Requirements on leptons:
  - P_T > 20 GeV/c
  - $|\eta|$ <1.1
- Study of the mean value of the leptons' P_T for the samples generated with the above top masses

Leptons' P_T

events generated with HERWIG

$$\sqrt{s} = 2\text{TeV}$$

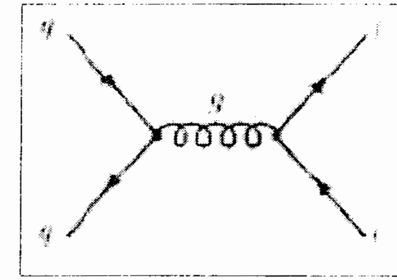

Top Quark Mass (GeV/c^2)	Lepton $\langle P_T \rangle$ (GeV/c)	$\langle P_T \rangle$ standard deviation (GeV/c)
130	50.59	26.15
150	53.33	28.43
160	55.08	30.39
170	56.78	31.55
180	58.17	32.10
190	58.91	31.73
200	60.83	34.21
210	62.72	34.73
230	67.11	37.64

Distributions of Leptons' P_T

events generated with HERWIG

$$\sqrt{s} = 2\text{TeV}$$

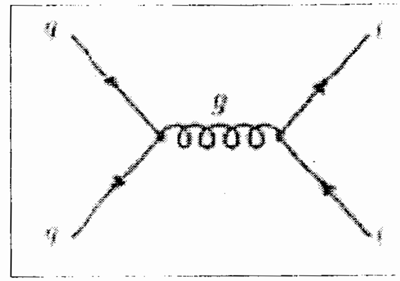

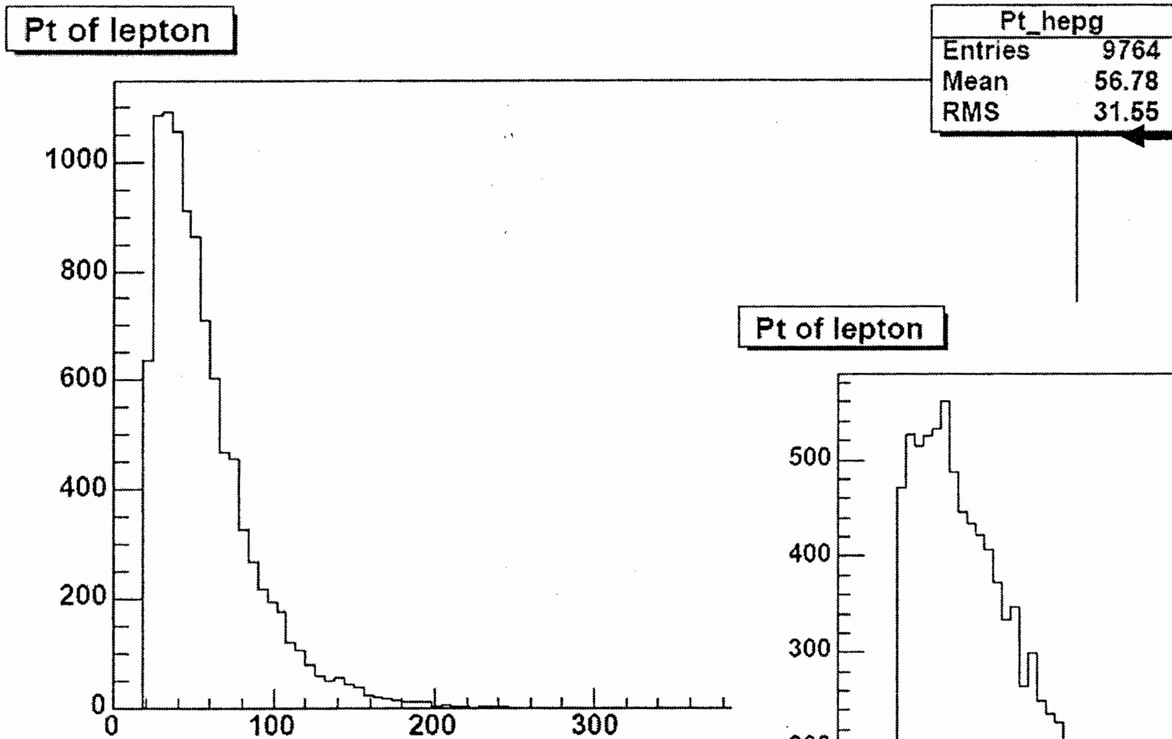

Mtop = 170 GeV/c^2

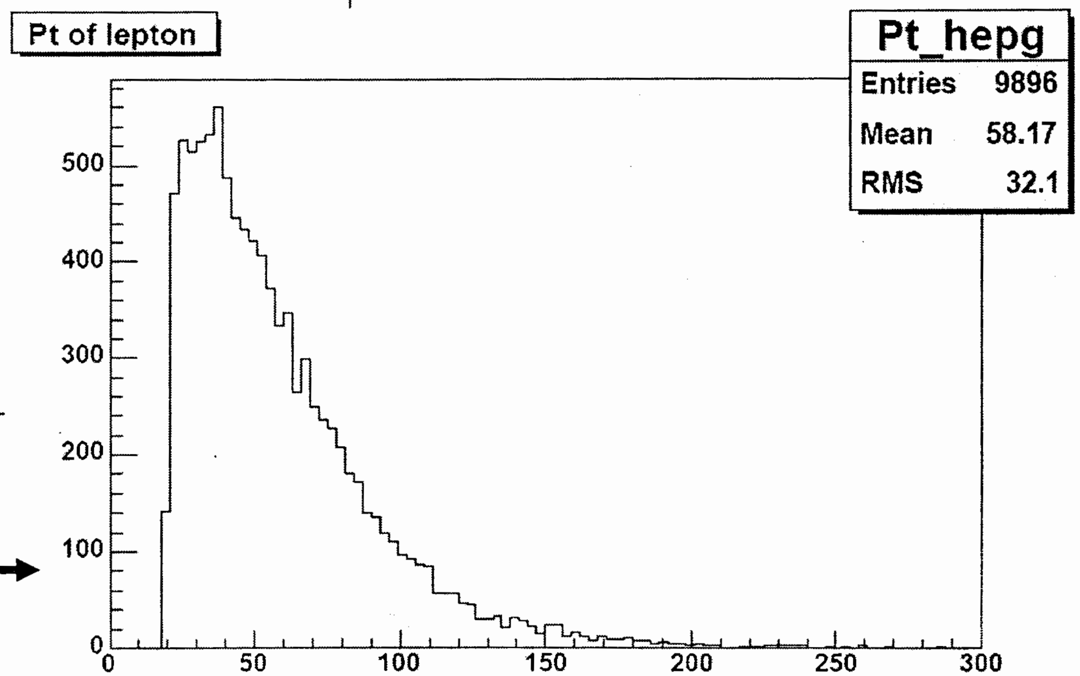

Mtop = 180 GeV/c^2

Leptons' P_T vs top mass

events generated with HERWIG

$\sqrt{s} = 2\text{TeV}$

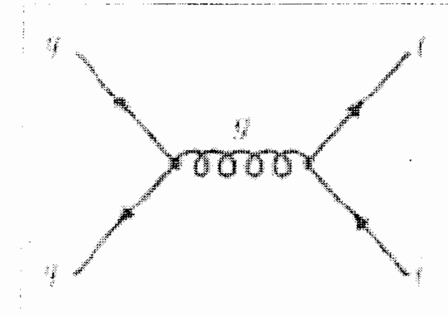

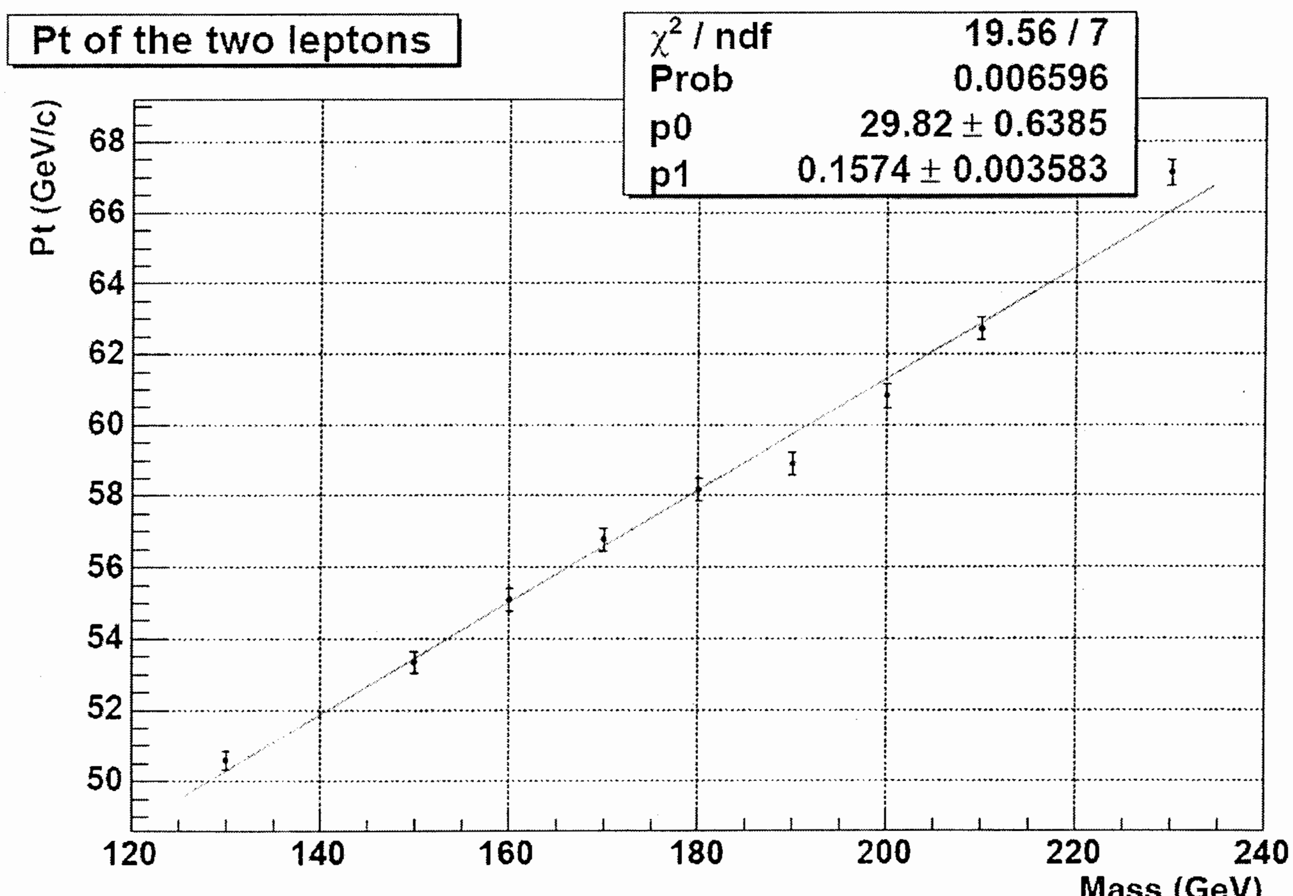

P_T

<u>sensitive</u> to the top quark mass

Fit to a straight line gives

slope: 0.16

Other kinematic variables vs top mass

events generated with HERWIG

$$\sqrt{s} = 2\,\mathrm{TeV}$$

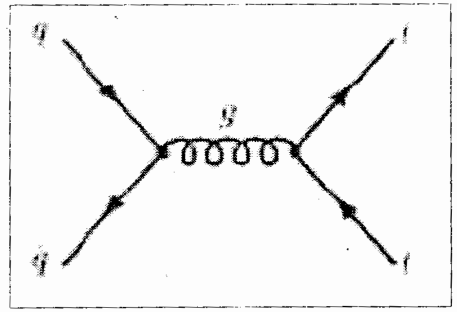

Kinematic Variable	Slope
P_T	0.1574±0.0036
P	0.1739±0.0042
Leading P_T	0.2278±0.0054
Leading P	0.2523±0.0064
Sum of P_T's	0.316±0.008
Sum of P's	0.3523±0.0092

Leptons' P_T

events generated with Pythia

$\sqrt{s} = 14\text{TeV}$

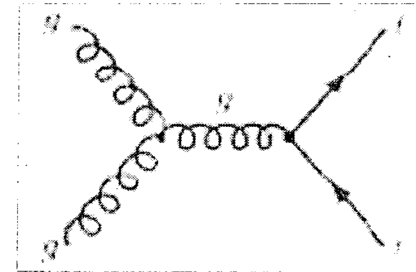

Top Quark Mass (GeV/c^2)	Lepton $\langle P_T \rangle$ (GeV/c)	$\langle P_T \rangle$ standard deviation (GeV/c)
130	54.99	33.13
140	55.5	33.47
150	57.37	35.75
160	59.37	37.1
170	61.69	38.97
180	63.89	40.83
190	66.28	43.91
200	67.63	44.52
210	69.81	45.11
220	72.67	47.32
230	75.65	51.03

Distributions of Leptons' P_T

events generated with Pythia

$\sqrt{s} = 14 TeV$

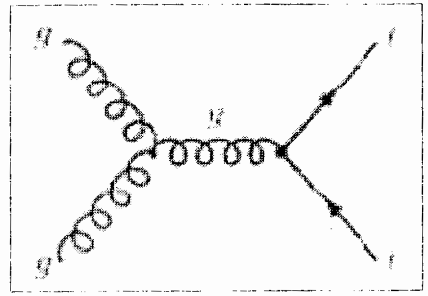

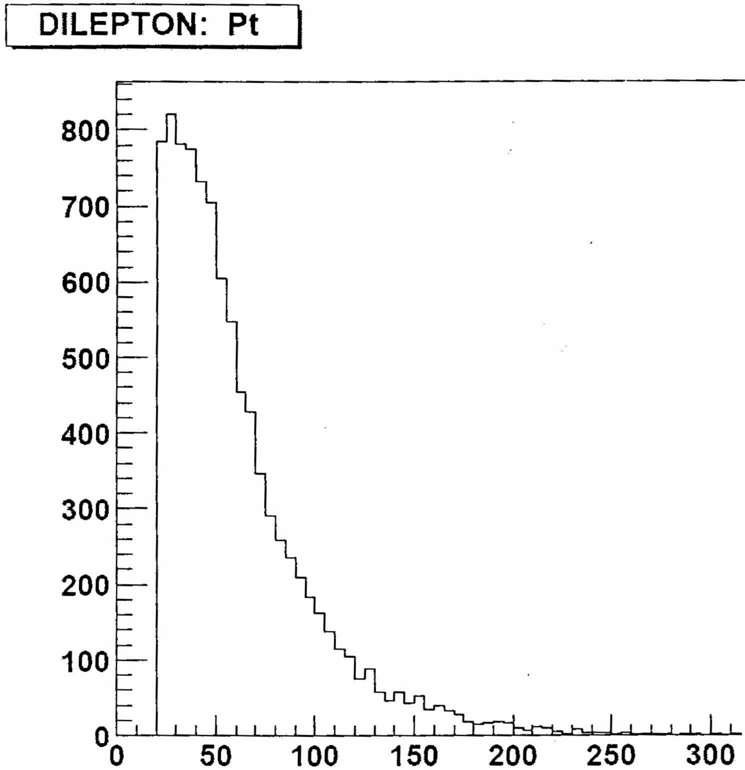

Mtop = 170 GeV/c^2

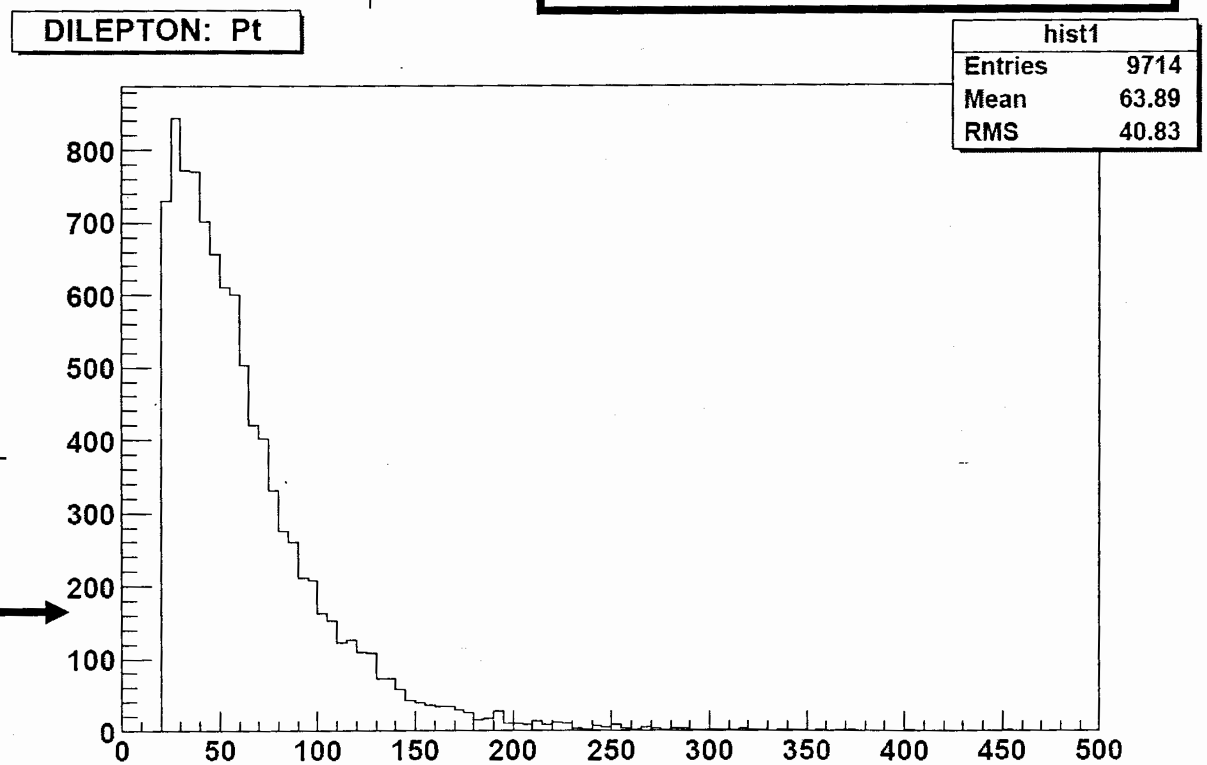

Mtop = 180 GeV/c^2

Leptons' P_T vs top mass

events generated with Pythia

$\sqrt{s} = 14\,\text{TeV}$

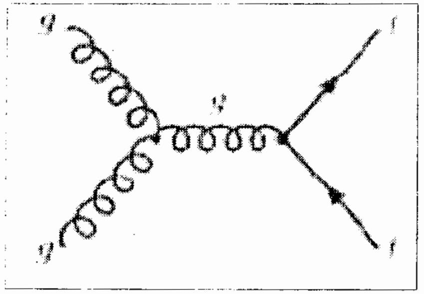

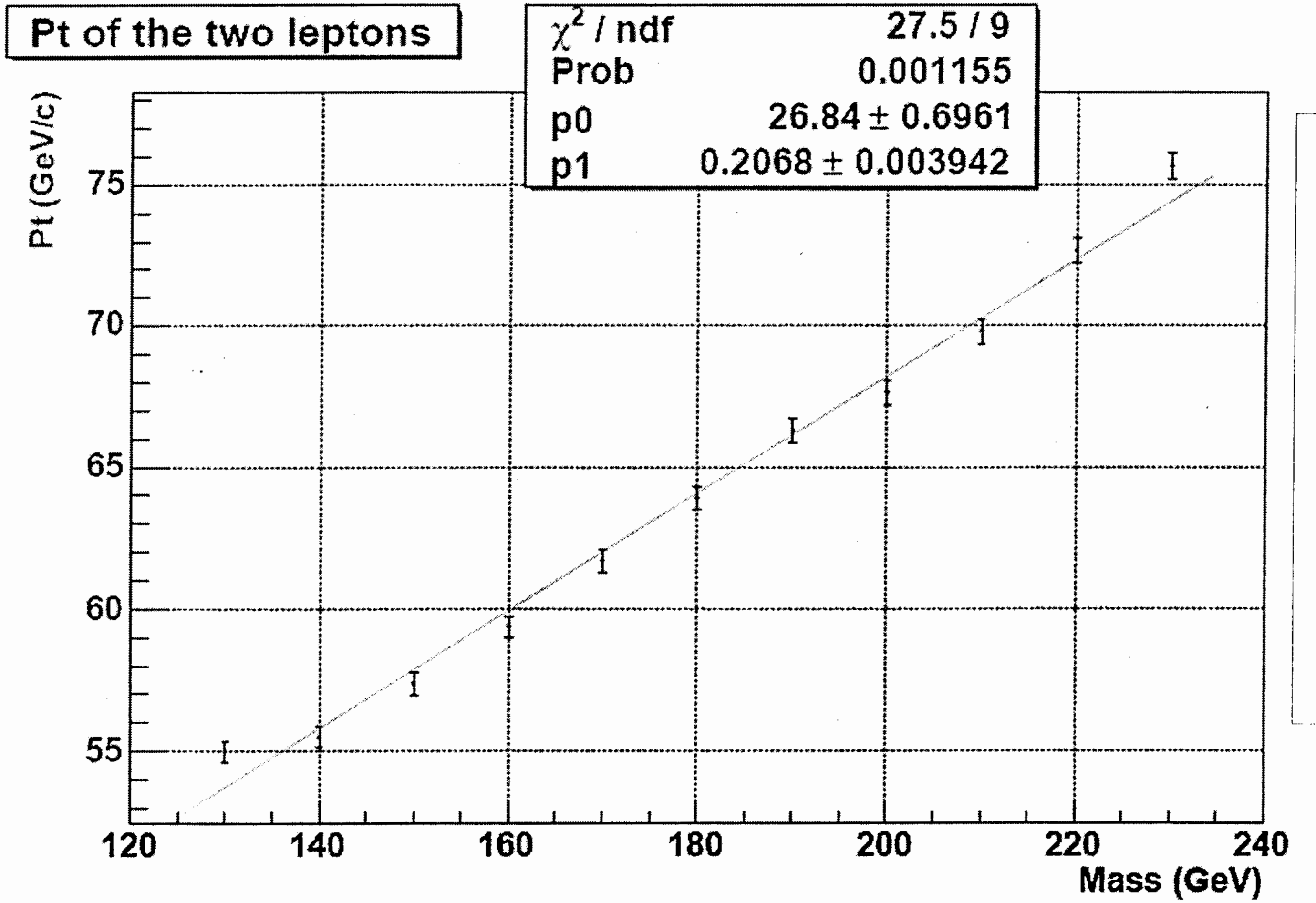

P_T

sensitive to the top quark mass

Fit to a straight line gives

slope: 0.21

Other kinematic variables vs top mass

events generated with Pythia

$\sqrt{s} = 14\text{TeV}$

Kinematic Variable	Slope
P_T	0.2068±0.0039
P	0.242±0.005
Leading P_T	0.2294±0.0062
Leading P	0.3526±0.0075
Sum of P_T's	0.381±0.008
Sum of P's	0.451±0.0010

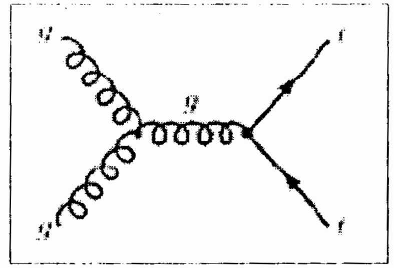

Again, the numbers for $\sqrt{s} = 2\text{TeV}$ →

Kinematic Variable	Slope
P_T	0.1574±0.0036
P	0.1739±0.0042
Leading P_T	0.2278±0.0054
Leading P	0.2523±0.0064
Sum of P_T's	0.316±0.008
Sum of P's	0.3523±0.0092

Leptons' P_T

events generated with HERWIG,
after simulation

$\sqrt{s} = 2\text{TeV}$

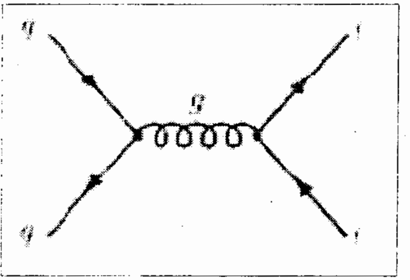

Top Quark Mass (GeV/c^2)	Lepton $\langle P_T \rangle$ (GeV/c)	$\langle P_T \rangle$ standard deviation (GeV/c)
130	54.43	30.00
150	57.24	31.94
160	59.54	33.55
170	60.99	34.12
180	63.43	35.47
190	62.85	34.82
200	65.86	37.86
210	66.54	47.58
230	70.17	38.79

Leptons' P_T vs top mass

events generated with HERWIG,
after simulation

$$\sqrt{s} = 2\,\mathrm{TeV}$$

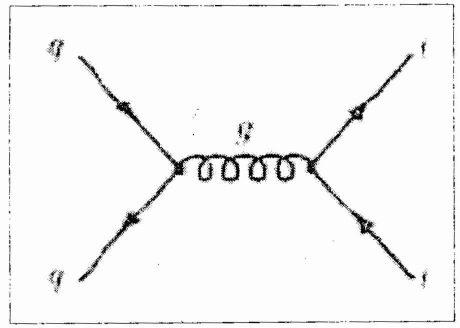

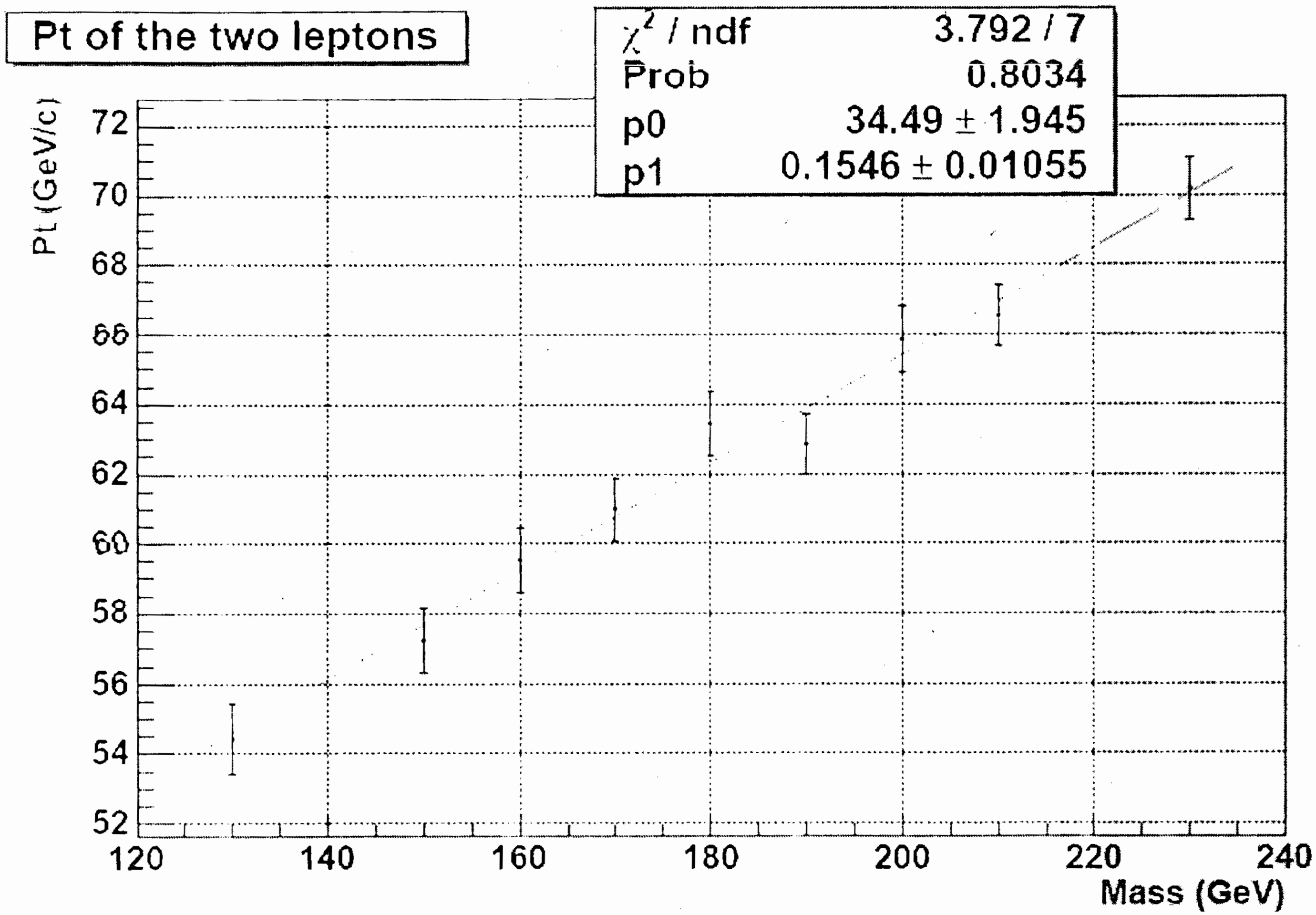

P_T

<u>sensitive</u> to the top quark mass

Fit to a straight line gives

slope: 0.15

Other kinematic variables vs top mass

events generated with HERWIG, after simulation

$$\sqrt{s} = 2\text{TeV}$$

Kinematic Variable	Slope
P_T	0.1546±0.0106
P	0.1667±0.0122
Leading P_T	0.2172±0.0157
Leading P	0.2309±0.0182
Sum of P_T's	0.3091±0.0237
Sum of P's	0.3317±0.0273

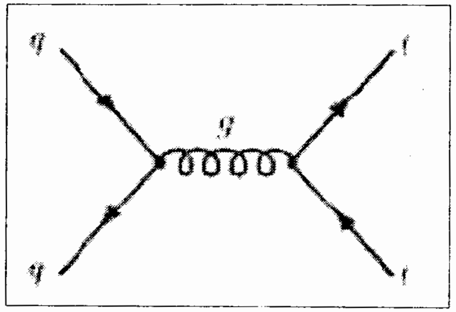

Again, the numbers in parton level →

Kinematic Variable	Slope
P_T	0.1574±0.0036
P	0.1739±0.0042
Leading P_T	0.2278±0.0054
Leading P	0.2523±0.0064
Sum of P_T's	0.316±0.008
Sum of P's	0.3523±0.0092

139

Estimation of the statistical error of the top mass (TEVATRON)

Expected statistical error in the top mass, as extracted from the Pt spectrum of the two leptons in the dilepton channel, as a function of Luminosity L

Top mass is linear dependent to the $\langle P_T \rangle$ → $\langle P_T \rangle = \lambda m_{top} + \kappa$

$$(\delta m_{top})_{stat} = \frac{(\delta < P_T >)_{stat}}{\lambda} = \frac{1}{\lambda} \times \frac{P_T^{rms}}{\sqrt{N}}$$

For TEVATRON

Integrated Luminosity	Expected by	Expected number of dilepton events	$(\delta M_{top})_{stat}$	
(pb^{-1})			(GeV/c^2)	(%)
193	Feb. 2003	10	51	28
400	Sep. 2004	21	35	20
1200	Dec. 2005	63	20	11
3000	Dec. 2006	158	13	7
8000	Dec. 2008	420	8	4

Estimation of the statistical error of the top mass (LHC)

Top mass is linear dependent to the $\langle P_T \rangle$ → $\langle P_T \rangle = \lambda m_{top} + \kappa$

$$(\delta m_{top})_{stat} = \frac{(\delta \langle P_T \rangle)_{stat}}{\lambda} = \frac{1}{\lambda} \times \frac{P_T^{rms}}{\sqrt{N}}$$

For LHC

Integrated Luminosity	Expected by	Expected number of dilepton events	$(\delta M_{top})_{stat}$	
(pb^{-1})			(GeV/c^2)	(%)
1000	End of 1^{st} year of operation	8000	1.6	0.8
10,000	End of 2^{nd} year of operation	80,000	0.5	0.3

Estimation of the systematic error of the top mass

Top mass is linear dependent to the
$\langle P_T \rangle \rightarrow \langle P_T \rangle = \lambda m_{top} + \kappa$

$$\underline{(\delta m_{top})_{syst}} = \frac{1}{\lambda} \times \sqrt{(\delta < P_T >)^2_{syst} + (\delta\kappa)^2 + m^2_{top}(\delta\lambda)^2}$$

Contributions to systematic error: uncertainties in

- the fit parameters due to finite MC statistics & omission of non linear terms
- the measurement of leptons' P_T
- the measurement of jets' Pt (MET also)
- the MC event generator
- the knowledge of background

Uncertainty	$(\delta\langle P_T\rangle)_{syst}$	$\delta\kappa$	$\delta\lambda$	$(\delta M_{top})_{stat}$	
	(Gev/c)	(Gev/c)		(GeV/c^2)	(%)
Leptons's P_T	0.05				
Linear fit					
Jet energy					
Monte Carlo					
Background					
Total					

Summary

- Top mass analysis, using only lepton P_T information in the ttbar→Dilepton channel, looks promising
- The method is applicable both in Tevatron and LHC experiments
- The systematic error of the top mass is expected to decrease considerably by this method
- The statistical error will also be very small at LHC

Status and Physical Program of Spectrometer with Vertex Detector

1. SVD history
2. SVD-2 setup
3. Experiment characteristics as from April'2002 run
4. Current status and physics program

P.F.Ermolov, A.V.Kubarovsky, V.V.Popov, L.A.Tikhonova, V.Yu.Volkov
SINP MSU Moscow

SVD-1 experiment

- Spectrometer with a Vertex Detector (SVD) on a proton beam channel #22 of Protvino 70 Gev accelerator went through few stages of development.
- SVD-1 used a fast cycling bubble chamber as a vertex detector and a magnetic spectrometer with MWPC
- With this setup, an estimate of near-threshold charm creation cross-section was obtained as

$$\sigma_{tot} = (1.7^{+1.2}_{-0.5})\mu b$$

SVD-1 → SVD-2

- To increase the rate of event collection, a bubble chamber was replaced by the MicroStrip Vertex Detector (MSVD) with 10,000 amplitude channels
- To register neutral particles: 1,500-channels γ-detector
- Particle identification: wide-aperture threshold Cerenkov detector

146

SVD-2 detector layout

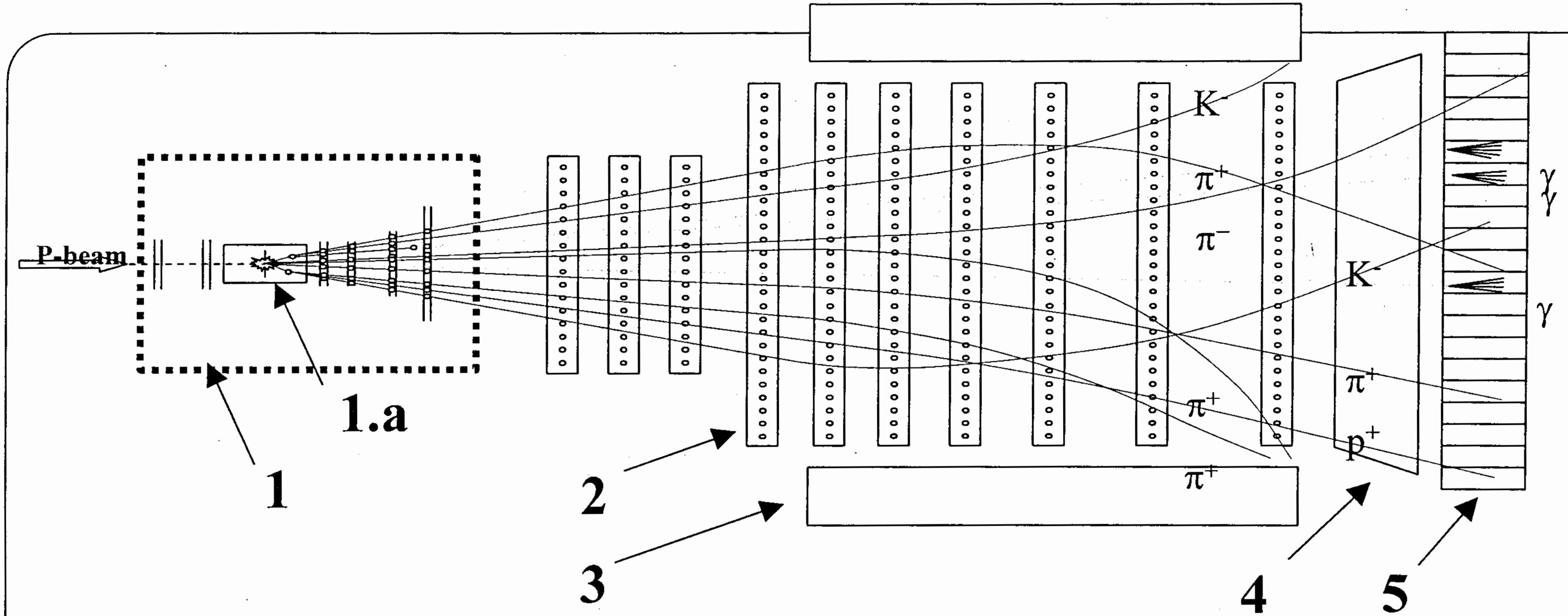

1 High precision microstrip vertex detector.

1a Active target with Si, C and Pb planes

2 Multiwire proportional chambers.

3 Magnet (1.18 T over 3m long region).

4 Multicell threshold Cherenkov counter.

5 Gamma detector.

147

SVD-2 tracking detector (cf. Karmanov's talk)

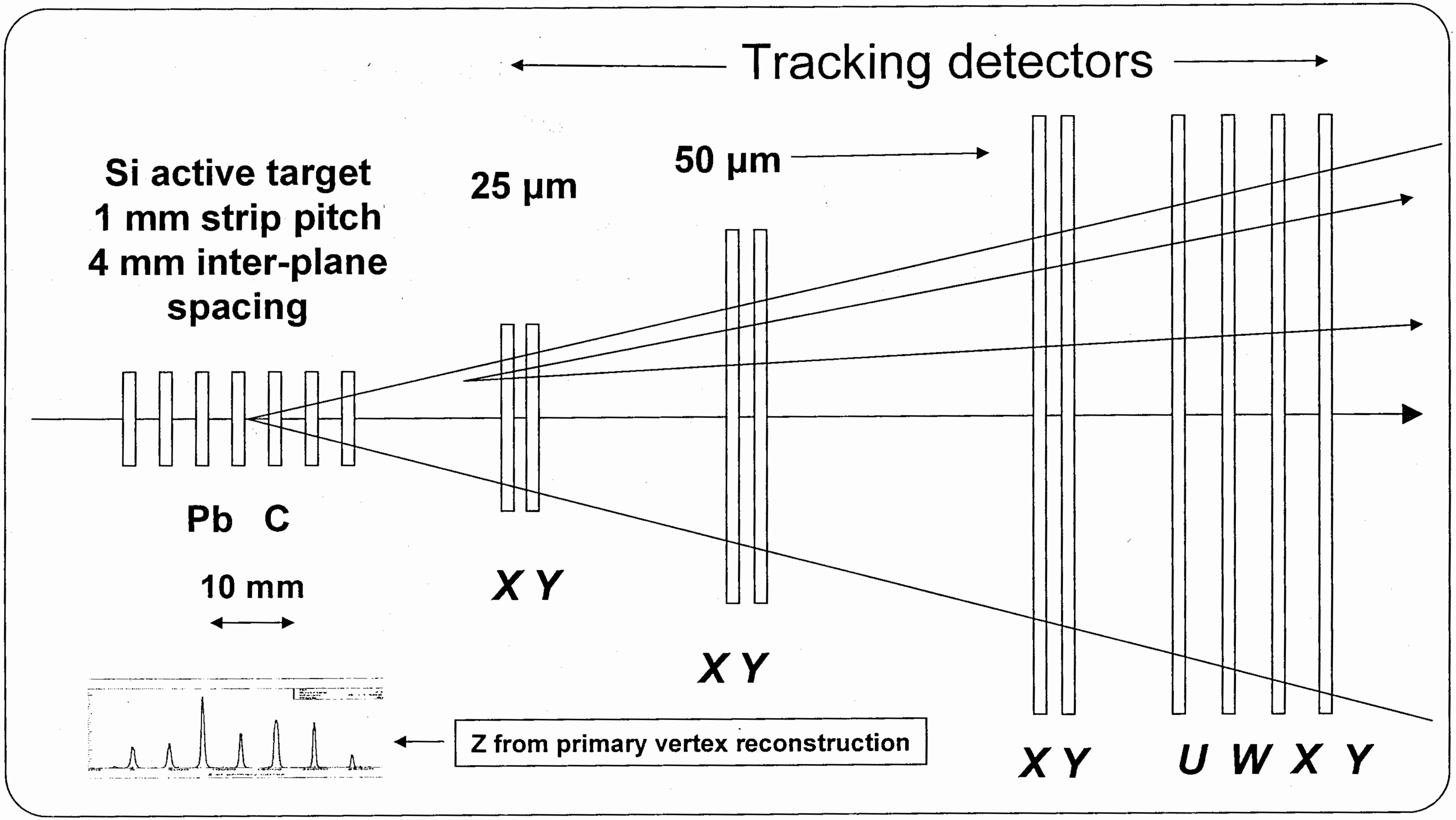

SVD-2 trigger

Level I

- Based on energy depositions in 5•8 ***Si*** active target strips
- Basic principle is to look for the >2...3 MIPs depositions in consecutive planes
- Decision time: 220 ns
- "Non-usable" events contamination: < 10%

Level II

- Not implemented yet...
- Basic idea - a search of "secondary" activity
- A simplified "fast" information from vertex tracking detector to be used

SVD-2 run I (April '2002)

- Intensity 500-600×10^3 protons/cycle (1.2 sec)
- Total target thickness ~0.5% of hadronic length
- 400-600 events/cycle registered
- 53,000,000 events stored
- Integral luminosity $L=1.6\ nb^{-1}$
- 3 target materials: Si, C and Pb

Experimental accuracies - geometry

- X,Y-resolutions for tracks fitted:
  - From MSVD — 8-10 μm
  - Secondary tracks from spectrometer — 700 μm
- Z-resolution:
  - for the primary vertex: — 70-140 μm
  - for the secondary vertex from MSVD: — 200-300 μm
- Impact parameter resolution: — ~ 14 μm

Experimental accuracies

- Momentum resolution for the 5 GeV tracks: 1%
- Effective mass resolution:
  - K^0: 4.4 MeV
  - Λ: 1.6 MeV
  - π^0 : 12 MeV
- Cerenkov detector efficiency : 70% for the pions in 3-20 GeV momentum region

SVD-2M

- 2003-2005 developments:

  1. Liquid hydrogen target
  2. A new vertex detector with a higher efficiency and a lower multiple scattering. New construction for replacing elements when needed
  3. Much better tracking in a forward part of spectrometer due to 9 double planes of straw tubes with a 200 μm resolution
  4. Increased intensity capabilities of proportional chambers by installing beam killers

SVD-2M (cont.)

5. New fast electronics for gamma-detector readout
6. Efficiency of Cerenkov detector increased to 85-90%
7. 2 different triggers on the high multiplicity events are being created

All these jobs are close to be finished soon and we hope for the successful tests during our end of 2005 run

Plans for 2005-2007

With a new setup we plan to make physics in 3 directions:

- High multiplicities in hadron collisions with hydrogen target (first priority)
- Near-threshold charm creation (Si, C, Pb targets)
- Searches for new hadron states (both types of targets)

The program is planned for years 2005-2007 with obtaining a total luminosity of ~ 50 nb^{-1}.

On results of the physics analysis

It will be discussed in more details in V.Popov talk. I would like to make a few comments.

1. High multiplicities. At this picture ,an event with 27 tracks in the vertex detector is presented.

On results of the physics analysis (cont.)

- At this picture, the multiplicity distribution for the proton-carbon interactions is presented. Some slope changes could be seen near the 30 tracks point.

On results of the physics analysis (cont.)

But Monte-Carlo simulations in Amelin model showed that there is a contribution to the multiplicity by the events with the ***secondary*** interactions in the same nucleus.

So, for the detailed investigations we need to use a pure hydrogen target.

158

On results of the physics analysis (cont.)

- 2. The main goal of the April'2002 run was to collect data on the charm creation cross sections near the threshold. An analysis proved to be rather complicated, and we hope to obtain a few hundred of events with D-mesons by the end of the year. We have already some events, and the little statistics is due to very rigid selection used by now.

On results of the physics analysis (cont.)

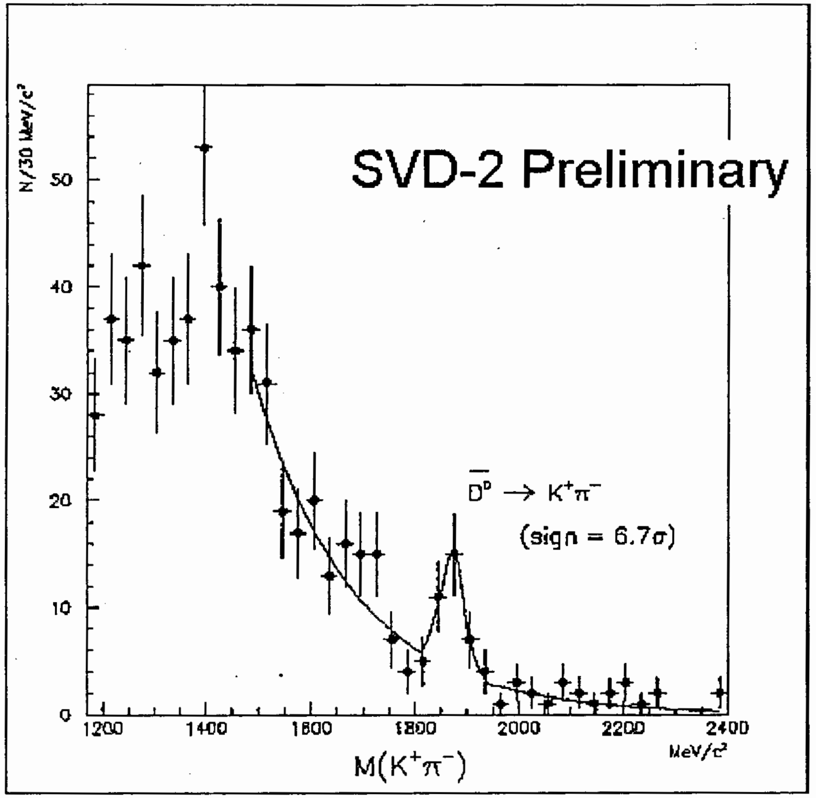

As an illustration, here is an invariant mass distribution for K+π- system with both tracks having large impact parameters in both x,y planes and its (secondary) vertex is within 3 mm from a primary one. Further analysis is going on.

On results of the physics analysis (cont.)

3. *Remarks on the pentaquark search*.

In 2004, SVD collaboration published the results on the search of the narrow resonance in $K^0{}_s p$ system. At the level of 5.5σ, we found a resonance with a Γ<25 MeV and a cross-section of 30-120 μb.

161

On results of the physics analysis (cont.)

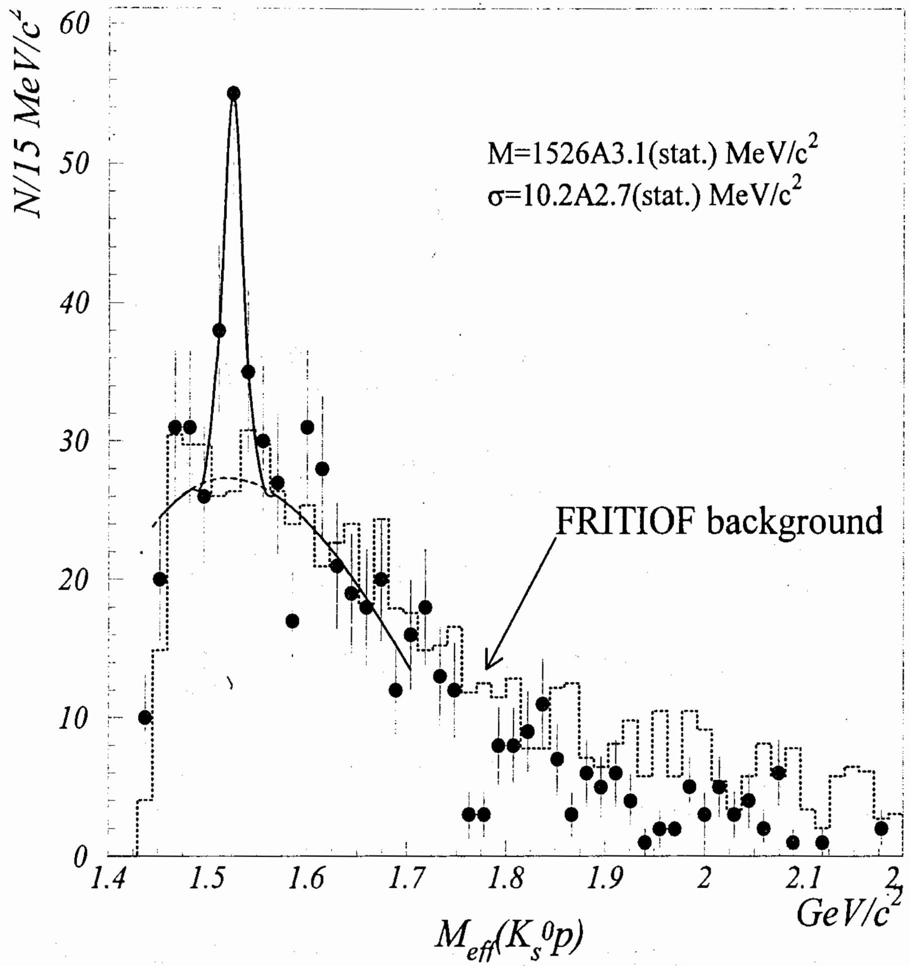

- At this picture, a result of a resonance search made in the beginning of 2004 is presented. Main criteria were:
  - Number of charged tracks in vertex detector ≤ 5
  - K0 registered if its decay length is ≤ 34 mm (average ~20 mm)
- With this criteria, ~ 5,000 events were selected and analyzed

New pentaquark analyzes (2004-2005)

- In the first one, the same K^0 decay region was used with another reconstruction method but without any selection criteria and without using Cerenkov detector information

  This resulted in a much higher number of K^0 to be analyzed

- The second one:
  K^0 decaying ***after*** the vertex detector (5-70 cm) were selected, using only spectrometer information to reconstruct tracks ("distant" K^0)

  Possibly much higher number of K^0 to be included into analysis

As a result, the total number of K^0 was increased by more than an order of magnitude

New pentaquark analyzes (cont.)

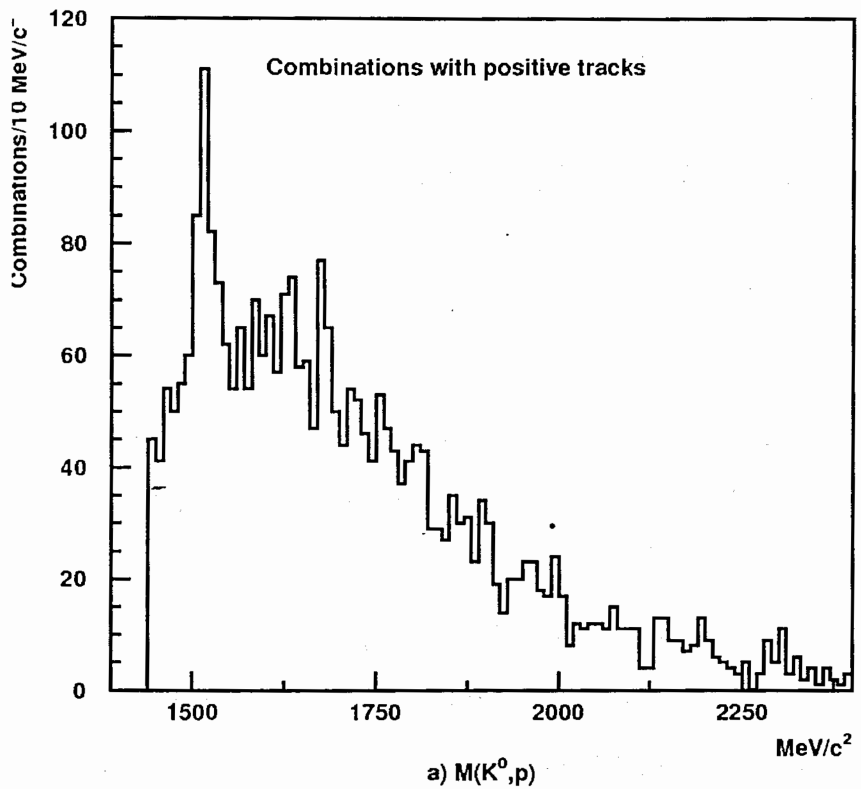

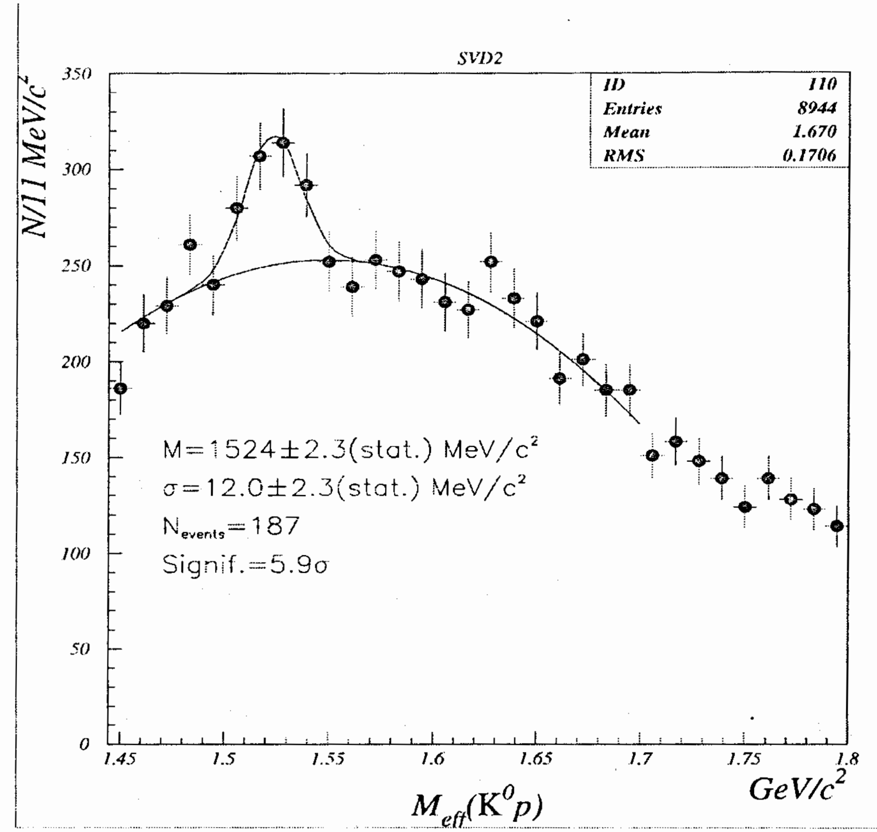

New pentaquark analyzes (2004-2005)

- At pictures, well pronounced peaks with a significance of about 6σ each can be seen in the mass region of 1522-1524 MeV.
- They are from ***two different samples*** , with a 300 events over background in total. Samples are not intersecting and are from the different kinematical regions.
- It doesn’t look at all as a statistical fluctuation.

New pentaquark analyzes (2004-2005)

We plan to make new cross-checks of our analysis, to study momentum and angular characteristics of this resonance and try to make conclusions on its creation mechanism

Very High Multiplicity Physics
Sixth International Workshop

Joint Institute for Nuclear Research

Dubna, 16-17 April 2005

А.Н.Алеев, С.Г.Басиладзе, Г.А.Богданова, А.М.Вишневская, В.Ю.Волков, Е.Г.Зверев, А.К.Лефлат, В.А.Крамаренко, Я.В.Гришкевич

Система запуска и аппаратура регистрации для координатных детекторов установки СВД-2

Аннотация

В сообщении описываются:
1) алгоритмы принятия решений и аппаратура системы запуска установки СВД-2;

2) состав детекторов, строение электронной регистрирующей аппаратуры и основные характеристики магнитного спектрометра на основе пропорциональных камер;

3) усилители для дрейфовых камер, программное обеспечение и результаты испытания модулей регистрации для дрейфовых камер разработки ОАЭ (ИФВЭ) на пучке ускорителя ИФВЭ.

Рассмотрены модификации системы запуска СВД-2 для отбора событий с большой множественностью вторичных частиц.

Обсуждаются вопросы модернизации электроники магнитного спектрометра и перечень мероприятий, необходимых для проведения тестов дрейфовых камер и регистрирующей электроники на пучке нуклотрона ОИЯИ.

1. Детекторы и системы регистрации установки СВД-2

Спектрометр с вершинным детектором (СВД), размещен на пучке протонов с импульсом 70 ГэВ/с на ускорителе У-70. Расположение основных детекторов установки схематически показано на рис.1. На первом этапе в качестве мишени использовалась быстроциклирующая пузырьковая камера.

В 1999 г СВД-объединение вышло с предложением о модернизации установки с целью измерения полного сечения образования очарованных частиц, измерения A-зависимости полного сечения на ядрах кремния, свинца, углерода и других элементов, а также поиска эффектов, связанных с механизмом высвобождения внутреннего очарования. Все перечисленные задачи потребовали многократного увеличения набираемой статистики и, как следствие, значительного увеличения быстродействия установки. Электроника регистрации магнитного спектрометра после проведенной модернизации способна принимать до 500 событий за сброс ускорителя. Быстроциклирующая пузырьковая камера заменена на прецизионный вершинный детектор с электронным съемом информации. Кроме того, разработана новая электроника системы синхронизации и запуска установки.

2. Система запуска установки

Для проведения эксперимента СВД-2, был выбран триггер, основанный на быстрой оценке амплитуд сигналов с МКД активной мишени [1]. Такая оценка позволяет также определить Z-координату взаимодействия. Активная мишень (АМ) сделана из пяти кремниевых пластин толщиной 300 мкм размером 8×8 мм, сегментированных на восемь полосок (стрипов) шириной 1 мм. Шаг установки всех плоскостей мишени составляет 4 мм по пучку. Детекторы активной мишени изготовлены в НИИМВ г.Зеленоград.

Расчеты, проведенные в [2], показывают, что если вторичные частицы регистрировать сцинтилляционном годоскопе (СГ), расположенном на некотором удалении от оси пучка, то можно обеспечить быстрый отбор событий, имеющих вторичные частицы с большим P_t. Это позволяет выделить события с $c\bar{c}$-парами уже на первом уровне запуска установки. СГ размещен на подвижной платформе γ-детектора на расстоянии примерно 8.3 м от мишени и состоит из двух плоскостей сцинтилляционных детекторов. Горизонтальная плоскость имеет 12 детекторов размером 200 x 2400 мм при толщине 10 мм. Вертикальная плоскость состоит из 14 детекторов 200 x 1400 мм.

Для запуска локальной системы SPECTRO сигнал триггера должен поступить в нее не позже 700 нс от момента прохождения пучковой частицы. Для запуска локальной системы VERTEX, основой системы регистрации которой являются усилители GASSIPLEX, триггерный сигнал должен приходить через 400÷500 нс относительно взаимодействия в АМ. Время от момента прохождения частицы через АМ до прихода тригерного сигнала в локальную систему DEGA не должно превышать 400 нс. Это самое критичное из условий работы системы запуска.

Взаимодействие модулей системы запуска. Схема системы запуска приведена на рис.2. Сигналы со сцинтилляционных детекторов формируются по амплитуде и длительности и подаются в модуль ТРС. Его выходной импульс поступает в модуль SYNCHRO-2, который вырабатывает сигнал, служащий строб-сигналом для модулей ААМ и RGH и стартовым сигналом для работы модулей ТРМ-2 и T-HOD. Параллельно сигналы со сцинтилляционного годоскопа формируются по длительности и записываются в регистры RGH. Сигналы с 16-разрядных выходов RGH поступают на входы модуля T-HOD, где производится одноуровневое табличное преобразование. Выходной сигнал модуля T-HOD, поступающий на вход модуля ТРМ, может быть выработан на основе ЛЮБОЙ комбинации входных сигналов.

Для выработки сигнала T1 сигналы с сегментов детекторов мишени усиливаются быстрыми малошумящими усилителями и подаются по коаксиальным кабелям в две группы модулей. Три модуля первой группы, аналого-цифровые преобразователи (АЦП), имеют по 16 каналов 12 разрядного аналого-цифрового преобразования. Пять модулей второй группы ААМ имеют по 8 каналов трехуровневой дискриминации.

Параллельно данные анализируются модулями ААМ, каждый канал которых содержит усилитель, три компаратора и приоритетный шифратор, и вырабатывает двухразрядное слово, так называемый статус канала. Результатом работы каждого модуля ААМ является 16 разрядное слово, содержащее информацию о восьми каналах амплитудного анализа и поступающее на выход с передней панели модуля.

Двухразрядный статус каждой пластины вырабатывается модулем ТРМ-2 в ОЗУ первого уровня на основе данных о каждом статусе канала:

00 - нет частицы (все сегменты 00),

01 - одна частица (все сегменты - 00, а один - 01),

10 - две частицы (есть один сегмент с кодом 10, или два сегмента с кодами 01),

11 - три частицы (есть один сегмент с кодом 11, или есть один сегмент с кодом 10, а другой сегмент имеет код 01, или есть два сегмента с кодами 10, или есть три сегмента с кодами 01).

Статус мишени вырабатывается в ОЗУ второго уровня на основе статуса каждой пластины. Сигналы статуса мишени и состояния годоскопа определяют выход триггера модуля ТРМ-2, Т1 – истинно или Т1-ложно.

Результаты применения триггера. Прототип системы синхронизации и запуска бал испытан на тестовом сеансе 1999 г [3].

Основная статистика на сеансе 2002 года была набрана при триггере, требующем наличие трех и более частиц в любой из пяти плоскостей активной мишени и наличие двух и более частиц в следующей за ней плоскости, при этом требовалось наличие срабатывания в двух пластинах СГ. Модули ААМ имели динамический диапазон, соответствующий пяти частицам. Пороги ААМ были настроены на одну, две и три частицы соответственно. События с вершиной в сцинтилляторе С4 не встречаются вследствие применения аналогового VETO на сигнал с С4. Таблицы, записываемые в модули ТРМ-2 и T-HOD, составлялись в виде текстовых файлов, содержащих построчно адрес и записываемое данное, при помощи пакета LabView 4.0. Таблицы заносились в память модулей однократно при старте основной программы сбора данных. Время принятия решения от момента поступления сигнала на вход модуля СИНХРОН до выдачи сигнала триггера с выхода модуля ТРМ-2 составило 200 нс. Задержка сигнала от момента прохождения частицы через мишень до появления сигнала триггера в локальной системе DEGA не превышала 350 нс, что обеспечило синхронную работу γ-детектора.

За 30 суток работы было набрано 50 млн событий с неупругими взаимодействиями [4,5]. На рис.3 показано пространственное распределение вдоль оси Z вершин взаимодействия, полученное с помощью восстановленных в ПВД треков. Явно видны взаимодействия как в кремнии, так и в пассивных углероде и свинце, в соответствии с количеством вещества в этих слоях.

3. Магнитный спектрометр установки СВД-2

Широко-апертурный магнитный спектрометр (ШАМС) производит съем и регистрацию сигналов с многопроволочных пропорциональных камер, сгруппированых в 10 блоков, 3 из которых установлены перед магнитом и 7 находятся в магните. В каждом блоке может быть от 2-х до 3-х плоскостей, общее количество плоскостей - 28, а общее количество сигнальных проволочек около 18 тысяч. В силу ограниченности места в магните (зазор между камерами и магнитом составляет 6 см) на самих камерах размещены только усилители-формирователи, а аппаратура регистрации сигналов находится в крейтах КАМАК. Длина соединительных кабелей составляет ~50 м.

Съем сигналов с пропорциональных камер. Съем импульсов с сигнальных проволочек пропкамер производится двумя типами усилителей-формирователей:

1) 16-канальными усилителями разработки ИЯФ СОАН (Новосибирск), основу которых составляет гибридная интегральная схема 155УД1 [6];
2) усилителями, на основе гибридной микросхемы УИ5, разработки ЛИЯФ (Ленинград) [7].

Входное сопротивление усилителей первого типа ~1 кОм, усиление по напряжению ~300; на выходе стоит ключ с общим эмиттером с регулируемым порогом срабатывания (от 300 до 700 мВ). Ради упрощения схем формирование выходных импульсов по длительности не производится.

Организация модулей регистрации. Модули регистрации сигналов с пропкамер имеют по 64 входа [8], в каждом крейте (см. рис.5) содержится от 10 до 11 модулей. Их основу составляет быстродействующее запоминающее устройство (ЗУ) на 16 64-разрядных слов, которое фиксирует наличие или отсутствие сигнала на каждом из входов модуля в тактах, повторяющихся с периодом 80 нс (12 МГц).

Тактовые импульсы генерируются в центральном управляющем крейте системы и затем распределяются в 2 этапа по всем крейтам с помощью 16-канальных разветвителей в уровнях NIM. Сигнал запуска распределяется по модулям регистрации из центрального крейта аналогичным образом через такие же разветвители (показаны на рис.5).

Организация считывания данных. Система считывания в ШАМС централизованная – рис.6, она имеет 3 иерархических уровня. Всего имеется 4 ветви (каждая со своим интерфейсным контроллером [9] в центральном крейте). Каждая ветвь имеет по 7 крейтов регистрации. К центральному крейту подключен он-лайн компьютер (IMB PC) через свой собственный интерфейсный контроллер [10]. В нем же находятся модули связи с системой запуска.

Фактором, определяющим скорость считывания, является физическое быстродействие магистрали ветви, цикл считывания одной координаты занимает ~4,5 мкс. Всего в событии считывается ~300 слов, т.е. время считывания одного события занимает ~1,2 мс. Таким образом, за время вывода пучка из ускорителя (~1 с) имеется возможность приема данных от ~700 событий.

4. Электронная аппаратура для дрейфовых камер

В настоящее время комплект аппаратуры для дрейфовых камер включает следующие электронные модули:

- 32-канальный усилитель-формирователь (разработки МГЭУ, Минск) с порогом 1 мкА;
- 64-канальные модули регистрации (TDC - время-цифровой преобразователь разработки ИФВЭ) с разрешением 2 нс;
- крейт-контроллер «Q-bus - МИСС» (разработки ИФВЭ) и картой адаптера «ISA – Q-bus» для персонального компьютера.

В декабрьском сеансе 2005г было проведено испытание одной плоскости дрейфовых трубок. Время фронта и спада на входе модулей регистрации (с учетом плоского кабеля длиной 15 м) составило приблизительно 12-15 нс. При испытаниях усилителей-дискриминаторов непосредственно на дрейфовых камерах *выявлена их склонность как к самовозбуждению, так и высокому уровню внешних наводок*. Различные методы заземления показали, что причиной этого является металлическая рама, на которой спроектированы собственно дрейфовые камеры. С целью устранения этого недостатка было установлено, что необходимо подключить раму к земле усилителей-дискриминаторов со стороны их входов, причем с увеличением количества контактов уровень наводок уменьшался. С целью дальнейшего уменьшения наводок необходимо подключить раму и к общей шине со стороны подачи высоковольтного напряжения, однако эффект уменьшения наводок меньше, чем со стороны усилителей.

При измерении линейности обнаружен эффект случайных отклонений отсчетов от набираемых «единичных» пиков; отклонения распределены не «по Гауссу» (имеются «торчки»), что возможно при аппаратных сбоях. Наличие flush-отклонений было подтверждено измерениями «на столе» в ОЭА.

Проводилось измерение плато по высоковольтному напряжению камеры; получено плато по напряжению не менее 250 В при эффективности выше 99%.

На рис.7 показан профиль пучка, зарегистрированный с помощью указанной аппаратуры и созданного к сеансу тестового программного обеспечения.

5. Задачи на ближайшее будущее

- измерение линейности (интегральной, дифференциальной) и стабильности работы время-цифровых преобразователей;

- испытание дрейфовых камер и электроники к ним в объеме 30-40% от полного на пучке нуклотрона ОИЯИ для исследования съема сигналов с трубок и пространственного разрешения аппаратуры;

- разработка структуры и логики работы подсистем синхронизации и считывания данных;

- создание программного обеспечения для считывания данных с дрейфовых камер в установку СВД-2.

6. Задачи к декабрьскому сеансу 2005г

- замена усилителей на одной плоскости магнитного спектрометра на новые (на основе усилителя-формирователя для дрейфовых трубок) и испытание их;

- сборка дрейфовых камер и электроники к ним в полном объеме, проведение предварительных испытаний;

- проведение ремонта вышедшей из строя аппаратуры (источники питания и вентиляторы КАМАК, модули регистрации, контроллеры, осциллографы).

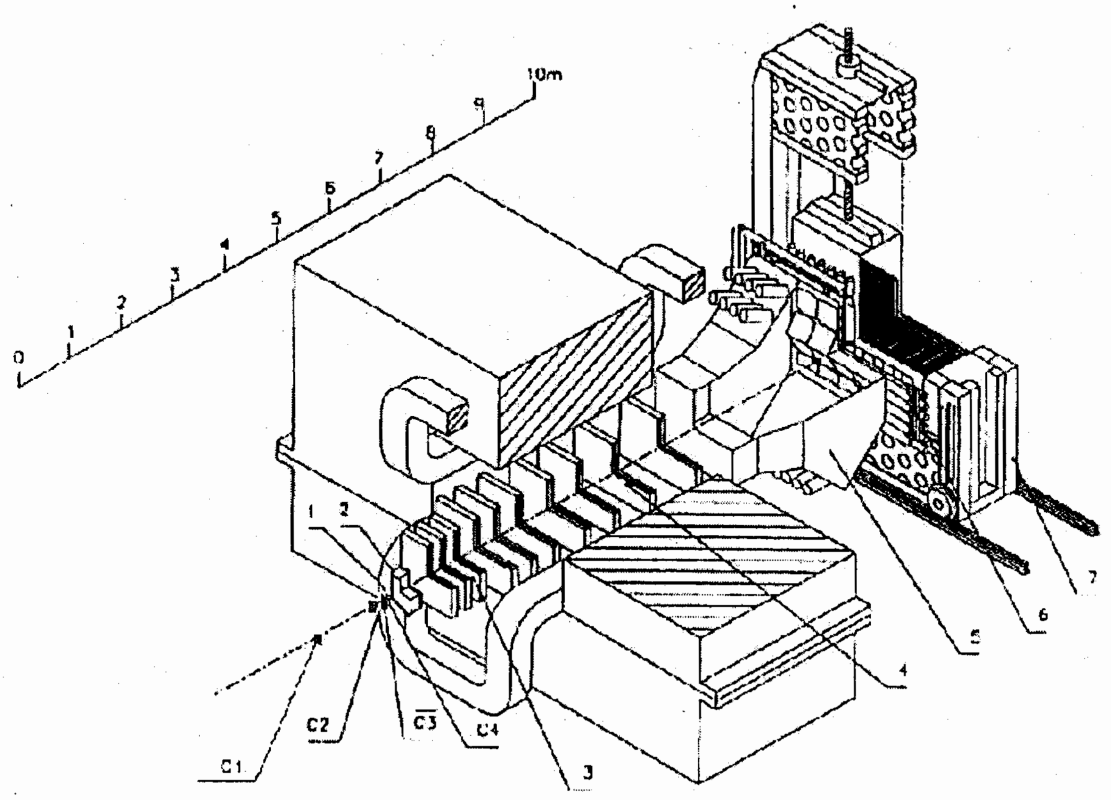

Рис.1. Детекторы установки СВД-2

<u>Цифрами обозначены</u>: 1 – активная мишень (АМ); 2 – прецизионный вершинный детектор (ПВД); 3 – блок минидрейфовых трубок (МД); 4 - магнитный спектрометр (МС); 5 – черенковский детектор (ЧД); 6 - сцинтилляционный годоскоп (СГ); 7 – детектор γ-квантов (ДЕГА).

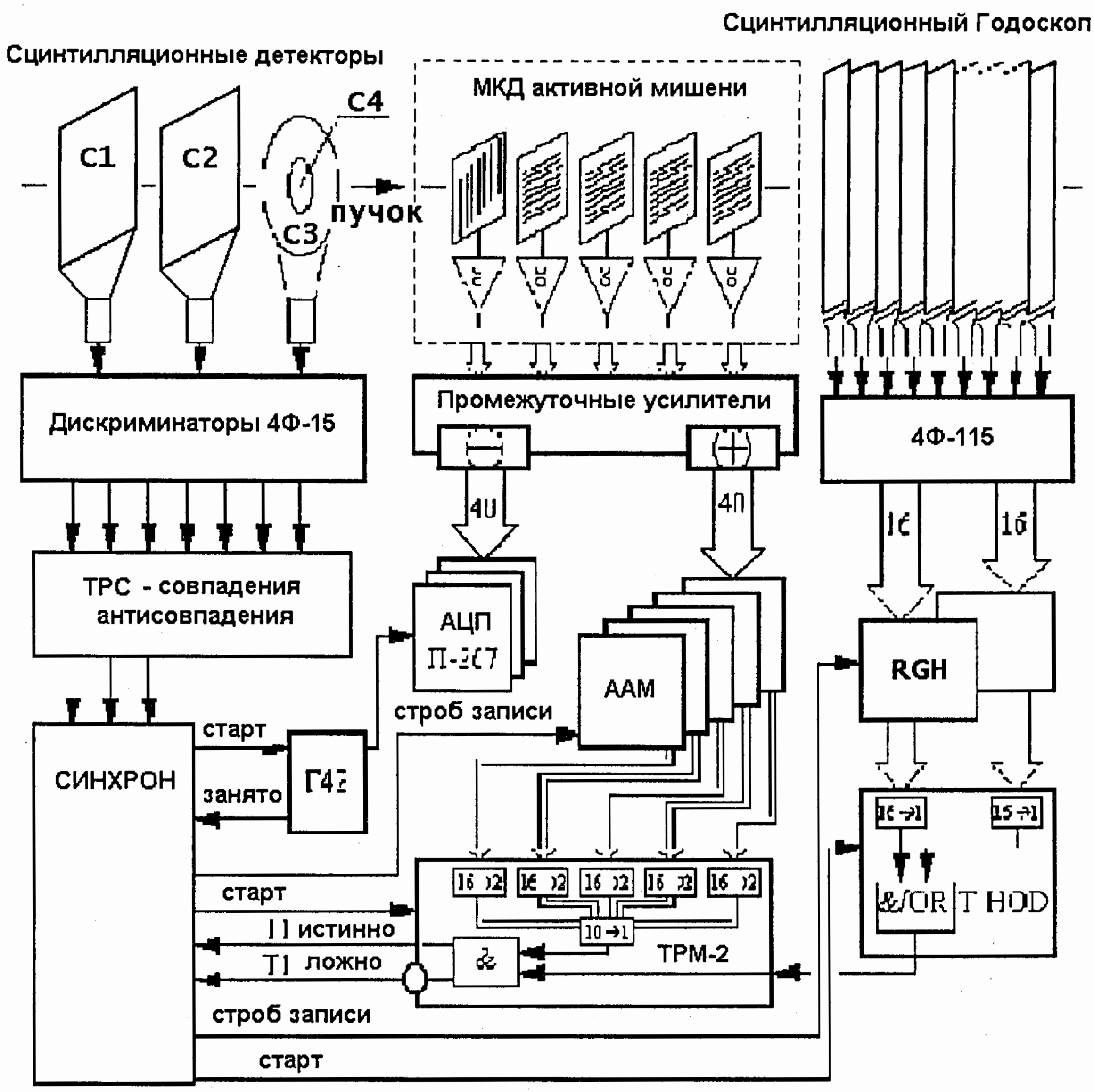

Рис.2. Функциональная схема взаимодействия модулей системы запуска

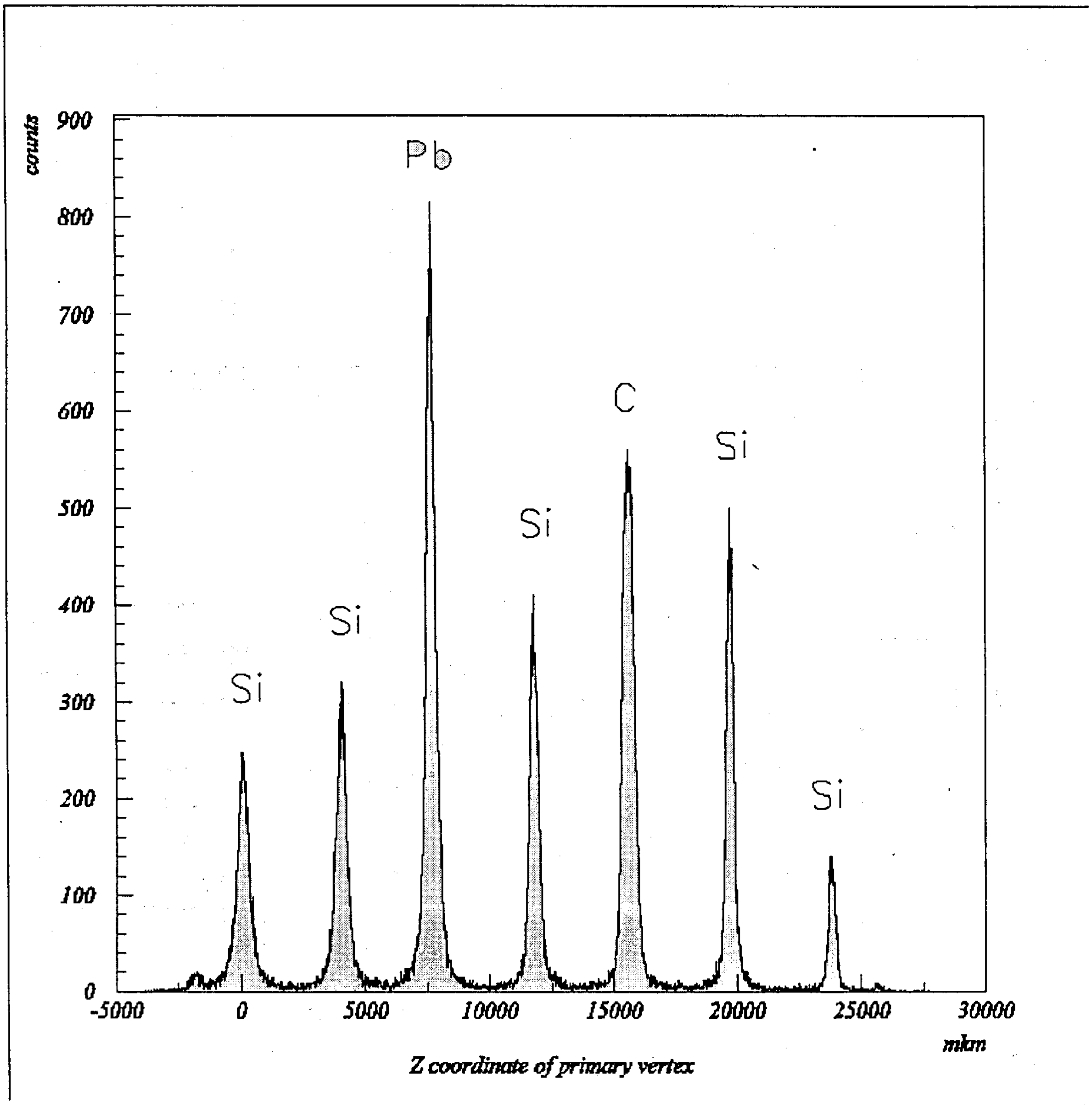

Рис.3. Пространственное распределение вершин взаимодействия вдоль оси Z в активной мишени

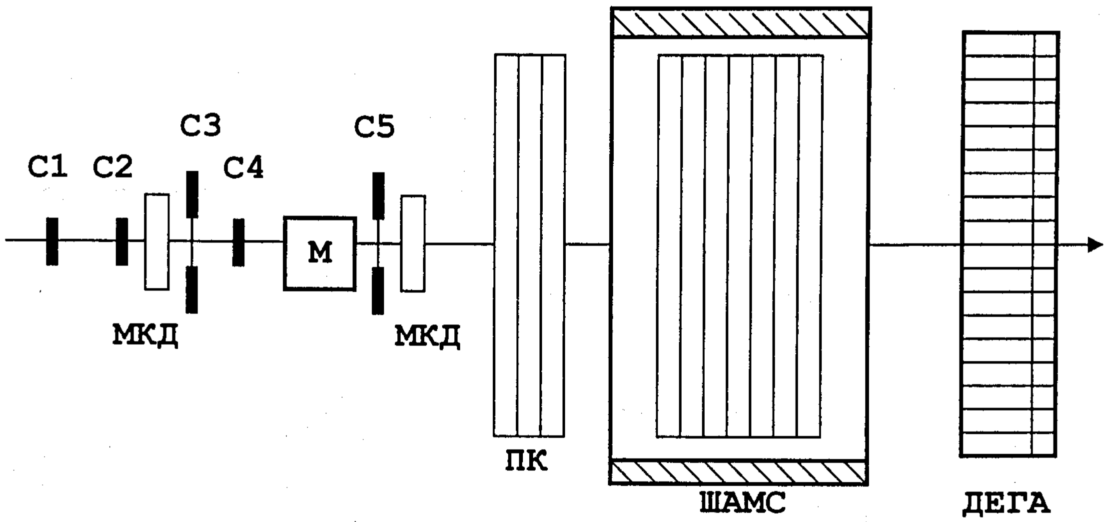

С1 – С5 – Сцинтилляционные детекторы
М – Мишень
МКД – МикроКремниевые Детекторы
ПК – Пропорциональные камеры
ШАМС – ШирокоАпертурный Магнитный Спектрометр
ДЕГА – Детектор ГАмма-квантов

Рис.4. Схема размещения пропорциональных камер магнитного спектрометра.

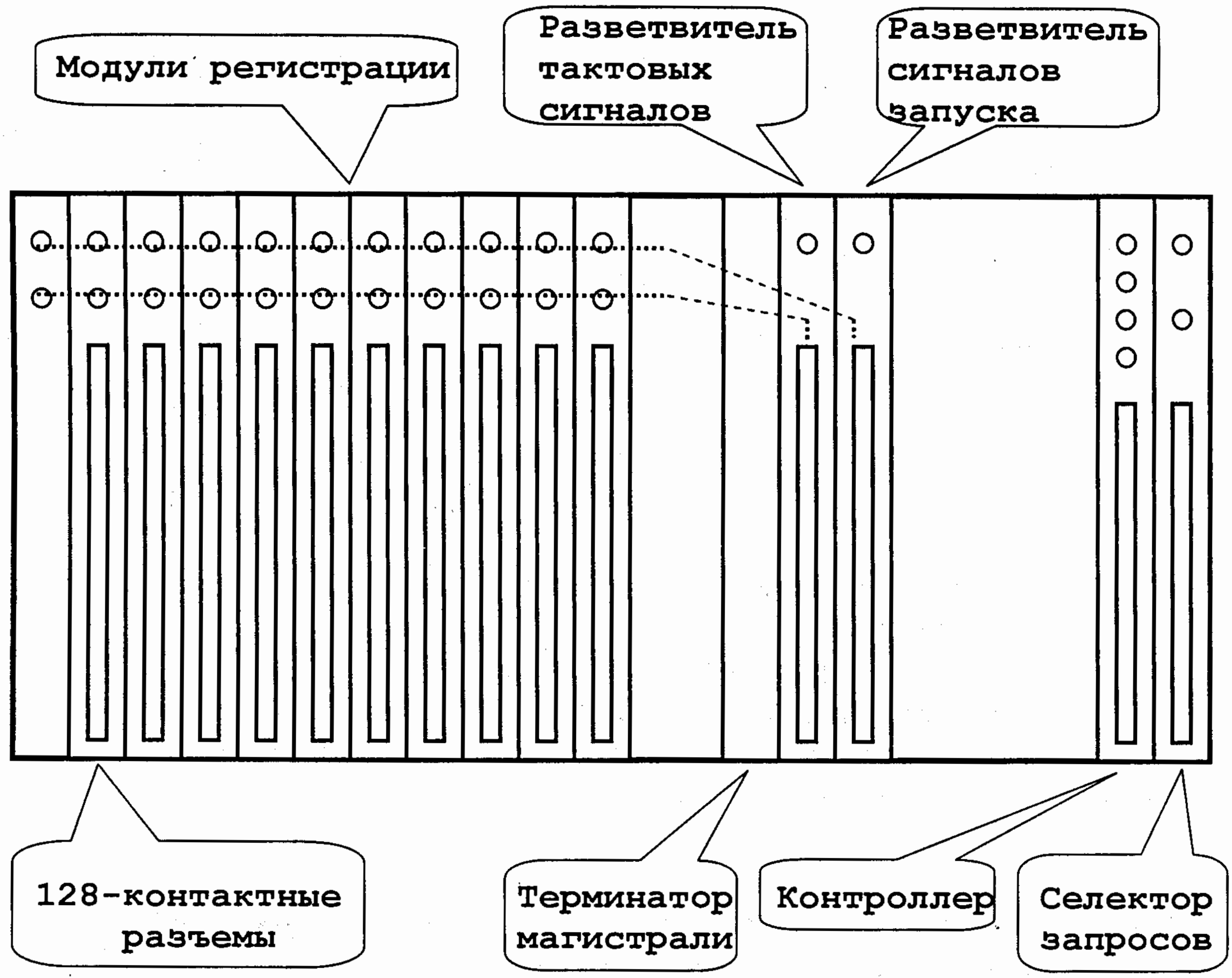

Рис.5. Расположение модулей в крейте регистрации

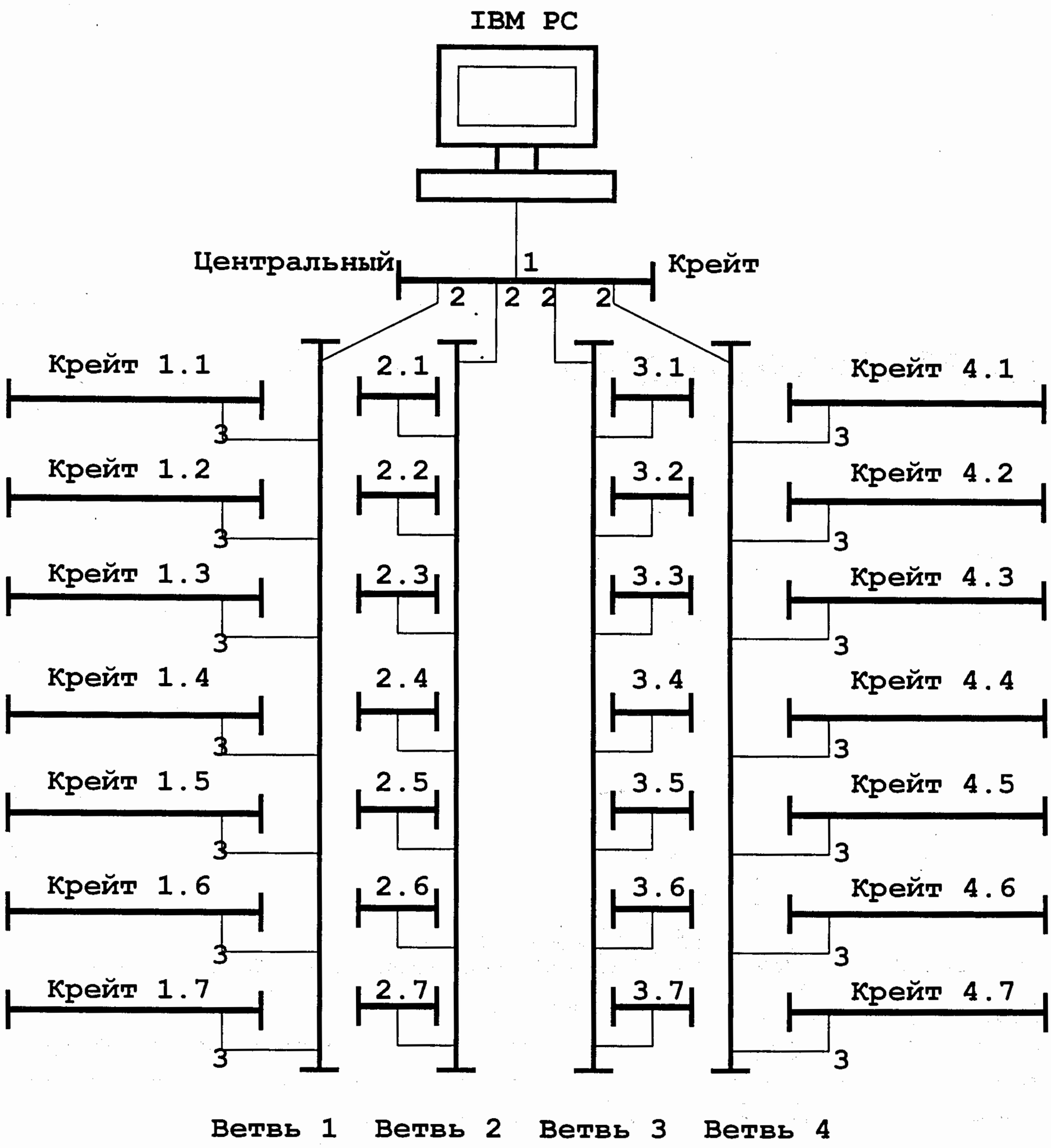

Интерфейсные контроллеры: 1 – контроллер IBM PC
2 – контроллер ветви
3 – контроллер крейта

Рис.6. Магистрали системы считывания магнитного спектрометра

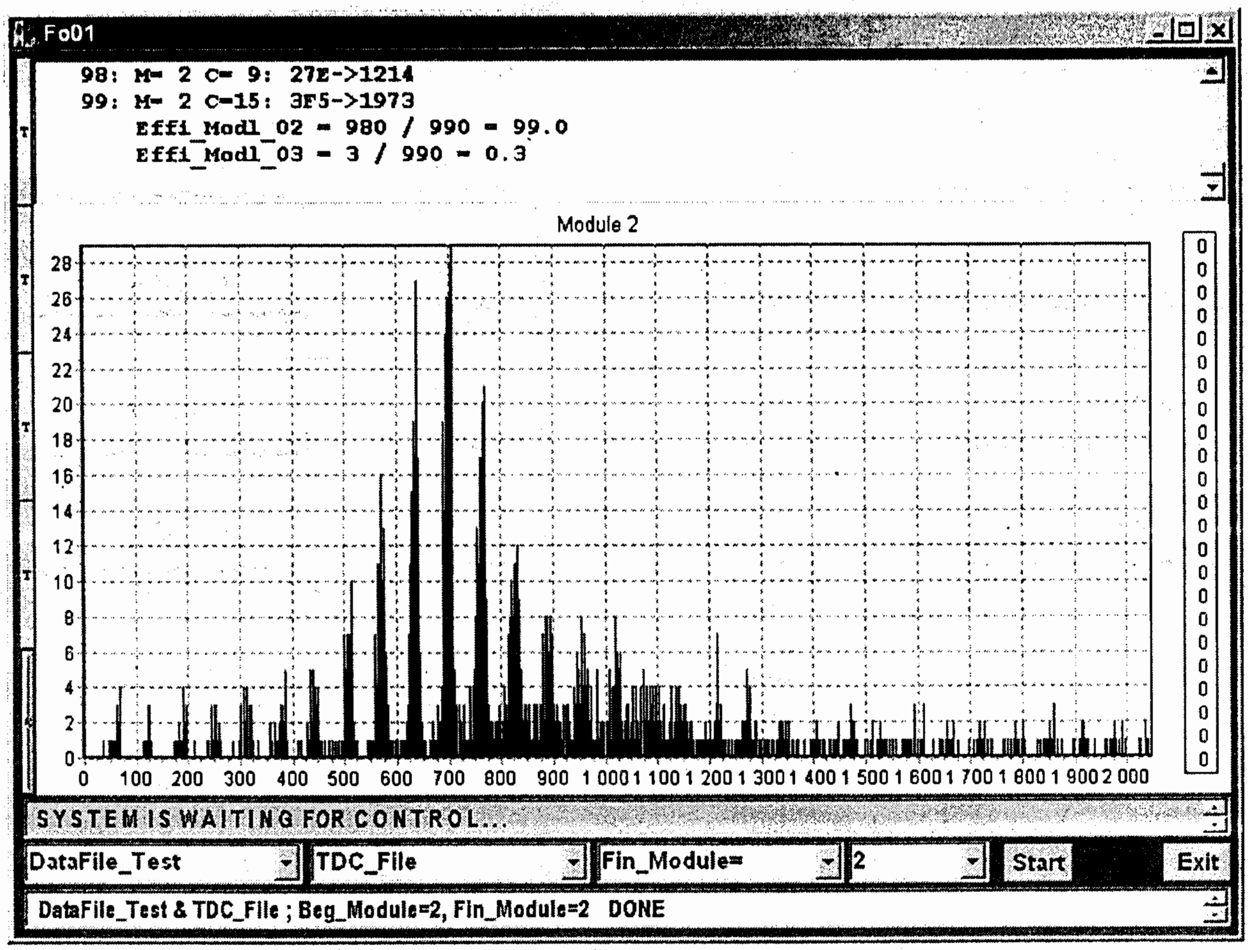

Рис.7. Профиль пучка в 32 каналах модуля регистрации для дрейфовых трубок

Литература:

1. С.Г.Басиладзе, А.П.Воробьев, П.Ф.Ермолов и др.
«Предложение эксперимента по изучению механизмов образования очарованных частиц в pA-взаимодействиях при 70 Гэв и их распадов» Препринт НИИЯФ МГУ-99-28/586 . Москва 1999 г.

2. Богданова Г.А. и др. «Оптимизированный 2-уровневый триггер для выделения событий с очарованными частицами в адрон-адронных взаимодействиях». Сообщение ОИЯИ Р1-95-451, Дубна 1995.

3. Г.А.Богданова, М.Ю.Волков, А.К.Лефлат и др. «Прототип системы синхронизации и запуска эксперимента Е-161 (СВД-2, спектрометр с вершинным детектором)» ПТЭ, 2001, №4, с.31-37.

4. A.Aleev, N.Amaglobeli, E.Ardashev, et. al. «STATUS OF THE EXPERIMENT ON CHARM PRODUCTION IN *pp* AND *pA* INTERACTIONS AT 70-GEV WITH SVD-2 SETUP AT IHEP ACCELERATOR.» Nucl.Phys.A699:352-355,2002.

5. А.Н.Алеев, Н.С.Амаглобели, Е.Н.Ардашев, и др.(коллаборация СВД) «Изучение узкого барионного резонанса, распадающегося по каналу pK_s^0 в *pA*-взаимодействиях при 70 Гэв/с на установке СВД-2». ЯФ,2005,т.68,№6,с.1040-1047; hep-ex/0401024.

6. С.Е.Бару, С.Г.Басиладзе, В.Р.Грошев, М.В.Гусак, М.И.Маркус, А.П.Онучин, Г.И.Провиз, Гибридная интегральная схема для пропорциональных камер, ПТЭ №4, 1975, с.105-107.

7. В.З.Беленький, Н.Ф.Бондарь, И.Б.Казаков, Н.Л.Нефедов, Л.Н.Уваров, Препринт ЛИЯФ 1049, Ленинград 1985 г.

8. С.Г.Басиладзе, О.З.Элоев, 64-канальный модуль регистрации сигналов с пропорциональных камер РПК-213, Разработка аппаратуры сопряжения ЭВМ с измерительными установками, Издательство МГУ 1985, с.61.

9. С.Г.Басиладзе, О.З.Элоев, Специализированный контроллер для отбора и считывания данных с пропорциональных камер КПК-671, Разработка аппаратуры сопряжения ЭВМ с измерительными установками, Издательство МГУ 1985, с.65.

10. А.Н.Алеев, С.Г.Басиладзе, А.Е.Селиков, Интерфейсный контроллер крейта для персонального компьютера, ПТЭ, в печати.

A. Aleev, V. Kireev, A. Yukaev

Spectrometer and Multichannel Cherenkov Counter of the SVD-2 experiment

- # 1. System of the proportional chambers.
- For a high multiplicity on SVD-2 experiment(fig. 1) is necessary to increase a beam intensity of the protons in the channel 22 of IHEP accelerator(U-70). Thus, for a reliable operation of the proportional chambers it was necessary to install beam-killer in region of the beam.
- The calculation of the beam killer coordinate from experimental dates is listed in Table.1. The installation work was made in 2004.
- The chambers was tested on the proton beam of IHEP accelerator(U-70) with intensity $3.0 \times 10^6 \div 1.0 \times 10^7$ p/cycle, and multiplicity >5.

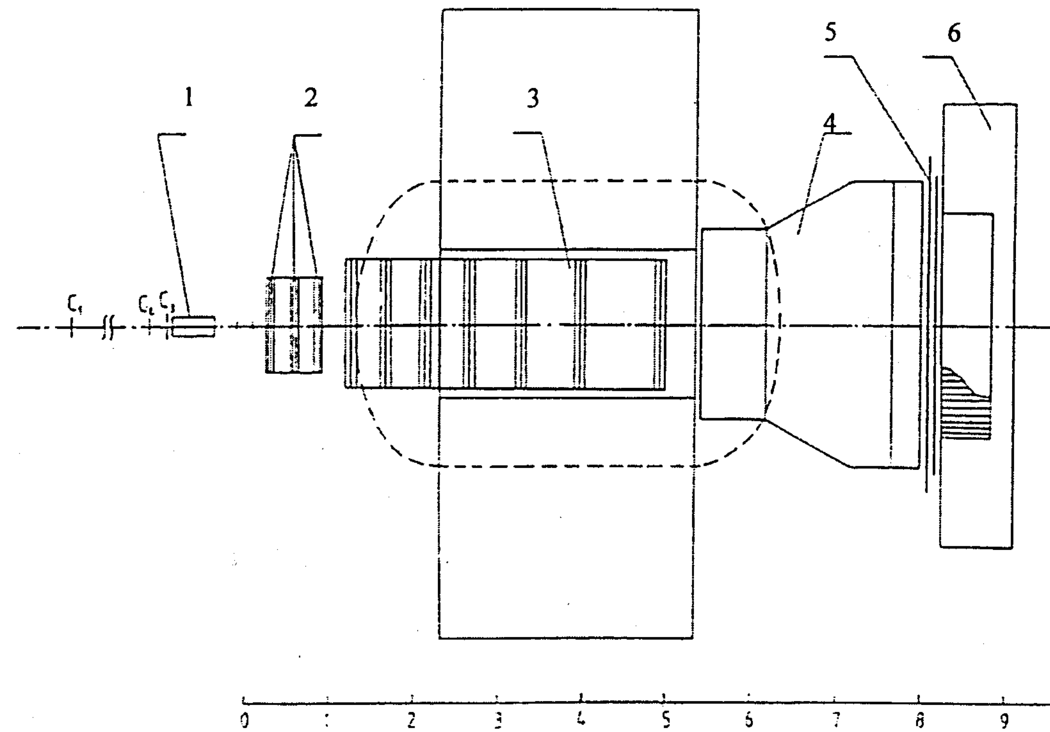

Fig.1.Schematic view of the SVD set-up for the second stage of the experiment E-161: 1-precision vertex detector; 2-block of the minidrift tubes; 3- central block of MWPC; 4-threshuld Čerenkov counter; 5-scintillation hodoscopes; 6-detector of the γ-quanta.

Камера	Горизонталь, проволочки						Размер заглушки, мм		Вертикаль	КАМЕРА		Z коорд.	Z отнoс У5 или относ. среза магн.
	Магнитное поле			Положение заглушки			Ширина заглушки, мм	Высота заглушки, мм	Положение заглушки				
	0,0	1/3max	Max	+	Центр, (проволки)				Центр, (мм)				
U4	278,5	279,0	279,9	284,00	279	274,00	20	20	Центр - 490	U4	1	1,679	-0,914
У4	327,8	328,5	329,9	334,00	329	324,00	20	20	Центр - 490	У4	2	1,908	-0,685
V4	277,1	277,7	278,8	283,00	278	273,00	20	20	491	V4	3	2,136	-0,457
U5	276,1	276,3	276,5	281,00	276	271,00	20	20	491	U5	4	2,365	-0,228
У5	325,7	326,4	327,6	332,00	327	322,00	20	20	491	У5	5	2,593	0
V5	275,0	275,7	276,9	281,50	276	270,50	22	20	492	V5	6	2,821	0,228
U6	273,8	274,2	275,0	281,00	275	269,00	24	20	492	U6	7		
У6	323,7	324,7	326,7	332,00	326	320,00	24	20	493	У6	8	3,278	0,685
V6	273,0	274,3	276,8	282,00	276	270,00	24	20	493	V6	9	3,507	0,914
U7	271,5	272,8	275,3	281,00	274	267,00	28	20	494	U7	10	3,721	1,128
У7	321,6	323,5	327,3	332,00	325	318,00	28	20	494	У7	11	3,986	1,393
V7	270,8	273,4	278,8	284,00	276	268,00	32	20	495	V7	12	4,251	1.658
U8	268,8	271,9	278,0	283,00	275	267,00	32	20	495	U8	13	4,516	1,923
У8	319,2	322,7	329,8	335,00	326	317,00	36	20	496	У8	14	4,781	2,188
V8	268,4	273,4	283,5	288,00	278	268,00	40	20	497	V8	15	5,046	2,453
U9	266,1	271,8	283,2	288,00	278	268,00	40	20	497	U9	16		
У9	316,8	322,6	334,1	338,00	328	318,00	40	20	498	У9	17	5,574	2,981

• Table.1.

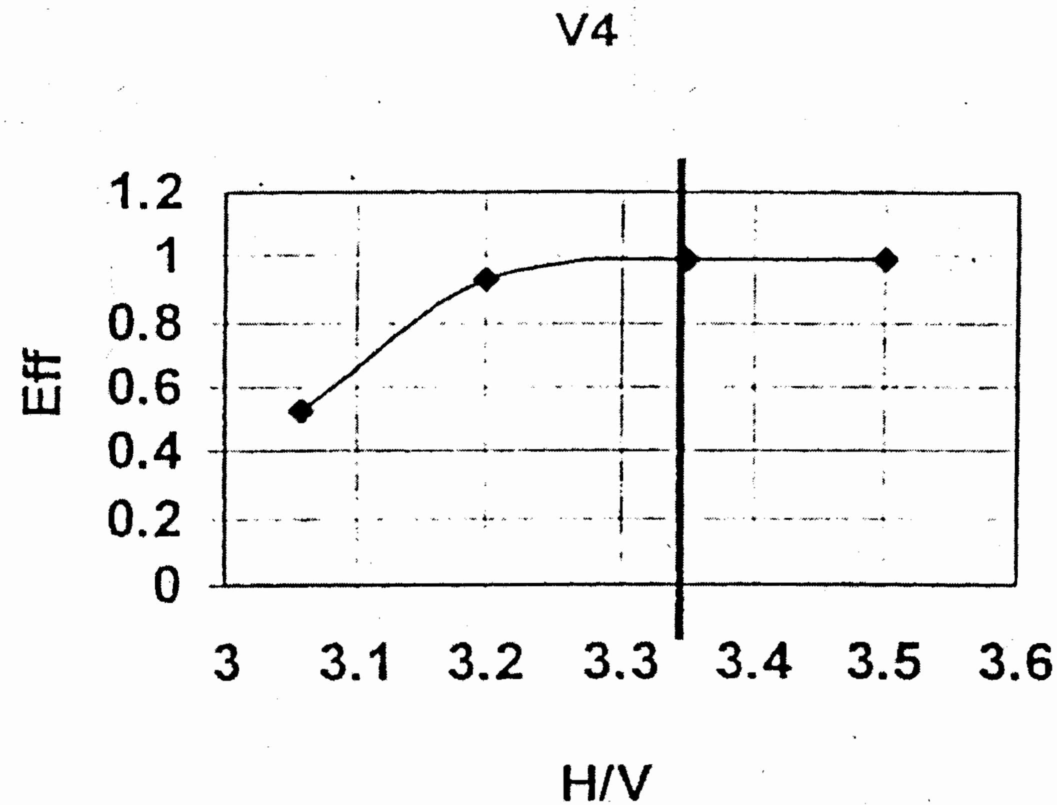

- Fig.2.
- The plateau for one chamber V4 with a proportion of gas:
- 82 % argon + 0.28 % alcohol + 0.52%freon +17.18 % isobutanes,
- is shown on Fig.2.

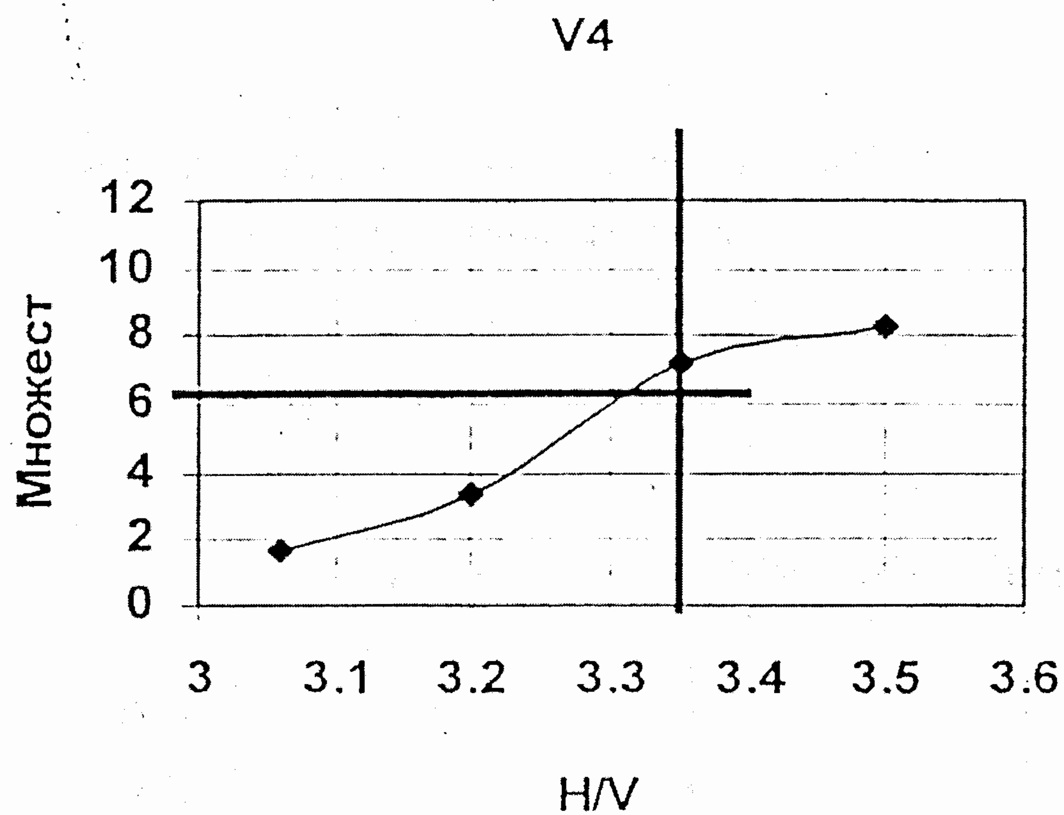

•

• Fig.3.

• The dependence of the multiplicity (number of the hits) from a high voltage on the chamber, is shown on Fig.3. The horizontal line indicates a average multiplicity for all chambers. The multiplicity varies from 6.1 up to 5.9 from the first chamber to the last, and correspond to the beginning of the plateau for each chamber.

V4, beam killer 271-282

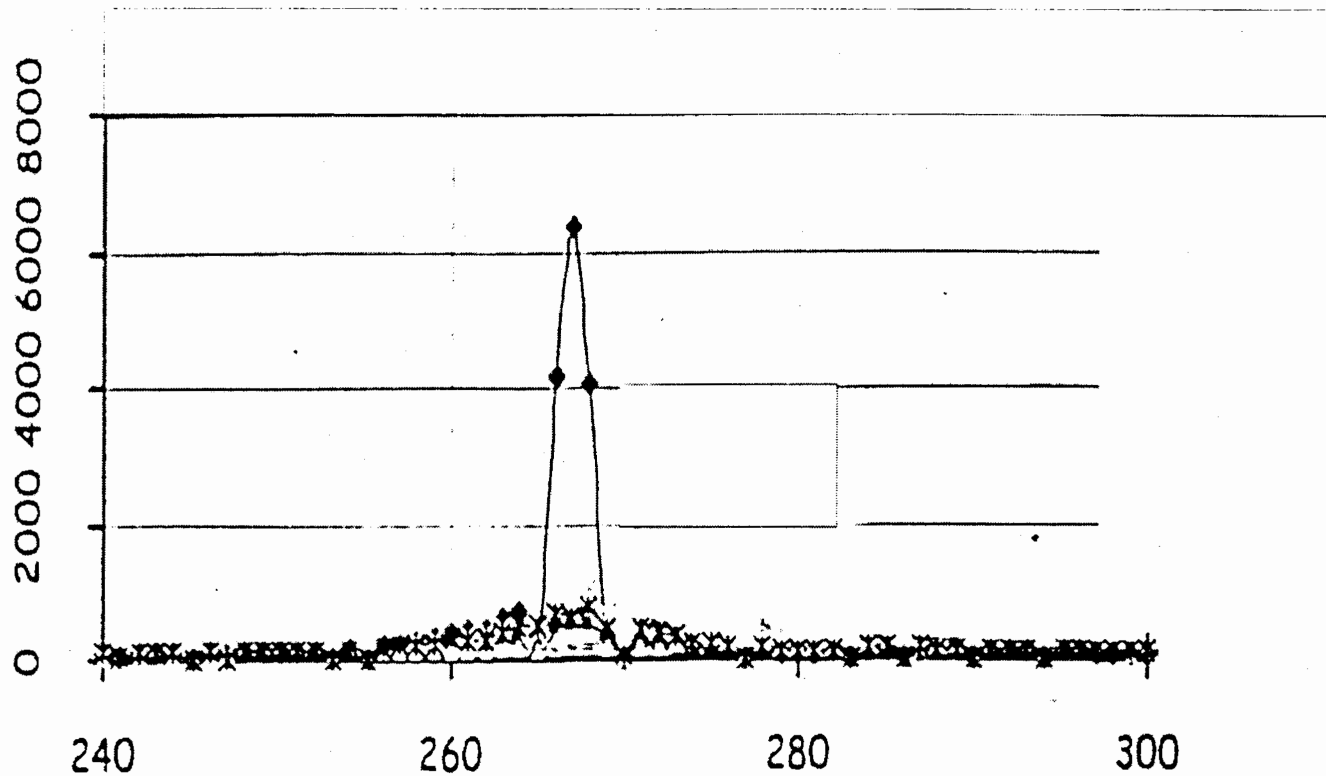

Fig.4.Dependence of the N tr. from numbers of the wires:
* - with beam killer
♦ - without beam killer

The beam in the beam killers area is killed up to a level of a background as shown on the Fig. 4.

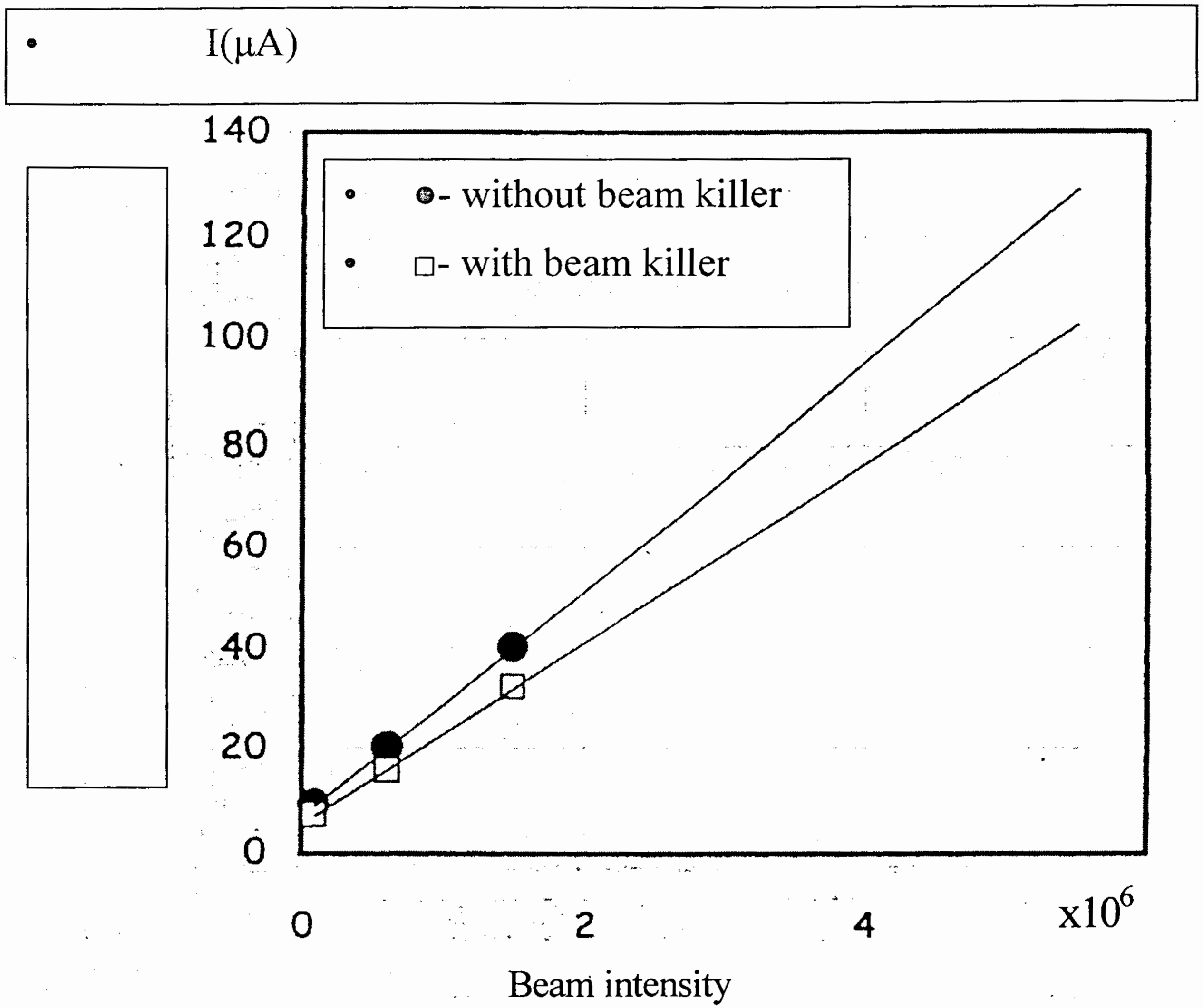

Fig.5. Dependence of the chamber current from a beam intensity.

2.The multichannel threshold Čerenkov counter (TCC).

- The counter is designed for charged particles identification, it has entrance aperture of 177x130cm². Four rows with 8 spherical mirrors in each one are arranged on the rear wall of the counter. When filled with freon at the atmospheric pressure and the temperature of 20°C, the counter provides the identification of pions in momentum range 4-21Gen/c with 70% efficiency(Fig.6.). For the greater efficiency of the counter the eight photomultipliers were replaced. For the best magnetic field compensation the inductance of the compensating coils in a central part of the Čerenkov counter were increased.

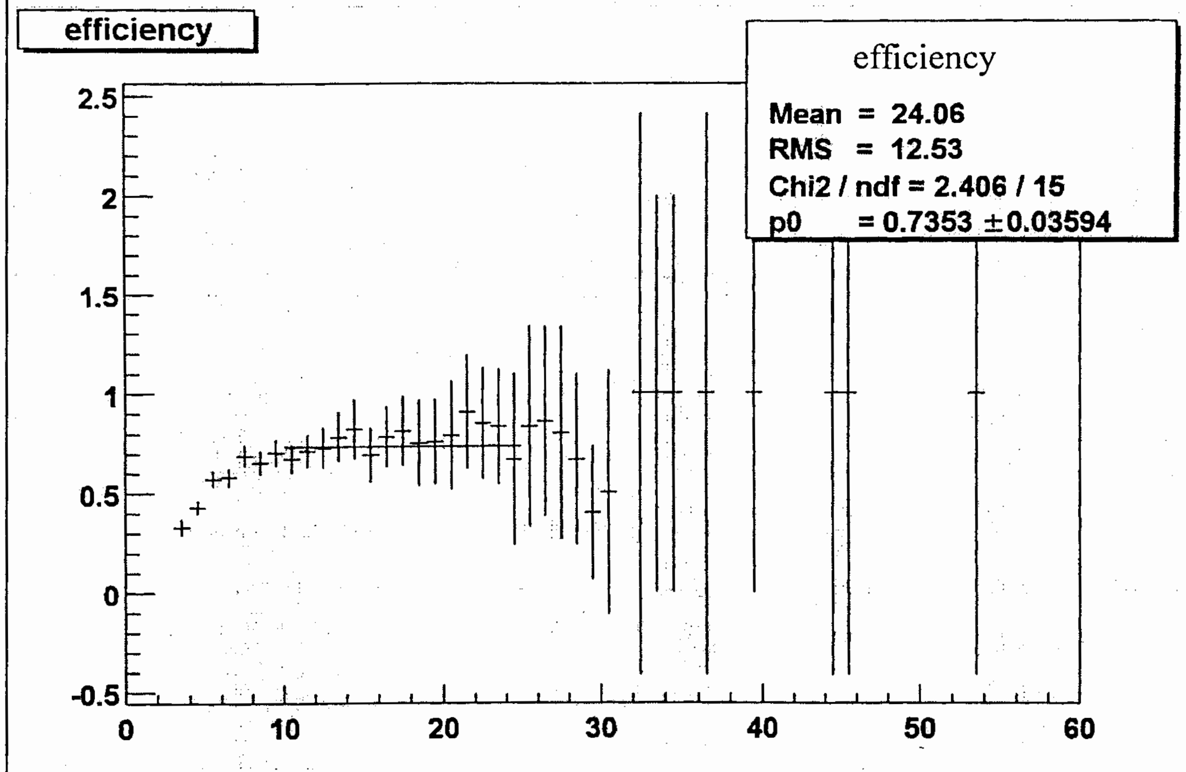

- Fig.6. Dependence of the particles registration efficiency from momentum.

Data analysis of April'2002 SVD-2 run. Pentaquark searches

1. Detection capabilities
2. Charmed mesons
3. Pentaquark searches

A.Kubarovsky, V.Popov, V.Volkov
SINP MSU Moscow

Talk at VHMP 2005, Dubna, Russia
16-17 April 2005

- 53,000,000 events collected
- ~7% are "beam only"/non-useable
- Basic way of pre-analysis:
  - Finding a primary vertex
  - Search for a secondary one(s) within different regions and with different detectors/methods to use/CPU time to be consumed ☺
- Average CPU time per event: up to 7 PIII-1000 seconds
- Facilities: SINP and SRCC MSU "old" clusters.

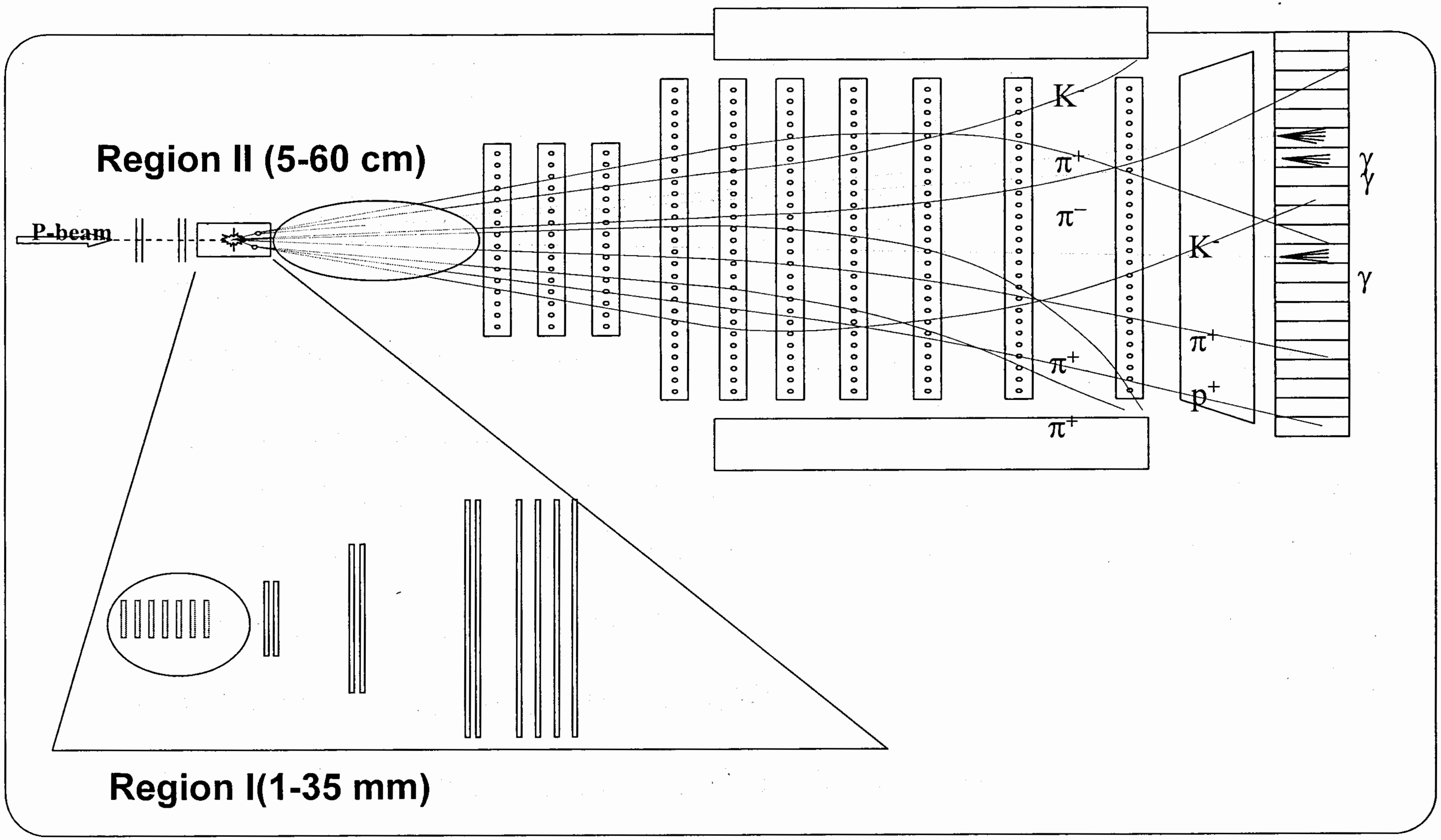

A.Kubarovsky, V.Popov,V.Volkov Data analysis of April'2002 SVD-2 run.
Pentaquark searches

VHMP
16 April 2005

Primary vertex Z-coordinate in SVD-2 active target

Si – 300μm; Pb – 220 μm; C – 500 μm

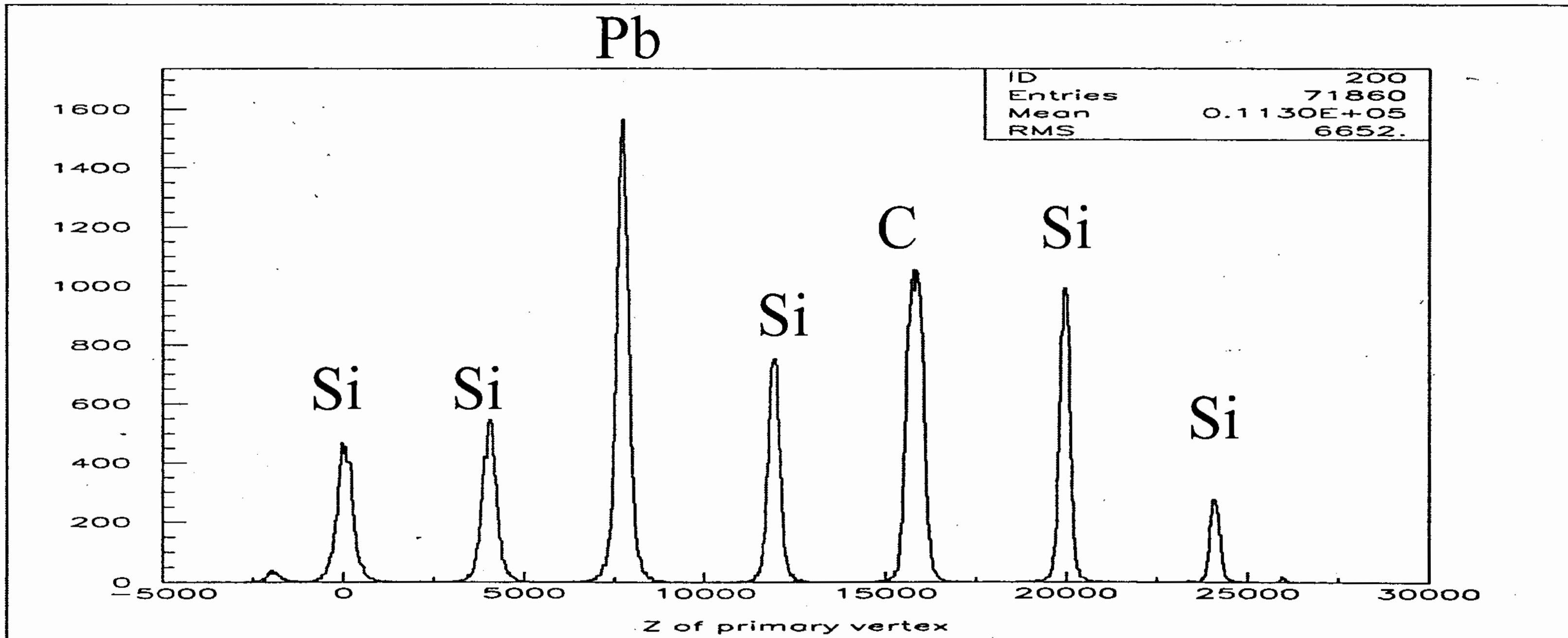

$\sigma_z = 70 \div 130 \mu m, \ \ \sigma_{x,y} = 7 \div 10 \mu m$

K^0_s and Λ^0 effective masses

- K^0_s M = 497.61 ± 0.09 (stat.), σ=4.4 MeV/c^2
- Λ^0 M = 1115.32 ± 0.05 (stat.), σ=1.6 MeV/c^2

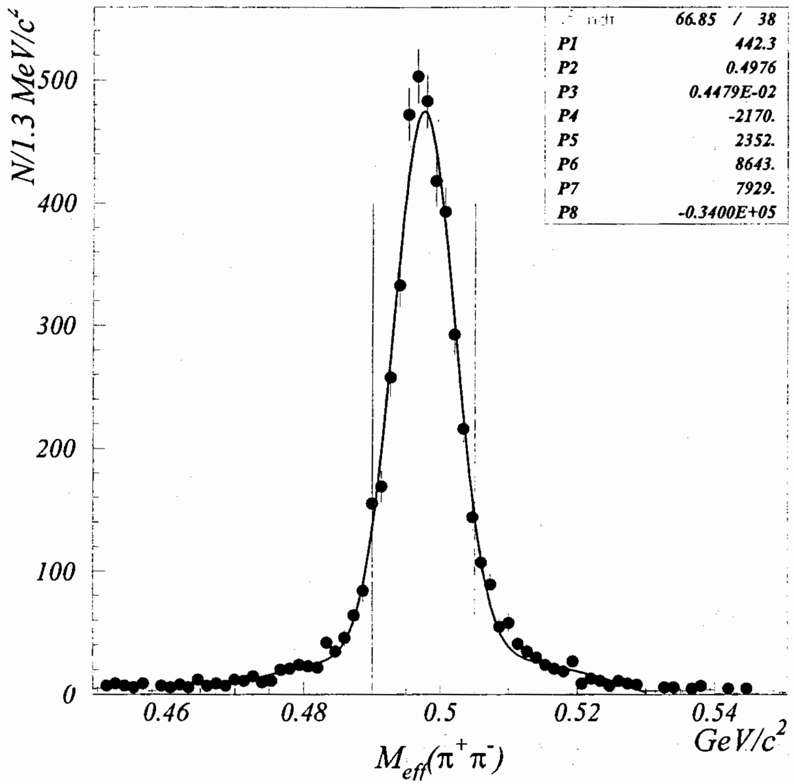

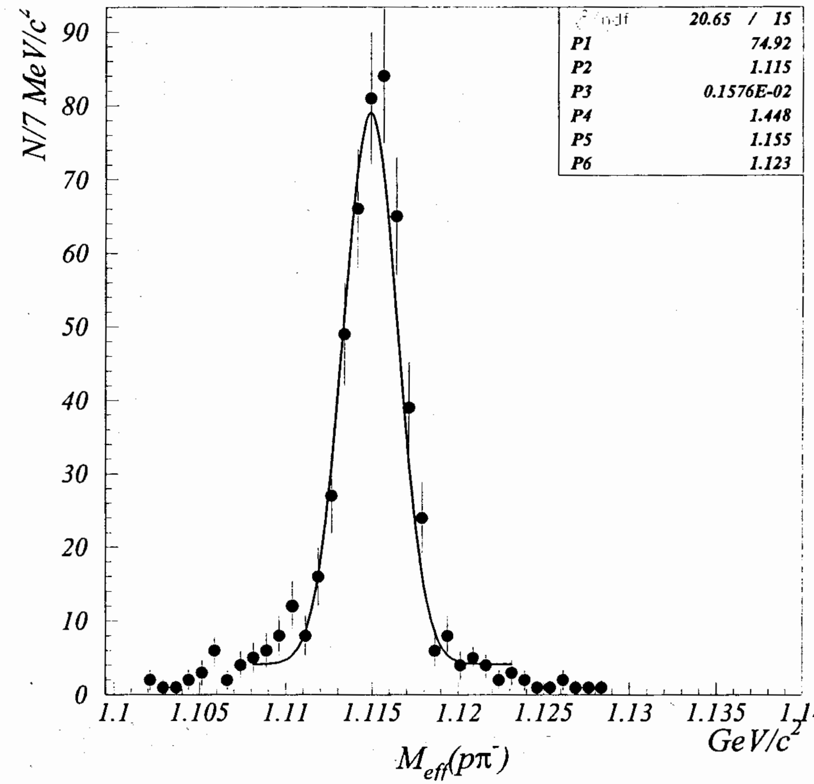

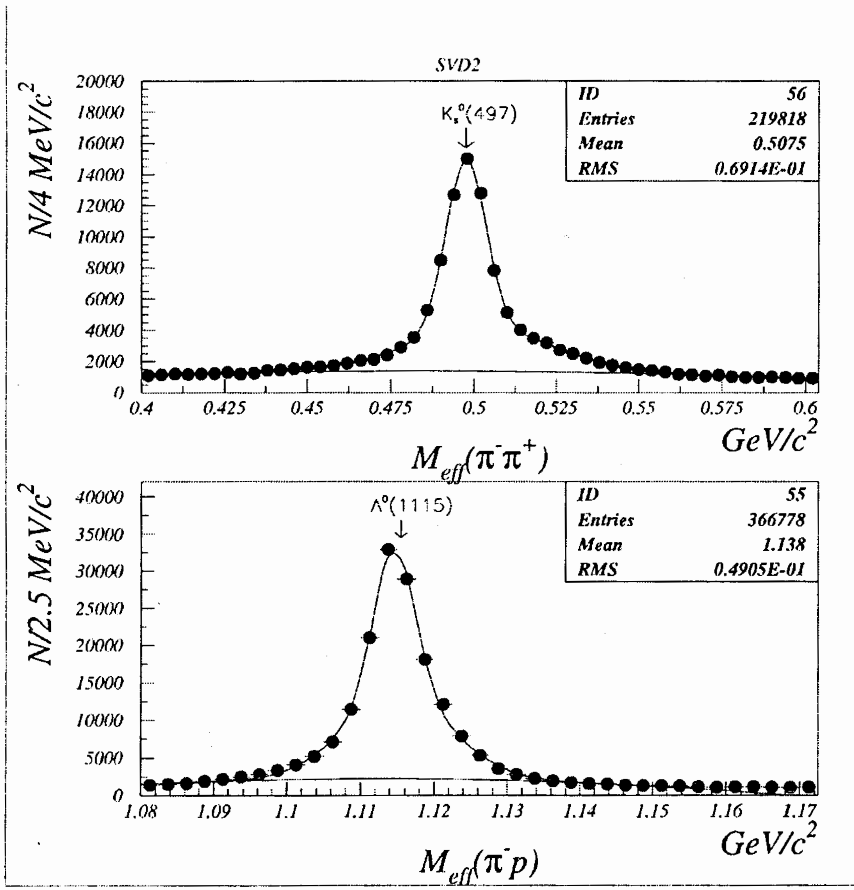

- Reconstruction of V0s with the spectrometer ("distant" ones):
  - K^0 : σ=5.8 MeV/c^2
  - Λ^0 : σ=3.0 MeV/c^2

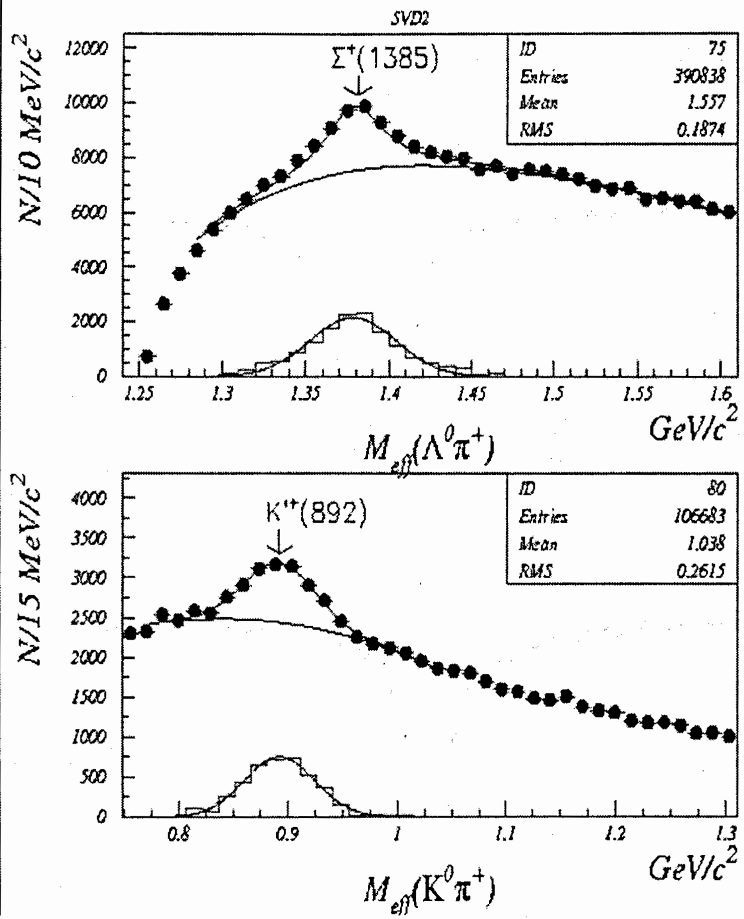

- The well-known resonances of the same topology as Θ^+
- Arrows correspond exactly to the PDG data

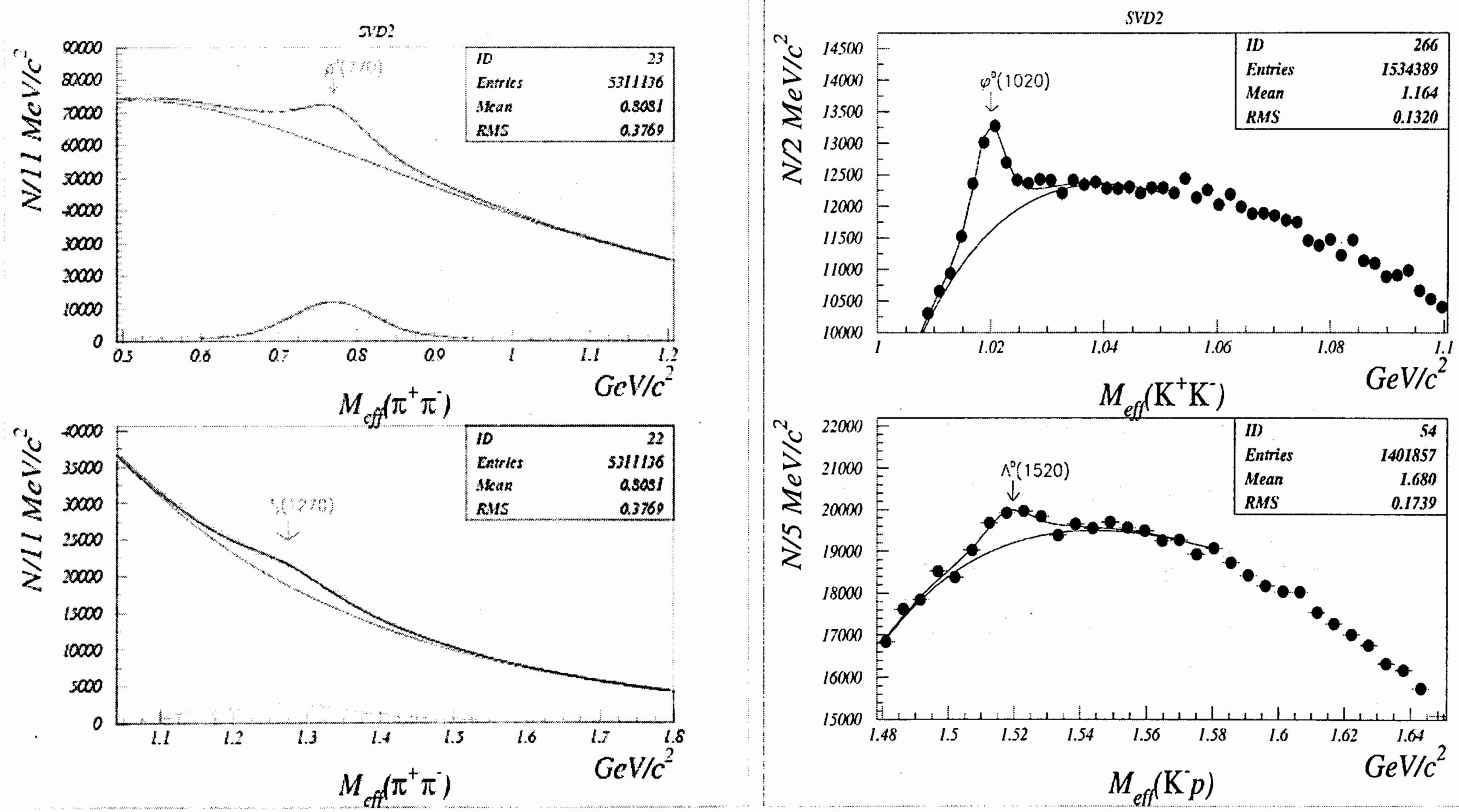

SVD

A.Kubarovsky, V.Popov,V.Volkov Data analysis of April'2002 SVD-2 run. Pentaquark searches

VHMP
16 April 2005

Near-threshold D^0 production

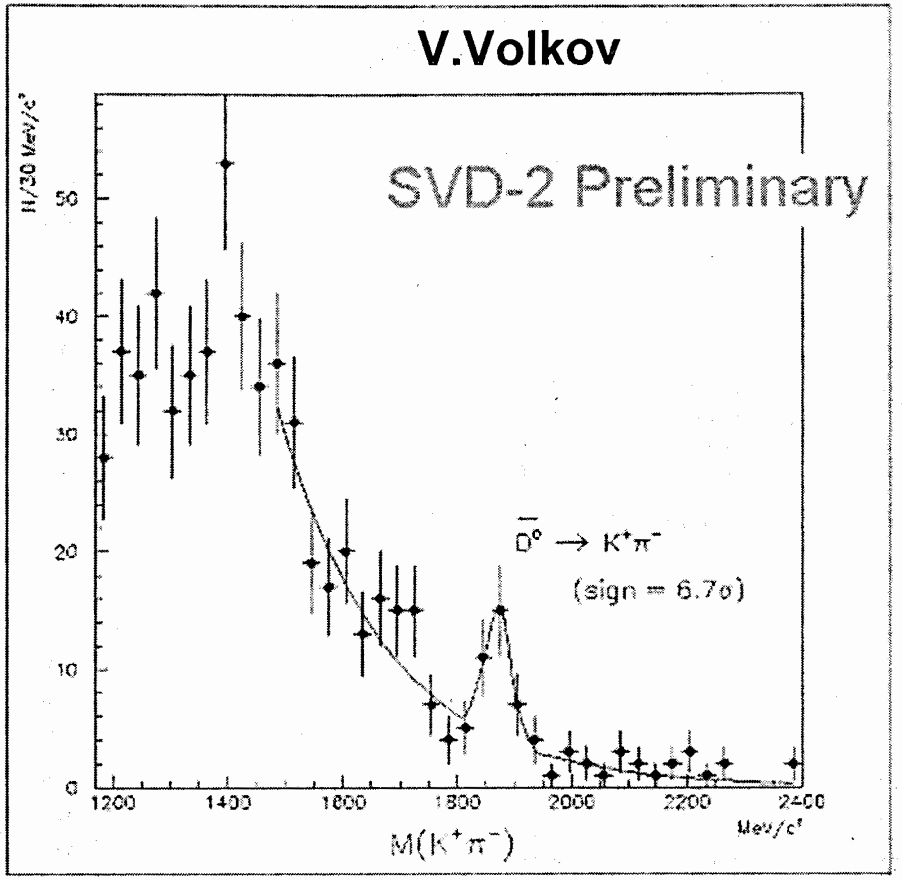

- Search for the $\overline{D^0} \to K^+\pi^-$ decays
- Different reconstruction methods used (not cross-checked yet…)
- 24 events over background of 12

A start of pentaquark history

- An idea of five-quark states was discussed since late 60's (Jaffe, Lipkin, Strotteman, …)
- First estimates in the Skyrme model (Chemtob, Praszalowicz, Walliser) – 1985...
- There were no conclusive results from experimental searches

"The general prejudice against baryons not made of three quarks and the lack of any experimental activity in this area make it likely that it will be another 15 years before the issue is decided". **(PDG, 1986)**

PDG – in "Particle listings under revision"

$\Theta(1540)^+$

$I(J^P) = 0(?^?)$ Status: ***

A REVIEW GOES HERE – Check our WWW List of Reviews

$\Theta(1540)^+$ MASS

As is done throught the *Review*, papers are listed by year, with the latest year first, and within each year they are listed alphabetically. NAKANO 03 was the earliest paper.

It is difficult to deny a status of three stars and a place in the Summary Tables for a state that six experiments claim to have seen. Nevertheless, as discussed in the above note, we believe it reasonable to have some reservations about the existence of this state on the basis of the present evidence.

In the '2003 fall...

- uudd$\bar{s}$ quark content
- Predicted by Diakonov,Petrov and Polyakov Z.Phys A 359, 305(1997)
- Supposed to be of 1530 MeV/c^2 mass, width <15 MeV/c^2 and to decay into nK^+ or pK^0
- Observed by several experiments (LEPS,DIANA,CLAS,…) in both decay modes
- The pK^0 mode can be searched for by SVD-2: good resolution for K^0_s and proton identification

Experiments zoo

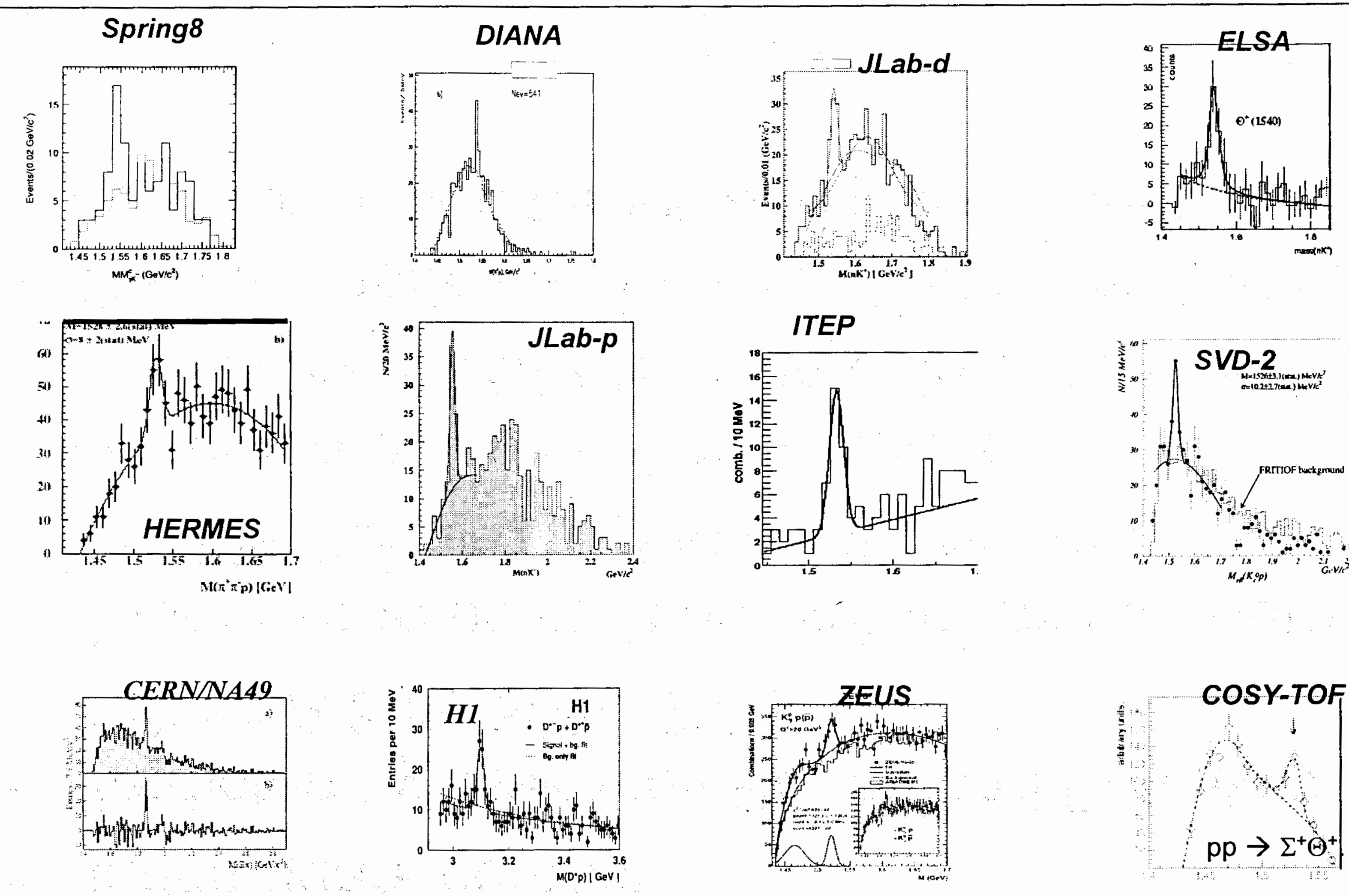

A.Kubarovsky, V.Popov,V.Volkov Data analysis of April'2002 SVD-2 run.
Pentaquark searches

VHMP
16 April 2005

PENTA-I : Data sample

- ~35,000 events sample for D-meson searches was used
- Primary selection mainly based on the presence of well-defined secondary vertices in the close-to-target region
- Secondary tracks are measured by vertex detector
- Allowed decay length is 1…35 mm (av. 20 mm), means that only ~10% of K^0_s to be reconstructed

Penta-I:Events selection

- $\leq$ 5 charged tracks from primary vertex to reduce combinatorial background
- K^0_s selection:
  - 2 oppositely charged tracks from secondary vertex
  - $490 \leq M_{\pi\pi} \leq 505$ MeV/c^2
  - $M_{p\pi} \geq 1120$ MeV/c^2 ($\rightarrow$ not Λ^0)
- Proton selection:
  - Positive track from primary vertex
  - Momentum of 4…21 GeV/c
  - Absence of a Cerenkov detector hit

Penta I : pK^0_s spectrum analysis

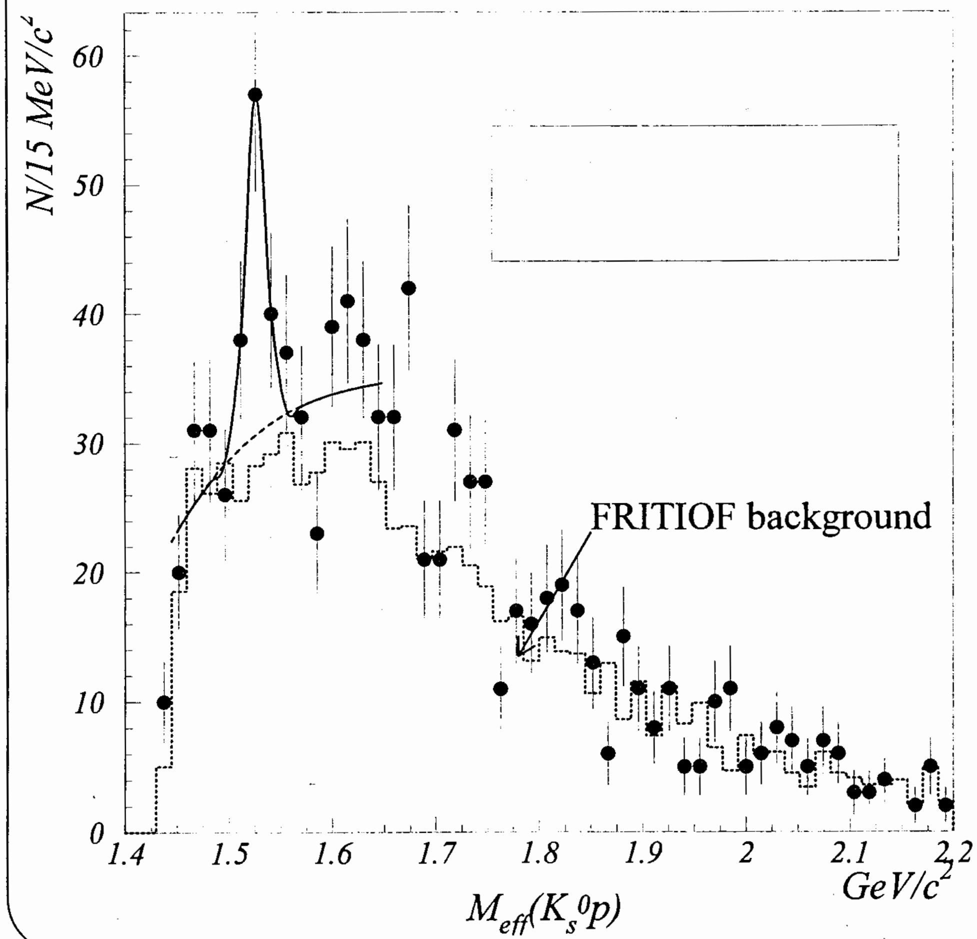

- Cut applied: pK^0_s system goes forward in center-of-mass system
- **Narrow peak at 1526 MeV/c² is observed**
- FRITIOF simulated background fails to reproduce the real shape
- Peaks in higher mass region can be attributed to Σ^{*+} bumps

Penta I : Cut applied: $P_p > P_{K0}$ to eliminate bumps
(cf. B.Levchenko, arXiv:hep-ph/0401122)

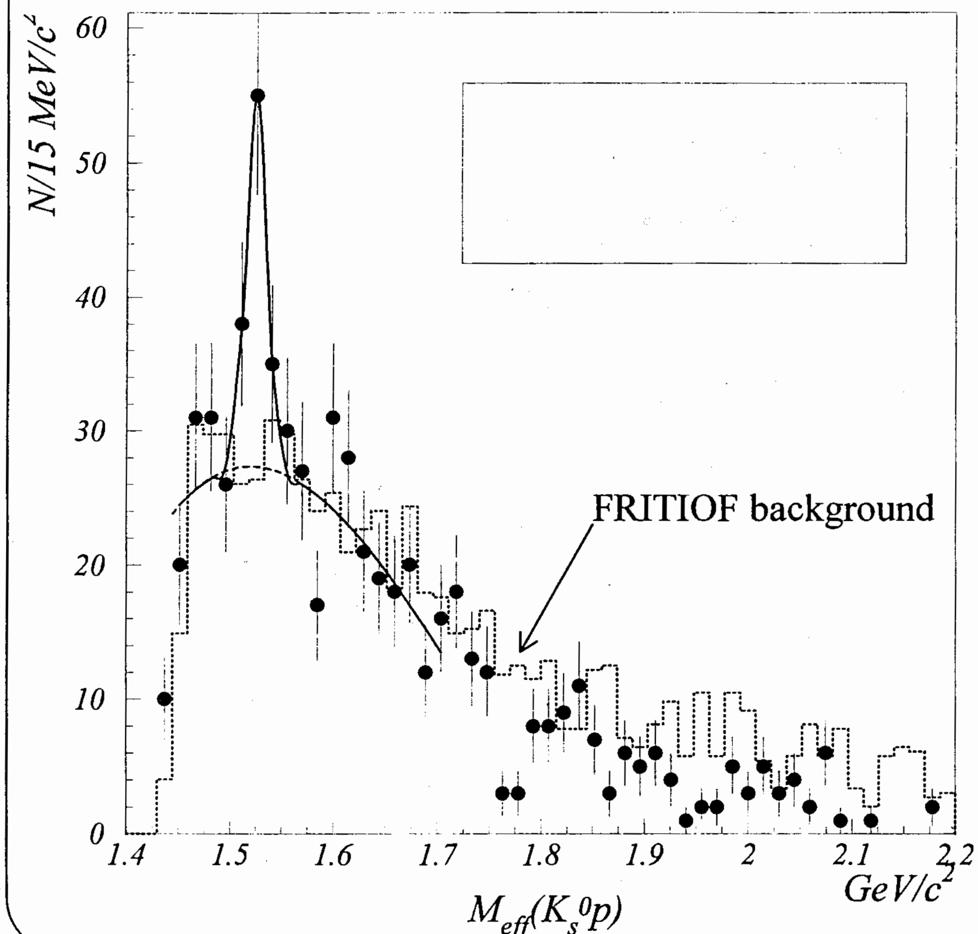

- Background can be described in different ways:
  - FRITIOF simulations
  - Plain polynom fitting
  - Random-star (not shown)
- All three give the shape compatible to the experimental one

Penta I : Pentaquark parameters at SVD-2

- Number of events within a peak: 50 over background of 78, gives a significance of 5.6 σ
- Mass: 1526 ± 3(stat.) ± 3(syst.) MeV/c^2
- Width Γ < 24 MeV/c^2 (below experimental resolution)
- Strangeness could not be defined directly, but there are no reported S= -1 states in this mass region

We interpret this state as Θ+ pentaquark

Penta I : Cross section and A-dependence

- We estimate the total cross-section of $pA \to \Theta^+ + X$ as $30 \div 120$ μb/nucleon
- We fail to find the difference in A-dependence of Θ^+ events from that of total for inelastic events ($\sim A^{0.7}$)

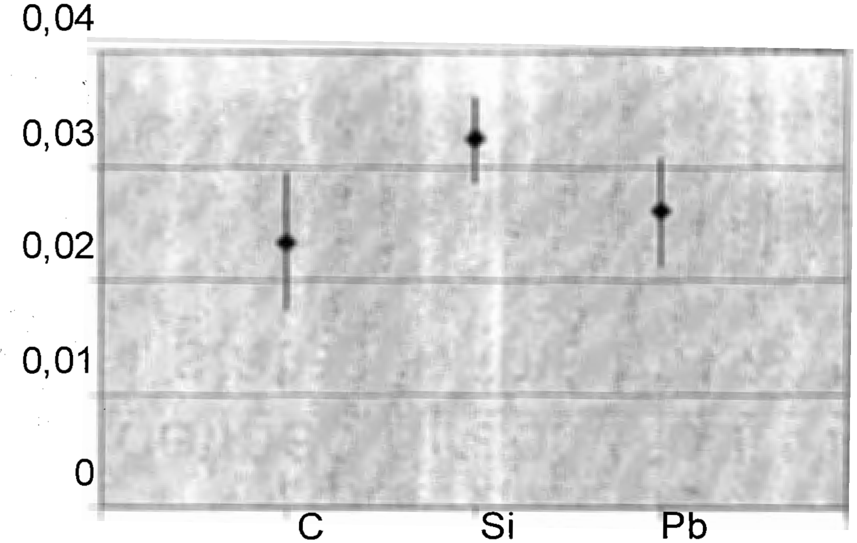

The ratio of Θ+ peak events to the total of K^0 events for different target materials

Theta masses from different experiments

- Certain mass shift can be observed between the K^+n and K^0p modes

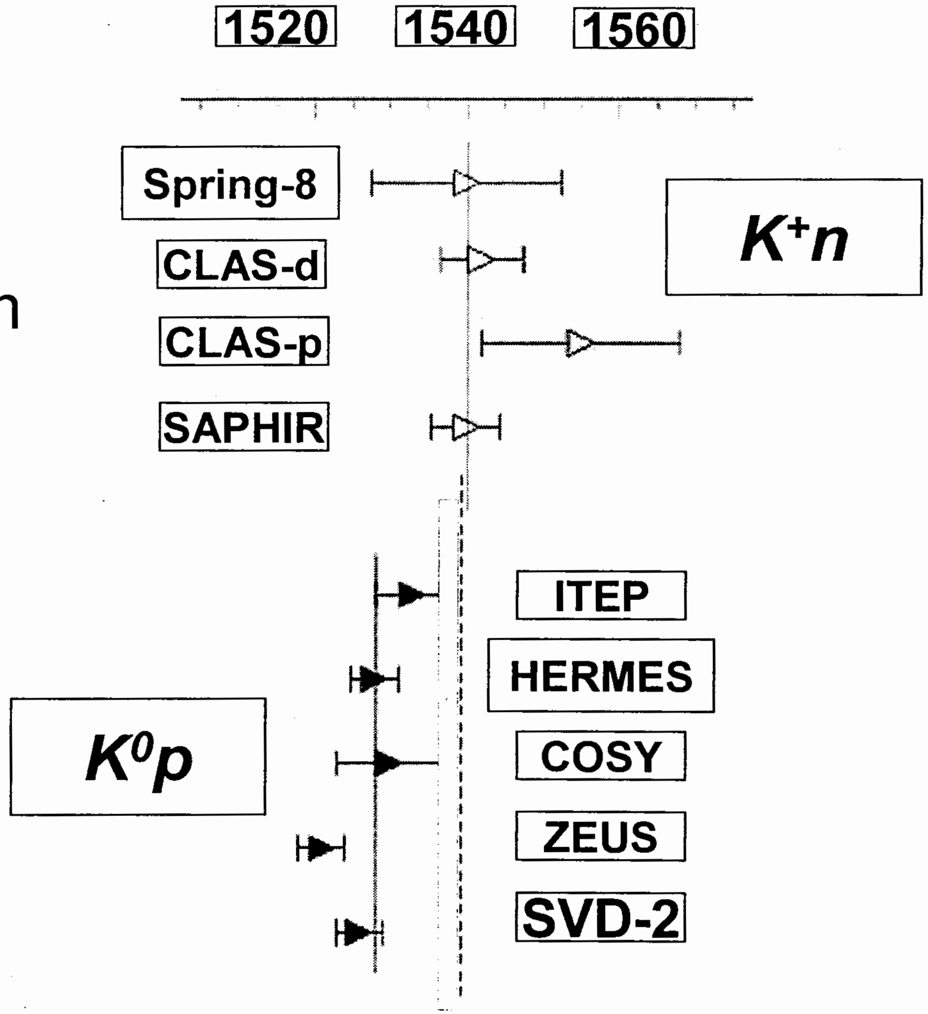

Penta I : second analysis

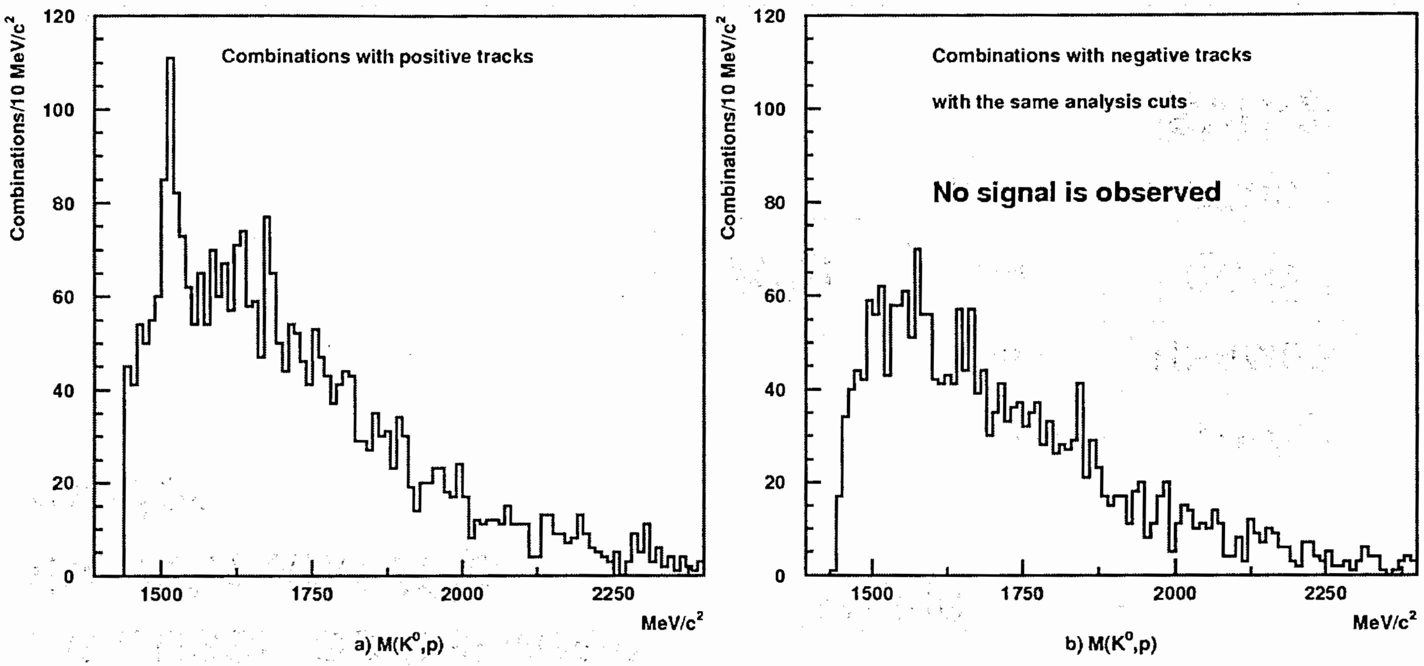

- **To be checked…**
- **Possibly could result in a much more narrow peak**

Penta II : event selection

- "Distant" K0 used
- Cuts applied:
  - Number of primary charged tracks: 4 to 6
  - Proton candidate momentum: $9 \leq P_p \leq 15$ GeV/c
  - No Cerenkov detector hit for a proton
- A total of 9,000 events selected

211

Penta II : results

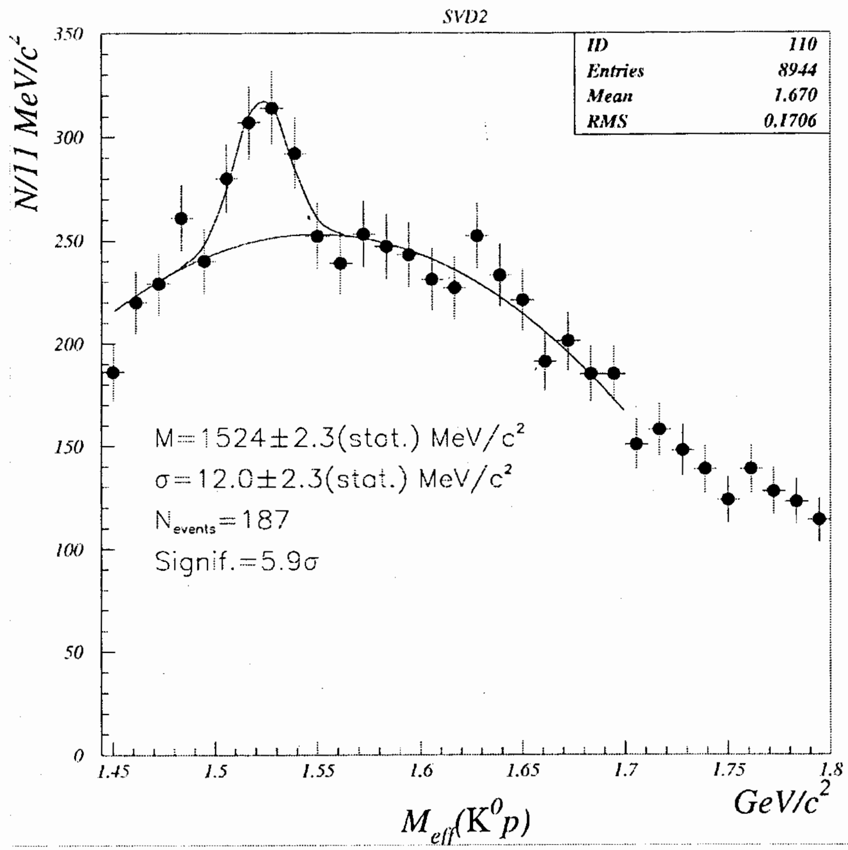

- Peak is well pronounced (6 σ)
- No significant change in the effective mass
- Cross-section and systematic errors are yet to be evaluated

Hadron nicknames

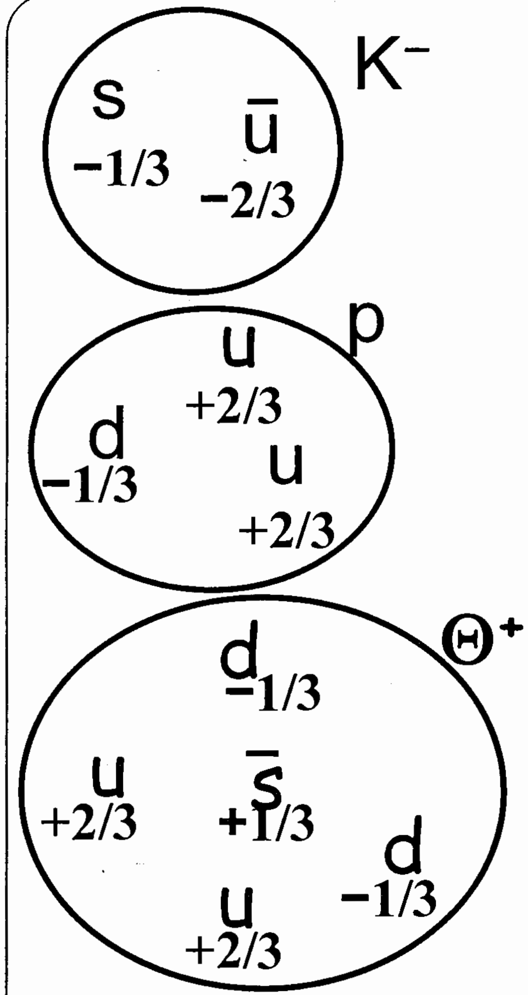

Meson: quark-antiquark

Baryon: three quarks

Pentaquark: 4 quarks + 1 antiquark

Exotic if antiquark is of the different flavour

Anti-decuplet of q4q-bar states

DPP model modified

(DP hep-ph/0310212)

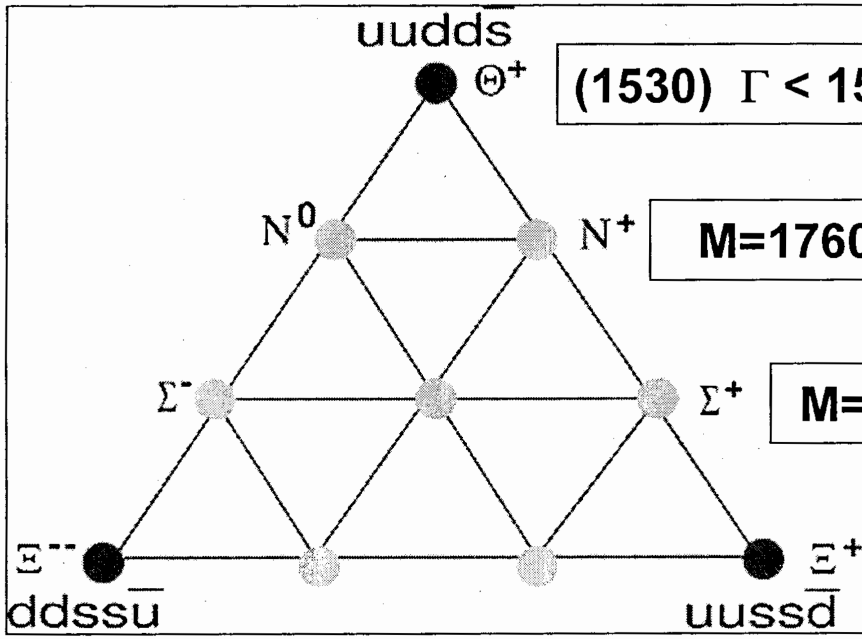

(1530) Γ < 15 MeV

M=1760-1810

M=1650-1690

M=1862 $\Gamma = 5\,\Gamma_{\Theta^+}$

214

H1: charmed pentaquark?

- M = 3099 ± 3 ± 5 MeV
- Minimal quark content: $uudd\bar{c}$
- To be confirmed!

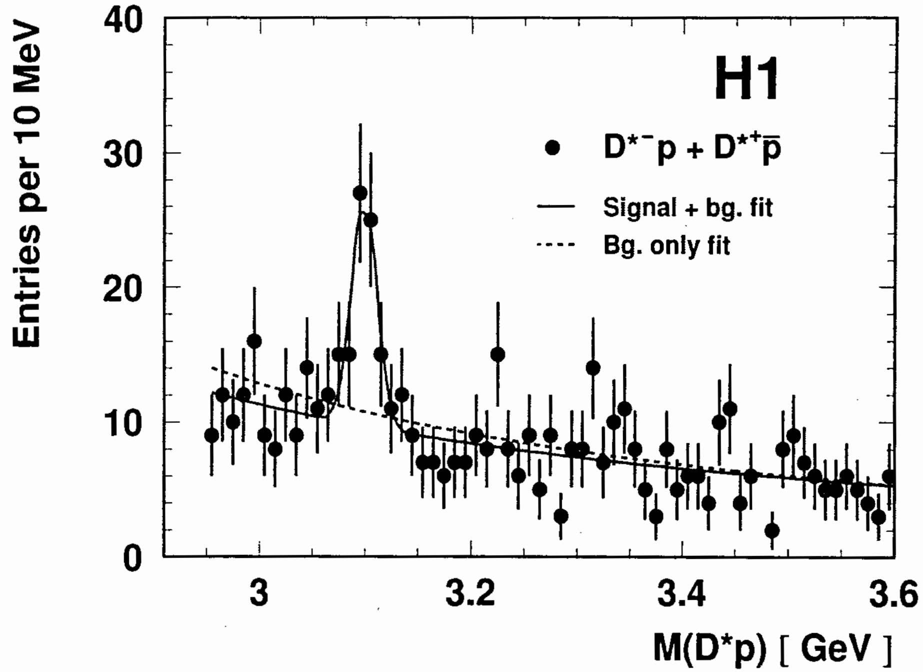

Exclusive reaction searches

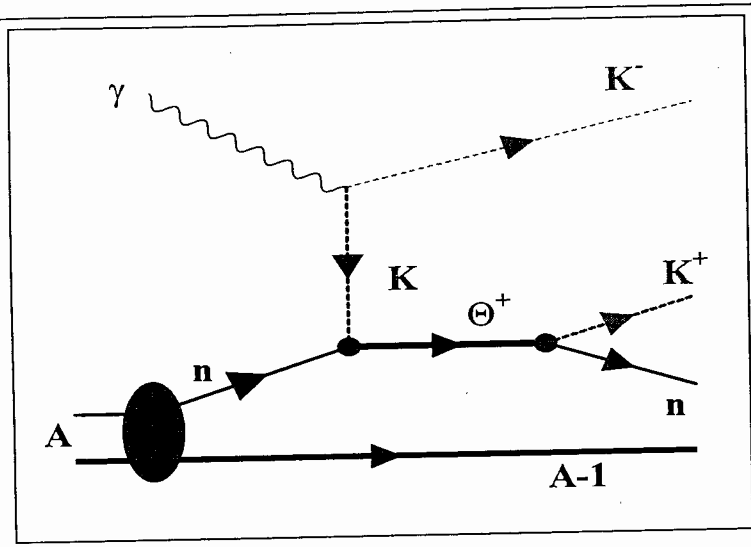

LEPS $\gamma n \rightarrow K^{+}K^{-}n$

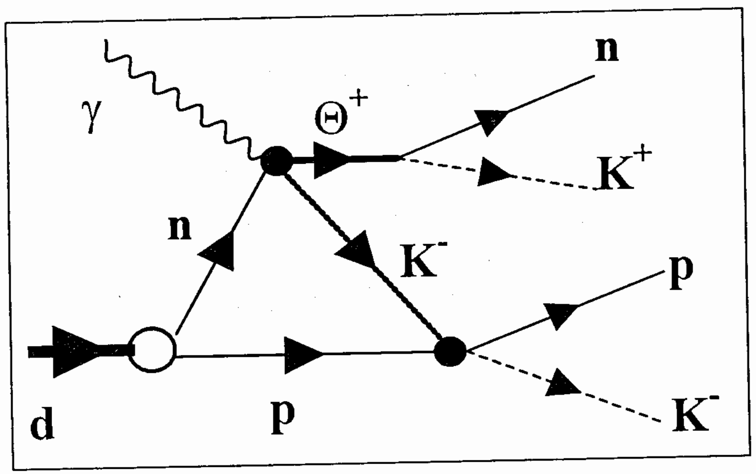

CLAS $\gamma d \rightarrow K^{+}K^{-}pn$

Pentaquark observations

Mass (MeV)	Width (MeV)	N_{event}	Statist. signif.	Reaction	Experiment
$\Theta^+(1540)$					
$1540 \pm 10 \pm 5$	< 25	19 ± 2.8	$\sim 2.7\sigma$	$\gamma C \to C' K^+ K^-$	LEPS
$1539 \pm 2 \pm 2$	< 9	29	$\sim 3.0\sigma$	$\gamma p \to n K^+ K^0_s$	DIANA
$1542 \pm 2 \pm 5$	< 21	43	$\sim 3.5\sigma$	$\gamma d \to p n K^+ K^-$	CLAS
$1540 \pm 4 (\pm 3)$	< 25	63 ± 13	4.8σ	$\gamma p \to n K^+ K^0_s$	SAPHIR
$1533 \pm 5 (\pm 3)$	< 20	27	$\sim 4.0\sigma$	ν–induced	CERN, FNAL
$1555 \pm 1 \pm 10$	< 26	41	$\sim 4.0\sigma$	$\gamma p \to n K^+ K^- \pi^+$	CLAS
1528 ± 4	< 19	~ 60	$\sim 4\sigma$	γ^*–induced	HERMES
$1526 \pm 3 \pm 3$	< 24	50	3.5σ	p-p reaction	SVD-2
1530 ± 5	< 18		3.7σ	p-p reaction	COSY
1545 ± 12	< 35	~ 100	$\sim 4\sigma$	p-A reaction	YEREVAN
$1521.5 \pm 1.5^{+2.8}_{-1.7}$	< 6	221	4.6σ	Fragmentation	ZEUS
$\Xi(1862)$					
1862	< 21		4.6σ	ν–induced	NA49
$\Theta_c(3099)$					
$3099 \pm 3 \pm 5$			5.4σ	γ^*–induced	HERA

A table from E.Klempt, hep-ph/0404270

Current status

- New analysis software is able to process "distant" V^0s :
  - K^0 - 10 times more statistics (for Θ^+ analysis and charm searches)
  - Λ – up to 100 times more statistics, allowing Ξ^- decays reconstruction to search for $\Xi_{3/2}$ pentaquark claimed by NA49
- Better kinematical fitting for secondaries to improve effective mass resolution

The end

Theta mass with another set of cuts applied

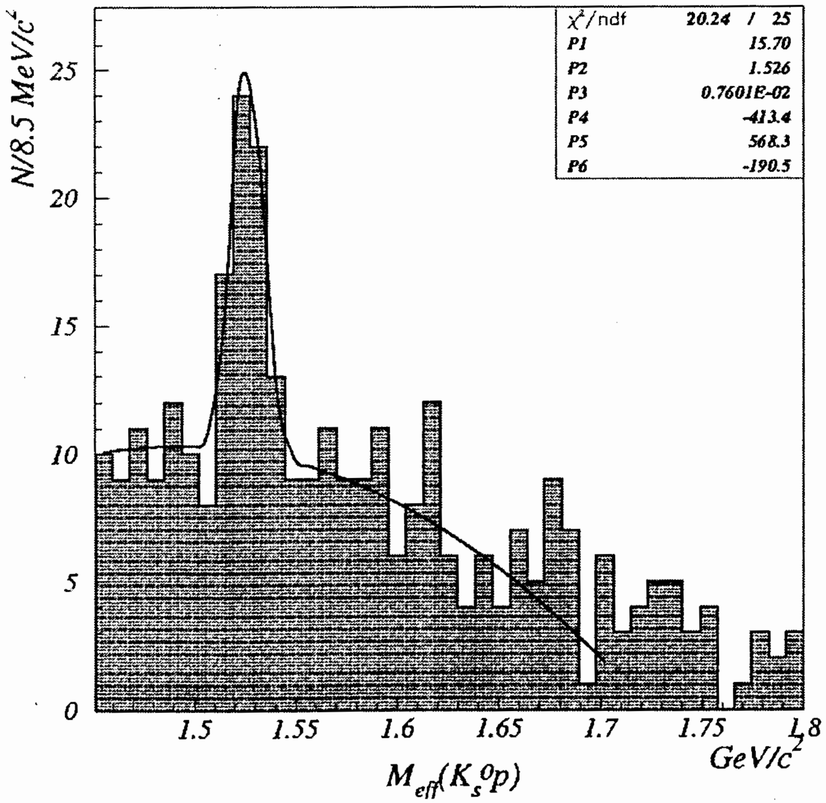

- Peak width:

24 → **18 *MeV/c²***

Pentaquark II (“distant” K^0)

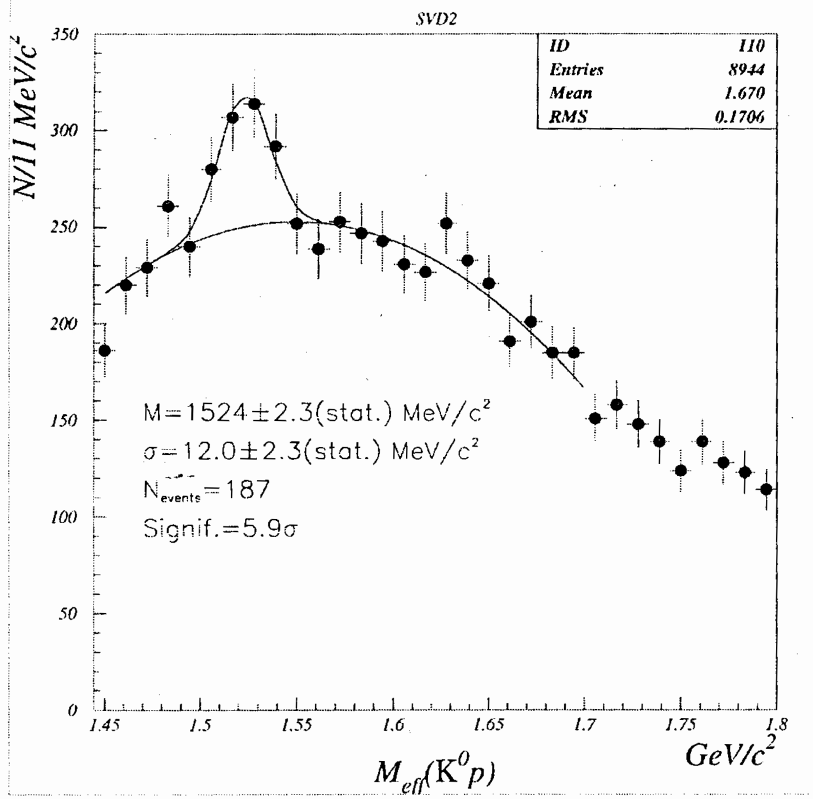

- $M=1524 \pm 2.3$ MeV/c^2
- $\sigma = 12.0 \pm 2.3$ MeV/c^2
- $N_{events} = 187$
- Significance 5.9 σ

No significant mass difference from the previous analysis

Silicon Microstrip Vertex Detector for Experiment SVD-2 (SINP MSU, Moscow & IHEP, Protvino, Russia)

1. **Detector description**
2. **Current status (April 2005).**

14.04.2005
SINP MSU
D.Karmanov

Detector description

Vertex detector for SVD-2 experiment will consist of the following parts:

- **3 Beam stations**, for position measurements (X,Y,Z) of primary particles before interaction with fix target.
- **Vertex Station** with **target**, some **silicon sensors for trigger** and **10 layers of microstrip silicon sensors** for precise measurements of position the products of interaction.

The sensitive elements of Beam Stations and Vertex Station are microstrip silicon sensors with different size and different strip pitch. The positions of each silicon sensor and their size and strip pitch are presented in Table 1 and on Fig. 1.

Two types of readout chips have been used for sensors readout. 16-th channel amplifiers “GASSIPLEX” used for all sensors readout in Beam Stations and for middle sensors (32 mm) in Vertex Station. The electronic boards with “GASSIPLEX” chips located outside the box of Stations.

The readout for the big sensors (52 mm) in Vertex Station provided by 128-th channels amplifier “VIKING”.

Detector description

- The **aperture** of Sensors in the Vertex Station should be **0.25÷0.17 rad.** depending on the interaction point position.

- Estimated **efficiency of registration** will be more then **97% for sensors with vertical strips and more then 96% for sensors with horizontal strips.**

- Estimated **accuracy of sensor's alignment** must be better than 300 μm in Z direction and **better than 10 μm in X (or Y) direction.**

Table 1. **Size, pitch and position of sensors.**

Sensor number	Station name	Strip direction	Active area size (horizontal× vertical, mm)	Z position (mm)	Strip pitch (um)
B1	Beam station	Vertical	16.0×6.4	-1000	25
B2	#1	Horizontal	6.4×16.0	-998	25
B3	Beam station	Vertical	16.0×6.4	-700	25
B4	#2	Horizontal	6.4×16.0	-698	25
B5	Beam station	Vertical	16.0×6.4	-400	25
B6	#3	Horizontal	6.4×16.0	-398	25
T1	Vertex station	Vertical	24.0×21.0	0	1000
T2	(sensors for trigger)	Vertical	24.0×21.0	4	1000
Vert-1	Vertex station	Vertical	32.0×32.0	22	50
Horiz-1		Horizontal	32.0×32.0	26	50
Vert-2	Vertex station	Vertical	32.0×32.0	46	50
Horiz-2		Horizontal	32.0×32.0	50	50
Vert-3	Vertex station	Vertical	51.2×51.2	68	50
Horiz-3		Horizontal	51.2×51.2	76	50
U1	Vertex station	Stereo Vertical (10.5°)	51.2×51.2	84	50
V1		Stereo Horizontal (10.5°)	51.2×51.2	92	50
Vert-4	Vertex station	Vertical	51.2×51.2	100	50
Horiz-4		Horizontal	51.2×51.2	108	50

Fig. 1. **Size and position of sensors in the Vertex Station.**

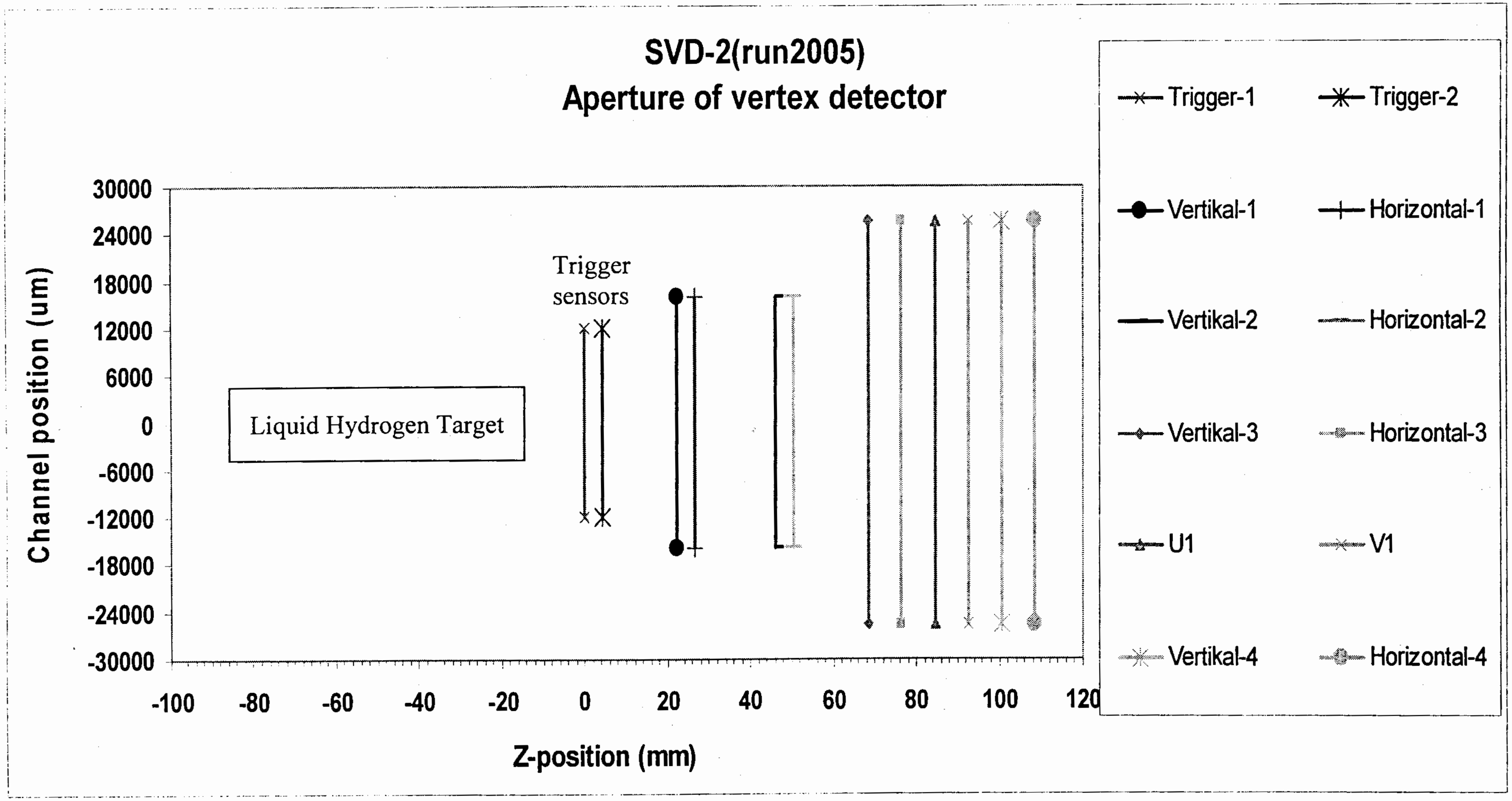

2. Current status.

- All elements of mechanical support for Beam Stations and Vertex Station are ready.

- All boards with sensors for Beam Stations are ready.
- **We hope to assemble all Beam Stations by the end of April 2005.**

- All sensors for the Vertex Station are ready (made and tested).

- 2 boards (of 4) with middle sensors (32 mm) are ready (made and tested) and 2 boards are at the final stage of assembling. **We hope to assemble boards with middle sensors in the end of May 2005.**
- 4 boards (of 6) for big sensors (52 mm) are in works. We are setting the "VIKING" chips on the boards and bonding them with the control electronics.

3. Problems.

- **The main problem is a bonding of "VIKING" chips.** We use manual ultrasonic bonder "UZSM-3M"(Russia) with aluminum wire with thickness 25 um. The yield of good chips after installation and bonding is less then 30%. It means that we need a lot of chips and a lot of time for assembling boards with big sensors.
- **The second problem is a initial quality of "VIKING" chips.** Unfortunately all our chips were not tested by manufacturer "IDEAS" (Norway). From the other hand we have not equipment for testing this unpackaged chips before installation on the board and bonding. So we don't know the real quality of chip before installation and we can not correct the process of bonding because, might be, we have bad chips initially.

Fig. 2. **Board with a small sensor for Beam Station.**

Sensor size 16×16 mm, 640 channels, 25 um pitch.

In the Beam Station we will use 256 strips from the center of sensor.

readout by “GASSIPLEX” amplifier.

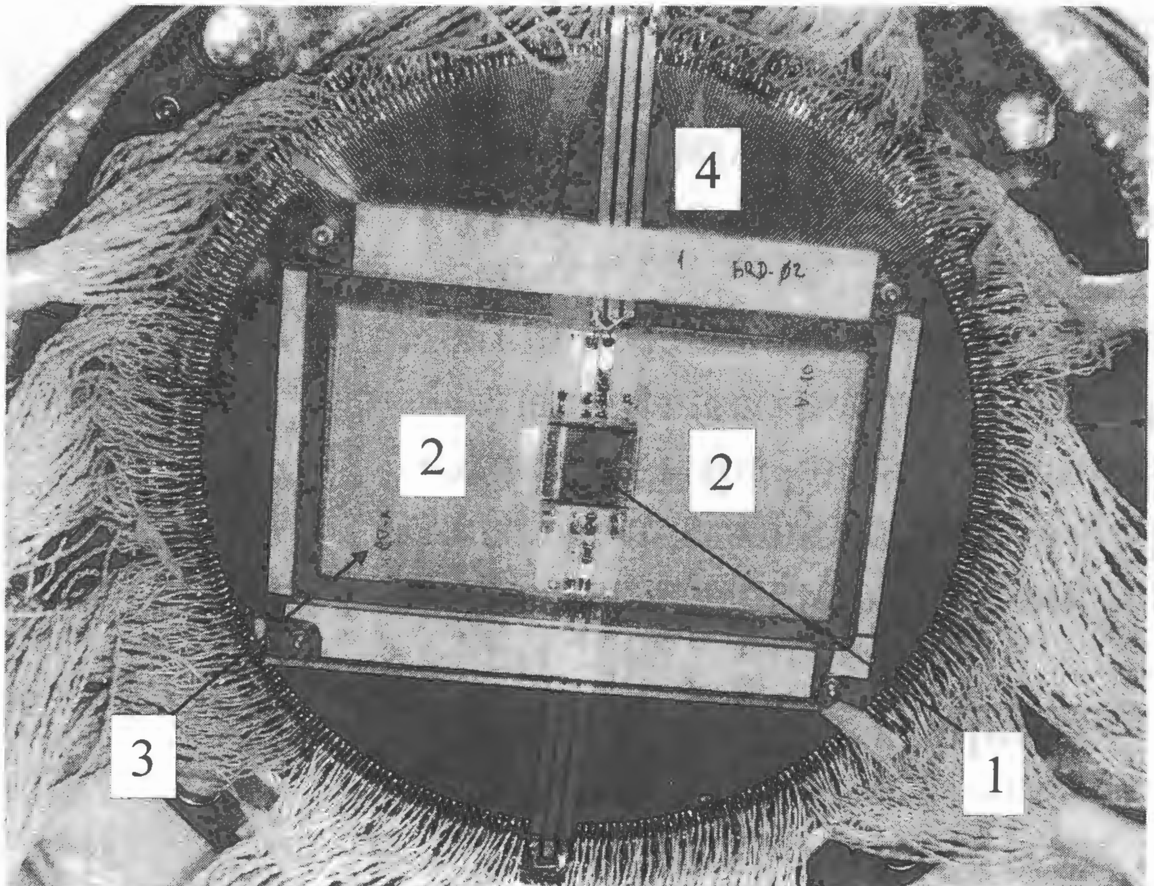

1 – Silicon sensor,

2 – Low capacitance pitch adapter from sensor to “J10” board,

3 – Ceramic board for sensor and adapters,

4 – “J10” board with output wires to outside readout boards with “GASSIPLEX” amplifiers.

Fig. 3. **Board with a medium sensor.**
Sensor size 32×32 mm, 640 channels, 50 um strip pitch.
for Beam Station. Readout by “GASSIPLEX” amplifier.

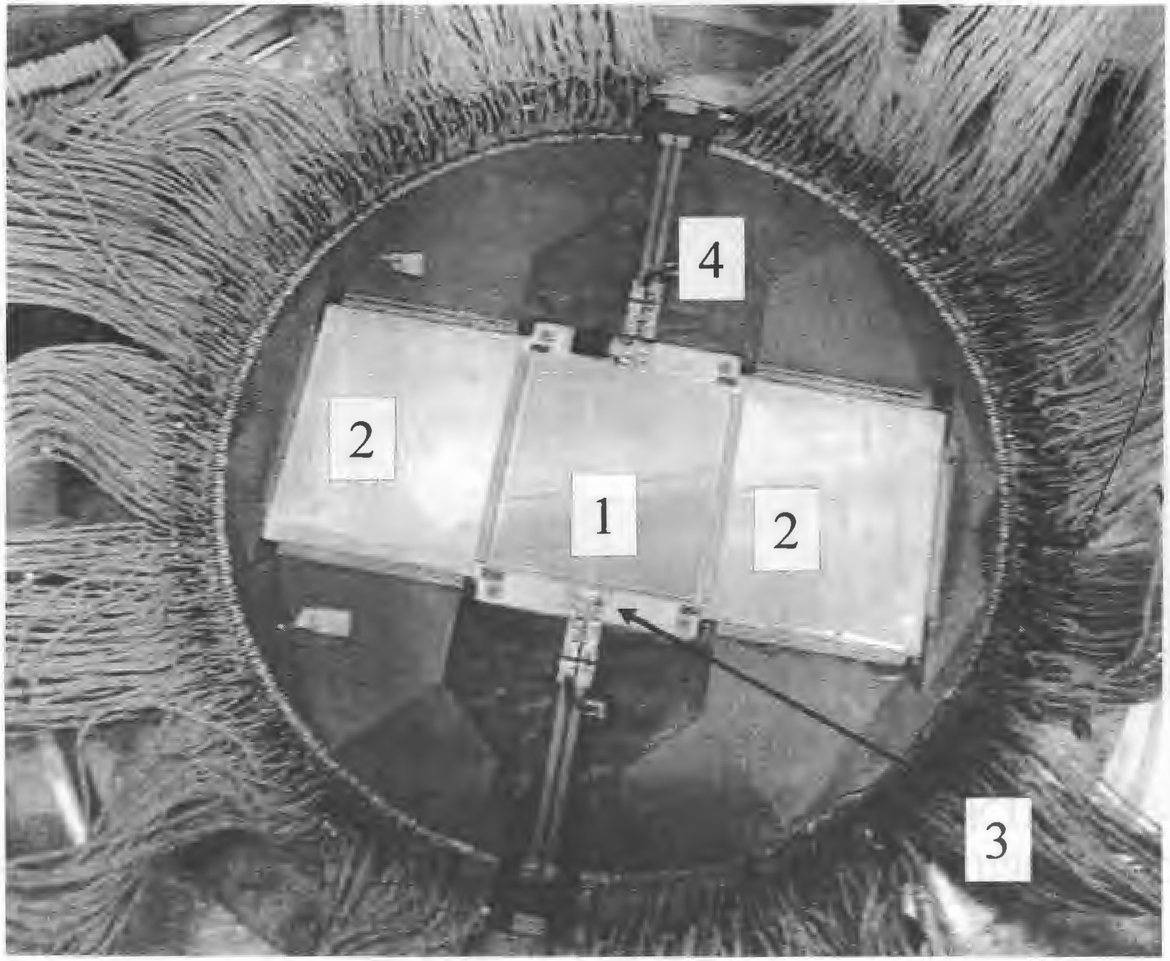

1 – Silicon sensor,
2 – Low capacitance pitch adapter from sensor to “J10” board,
3 – Ceramic board for senor and adapters,
4 – “J10” board with output wires to outside readout boards with “GASSIPLEX” amplifiers.

Fig. 4. **Board with a large sensor (project).**
Sensor size 52.2×52.2 mm, 1024 channels, 50 um strip pitch.
for Beam Station. Readout by “VIKING” amplifier.

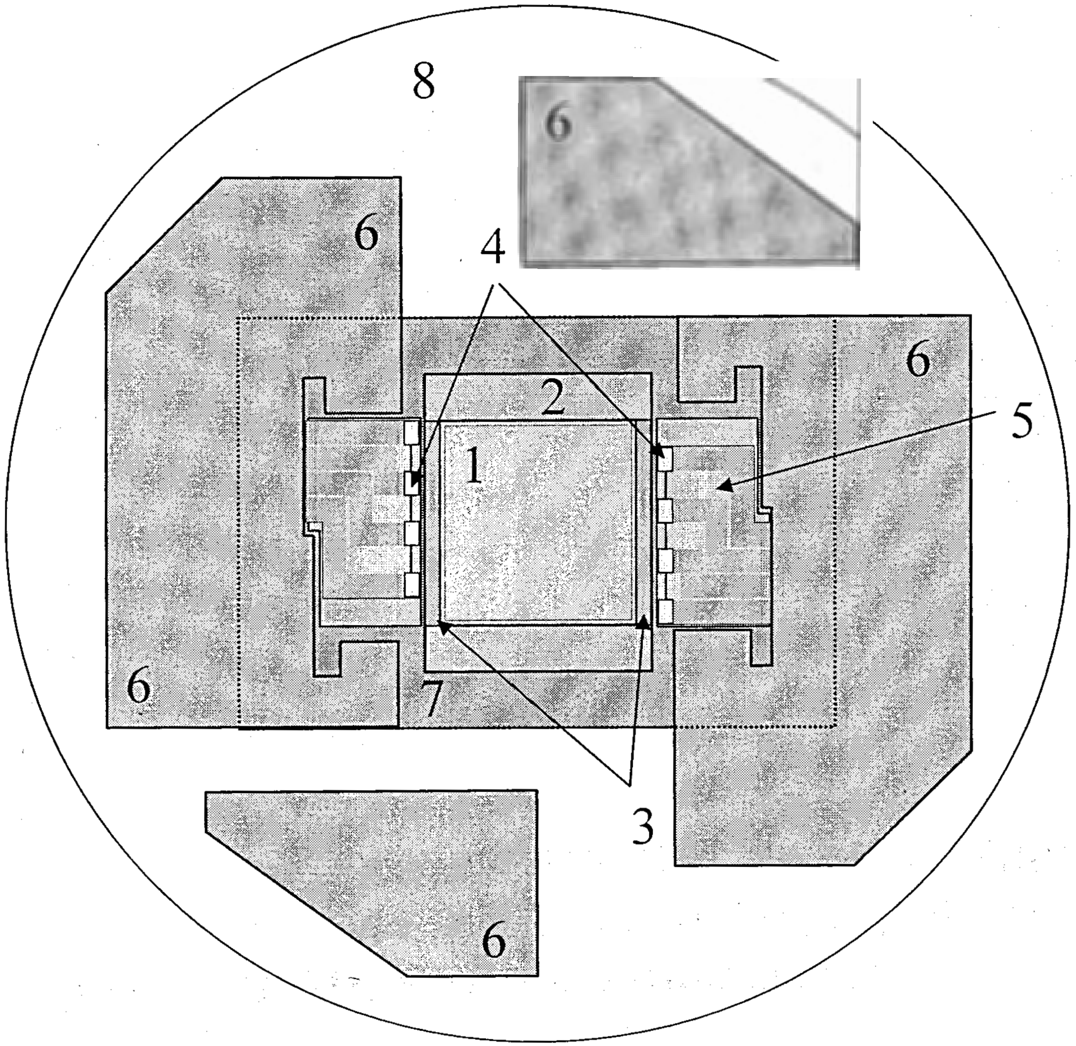

1 – Silicon sensor,
2 – Ceramic board for senor,
3 – Pitch adapter from sensor to chip “VIKING”,
4 – Chip “VIKING”,
5 – Board for chips “VIKING” (from polikor),
6 – control boards for chips “VIKING”,
7 – Titanium board,
8 – “J10” board with output wires and cables.

Fig. 5. **Beam Station**
(assembled).

SVD-2, Run December 2004.

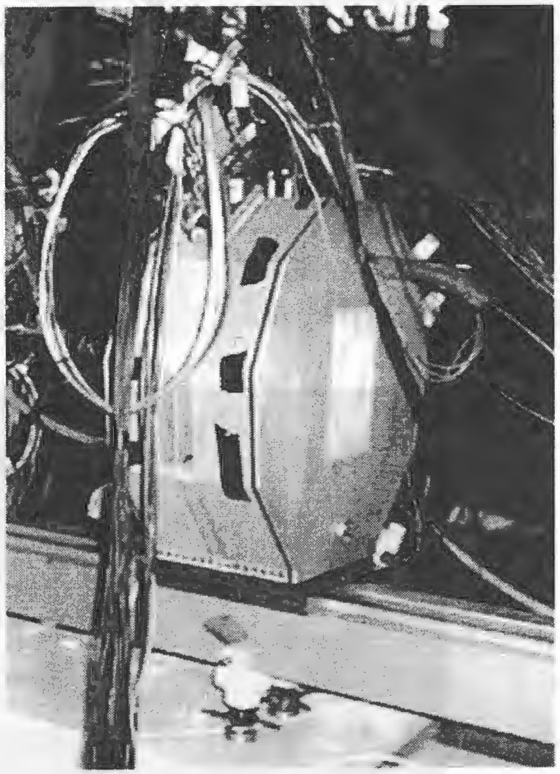

Fig. 6. **Vertex Station.**
(mechanical support
without sensor boards).
MSU April 2005.

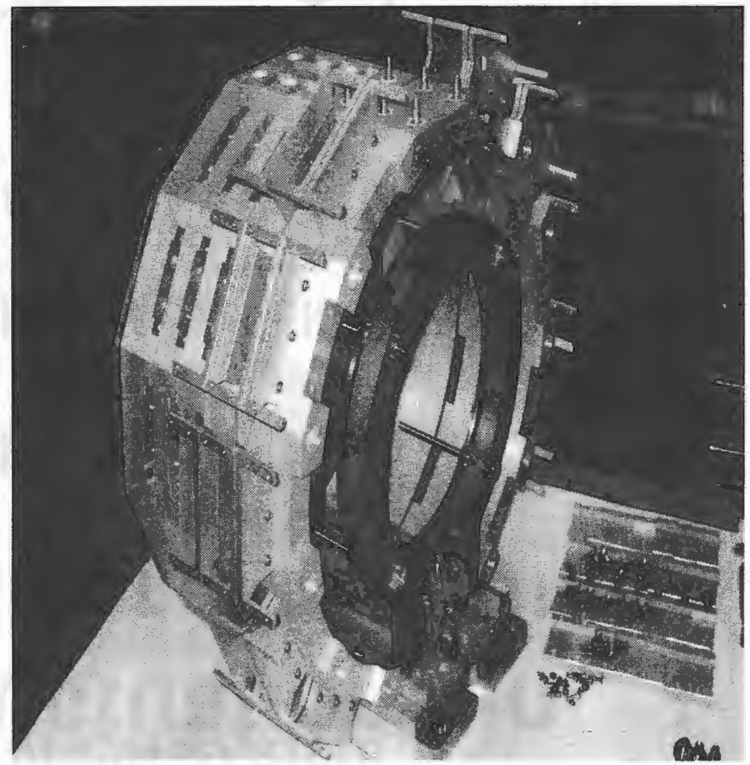

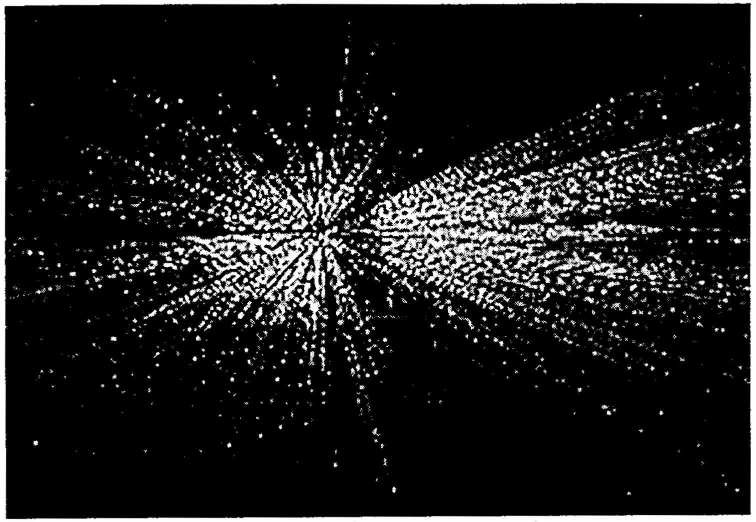

Nuclear Size Fluctuations in Nuclear Collisions

V.Uzhinsky, A.Galoyan

The first RHIC result – Large elliptic flow of particles

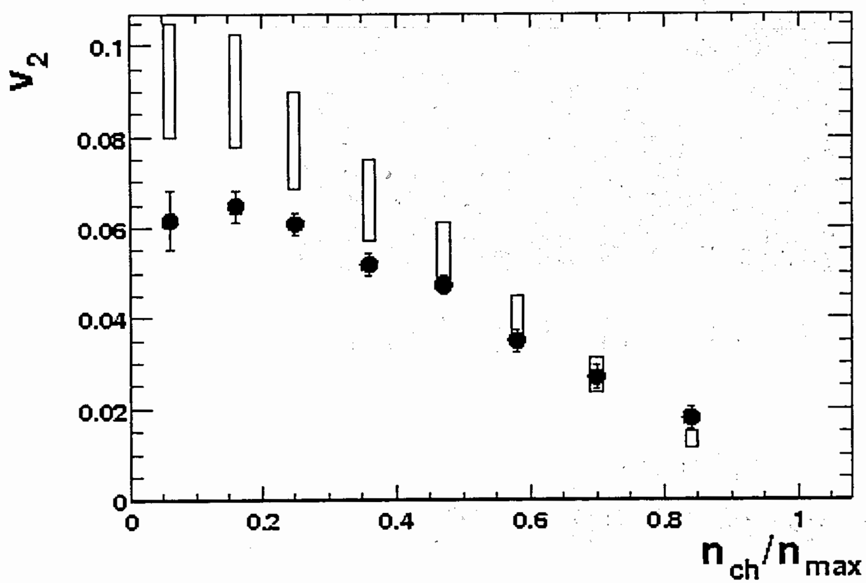

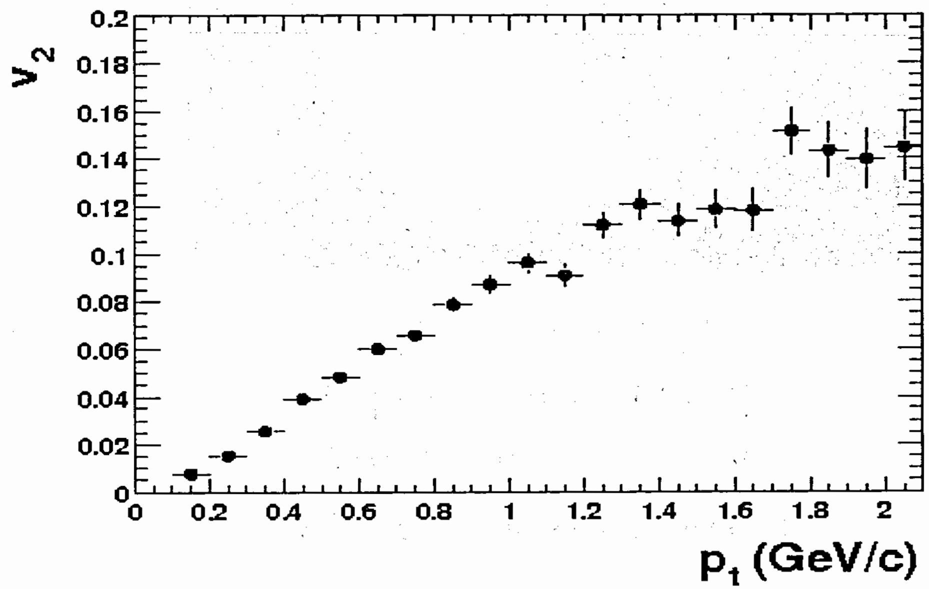

$$\frac{dN}{d(\phi-\Psi_R)} \propto \left(1+\sum_{n=1}^{\infty} 2v_n Cos(n(\phi-\Psi_R))\right) \qquad v_n = < Cos(n(\phi-\Psi_R)) >$$

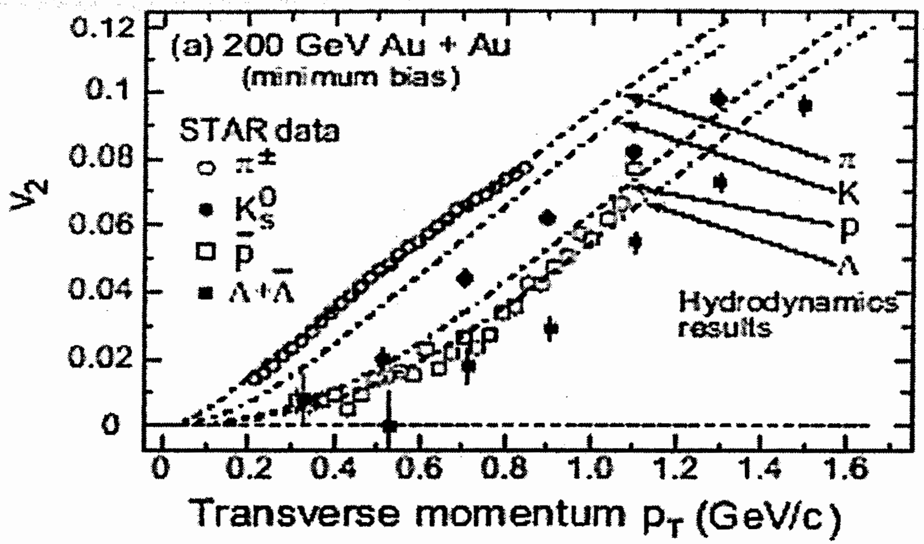

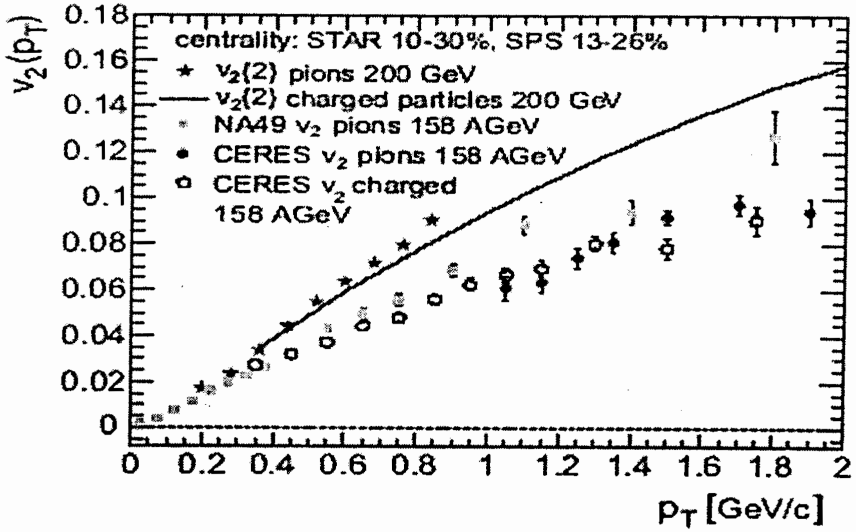

Hydrodynamic model

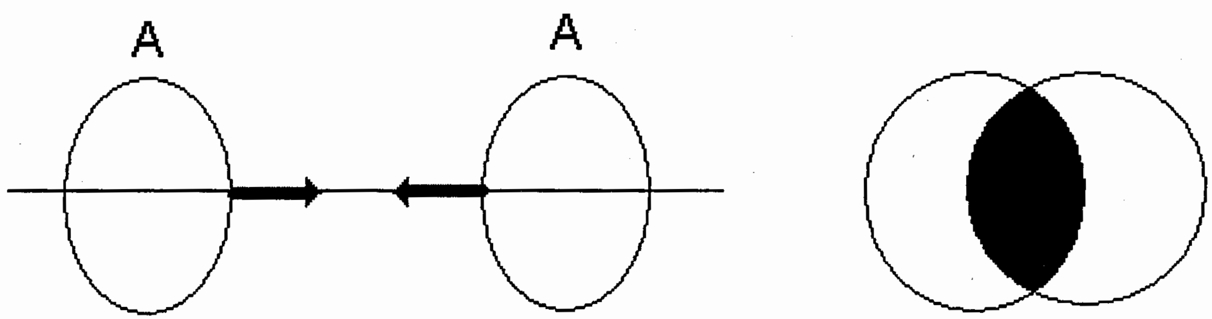

Nucleus is a quantum mechanical system.
How can one consider quantum fluctuations?
Especially size fluctuations.

$$|\Psi(\vec{r}_1, \vec{r}_2, ..., \vec{r}_A)|^2 = \prod_{i=1}^{A} \rho_A(\vec{r}_i)$$

$$\rho_A(r) = \frac{1}{4/3\pi R_A^3}\theta(R_A - r) \text{ – uniform sphere}$$

$$\rho(r) = Const/(1 + exp(\frac{r - R_A}{c})) \text{ -Saxon-Woods distribution}$$

Idea - A nucleus is a superposition of homogeneous spheres!

$$\rho_A(r) = \int f(R)\rho(r)dR$$
$$= \int f(R)\frac{1}{4/3\pi R^3}\theta(R - r)dR$$

$$\rho_A(r) = \frac{3}{4\pi}\int_r^\infty \frac{f(R)}{R^3}dR \quad f(R) = -\frac{4\pi R^3}{3}\rho'_A(R)$$

Pb-208, R_{Pb}=5.3 fm

Gaussian distribution

$$\rho_A(r) = \frac{1}{(\pi R_0^2)^{3/2}} e^{-r^2/R_0^2}$$

$$f(R) = \frac{8R^4}{3\sqrt{\pi}R_0^5} e^{-R^2/R_0^2}$$

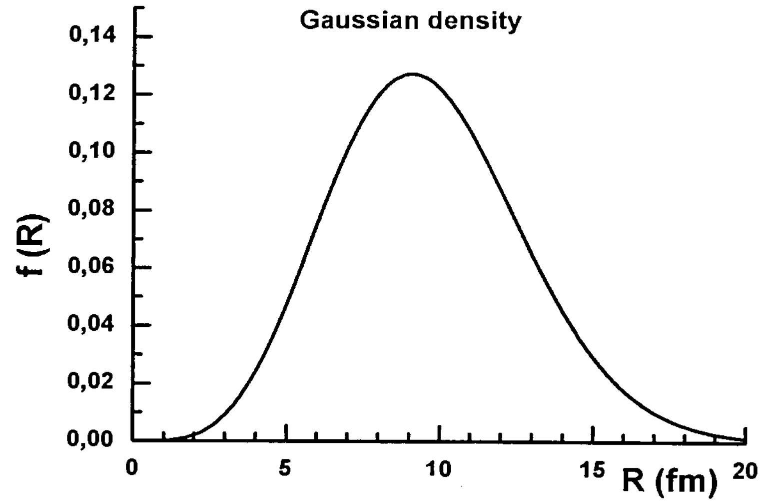

Saxon-Woods distribution

$$f(R) = Const\frac{4\pi R^3}{3c} e^{\frac{R-R_A}{c}} / (1 + e^{\frac{R-R_A}{c}})^2$$

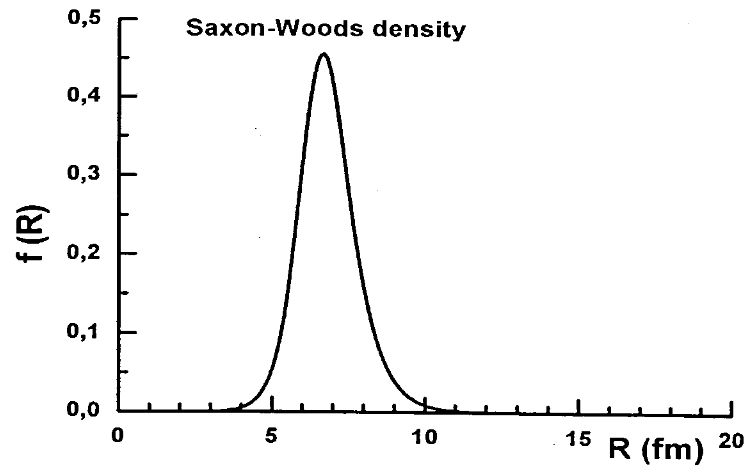

Size fluctuations are rather large! They must be taken into account in hydrodynamic calculations.

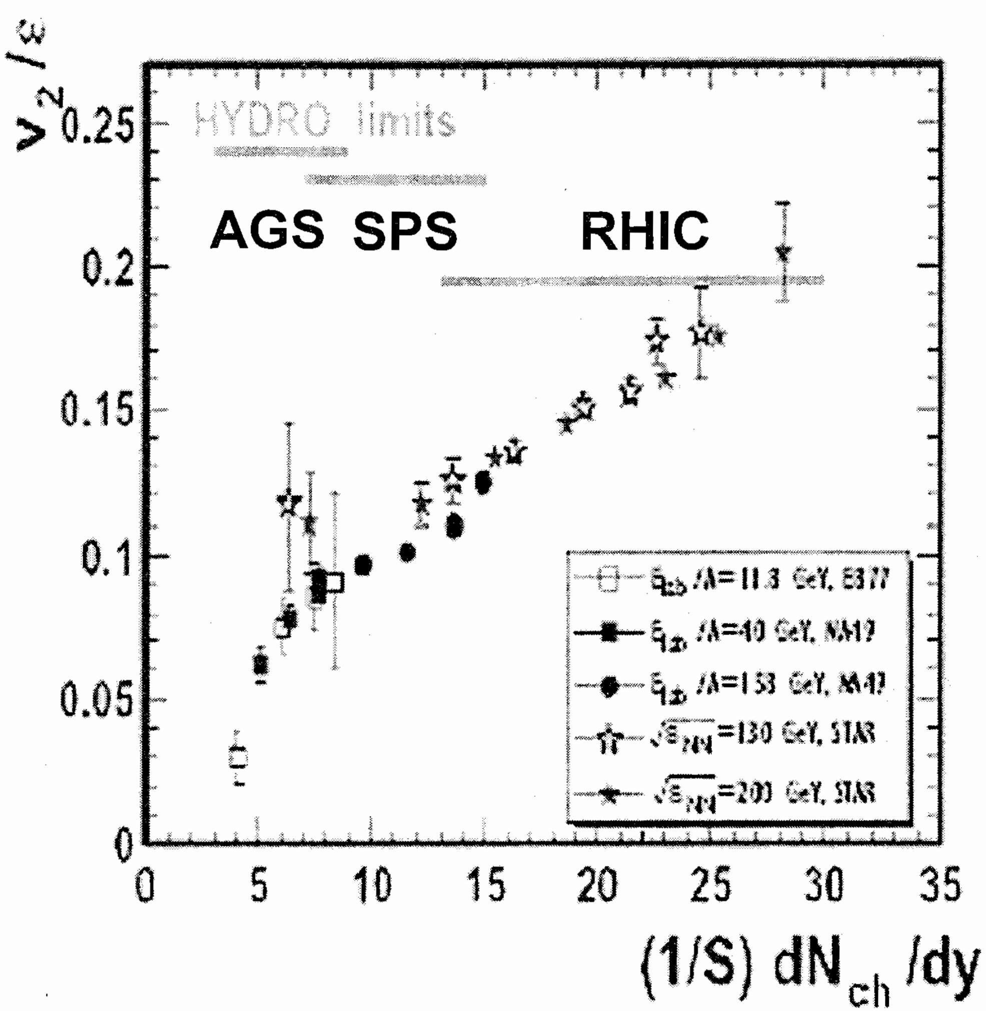

Mid-rapidity elliptic flow measurements from various energies and centralities combined in a single plot of v2 divided by relevant initial spatial eccentricity vs. charged-particle rapidity density per unit transverse area in the A + A overlap region. The figures, taken from Ref. [100], highlight the smooth behavior of flow vs. energy and centrality. The rightmost points represent near-central STAR results, where the observed v2/ϱ ratio becomes consistent with limiting hydrodynamic expectations for an ideal relativistic fluid. The hydrodynamic limits are represented by horizontal lines [100] drawn for AGS, SPS and RHIC energies (from left to right), for one particular choice of EOS that assumes no phase transition in the matter produced.

Where can it be used?

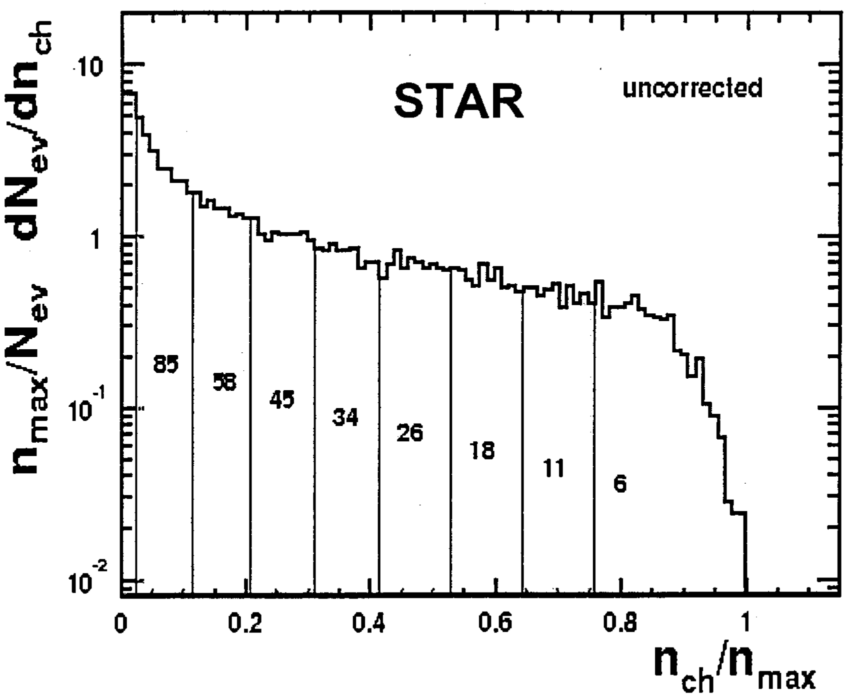

FIG. The primary track multiplicity distribution as a function of the number of tracks normalized by the maximum observed number of tracks. The eight centrality regions used in this analysis are shown. The integral under the curve is 1.0 and the cumulative fraction corresponding to the lower edge of each centrality bin is also indicated in percent.

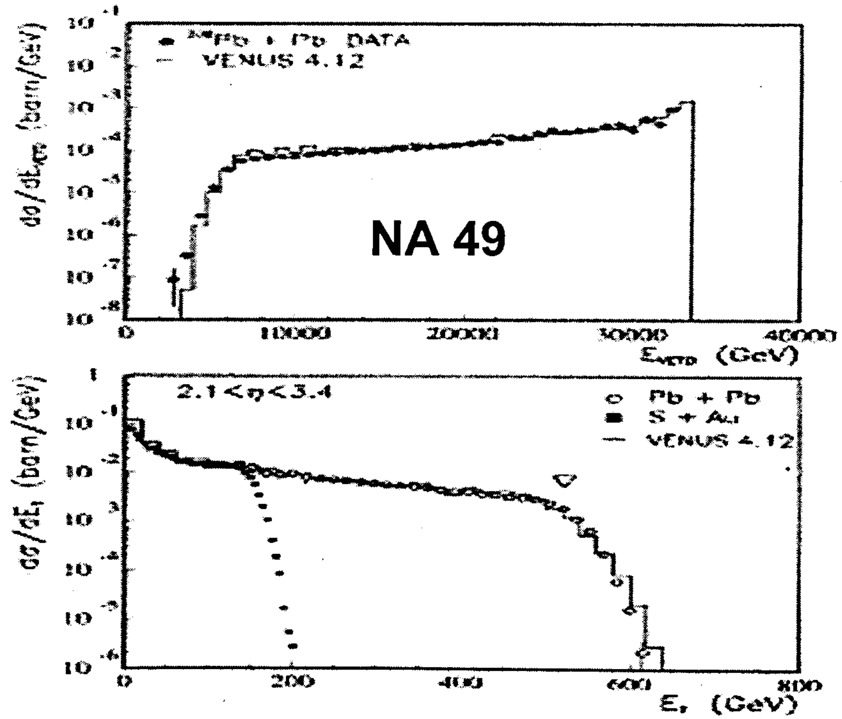

FIG. (top) Differential cross section of the energy measured in the veto calorimeter. Predictions of the VENUS model are also shown. (bottom) Differential cross section of the transverse energy produced in Pb + Pb and S + Au collisions, as measured by the ring calorimeter in the pseudorapidity range $2.1 < \eta < 3.4$. Results of the VENUS model are also shown. For explanation of the symbol ∇ see text.

What processes are dominated in high multiplicity events – multiple fluctuations in elementary (NN) collisions, or interactions of compact objects?

Sizes of interacting nuclei can be an essential parameter as the impact parameter.

Glauber approach

$$\sigma_{AB}^{in} = \int d^2b \left\{ 1 - \prod_{i=1}^{A} \prod_{j=1}^{B} \left[1 - \gamma\left(\vec{b} - \vec{s}_i + \vec{\tau}_j\right) - \gamma^*\left(\vec{b} - \vec{s}_i + \vec{\tau}_j\right) + \gamma\left(\vec{b} - \vec{s}_i + \vec{\tau}_j\right) \gamma\left(\vec{b} - \vec{s}_i + \vec{\tau}_j\right) \right] \right\} \cdot$$

$$\cdot \left\{ \prod_{i=1}^{A} \rho_A\left(\vec{s}_i, \vec{z}_i\right) d^3 r_i \right\} \left\{ \prod_{i=1}^{B} \rho_B\left(\vec{\tau}_i, \vec{\xi}_i\right) d^3 t_i \right\} \delta\left(\sum_{i=1}^{A} \vec{r}_i / A \right) \delta\left(\sum_{j=1}^{B} \vec{\tau}_j / B \right)$$

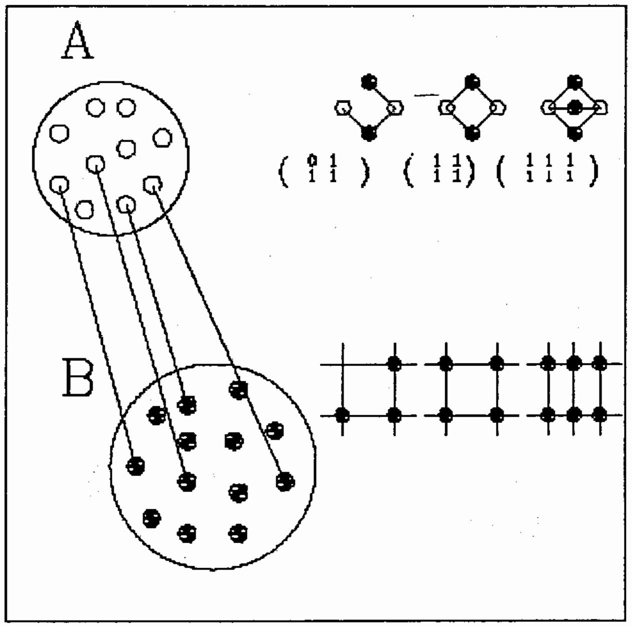

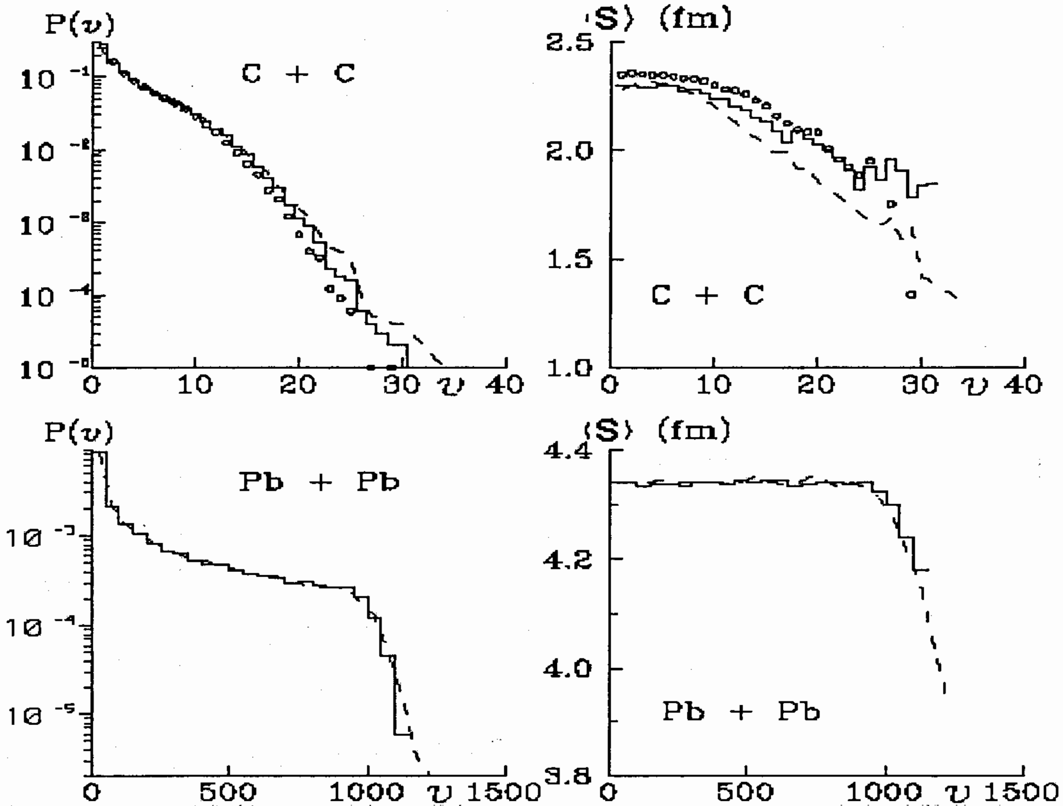

Size of a nucleus?

$$S = \sqrt{(\vec{r}_1^{\,2} + \vec{r}_2^{\,2} + ... + \vec{r}_A^{\,2})/A}$$

In case of deutron $S = r/2$

$$P(S) = \int \delta(S - \sqrt{(\vec{r}_1^{\,2} + ... + \vec{r}_A^{\,2})/A})\,|\Psi(\vec{r}_1, \vec{r}_2, ..., \vec{r}_A)|^2 d^3r_1 ... d^3r_A$$

$$|\Psi(\vec{r}_1, \vec{r}_2, ..., \vec{r}_A)|^2 = \prod_{i=1}^{A} \rho_A(\vec{r}_i)$$

$$\rho(r) = Const/(1 + exp(\frac{r - R_A}{c}))$$ -Saxon-Woods distribution

Standard Monte Carlo techniques

1) Sample nucleon coordinates according to the density;
2) Take center-of-mass correlations into account:
   - Shift center of mass of generated set to zero;
   - Sample for half of nucleons and ascribe to other half

$$\vec{R}_c = \frac{1}{A}\sum_{i=1}^{A} \vec{r}_i, \quad \vec{r}_i^{\,\prime} = \vec{r}_i - \vec{R}_c \qquad \{\vec{r}_i\}\ (i = 1...A/2),\ \ \vec{r}_i = \vec{r}_{i-A/2},\ \ (i = A/2 + 1...A)$$

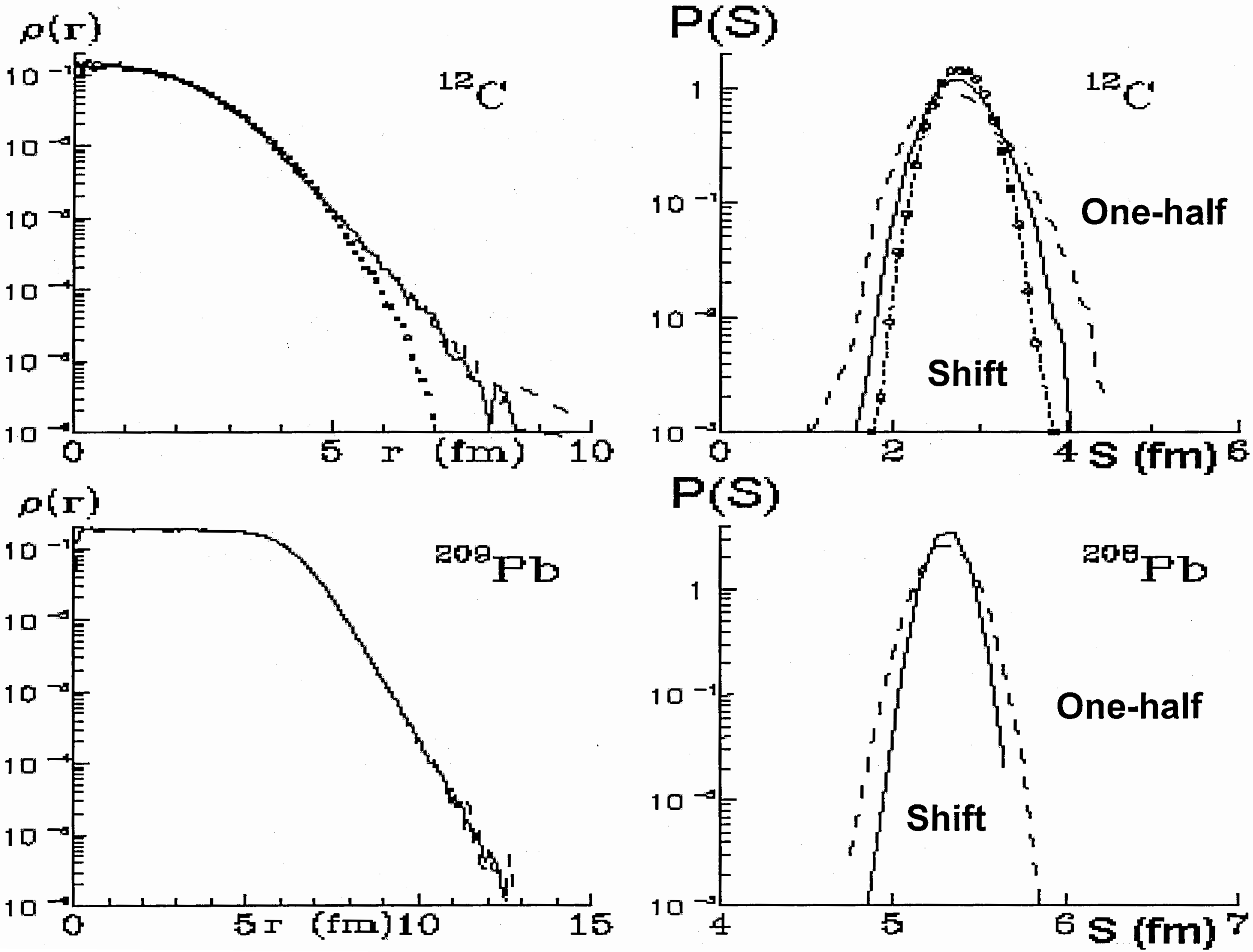
ρ(r)
^{12}C
r (fm)
P(S)
^{12}C
One-half
Shift
S (fm)
ρ(r)
^{208}Pb
r (fm)
P(S)
^{208}Pb
One-half
Shift
S (fm)

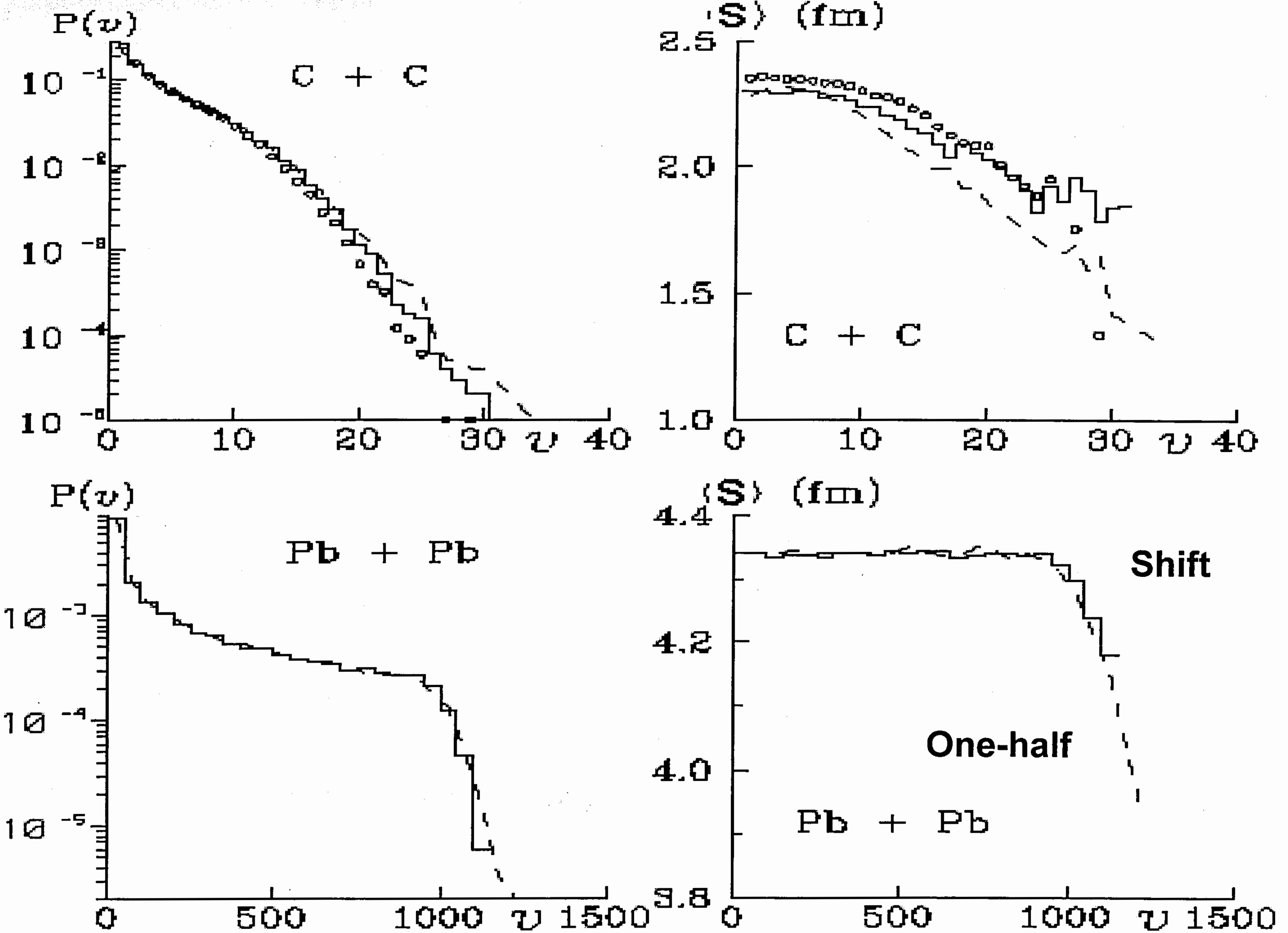
P(v)
C + C
10 -1
10 -2
10 -3
10 -4
10 -5
0 10 20 30 v 40
⟨S⟩ (fm)
2.5
2.0
1.5
1.0
C + C
0 10 20 30 v 40
P(v)
Pb + Pb
10 -3
10 -4
10 -5
0 500 1000 v 1500
⟨S⟩ (fm)
4.4
4.2
4.0
3.8
Shift
One-half
Pb + Pb
0 500 1000 v 1500

How can one simulate uniform distribution?

Standard procedure +/- CM correlations

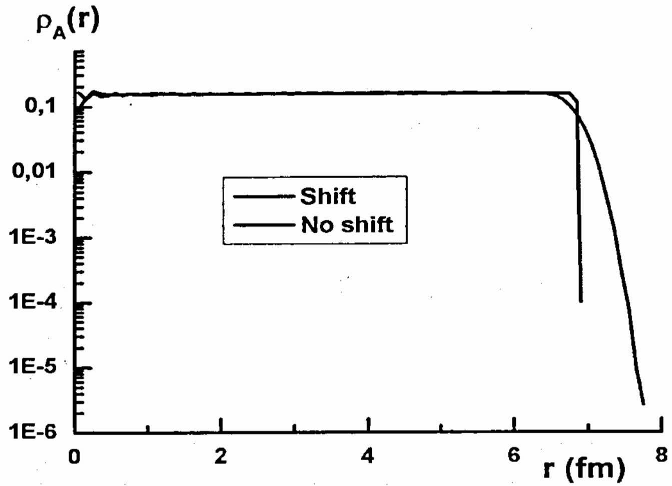

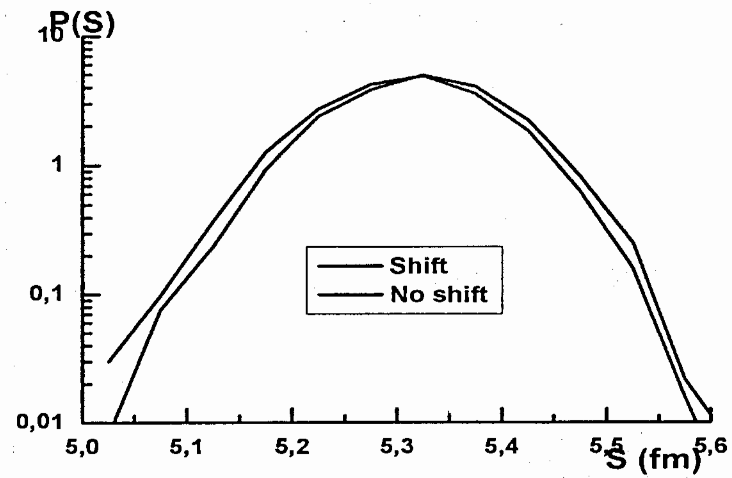

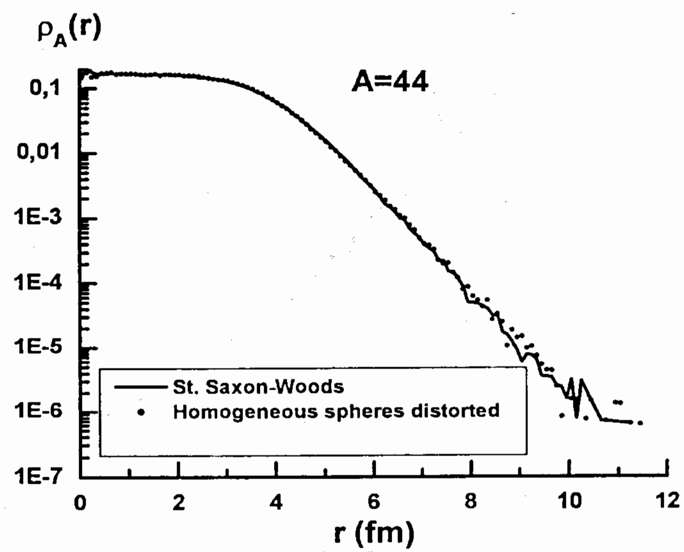

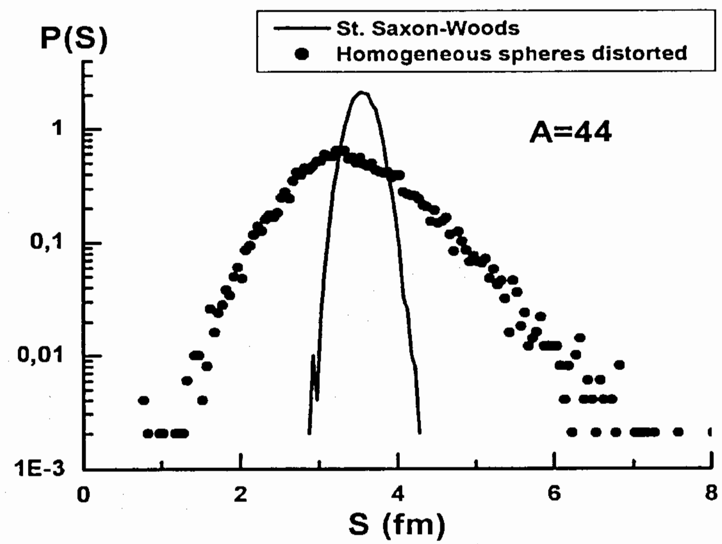

INTERACTIONS

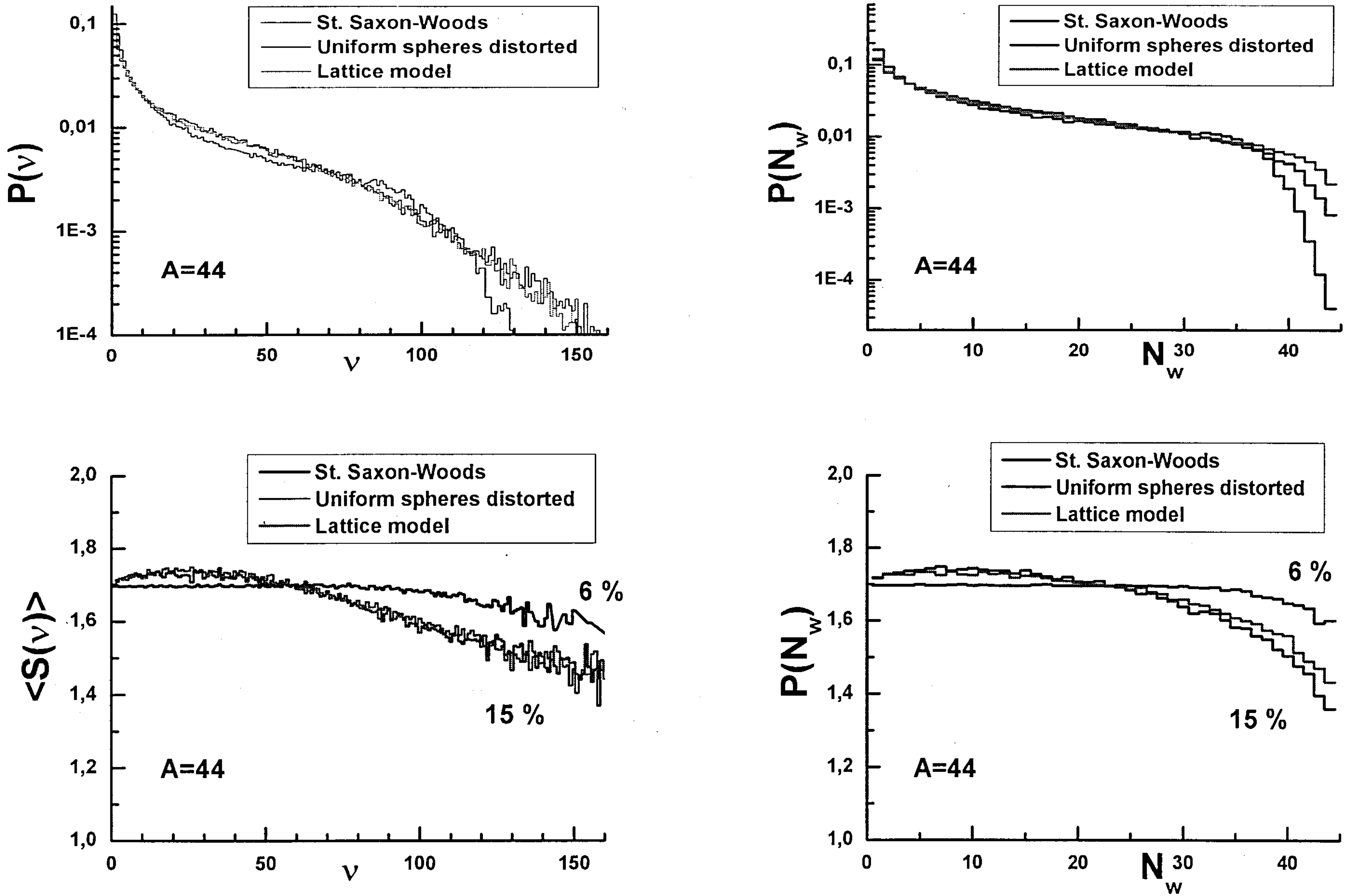

Lattice nucleus

N.D. Cook, T. Hayashi, Lattice model for quark, nuclear structure and nuclear reaction studies, J.Phys. G23: 1109-1126, 1997

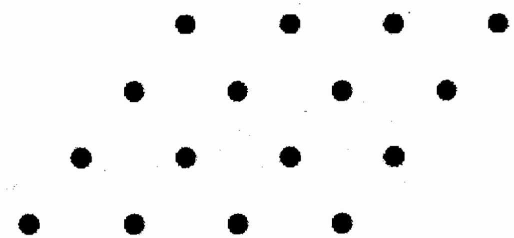

A=44

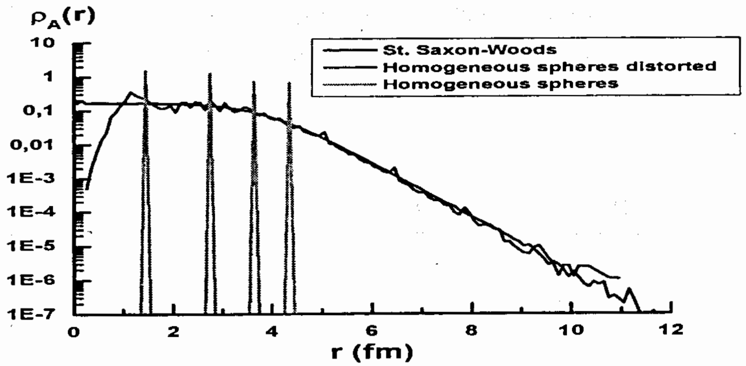

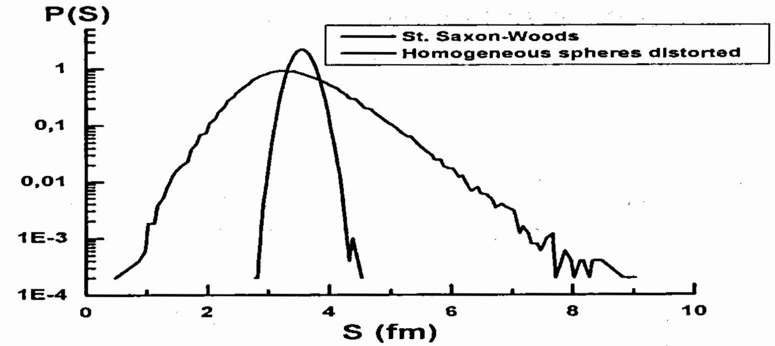

A=216

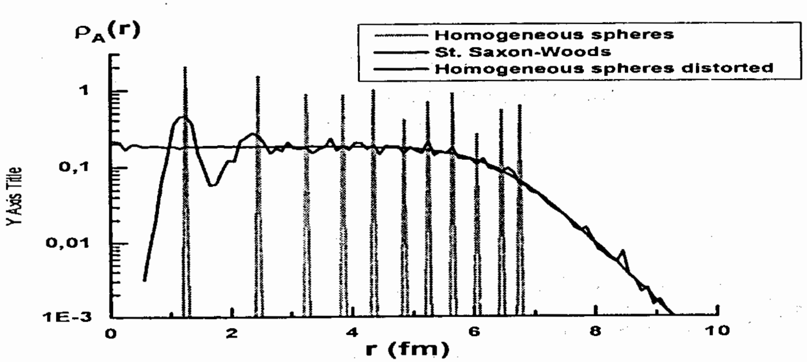

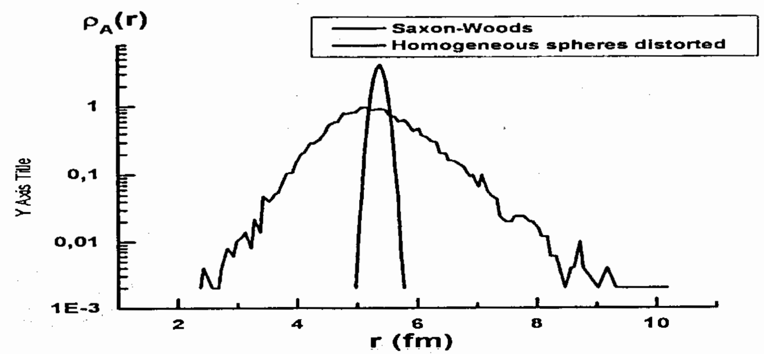

Weighted simulation

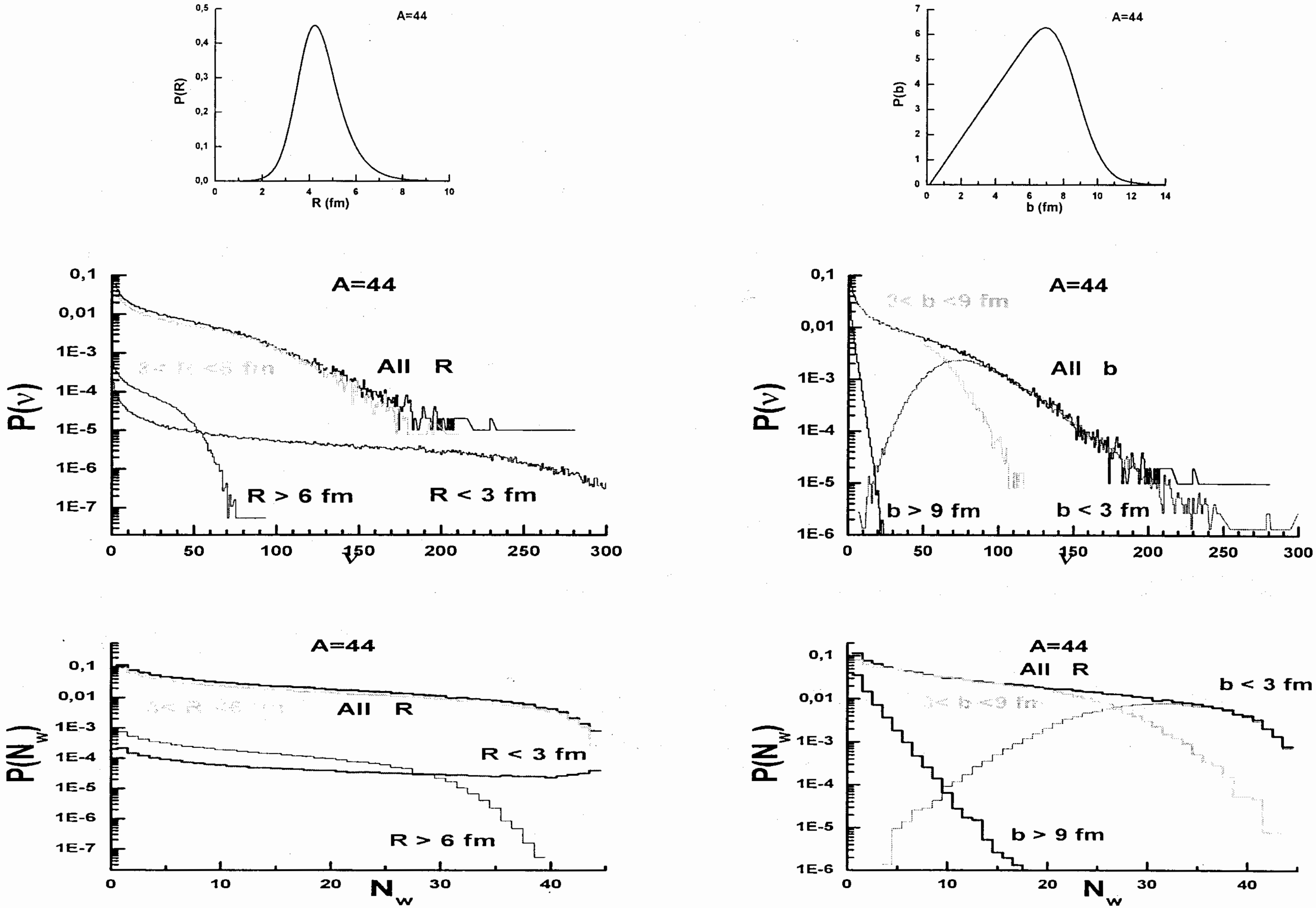

246

Conclusion

1. It is shown that nuclear size fluctuations are quite strong. They must be taken into account in hydrodynamic model.
2. According to the Glauber theory in ordinary approach the average nuclear size changes within 6-10 % in AA-interactions.
3. New method of weighted simulation of nucleus-nucleus interactions with high multiplicity of intra-nuclear collisions is proposed.
4. It is shown that in high multiplicity events nuclei with small sizes play essential role.
5. Effects of nuclear structure, especially nuclear size fluctuation, can be very important in nucleus-nucleus interactions with high multiplicity! (Multi-nucleon correlations)

PP-interaction

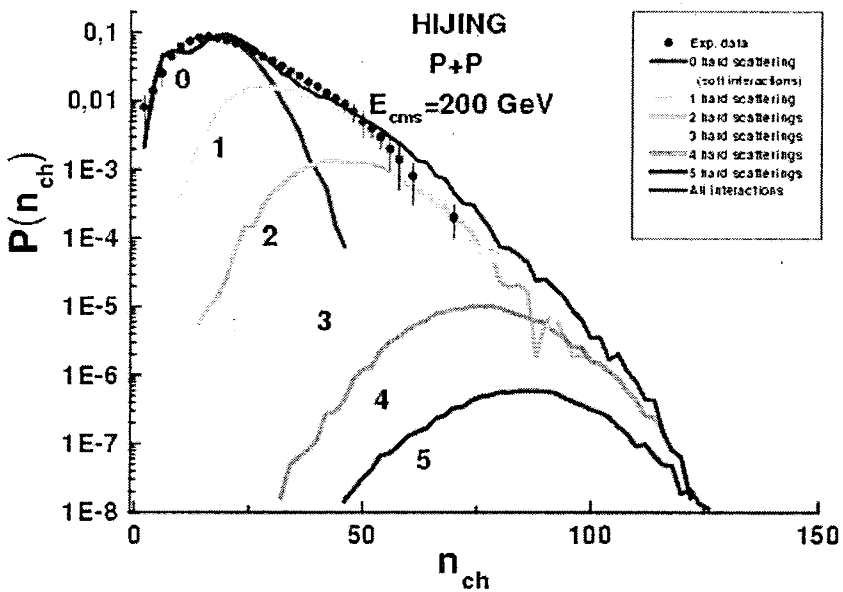

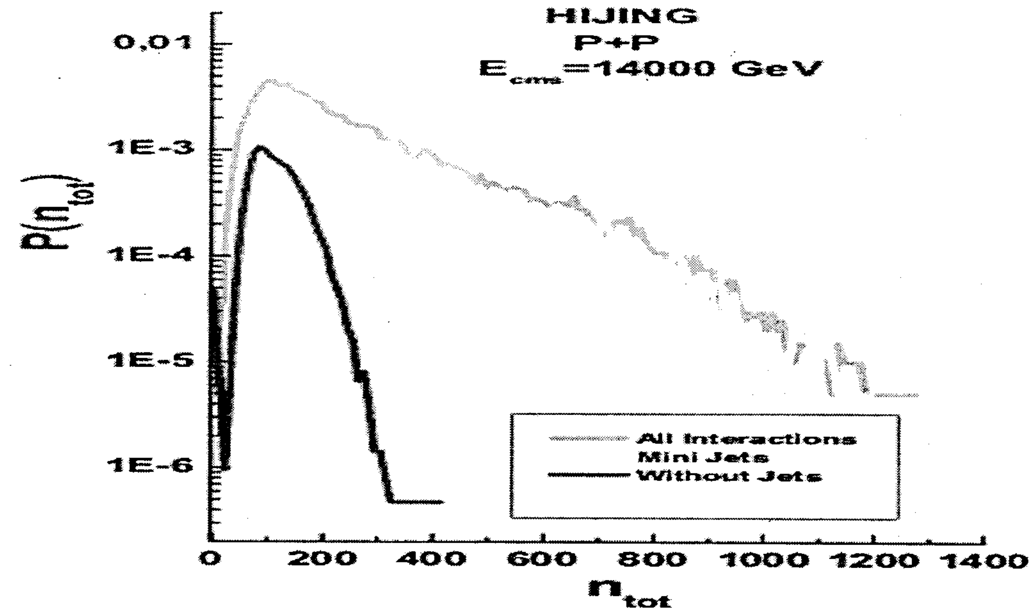

$P_{n\ jet}$ =?

A.Sissakian, J.Manjavidze

$P_{n\ jet} > O(e^{-n})$ (condensation)
$P_{n\ jet} = O(e^{-n})$ (Hard QCD)
$P_{n\ jet} < O(e^{-n})$ (Peripheral

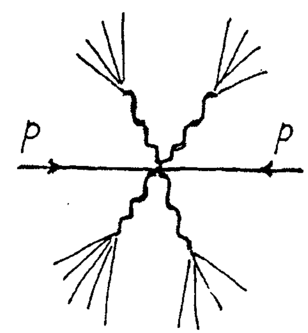

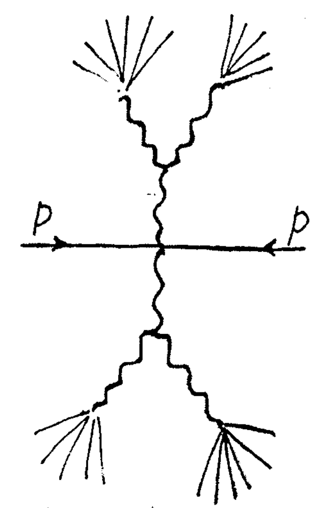

Jet energy measurement in CMS

Olga Kodolova, SINP MSU

Jet definition

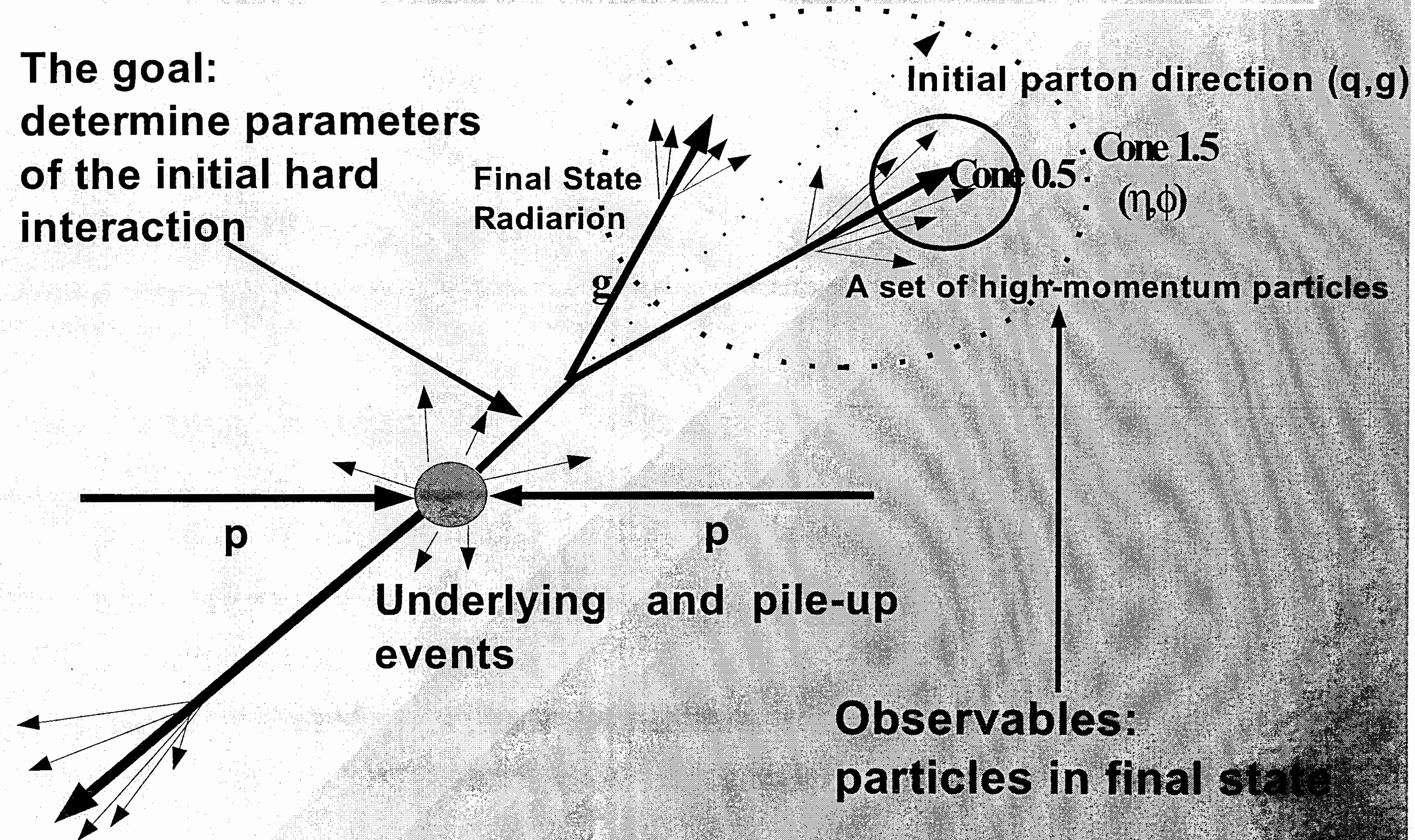

Jet definition - a set of high momentum particles

Factors influent on jet reconstruction

From jet physics (from parton to jet on particle level): previous slide

- Fragmentation
- ISR and FSR
- Underlying event
- Minimum bias (pile-up)

Leave for the physics channel study?

From detector performance (from jet on particle level to calorimeter jet):

- Magnetic field
- Electronic noise
- Dead materials and cracks
- Longatudinal leakage for high-Pt jets
- Shower size, out of cone loss, jet separations
- Calorimeter response to the particles

Develop common methodics?

CMS detector

CMS Longitudinal View

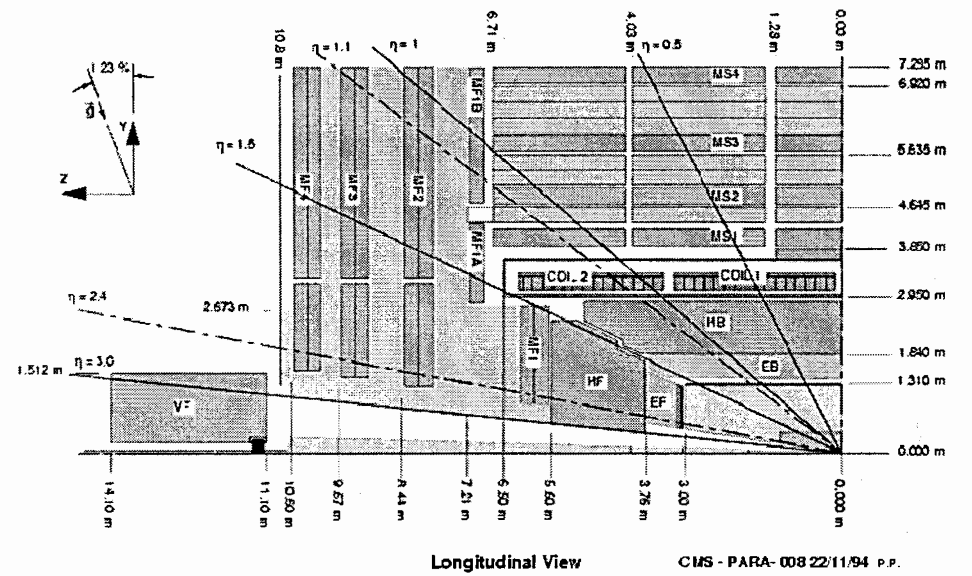

Tracker $|\eta|<2.5$

electromagnetic and hadronic calorimeters $|\eta|<3$

muon detector $|\eta|<2.4$

Very-Forward calorimeter $3<|\eta|<5$

4 Tesla magnetic field

Proposed additional calorimeter

CASTOR $5<|\eta|<7$

Detector effects influent on jet reconstruction

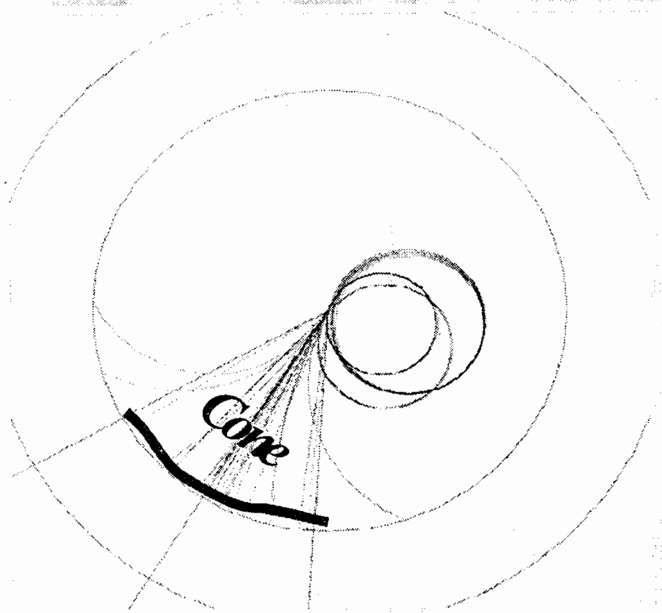

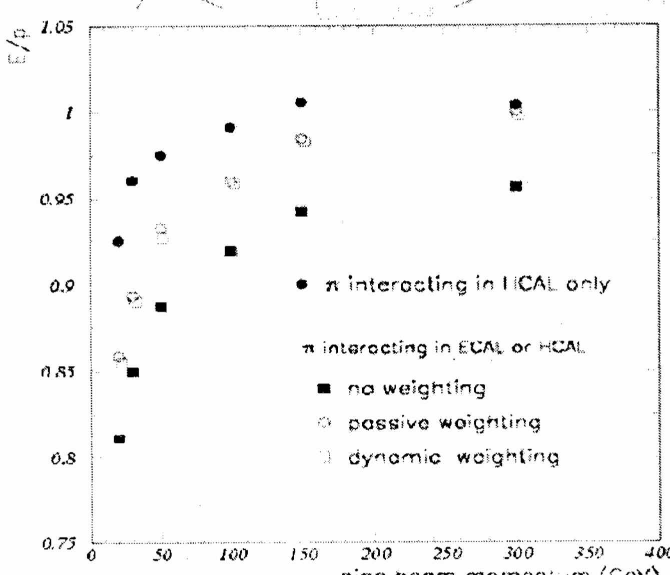

Magnetic field effect

Radius of ECAL front ~1.3m
Charged particles with Pt<0.8 GeV/c -> looper in barrel.
Charged particles with Pt<1.6GeV/c deflects by 0.5 radians.

Nonlinearity of calorimeter response

- Calorimeter consists of two compartments and both has different response to electrons and hadrons
- Jets have both hadronic (charged and neutrals) and e/γcomponents.

Cracks

Non-instrumental gaps between different part of calorimeters

Jet reconstruction procedure in CMS:
I) to find jet with one of the jet finding algorithms

1) Cone based

simple cone algorithm

iterative cone algorithm

midpoint cone algorithm

→ *Generated jet is considered as a set of particles (particle jet) at the vertex level in the definite cone R_{cone}^{gen}*

Reconstructed jet is considered as a set of calorimeter towers at the calorimeter level in the definite cone R_{cone}^{reco}

---

2) Kt algorithm

(with different stopping parameters)

→ *Generated jet is considered as a set of particles at the vertex level got with Kt algorithm*

Reconstructed jet is considered as a set of calorimeter towers at the calorimeter level got with Kt

---

Noise and pile-up have to be suppressed as the first step before any of these algorithms start.

Noise and pile-up events

Only noise is included

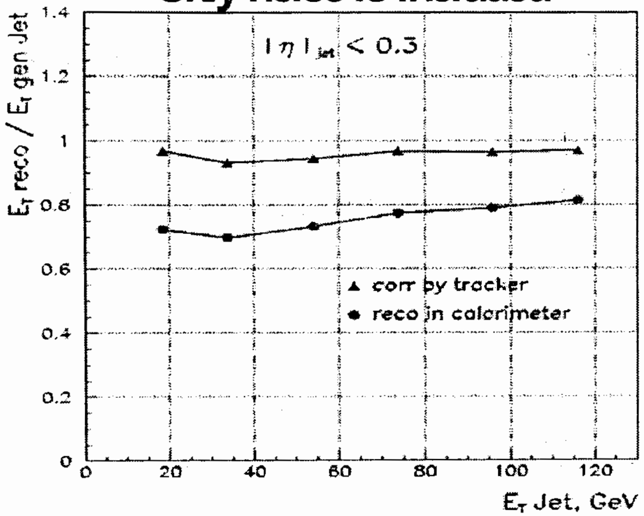

Pb-Pb central event

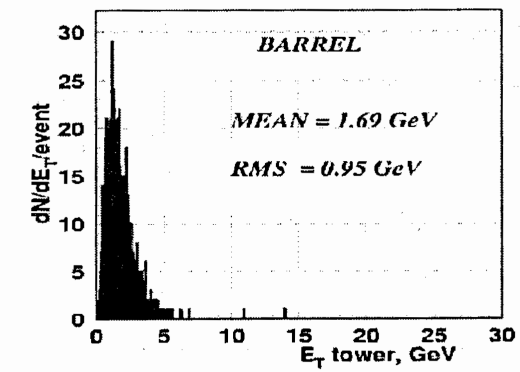

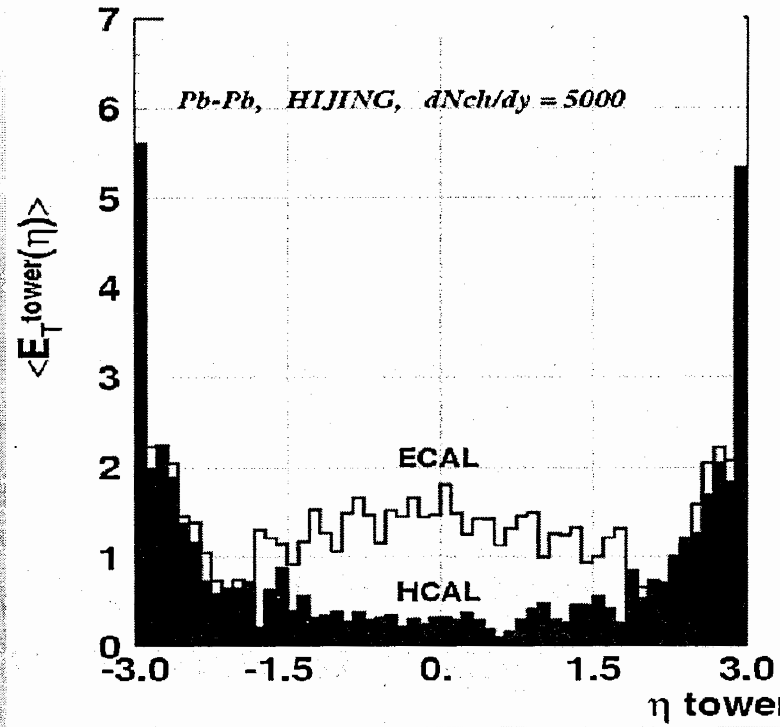

Electronic noise gives 5 GeV in cone 0.5 (η,ϕ)

Low luminosity pile-up gives >2.5 GeV in cone 0.5 in pp.

High luminosity pile-up gives >10 GeV in cone 0.5 in pp.

Number of pile-up events depends on time

Noise and pile-up suppression: <u>subtraction based on mean value</u>

mean value is determined over large min bias or QCD event sample:

- constant cut on tower energy (E cut - noise subtraction)
- constant cut on tower transverse energy (Et cut - noise and pile-up subtraction)
- sliding window (E cut depending on pseudorapidity - advanced noise and pile-up subtraction, possible taking into account geometry) Arno Heister

mean value is determined on event-by-event basis: pile-up subtraction algorithm

- calculate average energy and dispersion in tower (in eta rings) for each event
- subtract average energy and dispersion from each tower
- find jets with jet finder algorithm (any) using the new tower energies
- recalculate average energy and dispersion using towers free of jets
- recalculate jet energies

noise, pile-up, geometry are taking into account automaticaly

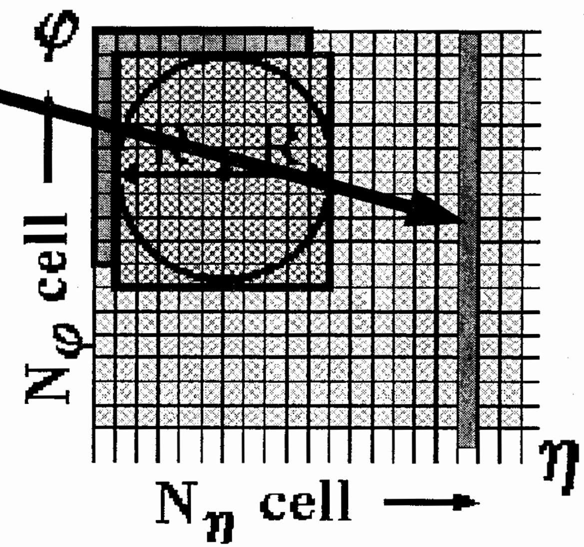

I.Vardanyan, A.Oulianov

Pile-up subtraction algorithm

I.Vardanyan
O.Kodolova
A.Oulianov

50 GeV jet
pp, $L=10^{34}$ $cm^{-2}s^{-1}$

Without pile-up subtr

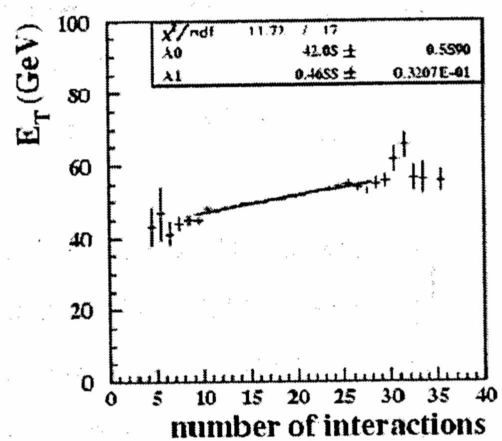

With pile-up subtr

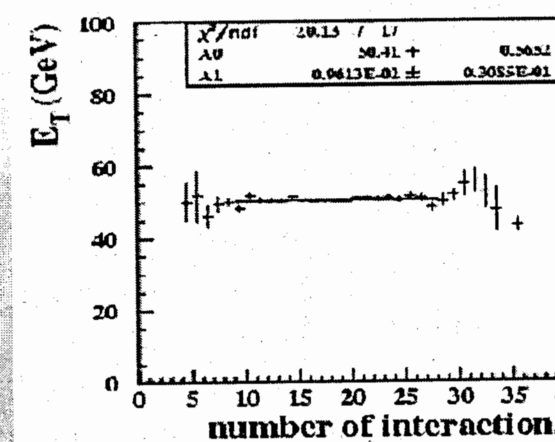

Pb+Pb
$dN_{ch}/dy=5000$

Without pile-up subtr

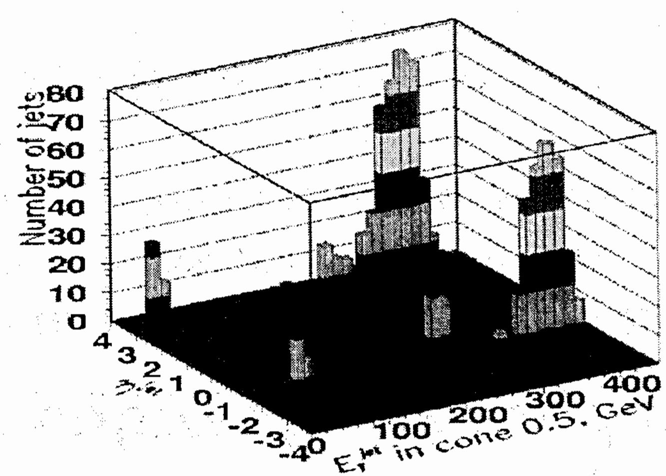

With pile-up subtr

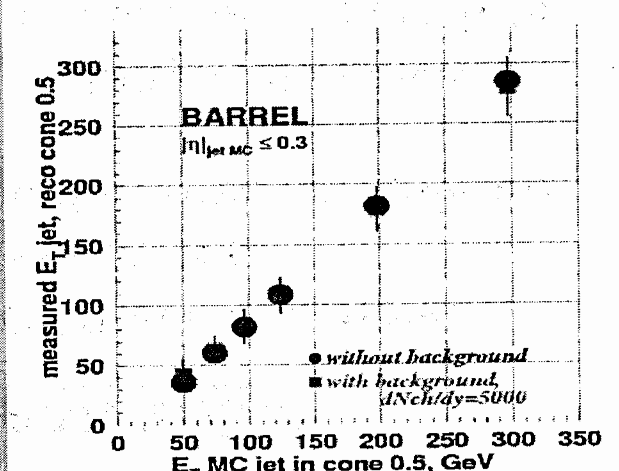

Linearity, resolution and efficiency before corrections

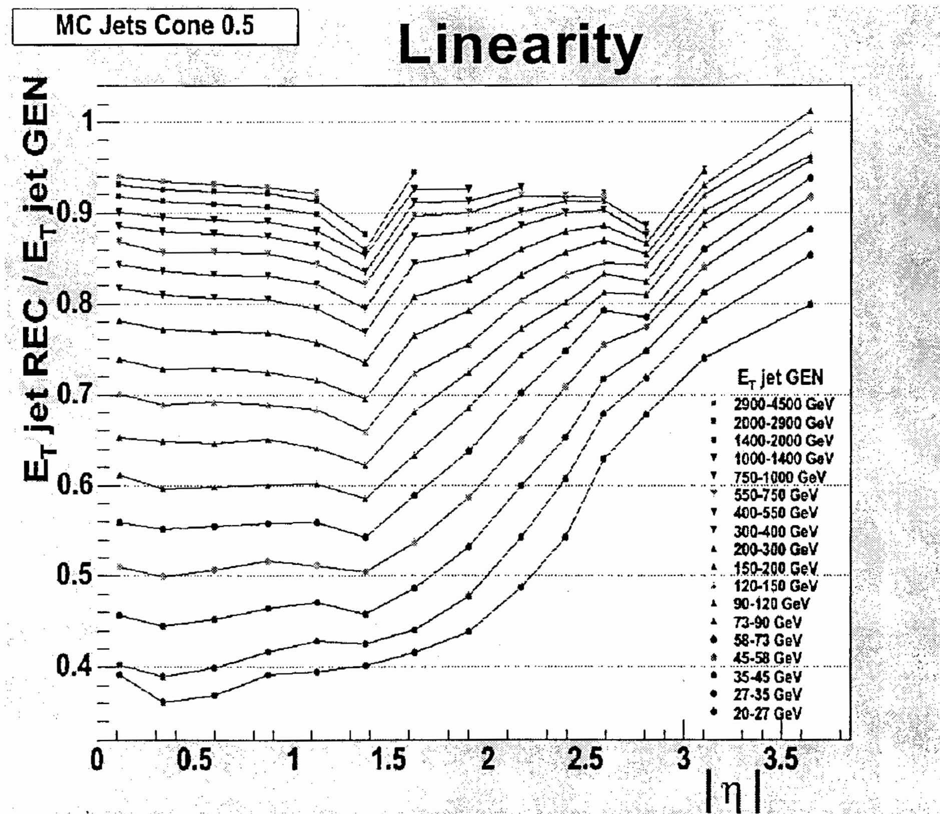

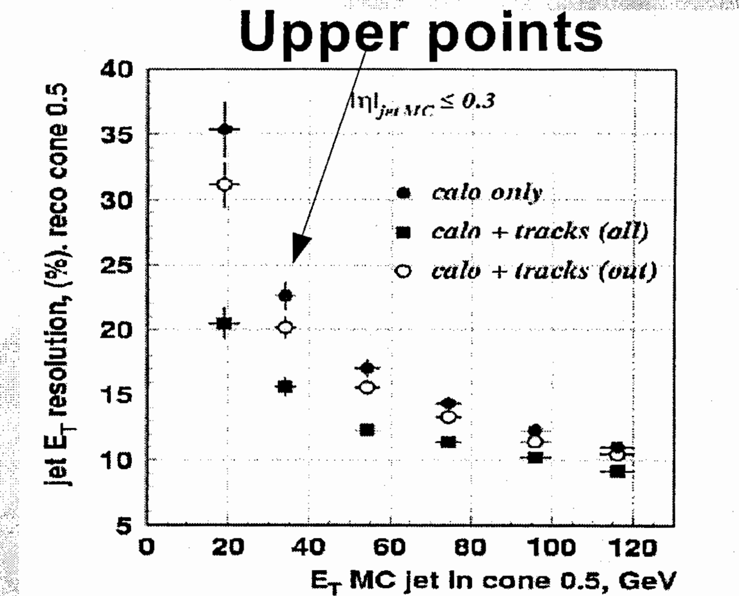

E_T jet resolution:

$\sigma(\langle E_T^{rec}/E_T^{MC}\rangle)/\langle E_T^{rec}/E_T^{MC}\rangle$

depending on E_T^{MC} of jet

120%/sqrt(E) without corrections

Efficiency and linearity depends on the cut on the tower, on the jet seed, on the reconstructed jets

Jet reconstruction procedure in CMS: II) To apply jet energy correction

Jet based ($|\eta|<4.5$):

1) $E = a \times (EC+HC)$, a depends on jet(E_T,η)

2) $E = a \times EC + b \times HC$, a, b depend on jet($E_T,\eta$)

from data: g/Z+jet, masses (Z,W,...)

from Monte-Carlo generators

Particle based ($|\eta|<4.5$):

3) $E = em + had$ (requires to separate em/had clusters)

$em = a \times EC$ for e/g

$had = b \times EC + c \times HC$, for had.

b (c) depend on EC (HC)

Use of tracks ($|\eta|<1.9$):

4) $E = E_0$ + (Tracks swept away by 4T field)

5) E = EC(e/g+neutral) + HC(neutral) + Tracks

QCD Monte-Carlo correction (jet based)

Robert Harris
S.Petrushanko

Response = ET_reconstructed_jet/ET_generated_jet

Correction = 1/Response as a function of E_T and η of jet

Application area:
QCD MC jet correction is applied to particle jet assuming that Monte-Carlo generator is adopted to the experiment.

Features:
QCD MC jet correction depends on the jet finding algorithm, on the cone size, on the level of noise and pile-up in event. -> a set of curves vs (P_T,η) has to be provided
QCD MC jet correction has systematics connected with parton species and selections to suppress background. In qcd jet sample there are 70% of g and 30% of q.

QCD Monte-Carlo correction (example)

S.Petrushanko

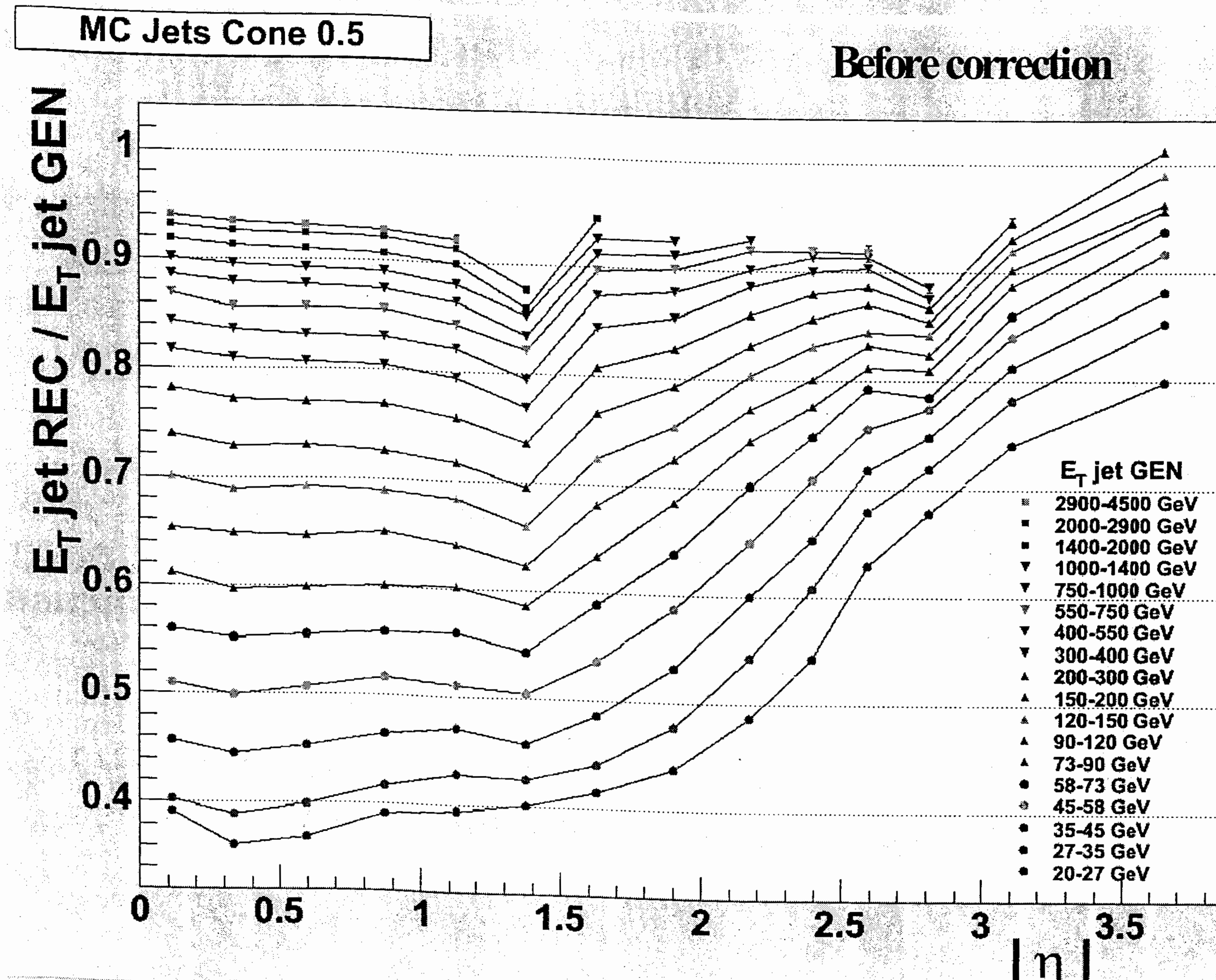

QCD Monte-Carlo correction (example)

S.Petrushanko

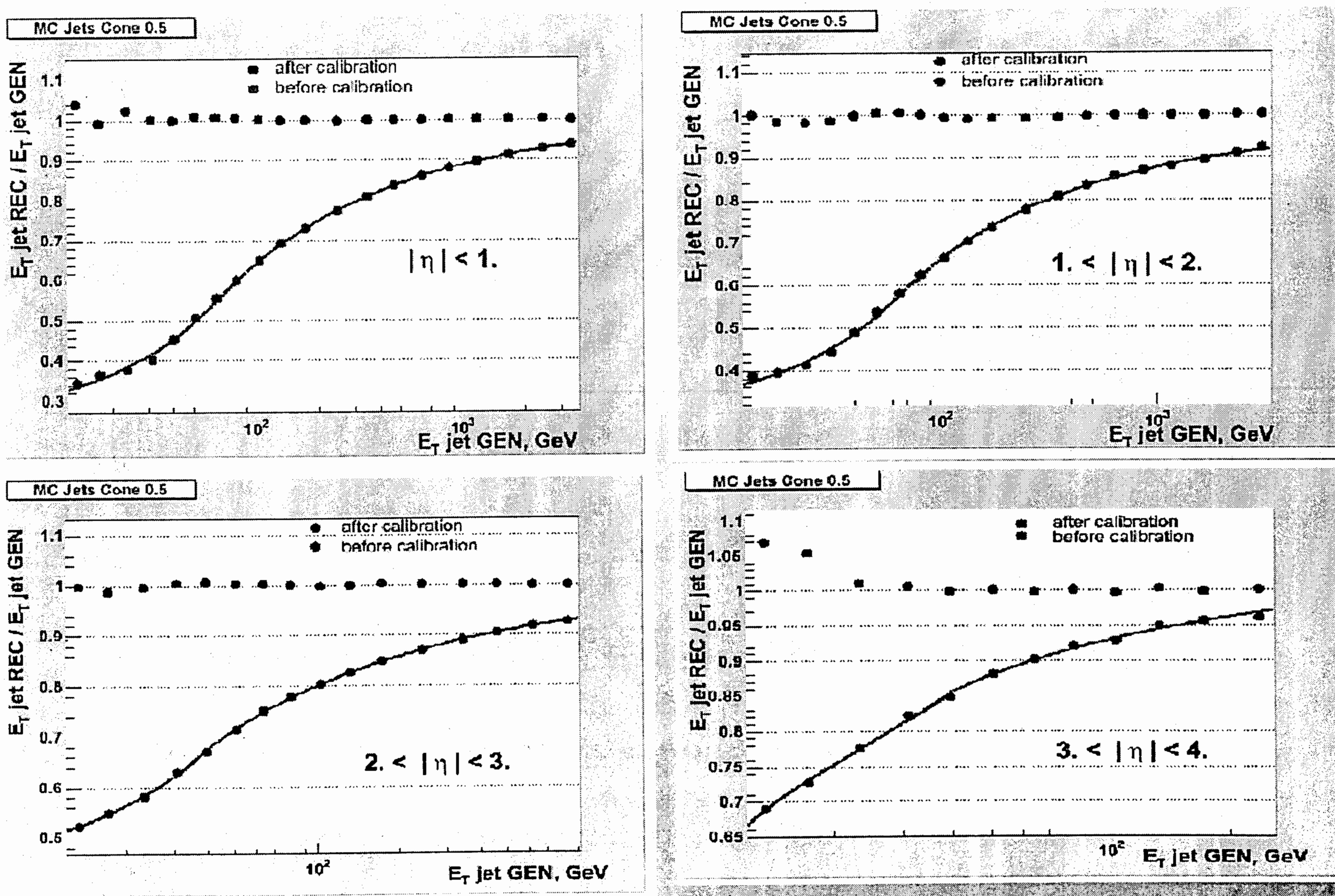

QCD Monte-Carlo correction (example)

After correction

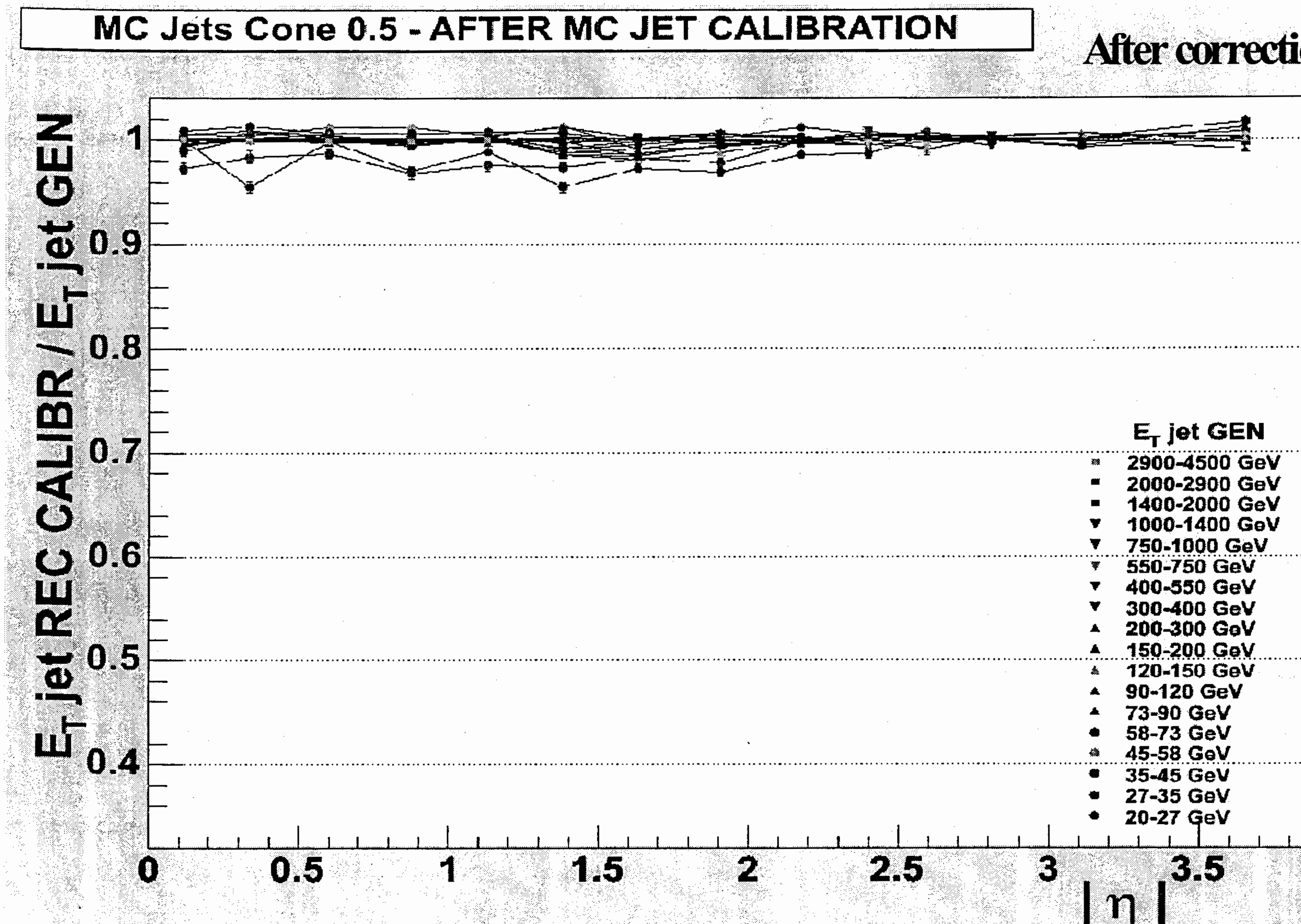

γ+jet correction (jet based)

Victor Konopliannikov
Alexei Oulianov

Tasks & strategy: parton energy scale

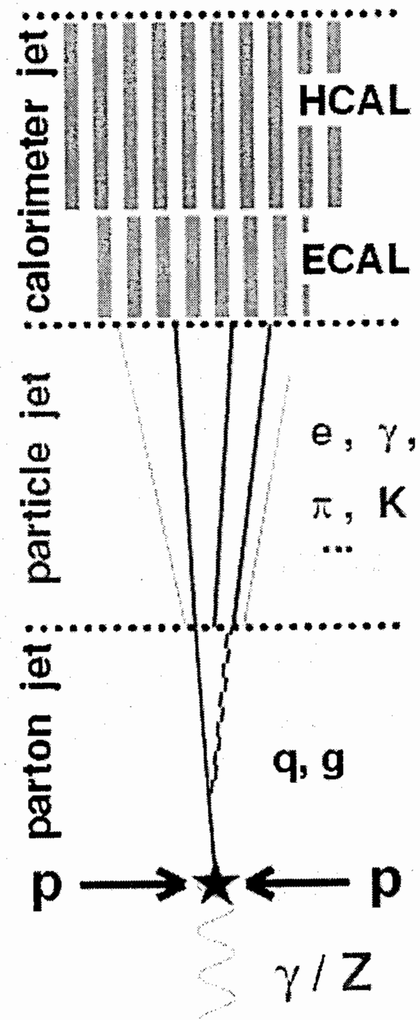

Calorimeter jet → parton: $E_{parton} = \dfrac{E^{reco}_{jet}}{k_{jet}}$

Parton jet correction

$$k_{jet} \equiv \frac{P^{reco}_{T\,jet}}{P_{T\,parton}} \approx \frac{P^{reco}_{T\,jet}}{P_{T\,\gamma/Z}}$$

using P_T-balance between parton and γ / Z:

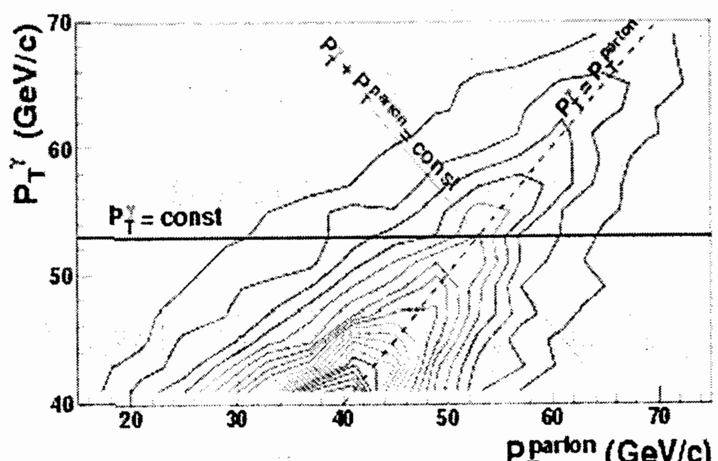

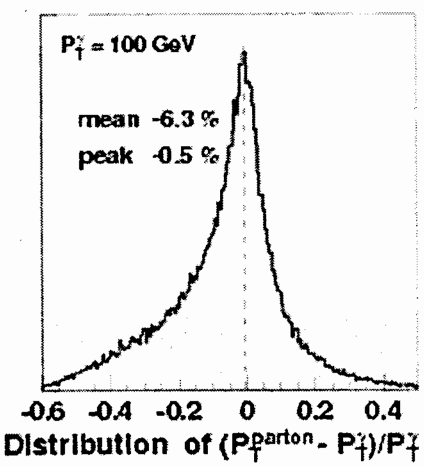

γ+jet correction (jet based)

Tasks & strategy: particle jet energy scale

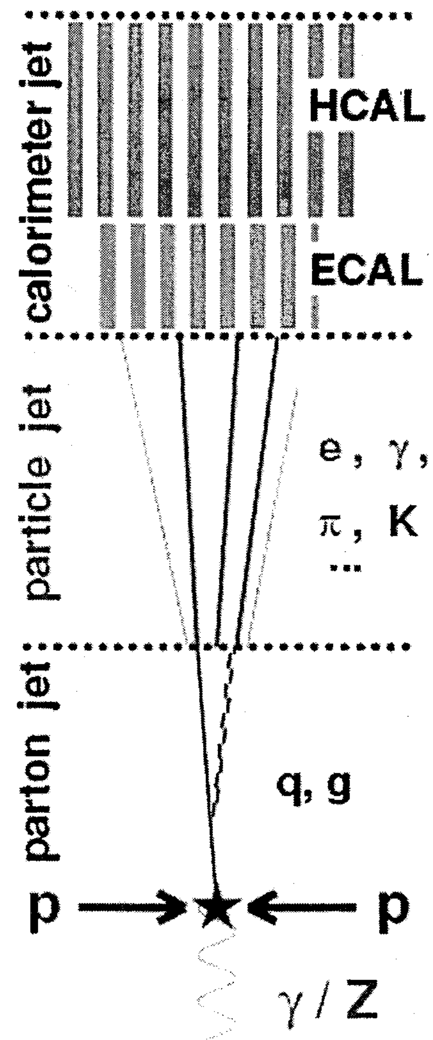

Parton → particle jet:

$$E_{jet}^{ptcl} = E_{parton} k_{ptcl} = \frac{E_{jet}^{reco}}{k_{jet}} k_{ptcl},$$

$$k_{ptcl} \equiv \frac{P_{Tjet}^{ptcl}}{P_{Tparton}}$$

k_{ptcl} **is MC-coefficient**

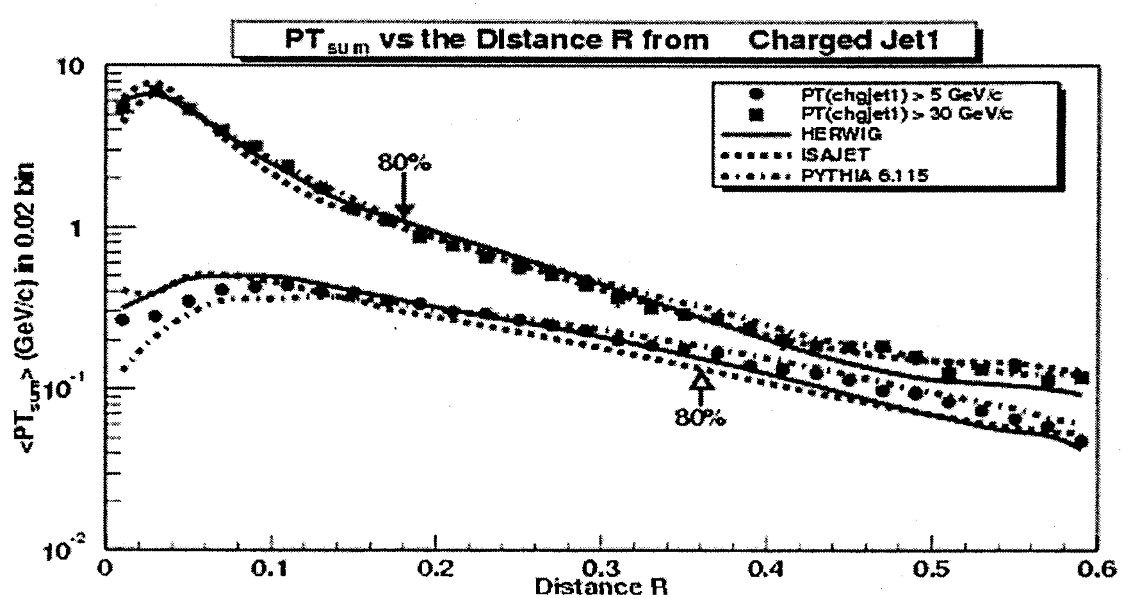

γ+jet correction (jet based)

V.Konopliannikov
A.Oulianov

Application area:

γ+jet correction is applied to parton (direct use of the initial γ-jet E_T balance)

γ+jet correction is applied to particle jet with the additional MC correction taken into account the difference between parton and particle jet.

Features:

γ+jet correction depends on the jet finding algorithm, on the cone size, on the level of noise and pile-up in event. -> a set of curves vs (P_T,η) is needed

γ+jet correction has systematics connected with parton species and selections to suppress background. In γ+jet sample there are 90% of q and 10% of g. There is a background from the dijet events (with leading π^0).

Response subtraction algorithm (use of tracks)

Jet energy=Response_charged+Response (e/γ)+Response (neutral)

- **Replace response of charged hadron of jet in reconstruction cone with energy of charged from Tracker.**

Jet energy=sum(Pin) + sum(Pout)+ Response (e/γ+neutral)_ECAL + Response (neutral)_HCAL

- **Add tracks out of reconstruction cone**

Expected response of charged particles can be calculated in different ways: e/π technique, library of responses, matched clusters (not implemented yet)

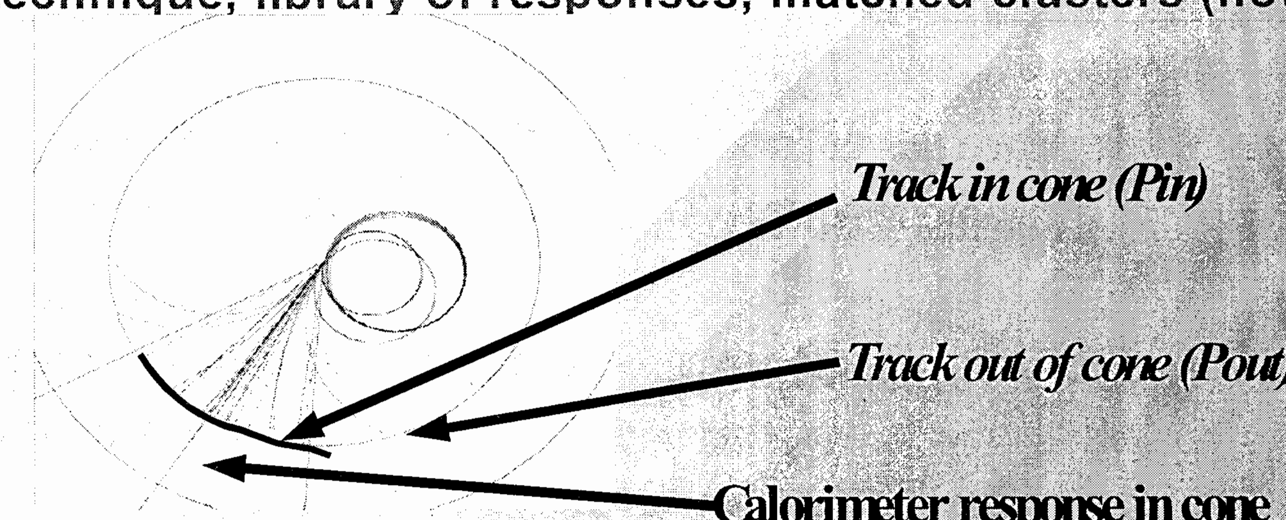

Remark: e/π technique (Dan Green, Energy flow in CMS Calorimetry, Fermilab-FN-0709, V.V.Abramov et al, CMS NOTE 2000/003)

Jet energy correction using tracker measurements (response subtraction procedure, CMS NOTE 2004/015, Accepted for publication in EPJC).

Single jets: linearity

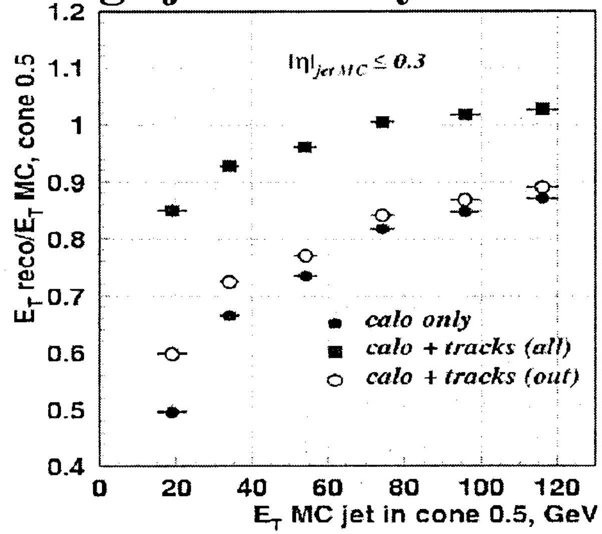

resolution

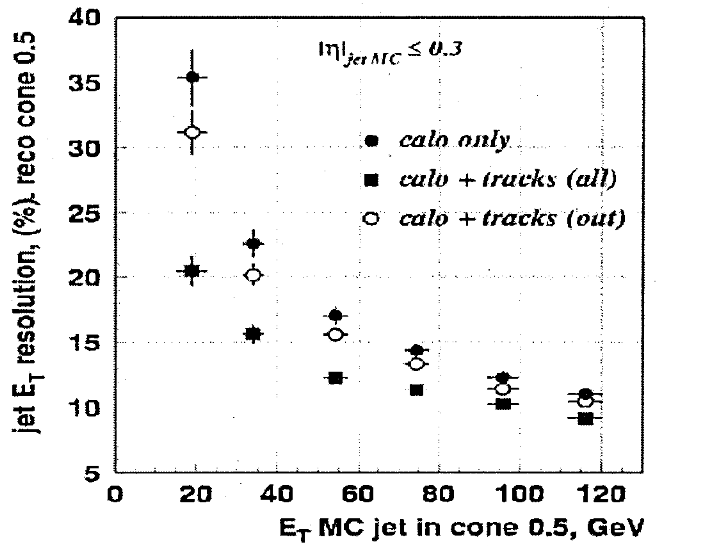

I.Vardanyan
O.Kodolova
A.Nikitenko
and G.Bruno
L.Fano

Mass of Z' (120 GeV)

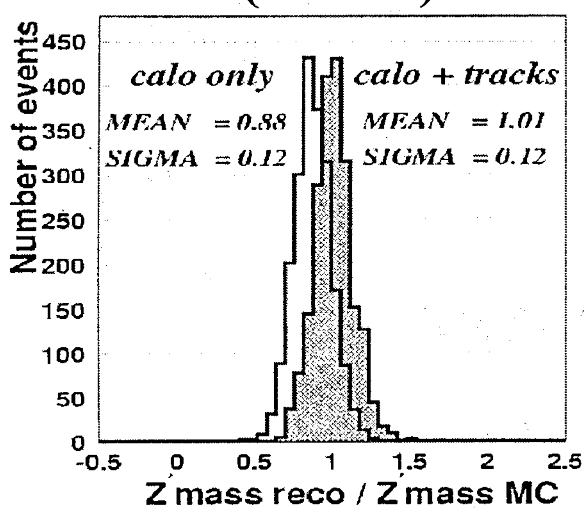

$L = 2x10^{33} cm^{-2} s^{-1}$

Resonance	Calo	Calo + tracks
Z' (120 GeV)	0.88+-0.12	1.01+-0.12
H (125 GeV)	0.84+-0.11	1.006+-0.11

Improvement in resolution

(sigma(<Mrec>/<Mmc>)/<Mrec/Mmc>) ~15%

ORCA:Jets/JetCalibration

Pile-up subtraction and tracker correction (on going study)

I.Vardanyan

100 GeV jet superimposed with AA event.

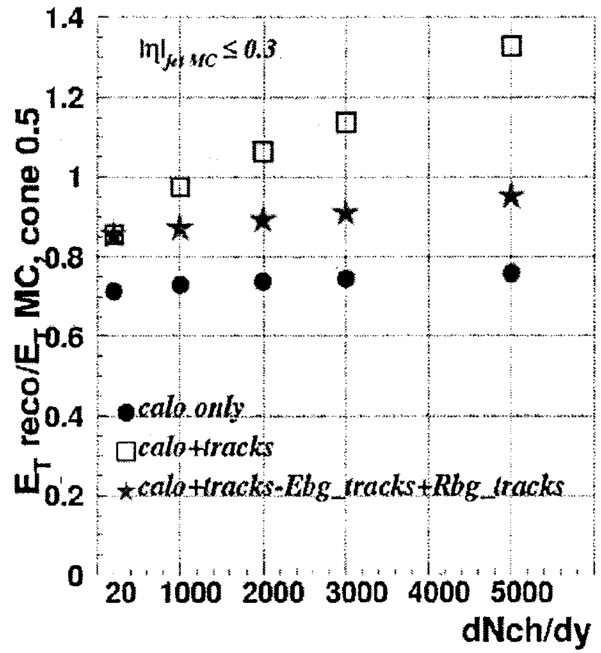

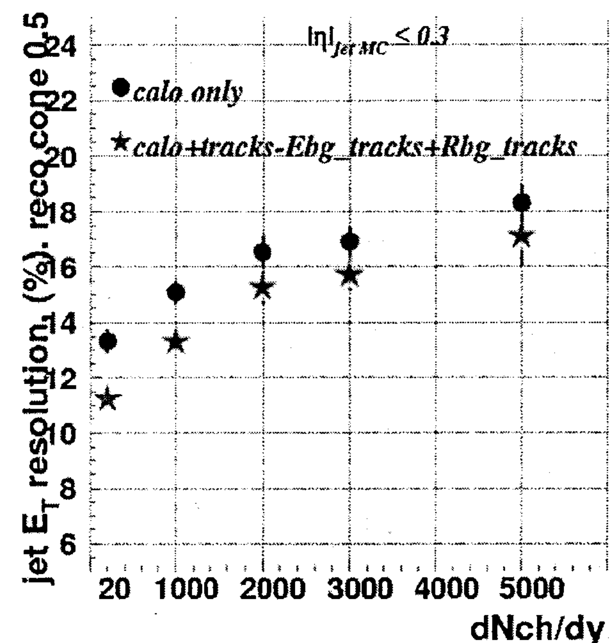

Ejet_corr = Ejet_calo - (Rtrack_jet+Rtrack_bg) + (Etrack_jet + Etrack_bg) - <Etrack_bg> +<Rtrack_bg>

The additional subtraction of background tracks

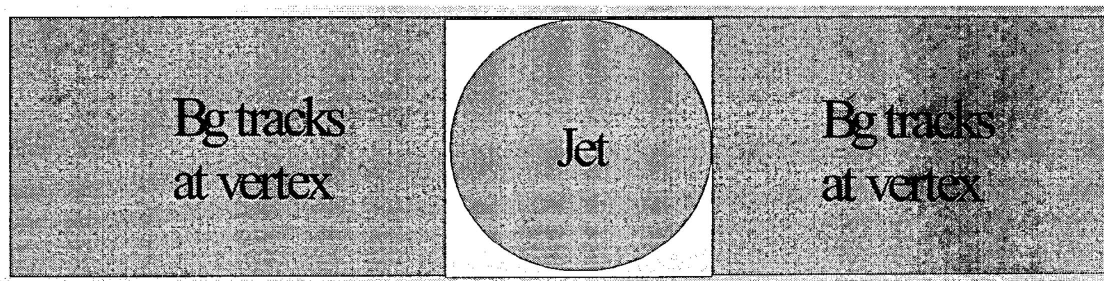

The identification of primary jet vertex with use of tracker and muon chambers

N.Ilyina
A.Krokhotin
V.Gavrilov

Jet veto I (for Low Luminosity condition).

- the ratio of the sum of transverse momenta of all tracks found inside the jet cone and having the same vertex as the signal muon to the transverse momentum of jet ($\alpha = \mathrm{sum}(P_{T\,jet}^{track})/P_T^{jet}$) is calculated.

  The jet vertex should satisfy: $|Z_{vertex}^{track} - Z_{vertex}^{m}| < dZ$
- the vertex is considered as primary if $\alpha > \alpha_0$

Jet veto 2 (for High Luminosity condition)

- the ratio ($\beta = \mathrm{sum}(P_{T\,jet}^{track})/P_{T\,all}^{track}$) is calculated.
- the vertex is considered as primary if $\beta > \beta_0$

	Particle level only signal jet	Calortimeters only		Calorimeters and tracker	
		Low Lumi	High Lumi	Low Lumi	High Lumi
Fraction of events that satisfy central jet veto	0.8	0.21	0.09	0.53	0.45

Fake jets suppression

Summary

Jet measurements include three steps:
- noise and pile-up suppression
- jet finding
- jet energy correction
  and jet direction correction ($|\eta|<2.4$)

Jet energy and direction correction
- jet based (γ/Z+jet, W->jj, dijet, Monte-Carlo)
- using information of tracker detectors

Jet measurements requires simultanious monitoring and recalibration during data taking:
- monitoring with off-line processes
- recalibration with off-line processes:
  isolated particles, γ/Z+jet, min bias, ...

MULTIPARTICLE DYNAMICS STUDY by GLUON DOMINANCE MODEL

***Kokoulina E.**, Nikitin V.*

GSTU, Belarus & JINR,Dubna

The unified approach to multiplicity distribution (MD) description in high energy interactions:

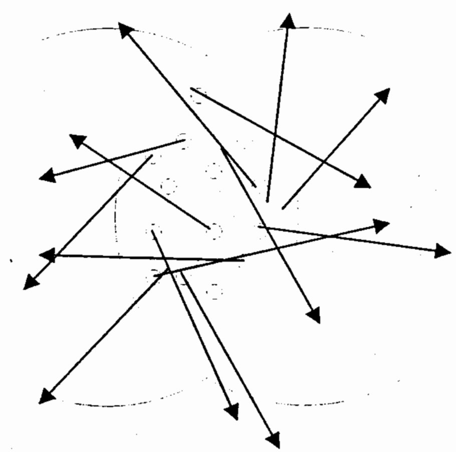

e^+e^- - annihilation,

Proton (nucleus) collisions

Proton-antiproton-annihilation

The region of high multiplicity (HM): $n \gg \bar{n}(s)$ – mean muliplicity.

Pn - multiplicity distribution (MD), Q(s,z) - generating function (GF)

$Q(s,z) = \mathrm{S}\ Pn\ (s)\ z^{n}$.

- $e^{+}e^{-}$-annihilation - MD, moments… (the QCD Markov branching process + hadronization);

Kuvshinov V. and Kokoulina E. Acta Phys.Polon.B13(1982) 533.

- pp- interactions from 69 to 800 GeV/c by two schemes with and without gluon branch on 1st stage, modification of 2nd scheme by clan mechanism at higher energies;
- $p\bar{p}$ -annihilation (~10-100 GeV/c).

$$e^+e^- \to \gamma(Z^0) \to q\bar{q} \to (q,g) \to ? \to hadrons$$

First stage (cascade):

a) gluon fission; b) quark bremsstrahlung; c) quark pair creation.

Second stage:

Hadronization. BD

$$Q_p^H = \left[1 + \frac{\bar{n}_p^h}{N_p}(z-1)\right]^{N_p}.$$

K.Konishi et.al.NPB157(1979)45
A.Giovannini.NPB161(1979)429.

$$\frac{dQ^{(q)}}{dY} = \tilde{A}Q^{(q)}(Q^{(g)}-1),$$

$$\frac{dQ^{(g)}}{dY} = A(Q^{(g)2}-Q^{(g)}) + B(Q^{(q)2}-Q^{(g)}).$$

Convolution: of two stages

quark fission -> NBD

$$P_m = \frac{k_p(k_p+1)\ldots(k_p+m-1)}{m!}\left(\frac{\bar{m}}{\bar{m}+k_p}\right)^m \left(\frac{k_p}{\bar{m}+k_p}\right)^{k_p}.$$

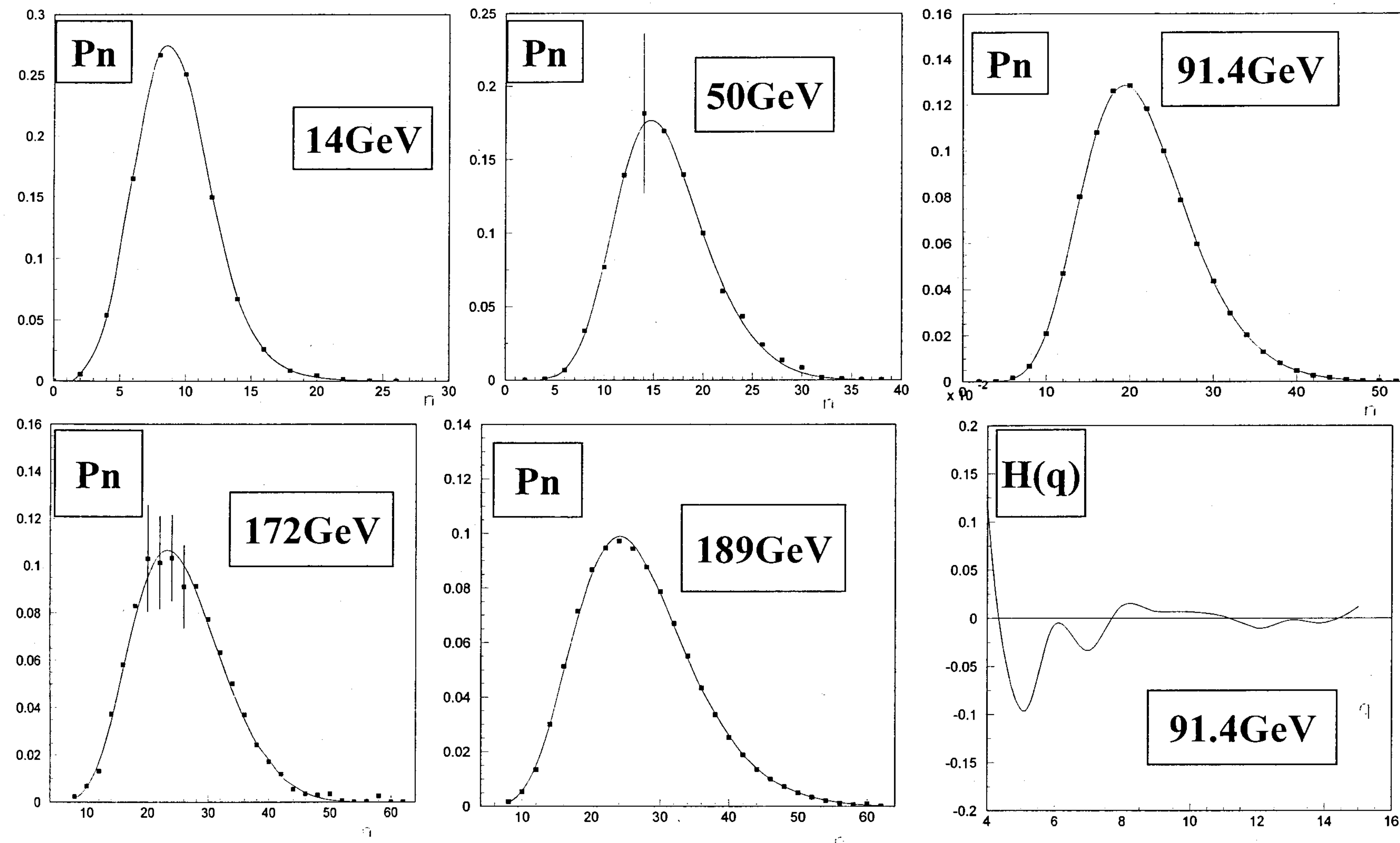

Pn in e^+e^--annihilation at 14, 50, 91.4, 172 and 189 GeV; H(q) at 91.4 GeV.

E. Kokoulina. Minsk, NPCS (2002)[hep-ph/0209334]; ISMD32,2002.

hadronization gluon parameters ($N_g, \overline{n}_g^h$), 14 -189 GeV.

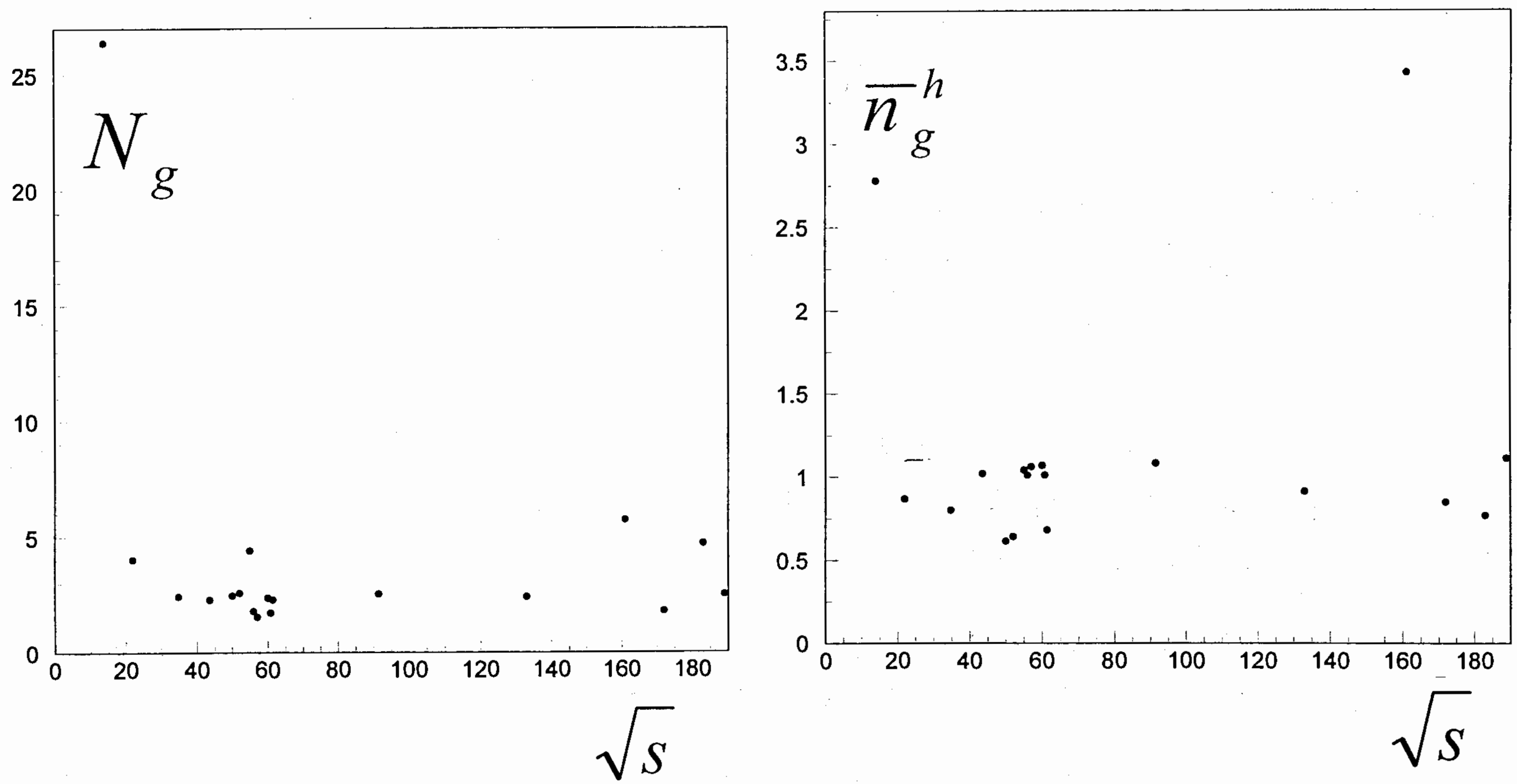

$N_g(\overline{n}_g^h)-$ maximal (mean) multiplicity of hadrons are formed from gluon on the stage of hadronization.

$N_g / N_q \sim .2-$ hadronization of gluon are softer than quark.

Project "THERMALIZATION"
(JINR , IHEP, SINP MSU, GGTU)

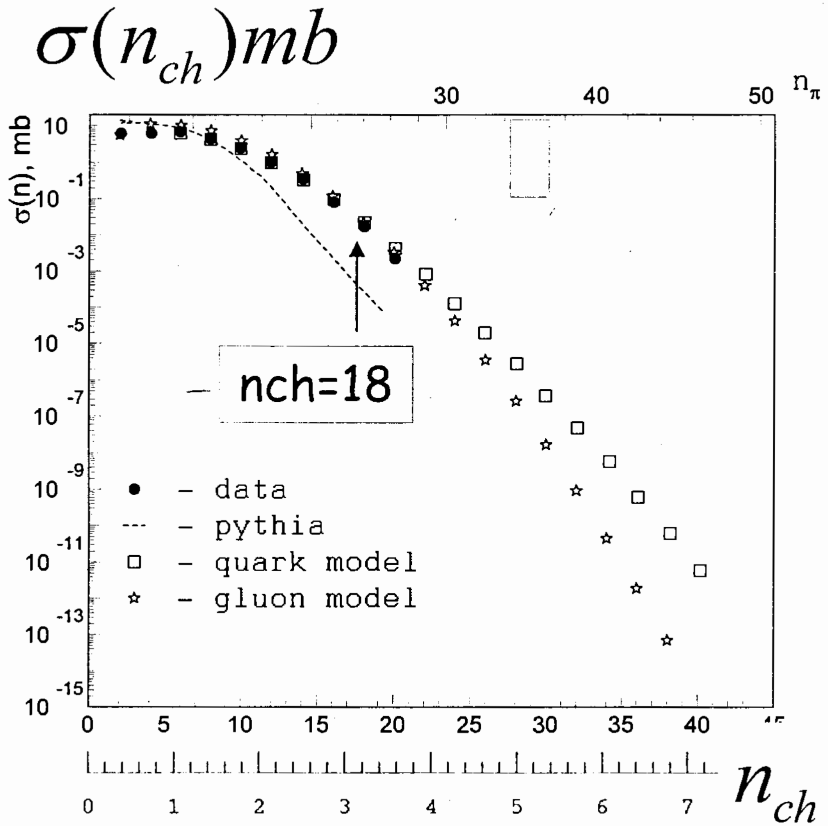

1. Experimental data pp (70 GeV).
2. Quark model. Yad.Fiz. 55 (1992) 820. Collisions of quark pair.
3. MC PHYTHIA code underestimates the **s**(nch) by two orders of magnitude at nch=18.

The goal:

The study of MP at pp (pA) interactions in HM region: nch>20-30.

$$z = n_{ch} / \overline{n}_{ch}(s)$$

Gluon Dominance model (GDM)

- After an inelastic collision of two protons the part of energy are converted into the thermal and one or few gluons become free,
- Gluons may give cascade – I stage;
- Some of gluons (not of all) leave Quark-Gluon System (QGS) – are evaporated and are converted to hadrons – II stage.

<u>Our model investigations had shown</u> :
quarks of initial protons are staying
in leading particles (from 70 to 800 GeV/c).
Multiparticle production (MP) is realized
by gluons. We name them active.

P.Carruthers about a passive role quarks:

"...labels and sources of colour perturbation in the vacuum: meanwhile the gluons dominates in collisions and multiparticle production." (1984)

The domination of gluons was first proposed by S.Pokorski and L.Van Hove (1975).

The Multiplicity Distributions (MD) analysis are used to study MP-processes.

Model with the gluon branch in QGS - **branch model** (TSMB)

or

Model without the gluon branch - **Thermodynamic model** (TSMT)

E.Kokoulina, V.Nikitin. 7th Int. school-seminar The actual problems of Microworld Physics, Gomel, Belarus V.1 (2004) [hep-ph/0308139]

TSMB -convolution gluon and hadron MD

- **MD for active gluons at the moment of impact – Poisson** $e^{-\bar{k}}\bar{k}^{k}/k!$
- **MD for branch of gluons – Farry**

$$\frac{1}{\bar{m}^{k}}\left(1-\frac{1}{\bar{m}}\right)^{m-k}\frac{(m-1)(m-2)...(m-k+1)}{(k-1)!}$$

- **MD for hadronization stage – Binomial (BD)**

$$C_{\alpha mN}^{n-2}\left(\frac{\bar{n}_{h}}{N}\right)^{n-2}\left(1-\frac{\bar{n}_{h}}{N}\right)^{\alpha mN-(n-2)}$$

Scheme with branch:

$$P_n = \sum_{k=0}^{Mk} \frac{e^{-\bar{k}}\bar{k}^k}{k!} \sum_{m=k}^{Mg} \frac{1}{\bar{m}^k} \frac{(m-1)(m-2)...(m-k+1)}{(k-1)!} \left(1-\frac{1}{\bar{m}}\right)^{m-k} C_{\alpha m N}^{n-2} \left(\frac{\bar{n}^h}{N}\right)^{n-2} \left(1-\frac{\bar{n}^h}{N}\right)^{\alpha m N-(n-2)}.$$

α - ratio of evaporated gluons to all active ones

$\bar{n}^h$, N – parameters of hadronization for gluon

$(\alpha < 1)$ Some of active gluons (<50%) are staying inside QGS and don't give hadron jets. New formed hadrons catching up them, are excited and throw down excess of energy by soft photons (SP).

We found weak branching of active gluons at 69 GeV/c.

TSMT - gluons leave QGS and fragment to hadrons (without branch):
MD = Poisson & Binomial

$$P_n = \sum_{m=0}^{Me} \frac{e^{-\overline{m}}\,\overline{m}^m}{m!} C_{mN}^{n-2} \left(\frac{\overline{n}^h}{N}\right)^{n-2} \left(1 - \frac{\overline{n}^h}{N}\right)^{mN-(n-2)}, \quad (n > 2).$$

M - max number of evaporated gluons is rising (from 6 to 10)
max number of hadrons is limited by M*N
(~ 24-26 for charged particles at 69 GeV/c)

Kokoulina E. Acta Phys.Polon. B35(2004)295

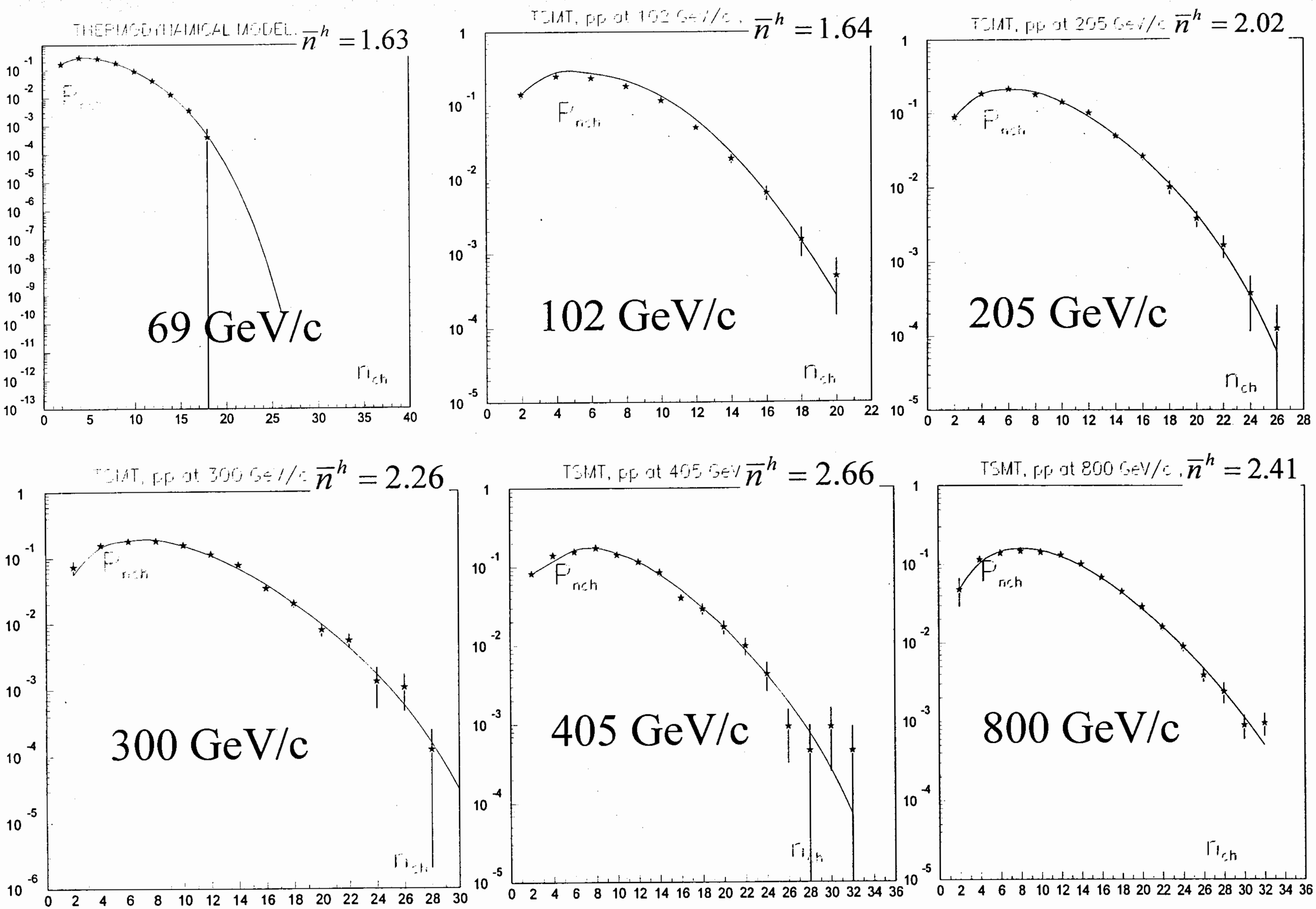
THERMODYNAMICAL MODEL $\overline{n}^h = 1.63$
69 GeV/c
TSMT, pp at 102 GeV/c $\overline{n}^h = 1.64$
102 GeV/c
TSMT, pp at 205 GeV/c $\overline{n}^h = 2.02$
205 GeV/c
TSMT, pp at 300 GeV/c $\overline{n}^h = 2.26$
300 GeV/c
TSMT, pp at 405 GeV $\overline{n}^h = 2.66$
405 GeV/c
TSMT, pp at 800 GeV/c $\overline{n}^h = 2.41$
800 GeV/c
P_{nch}
n_{ch}

Comparisons:

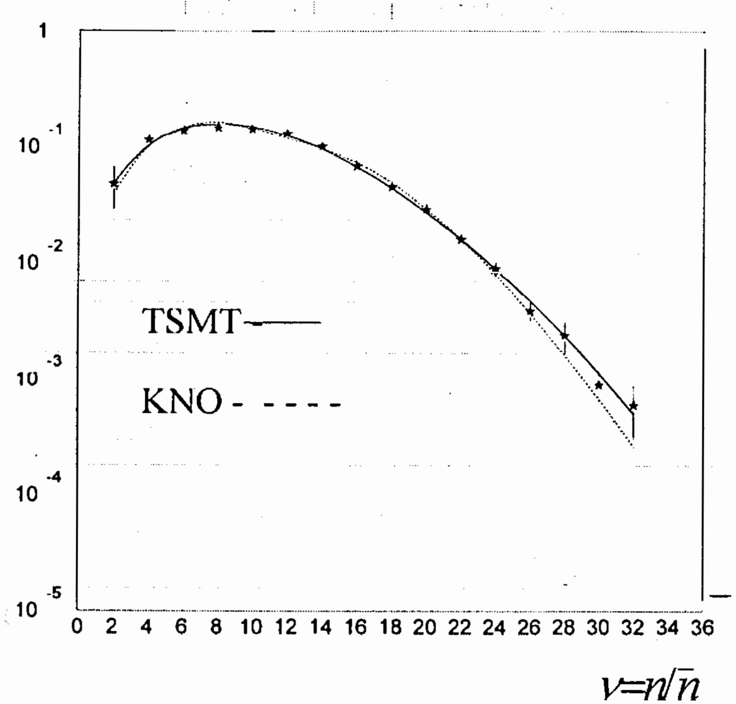

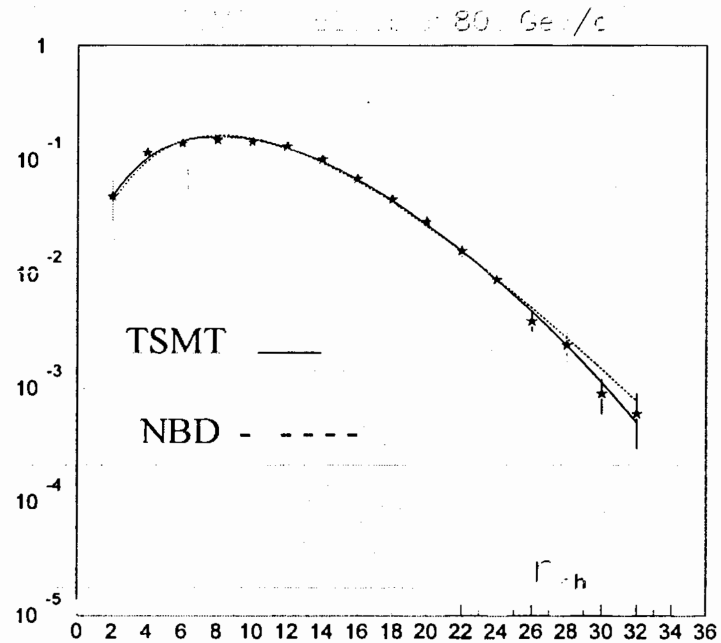

$$\psi(\nu) = (0.1/\nu^2 + 18.85\,\nu^4 + 9.39\,\nu^{10}) \cdot$$
$$\cdot \exp(-8.25\,\nu - 1.35/\nu + 6.628),$$

$$P_n = \frac{k(k+1)\ldots(k+n-1)}{n!}\,\frac{k^k \bar{n}^n}{(k+\bar{n})^{k+n}}$$

Semenov S. et al. Sov.J. Nucl Phys.22(1975) 792

Clan as independent intermediate gluon source.

A.Giovannini, R.Ugocioni [hep-ph/0405251]

Ln (NBD) ~ Farry (TSMB)

Ln (NBD) ~ Binom. (TSMT)

<u>Our results:</u> clans consist from gluons! Change of fragmentation (e^+e^-) to recombination mechanism (hh, AA) .

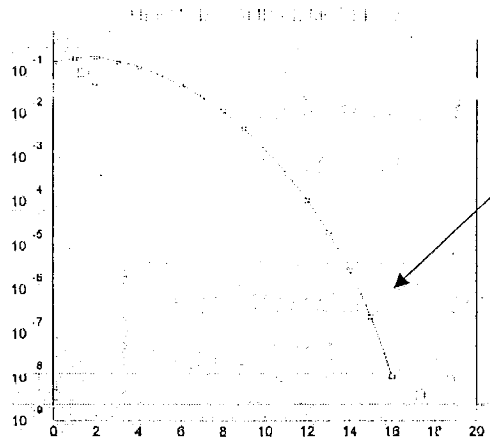

MD of neutral mesons at 69 GeV/c

The simplification on the second stage of TSM:

$$\frac{\overline{n}_{ch}}{N_{ch}} \approx \frac{\overline{n}_{0}}{N_{0}} \approx \frac{\overline{n}_{tot}}{N_{tot}}$$

<u>Our results</u>: max of neutral mesons	**= 16**
max of total multiplicity	**=42**

Mean multiplicity of neutral mesons versus the number of charged particles

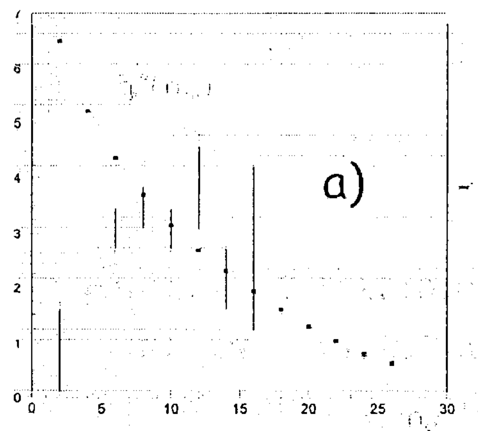

$$\overline{n}_0(n_{ch}) = \sum_{n_{tot}=n_1}^{n_2} P_{n_{tot}} \cdot (n_{tot} - n_{ch}) \Big/ \sum_{n_{tot}=n_1}^{n_2} P_{n_{tot}}$$

a) top and bottom limits is determined by condition:

$$n_{ch} + n_0 = 42$$

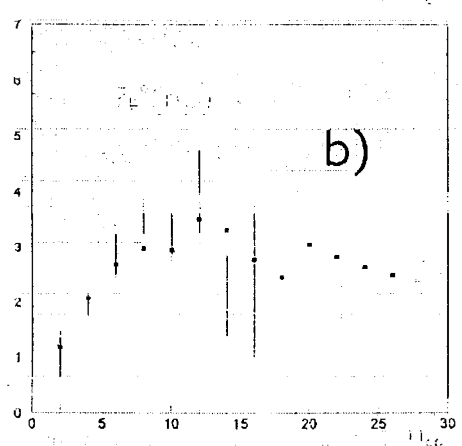

b) The noticeable improvement is reached if we decrease top limit at charged multiplicities <10 to

$$n_2 = 2n_{ch}\,(n_o \le n_{ch})$$

<u>Our result:</u> *Centaur events may be realized in the region of HM. AntiCentaur events must be absent.*

pp -> n ch, ISR (30-60 GeV)

Modification.
Superposition of clans:
clans consist from one, two (or more) gluons of fission:

$$P_n(s) = \alpha_1 \sum_{m_1}^{M_1} \frac{e^{-\overline{m}_1}\,\overline{m}_1^{\,m_1}}{m_1!} C_{m_1 N}^{n-2} \left(\frac{\overline{n}^h}{N}\right)^{n-2} \left(1 - \frac{\overline{n}^h}{N}\right)^{m_1 N-(n-2)} +$$

$$+\alpha_2 \sum_{m_2}^{M_2} \frac{e^{-\overline{m}_2}\,\overline{m}_2^{\,m_2}}{m_2!} C_{2m_2 N}^{n-2} \left(\frac{\overline{n}^h}{N}\right)^{n-2} \left(1 - \frac{\overline{n}^h}{N}\right)^{2m_2 N-(n-2)} .$$

$$(\alpha_1 + \alpha_2 = 1)$$

$$\overline{m}_1 = 3.59 \pm 0.03,\ \overline{m}_2 = 1.15 \pm 0.25,$$
$$\alpha_1/\alpha_2 \sim 1.8,\ \chi^2/ndf = 9/13.$$

Soft (α_1) & semi-hard (α_2) components, and so on.

Kokoulina E., Nikitin V. et al. ISHEPP2004.hep-ph/0503254.

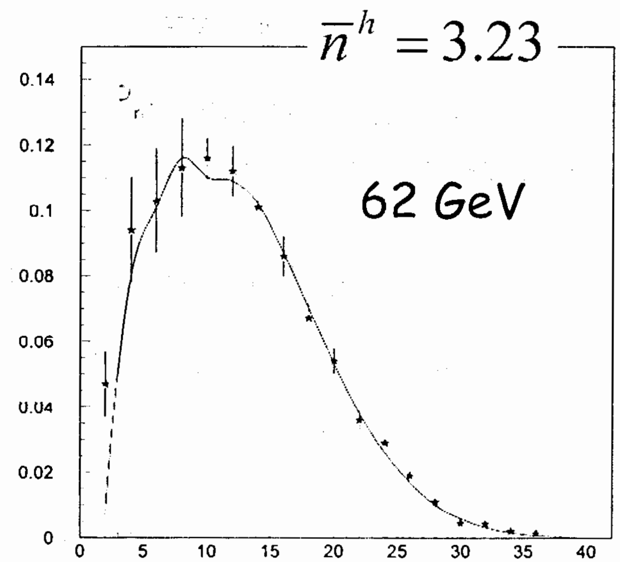

From GDM the ratio of charged hadrons to neutral mesons in p+p is:

70 GeV/c: 1.19+/-0.25;

800 GeV/c: 1.49+/-0.33;

(cms) 62 GeV : ~ 1.6 ( )

The ratio of h/ **p=1.6** is the value measured in experiment : p+p reactions (53 GeV) and

Au-Au (200 GeV/N) peripheral interactions (60-92%) RHIC.

PHENIX [nucl-exp/0410003];
X.Zhang, G.Fai.[hep-ph/0306227]

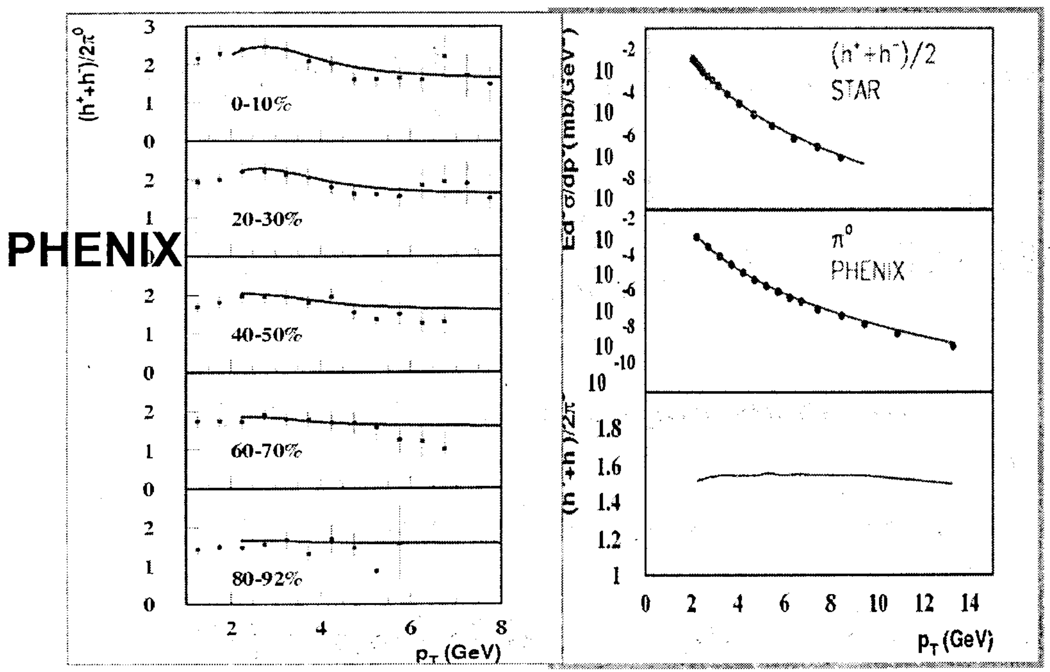

<u>The assumption:</u> The specific feature of our GDM approach is the dominance of a lot of active gluons at MP. We expect the emergence of them in nucleus collisions (RHIC) and the formation of new kind of matter QGP.

Soft Photons - the signature of hadronization

$$\sigma_\gamma \approx 4mb,\ \sigma_{in} \approx 40mb,\ \sigma_\gamma \approx n_\gamma(T)\cdot\sigma_{in} \rightarrow n_\gamma \approx 0.1$$

The black body emission spectrum: $$\frac{dn_\gamma}{d\nu} = \frac{8\pi}{c^3}\frac{\nu^3}{e^{\frac{h\nu}{T}}-1}$$

$$n_\gamma(T) = 0.244\cdot V\left(\frac{2\pi kT}{hc}\right)^3,\quad T_r = 2.725K\,(MVB) \rightarrow n_\gamma(T_r)/V = 4.112\cdot 10^8 m^{-3}$$

$$n_\gamma(T) = n_\gamma(T_r)\cdot\left(\frac{T}{T_r}\right)^3,\ \rho(T) = n_\gamma(T)/V = 4.112\cdot 10^8\cdot 10^{-6}\cdot 10^{-39}\left(\frac{T}{T_r}\right)^3 fm^{-3}\text{(the density)}$$

Excess of soft photons: $p_t \sim 10-50(MeV)\ (1MeV = 1.16\cdot 10^{10}K)$

$$T = p \approx p_t\cdot\sqrt{2}$$

$$L^3\cdot\rho(T) \approx n_\gamma \rightarrow L(T)$$

p_t	L(fm)	p_t	L(fm)
10	11.	30	3.5
15	6.9	40	2.6
25	4.1	50	2.0

Our result: L - the size of hadronization region

M.Volkov,E.Kokoulina, E.Kuraev.
Part. and Nucl., Let., №5(2004)122. [hep-ph/0402163]

$p\bar{p}$ -annihilation (exper.data):

J.Rushbrooke and B.Webber.
Phys.Rep. C44(1978)1

1) The second correlation moment of negative hadrons (f_2^{--}) in pp-interactions and $p\bar{p}$ -annihilation.

2) The differences $\sigma_n(p\bar{p}) - \sigma_n(pp)$ at 14.75, 22, 32 and 100 GeV/c remain significant for all multiplicities and have local max and min.

GDM:

1) $$Q(m,z) = Q(1,z)^m = \left[1 + \bar{n}^h / N(z-1)\right]^{mN}$$

2) $$Q(z) = c_0 \sum_m P_m^G \left[1 + \frac{\bar{n}^h}{N}(z-1)\right]^{mN} + c_2 z^2 \sum_m P_m^G \left[1 + \frac{\bar{n}^h}{N}(z-1)\right]^{mN} +$$

$$+ c_4 z^4 \sum_m P_m^G \left[1 + \frac{\bar{n}^h}{N}(z-1)\right]^{mN}.$$

GDM

$p\,\overline{p}$ - annihilation (10 - 100 GeV/c)

a) second Correlative moments of negative charged particles:

$$f_2^{--} = \overline{n_-(n_- - 1)} - \overline{n}_-^2 \sim -m_G(\overline{n}^h)^2 / N$$

b) differences between *pp* and $p\overline{p}$ inelastic topological cross sections:

GDM - 14.75 GeV/c

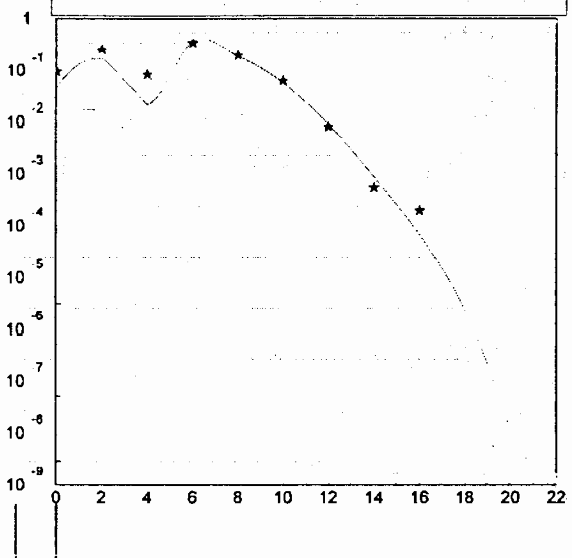

$$\boxed{\Delta\sigma_n(p\overline{p} - pp) = \sigma_n(p\overline{p}) - \sigma_n(pp)}$$

Pn = $\Delta\sigma_n / \Sigma\Delta\sigma_n$ $\quad c_0 : c_2 : c_4 = 15:40:0.05,$

$\overline{m} = 3.36 \pm 0.18,\ \overline{n}^h = 1.74 \pm 0.61.\ \chi^2 / ndf \sim 1.5.$

Superposition of intermediate topologies ("0", "2" -valent q's, "4"- valent + vacuum q's)

\+ GDM → Pn-description.

"The search for signatures of quark-gluon dynamics in NN annihilation is somewhat analogous to the search of the phase transition from a hadron gas to a quark-gluon plasma in relativistic ion transitions. The signal must be isolated from background of statistical processes characteristic of a system with many degrees of freedom. ..."

C.Dover. Prog. Part. Nucl. Phys. 29(1992)87.

"... series of experimental facts and theoretical ideas which might, hopefully, transform an enigma in a Ariadna thread in the labyrinth of multiparticle dynamics in its awkward journey toward QCD and open new perspectives in pp and heavy ion collisions in the TeV energy domain."

A.Giovannini (2004).

Conclusions:

- **MD charged and neutral (69 - 800 GeV/c) ;**
- **the thermodynamic picture of the gluon escape (evaporation);**
- **the active role of gluons;**
- **the charged hadron/ neutral pion ratio;**
- **estimates of the soft photon number and the size region of emission;**
- **2nd correl. moment in $p\bar{p}$-annihilation.**

Outlook:

- **the description of MD at higher energies;**
- **the inclusion momentum distribution in TSM;**
- **the investigation of gluon structure of clans;**
- **the employment GDM for the description of $p\bar{p}$ - annihilation;**
- **the hA- and AA- processes at 70 GeV/c and higher in the region of high multiplicity.**

There is no higher or lower knowledge, but one only, flowing out of experimentation.

Leonardo da Vinci

Statistical Fluctuations in Different Ensembles

Begun Victor

Bogolyubov Institute for Theoretical Physics

Ukraine

Motivation

1. Surprising success of statistical models for particle production in A+A collisions.
2. New data on fluctuations are coming.
3. Particle number fluctuations in different statistical ensembles were not studied up to now !?
4. We have found that they are different even in the thermodynamic limit!

Contents

1. GCE,
2. **CE: $Q=0$, $Q\neq0$,**
3. **MCE** neutral,
4. **MCE $Q=0$,**
5. Quantum statistics effects,
6. Acceptance.

1. V.V. Begun, M. Gaździcki, M.I. Gorenstein, O.S.Zozulya, "Particle Number Fluctuations in a **Canonical Ensemble", Phys. Rev. C70** (2004) 034901; nucl-th/0404056, **Apr 2004**.

2. V.V.Begun, M.I.Gorenstein, A.P.Kostyuk, O.S.Zozulya, "Particle Number Fluctuations in the **Microcanonical Ensemble"**, nucl-th/0410044, **Phys. Rev. C,** in print.

3. V.V. Begun, M.I. Gorenstein, O.S. Zozulya, "Fluctuations in the **Canonical Ensemble**", nucl-th/0411003.

4. A. Keranen, F. Becattini, V.V. Begun, M.I. Gorenstein, O.S. Zozulya, "Particle Number Fluctuations in Statistical Model with Exact Charge Conservation Laws‟, nucl-th/0411116

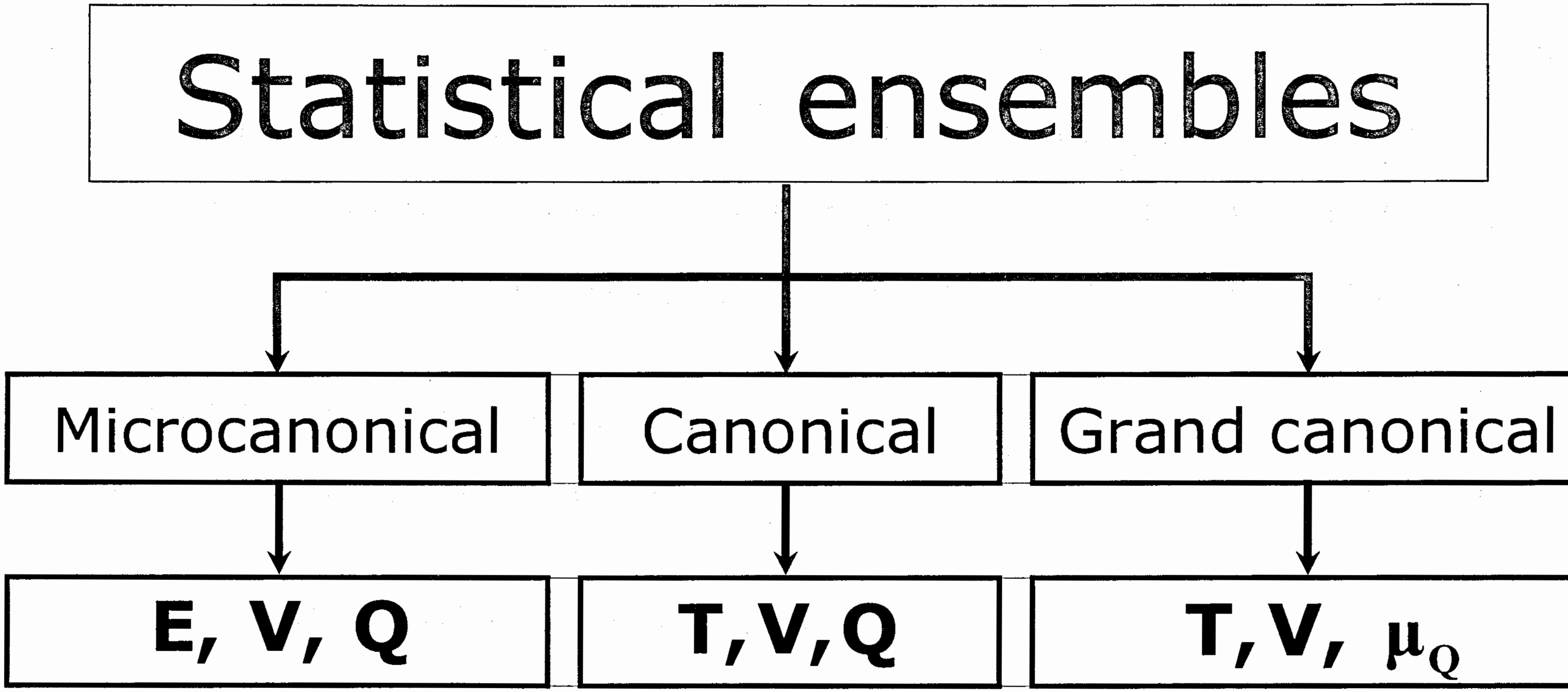

$\mathbf{E} \rightarrow \mathbf{T}$ $\qquad$ $\mathbf{Q} \rightarrow \mu_Q$

Victor Begun

$$z_j = \frac{g_j V}{(2\pi)^3} \int \exp[-\varepsilon_p / T]\, d^3p$$

$$= \frac{g_j V}{2\pi^2} T m_j^2 K_2\left(\frac{m_j}{T}\right)$$

$$\varepsilon_p = \sqrt{p^2 + m_j^2}$$

where j numerates the species, $\lambda_{j\pm} = \exp(\pm\mu/T)$

z_j is a single particle partition function, $z = \sum_j z_j$

$$\mathbf{V} \rightarrow \infty \quad \Rightarrow \quad \mathbf{z} \rightarrow \infty$$

Partition function in GCE

$$Z_{\text{g.c.e.}}(V,T,\mu) = \sum_{N_{1+},N_{1-}=0}^{\infty} \cdots \sum_{N_{j+},N_{j-}=0}^{\infty} \cdots$$

$$\times \frac{(\lambda_{1+}z_1)^{N_{1+}}}{N_{1+}!} \frac{(\lambda_{1-}z_1)^{N_{1-}}}{N_{1-}!} \cdots \frac{(\lambda_{j+}z_j)^{N_{j+}}}{N_{j+}!} \frac{(\lambda_{j-}z_j)^{N_{j-}}}{N_{j-}!} \cdots$$

$$= \prod_j \exp(\lambda_{j+}z_j + \lambda_{j-}z_j) = \exp\left[2z\cosh\left(\mu/T\right)\right]$$

Partition function in CE

$$Z_{\text{c.e.}}(V,T,Q) = \sum_{N_{1+},N_{1-}=0}^{\infty} \cdots \sum_{N_{j+},N_{j-}=0}^{\infty} \cdots$$

$$\times \frac{(\lambda_{1+}z_1)^{N_{1+}}}{N_{1+}!} \frac{(\lambda_{1-}z_1)^{N_{1-}}}{N_{1-}!} \cdots \frac{(\lambda_{j+}z_j)^{N_{j+}}}{N_{j+}!} \frac{(\lambda_{j-}z_j)^{N_{j-}}}{N_{j-}!} \cdots$$

$$\times \delta\left[\left(N_{1+} + \ldots + N_{j+} + \ldots - N_{1-} - \ldots - N_{j-} - \ldots\right) - Q\right]$$

$$= I_Q(2z)$$

K. Redlich, L. Turko, Z. Phys. C 5 (1980) 541; J. Rafelski, M. Danos, Phys. Lett. B 97 (1980) 279.

The microcanonical partition function (m=0)

$$W_N(E,V) = \frac{1}{N!}\left[\frac{gV}{2\pi^3}\right]^N \int d^3p^{(N)} \ldots \int d^3p^{(1)}$$

$$\times\ \delta(E - \sum_{k=1}^{N} |\vec{p}^{(k)}|) = \frac{1}{E}\frac{x^N}{(3N-1)!N!}\ ,$$

$$W(E,V) \equiv \sum_{N=1}^{\infty} W_N(E,V) = \frac{x}{2E}\ {}_0F_3\left(;\frac{4}{3},\frac{5}{3},2;\frac{x}{27}\right)$$

where $x \equiv \dfrac{gVE^3}{\pi^2}$.

V.V.Begun *et al.*, PRC in print, nucl-th/0410044

CE/GCE ratio

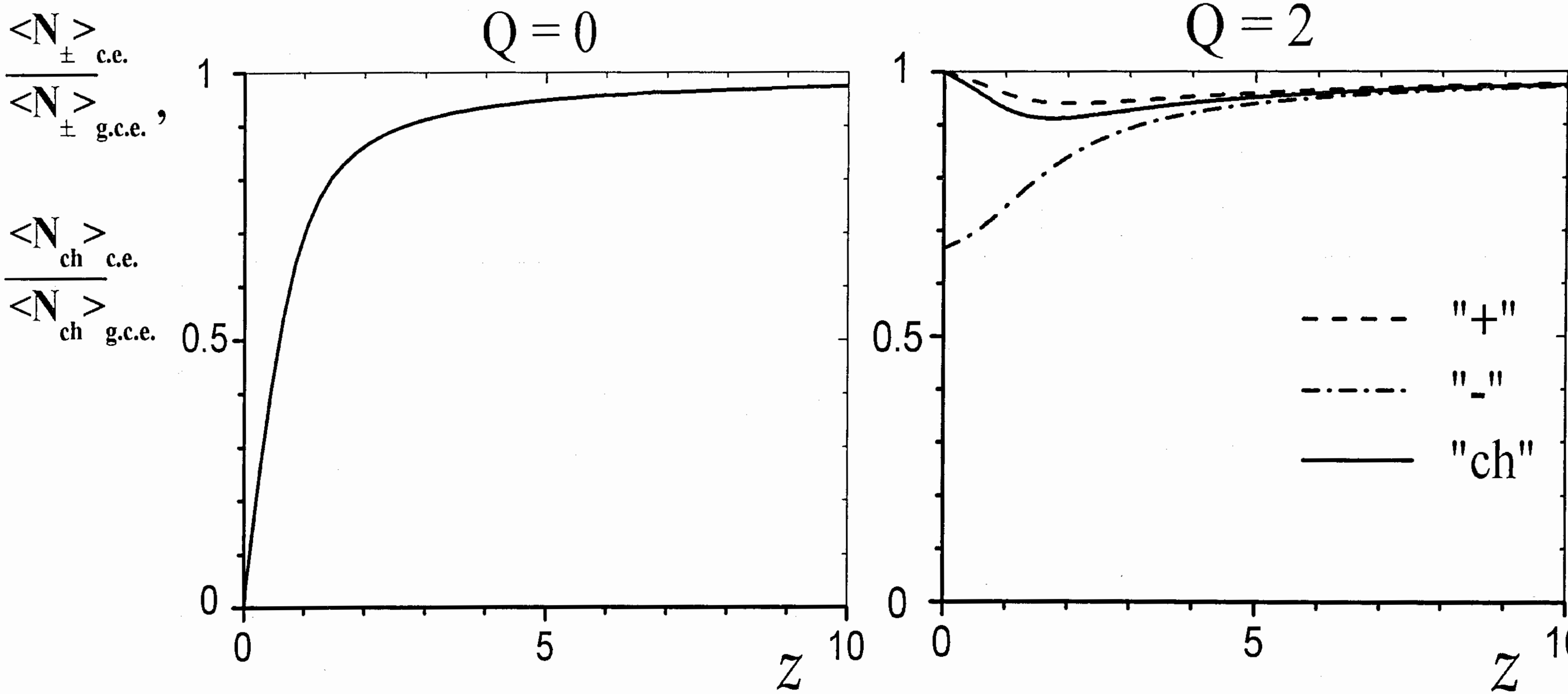

$$< N_{j\pm} > = a_\pm \, z_j, \qquad a_\pm^{g.c.e.} = \exp(\pm\mu/T), \quad a_\pm^{c.e.} = \frac{I_{Q\mp1}(2z)}{I_Q(2z)}.$$

M.Gorenstein, M.Gaździcki, W.Greiner, PLB 483 (2000) 60.

Victor Begun

MCE/GCE ratio (m=0)

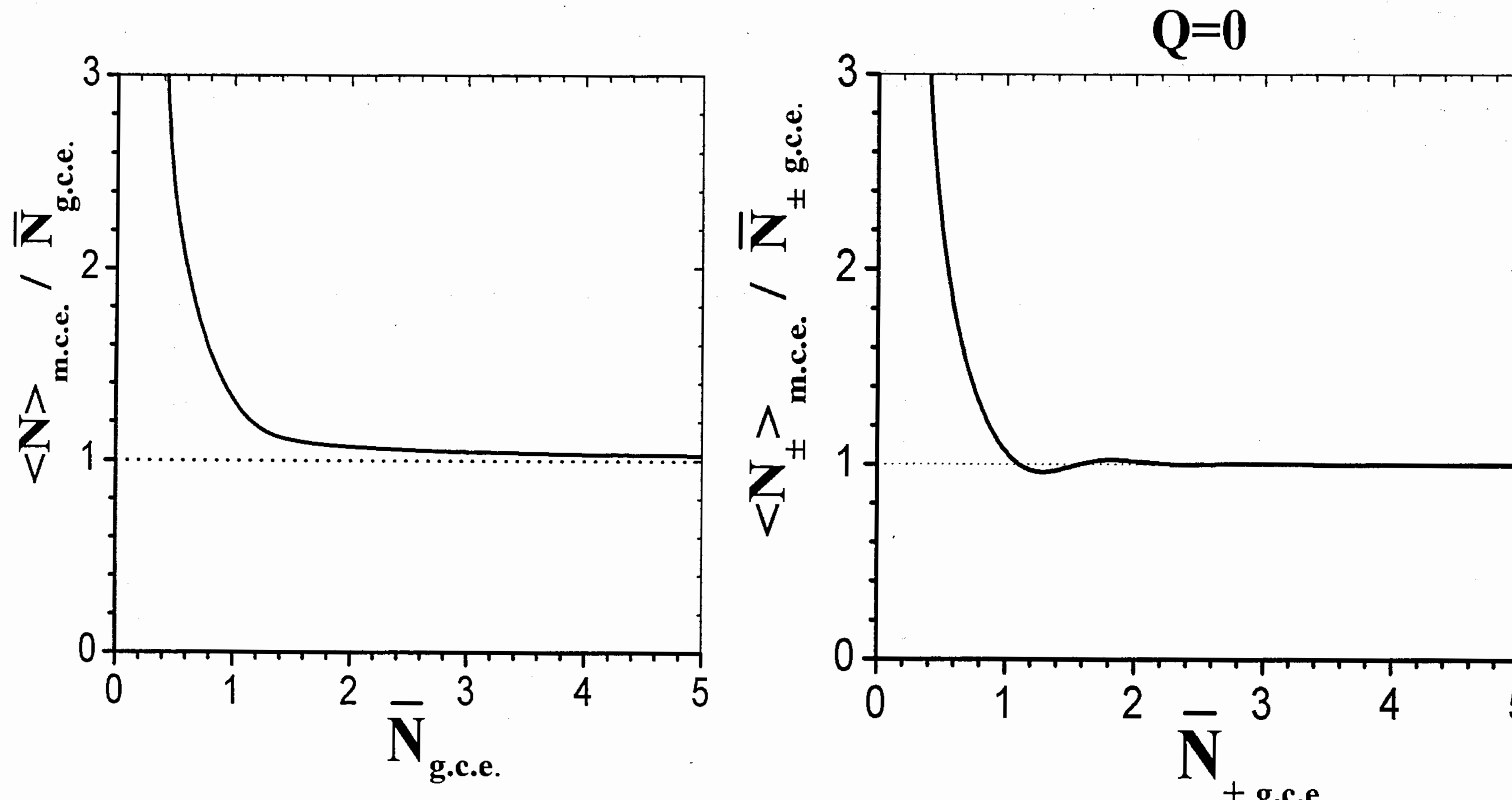

$$< N >_{m.c.e.} \approx \overline{N}\left(1+\frac{1}{8\,\overline{N}}+\dots\right), \qquad < N_\pm >_{m.c.e.} \approx \overline{N}_\pm\left(1+\frac{49}{2304\ \overline{N}_\pm^2}+\dots\right).$$

Victor Begun

Fluctuations

Variance: $V(N) \equiv \langle N^2 \rangle - \langle N \rangle^2$

Scaled variance: $\boldsymbol{\omega \equiv \dfrac{\langle N^2 \rangle - \langle N \rangle^2}{\langle N \rangle}}$

$\mathbf{N} = N,\ N_+,\ N_-,\ N_{ch}=N_+ + N_-,$

$$\omega_{g.c.e.} = \omega^{+}_{g.c.e.} = \omega^{-}_{g.c.e.} = \omega^{ch}_{g.c.e.} = 1$$

Victor Begun

CE fluctuations

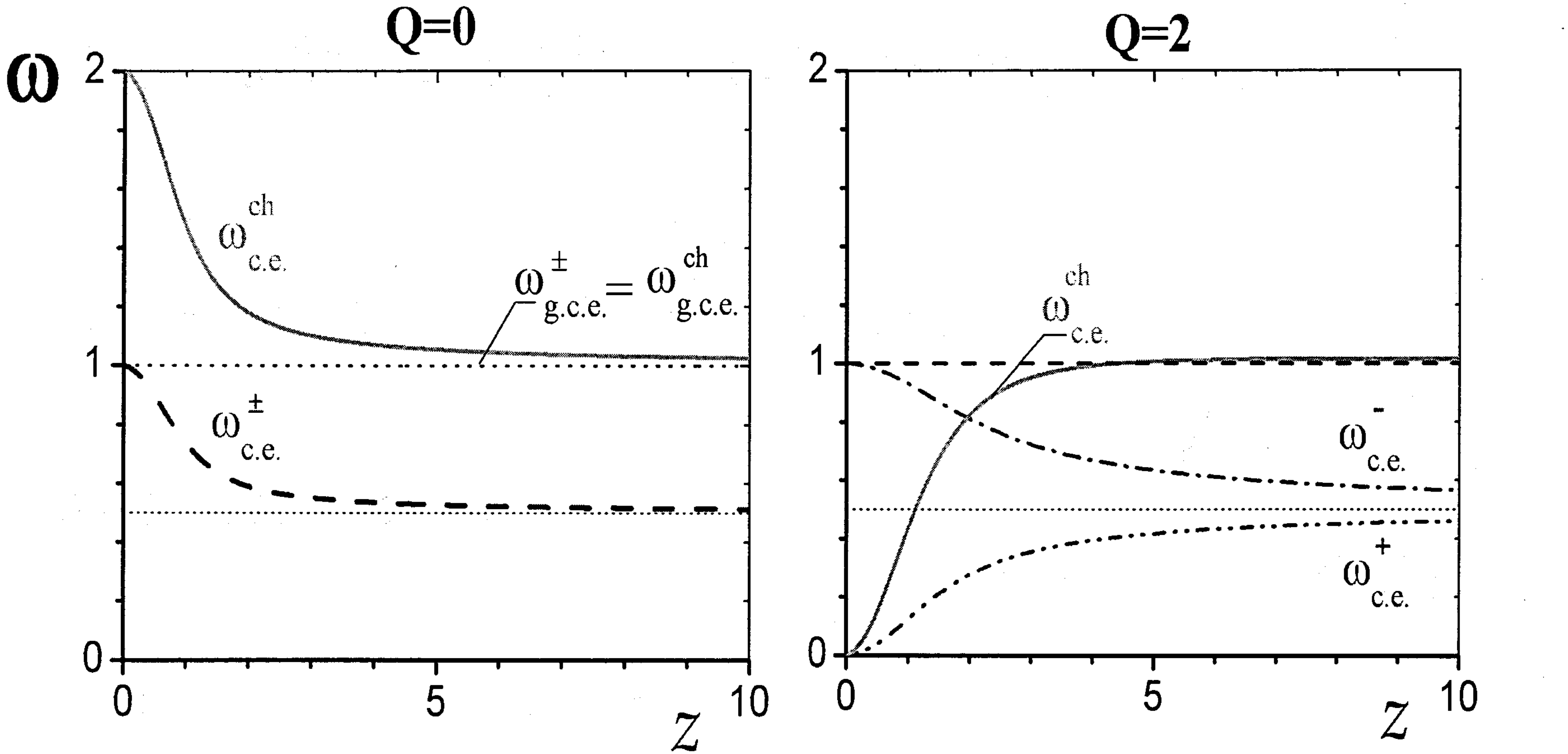

306

V.V. Begun, M. Gaździcki, M.I. Gorenstein, O.S.Zozulya, Phys. Rev. C70 (2004) 034901; nucl-th/0404056.

CE fluctuations, Q>0

$$y = \frac{Q}{2z}$$

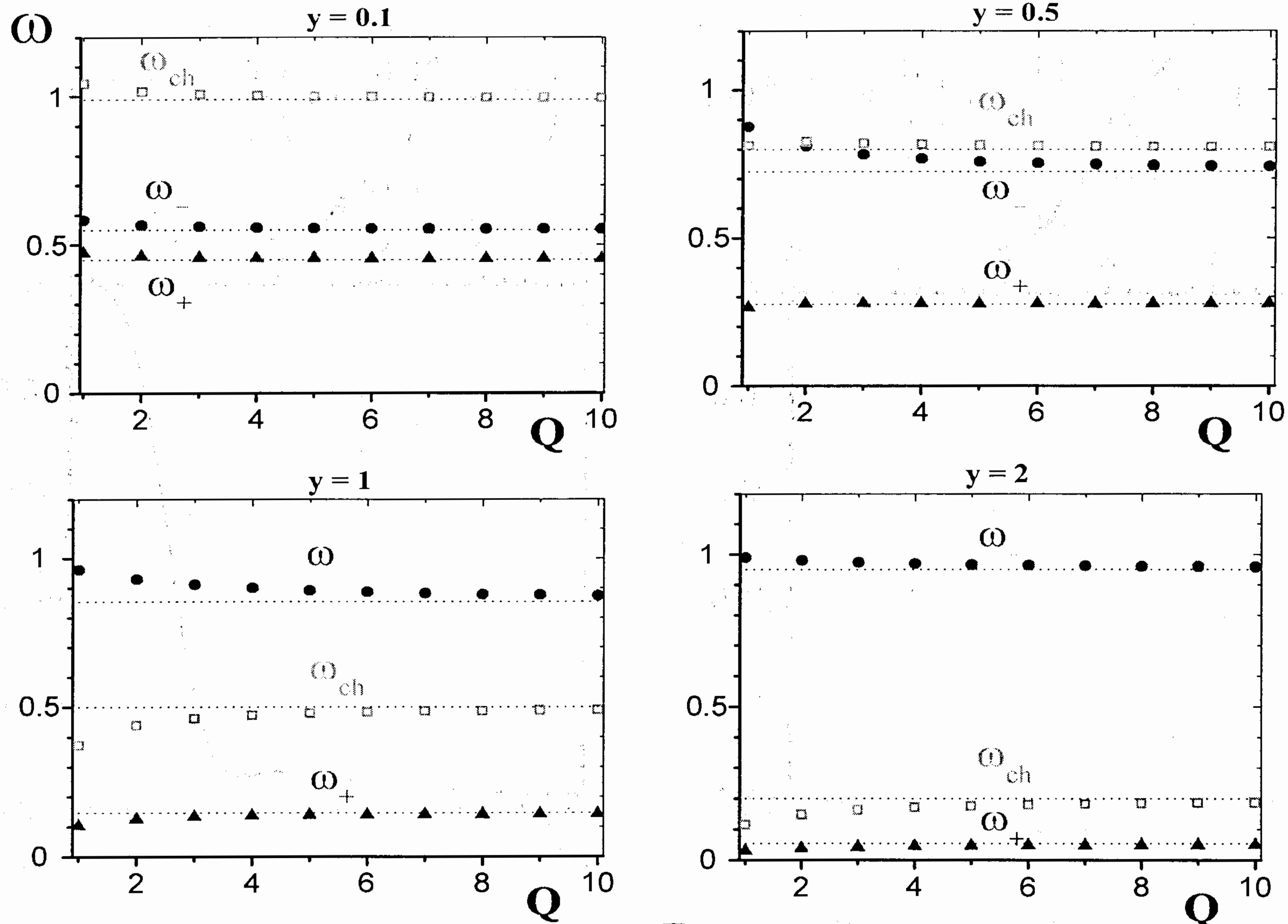

V.V. Begun, M.I. Gorenstein, O.S. Zozulya, nucl-th/0411003

Victor Begun

MCE fluctuations (m=0)

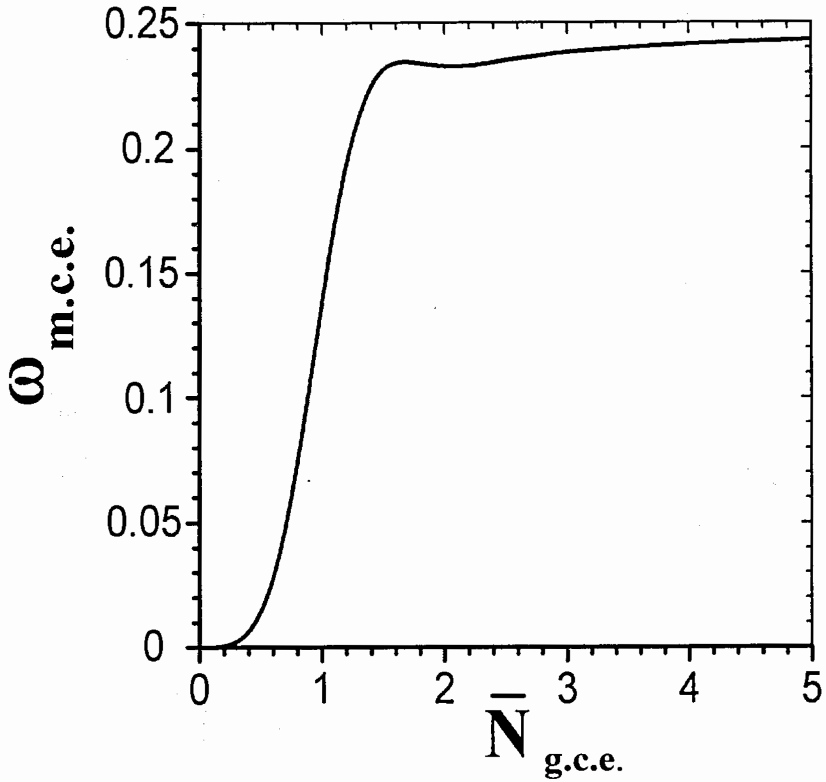

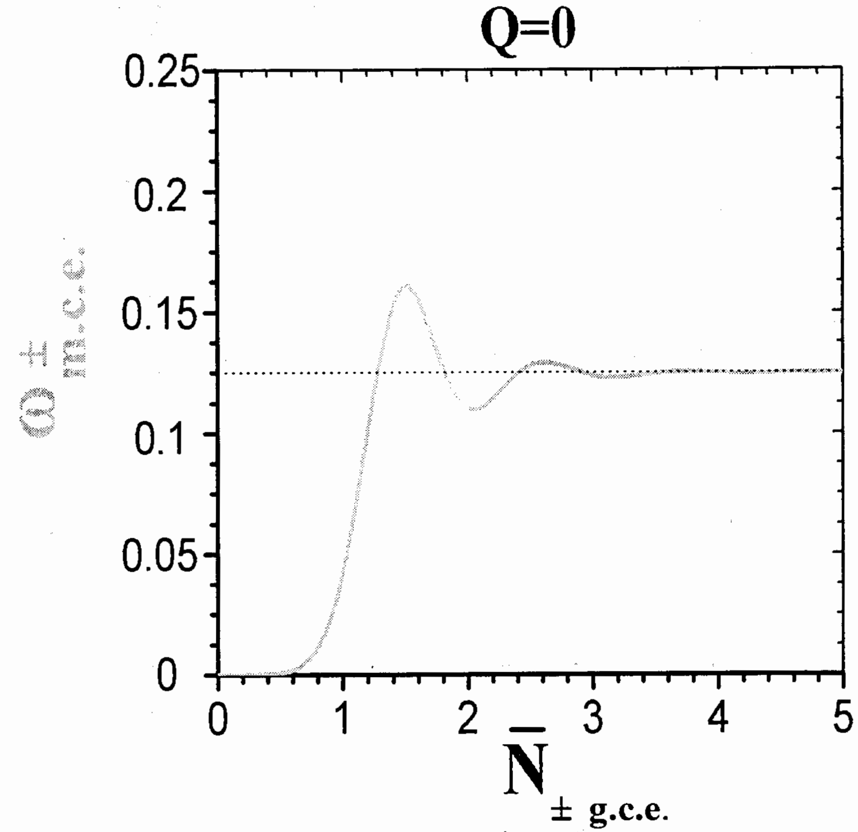

$$\omega_{\mathrm{m.c.e.}} \approx \frac{1}{4}\left(1 - \frac{1}{8\,\overline{N}} + \ldots\right), \qquad \omega^{\pm}_{\mathrm{m.c.e.}} \approx \frac{1}{8}\left(1 - \frac{49}{1152\,\overline{N}^{2}_{\pm}} + \ldots\right)$$

V.V.Begun *et al.*, PRC in print, nucl-th/0410044

Victor Begun

Quantum statistics effects

$$< n_p^\pm > = \frac{1}{\exp\left[\left(\sqrt{p^2+m^2} \mp \mu\right)/T\right] - \gamma}, \qquad \upsilon_p^2 \equiv <(n_p^\pm)^2> - <n_p^\pm>^2 \equiv <n_p^\pm>(1+\gamma <n_p^\pm>)$$

$$W_{g.c.e.}(\{n_p\}) = \prod_p w_p(n_p),$$

$$W_{c.e.}(\{n_p\}) = \prod_p w_p(n_p)\ \delta\left(\sum_{p,\alpha} q^\alpha \Delta n_p^\alpha\right), \qquad \boldsymbol{\alpha = \pm 1}$$

$$W_{m.c.e.}(\{n_p\}, Q=0) = \prod_p w_p(n_p)\ \delta\left(\sum_{p,\alpha} \varepsilon^\alpha \Delta n_p^\alpha\right)\ \delta\left(\sum_{p,\alpha} q^\alpha \Delta n_p^\alpha\right).$$

M.Stephanov, K.Rajagopal, E.Shuryak, Phys.Rev. D60 (1999) 114028

GCE

CE

$\mu = 0$

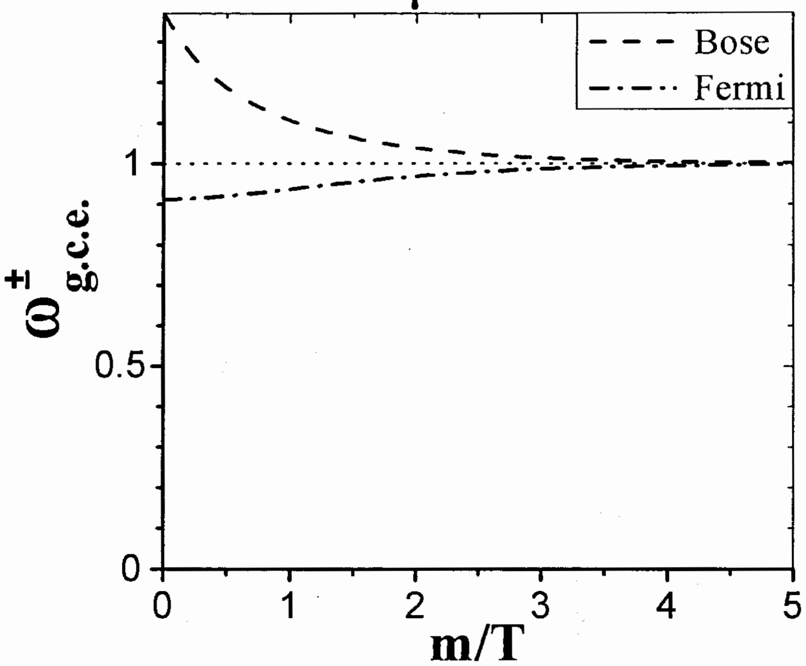

Q=0

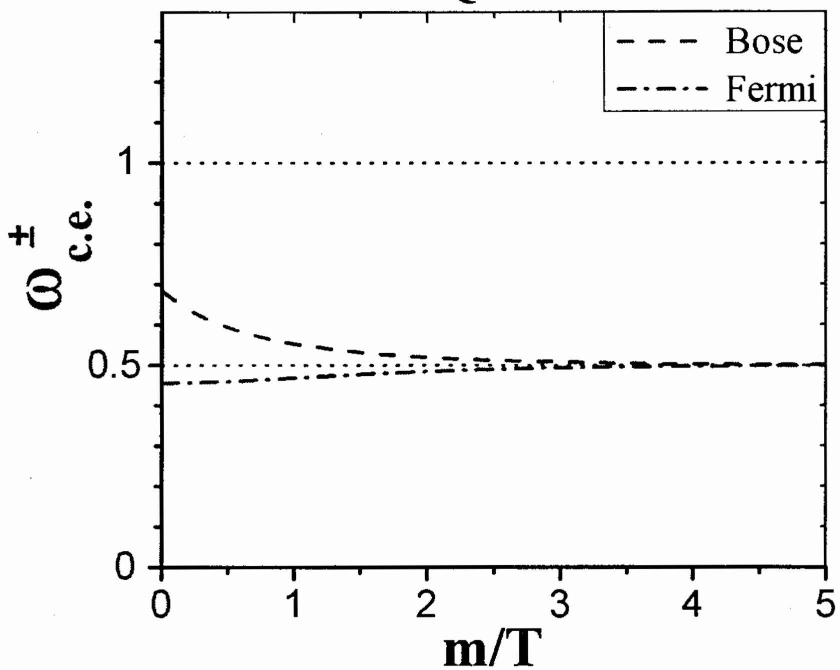

m=0:

$$\omega^{\pm B}_{g.c.e.} \approx 1.368,$$

$$\omega^{\pm}_{g.c.e.} \equiv \mathbf{1},$$

$$\omega^{\pm F}_{g.c.e.} \approx 0.912,$$

$$\omega^{\pm B}_{c.e.}(Q=0) \approx 0.684,$$

$$\omega^{\pm}_{c.e.}(Q=0) = \mathbf{1/2} = 0.5,$$

$$\omega^{\pm F}_{c.e.}(Q=0) \approx 0.456,$$

V.V. Begun, M.I. Gorenstein, O.S. Zozulya, nucl-th/0411003

MCE

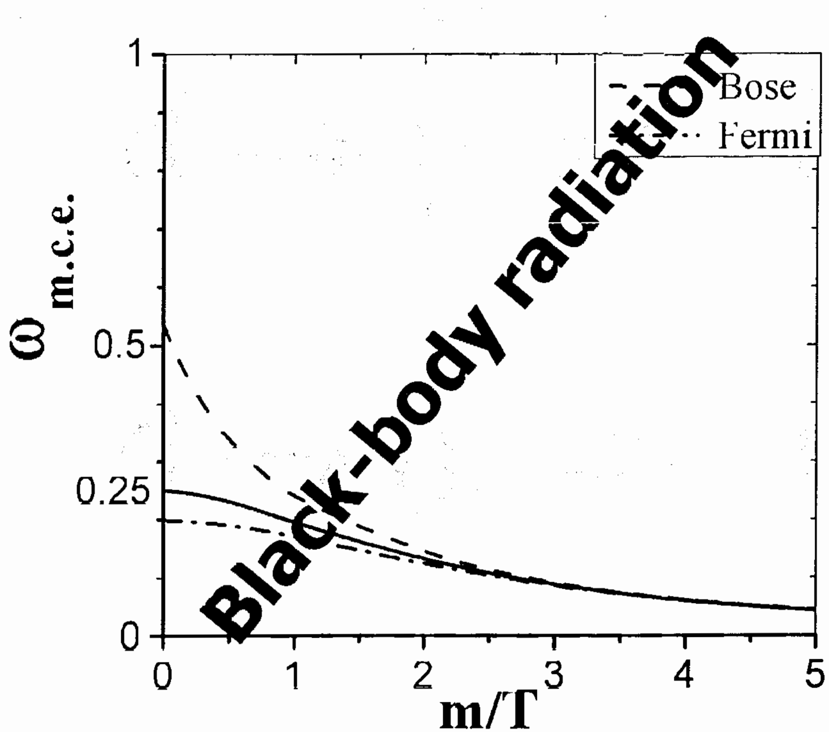

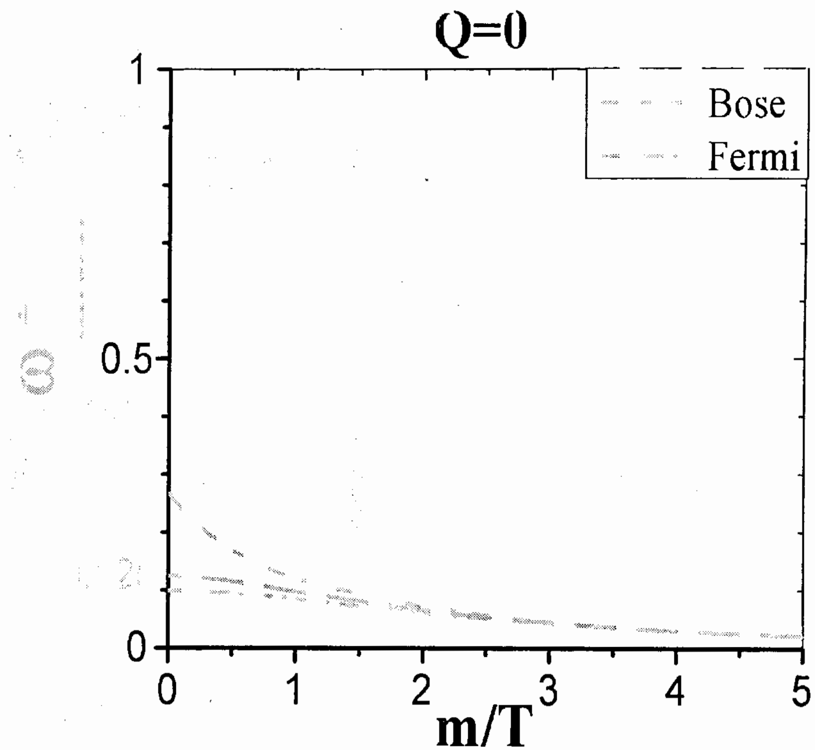

m=0:

$\omega^{B}_{m.c.e.} \approx 0.535,$ $\omega^{\pm B}_{m.c.e.}(Q=0) \approx 0.268,$

$\omega_{m.c.e.} = \mathbf{1/4} = 0.25,$ $\omega^{\pm}_{m.c.e.}(Q=0) = \mathbf{1/8} = 0.125,$

$\omega^{F}_{m.c.e.} \approx 0.198,$ $\omega^{\pm F}_{m.c.e.}(Q=0) \approx 0.099.$

V.V.Begun *et al.*, PRC in print, nucl-th/0410044

Victor Begun

Limited kinematical acceptance

$$\omega_{acc} = q \cdot \omega + (1 - q)$$

$$q \to 0 \Rightarrow \omega_{acc} = 1$$

$$\boxed{q \to 1 \Rightarrow \omega_{acc} = \omega}$$

Summary

1. Particle number fluctuations calculated in the CE and MCE **for the first time!**

2. $\omega \neq \omega^{+} \neq \omega^{-} \neq \omega^{ch}$

3. Conservation laws reduce fluctuations!

4. In the limit $\mathbf{V}\rightarrow\infty$

	GCE	**CE**	**MCE**
neutral	1	1	**1/4**
Q=0	1	**1/2**	**1/8**

5. Large acceptance is required.

Examples when exact conservation laws are required

- pp, $p\bar{p}$, e^+e^- collisions,
- Strangeness production in A+A collisions at low energies,
- Antiproton production in peripheral A+A collisions,
- Charm and charmonium production.

Gaździcki, NA49, QM 2004:

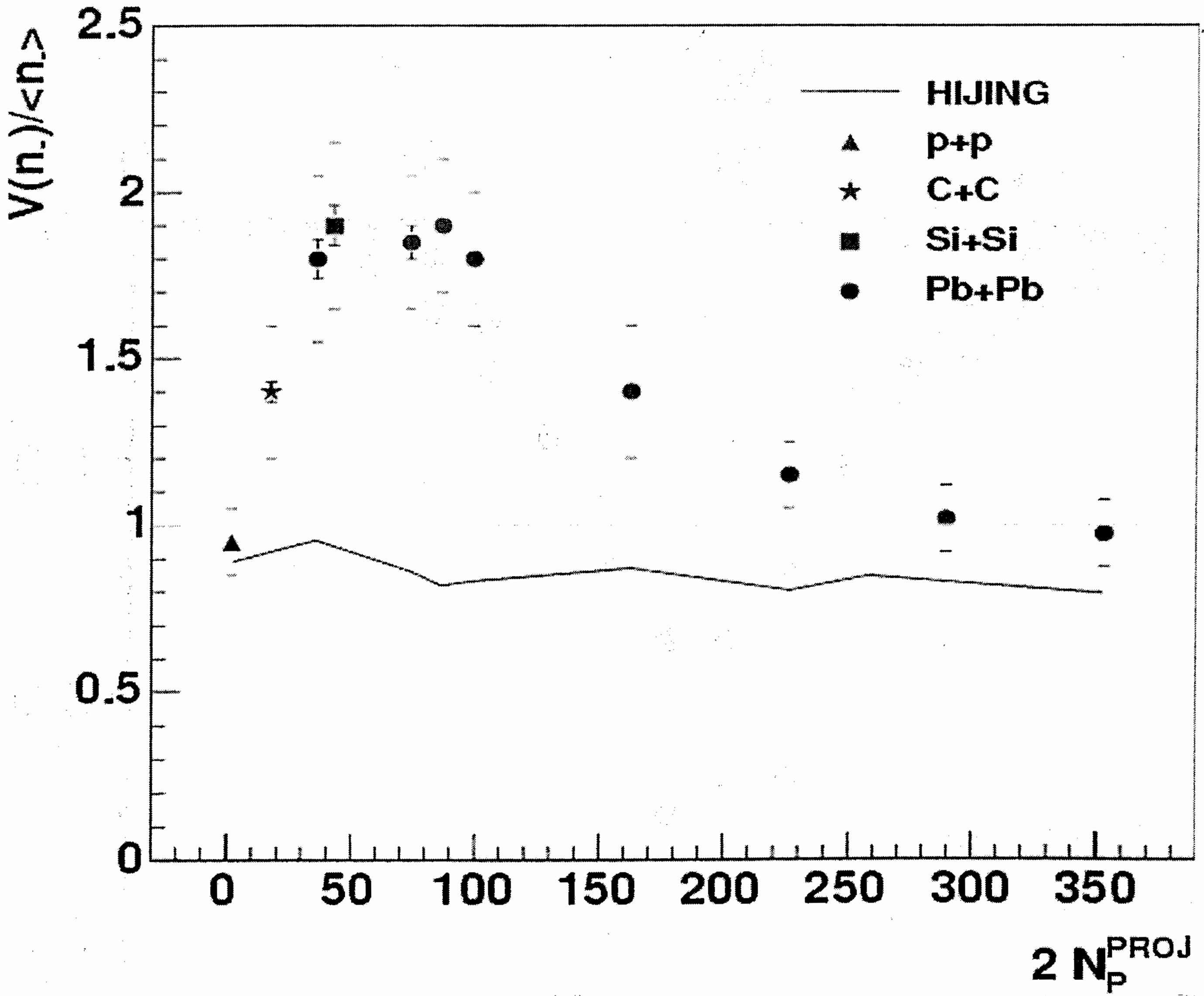

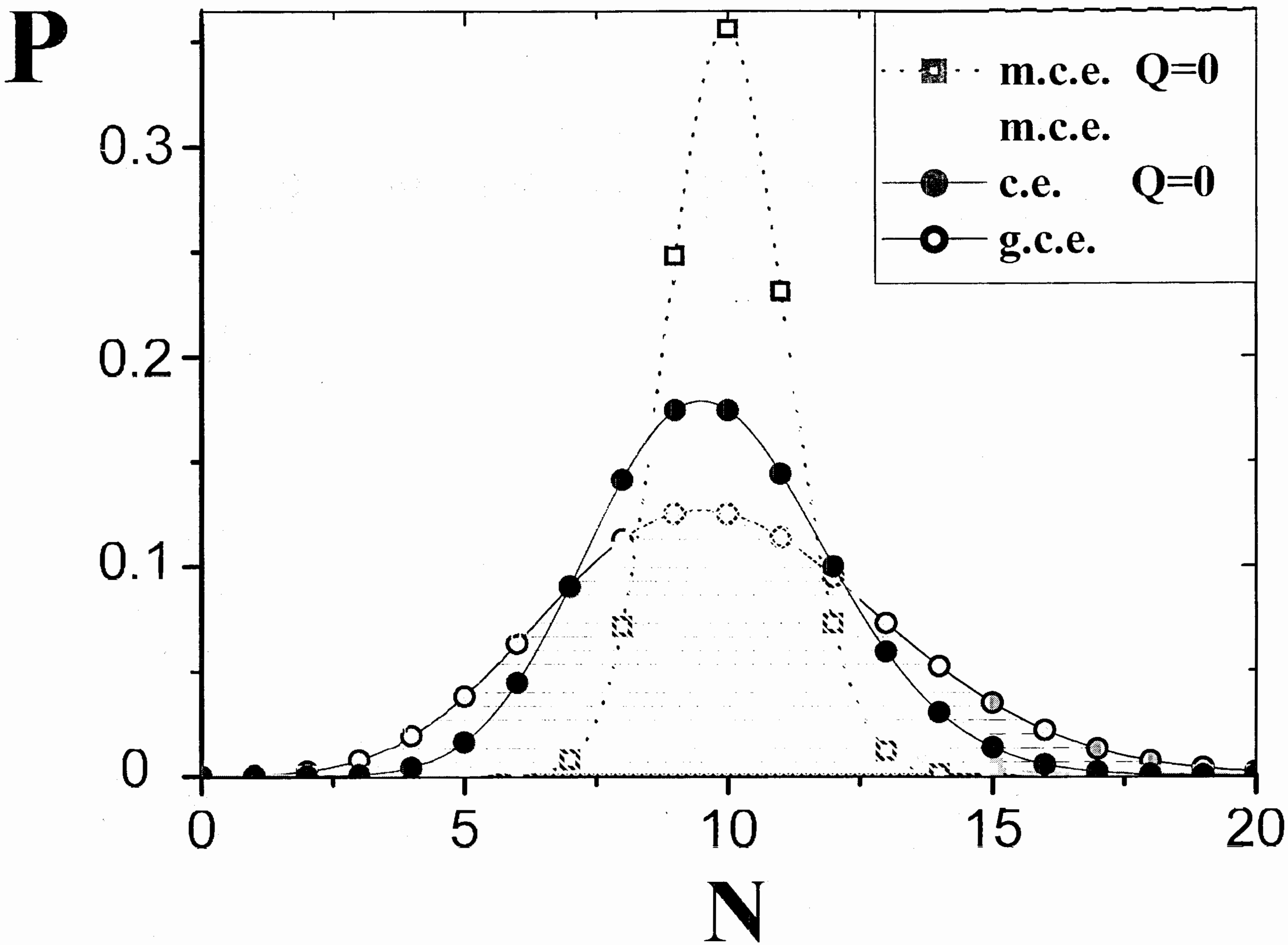
P
0.3
0.2
0.1
0
m.c.e. Q=0
m.c.e.
c.e. Q=0
g.c.e.
0
5
10
15
20
N

A system with two conserved charges (p,n,π-gas)

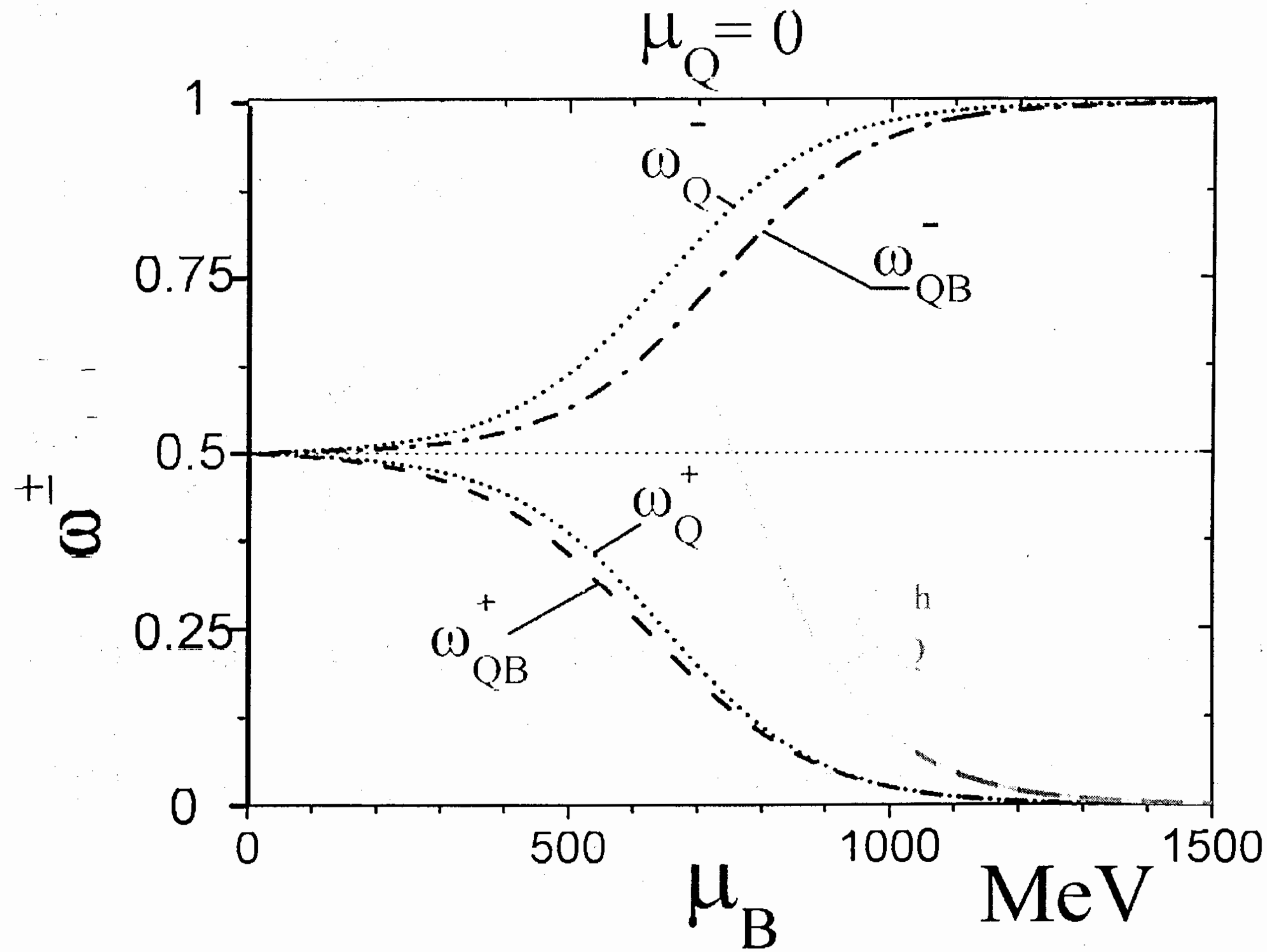

Victor Begun

Definitions of Fluctuations

1. Standard textbooks in statistical physics:

   a) Non-relativistic case: $N_{c.e.}, N_{m.c.e.}$=const,

   b) $$\delta \equiv \frac{\sqrt{<\Delta N^2>}}{<N>} \sim \frac{1}{\sqrt{<N>}} \to 0, \quad N \to \infty.$$

2. Scaled variance:

$$\omega \equiv \frac{<\Delta N^2>}{<N>} \qquad \omega^{\pm}_{g.c.e.} = \omega^{ch}_{g.c.e.} \equiv 1\,.$$

Conclusions

1. $\omega_{g.c.e.} = \omega^{+}_{g.c.e.} = \omega^{-}_{g.c.e.} = \omega^{ch}_{g.c.e.} = 1,$

2. $\omega^{\pm B}_{g.c.e.} \approx 1.368, \qquad \omega^{\pm F}_{g.c.e.} \approx 0.912,$

3. **Q=0,** $\Rightarrow \quad \omega = 1/2,$

4. **Q>0,** $\Rightarrow \quad \omega^{+} < \omega^{-},$

5. **E=const,** $\Rightarrow \quad \omega = 1/4,$

6. **E=const, Q=0** $\Rightarrow \quad \omega^{\pm} = 1/8,$

7. **Large acceptance is required.**

Victor Begun

Thermodynamics

J.Manjavidze
LPP, JINR (Dubna)

- ***Introductory comments***
- ***S-matrix interpretation of thermodynamics***
- ***Connection with Schwinger-Keldysh and Matsubara thermodynamics***
- ***Range of validity of thermodynamic description***
- ***Conclusions***

VHM region: The phase space structure

- “Regge” (BFKL, ...)

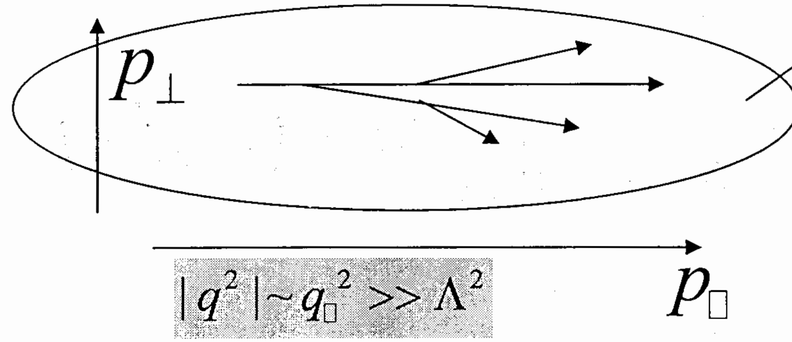

$$\boxed{|K_3|/|K_2|^{3/2} \sim 1/n}$$

•“VHM” – low-x: $|K_3|/|K_2|^{3/2} \ll 1$

•L.Gribov et al.; L.Lipatov;

•J.Manjavidze & A.Sissakian;

•L.MacLerran, D.Kharzeev

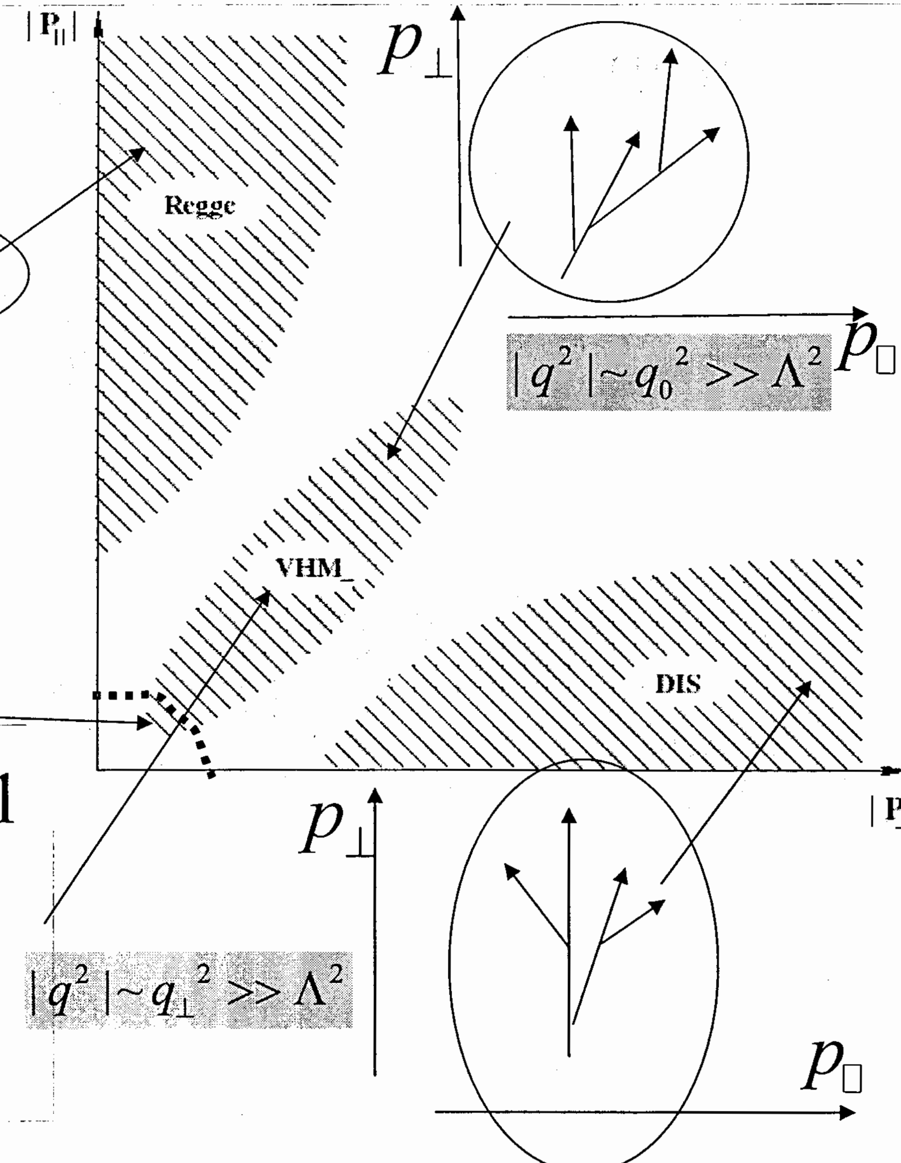

•“DIS” (DGLAP;...)

Weak coupling perturbation theory

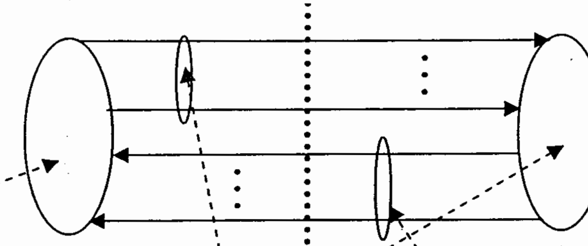

•Weak-coupling theory:

$$i\tilde{D}(q,\beta,z)=\begin{bmatrix} \dfrac{i}{q^2-m^2+i\varepsilon} & 0 \\ 0 & -\dfrac{i}{q^2-m^2-i\varepsilon} \end{bmatrix}+2\pi\delta(q^2-m^2)\begin{bmatrix} 0 & -z_i(q)e^{-\beta_i\varepsilon(q)} \\ z_f(q)e^{-\beta_f\varepsilon(q)} & 0 \end{bmatrix}$$

$$R(\beta,z)=e^{-i\mathrm{V}(-i\hat{\mathrm{j}}_f)+i\mathrm{V}(-i\hat{\mathrm{j}}_i)}\,e^{i\int dx\, j_l(x)D_{lm}(x-y;\beta,z)\,j_m(y)}$$

•Mahanthappa (61)

$$\boxed{\hat{j}\equiv\frac{\delta}{\delta j}}$$

$$\boxed{\text{CMframe:}\quad \alpha=(\mathrm{i}\beta,\vec{0})}$$

The black-body environment

$$z_i = z_f = 1$$

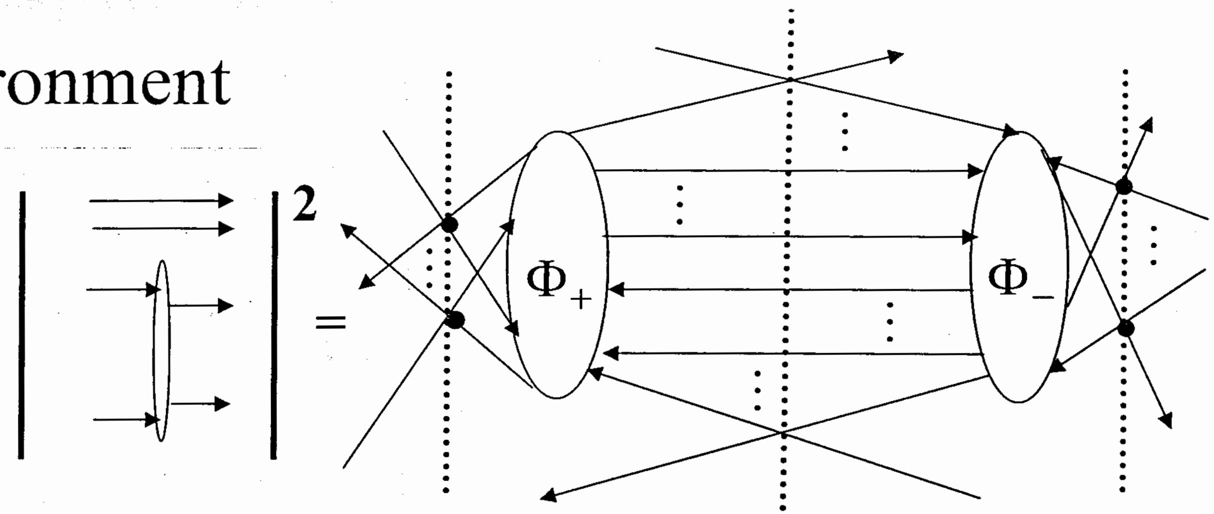

$$iG_s(q;\beta_i,\beta_f,z=1)=\begin{bmatrix} iG_F(q) & 0 \\ 0 & -iG_F{}^*(q)\end{bmatrix}+2\pi\delta(q^2-m^2)\begin{bmatrix}\overline{n}_{++} & -\overline{n}_{+-} \\ -\overline{n}_{-+} & \overline{n}_{--}\end{bmatrix}$$

$$\overline{n}_{++}(q_0)=\overline{n}_{--}(q_0)=\overline{n}\left(\frac{\beta_i+\beta_f}{2}\,|\,q_0\,|\right)$$

Occupation number

$$\overline{n}(\beta q_0)=\frac{1}{e^{\beta q_0}-1}$$

$$\overline{n}_{+-}(q_0)=\Theta(q_0)(1+\overline{n}(q_0\beta_i))+\Theta(-q_0)\overline{n}(-q_0\beta_i)$$

$$\overline{n}_{-+}(q_0)=\Theta(q_0)\overline{n}(q_0\beta_f)+\Theta(-q_0)(1+\overline{n}(-q_0\beta_f))$$

•Schwinger (61), Mahanthappa(61), Keldysh (64), Niemi &Semenoff (84),… $:\beta_i=\beta_f=\beta$

Equilibrium condition

$$\rho(P;z)=\sum_{m,n}\frac{1}{m!n!}\int d\upsilon_m(q,z_i)d\upsilon_n(p,z_f)\delta(P-\sum_{i=1}^{m}q_i)\delta(P-\sum_{i=1}^{n}p_i)\,|a_{mn}|^2$$

$$\rho(P;z)=\int\frac{d^4\alpha_i}{(2\pi)^4}e^{i\alpha_i P}\frac{d^4\alpha_f}{(2\pi)^4}e^{i\alpha_f P}R(\alpha,z):\alpha\to(-i\beta,\vec{0})$$

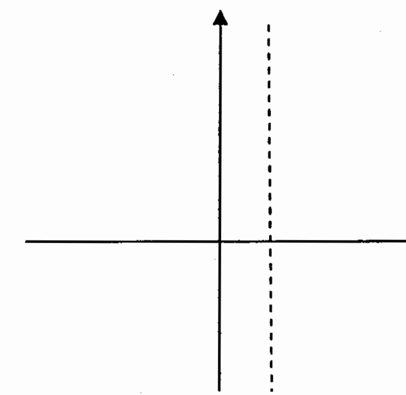

$$\rho(E;z)=\int\frac{d\beta}{2\pi i}e^{+\beta E+\ln R(\beta,z)}:\frac{\partial}{\partial\beta}(\beta E+\ln R(\beta,z))=0,$$

$$E=-\frac{\partial\ln R(\beta,z)}{\partial\beta}:\beta_c(E,z)\to\beta_c(E,n)$$

$$\rho_l\sim\sum_{k=0}^{\infty}(lk)!(K_l/K_2{}^{l/2})^k$$

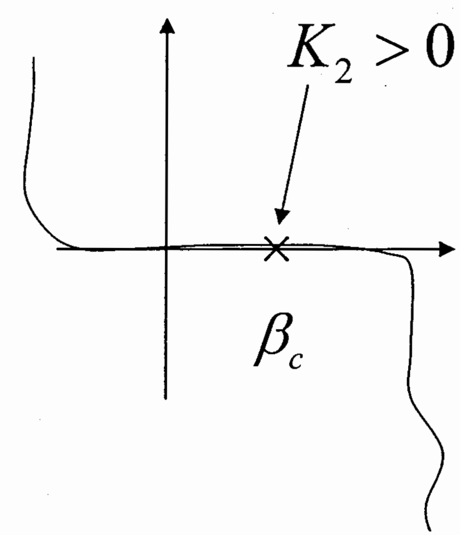

$$K_2=\frac{R''-R'^2}{R^2}$$

$$K_l(E,n)=\frac{\partial^l\ln R(\beta_c,n)}{\partial\beta_c{}^l}:$$

$$K_3=\frac{R'''-3R''R'+2R'^3}{R^3}$$

Local equilibrium

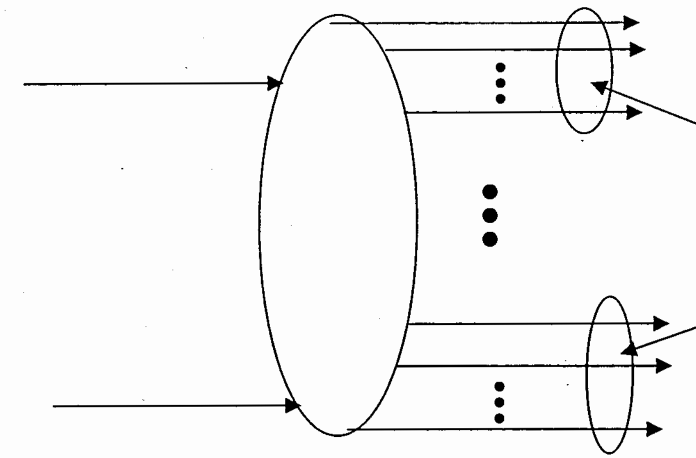

$$\delta(P-\sum_{k=1}^{n} q_k) =$$

$$= \int \prod_{j=1}^{N} \{dQ_j \delta(Q_j - \sum_{k=1}^{n_j} q_{k,j})\} \delta(P - \sum_{j=1}^{N} Q_j)$$

$$R(\{\alpha,z\}^i,\{\alpha,z\}^f;\phi) = \exp\Big\{ i \sum_{j=1}^{N} \Big[\int dx dx' \widehat{\phi}_+(x) D_{+-}(x-x';\alpha_j^i, z_j^i) \widehat{\phi}_-(x') -$$

$$- \int dx dx' \widehat{\phi}_-(x) D_{+-}(x-x';\alpha_j^f, z_j^f) \widehat{\phi}_+(x') \Big] \Big\} R_0(\phi)$$

$$R(\{\alpha,z\}^i,\{\alpha,z\}^f;\phi) = \exp\Big\{ i \int dx dx' \widehat{\phi}_-(x) D_{+-}(x-x';\alpha^i, z^i) \phi_+(x')$$

$$- \int dx dx' \widehat{\phi}_-(x) D_{-+}(x-x';\alpha^f, z^f) \phi_+(x') \Big\} R_0(\phi)$$

Wigner functions

(x+x')=2R

(x-x')=r ⟶ q

y=R!

$$\{q,R\}=\hbar:$$

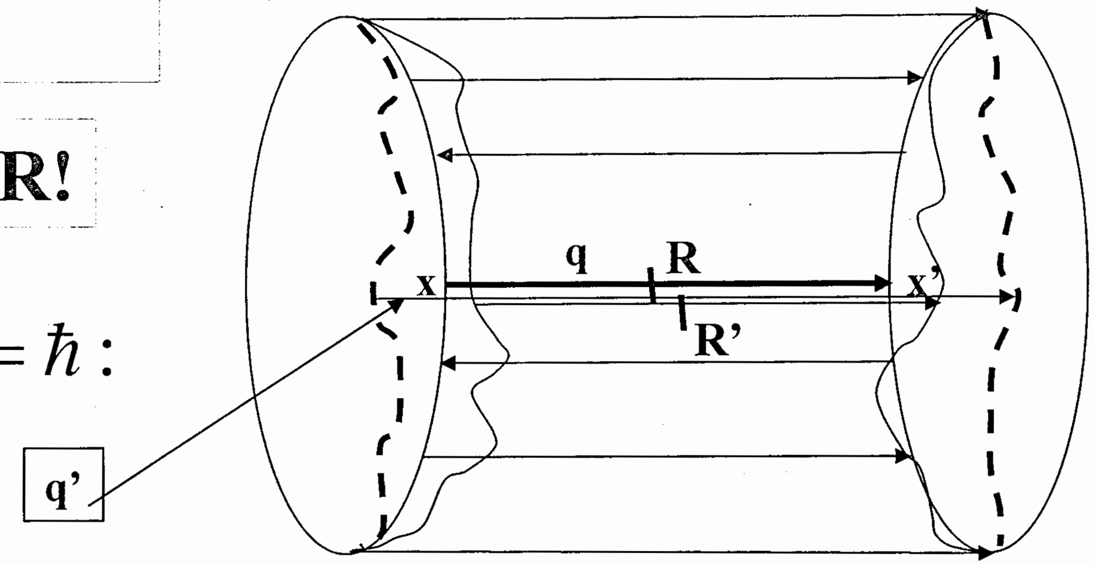

$$R(\{\alpha,z\}^i,\{\alpha,z\}^f;\phi)=\exp\Big\{i\sum_{j=1}^{N}\Big[\int dxdx'\,\widehat{\phi}_+(x)D_{+-}(x-x';\alpha_j^i,z_j^i)\widehat{\phi}_-(x')-$$

$$-\int dxdx'\,\widehat{\phi}_-(x)D_{+-}(x-x';\alpha_j^f,z_j^f)\widehat{\phi}_+(x')\Big]\Big\}R_0(\phi)$$

$$W_1(\{\beta,z\}^i,\{\beta,z\}^f;q,R)=\int dr e^{iqr}e^{-\beta^f(R)\varepsilon(q)}\times$$

$$\times\frac{\delta}{\delta\phi^i(R-r/2)}\frac{\delta}{\delta\phi^f(R+r/2)}R(\{\beta,z\}^i,\{\beta,z\}^f;\phi)\,|_{\phi=0}$$

Local equilibrium: S-matrix

$$R(\{\alpha, z\}^i, \{\alpha, z\}^f) =$$

$$= \exp\Big\{ i\Big[\int dx dx' \widehat{\phi}_+(x) D_{+-}(x-x'; \alpha^i(\frac{x+x'}{2}), z^i(\frac{x+x'}{2}))\phi_-(x') -$$

$$- \int dx dx' \widehat{\phi}_-(x) D_{+-}(x-x'; \alpha^f(\frac{x+x'}{2}), z^f(\frac{x+x'}{2}))\phi_+(x')\Big]\Big\} R_0(\phi)|_{\phi=0}$$

$$R_0(\phi) = Z(\phi_+) Z^*(\phi_-)$$

"Correlators" in processes with the high multiplicity

S.S. Shimanskiy (JINR)

Plan

- “Correlators” in HM processe
- Mathematical trick
- Asymptotic

A. Bialas, V. Koch, Event by Event fluctuations and Inclusive Distributions, Physics Letters B 456 (1999) 1-4

2. Let us consider a variable $x(p)$ which depends on momentum of one particle. We shall discuss event-by-event fluctuations of the quantity

$$S(x) = \sum_{i=1}^{N} x(p_i) \equiv \sum_{i=1}^{N} x(i) \tag{1}$$

where N is the multiplicity of the event.

The *event averaged* moments of this quantity can be expressed as

$$< S^k >= \frac{1}{M} \sum_{m=1}^{M} \sum_{i_1=1}^{N_m} ... \sum_{i_k=1}^{N_m} x_m(i_1)...x_m(i_k) \tag{2}$$

where m labels the different events and M is their total number. N_m is the multiplicity of the event labelled by m.

On the other hand, the moments of $x(p)$ calculated from n-particle inclusive distribution $\rho_n(p_1, ..., p_n)$ are defined as

$$\int dp_1 ... dp_n \rho_n(p_1, ..., p_n)[x(p_1)]^{k_1} ... [x(p_n)]^{k_n} =$$
$$\frac{1}{M} \sum_{m=1}^{M} \sum_{i_1=1}^{N_m} ... \sum_{i_n=1}^{N_m} [x_m(i_1)]^{k_1} ... [x_m(i_n)]^{k_n} \tag{3}$$

where the sums over $i_1 ... i_n$ include only the terms for which all indices $i_1 ... i_n$ are different from each other.

One sees immediately that (2) and (3) are related.

$$< S >= \int dp \rho_1(p) x(p) \tag{4}$$

$$< S^2 >= \int dp_1 dp_2 \rho_2(p_1, p_2) \, x(p_1) x(p_2) + \int dp \rho_1(p) \, [x(p)]^2 \tag{5}$$

$$\begin{aligned} < S^3 > \;\; &= \int dp_1 dp_2 dp_3 \rho_3(p_1, p_2, p_3) \, x(p_1) x(p_2) x(p_3) \\ &+ 3 \int dp_1 dp_2 \rho_2(p_1, p_2) \, x(p_1) [x(p_2)]^2 \\ &+ \int dp \rho_1(p) \, [x(p)]^3 \end{aligned} \tag{6}$$

Similar formulae can be derived for higher moments of S.

Flow at 130 and 200 GeV

Sergei Voloshin

Wayne State University

Outline:

1. Analyses related to flow
2. v_2/ε, the last figure in the flow PRC draft
3. **Flow at $\sqrt{s}$ = 20, 130 and 200 GeV/c.** Centrality determination. 4-particle correlations without generating functions.
4. K^0 and Lambda flow
5. FTPC

Q-vector products and multiparticle correlations

$$u = e^{if}; \quad Q = \sum u; \quad Q_2 = \sum u^2$$

$$\langle u_i u_j^* \rangle = \left\langle \frac{1}{N(N-1)}(QQ^* - N) \right\rangle$$

$$\langle u_i u_j u_k^{*2} \rangle = \left\langle \frac{1}{N(N-1)(N-2)} \left[(Q^2 Q_2^* - N) - (Q_2 Q_2^* - N) - 2(QQ^* - N) \right] \right\rangle$$

$$\begin{aligned} \langle u_i u_j u_k^* u_l^* \rangle = \Bigg\langle \frac{1}{N(N-1)(N-2)(N-3)} \Big[& (Q^2 Q^{*2} - N) - 2N(N-1) \\ & - 4(N-2)(QQ^* - N) - 2(Q^2 Q_2^* - N) + (Q_2 Q_2^* - N) \Big] \Bigg\rangle \end{aligned}$$

Шиманский

ЯДЕРНАЯ ФИЗИКА, 2004, том 67, № 1, с. 70–72

VERY HIGH MULTIPLICITY PHYSICS

ON CORRELATORS FOR HIGH MULTIPLICITY EVENTS

© 2004 J. A. Budagov, Y. A. Kulchitsky[1]*, J. Manjavidze, N. A. Russakovich, A. N. Sissakian
Joint Institute for Nuclear Research, Dubna, Russia

Received May 21, 2003

We present the results of the study of the energy correlators $K_2(n)$, $K_3(n)$ and their ratio $R_3(n)$ in dependence on the hadron multiplicity at the LHC. The PYTHIA generator has been used. The PYTHIA predicts that $R_3(n)$ is not dependent from multiplicity. The $K_2(n)$, $K_3(n)$ and $R_3(n)$ ratio can be studied at ATLAS.

The investigation of the very high multiplicity (VHM) events is a very important task for high energy physics [1]. The purpose of this study is to calculate the energy correlators $K_2(n,s)$, $K_3(n,s)$ and the ratio $R_3(n,s) = |K_3(n,s)|^{2/3}/|K_2(n,s)|$ as a function of hadron multiplicity at ATLAS [2]. The theory predicts that the $R_3(n,s)$ ratio has tendency to equilibrium for the VHM events [1].

We will call the very high multiplicity events the ones for which the condition $n(s) \gg \bar{n}(s)$ is fulfilled, where n is the number of hadrons in an event, $\bar{n}$ is the mean multiplicity of hadrons, and $\sqrt{s}$ is the c.m.s. energy. Figure 1 shows the distribution of $\langle n\rangle P(n)$, where $P(n) = \sigma_n/\sigma_{\rm tot}$, as a function of the secondary particles multiplicity represented in the units of the mean multiplicity. The points are the results of the E735 (FNAL) experiment at 1.8 TeV with $\langle n\rangle = 44$ [3]. The A region corresponds to the multiperipheral kinematics where $n \sim \bar{n}(s)$. The B region is the thermodynamical region corresponding to the approximation of the noninteracting gas where $n \to n_{\max}(s)$. The maximum possible number of hadrons is equal to $n_{\max}(s) = \sqrt{s}/m_\pi$, where m_π is the pion mass. The C region corresponds to the VHM events. The cross section of such a process is significantly smaller than $10^{-7}\sigma_{\rm tot}$ at 2 TeV. The thermodynamical description of the final state events in the high energy physics is possible at the fulfillment of the condition of Bogolyubov's principle of vanishing the correlators [4]: $R_l(n,s) = |K_l(n,s)|^{2/l}/|K_2(n,s)| \ll 1$, where $l = 3, 4, \ldots$, $K_l(n,s)$ is the l-particle energy correlator for the n-particle event. Two and three particle correlators are defined as

$$K_2(n,s) = \langle([\varepsilon_1;n,s] - \langle\varepsilon;n,s\rangle)([\varepsilon_2;n,s] - \langle\varepsilon;n,s\rangle)\rangle,$$

$$K_3(n,s) = \langle([\varepsilon_1;n,s] - \langle\varepsilon;n,s\rangle)([\varepsilon_2;n,s] - \langle\varepsilon;n,s\rangle)([\varepsilon_3;n,s] - \langle\varepsilon;n,s\rangle)\rangle,$$

where ε_i is energy of i-particle and $\langle\varepsilon;n,s\rangle$ is the mean energy.

The PYTHIA has been used for this investigation [5]. For the simulation of the trigger events the hard processes have been used : $q_iq_j \to q_iq_j$, $q_i\bar{q}_i \to q_j\bar{q}_j$, $q_i\bar{q}_i \to gg$, $q_ig \to q_ig$, $gg \to q_i\bar{q}_i$, $gg \to gg$, where q are quarks and g are gluons. The main background for the VHM events at the LHC will be the soft processes. There will be ≈ 23 pp-interaction in the 25 ns of one interaction of bunches at the full LHC luminosity (10^{34} cm^{-2} s^{-1}). The time of the data collection will be 125 ns, for example for the electromagnetic calorimeter. Therefore, there will be written about 115 soft background events, which are called "pile-up", simultaneously with the trigger event. The inelastic processes have been used for the simulation of pile-up events.

Figure 2 (left) shows the results of calculations of the average energy and the correlators $\sqrt{K_2(n)}$, $\sqrt[3]{K_3(n)}$ in the GeV scale as a function of the hadrons multiplicity at 14 TeV. The values of $\sqrt{K_2(n)}$ have signs of $K_2(n)$. As can be seen the $K_2(n)$ and $K_3(n)$ tend to zero at $n_h \to 500$. The dependence of the $R_3(n)$ ratio on n_h is given in Fig. 2 (right). The PYTHIA predictions are given for the A region shown in Fig. 1. The average value of the $R_3(n)$ ratio does not depend on the hadron multiplicity and equals to 1.23. There is no tendency to equilibrium in this region. This can be understood as the PYTHIA is based on the multiperipheral model [1].

[1] Joint Institute for Nuclear Research, Dubna, Russia and Institute of Physics, National Academy of Sciences, Minsk, Belarus

*E-mail: Iouri.Koultchitski@cern.ch

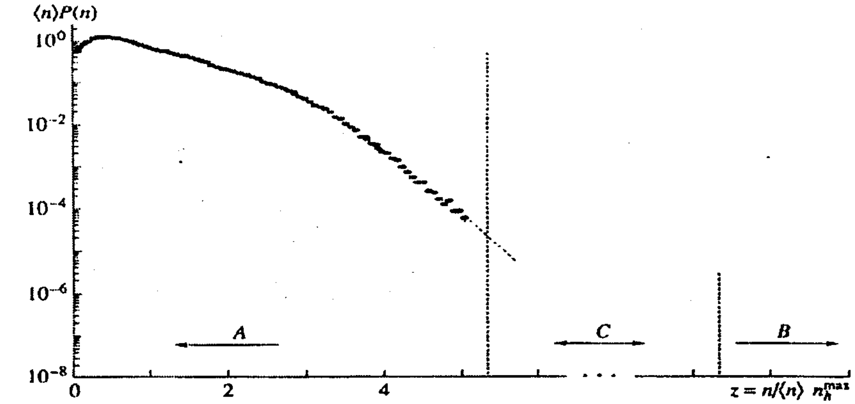

Fig. 1. Multiplicity distribution $\langle n\rangle P(n)$ in the KNO scaling form at 1.8 TeV.

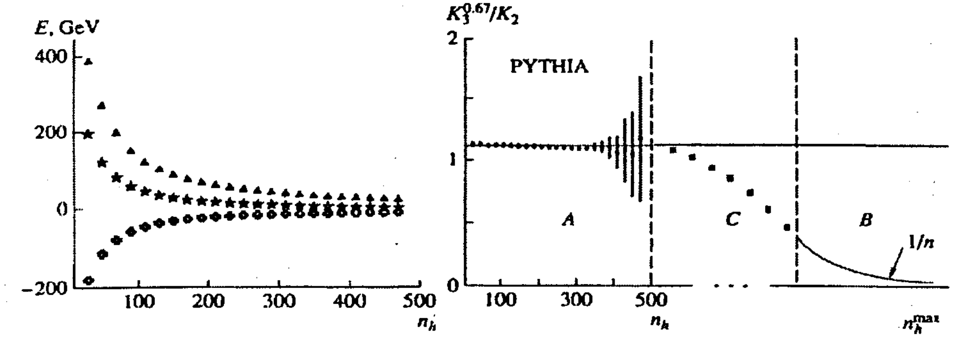

Fig. 2. The average energy (triangulars), the correlators $\sqrt{K_2(n)}$ (crosses), $\sqrt[3]{K_3(n)}$ (stars) on the left side and the $R_3(n)$ ratio (black circles) on the right side as a function of the multiplicity at 14 TeV. The black squares on the right side are the theory supposition for very high multiplicity region.

Harder events have been selected taking into account the experimental trigger conditions. The requirement on the transverse parton momentum $p_t^q \geq p_t^{q,\min}$ has been used, where $p_t^{q,\min} \geq 500$ GeV. This has led to the multiplicity increasing to $\approx$800. However, the tendency to equilibrium is not observed although the $R_3(n)$ ratio decreases to 1.1 for $p_t^q \geq$ ≥ 2000 GeV.

The investigation of behaviour of the VHM events is planned out on the ATLAS (LHC) [2] by using its calorimeter [6]. This calorimeter has beautiful energy resolution $\sigma/E = (42\%/\sqrt{E} + 1.8\%) \oplus 1.8/E$ in the barrel region [7]. Only charged particles with the transverse momentum more than $\approx$1.5–2 GeV reach the calorimeter because of the strong magnetic field (2 T) of the solenoidal magnet. Therefore, only hadrons with $p_t \geq 2$ GeV in the region $|\eta| \leq 2.5$ have been selected. The physics events satisfied the condition $p_t^q \geq p_t^{q,\min}$ for partons have been simulated for the decreasing of the background pile-up events. The obtained distributions of the correlators $K_2(n)$ and $K_3(n)$ as a function of multiplicity taking into account the pile-up are similar of the ones shown in Fig. 2 (left). As a result of using the cuts $p_t \geq 2$ GeV and $|\eta| \leq 2.5$ the maximum multiplicity decreases to $\approx$300 hadrons per event. As before, there is no tendency to equilibrium for the $R_3(n)$ ratio, $R_3(n) =$ $= 1.21$ for $p_t^q \geq 2000$ GeV. It is important to note, that

Mathematical trick

Let $y_1, \ldots, y_N$ be real numbers (a sample).

For each $L \geq 1$ consider

$$S_L = \sum_{i=1}^{N} y_i^L$$

and

$$D_L = \sum_{i_1 < \cdots < i_L} y_{i_1} \cdots y_{i_L}$$

where the sum is taken over all combinations of L distinct indices $i_1, \ldots, i_L$, and each combination is used exactly once.

It is important to note that

$$y_1 + \cdots + y_L = S_1 \tag{1}$$

Squaring this equation gives

$$\sum_{i=1}^{2} y_i^2 + 2\sum_{i<j} y_i y_j = S_1^2.$$

hence

$$S_2 + 2D_2 = S_1^2, \qquad D_2 = \frac{1}{2}S_1^2 - \frac{1}{2}S_2,$$

which is our desired relation for $L = 2$.

Now consider the case $L \geq 3$. First, note that

$$D_L = \frac{1}{L!} \sum_{i_1 \neq \cdots \neq i_L} y_{i_1} \cdots y_{i_L}, \tag{2}$$

where the sum is taken over all combinations of L distinct indices $i_1, \ldots, i_L$ (because there are $L!$ permutations of L distinct indices). Summing over i_L gives

$$\sum_{i_L \notin \{i_1, \ldots, i_{L-1}\}} y_{i_L} = S_1 - y_{i_1} - \cdots - y_{i_{L-1}} \quad .$$

because of (1). This allows us to eliminate y_{i+L} and reduce the summation in (2). **This is the main principle.**

For $L = 3$, we get

$$\begin{aligned}
D_3 &= \frac{1}{3!} \sum_{i \neq j \neq k} y_i y_j y_k \\
&= \frac{1}{3!} \sum_{i \neq j} y_i y_j (S_1 - y_i - y_j) \\
&= \frac{1}{3!} (S_1 \sum_{i \neq j} y_i y_j - \sum_{i \neq j} y_i^2 y_j - \sum_{i \neq j} y_i y_j^2) \\
&= \frac{1}{3!} (S_1 \sum_{i} y_i (S_1 - y_i) - \sum_{i \neq j} y_i^2 (S_1 - y_i) - \sum_{i \neq j} (S_1 - y_j) y_j^2) \\
&= \frac{1}{3!} (S_1^2 \sum_{i} y_i - S_1 \sum_{i} y_i^2 - 2(S_1 \sum_{i} y_i^2 - \sum_{i} y_i^3)) \\
&= \frac{1}{3!} (S_1^3 - 3S_1 S_2 + 2S_3).
\end{aligned}$$

REDUCE CODE

- input_case nil$
- operator S;

- procedure p3(x,l,r);
- if r={} then s(reverse(x.l))
- else if first(r)>x then s(append(reverse(x.l),r))
- else p3(x,first(r).l,rest(r))$

- procedure p2(x,l,r,z);
- if r={} then z
- else p2(x,first(r).l,rest(r),z-p3(x+first(r),l,rest(r)))$

- procedure s(l);
- if rest(l)={} then S(first(l))
- else p2(first(l),{},rest(l),else S(first(l))*s(rest(l))$

- procedure D(n);
- s(for i:=1:n collect 1)/factorial(n);

- end;

As example D(5):

$$D_5 = \frac{1}{5}S_5 - \frac{1}{4}S_4S_1 - \frac{1}{6}S_3S_2 + \frac{1}{6}S_3S_1^2 + \frac{1}{8}S_2^2S_1 - \frac{1}{12}S_2S_1^3 + \frac{1}{120}S_1^5$$

Шиманский

ЯДЕРНАЯ ФИЗИКА, 2004, том 67, № 1, с. 70–72

ON CORRELATORS FOR HIGH MULTIPLICITY EVENTS

© 2004 J. A. Budagov, Y. A. Kulchitsky[1]*, J. Manjavidze, N. A. Russakovich, A. N. Sissakian

Joint Institute for Nuclear Research, Dubna, Russia

Received May 21, 2003

We present the results of the study of the energy correlators $K_2(n)$, $K_3(n)$ and their ratio $R_3(n)$ in dependence on the hadron multiplicity at the LHC. The PYTHIA generator has been used. The PYTHIA predicts that $R_3(n)$ is not dependent from multiplicity. The $K_2(n)$, $K_3(n)$ and $R_3(n)$ ratio can be studied at ATLAS.

The investigation of the very high multiplicity (VHM) events is a very important task for high energy physics [1]. The purpose of this study is to calculate the energy correlators $K_2(n,s)$, $K_3(n,s)$ and the ratio $R_3(n,s) = |K_3(n,s)|^{2/3}/|K_2(n,s)|$ as a function of hadron multiplicity at ATLAS [2]. The theory predicts that the $R_3(n,s)$ ratio has tendency to equilibrium for the VHM events [1].

We will call the very high multiplicity events the ones for which the condition $n(s) \gg \bar{n}(s)$ is fulfilled, where n is the number of hadrons in an event, $\bar{n}$ is the mean multiplicity of hadrons, and $\sqrt{s}$ is the c.m.s. energy. Figure 1 shows the distribution of $\langle n\rangle P(n)$, where $P(n) = \sigma_n/\sigma_{\rm tot}$, as a function of the secondary particles multiplicity represented in the units of the mean multiplicity. The points are the results of the E735 (FNAL) experiment at 1.8 TeV with $\langle n\rangle = 44$ [3]. The A region corresponds to the multiperipheral kinematics where $n \sim \bar{n}(s)$. The B region is the thermodynamical region corresponding to the approximation of the noninteracting gas where $n \to n_{\max}(s)$. The maximum possible number of hadrons is equal to $n_{\max}(s) = \sqrt{s}/m_\pi$, where m_π is the pion mass. The C region corresponds to the VHM events. The cross section of such a process is significantly smaller than $10^{-7}\sigma_{\rm tot}$ at 2 TeV. The thermodynamical description of the final state events in the high energy physics is possible at the fulfillment of the condition of Bogolyubov's principle of vanishing the correlators [4]: $R_l(n,s) = |K_l(n,s)|^{2/l}/|K_2(n,s)| \ll 1$, where $l = 3, 4, \ldots$, $K_l(n,s)$ is the l-particle energy correlator for the n-particle event. Two and three particle correlators are defined as

$$K_2(n,s) = \langle([\varepsilon_1;n,s] - \langle\varepsilon;n,s\rangle)([\varepsilon_2;n,s] - \langle\varepsilon;n,s\rangle)\rangle,$$

$$K_3(n,s) = \langle([\varepsilon_1;n,s] - \langle\varepsilon;n,s\rangle)([\varepsilon_2;n,s] - \langle\varepsilon;n,s\rangle)([\varepsilon_3;n,s] - \langle\varepsilon;n,s\rangle)\rangle,$$

where ε_i is energy of i-particle and $\langle\varepsilon;n,s\rangle$ is the mean energy.

The PYTHIA has been used for this investigation [5]. For the simulation of the trigger events the hard processes have been used: $q_iq_j \to q_iq_j$, $q_i\bar{q}_i \to q_j\bar{q}_j$, $q_i\bar{q}_i \to gg$, $q_ig \to q_ig$, $gg \to q_i\bar{q}_i$, $gg \to gg$, where q are quarks and g are gluons. The main background for the VHM events at the LHC will be the soft processes. There will be ≈ 23 pp-interaction in the 25 ns of one interaction of bunches at the full LHC luminosity (10^{34} cm^{-2} s^{-1}). The time of the data collection will be 125 ns, for example for the electromagnetic calorimeter. Therefore, there will be written about 115 soft background events, which are called "pile-up", simultaneously with the trigger event. The inelastic processes have been used for the simulation of pile-up events.

Figure 2 (left) shows the results of calculations of the average energy and the correlators $\sqrt{K_2(n)}$, $\sqrt[3]{K_3(n)}$ in the GeV scale as a function of the hadrons multiplicity at 14 TeV. The values of $\sqrt{K_2(n)}$ have signs of $K_2(n)$. As can be seen the $K_2(n)$ and $K_3(n)$ tend to zero at $n_h \to 500$. The dependence of the $R_3(n)$ ratio on n_h is given in Fig. 2 (right). The PYTHIA predictions are given for the A region shown in Fig. 1. The average value of the $R_3(n)$ ratio does not depend on the hadron multiplicity and equals to 1.23. There is no tendency to equilibrium in this region. This can be understood as the PYTHIA is based on the multiperipheral model [1].

[1] Joint Institute for Nuclear Research, Dubna, Russia and Institute of Physics, National Academy of Sciences, Minsk, Belarus

* E-mail: Iouri.Koultchitski@cern.ch

For case when S_1=0:

$$\begin{aligned}
D_2 &= -\frac{1}{2}S_2 \\
D_3 &= \frac{1}{3}S_3 \\
D_4 &= -\frac{1}{4}S_4 + \frac{1}{8}S_2^2 \\
D_5 &= \frac{1}{5}S_5 - \frac{1}{6}S_2S_3 \\
D_6 &= -\frac{1}{6}S_6 + \frac{1}{8}S_4S_2 + \frac{1}{18}S_3^2 - \frac{1}{48}S_2^3 \\
D_7 &= \frac{1}{7}S_7 - \frac{1}{10}S_5S_2 - \frac{1}{12}S_4S_3 + \frac{1}{24}S_3S_2^2 \\
D_8 &= -\frac{1}{8}S_8 + \frac{1}{12}S_6S_2 + \frac{1}{15}S_5S_3 + \frac{1}{32}S_4^2 - \frac{1}{32}S_4S_2 - \frac{1}{36}S_3^2S_2 + \frac{1}{384}S_2^4
\end{aligned} \tag{2}$$

Density function - $f(x)$

$$1 = \int f(x)dx \qquad 1 = \frac{1}{N}\sum i$$

$$\overline{x} = \int x \cdot f(x)dx \qquad \overline{x} = \frac{1}{N}\sum x_i$$

Central moments -

$$\mu_L = \int (x - \overline{x})^L \cdot f(x)dx \qquad \mu_L = \frac{1}{N}\sum (x_i - \overline{x})^L$$

Let's be K_L-**correlators**, through D_L:

$$K_L = \bar{D}_L = \frac{1}{C_N^L} D_L$$

— correlator power L, where

$$C_N^L = \frac{N!}{L!(N-L)!} \sim N^L$$

— term number in D_L.

μ_L it is **central moments**

$$\mu_L = \frac{1}{N} S_L$$

Asymptotic for K_L

$$L = 2n+1 \qquad K_{2n+1} \sim \frac{S_2^{n-1} \cdot S_3}{N^{2n+1}} \sim \frac{\mu_2^{n-1} \cdot \mu_3}{N^{n+1}}$$

$$L = 2n \qquad K_{2n} \sim \frac{S_2^{n}}{N^{2n}} \sim \frac{\mu_2^{n}}{N^{n}}$$

$$K_2 \sim -\frac{\mu_2}{N}$$

$$K_3 \sim \frac{\mu_3}{N^2}$$

$$K_4 \sim \frac{\mu_2^2}{N^2}$$

343

Asymptotic for ratio:

$$f_L = \frac{|K_L|^{\frac{2}{L}}}{|K_2|},$$

$$L = 2n+1 \qquad f_{2n+1} \sim \frac{1}{N^{\frac{1}{2n+1}}}$$

$$L = 2n \qquad f_{2n} \sim const$$

Average on set of "events":

$$\overline{x_m} = \frac{1}{N} \sum_{i=1}^{N} x_{m,i}$$

$$\tilde{x} = \frac{1}{M} \sum_{m=1}^{M} \overline{x_m}$$

Then, if $y_{m,i} = x_{m,i} - \overline{x_m}$ will be

$$\sum_{i=1}^{N} y_{m,i} = 0. \tag{1}$$

Introduce:

$$\widetilde{y_{m,i}} = x_{m,i} - \tilde{x} = (x_{m,i} - \overline{x_m}) + (\overline{x_m} - \tilde{x}) = y_{m,i} + \Delta_m$$

$$\sum_{i=1}^{N} \widetilde{y_{m,i}} = \sum_{i=1}^{N} (y_{m,i} + \Delta_m) = N \cdot \Delta_m$$

Let's receive connection $\widetilde{D_{m,L}}$ with old ones(event case) $D_{m,L}$ for which we have known asymptotic. For two tracks event we will have:

$$\widetilde{D_{m,2}} = \widetilde{y_{m,1}} \cdot \widetilde{y_{m,2}} = (y_{m,1}+\Delta_m)\cdot(y_{m,2}+\Delta_m) = y_{m,1}\cdot y_{m,2}+2\cdot\Delta_m\cdot(y_{m,1}+y_{m,2})+\Delta_m^2 = D_{m,2}+\Delta_m^2$$

It is trivial the general formula turns out.

$$\widetilde{D_{m,L}} = \sum_{i=0}^{L} {C'}_{N_m-i}^{L-i} \cdot D_{m,i} \cdot \Delta_m^{L-i} = {C'}_{N_m}^{L} \cdot \Delta_m^L + \sum_{i=2}^{L} {C'}_{N_m-i}^{L-i} \cdot D_{m,i} \cdot \Delta_m^{L-i}$$

$$\widetilde{D_{m,2}} = {C'}_{N_m}^{2} \cdot \Delta_m^2 + D_{m,2} = {C'}_{N_m}^{2} \cdot \Delta_m^2 - \frac{1}{2} S_{m,2}$$

$$\widetilde{K_{m,L}} = \frac{\widetilde{D_{m,L}}}{{C'}_{N_m}^{L}} = \Delta_m^L + O(\frac{1}{N_m})$$

$$\widetilde{K_{m,2}} = \Delta_m^2 - \frac{\mu_{m,2}}{(N-1)}$$

$$\frac{\widetilde{K_{m,L}}}{\widetilde{K_{m,2}}^{\frac{L}{2}}} \sim \frac{\Delta_m^L}{(\Delta_m^2)^{\frac{L}{2}}}$$

"Correlators" and "Moments",
Stadnik A.V., Chernov N.I.,Shimanskiy
Communication of the JINR, P11-2003-143

- Shimanskiy S.S.
  Seminar VBLHE, October, 27 2004
  Seminar VBLHE-LPP, March, 11, 2005

- REDUCE programs by Grozin A.G. (BINP,Novosibirsk)

Thank you!

"Polarization studies as additional tool to search and study of the quark-gluon plasma"

S.S. Shimanskiy (VBLHE, JINR)

QGP'2000 at CERN

A common assessment of the collected data leads us to conclude that we now have compelling evidence that a new state of matter has indeed been created, at energy densities which had never been reached over appreciable volumes in laboratory experiments before and which exceed by more than a factor 20 that of normal nuclear matter. The new state of matter found in heavy ion collisions at the SPS features many of the characteristics of the theoretically predicted quark-gluon plasma.

QGP'2003 at BNL

TJH RHIC PAC 9/29-30, 2003 TJH RHIC PAC 9/29-30, 2003

- ***Conclusions About Matter at RHIC:***
  - **The data on high pt suppression and correlations support the conclusion that we have produced a medium that:**
    - **- is dense; (pQCD theory →many times cold nuclear matter density)**
    - **- is dissipative(very strongly interacting)**
  - **We need to show that:**
    - **- dissipation and collective behavior occur at the partonic stage**
    - **- the system is deconfined and thermalized**
    - **- a transition occurs: can we turn the effects off ?**
  - **We need:**
    - **- extended AuAu run needed to address several important probes that need large data sets (e.g., pT-dependence of suppression; J/ψ, ϒ, open charm, heavy baryon / meson flow); also, species and energy scans to map the evolution of key observables**
    - **- more guidance from theory (!) particularly on what to expect from hadronic scenarios**

QGP + SPIN

How we can use SPIN to find thermalization?

the system is thermalized $\equiv$ in the plasma rest frame there is no preferred direction, no polarization

Paul Hoyer, Physics Letters B,v.187 (1987)162
Particle polarization as a signal of plasma formation

“Heavy ion collisions leading to the formation of quark-gluon plasma are characterized by an isotropic distribution of the parton momenta in the plasma rest frame. We discuss the restrictions that this isotropy imposees on the polarizations of plasma-produced virtual photons, hyperons and hadronic resonances. “

(October 5, 2001)

Λ transverse polarization measurement at mid-rapidity from Au+Au collisions at $\sqrt{s_{\mathrm{NN}}} = 130$ GeV

Maria Castro and Rene Bellwied (Wayne State University)

Abstract

We report first results on transverse polarization of Λ hyperons at mid-rapidity in Au+Au collisions at $\sqrt{s_{NN}} = 130$ GeV using the STAR TPC at RHIC. Our measurements of the Λ polarization, P, measured over the full kinematic range of $|x_f| < 0.03$ and $p_t < 5$ GeV/c is consistent with zero within 2σ. The Λ sample has also been binned in p_t. Again, the polarization measurement in each bin shows no significant deviation from zero.

TABLE II: **Polarization for each p_t range and rapidity range**

p_t (GeV/c)	P(-0.5<y<0.5)	χ^2/dof	P(y>0)	χ^2/dof	P(y<0)	χ^2/dof
0-5	-0.0165 ± 0.0154	23.93/18	0.0274 ± 0.0219	26.1/18	-0.0575 ± 0.0216	17.23/18
0-0.5	-0.126 ± 0.147	8.018/8	-0.143 ± 0.205	2.911/8	-0.0843 ± 0.222	8.369/8
0.5-1	-0.0573 ± 0.0286	3.802/8	-0.0225 ± 0.0262	5.126/8	-0.0941 ± 0.0402	4.688/8
1-1.5	-0.00137 ± 0.0249	12.13/18	0.0231 ± 0.0356	13.01/18	-0.0252 ± 0.0349	14.9/18
1.5-2	0.0203 ± 0.0337	25.7/18	0.0806 ± 0.0472	15.06/18	-0.0339 ± 0.0482	25.85/18
2-5	-0.0106 ± 0.0450	20.65/18	0.0956 ± 0.0633	14/18	-0.0286 ± 0.0644	18.46/18

TABLE III: **Polarization for each p_t range**

p_t (GeV/c)	$\frac{P(y>0)-P(y<0)}{2}$
0-5	0.0423 ± 0.0154
0-0.5	-0.0293 ± 0.1511
0.5-1	0.0358 ± 0.0240
1-1.5	0.0242 ± 0.0249
1.5-2	0.0573 ± 0.0337
2-5	0.0621 ± 0.0452

Dileptons as an unique probes for QGP

- **Haven’t strong interaction.**
- **Come out from all evolution stages.**

CERES/NA45 data

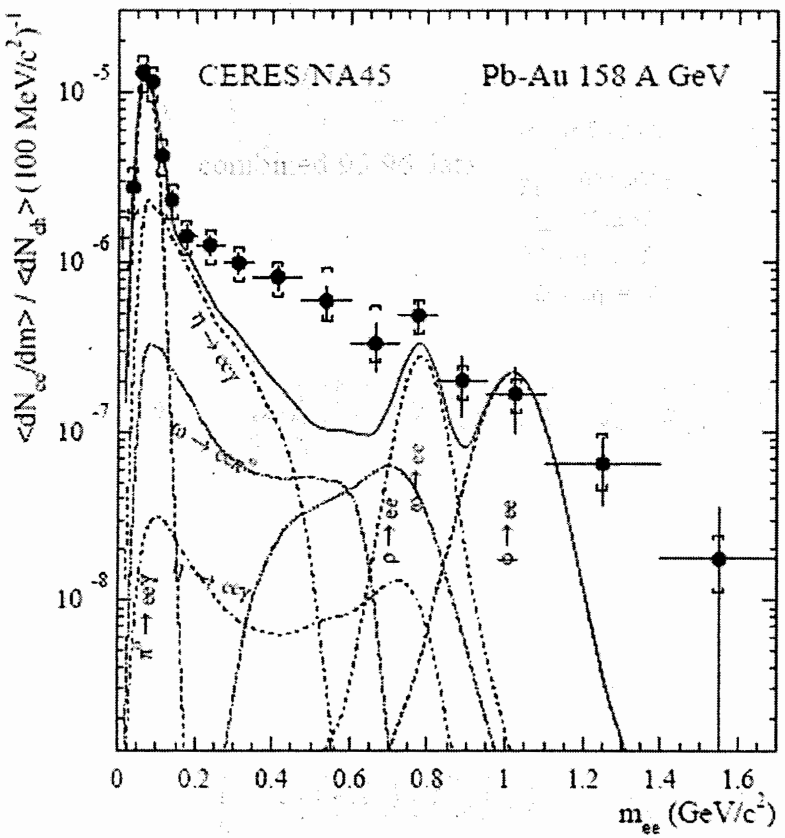

(# of pairs) with $m > 0.2$ GeV/c^2: 2670±260
combined signal/background: 1/12

Electron-Pair Spectrum at 40 AGeV/c

S. Damjanovic

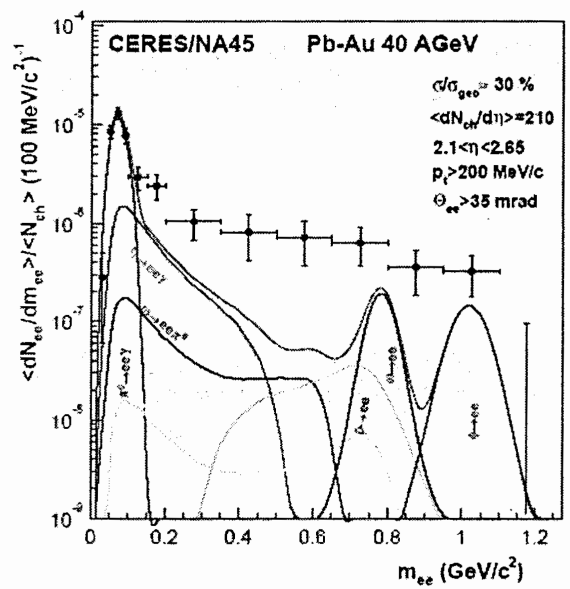

mass range	# of pairs	S/B	syst. err.
$m_{ee} < 0.2\,GeV/c^2$	249±28	1/1	16%
$m_{ee} > 0.2\,GeV/c^2$	185±48	1/6	26%

- particle ratios from thermal model fit to PbPb data
- rapidity and p_t distributions from PbPb systematics
- folded with experimental mass resolution 4.2% (ω)

Enhancement for $m_{ee} > 0.2\,GeV/c^2$ compared to cocktail:
5.1±1.3(stat)±1.0(syst)

Dileptons Anisotropies. How we can resolve sub processes using its?

The simple examples.

For

$$q\bar{q} \rightarrow e^+ \ e^-$$

will be the following angular distribution

$$\frac{d\sigma}{dcos\theta} \sim 1 + B \cdot cos^2\theta.$$

but for

$$\pi^+ \ \pi^- \rightarrow e^+ \ e^-$$

will be

$$\frac{d\sigma}{dcos\theta} \sim 1 - B \cdot cos^2\theta.$$

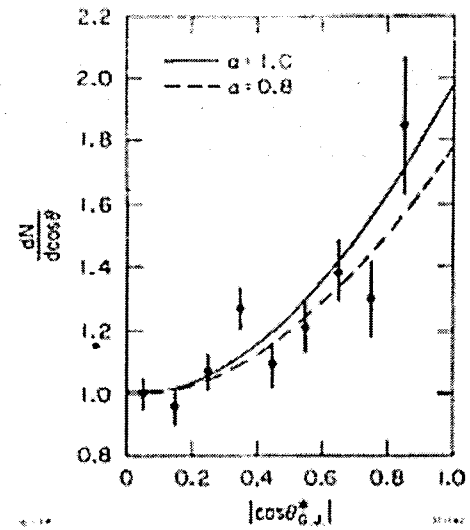

Fig. 2. Distribution of $\cos\theta^*$ for $\pi^- N \rightarrow \mu^+\mu^- X$ at 200 GeV/c with $4 < M < 6$ GeV and $p_T < 1$ GeV/c. The two curves correspond to formula (4) description of the data.

Integration over either polar or azimuthal angle gives:

$$W_1(\theta^*) \sim 1 + \alpha\cos^2\theta^*$$

$$W_2(\phi) \sim 1 + \beta\cos 2\phi$$

where both α and β may vary between -1 and +1.

NN-reactions

TRANSPARENCES

e+e- anisotropy (theory)

E.L. Bratkovskaya, O.V. Teryaev, V.D. Toneev from JINR

Phys. Lett. B 348 (1995) 283.

E.L. Bratkovskaya, O.V. Teryaev, V.D. Toneev +

W. Cassing, U. Mosel, M. Schafer from Giessen

Phys. Lett. B 348 (1995) 325.

W. Cassing, E.L. Bratkovskaya

Physics Reports 308 (1999) 65-233.

GSI and more energies

Bratkovskaya E.L. et al., Z. Phys. C 75, 119.126 (1997)

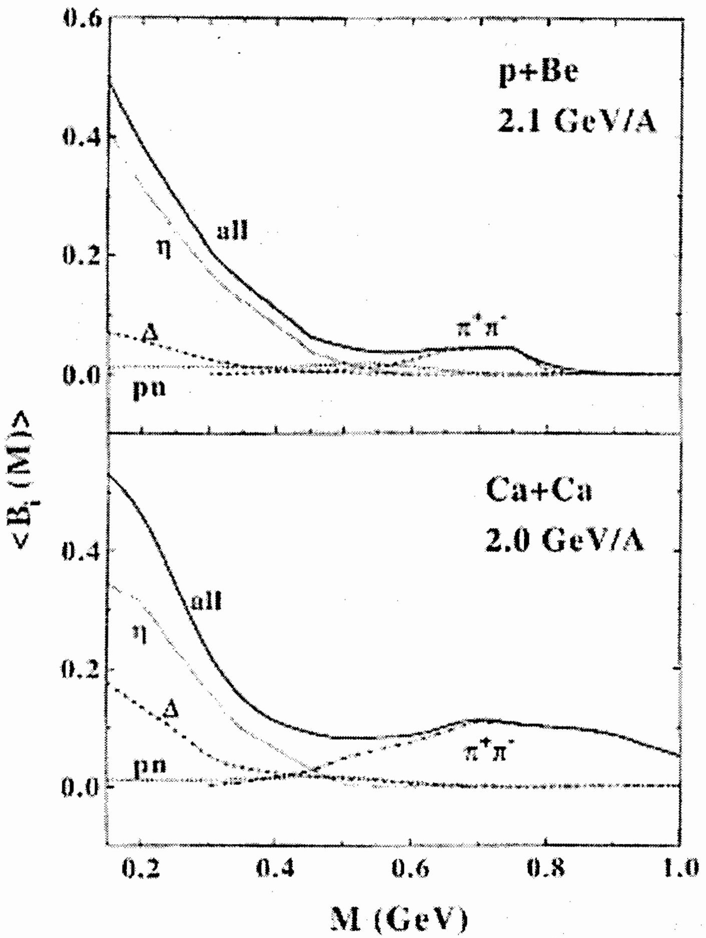

Fig. 1. The weighted anisotropy coefficients $\langle B_i(M)\rangle$ for p + Be collisions at the bombarding energy of 2.1 GeV and Ca + Ca collisions at the bombarding energy of 2.0 GeV/A. The "η" denotes the contribution of the η-channel, the "Δ" labels the contribution of the Δ Dalitz decay, "pn" the proton-neutron bremsstrahlung, and "$\pi^+\pi^-$" the pion annihilation channel. The solid curves (denoted by "*all*") show the sum of all sources

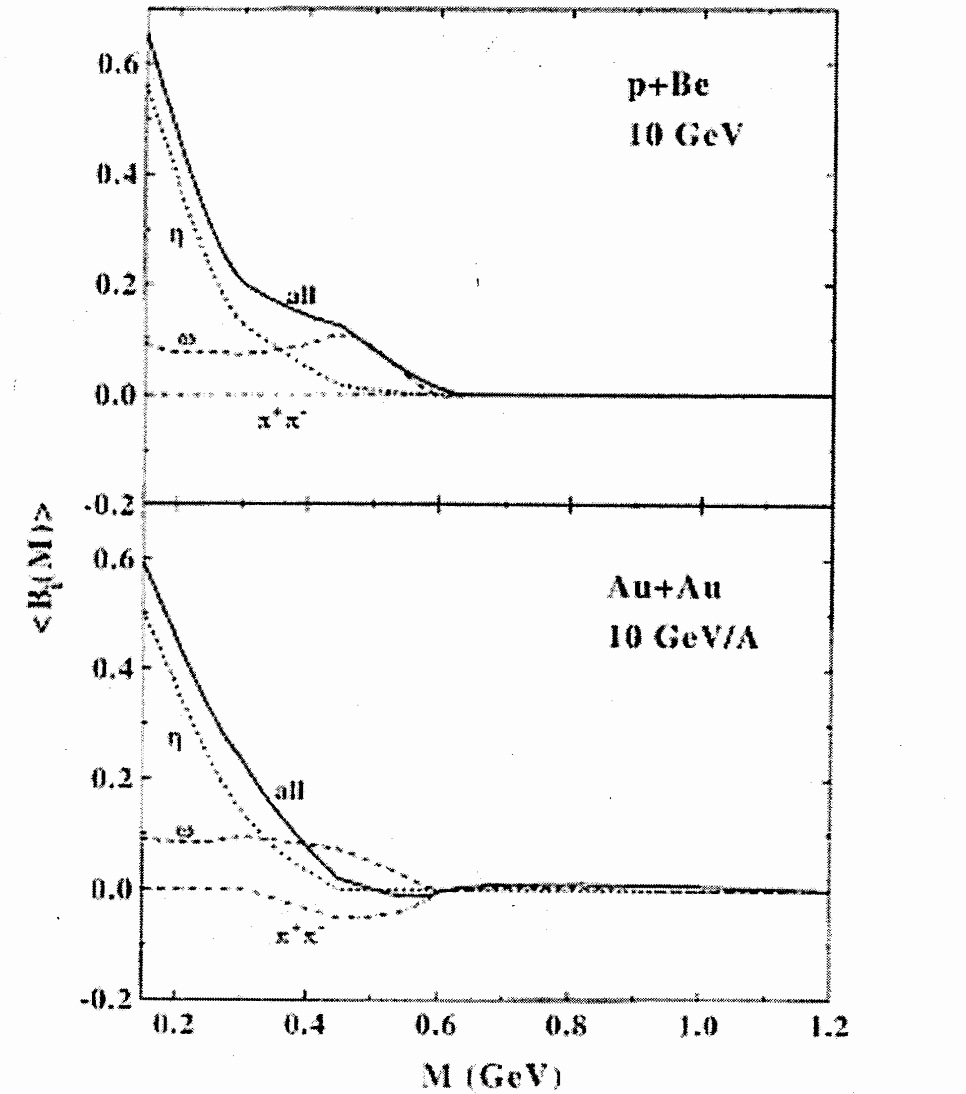

Fig. 3. The weighted anisotropy coefficients $\langle B_i(M)\rangle$ for p + Be and central Au + Au collisions at 10 GeV/A. The notation is the same as in Fig. 2

SPS energy

Bratkovskaya E.L. et al., Z. Phys. C 75, 119.126 (1997)

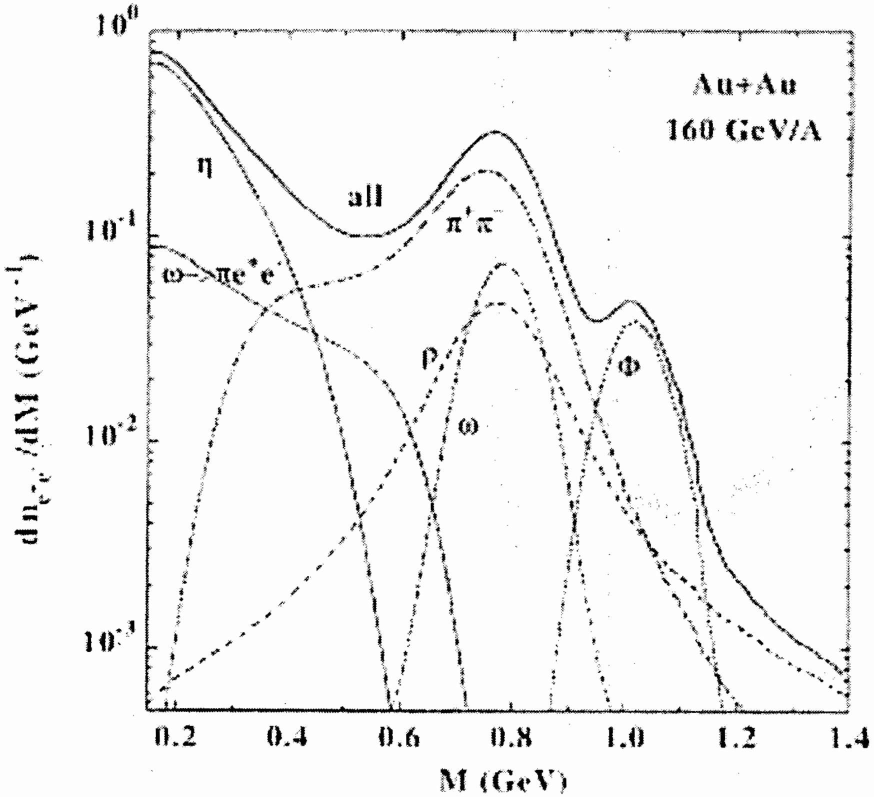

Fig. 5. The differential multiplicity $dn_{e^+e^-}/dM$ for a central Au + Au collision at 160 GeV/A. The notation is the same as in Fig. 2

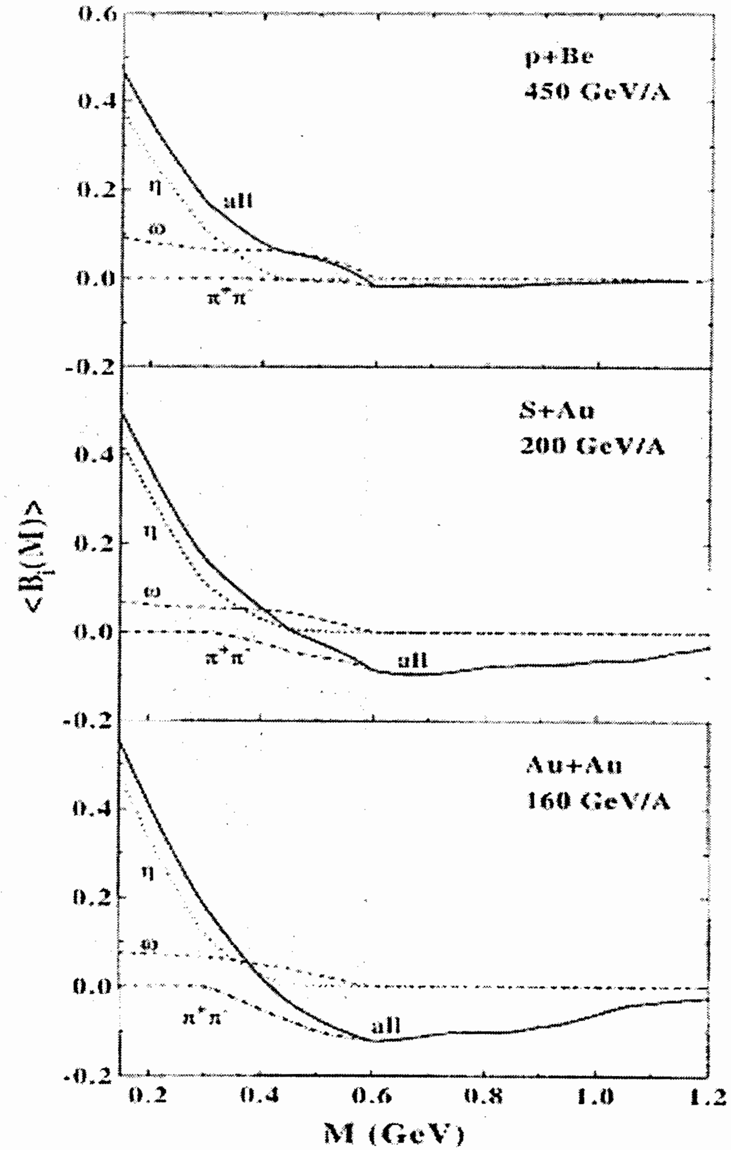

Fig. 6. The weighted anisotropy coefficients $\langle B_i(M) \rangle$ for p + Be collisions at 450 GeV/A, S + Au at 200 GeV/A and Au + Au at 160 GeV/A. The notation is the same as in Fig. 2

SPS energy II

Rapp R., hep-ph/0201101

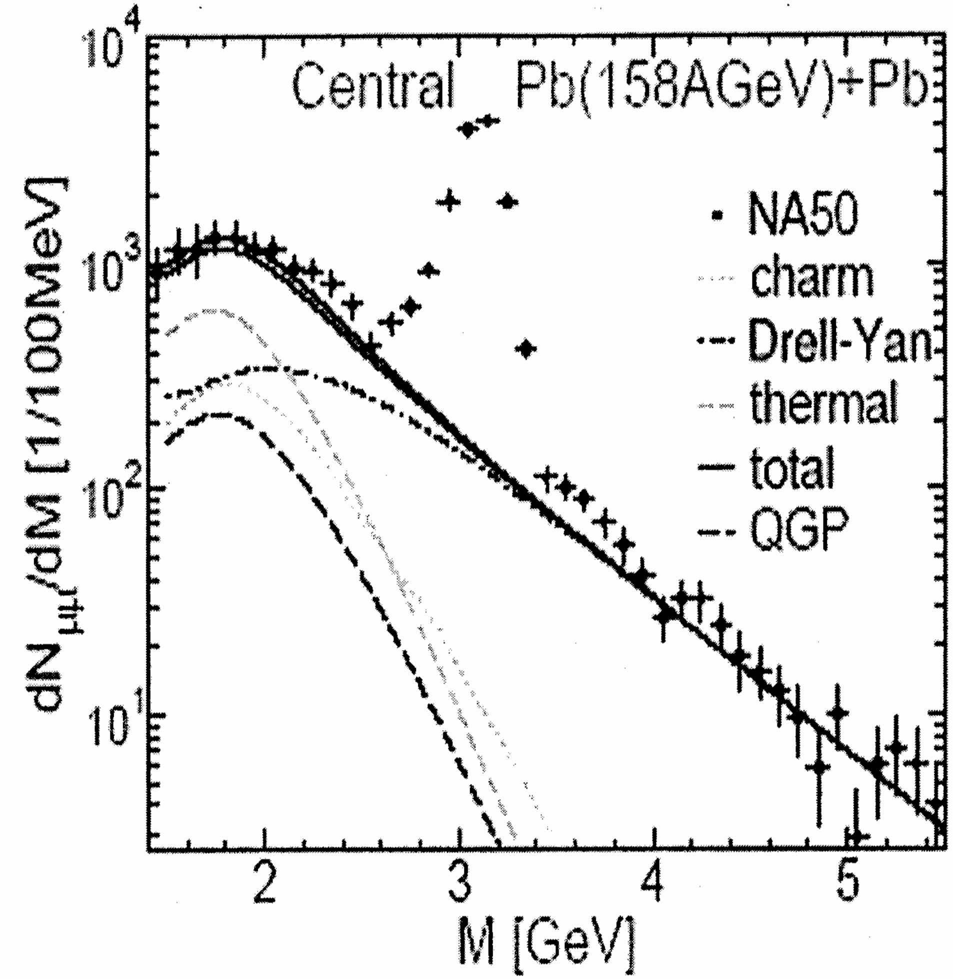

FIG. 6. Thermal fireball calculations [26] compared to NA50 data [3]. Upper and lower total yields correspond to $T_0 = 195$ MeV and 220 MeV, respectively.

The STAR Barrel TOF MRPC Prototype

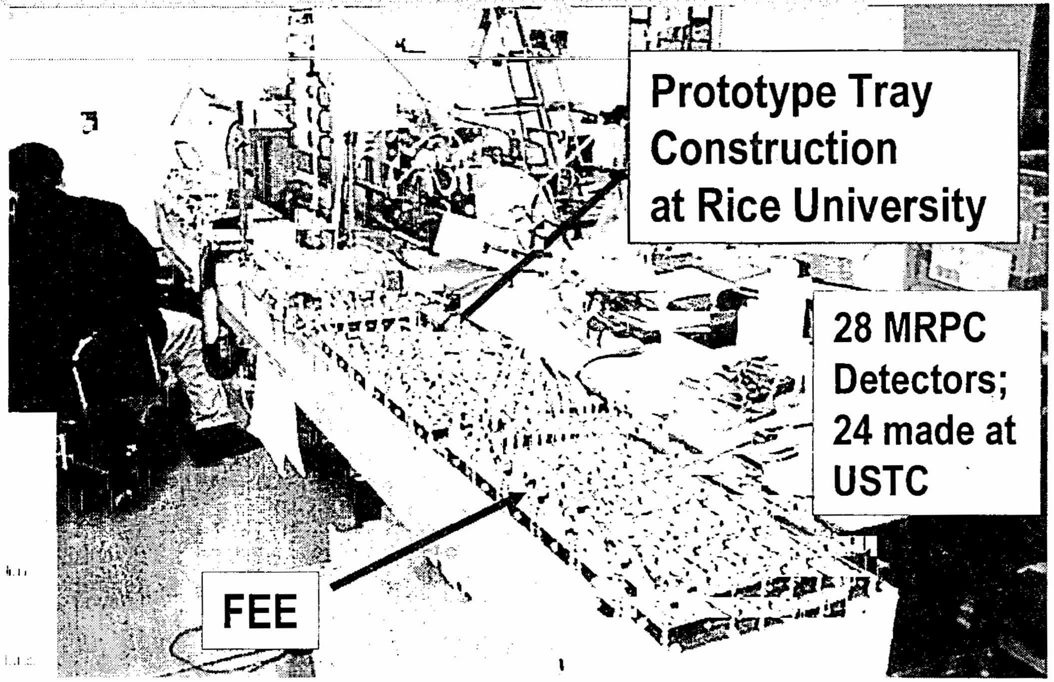

MRPC design developed at CERN, built in China

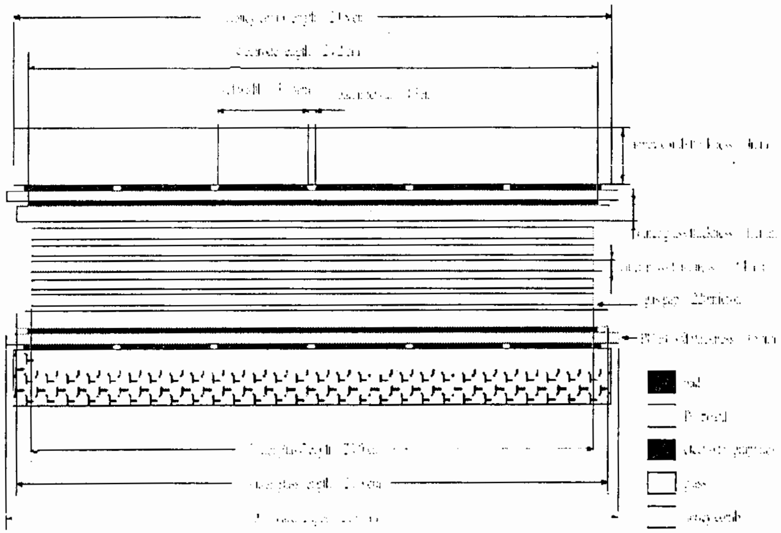

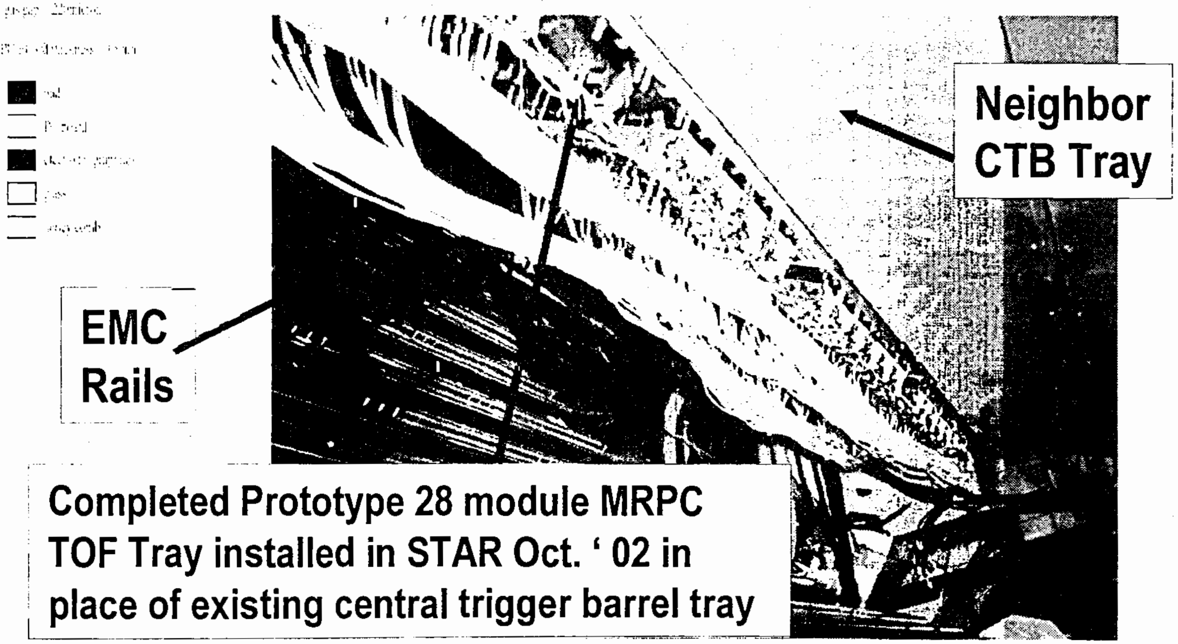

$\sigma \sim 70$ ps, 2 meter path

Strong team including 6 Chinese Institutions in place

Examples of Benefit of TOF

Open Charm and Resonances in central Au-Au collisions

	p_T (GeV/c)	FOM
D^o	All	4.6
D^o	2-4	2.6
D^o	4-6	2.0
D^o	>6	1.0
K^{*o}	0-1	2.0
K^{*o}	1-2	1.85
K^{*o}	2-3	1.74
K^{*o}	3-5	1.39
ϕ(1020)	0-2	5.0
ϕ(1020)	2-5	3.4
Λ (1520)	0-1.6	11.4

FOM (figure of merit) = reduction in required data set by using TOF PID

TOF PID also reduces systematic errors from correlated back-ground due to misidentified particles

Certain measurements are impossible without TOF – unlike particle correlations (Ξ–π), scale dependent correlation studies (velocity vs momentum correlations), exotic searches…

TOF + TPC electron Tag

- Works well at low energy – complements calorimeter
- Gives access to vector meson ($\rho,\omega,\phi,J/\Psi$) e+e- decays
- Thermal dileptons
- Single electron spectrum
- D meson yield, flow

363

RHIC energy

Rapp R., hep-ph/0201101

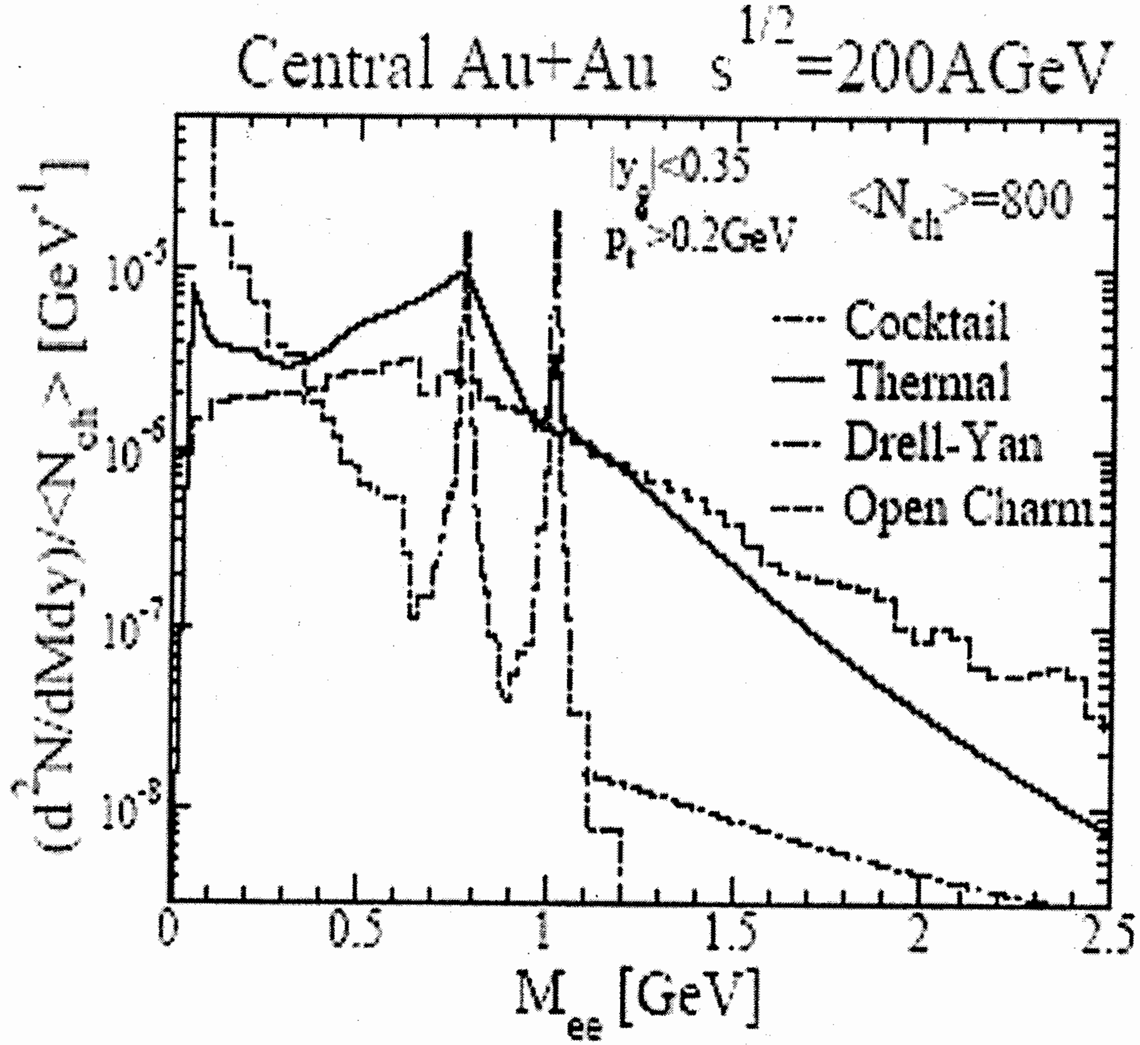

FIG. 8. Dilepton spectra from central Au+Au collisions at full RHIC energy.

J/Ψ polarization

Ioffe B.L., hep-ph/0310343
Dubna, SPIN 2003

Let is now dwell upon the J/ψ production in heavy ion collisions. Let us assume that at sufficiently high collision energy the quark–gluon plasma is formed. Due to the arguments presented above, the formation of quarkonia will thus take place in the plasma (this will of course result in the suppression of the formation probability [14]). The non–perturbative effects should thus be absent (or small), and we are left only with the perturbative mechanism. Then, according to the third row of Table 1, about one half of J/ψ's will be produced directly and another one half via $\chi_2 \to J/\psi + \gamma$. (The approximate equality of these contributions stems from the fact that the extra power of α_s in the direct production cross section is compensated by a relatively small branching ratio – about 20% – of the $\chi_2 \to J/\psi + \gamma$ decay.) We thus expect that the asymmetry coefficient of the electron (muon) angular distribution in the $J/\psi \to e^+e^-(\mu^+\mu^-)$ decay in the case of quark–gluon plasma formation will increase from zero to about (at $p_t = 0$) $\alpha \simeq 0.6$. The account of the initial transverse momentum distribution of gluons as discussed above reduces asymmetry coefficient to

$$\alpha \simeq 0.35 \div 0.4. \tag{7}$$

Conclusion. In case of quark-gluon plasma formation in heavy ion collisions, one may expect an essential increase of J/ψ polarization in comparison with that in hadronic collisions. Therefore, the measurement of electron (muon) angular asymmetry of $J/\psi \to e^+e^-(\mu^+\mu^-)$ decay is an effective tool of detection of quark-gluon plasma formation in heavy ion collisions.

JINR

What will be interesting for investigations ?

(Will need to compare pp and AA data, energy and impact parameter dependences)

CORRELATOR ANALYSIS OF MULTIPARTICLE EVENTS

P. Filip, R. Lednicky, M. Pachr and N. Amelin

JINR, Dubna

April 16, 2005

1 Motivation

Particle production probability

By definition the probability to produce system of identical n-particles in given phase-space cells

$$P_n(\sqrt{s}) \sim \int |M_n|^2 dW_n. \tag{1}$$

In Eq. (1) $|M_n(p_1, p_2, ..., p_n)|^2$ is squared matrix elements and dW_n is Lorentz invariant relativistic phase-space factor.

The Lorentz invariant relativistic phase-space factor is defined as

$$dW_n = \{\prod_{i=1}^{n} \frac{d^3\mathbf{p}_i}{(2\omega_i)}\}\delta^4(\sum_{i=1}^{n} p_i - P_0), \tag{2}$$

where $P_0 = (\mathbf{P}_0, E_n)$ and $p_n = (\mathbf{p}_n, \omega_n)$ are initial 4-momentum and outgoing particle 4-momenta,respectively.

Removing δ-functions from (1) by the Laplace transform we can introduce a function $\rho_n(\beta)$ of the complex variable β .

Note! The function $\rho_n(\beta)$ plays the role of partition function for canonical ensemble of particles, when the total energy fluctuates and there are no correlations among particles due to the energy conservation.

Then probability $P_n(\sqrt{s})$ may be obtained through the inverse Laplace transform

$$P_n(\sqrt{s}) = \frac{1}{2\pi} \int_{-i\infty}^{+i\infty} d\beta e^{F(\beta)}, \tag{3}$$

where

$$F(\beta) = \ln(e^{\beta\sqrt{s}} \rho_n(\beta)). \tag{4}$$

The integral (3) may be estimated by the saddle-point method, if saddle point β_m, where function $F(\beta)$ has maximum at $Im\beta_m$ and $F(\beta)$ has minimum at $Re\beta_m$, exists. The value β_m can be found solving the equation

$$\frac{dF(\beta)}{d\beta} = 0. \tag{5}$$

One may expand $F(\beta)$ near β_m:

$$F(\beta) = A + \frac{1}{2}K_2^M(\beta - \beta_m)^2 + \frac{1}{6}K_3^M(\beta - \beta_m)^3 + ..., \tag{6}$$

where linear term over β dissapears due to the condition (6) and

$$K_2^M = \frac{d^2F(\beta_m)}{d^2\beta} = \frac{d^2 \ln \rho(\beta_m)}{d^2\beta} \tag{7}$$

and

$$K_3^M = \frac{d^3F(\beta_m)}{d^3\beta} = \frac{d^3\ ln\rho(\beta_m)}{d^3\beta}. \tag{8}$$

Thermalization

If we will keep only two first terms in the equation (6) and K_2^M is positive then distribution $e^{F(\beta)}$ over β has Gaussian form with maximum at $Im\beta_m$.

J. Manjavidze and A. Sissakian (Phys. Rep. **346** 1, 2001) suggested to check validity of the Gaussian approximation of (6) experimentally by measuring of the ratio, which must be

$$\frac{(K_3^M)^{2/3}}{K_2^M} << 1, \tag{9}$$

and its dependence from multiplicity of the produced particles.

The validity of such approximation was referred by them as a *thermalization* of particle system.

Canonical phase space example

Let us consider the meaning of the expansion coefficients K_2^M and K_3^M coefficients in more details, starting from the pure phase space consideration.

If $|M_n|^2 = 1$ then $\rho_n(\beta)$ can be considered as canonical distribution function of relativistic ideal gas with the temperature $T = 1/|\beta|$.

Let us write $\rho_n(\beta)$ explicitly

$$\rho_n(\beta) = \int \prod_{i=1,n} \{\frac{d^3p_i \exp(-\beta\omega_i)}{(2\pi)^3 2\omega_i}\}. \tag{10}$$

For identical particles with mass m:

$$\rho_n(\beta) = \frac{1}{(2\pi)^{2n}} (\int_m^\infty d\omega \sqrt{\omega^2 - m^2} \exp(-\beta\omega))^n. \tag{11}$$

We may also calculate k-th derivatives of the $\ln \rho_n(\beta)$ over β . For example, let us define three first derivatives of $\ln \rho_n$:

$$\frac{d \ln \rho_n(\beta)}{d\beta} = \frac{1}{\rho_n(\beta)} \rho_n^{(1)}(\beta). \tag{12}$$

$$\frac{d^2 \ln \rho_n(\beta)}{d^2\beta} = -(\frac{1}{\rho_n(\beta)})^2 (\rho_n^{(1)}(\beta))^2 + \frac{1}{\rho_n(\beta)} \rho_n^{(2)}(\beta). \tag{13}$$

and

$$\frac{d^3 \ln \rho_n(\beta)}{d^3\beta} = 2(\frac{1}{\rho_n(\beta)})^3 (\rho_n^{(1)}(\beta))^3 - 3(\frac{1}{\rho_n(\beta)})^2 \rho_n^{(2)}(\beta) \rho_n^{(1)}(\beta) + \frac{\rho_n^{(3)}(\beta)}{\rho_n(\beta)} \tag{14}$$

From the above formulae we may conclude that mean value of energy is

$$M_1 =< \omega >= -\frac{1}{n} \frac{d \ln \rho_n(\beta)}{d\beta} = \frac{\int_m^\infty d\omega \omega \sqrt{\omega^2 - m^2} \exp(-\beta\omega)}{\int_m^\infty d\omega \sqrt{\omega^2 - m^2} \exp(-\beta\omega)}. \tag{15}$$

example, let us define three first derivatives of $\ln \rho_n$:

$$\frac{d \ln \rho_n(\beta)}{d\beta} = \frac{1}{\rho_n(\beta)} \rho_n^{(1)}(\beta). \tag{12}$$

$$\frac{d^2 \ln \rho_n(\beta)}{d^2\beta} = -(\frac{1}{\rho_n(\beta)})^2 (\rho_n^{(1)}(\beta))^2 + \frac{1}{\rho_n(\beta)} \rho_n^{(2)}(\beta). \tag{13}$$

and

$$\frac{d^3 \ln \rho_n(\beta)}{d^3\beta} = 2(\frac{1}{\rho_n(\beta)})^3 (\rho_n^{(1)}(\beta))^3 - 3(\frac{1}{\rho_n(\beta)})^2 \rho_n^{(2)}(\beta) \rho_n^{(1)}(\beta) + \frac{\rho_n^{(3)}(\beta)}{\rho_n(\beta)} \tag{14}$$

From the above formulae we may conclude that mean value of energy is

$$M_1 =< \omega >= -\frac{1}{n} \frac{d \ln \rho_n(\beta)}{d\beta} = \frac{\int_m^\infty d\omega \omega \sqrt{\omega^2 - m^2} \exp{(-\beta\omega)}}{\int_m^\infty d\omega \sqrt{\omega^2 - m^2} \exp{(-\beta\omega)}}. \tag{15}$$

Similarly we obtain

$$M_2 =< \omega^2 > - < \omega >^2 = \frac{1}{n}\frac{d^2 \ln \rho_n(\beta)}{d^2\beta}, \tag{16}$$

where

$$< \omega^2 > = \frac{\int_m^\infty d\omega \omega^2 \sqrt{\omega^2 - m^2} \exp(-\beta\omega)}{\int_m^\infty d\omega \sqrt{\omega^2 - m^2} \exp(-\beta\omega)}, \tag{17}$$

and

$$M_3 =< \omega^3 > -3 < \omega^2 >< \omega > +2 < \omega >^3 = -\frac{1}{n}\frac{d^3 \ln \rho_n(\beta)}{d^3\beta}, \tag{18}$$

where

$$< \omega^3 > = \frac{\int_m^\infty d\omega \omega^3 \sqrt{\omega^2 - m^2} \exp(-\beta\omega)}{\int_m^\infty d\omega \sqrt{\omega^2 - m^2} \exp(-\beta\omega)}. \tag{19}$$

Thus, the expansion coefficients K_2^M and K_3^M are central moments M_2 and M_3 that multiplied on n and $-n$, respectively.

Mean energy fluctuations

From more general consideration one may understand that $k-th$ expansion coefficients has the meaning of $k-th$ power of the mean value fluctuation of particle energy.

The sources of the fluctuations are single particle distributions that can be characterized by central moments and particle correlations (see, e.g. N.N.Bogolubov, Selected papers on statistical physics, Nauka, 1967, p. 13).

In the canonical phase space case the energy correlators are equal to zero and the expansion coefficients has the meaning of $k-th$ energy central moments multiplied on n.

If the moments of the single-particle distribution weakly vary with the number n, the fluctuations for high enough n are "mostly" provided by the correlations, i.e. the expansion coefficients have the meaning of the correlators that multiplied on the $n(n-1)...(n-k-1)$.

Talk overview

- In this talk we consider integral characteristics of particle correlations, namely the correlators for a given particle observable (e.g., the particle energy E, transverse momentum p_t or rapidity y).
- We investigate their properties, including the connection with the event-to-event fluctuations.
- We suggest a fast procedure how to construct the correlators.
- We demonstrate their ability to reflect underlying mechanisms in the case of several models.

2 Correlator definition

Probability distribution function

Let us consider events of produced particles with fixed multiplicity n. The inclusive or exclusive production probability of $\nu \leq n$ identical particles can be described by a probability distribution function (PDF) $f_\nu^{(n)}(x_1, \ldots, x_\nu)$ of a given observable x. $f_\nu^{(n)}$ is a symmetric function normalized to unity. The PDF can be characterized by the mean value

$$\bar{x}^{(n)} = \int x f_1^{(n)}(x) dx, \tag{20}$$

and - by the l-order moment-type quantities

$$C_{i_1,\ldots,i_l}^{(n,x)} = \int (x_{i_1} - \bar{x}^{(n)}) \ldots (x_{i_l} - \bar{x}^{(n)}) f_n^{(n)}(x_1, \ldots, x_n) dx_1 \ldots dx_n. \tag{21}$$

Due to the PDF symmetry, all the quantities $C_{i_1,\ldots,i_l}^{(n,x)}$ coincide for any permutation of indexes.

Correlators and central moments

For independent particle production, neglecting correlations due to quantum statistics and final state interaction, the multivariate PDF reduces to the product of the same one-particle distribution functions:

$$f_\nu^{(n)}(x_1, \ldots, x_\nu) = f_1^{(n)}(x_1) \ldots f_1^{(n)}(x_\nu). \tag{22}$$

Obviously, in this case $C^{(n,x)}_{i_1,i_2,\ldots i_l} = 0$ for $i_1 \neq i_2 \ldots \neq i_l$.

The quantities $C^{(n,x)}_{i_1,i_2,\ldots,i_l}$ for $i_1 \neq i_2 \ldots \neq i_l$ thus measure a correlation among produced particles and we will call them correlators. Since the correlators do not depend on the concrete set of the l mutually different indexes, we will use for them the simple notation $C_l^{(n,x)}$.

Note that for equal indexes $i_1 = i_2 = \ldots = i_l, C^{(n,x)}_{i_1,i_2,\ldots i_l} \equiv M_l^{(n,x)}$ represents the l-th central moment of the one-particle PDF.

Correlators for fluctuating events

In practice, the PDF can depend on all the event characteristics α, including the observed multiplicity, the particle composition or the selected range of the impact parameters. So one has to introduce the corresponding probabilities p_α. The equations for the mean value and correlators should be then generalized.

Particularly,

$$\langle \bar{x} \rangle = \left\langle \bar{x}^{(n)} \right\rangle = \sum_\alpha p_\alpha \bar{x}^{(\alpha)} / \sum_\alpha p_\alpha = \sum_\alpha p_\alpha \int x f_1^{(\alpha)}(x) dx / \sum_\alpha p_\alpha . \tag{23}$$

Using the identity

$$x_k - \langle \bar{x} \rangle = (x_k - \bar{x}^{(\alpha)}) + (\bar{x}^{(\alpha)} - \langle \bar{x} \rangle), \tag{24}$$

one can rewrite the "global" correlator $C_l^{(x)}$ in terms of the

α-dependent correlators

$$C_l^{(\alpha,x)} = \int (x_1 - \langle \bar{x}^{(\alpha)} \rangle) \ldots (x_l - \langle \bar{x}^{(\alpha)} \rangle) f_l^{(\alpha)}(x_1, \ldots, x_l) dx_1 \ldots dx_l \tag{25}$$

and the fluctuations of the observable mean $\bar{x}^{(\alpha)}$ at a given α around the "global" mean $\langle \bar{x} \rangle$:

$$C_l^{(x)} = \sum_\alpha p_\alpha \sum_{\lambda=0}^{l} \binom{l}{\lambda} C_\lambda^{(\alpha,x)} (\bar{x}^{(\alpha)} - \langle \bar{x} \rangle)^{l-\lambda} / \sum_\alpha p_\alpha .$$

Correlator definition

$$C_l^{(x)} = \left\langle \sum_{\lambda=0}^{l} \binom{l}{\lambda} C_\lambda^{(\alpha,x)} \left(\bar{x}^{(\alpha)} - \langle \bar{x} \rangle\right)^{l-\lambda} \right\rangle , \tag{26}$$

where $C_0^{(\alpha,x)} = 1, C_1^{(\alpha,x)} = 0$.

As follows from this equation the absence of the correlation at any α (i.e. $C_l^{(\alpha,x)} = 0$ for $l > 1$) does not lead to a vanishing global correlator. It is solely determined by the fluctuation of the α-dependent observable mean: $C_l^{(x)} = \langle (\bar{x}^{(\alpha)} - \langle \bar{x} \rangle)^l \rangle$.

Non-identical particles example

For two types of particles, say those characterized by positive $(+)$ and negative $(-)$ charge, one has to make the substitutions $l \rightarrow l_+, l_-$, $x \rightarrow x_+$ and x_-. Particularly,

$$\bar{x}_+^{(\alpha)} = \int x_+ f_{1,0}^{(\alpha)}(x_+) dx_+, \quad \bar{x}_-^{(\alpha)} = \int x_- f_{0,1}^{(\alpha)}(x_-) dx_-, \tag{27}$$

$$C_{l_+,l_-}^{(\alpha,x)} =$$

$$\int (x_{+_1} - \langle \bar{x}_+^{(\alpha)} \rangle) \ldots (x_{+_{l_+}} - \langle \bar{x}_+^{(\alpha)} \rangle)(x_{-_1} - \langle \bar{x}_-^{(\alpha)} \rangle) \ldots (x_{-_{l_-}} - \langle \bar{x}_-^{(\alpha)} \rangle) \cdot$$

$$f_{l_+,l_-}^{(\alpha)}(x_{+_1}, \ldots, x_{+_{l_+}}; x_{-_1}, \ldots, x_{-_{l_-}}) dx_{+_1} \ldots dx_{+_{l_+}} dx_{-_1} \ldots dx_{-_{l_-}} . \tag{28}$$

We express the correlator $C_2^{(x)} \equiv C_{cc}^{(x)}$ of two charged particles in the events with $n = n_+ + n_-$ selected particles through the correlators $C_{2,0}^{(x)} \equiv C_{++}^{(x)}$, $C_{0,2}^{(x)} \equiv C_{--}^{(x)}$ and $C_{1,1}^{(x)} \equiv C_{+-}^{(x)}$. Using the identity

$$\bar{x} = \bar{x}_\pm - (\bar{x}_\pm - \bar{x}) \equiv \bar{x}_\pm - \Delta\bar{x}_\pm, \tag{29}$$

one can write

$$C_{cc}^{(x)} = \frac{n_{++}}{n_{cc}}[C_{++}^{(x)} + \Delta\bar{x}_+{}^2] + \frac{n_{--}}{n_{cc}}[C_{--}^{(x)} + \Delta\bar{x}_-{}^2] + \frac{n_{+-}}{n_{cc}}[C_{+-}^{(x)} + \Delta\bar{x}_+\Delta\bar{x}_-], \tag{30}$$

where

$$n_{cc} = n_{++} + n_{--} + n_{+-} = n_+(n_+ - 1)/2 + n_-(n_- - 1)/2 + n_+n_- \tag{31}$$

is the number of charged pairs.

Again even in the absence of correlations of particles of given charges, i.e. $C^{(x)}_{++} = C^{(x)}_{--} = C^{(x)}_{+-} = 0$, the correlator $C^{(x)}_{cc}$ can be non-zero provided $\bar{x}_+ \neq \bar{x}_-$. In particular, for $n_+ = n_- = n/2$,

$$\bar{x} = \frac{n_+}{n}\bar{x}_+ + \frac{n_-}{n}\bar{x}_- = \frac{1}{2}(\bar{x}_+ + \bar{x}_-), \quad \Delta\bar{x}_+ = -\Delta\bar{x}_- = \frac{1}{2}(\bar{x}_+ - \bar{x}_-) \tag{32}$$

and, in the absence of correlations,

$$C^{(x)}_{cc} = -\frac{(\bar{x}_+ - \bar{x}_-)^2}{4(n-1)} \leq 0. \tag{33}$$

3 Correlator estimates

Correlator estimates from the events with fixed multiplicity

In the case of n_{evt} experimental events with a fixed multiplicity n, the mean value of the observable x can be estimated as

$$\langle \bar{x} \rangle = \frac{1}{n_{\text{evt}}} \sum_{i=1}^{n_{\text{evt}}} \bar{x}^{(i)}, \tag{34}$$

where $\bar{x}^{(i)}$ is the estimate of the observable mean in the i-th event:

$$\bar{x}^{(i)} = \frac{1}{n} \sum_{j=1}^{n} x_j^{(i)}. \tag{35}$$

Similarly, the correlator $C_l^{(x)}$ can be estimated as

$$C_l^{(x)} = \frac{1}{n_{\rm evt}} \sum_{i=1}^{n_{\rm evt}} C_l^{(i,x)}, \tag{36}$$

where $C_l^{(i,x)}$ is the estimate of the correlator in the i-th event:

$$C_l^{(i,x)} = \frac{1}{n_l} \sum (x_{i_1}^{(i)} - \langle \bar{x} \rangle) \ldots (x_{i_l}^{(i)} - \langle \bar{x} \rangle); \tag{37}$$

the sum in Eq. (37) runs over the n_l l-particle sets chosen from all n particles in the event. One can sum either over $n_l = \binom{n}{l} = n(n-1)\ldots(n-l+1)/l!$ of the sorted sets $i_1 < i_2 < \ldots < i_l$ or over $n_l = n(n-1)\ldots(n-l+1)$ of the unsorted sets $i_1 \neq i_2 \neq \ldots \neq i_l$. In the latter case, each of the unsorted sets gives rise to the $l!$ of identical terms in the sum.

Correlator estimates from the events with fluctuating multiplicity

In the case of a mixture of events with different multiplicities $n^{(i)}$, one can estimate the observable mean and the correlators in a similar way as in the two-step averaging procedure considered before.

One should only make the substitutions $n \to n^{(i)}$, $n_l \to n_l^{(i)}$ in Eqs. (35), (37) and take into account that the single-event averages enter into Eqs. (34) and (36) multiplied by the weights proportional to $n^{(i)}$ and $n_l^{(i)}$, respectively:

$$\langle \bar{x} \rangle \equiv \left\langle \bar{x}^{(i)} \right\rangle = \frac{1}{N} \sum_{i=1}^{n_{\mathrm{evt}}} n^{(i)} \bar{x}^{(i)}, \quad N = \sum_{i=1}^{n_{\mathrm{evt}}} n^{(i)}, \tag{38}$$

$$C_l^{(x)} \equiv \left\langle C_l^{(i,x)} \right\rangle_l = \frac{1}{N_l} \sum_{i=1}^{n_{\mathrm{evt}}} n_l^{(i)} C_l^{(i,x)}, \quad N_l = \sum_{i=1}^{n_{\mathrm{evt}}} n_l^{(i)}. \tag{39}$$

The same result can be obtained by averaging simply over all N collected particles or all N_l l-particle sets (formed from particles within the same event only):

$$\langle \bar{x} \rangle = \frac{1}{N} \sum_{j=1}^{N} x_j, \tag{40}$$

$$C_l^{(x)} = \frac{1}{N_l} \sum (x_{i_1} - \langle \bar{x} \rangle) \ldots (x_{i_l} - \langle \bar{x} \rangle), \tag{41}$$

where the sum in Eq. (41) runs over all N_l sets.

Correlator estimates for non-identical particles

The generalization of Eqs. (34)-(41) to two or more particle species is straightforward. For example, for two types of particles characterized by positive and negative charge, one has to make substitutions $l \to l_+, l_-$, $n \to n_+, n_-$, $n_l \to n_{l_+}, n_{l-}$, $N_l \to \sum_i n_{l_+}^{(i)} n_{l-}^{(i)}$ and $x \to x_+, x_-$. Particularly,

$$C_{1,1}^{(i,x)} = (\bar{x}_+^{(i)} - \langle x_+ \rangle)(\bar{x}_-^{(i)} - \langle x_- \rangle), \quad C_{l_+,l_-}^{(i,x)} = C_{l_+}^{(i,x_+)} C_{l_-}^{(i,x_-)}. \quad (42)$$

Correlator estimate errors

We can split all the events into n_g subgroups, each with about the same number of events, and estimate the correlator $C^{(m)}$ in the m-th subgroup using the global estimate of the mean value $\langle x \rangle$. The global estimate of the correlator is then given by the mean of the group values:

$$C = \frac{1}{n_g} \sum_{m=1}^{n_g} C^{(m)}. \tag{43}$$

The dispersion of the group values is

$$D = \frac{1}{n_g - 1} \sum_{m=1}^{n_g} (C^{(m)} - C)^2, \tag{44}$$

where the sum of the deviations squared is divided by $n_g - 1$ since one degree of freedom is used for the global estimate of the correlator according to Eq. (43).

Neglecting a small correlation of the group correlators due to the use of the global estimate of $\langle x \rangle$, one can calculate the error in the global correlator estimate as

$$\sigma(C) = (D/n_g)^{1/2} = \left(\frac{1}{n_g(n_g - 1)} \sum_{m=1}^{n_g} (C^{(m)} - C)^2 \right)^{1/2}. \tag{45}$$

4 Correlators and fluctuations

Relation of correlators and fluctuations

To relate the correlator $C_l^{(x)}$ with the event-to-event fluctuation of the observable single-event mean $\bar{x}^{(i)}$, one can again use the identity

$$x_k^{(i)} - \langle \bar{x} \rangle = (x_k^{(i)} - \bar{x}^{(i)}) + (\bar{x}^{(i)} - \langle \bar{x} \rangle), \tag{46}$$

and write the estimate of the single-event correlator in the form

$$C_l^{(i,x)} = \sum_{\lambda=0}^{l} \binom{l}{\lambda} c_\lambda^{(i,x)} (\bar{x}^{(i)} - \langle \bar{x} \rangle)^{l-\lambda}, \tag{47}$$

where $c_0^{(i,x)} = 1, c_1^{(i,x)} = 0$ and $c_l^{(i,x)}$ for $l \geq 2$ is defined as

$$c_l^{(i,x)} = \frac{1}{n_l^{(i)}} \sum (x_{i_1}^{(i)} - \bar{x}^{(i)}) \ldots (x_{i_l}^{(i)} - \bar{x}^{(i)}). \tag{48}$$

The estimate of the correlator can then be written in the form

$$C_l^{(x)} = \left\langle \sum_{\lambda=0}^{l} \binom{l}{\lambda} c_\lambda^{(i,x)} (\bar{x}^{(i)} - \langle \bar{x} \rangle)^{l-\lambda} \right\rangle_l , \tag{49}$$

where the l-dependent averaging is defined in Eq. (39). Introducing the notation for the event-to-event fluctuation of the observable single-event mean $\bar{x}^{(i)}$

$$\Delta \bar{x}^{(i)} = \bar{x}^{(i)} - \langle \bar{x} \rangle \tag{50}$$

and omitting the event indexes, Eq. (49) particularly yields:

$$C_2^{(x)} = \langle c_2^{(x)} + \Delta \bar{x}^2 \rangle_2, \tag{51}$$

$$C_3^{(x)} = \langle c_3^{(x)} + 3c_2^{(x)} \Delta \bar{x} + \Delta \bar{x}^3 \rangle_3, \tag{52}$$

$$C_4^{(x)} = \langle c_4^{(x)} + 4c_3^{(x)} \Delta \bar{x} + 6c_2^{(x)} \Delta \bar{x}^2 + \Delta \bar{x}^4 \rangle_4. \tag{53}$$

Non-identical particles example

For two different particle species + and −, The Eqs.

$$C_{1,1}^{(i,x)} = (\bar{x}_+^{(i)} - \langle x_+ \rangle)(\bar{x}_-^{(i)} - \langle x_- \rangle), \quad C_{l_+,l_-}^{(i,x)} = C_{l_+}^{(i,x+)} C_{l_-}^{(i,x-)}. \tag{54}$$

and

$$C_l^{(x)} = \left\langle \sum_{\lambda=0}^{l} \binom{l}{\lambda} c_\lambda^{(i,x)} (\bar{x}^{(i)} - \langle \bar{x} \rangle)^{l-\lambda} \right\rangle_l \tag{55}$$

yield, e.g.:

$$C_{1,1}^{(x)} \equiv C_{+-}^{(x)} = \langle \Delta\bar{x}_+ \Delta\bar{x}_- \rangle_{1,1}, \quad C_{2,1}^{(x)} \equiv C_{++-}^{(x)} = \langle (c_2^{(x+)} + \Delta\bar{x}_+{}^2) \Delta\bar{x}_- \rangle_{2,1}. \tag{56}$$

Meaning of the quantities $c_l^{(x)}$

We can prove that these quantities can be expressed through the estimates of the moments of the single-particle x-distribution in a given event:

$$m_\lambda^{(x)} = \frac{1}{n}\sum_{j=1}^{n}(x_j - \bar{x})^\lambda. \tag{57}$$

Particularly,

$$c_2^{(x)} = -\frac{m_2^{(x)}}{n-1}, \tag{58}$$

$$c_3^{(x)} = \frac{2m_3^{(x)}}{(n-1)(n-2)}, \tag{59}$$

$$c_4^{(x)} = \frac{3n\left(m_2^{(x)}\right)^2 - 6m_4^{(x)}}{(n-1)(n-2)(n-3)}, \tag{60}$$

One can conclude from the above consideration:

1. The quantities $c_l^{(x)}$ are determined by the shape of the single-particle x-distribution and the number of the detected (n) or selected $(n \to \nu \leq n)$ particles in a given event. Therefore, they are sensitive only to a part of the correlation related to this shape; an example is the correlation due to energy-momentum conservation (see the 4-th item). The remaining part is contained in the event-to-event fluctuations of the observable mean in accordance with Eqs. (49)-(56).

2. The magnitude of the quantities $c_l^{(\nu,x)}$ decreases with the increasing number ν of selected particles. This decrease should be compensated by the ν-dependence of the fluctuations to guarantee the ν-independence of the correlators. Particularly, $\langle \Delta \bar{x}^2 \rangle_2^{(\nu)} = \langle m_2^{(x)} \rangle_2 / (\nu - 1)$ for uncorrelated production $(C_l^{(x)} = 0)$.

3. Assuming the moments $m_l^{(x)}$ of the single-particle distribution weakly varying with the number n of observed particles, the correlators for high enough n may dominate by the event-to-event fluctuations, i.e. $C_l^{(x)} \to \langle \Delta \bar{x}^l \rangle_l$.

4. For a conserved additive observable x (e.g., particle energy), considering particles of any kind and assuming that all n_{tot} particles are observed ($n = n_{\mathrm{tot}}$), the mean $\bar{x}$ does not fluctuate so $C_l^{(x)} = \langle c_l^{(x)} \rangle_l$. Particularly, $C_2^{(x)} = -\langle m_2^{(x)} \rangle_2 / (n_{\mathrm{tot}} - 1)$ and $C_3^{(x)} = 2\langle m_3^{(x)} \rangle_3 / [(n_{\mathrm{tot}} - 1)(n_{\mathrm{tot}} - 2)]$ for the events with about the same numbers of produced particles.

5. The use of Eqs. (58)-(60) can save substantial amount of computing time compared with the direct evaluation of the correlator estimates according to Eq. (41). In the former case the number of operations is $\propto n$ while in the latter case it is $\propto n^l$.

5 Correlator estimates from one event

In the case of uncorrelated particle production, the event-to-event fluctuations of the observable mean are solely determined by the quantities $c_l^{(x)}$.

Such "standard" fluctuations are thus related to the single-particle distributions and can be estimated by the event-mixing techniques.

The eventual deviation from the "standard" or "statistical" fluctuations then signals the presence of correlations or - a mixture of the events with different single-particle distributions.

Therefore, to clarify the origin of the "non-standard" or "non-statistical" fluctuations, it is desirable to estimate the correlators for the events with similar characteristics α. The ultimate solution is to use the information from a given event only.

To do so, one has to destroy the equality in

$$\sum_{j=1}^{n}(x_j - \bar{x}) \equiv 0, \tag{61}$$

i.e. decouple as much as possible the observables x_j entering into the correlator estimate from the observable mean $\bar{x}$ in a given event.

In the case of sufficiently large multiplicity, it can be easily achieved by splitting the event in a number of sub-events $s = 1, 2, \ldots, n_{\mathrm{sevt}}$ with about the same multiplicities $n^{(s)}$. One can then estimate the correlators according to Eqs. (34)-(41) or (51)-(56) and (57)-(60), making the substitutions $i \to s$ and $n_{\mathrm{evt}} \to n_{\mathrm{sevt}}$.

6 Different model examples

"Analytical" example

Let us first consider simple PDF's characterized by the parameters T,T_1 and A:

$$f_3^{(3)}(x_1, x_2, x_3) \propto e^{-|\frac{x_1-x_2}{T_1}|} e^{-|\frac{x_1-x_3}{T_1}|} e^{-|\frac{x_2-x_3}{T_1}|}), \tag{62}$$

$$f_n^{(n)}(x_1, x_2, ..., x_n) \propto \prod_{i=1}^{n} e^{-\frac{x_i}{T}} (1 + A \sum_{i<j\leq n} e^{-|\frac{x_i-x_j}{T_1}|}), \tag{63}$$

The allowed interval of the variable x was 0-150, the parameters $T = 150$, $T_1 = 25$ and $A = 0, 1, 2$.

Table 1: The correlators corresponding to PDF's in Eqs. (62) (the first two lines) and (63). The results of numerical integration are compared with the estimates obtained from n_{evt} simulated events.

Correlator	$C_2^{(x)}$	$C_3^{(x)}$	$C_4^{(x)}$
	1312.5	0.	
$n_{\mathrm{evt}} = 5 \cdot 10^5$	1313.4 ± 1.8	$61. \pm 108.$	
$n = 3, A = 0$	0.	0.	
$n_{\mathrm{evt}} = 5 \cdot 10^5$	-0.3 ± 1.4	$21. \pm 70.$	
$n = 3, A = 2$	229.0	1771.5	
$n_{\mathrm{evt}} = 5 \cdot 10^5$	229.9 ± 1.4	$1779. \pm 110.$	
$\mathrm{n} = 4,\ \mathrm{A} = 1$	113.8	707.	2913.
$n_{\mathrm{evt}} = 3 \cdot 10^6$	114.4 ± 0.7	$666. \pm 43.$	$3890. \pm 1836.$

"Microcanonical" example

We consider the energy correlators estimated from the "microcanonical" ensemble of events simulated according to the non-relativistic phase space using Metropolis algorithm to redistribute the particle energies via binary energy-conserving collisions.

The total amount of energy distributed among $n_{\rm tot}$ particles is $X_{\rm tot} = n_{\rm tot}\bar{x}$, where $\bar{x}$ is the mean particle energy. We have put $\bar{x} = 100$ in arbitrary units. Assuming that all $n_{\rm tot}$ particles are observed, the mean particle energy does not fluctuate ($\Delta\bar{x} = 0$) and the correlators $C_l^{(x)}$ are then given by Eqs. (58)-(60) with $n = n_{\rm tot}$. Particularly, $C_2^{(x)}$ and $C_3^{(x)}$ vanish at large $n_{\rm tot}$ as $1/n_{\rm tot}$ and $1/{n_{\rm tot}}^2$ respectively. The results shown in table 2 confirm this behavior.

Table 2: The correlators $C_2^{(x)}$ and $C_3^{(x)}$ estimated from the "microcanonical" ensemble of events with fixed mean particle energy $\bar{x} = 100$ in arbitrary units, each consisting of $2 \cdot 10^4$ events with fixed particle multiplicity n_{tot}. All particles are assumed to be observed, i.e. $n = n_{\text{tot}}$.

n_{tot}	5	10	15	20	100
$C_2^{(x)}$	-1181 ± 20	-624 ± 11	-426 ± 5	-323 ± 1	-66.2 ± 0.1
$C_3^{(x)}$	49900 ± 200	14730 ± 50	6940 ± 20	4041 ± 6	174 ± 1

Table 3: The same as in table 2 for $n_{\mathrm{tot}} = 100$ and different numbers ν of selected particles.

ν	5	10	15	20
$C_2^{(x)}$	-75 ± 8	-63 ± 3	-68 ± 2	-66 ± 2
$C_3^{(x)}$	200 ± 500	300 ± 100	220 ± 70	170 ± 50

In table 3, we show the same correlators as in table 2 for $n_{\mathrm{tot}} = 100$, but now calculated for different numbers of selected particles $\nu < n_{\mathrm{tot}}$. One may see that within the errors the correlator estimates are ν-independent. This confirms the conclusion about the compensation of the ν-dependence of the quantities $c_l^{(\nu,x)}$ by that of the $\bar{x}$ fluctuations.

"Parton string model" example

We have estimated the pion transverse momentum correlators $C_2^{(p_t)}$, $C_3^{(p_t)}$ and $C_4^{(p_t)}$ using $2 \cdot 10^3$ central (impact parameter $b = 0$ fm) events of $Pb + Pb$ collisions at total c.m. energy $\sqrt{s} = 200$ AGeV simulated in the parton string model (PSM) (N. Amelin, N. Armesto, C. Pajares and D. Sousa, Eur. Phys. J. **C22**(2001) 149).

In this phenomenological model, the soft and semihard parton collisions initiate the formation of color strings and the subsequent string breaking leads to the production of stable (with respect to strong interaction) hadrons and resonances (lowest SU(3) multiplets) that are forced to decay.

We have divided the simulated events into 100 subgroups and selected $\nu = 1900$ pions of a given charge in each event.

Table 4: The pion transverse momentum correlators obtained from central PSM events of $Pb+Pb$ collisions at $\sqrt{s} = 200$ AGeV.

π's	$C_2^{(p_t)}$, $(\mathrm{GeV/c})^2$	$C_3^{(p_t)}$, $(\mathrm{GeV/c})^3$	$C_4^{(p_t)}$, $(\mathrm{GeV/c})^4$
π^+	$(44.0 \pm 6.6) \cdot 10^{-6}$	$(-7.4 \pm 12.1) \cdot 10^{-8}$	$(8.7 \pm 3.3) \cdot 10^{-9}$
π^-	$(44.6 \pm 6.0) \cdot 10^{-6}$	$(7.8 \pm 12.5) \cdot 10^{-8}$	$(9.5 \pm 4.6) \cdot 10^{-9}$
π^0	$(71.2 \pm 7.6) \cdot 10^{-6}$	$(3.0 \pm 2.7) \cdot 10^{-7}$	$(34.3 \pm 9.5) \cdot 10^{-9}$
$\pi^\pm$	$(52.6 \pm 4.2) \cdot 10^{-6}$	$(-1.5 \pm 7.1) \cdot 10^{-8}$	$(9.0 \pm 2.0) \cdot 10^{-9}$
$\pi^{\pm,0}$	$(59.6 \pm 3.5) \cdot 10^{-6}$	$(2.1 \pm 5.3) \cdot 10^{-8}$	$(11.2 \pm 1.6) \cdot 10^{-9}$

We have also selected $\pi^+\pi^-$ pairs only and estimated $C_{+-}^{(p_t)} = (61.9 \pm 4.4) \cdot 10^{-6} (GeV/c)^2$.

As was mentioned before the correlators for very high multiplicity n may dominate by the event-to-event fluctuations, i.e. $C_l^{(p_t)} \to \langle \Delta\bar{p_t}^l \rangle_l$, if the moments $m_l^{(p_t)}$ of the single-particle p_t distribution weakly varying with the number n of observed particles.

The found PSM correlators $C_3^{(p_t)}$ are consistent with zero within the errors. It means that we have deal with close to symmetrical distribution function for $\Delta\bar{p}_t$.

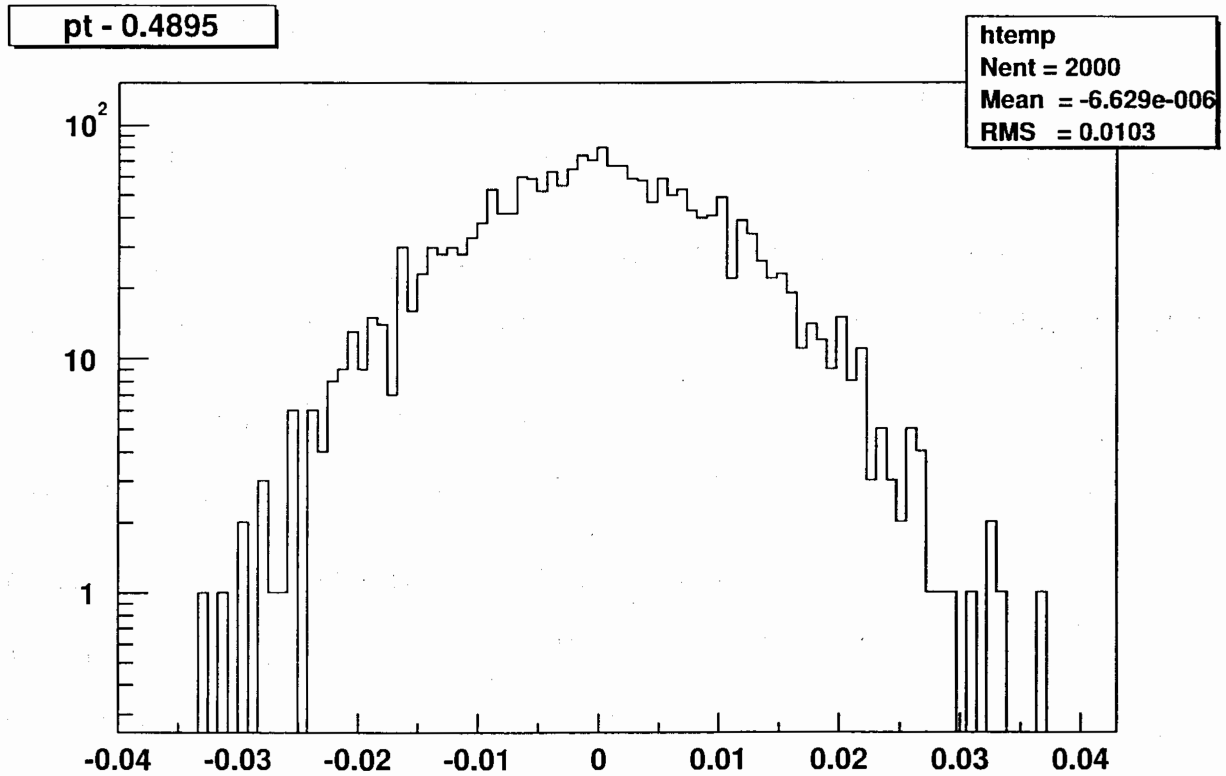

Figure 1: Event-to-event mean p_t fluctuation distribution.

7 Conclusion

- We have developed a fast procedure allowing one to calculate, for a reasonable computer time, the particle correlators of any order and estimate their errors (an example of the corresponding C++ code can be found on the web-page "alice-hbt.jinr.ru").
- We have suggested the extension of this procedure for the event-by-event approach as well.
- We have clarified a close relation between the correlators and fluctuations of the observable event-mean values.
- We have applied the procedure to the events simulated within various models and demonstrated the usefulness of the two-, three- and four-particle correlators. The measurement of the higher-order correlators is rather difficult as it requires very high statistics.

Multiparticle production processes from the Information Theory point of view

O.Utyuzh

The Andrzej Sołtan Institute for Nuclear Studies (SINS),
Warsaw, Poland

Why and **When** of information theory in multiparticle production

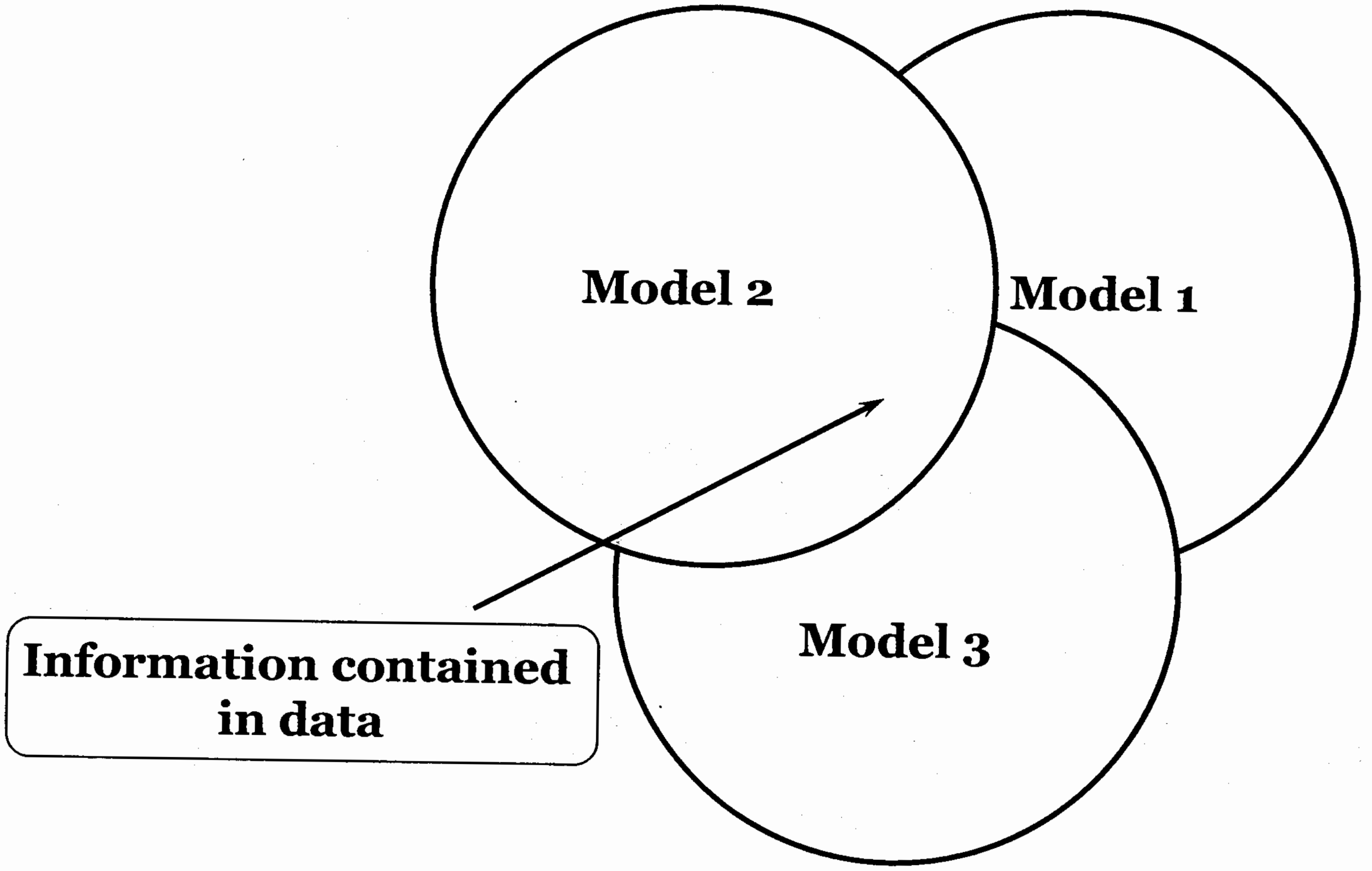

Which model is correct?

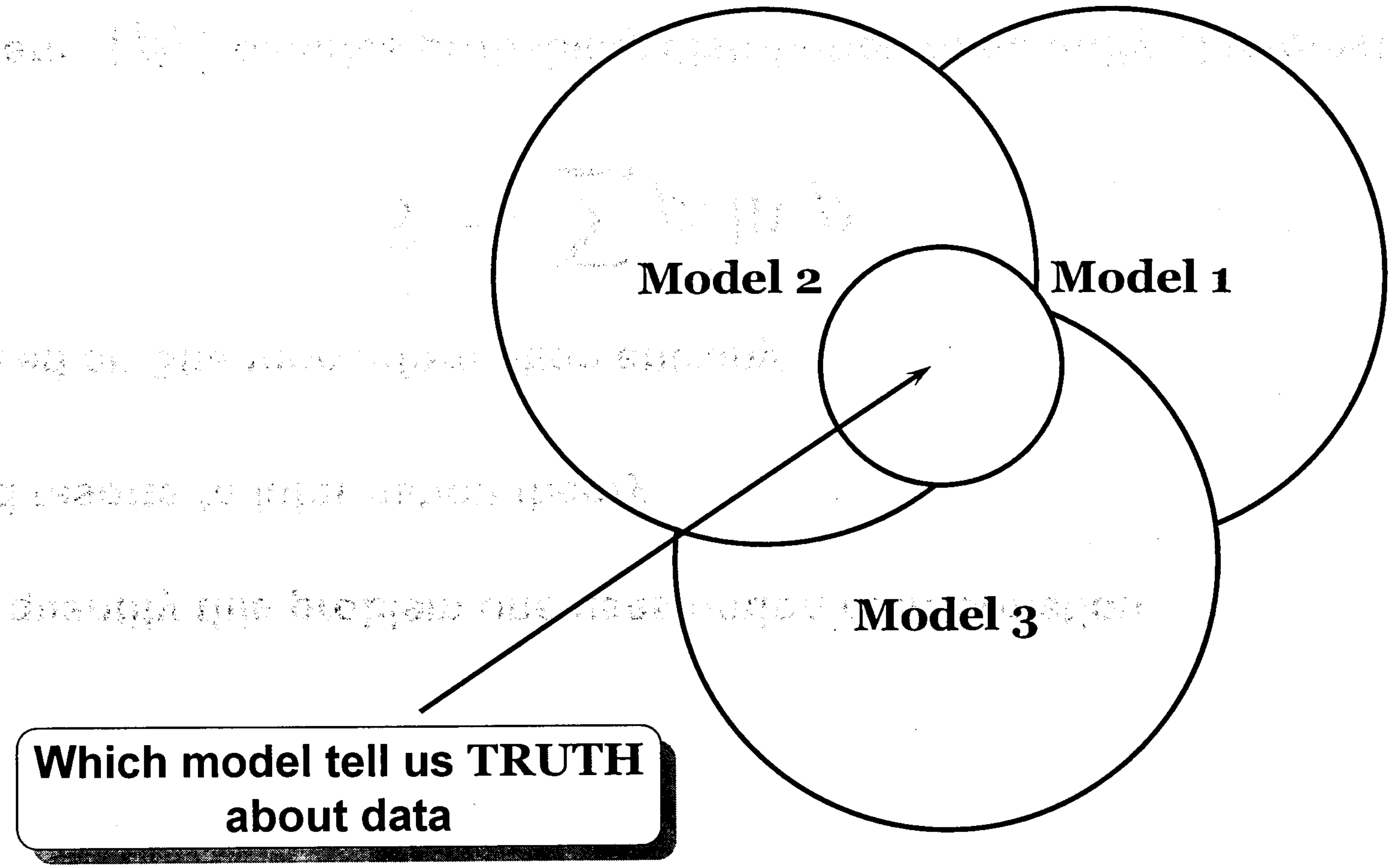

- To quantify this problem one uses notion of information
- and resorts to information theory
- based on Shannon information entropy

$$S = -\sum p_i \ln p_i$$

- where $\{p_i\}$ denotes probability distribution of quantity of interest

This probability distribution must satisfy the following:

- to be normalized to unity: $\sum_i p_i = 1$

- to reproduce results of experiment: $\sum_i p_i \cdot R_k(x_i) = \langle R_k \rangle$

- to maximize (under the above constraints) information entropy

$$S = -\sum p_i \ln p_i$$

-with $\{\lambda_k\}$ **uniquely given by the experimental constraint equations**

$$p_i = \exp\left[-\sum_i \lambda_k \cdot R_k(x_i)\right]$$

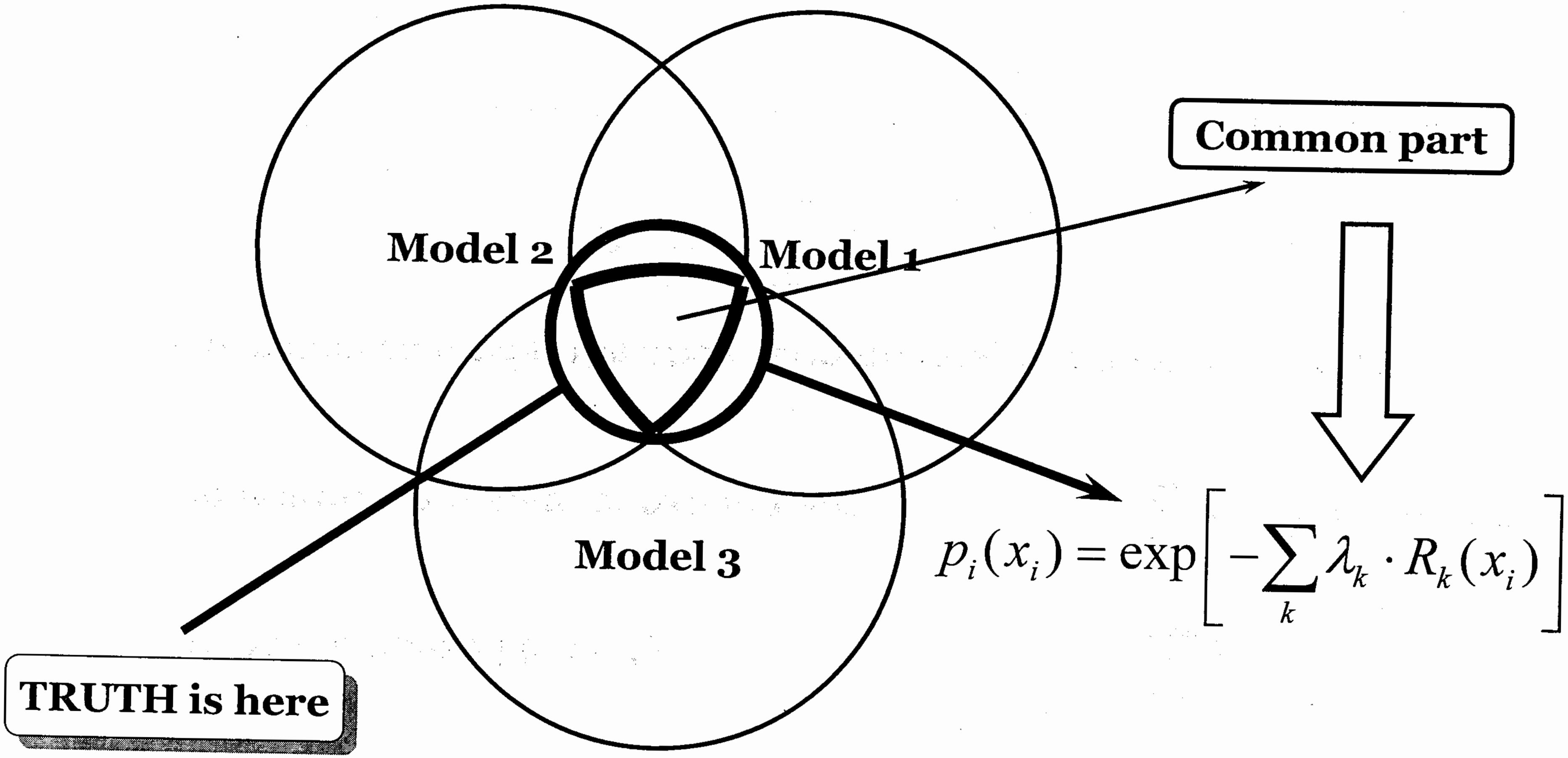
Common part
Model 2
Model 1
Model 3
$p_i(x_i) = \exp\left[-\sum_k \lambda_k \cdot R_k(x_i)\right]$
TRUTH is here

notice

If some new data occur and they turn out to disagree with

$$p_i(x_i) = \exp\left[-\sum_k \lambda_k \cdot R_k(x_i)\right]$$

it means that there is more information which must be accounted for :

- **either by some new** $\lambda = \lambda_{k+1}$
- **or by recognizing that system in nonextensive and needs a new form of** $exp(...) \rightarrow exp_q(...)$
- **or both ....**

Some examples (multiplicity)

knowledge of only $\langle n_{ch} \rangle$ +	most probable distribution
- fact that particles are distinguishable	geometrical (Bose-Einstein)
- fact that particles are nondistinguishable	Poissonian
- fact that particles are coming from k independent, equally strongly emitting sources	Negative Binomial
- second moment $\langle n^2 \rangle$	Gaussian

Rapidity distribution

- **we are looking for**

$$f_N(y) = \frac{1}{N}\frac{dN}{dy} = \frac{1}{\sigma_N N}\int d^2 p_T \left[\frac{E d\sigma}{d^3 p}\right]$$

- **by maximizing**

$$S = -\int_{-Y_M}^{Y_M} dy \cdot f_N(y) \cdot \ln[f_N(y)]$$

- **under conditions**

$$\int_{-Y_M}^{Y_M} dy \cdot f_N(y) = 1 \qquad \int_{-Y_M}^{Y_M} dy \cdot E \cdot f_N(y) = \mu_T \int_{-Y_M}^{Y_M} dy \cdot \cosh(y) \cdot f_N(y) = \frac{M}{N}$$

G.Wilk, Z.Włodarczyk, *Phys. Rev.* **43** (1991) 794

As most probable distribution we get

$$f_N(y) = \frac{1}{Z} \cdot \exp\left[-\beta\mu_T \cdot \cosh(y)\right]$$

where $$Z = Z(M, N, \mu_T) = \int_{-Y_M}^{Y_M} dy \cdot \exp\left[-\beta\mu_T \cdot \cosh(y)\right]$$

$$Y_M = \ln\left\{\frac{M'}{2\mu_T}\left[1 + \left(1 - \frac{4\mu_T^2}{M'^2}\right)^{1/2}\right]\right\}$$ and $$\beta = \beta(\mathrm{W;N,}\mu_\mathrm{T})$$

$$f_N(y) = \frac{1}{Z} \cdot \exp\left[-\beta\mu_T \cdot \cosh(y)\right]$$

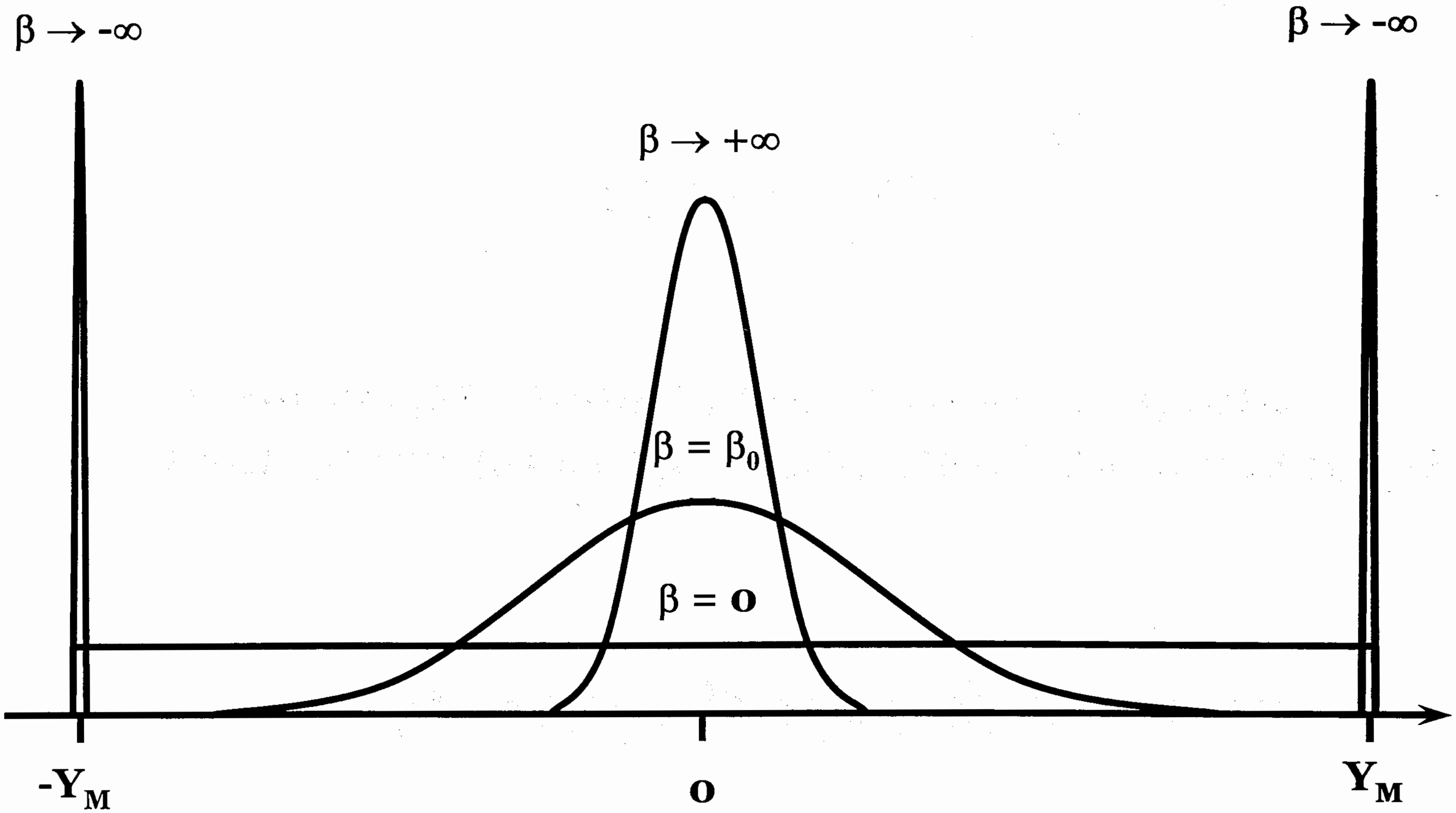

Another point of view ...

Fact: In multiparticle production processes many observables follow simple exponential form:

$$f(x) \approx \exp[-\frac{x}{\Lambda}]$$

"thermodynamics" (i.e, $\Lambda \approx T$)

N-particle system

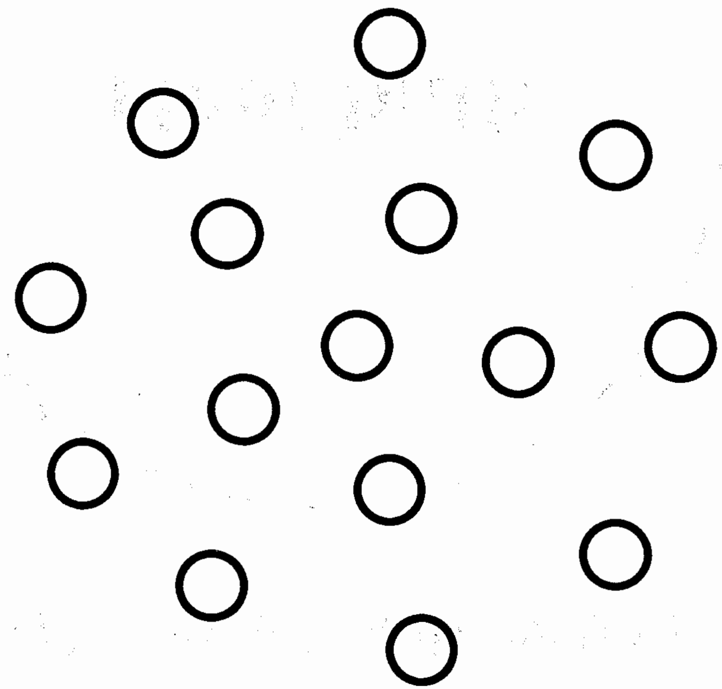

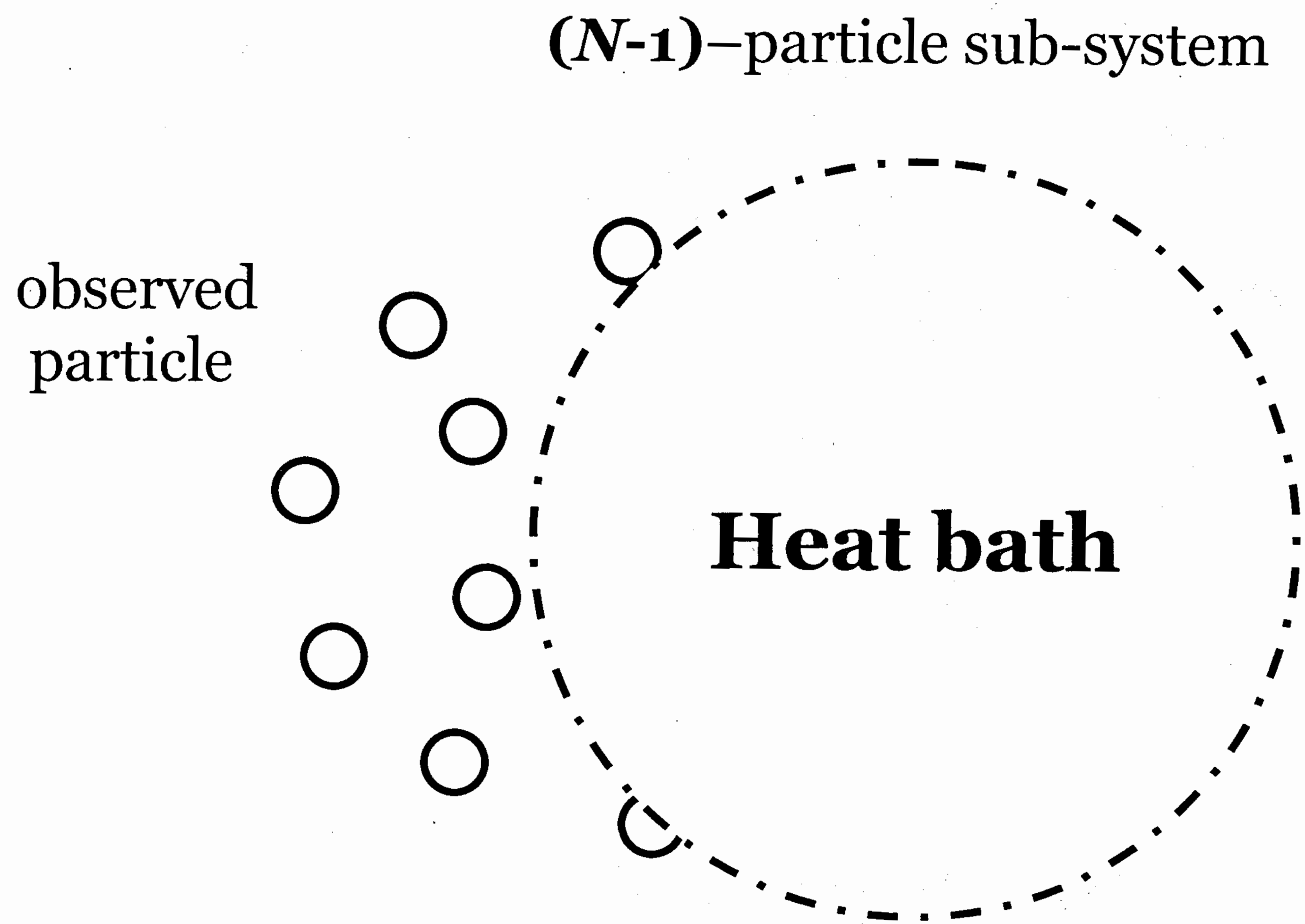
(N-1)–particle sub-system
observed
particle
Heat bath

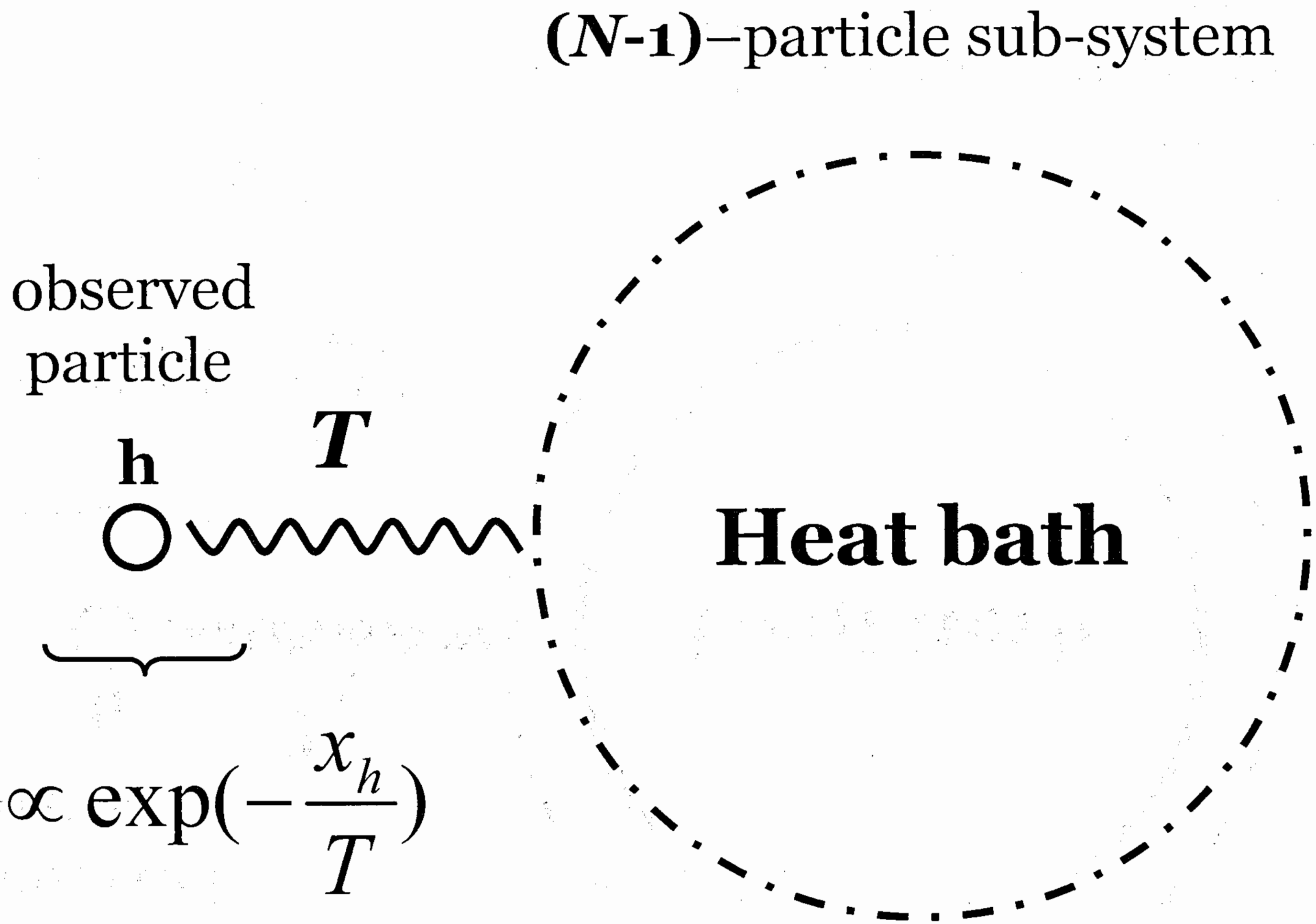

$$f(x_h) \propto \exp(-\frac{x_h}{T})$$

L.Van Hove, *Z.Phys.* **C21** (1985) 93,
Z.Phys. **C27** (1985) 135.

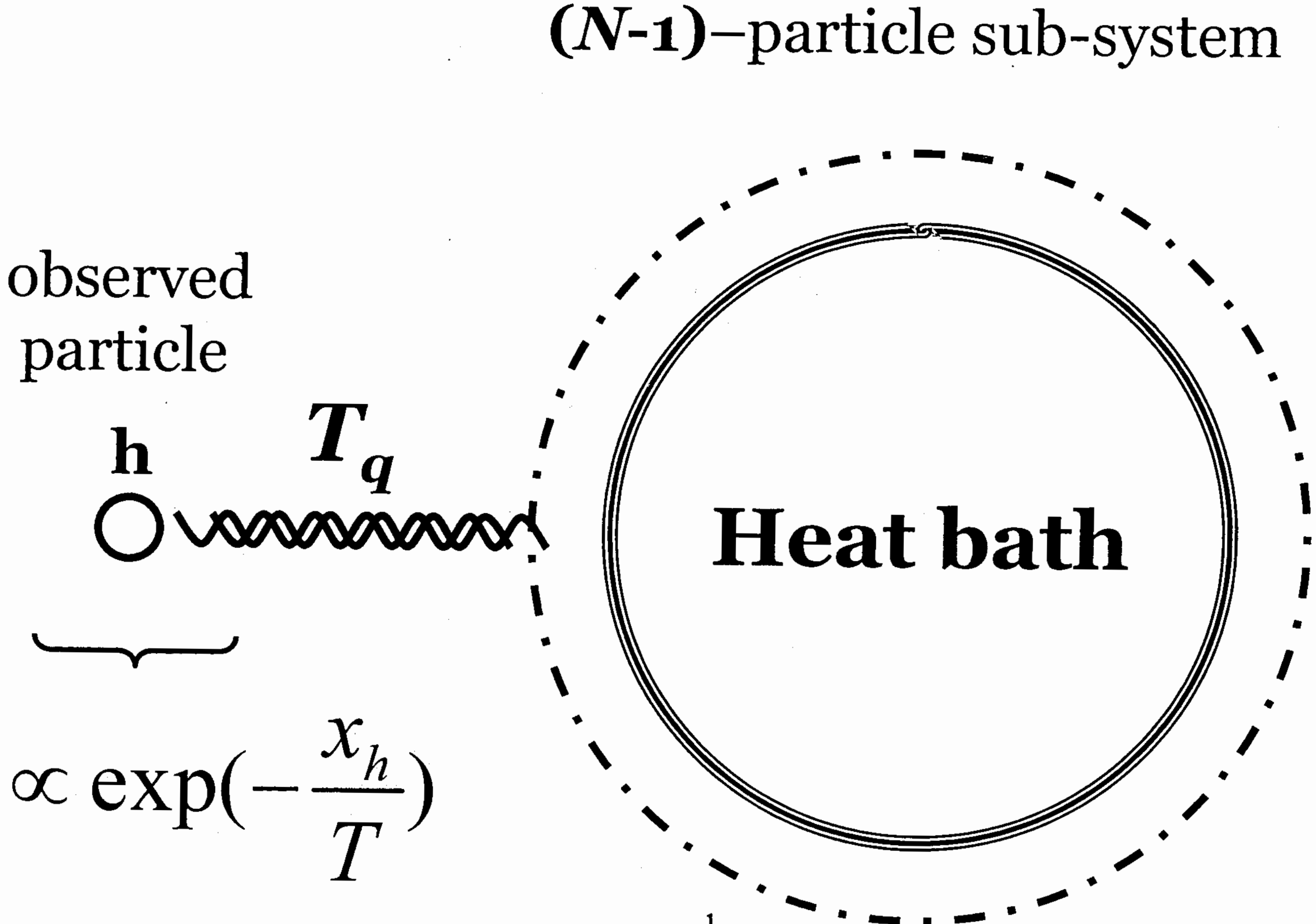

$$f(x_h) \propto \exp(-\frac{x_h}{T})$$

where $$\exp_q(-\frac{x_h}{T_q}) \equiv [1-(1-q)\cdot\frac{x_h}{T_q}]^{\frac{1}{1-q}}$$

nonextensivity

Nonextensive (Tsallis) entropy:

$$S_q = \frac{1 - \sum_i p_i^q}{q-1}$$

is nonextensive because of

$$S_q(A \oplus B) = S_q(A) + S_q(B) - (q-1) S_q(A) \cdot S_q(B)$$

***q*-biased probabilities:**

$$\tilde{p}_i = \frac{p_i^{\,q}}{\sum_i p_i^{\,q}}$$

***q*-biased averages:**

$$\langle E \rangle = \sum_i \tilde{p}_i E_i$$

$$\langle N \rangle = \sum_i \tilde{p}_i N_i$$

Another origin of q: fluctuations present in the system...

Fluctuations of temperature:

$$T = T(E) = T_0 + a \cdot (E - E_0)$$

with

$$a = \frac{1}{C_V},$$

then the equation on probability *P(E)* that a system *A* interacting with the heat bath *A'* with temperature *T* has energy *E* changes in the following way

$q = 1 + a:$

$$d\ln[P(E)] \approx \frac{dE}{T} \Rightarrow P(E) \approx \exp\left(-\frac{E}{T}\right)$$

$$d\ln[P(E)] \approx \frac{dE}{T_0 + a(E - E_0)} \Rightarrow P(E) \approx \left[1 - (1-q)\frac{E - E_0}{T_0}\right]^{\frac{1}{1-q}}$$

M.P.Almeida, *Physica* **A325** (2003) 426

Summarizing: 'extensive' ⇔ 'nonextensive'

$$L = \exp\left(-\frac{x}{\lambda_0}\right) \quad \Longrightarrow \quad L_q = \exp_q\left(-\frac{x}{\lambda_0}\right) = \left\langle \exp\left(-\frac{x}{\lambda}\right)\right\rangle$$

where *q* measures amound of fluctuations

and

<….> denotes averaging over (Gamma) distribution in (*1/λ*)

$$q = 1 \pm \omega = 1 \pm \frac{\left\langle \left(\frac{1}{\lambda}\right)^2 \right\rangle - \left\langle \frac{1}{\lambda} \right\rangle^2}{\left\langle \frac{1}{\lambda} \right\rangle^2}$$

G.Wilk, Z.Włodarczyk, *Phys. Rev. Lett.* **84** (2000) 2770; *Chaos,Solitons and Fractals* **13/3** (2001) 581

436

Summary (known origins of nonextensivity)

- **existence of long range correlations**
- **memory effect**
- **fractality of the available phase space**
- **intrinsic fluctuations existing in the system**
- **..... others ....**

Applications: pp

- input: $\sqrt{s}, \mu_T, \langle N_{ch} \rangle$

-fitted parameters: q, κ_q

$$p_q(y) = \frac{1}{N}\frac{dN_q}{dy} = \frac{1}{Z_q}\exp\left(-\beta_q \mu_T \cosh y\right)$$

$$\int_{-Y_m}^{Y_m} dy \cdot \mu_T \cosh y \left[p_q(y)\right]^q = \frac{\kappa_q \sqrt{s}}{N} \quad \Rightarrow \beta_q$$

$$K_q = \frac{N}{\sqrt{s}}\langle E \rangle_q = \frac{N}{\sqrt{s}}\int_{-Y_m}^{Y_m} dy \cdot \mu_T \cosh y \left[p_q(y)\right]^q \approx \frac{\kappa_q}{3-q}$$

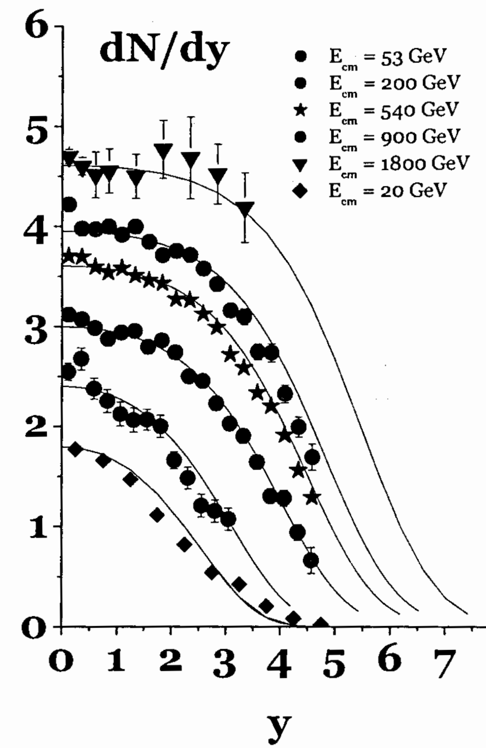

NUWW *PR* **D67** (2003) 114002

inelasticity

NUWW *PR* **D67** (2003) 114002

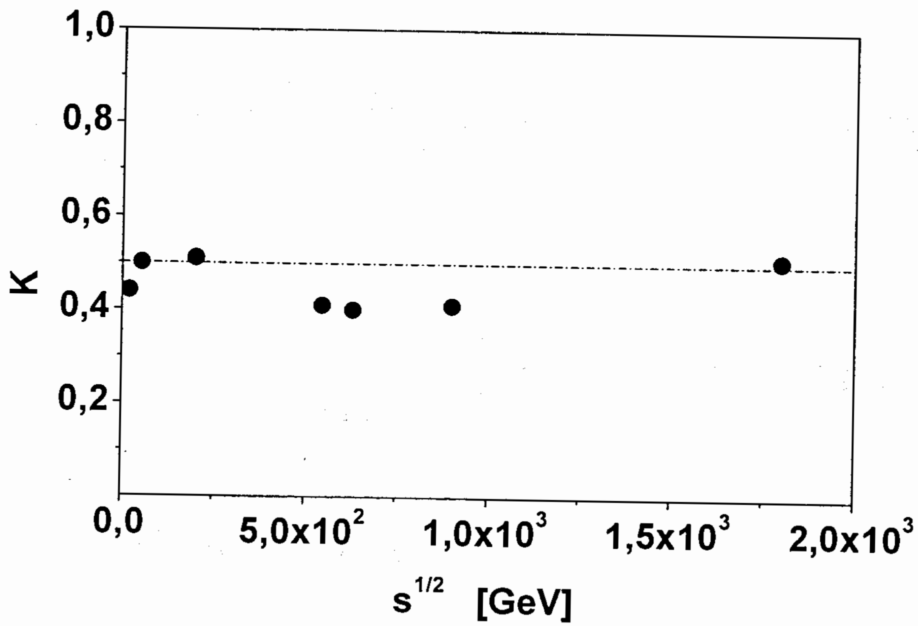

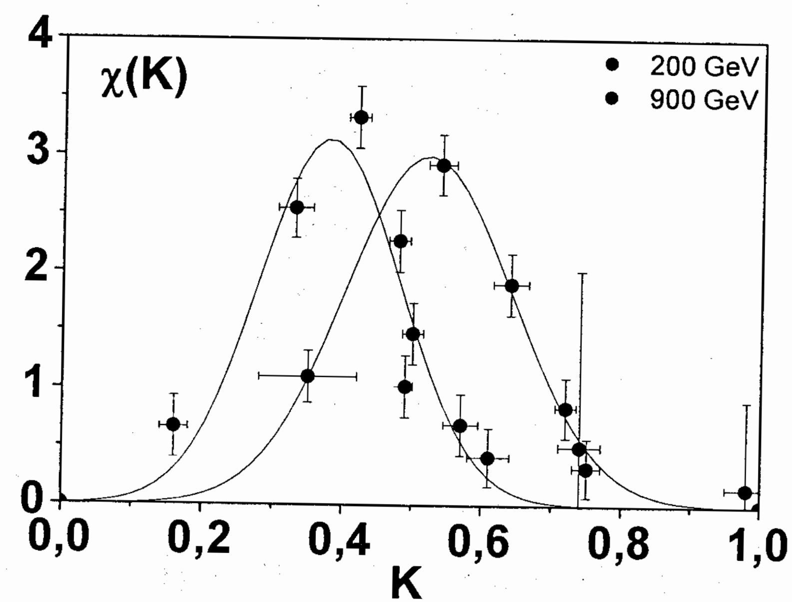

From fits to rapidity distribution data one gets:

(*) y - distribution $\Leftrightarrow$ 'partition temperature'

$$T \approx \frac{K \cdot \sqrt{s}}{\langle N_{ch} \rangle}$$

(*) q $\Leftrightarrow$ fluctuating T

$q \Leftrightarrow$ fluctuating $\langle N_{ch} \rangle$

Conjecture: $q-1$ should measure amount of fluctuation in $P(N_{ch})$

It does so, indeed, see Fig. where data on q obtained from fits are superimposed with fit to data on parameter k in **Negative Binomial Distribution!**

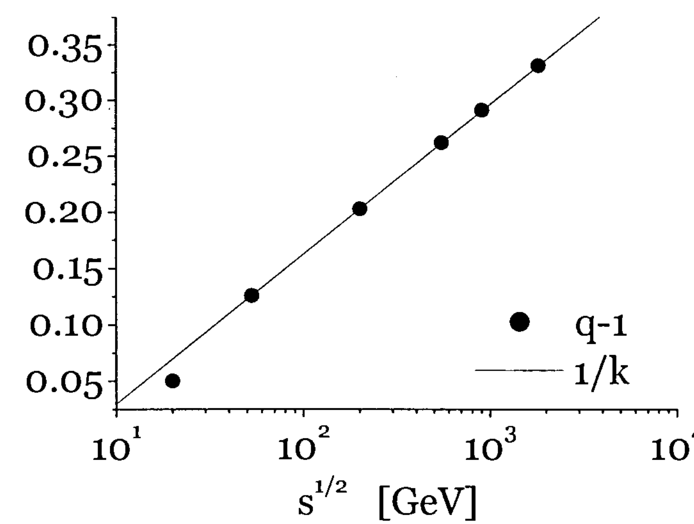

- **Experiment:** $P(N_{ch}) = P_{NB}(\langle N_{ch}\rangle;\{k(k\geq 1)\})$

$$\frac{1}{k} = \frac{\sigma^2(N_{ch})}{\langle N_{ch}\rangle^2} - \frac{1}{\langle N_{ch}\rangle}$$

- $\frac{1}{k}$ **is measure of fluctuations**

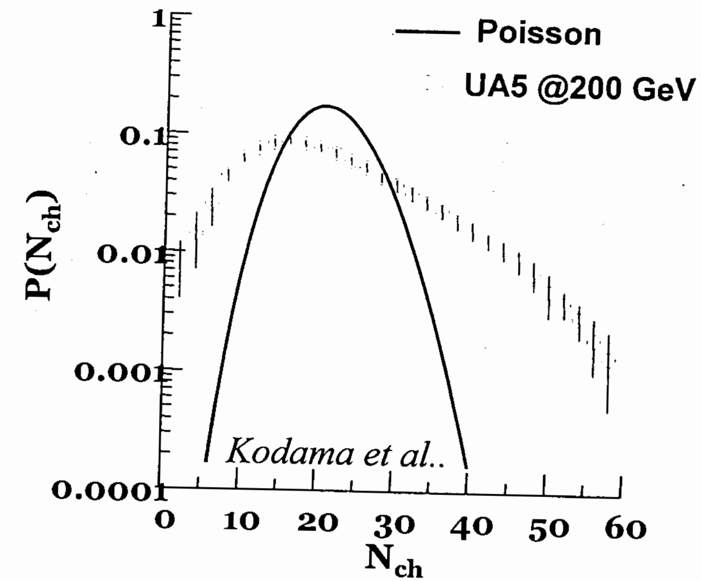

$$P(N) = \int_0^\infty d\bar{n}\,\frac{\bar{n}^n\exp(-\bar{n})}{n!}\cdot\frac{\gamma^k\bar{n}^{k-1}\exp(-\gamma\bar{n})}{\Gamma(k)} \Rightarrow \frac{\Gamma(k+n)}{\Gamma(1+n)\Gamma(k)}\cdot\frac{\gamma^k}{(\gamma+1)^{k+n}}$$

with $\gamma = \frac{k}{<\bar{n}>}$

$$\frac{1}{k} = q - 1$$

P.Carruthers,C.C.Shih, *Int. J. Phys.* **A4** (1989) 5587

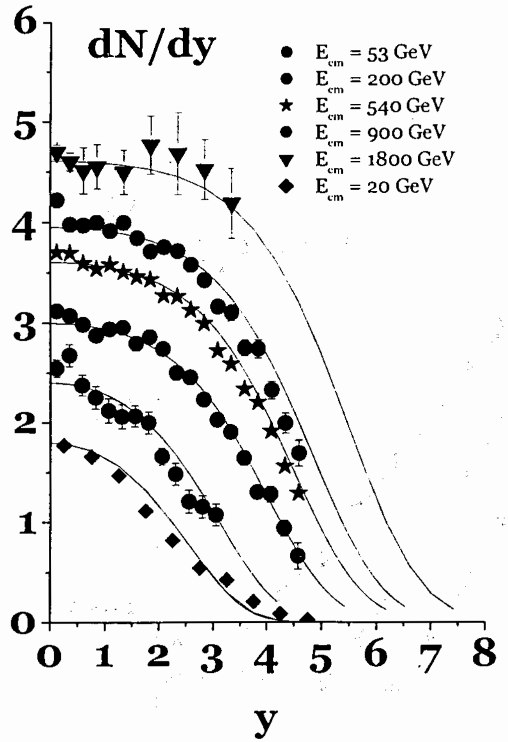

NUWW Physica **A300** (2004) 467

$$q = \frac{q_L T_L^2 + q_T T_T^2}{T^2} - \frac{T_L^2 + T_T^2}{T^2} + 1$$

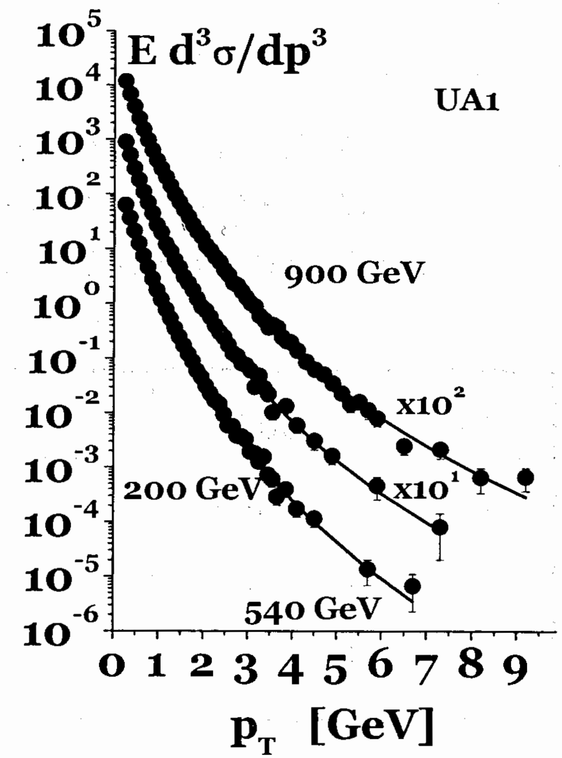

$S^{1/2}$	q_L	$T_L=1/\beta_L$
200	1.203	12.12
546	1.262	22.38
900	1.291	29.47

$$\sigma^2(T) = \sigma^2(T_L) + \sigma^2(T_T)$$

$S^{1/2}$	q_T	$T_T=1/\beta_T$
200	1.095	0.134
546	1.105	0.135
900	1.110	0.140

Applications: AA

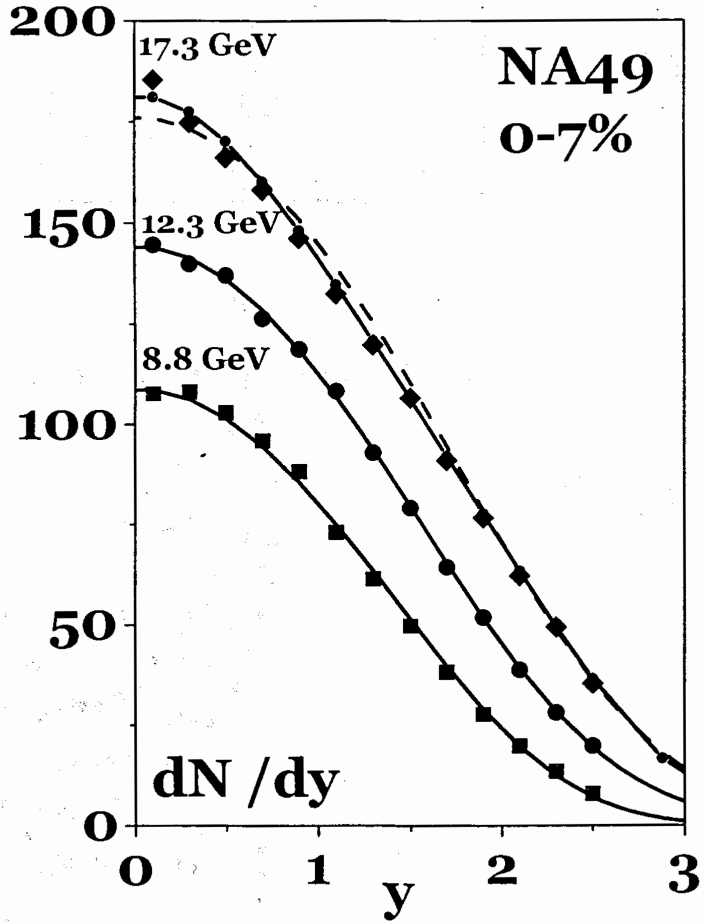

Example of use of MaxEnt method applied to some *NA49* data for π^- production in PbPb collisions (centrality 0-7%):

- **(blue lines)**

$S^{1/2}$	q	K_q
8.8	1.040	0.22
12.3	1.164	0.30
17.3	1.200	0.33

- **(orange line)** ***q=1*, two sources of mass *M=6.34 GeV* located at *|y|=0.83***

this is example of adding new dynamical assumption

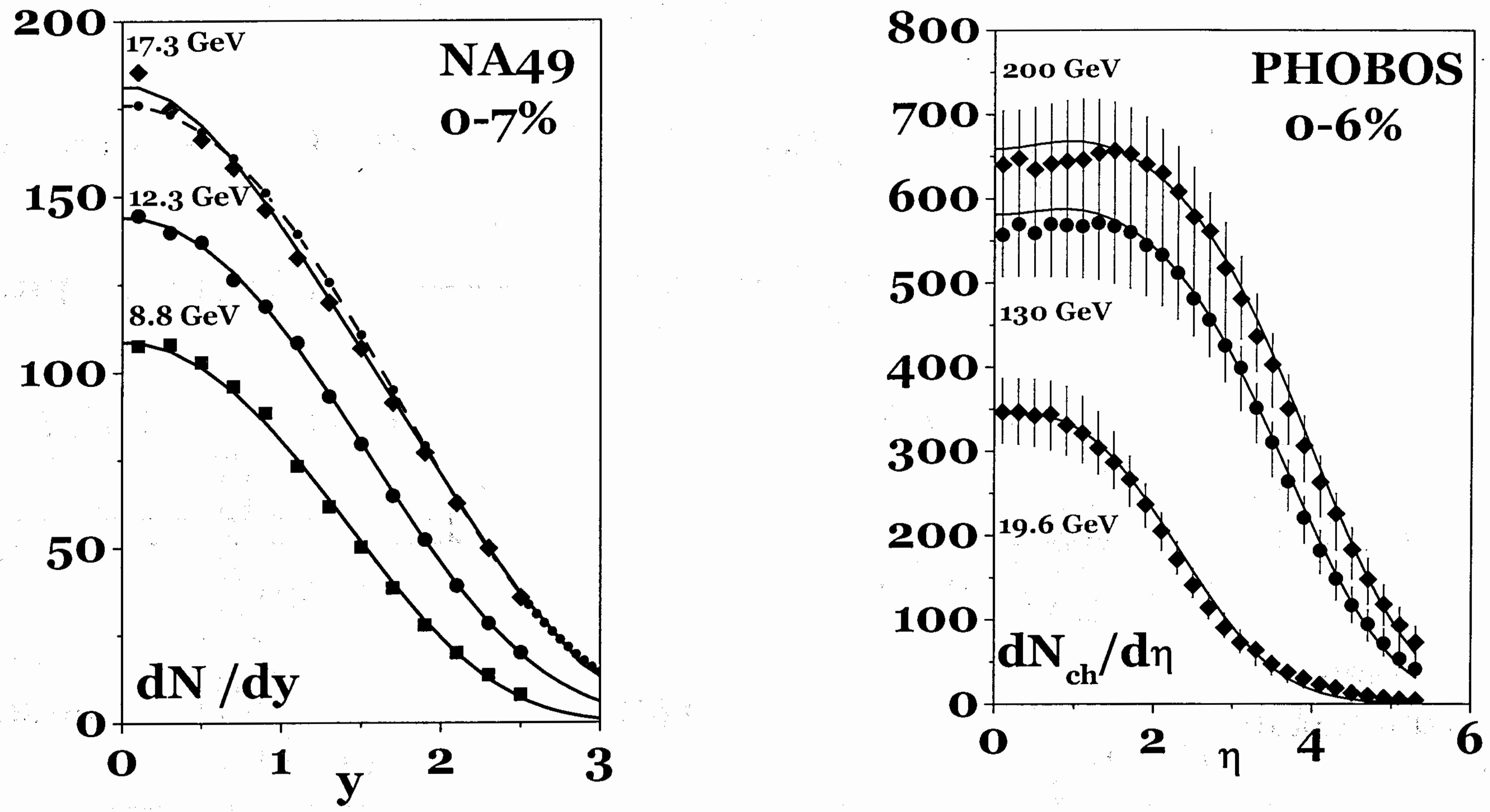

200
150
100
50
0
17.3 GeV
12.3 GeV
8.8 GeV
NA49
0-7%
dN /dy
0
1
y
2
3
800
700
600
500
400
300
200
100
0
200 GeV
130 GeV
19.6 GeV
PHOBOS
0-6%
dN_{ch}/dη
0
2
η
4
6

Applications: pA

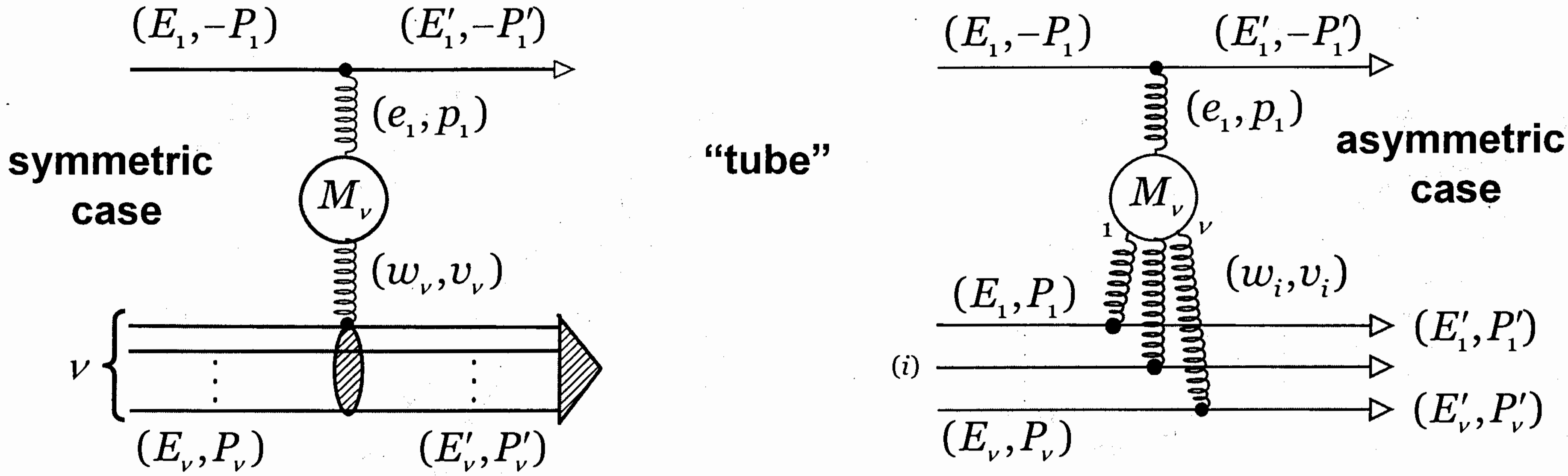

- input: $\sqrt{s},\mu_T,\langle N_{ch}\rangle \longrightarrow \sqrt{s_\nu},\mu_T,\bar{N}_\nu$

$$s_\nu = \nu s + (\nu-1)^2 m^2 \quad \textbf{with} \quad s = 2m^2 + 2m\sqrt{p_{LAB}^2 + m^2}$$

$$\bar{N}_\nu = \frac{1}{2}(1+\langle\nu\rangle)\bar{N}$$

W.Busza, Acta Phys. Polon. **B8** *(1977) 333,*
C.Halliwell et al., Phys. Rev. Lett. **39** (1977) 1499

Rapidity distribution

- **we are looking for**

$$f_N(y) = \frac{1}{N}\frac{dN}{dy} = \frac{1}{\sigma_N N}\int d^2 p_T \left[\frac{Ed\sigma}{d^3p}\right]$$

- **by maximizing**

$$S = -\int\limits_{-Y_{\min}^{(\nu)}}^{Y_{\max}^{(\nu)}} dy \cdot f_N(y)\cdot \ln\left[f_N(y)\right]$$

- **under conditions**

$$\int\limits_{-Y_{\min}^{(\nu)}}^{Y_{\max}^{(\nu)}} dy \cdot f_N(y) = 1$$

$$P \neq 0 \Rightarrow \begin{cases} \int\limits_{-Y_{\min}^{(\nu)}}^{Y_{\max}^{(\nu)}} dy \cdot E \cdot f_N(y) = \mu_T \int\limits_{-Y_{\min}^{(\nu)}}^{Y_{\max}^{(\nu)}} dy \cdot \cosh(y)\cdot f_N(y) = \frac{W_\nu}{N_\nu} \\ \int\limits_{-Y_{\min}^{(\nu)}}^{Y_{\max}^{(\nu)}} dy \cdot P \cdot f_N(y) = \mu_T \int\limits_{-Y_{\min}^{(\nu)}}^{Y_{\max}^{(\nu)}} dy \cdot \sinh(y)\cdot f_N(y) = \frac{P_\nu}{N_\nu} \end{cases}$$

$$W_\nu = (\nu R + K)\cdot\frac{\sqrt{s}}{2} \qquad \text{and} \qquad P_\nu = -(\nu R - K)\cdot\frac{\sqrt{s-4m^2}}{2}$$

$$M_\nu = \sqrt{W_\nu^2 - P_\nu^2} = \sqrt{KR\nu s + (\nu R - K)^2 m^2} \xrightarrow{R=K} K\sqrt{s}$$

As most probable distribution we get

$$f_\nu(y) = \frac{1}{Z_\nu}\cdot\exp\left[-\beta_\nu\mu_T\cdot\cosh(y) - \lambda_\nu\mu_T\cdot\sinh(y)\right]$$

where $Z_\nu = Z_\nu(W_\nu, P_\nu, N_\nu, \mu_T)$

$$= \int_{-Y_{\min}^{(\nu)}}^{Y_{\max}^{(\nu)}} dy\cdot\exp\left[-\beta_\nu\mu_T\cdot\cosh(y) - \lambda_\nu\mu_T\cdot\cosh(y)\right]$$

“symmetric”

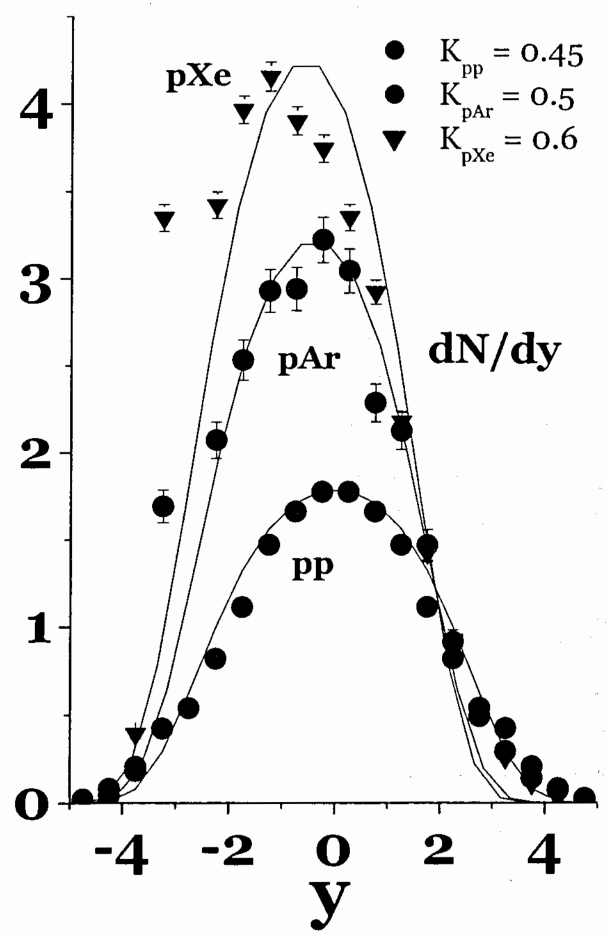

“asymmetric”

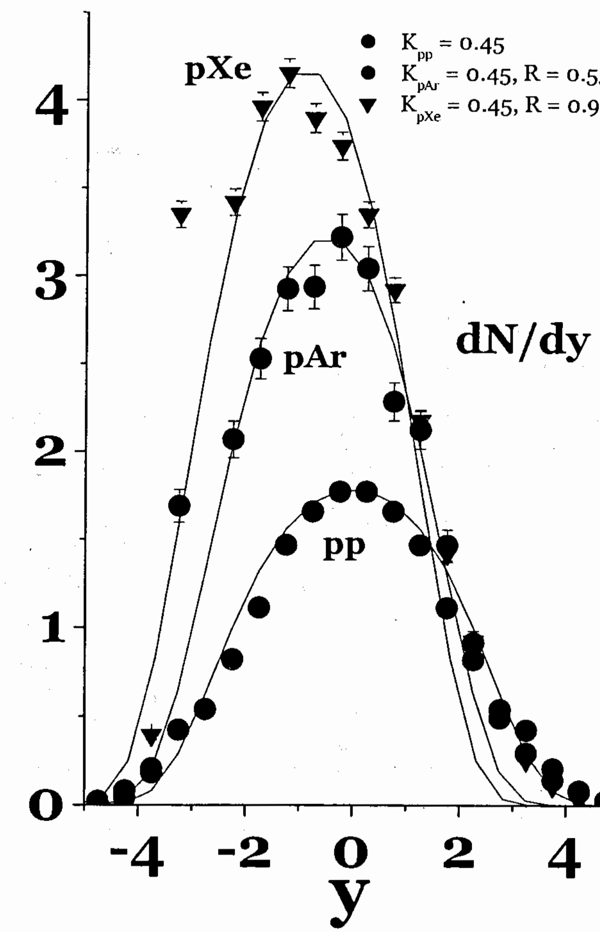

“sequential”

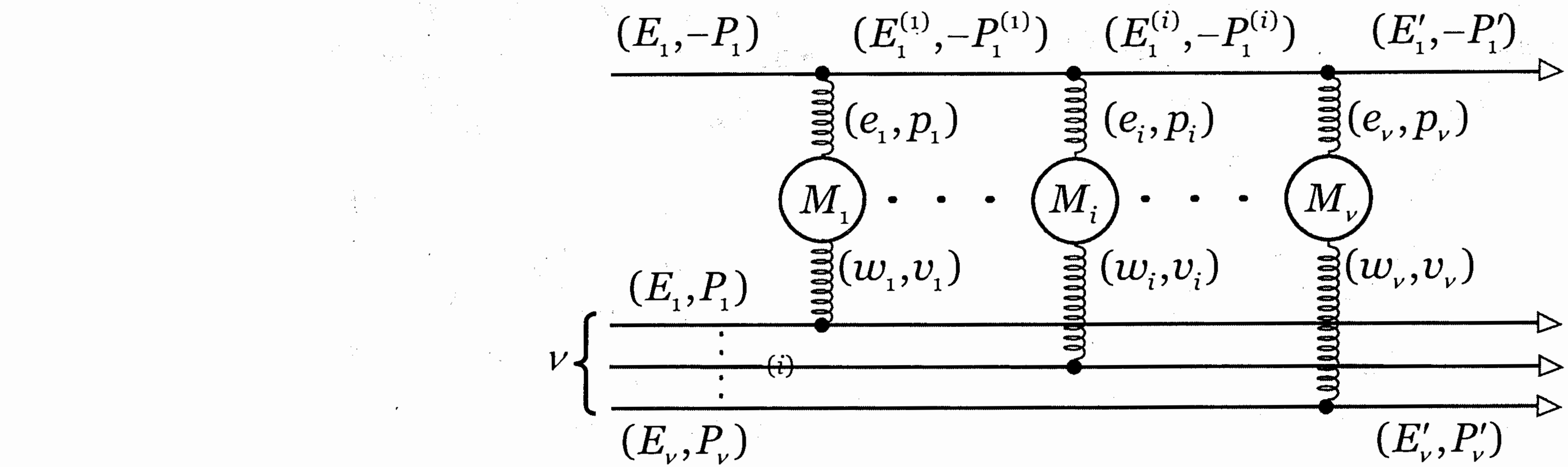

$$f_\nu(y) = \sum_{i=1}^{\nu} f_i(y)$$

can be visualized $\bar{N}_\nu = \bar{N}_1 + \frac{1}{2}(\nu-1)\bar{N}_2$

where $\bar{N}_{1,2}$ **are such that** $2\bar{N}_1 + (\nu-1)\cdot\bar{N}_2 = (\nu+1)\cdot\bar{N}_\nu$

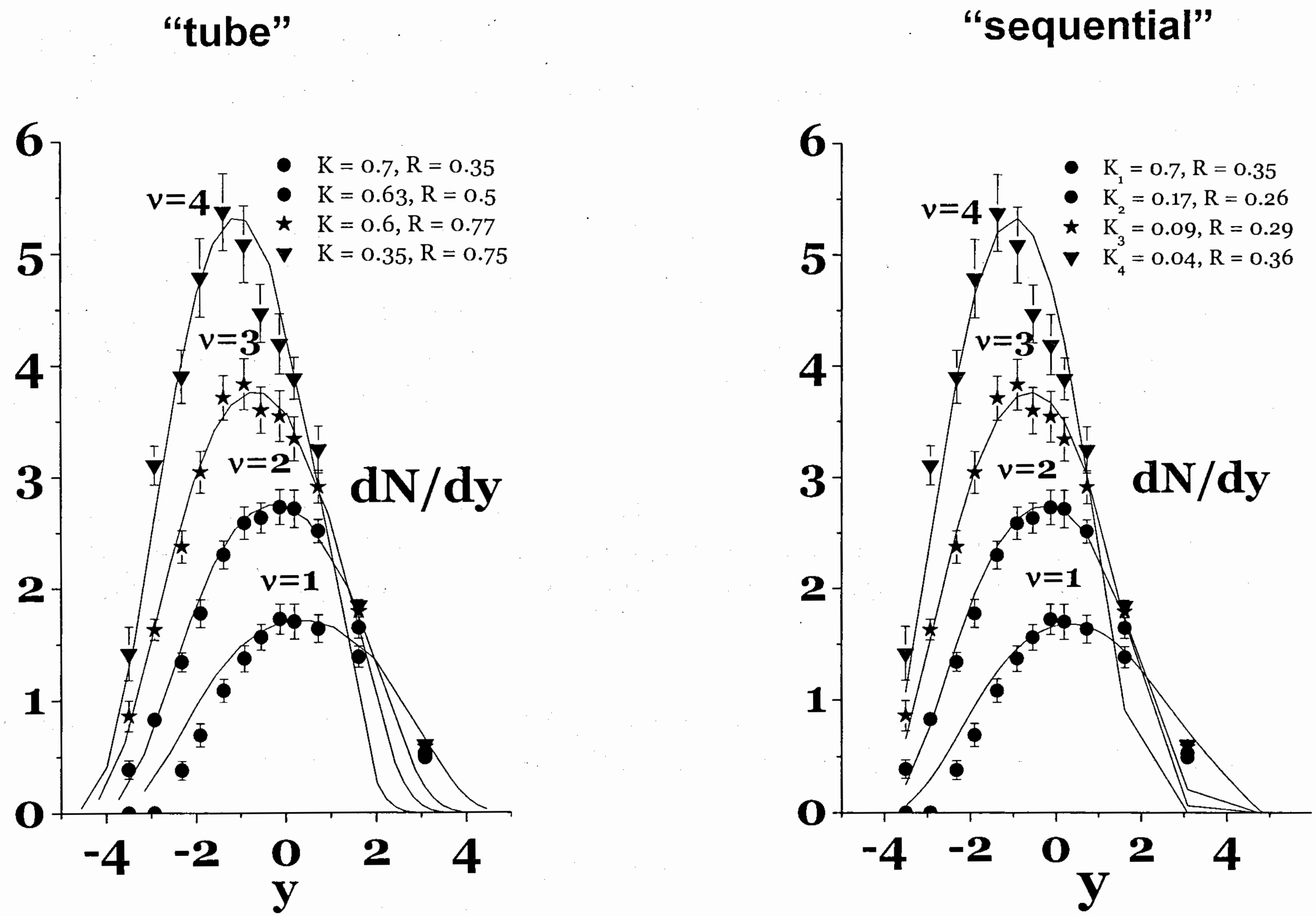
"tube"
"sequential"
K = 0.7, R = 0.35
K = 0.63, R = 0.5
K = 0.6, R = 0.77
K = 0.35, R = 0.75
K_1 = 0.7, R = 0.35
K_2 = 0.17, R = 0.26
K_3 = 0.09, R = 0.29
K_4 = 0.04, R = 0.36
ν=4
ν=3
ν=2
ν=1
dN/dy
y
0
1
2
3
4
5
6
-4
-2
0
2
4

summary

- **In many places one observes simple "exponential" or "exponential-like" behaviour of some selected distributions**

- **Usually regarded to signal some "thermal" behaviour they can also be considered as arising because insufficient information which given experiment is providing us with**

- **When treated by means of information theory methods (MaxEnt approach) the resultant formula are formally identical with those obtained by thermodynamical approach but their interpretation is different and they are valid even for systems which cannot be considered to be in thermal equilibrium.**

- **It means that statistical models based on this approach have more general applicability then naively expected.**

summary

- **Therefore: Statistical models of all kinds are widely used as source of some quick reference distributions. However, one must be aware of the fact that, because of such (interrelated) factors as:**
  - fluctuations of intensive thermodynamic parameters
  - finite sizes of relevant regions of interaction/hadronization
  - some special features of the „heath bath" involved in a given process the use of only one parameter *T* in formulas of the type

$$\exp(-\frac{x}{T})$$

is not enough and, instead, one should use two (... at least...) parameter formula

$$\exp_q(-\frac{x}{T}) = [1-(1-q)\frac{x}{T}]^{\frac{1}{1-q}}$$

with q accounting summarily for all factors mentioned above.

Back-up Slides

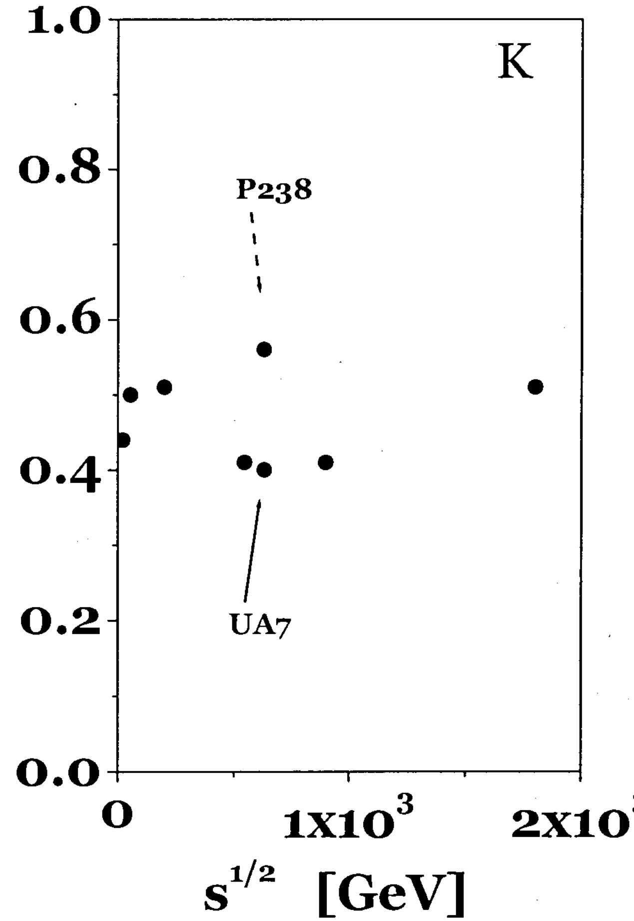
K
P238
UA7
1.0
0.8
0.6
0.4
0.2
0.0
0
1X10³
2X10³
s^1/2 [GeV]

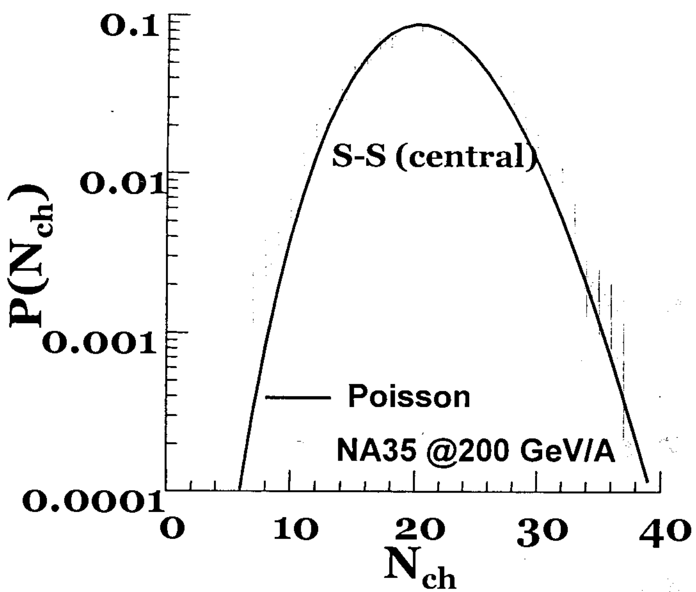
0.1
0.01
0.001
0.0001
P(N_ch)
S-S (central)
Poisson
NA35 @200 GeV/A
0
10
20
30
40
N_ch

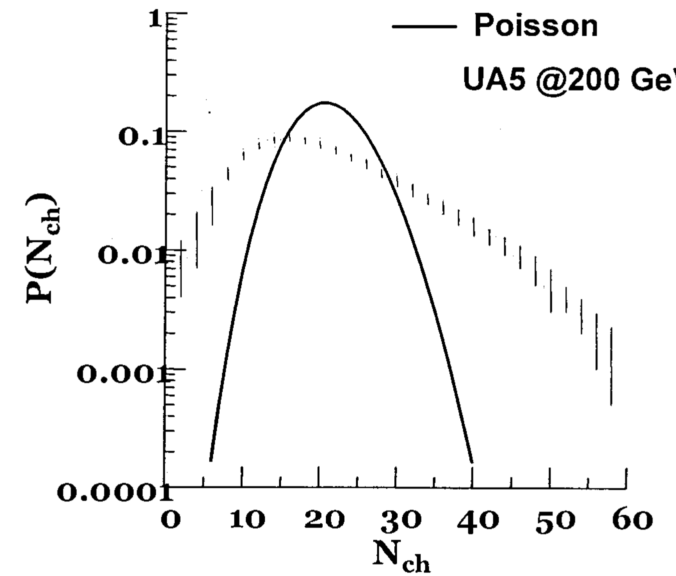
1
0.1
0.01
0.001
0.0001
P(N_ch)
Poisson
UA5 @200 GeV
0
10
20
30
40
50
60
N_ch

Back-up Slides

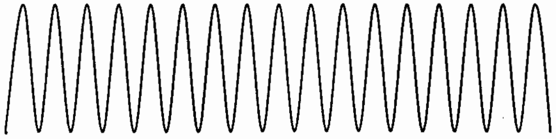

High-Energy collisions ...

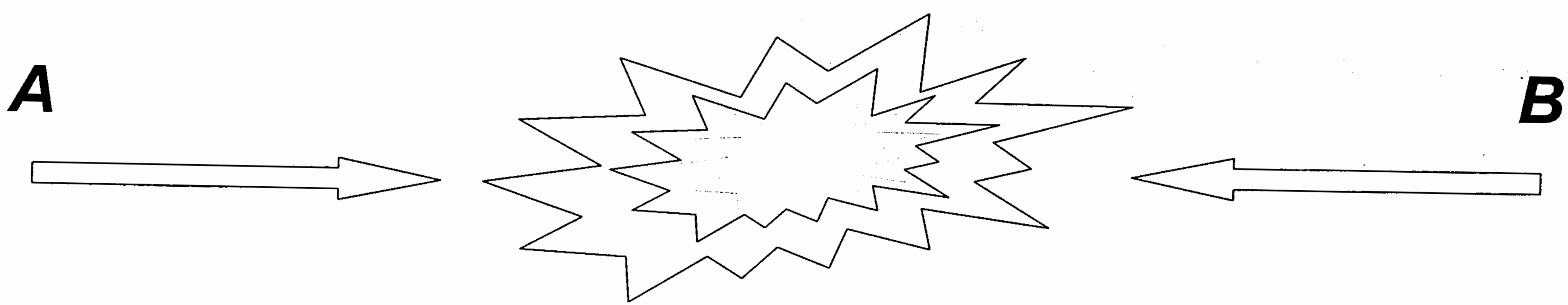

High-Energy collisions ...

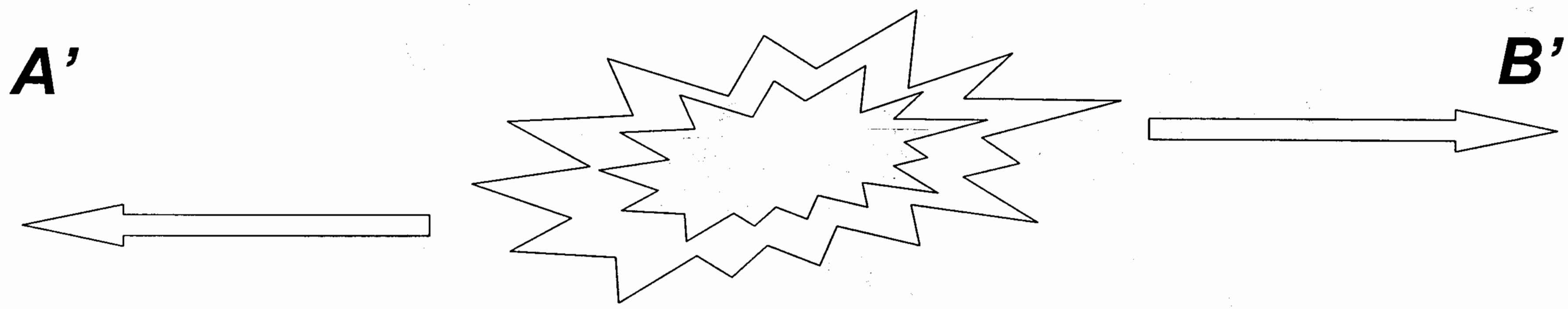

High-Energy collisions ...

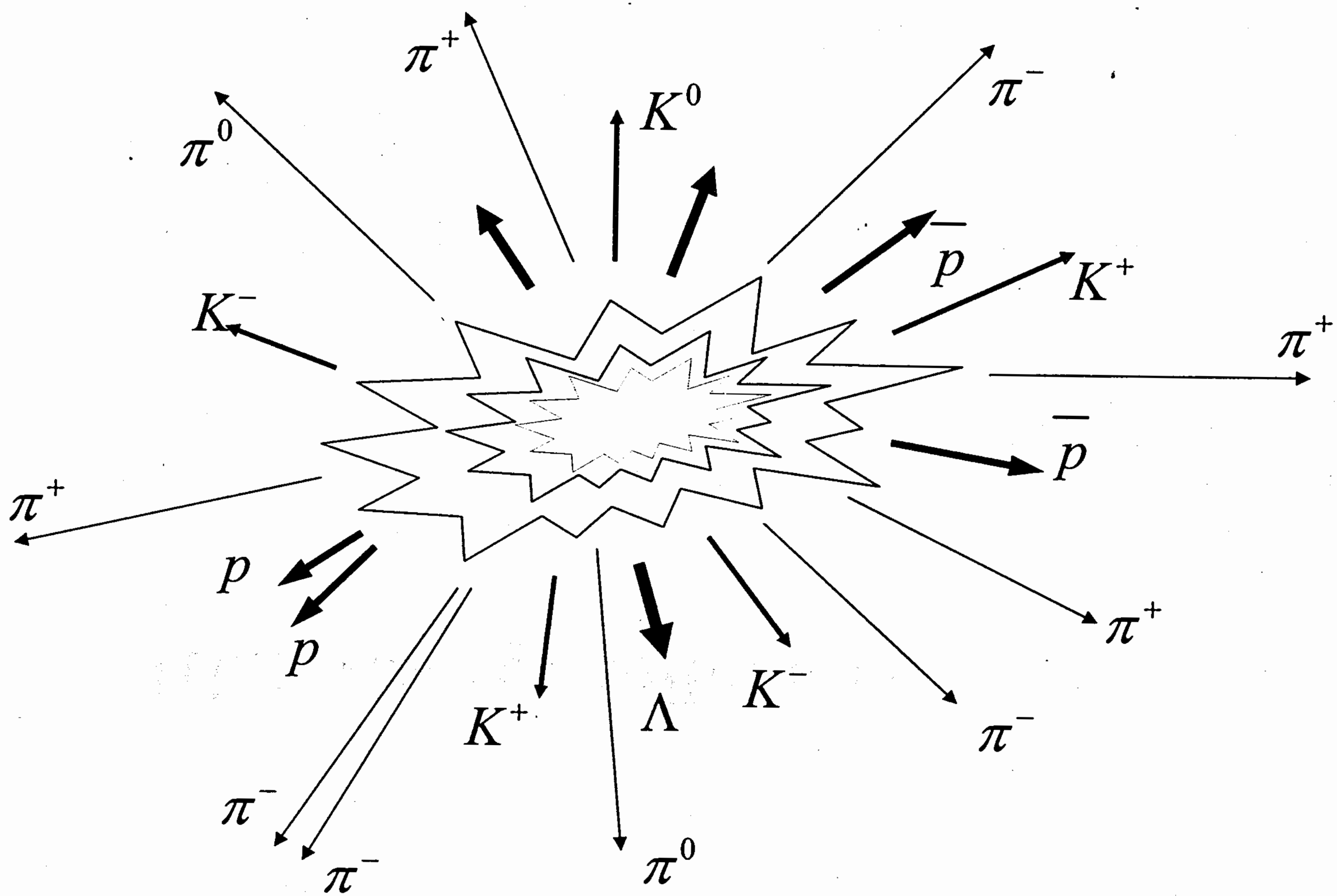

summary

- **Therefore: Statistical models of all kinds are widely used as source of some quick reference distributions. However, one must be aware of the fact that, because of such (interrelated) factors as:**

  - fluctuations of intensive thermodynamic parameters
  - finite sizes of relevant regions of interaction/hadronization
  - some special features of the „heath bath" involved in a given process the use of only one parameter T in formulas of the type

$$\exp(-\frac{x}{T})$$

is not enough and, instead, one should use two (... at least...) parameter formula

$$\exp_q(-\frac{x}{T}) = [1-(1-q)\frac{x}{T}]^{\frac{1}{1-q}}$$

with q accounting summarily for all factors mentioned above.

- **In general, for small systems, microcanonical approach would be preferred (because in it one effectively accounts for all nonconventional features of the heat bath...)** *(D.H.E.Gross, LNP 602)*

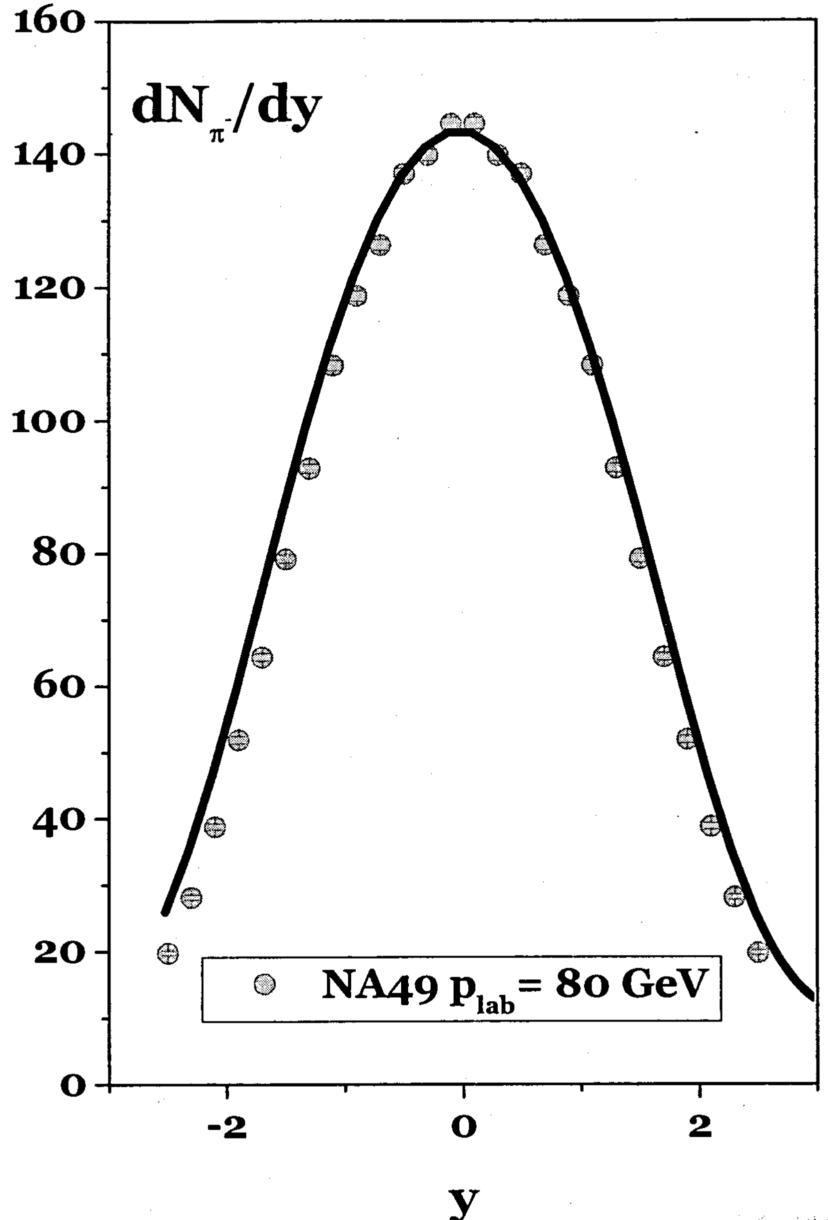

Example of use of MaxEnt method applied to some NA49 data for π^- production in PbPb collisions (centrality 0-7%) - (I) :

(*) the values of parameters used:
q=1.164 and K=0.3

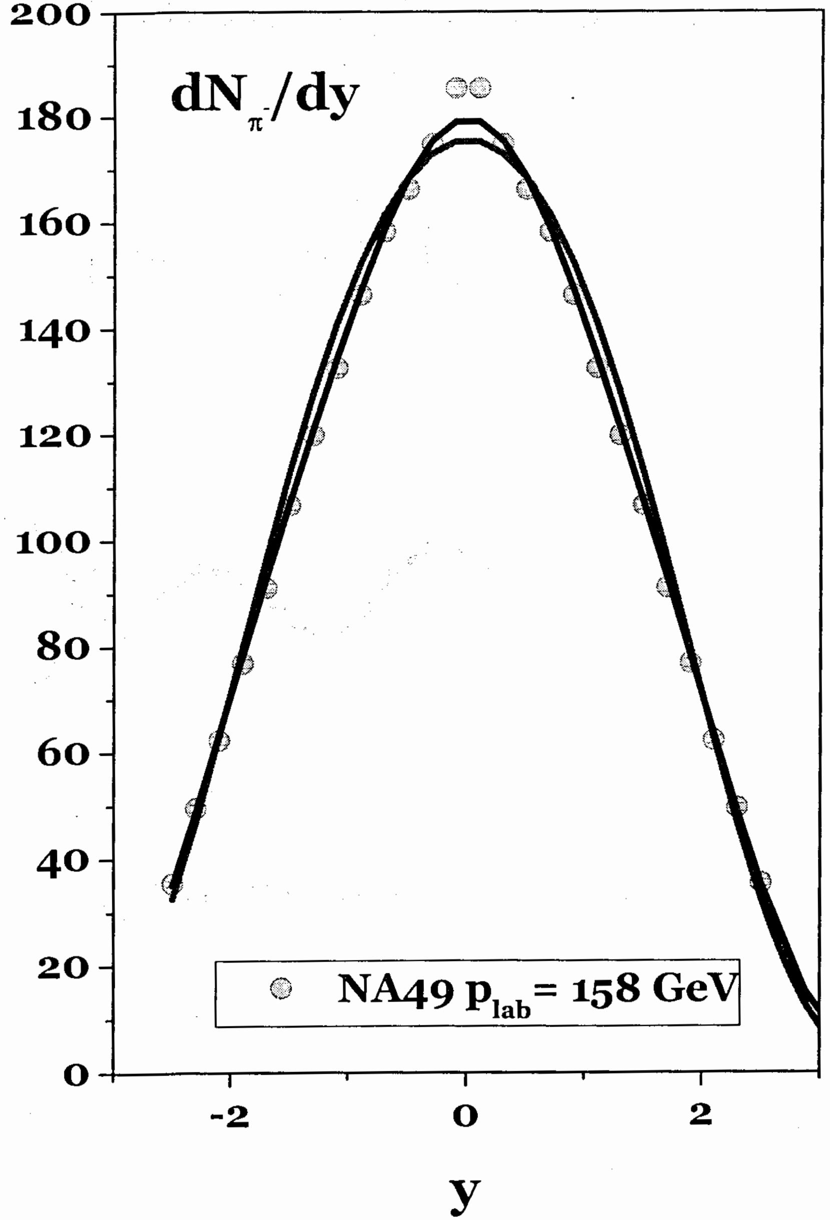

Example of use of MaxEnt method applied to some NA49 data for π^- production in PbPb collision (centrality 0-7%) - (I) :

(*) the values of parameters use (red line): q=1.2 and K=0.33

(*) q=1, two sources of mass M=6.34 GeV located at |y|=0.83

$\underbrace{\hspace{10em}}$

this is example of adding new dynamical assumption

(*) ***Nonextensivity – its possible origins .... "thermodynamics"***

T varies $\Leftrightarrow$

fluctuations...

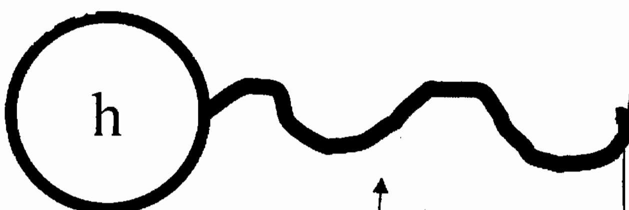

$T_0=\langle T\rangle$, q

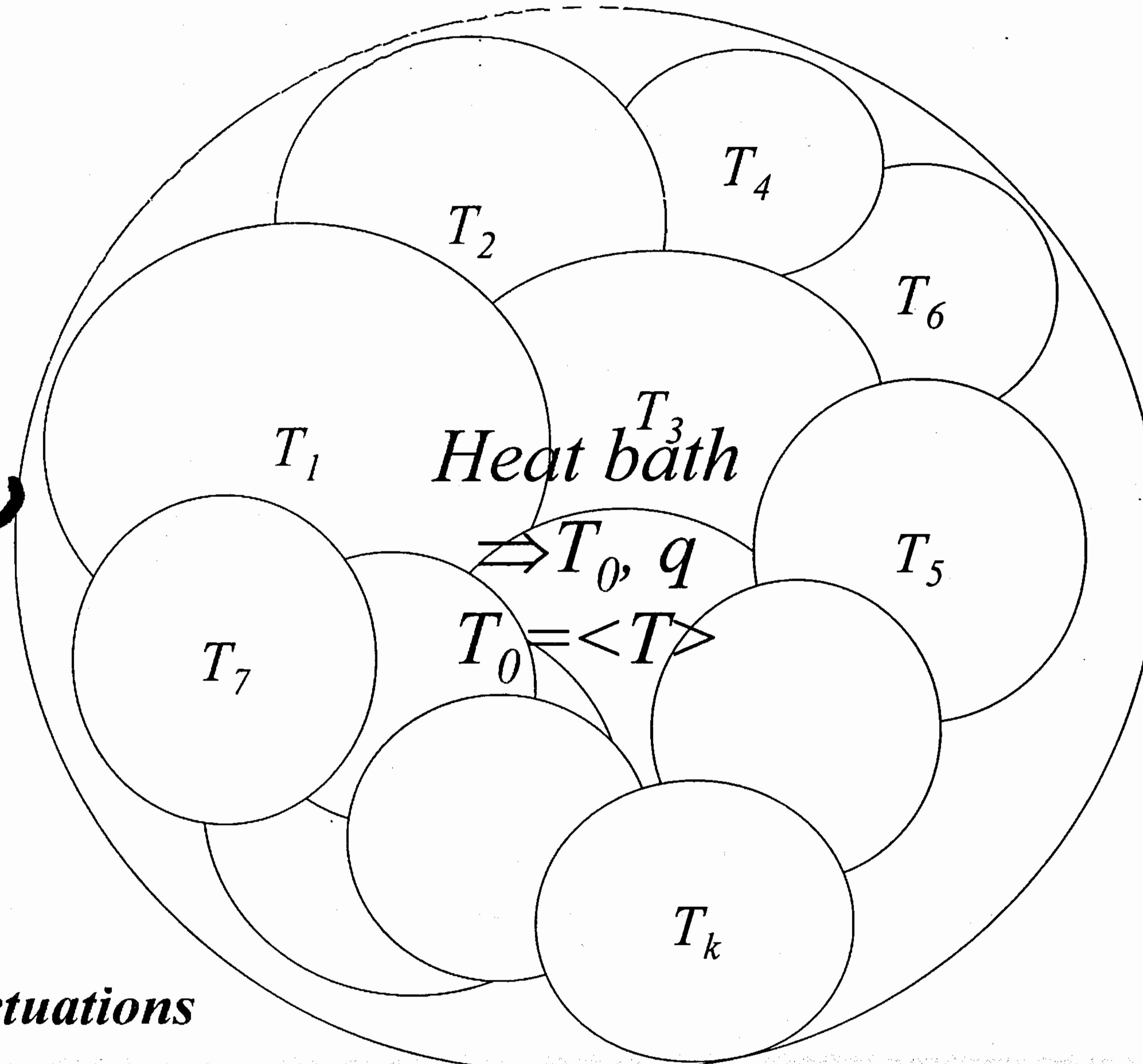

q - measure of fluctuations

Historical example:

(*) observation of deviation from the expected exponential behaviour
(*) successfully intrepreted (*) in terms of cross-section fluctuation:

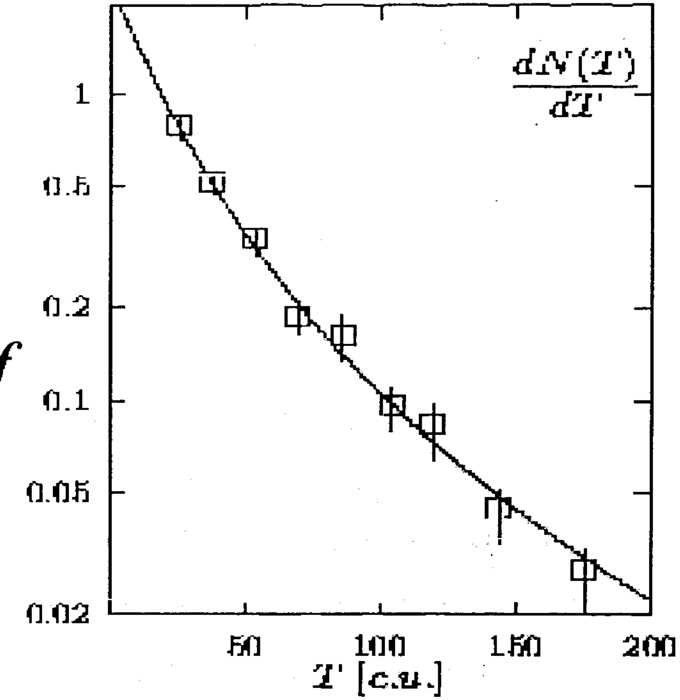

(*) can be also fitted by:

$$\frac{dN}{dT} = const \cdot \exp\left(-\frac{T}{\lambda}\right) \Rightarrow$$

$$\frac{dN}{dT} = const \cdot \left[1-(1-q)\frac{T}{\lambda}\right]^{\frac{1}{1-q}}; q = 1.3$$

Depth distributions of starting points of cascades in Pamir lead chamber Cosmic ray experiment (WW, NPB (Proc.Suppl.) A75 (1999) 191

(*) WW, PRD50 (1994) 2318

(*) immediate conjecture:
q ⇔ fluctuations present in the system

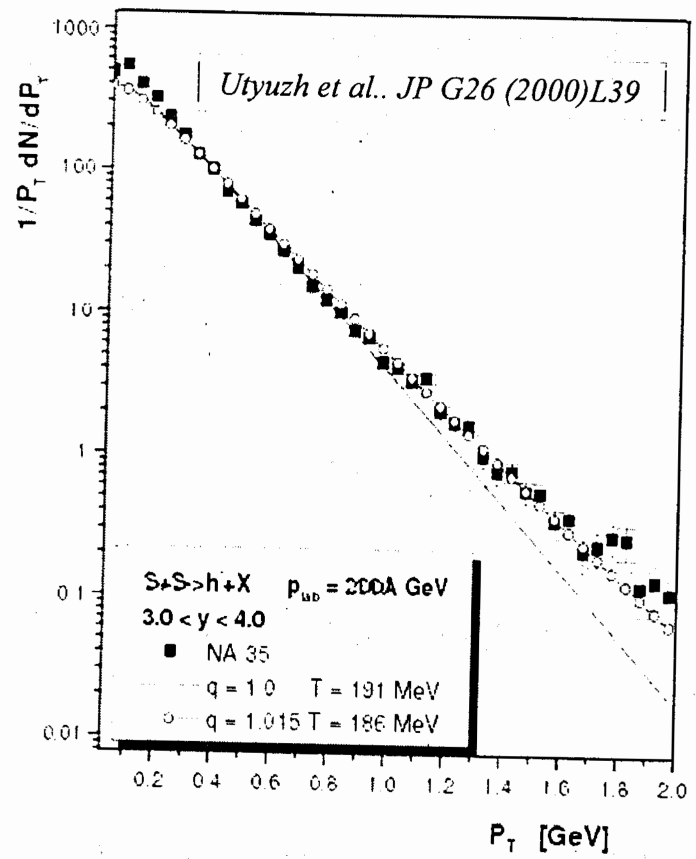

Fig.2

Some comments on T-fluctuations:

(*) Common expectation: slopes of p_T distributions $\Rightarrow$ information on T

(*) Only true for q=1 case, otherwise it is <T>, |q-1| provides us additional information

(*) Example: $|q-1|=0.015 \Rightarrow \Delta T/T \approx 0.12$

(*) Important: these are fluctuations existing in small parts of the hadronic system with respect to the whole system rather than of the event-by-event type for which $\Delta T/T = 0.06/\sqrt{N} \to 0$ for large N

Such fluctuations are potentially very interesting because they provide a direct measure of the total heat capacity of the system $\Rightarrow$ $$\frac{\sigma^2(\beta)}{<\beta>^2} = \frac{1}{C} = \omega = q - 1$$

$\Rightarrow$ ***Prediction: C ~ volume of reaction V, therefore q(hadronic)>>q(nuclear)***

Rapidity distributions:

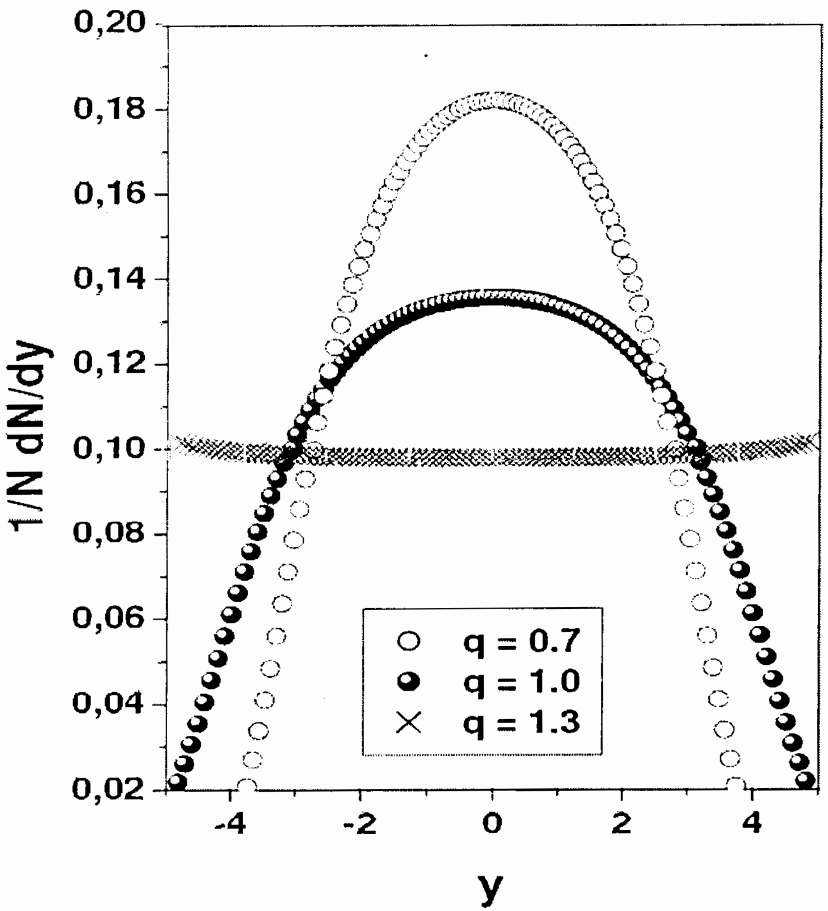

$$\frac{dN}{dy} = \frac{1}{Z_q} \cdot \left[1-(1-q)\cdot\beta_q\cdot\mu_T \cosh y\right]^{\frac{1}{1-q}}$$

$$Z_q = \int dy \left[1-(1-q)\cdot\beta_q\cdot\mu_T \cosh y\right]^{\frac{1}{1-q}}$$

Features:

(*) two parameters: $\beta_q=1/T_q$ and q
$\Rightarrow$ shape and height are strongly correlated

(*) in usual application only $\beta=1/T$
- but in reality (•) $1/Z_{q=1}$ is always used as another independent parameter $\Rightarrow$ height and shape are fitted independently

(*) in q-approch they are correlated

(•) T.T.Chou, C.N.Yang, PRL 54 (1985) 510; PRD32 (1985) 1692

Multiplicity Distributions: (UA5, DELPHI, NA35)

Kodama et al..

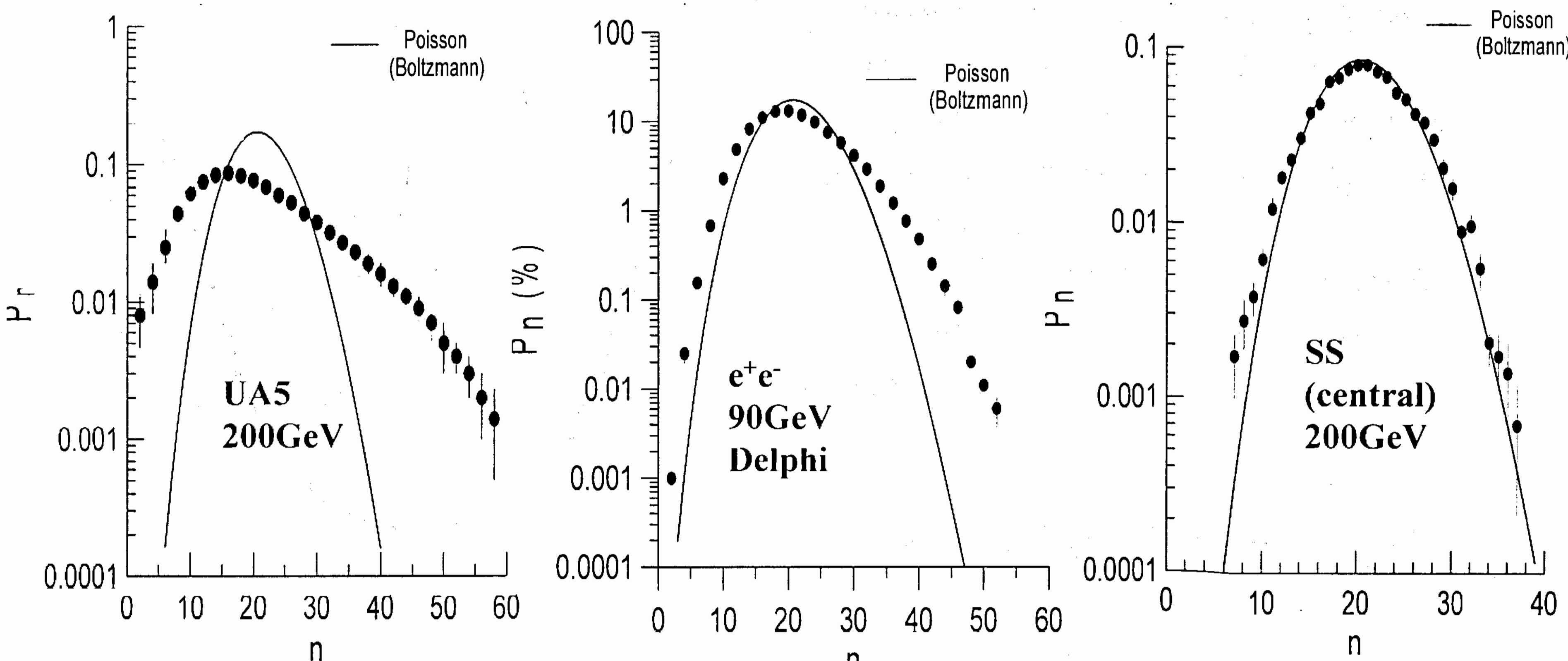

$\langle n \rangle =$ **21.1; 21.2; 20.8**

$D^2 = \langle n^2 \rangle - \langle n \rangle^2 =$ **112.7; 41.4; 25.7**

➔ ***Deviation from Poisson: 1/k***

$1/k = [D^2 - \langle n \rangle]/\langle n^2 \rangle =$ **0.21; 0.045; 0.011**

Recent example from AA -(1) (RWW, APP B35 (2004) 819)

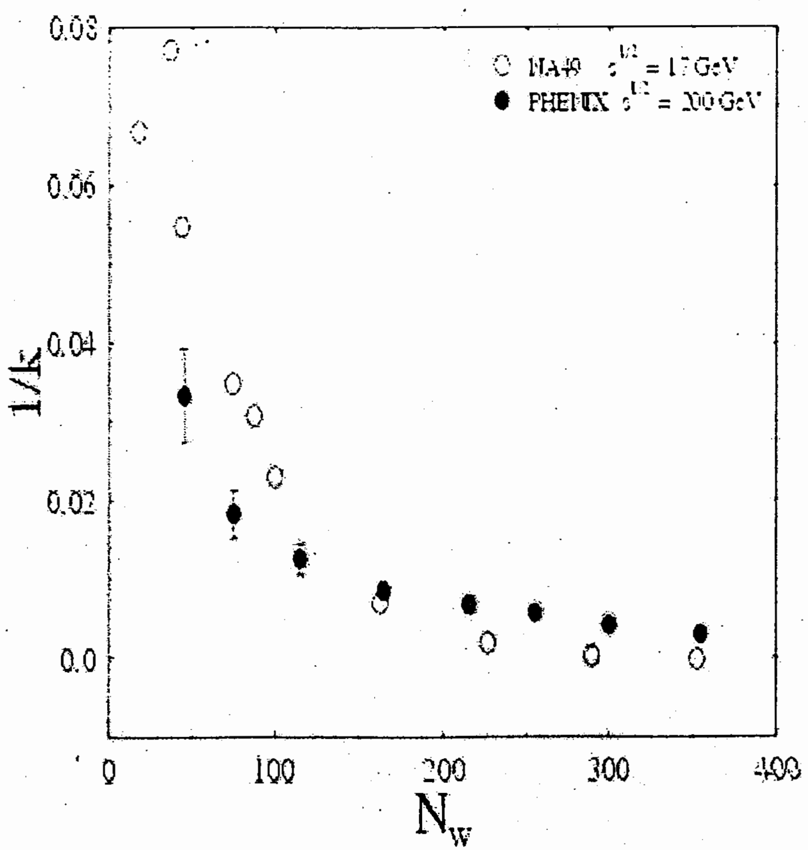

Dependence of the NBD parameter 1/k on the number of participants for NA49 and PHENIX data

With increasing centrality fluctuations of the multiplicity become weaker and the respective multiplicity distributions approach Poissonian form.

???

Perhaps: smaller $N_W \Rightarrow$ smaller volume of interaction $V \Rightarrow$ smaller total heat capacity $C \Rightarrow$ greater $q=1+1/C \Rightarrow$ greater $1/k = q-1$

Recent example from AA – (2) (RWW, APP B35 (2004) 819)

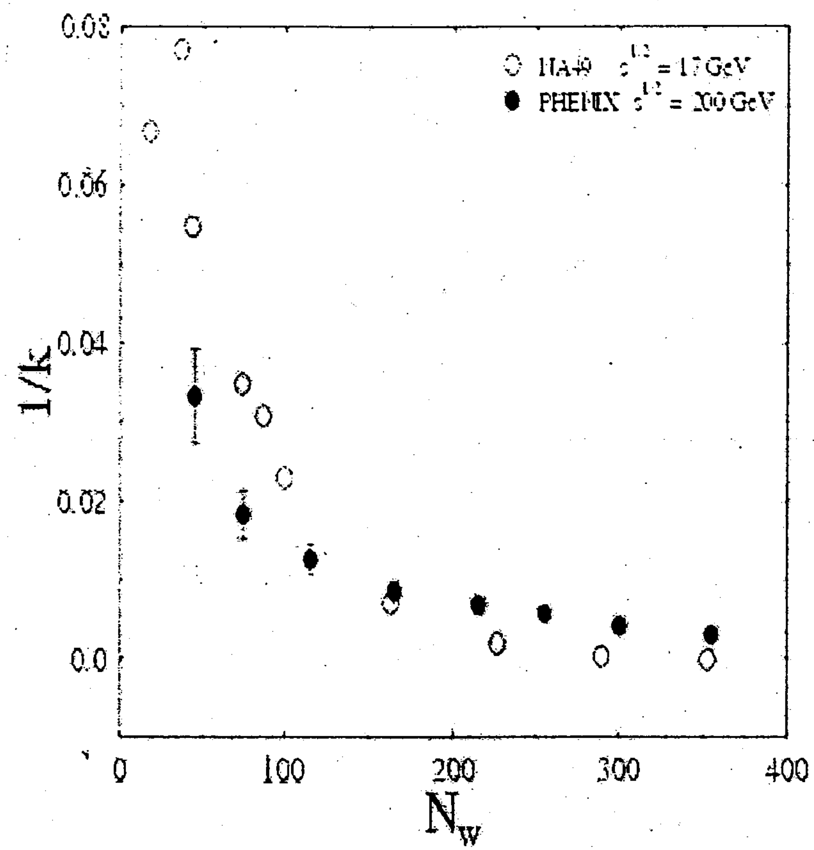

Dependence of the NBD parameter 1/k on the number of participants for NA49 and PHENIX data

In this case it can be shown that:

$$\frac{1}{k} = \frac{D^2(N)}{<N>^2} = R(q-1) \Rightarrow D(N) \approx \sqrt{R(q-1)}$$

$$R(q-1) \approx 0.33 \qquad (\leftarrow \textit{ Wróblewski law })$$

$$R = \frac{(\delta S)^2 / S^2}{(\delta E)^2 / E^2} \approx 0.56 \qquad (\leftarrow \textit{for } p/e = 1/3)$$

$\Rightarrow q \approx 1.59$ which apparently (over)saturates the limit imposed by Tsallis statistics: $q \leq 1.5$. For $q=1.5$ one has:

0.33 → 0.28 (in WL)

or

1/3 → 0.23 (in EoS)

$$\boxed{p_i = \exp[-\sum \lambda_k \bullet R_k(x_i)]}$$

This is distribution which:

(*) tells us "the truth, the whole truth" about our experiment, i.e., it reproduces known information

(*) tells us "nothing but the truth" about our experiment, i.e., it conveys the least information (= only those which is given in this experiment, nothing else)

⇨ it contains maximum missing information

G. Wilk, Z. Włodarczyk, Phys. Rev. 43 (1991) 794

Example *(from Y.-A. Chao, Nucl. Phys. B40 (1972) 475)*

Question: what have in common such successful models as:

(*) multi-Regge model

(*) uncorrelated jet model

(*) thermodynamical model

(*) hydrodynamical model

(*) ....

Answer: ***they all share common (explicite or implicite) dynamical assumptions that:***

(*) only part of initial energy of reaction is used for production of particles $\leftrightarrow$ ***existence of inelasticity of reaction, K~0.5***

(*) transverse momenta of produced secondaries are cut-off $\leftrightarrow$ ***dominance of the longitudinal phase-space***

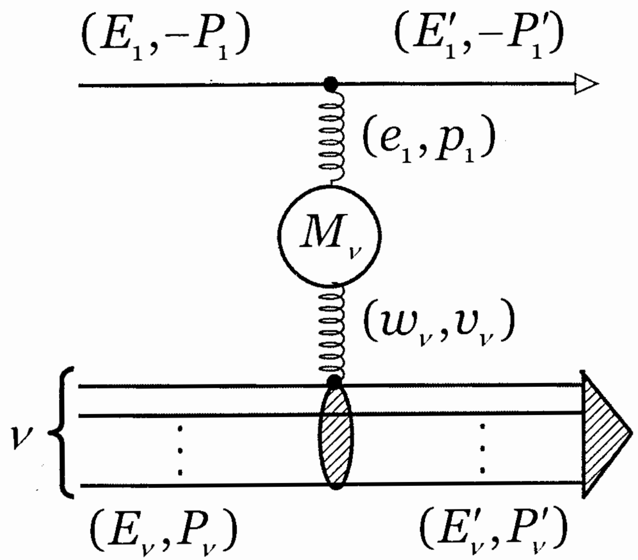
$(E_1,-P_1)$
$(E'_1,-P'_1)$
(e_1,p_1)
M_ν
(w_ν,v_ν)
ν
(E_ν,P_ν)
(E'_ν,P'_ν)

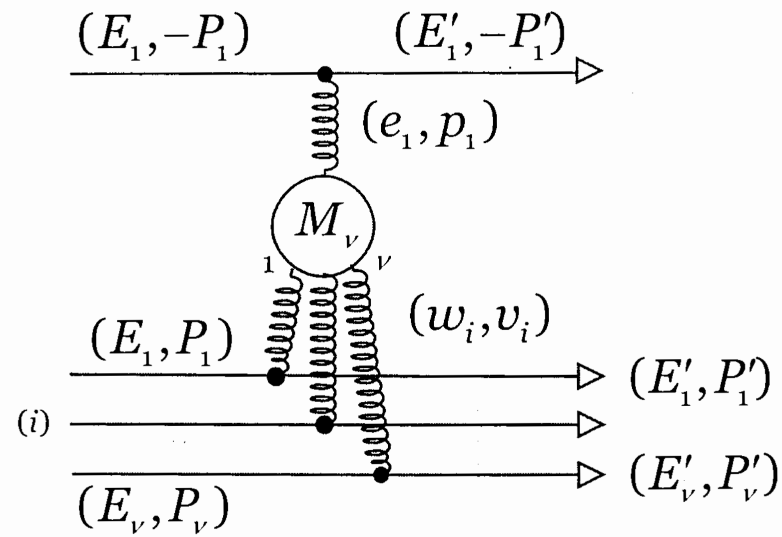
$(E_1,-P_1)$
$(E'_1,-P'_1)$
(e_1,p_1)
M_ν
1
ν
(w_i,v_i)
(E_1,P_1)
(E'_1,P'_1)
(i)
(E'_ν,P'_ν)
(E_ν,P_ν)

summary

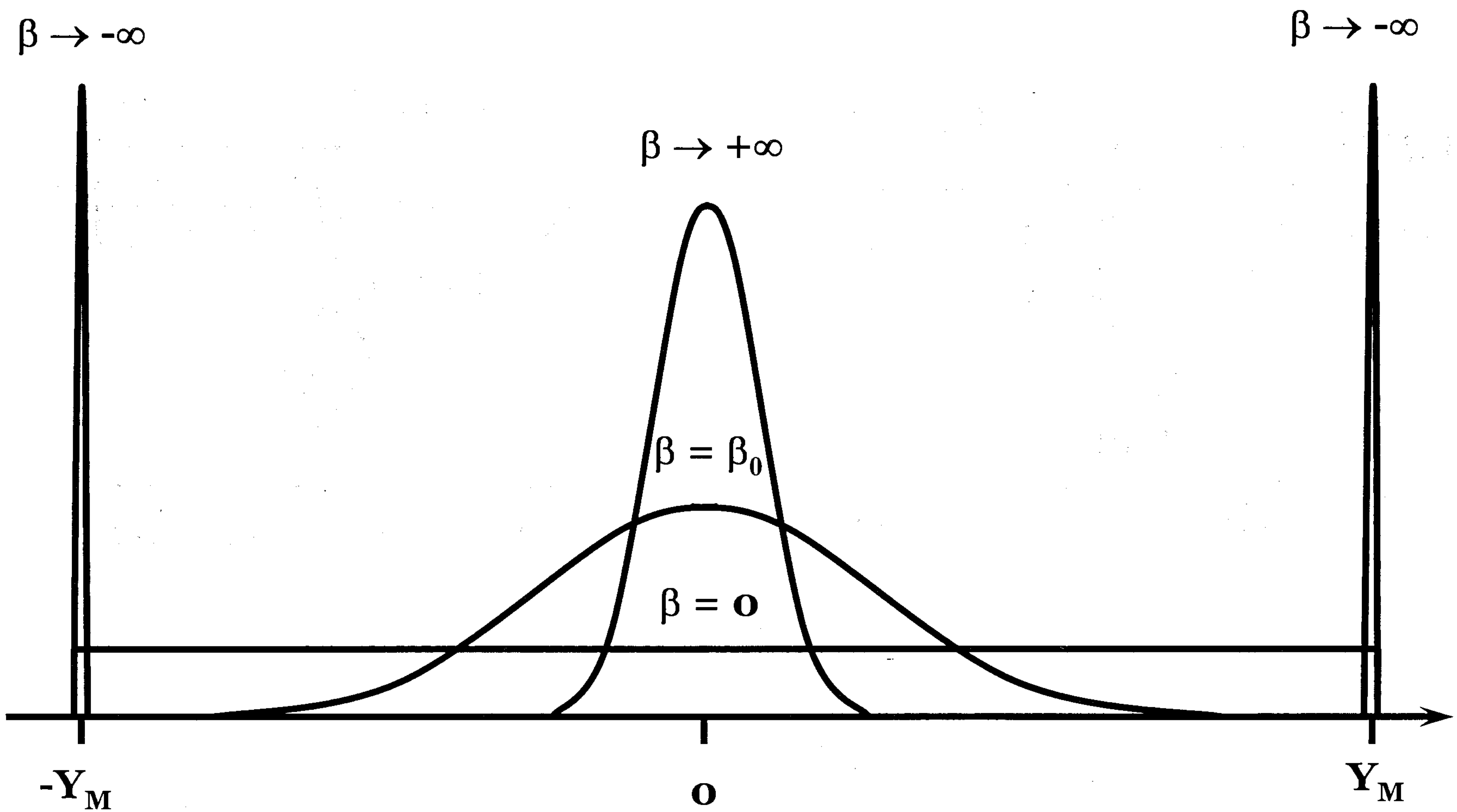

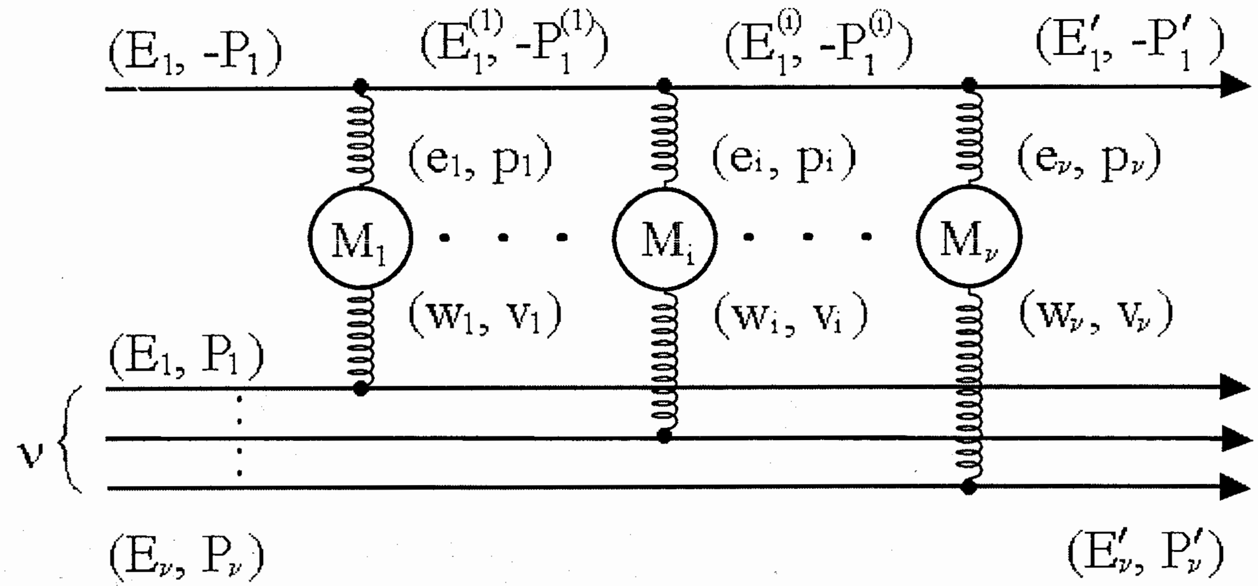

$(E_1, -P_1)$
$(E_1^{(1)}, -P_1^{(1)})$
$(E_1^{(i)}, -P_1^{(i)})$
$(E_1', -P_1')$
(e_1, p_1)
(e_i, p_i)
(e_ν, p_ν)
M_1
M_i
M_ν
(w_1, v_1)
(w_i, v_i)
(w_ν, v_ν)
(E_1, P_1)
ν
(E_ν, P_ν)
(E_ν', P_ν')

Events generator for pp collisions at $E_{lab} = 70$ GeV

N. Shubitidze

$$p+p \rightarrow p+p+\underbrace{\pi^{\pm}+\ldots+\pi^{\pm}}_{\eta}+\underbrace{\pi^{0}+\ldots+\pi^{0}}_{\lambda}$$

$$\eta = 2, 4, \ldots \qquad E_{lab} = 70 GeV$$

$$Z_N = \int \left\{ \prod_{i=1}^{N} \frac{d^3 k_i \exp[-r_0^2 k_{t,i}^2]}{2\sqrt{k_i^2 + m_i^2}} \right\} \delta\left(E - \sum_{i=1}^{N} \sqrt{k_i^2 + m_i^2}\right) \times$$

$$\times \delta\left(\sum_{i=1}^{N} k_{i,x}\right) \delta\left(\sum_{i=1}^{N} k_{i,y}\right) \delta\left(\sum_{i=1}^{N} k_{i,z}\right)$$

$k_{t,i}$ - transverse momentum, $\quad N = \eta + \lambda + 2$

r_0 - cutting parameter, phenomenological constant

$$k_{N,x} = -\sum_{i=1}^{N-1} k_{i,x}, \quad k_{N,y} = -\sum_{i=1}^{N-1} k_{i,y}, \quad k_{N,z} = -\sum_{i=1}^{N-1} k_{i,z}$$

$$(k_{i,x}, k_{i,y}, k_{i,z}) \Rightarrow (k_i, \theta_i, \varphi_i)$$

$$\theta_i = \mu_i \pi, \quad \varphi_i = \nu_i 2\pi$$

$$k_1 = \rho f_1(\eta_1, \eta_2, \ldots, \eta_{N-2})$$

$$k_2 = \rho f_2(\eta_1, \eta_2, \ldots, \eta_{N-2})$$

$$\vdots$$

$$k_{N-1} = \rho f_{N-1}(\eta_1, \eta_2, \ldots, \eta_{N-2})$$

$$\psi(\rho) = E - \sum_{i=1}^{N} \sqrt{\rho^2 f_i^2 + m_i^2} = 0$$

$$\delta\left(E - \sum_{i=1}^{N} \sqrt{k_i^2 + m_i^2}\right) = \frac{1}{\left|\psi'(\rho_0)\right|}$$

N = 8

$$k_1 = \rho \quad \eta_6 \quad \eta_5 \quad \eta_4$$

$$k_2 = \rho \quad \eta_6 \quad \eta_5 \quad (1-\eta_4)$$

$$k_3 = \rho \quad \eta_6 \quad (1-\eta_5) \quad \eta_3$$

$$k_4 = \rho \quad \eta_6 \quad (1-\eta_5)(1-\eta_3)$$

$$k_5 = \rho(1-\eta_6) \quad \eta_2 \quad \eta_1$$

$$k_6 = \rho(1-\eta_6) \quad \eta_2 \quad (1-\eta_1)$$

$$k_7 = \rho(1-\eta_6)(1-\eta_2)$$

P. L'Ecuyer, ``Tables of Maximally-Equidistributed Combined LFSR Generators", Mathematics of Computation, 68, 225 (1999), 261--269

V.V.Babintsev et al. Prepr. IHEP M-25,1976

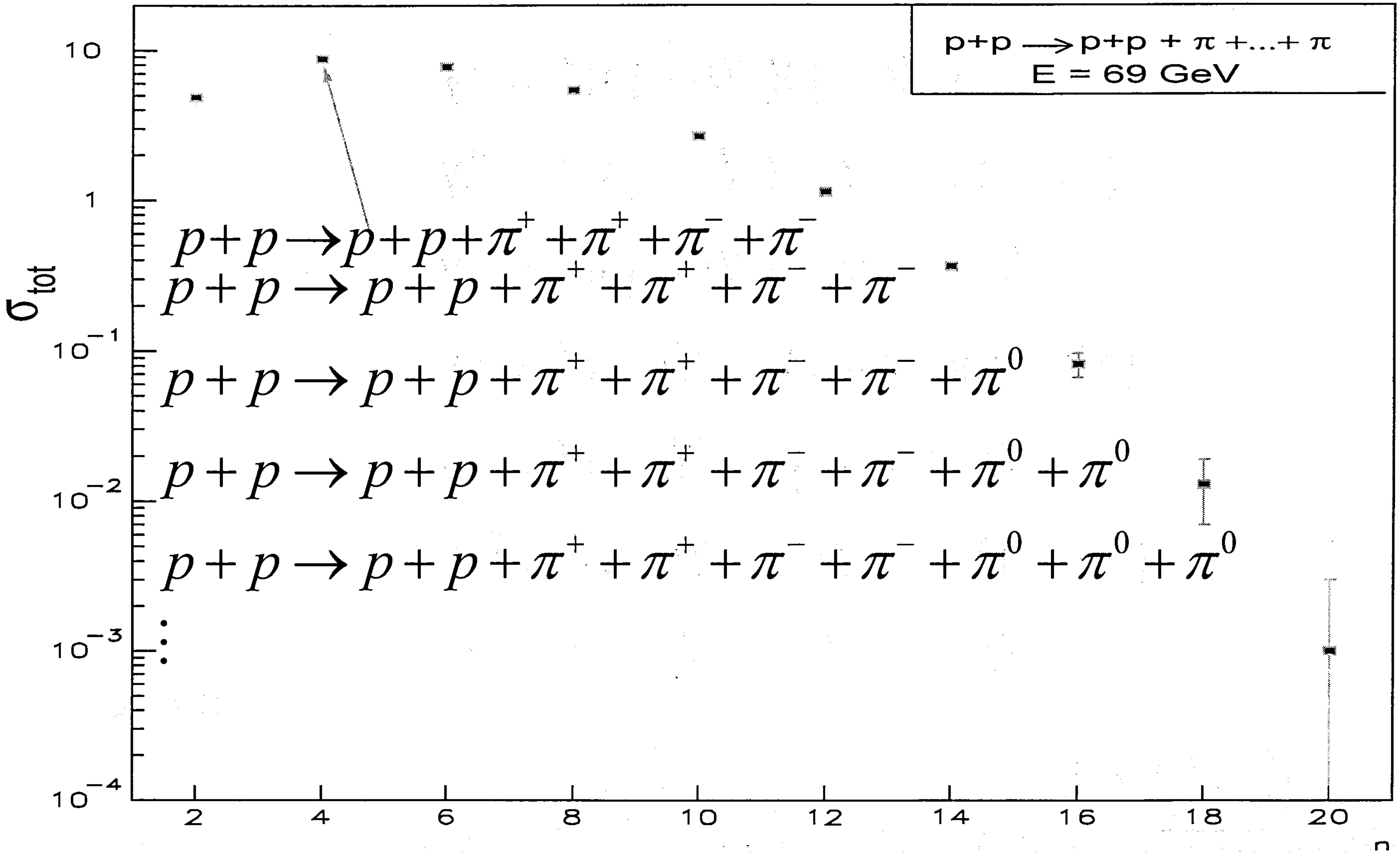

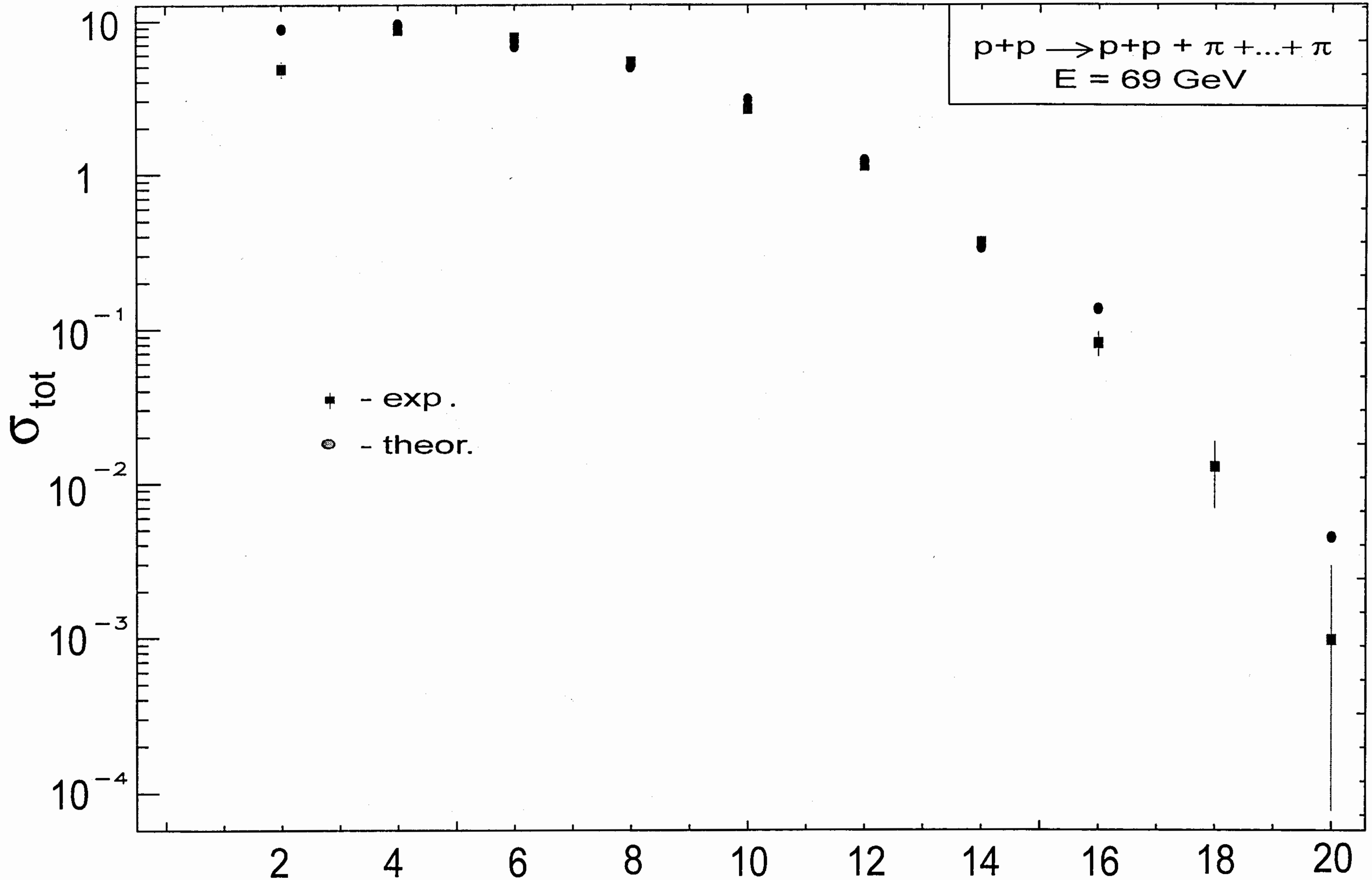
p+p → p+p + π +...+ π
E = 69 GeV
- exp.
- theor.
σ_{tot}
10
1
10^{-1}
10^{-2}
10^{-3}
10^{-4}
2
4
6
8
10
12
14
16
18
20

Definition a number of charged mezons:

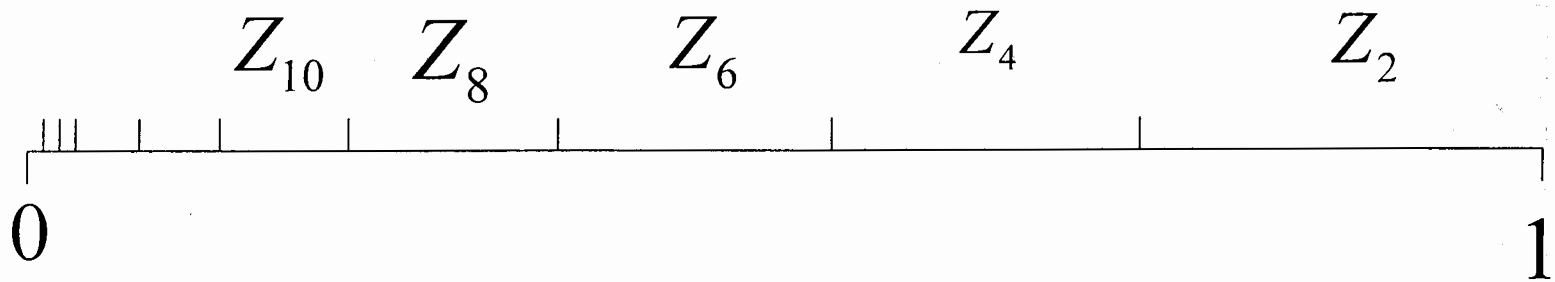

$$Z_{\eta} = \frac{\sigma_{\eta\pi}}{\sigma_{2\pi}+\sigma_{4\pi}+\sigma_{6\pi}+\ldots+\sigma_{68\pi}}$$

Definition a number of neutral mezons:

$$Z_{\eta,\lambda} = \frac{\sigma_{2\_\eta\_\lambda}}{\sigma_{2\_\eta\_0}+\sigma_{2\_\eta\_1}+\sigma_{2\_\eta\_2}+\ldots+\sigma_{2\_\eta\_\lambda_{\max}}}$$

$$\frac{1}{2}\,\frac{k\,p\,Sin(\theta)\,Exp(-k^2\,p^2\,Sin^2(\theta))}{F(k\,p)}$$

$F(z)$ - Dawson's integral

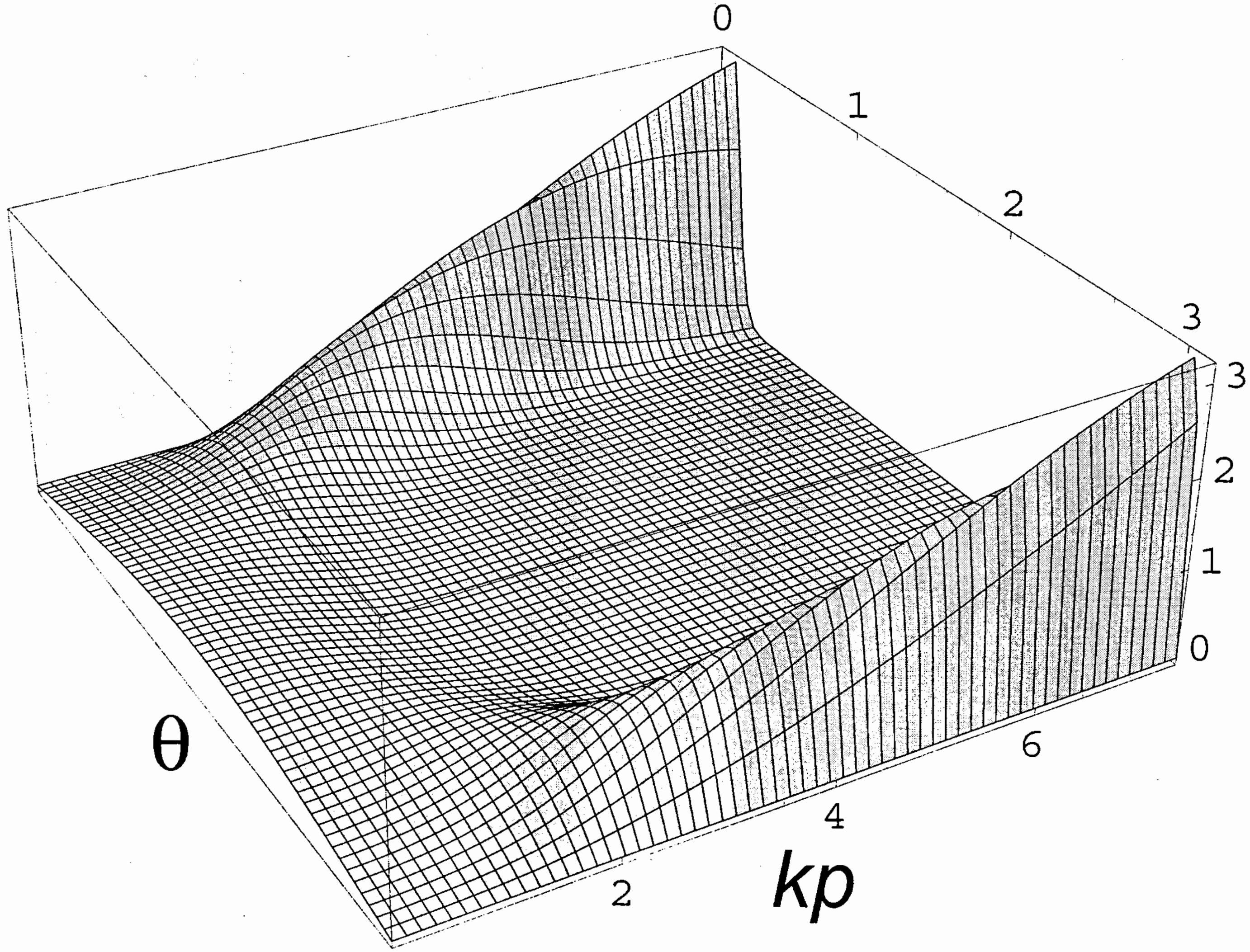

$k = 3.79$

$$\int_{y_{\min}}^{y_{\max}} \int_{x_{\min}}^{x_{\max}} P(x, y)\,dx\,dy = 1$$

$$0 < u, v < 1$$

$$u = \int_{y_{\min}}^{y} dy' \int_{x_{\min}}^{x_{\max}} P(x', y')\,dx' \Rightarrow y = y_0$$

$$v = \int_{x_{\min}}^{x} P(x', y_0)\,dx' \bigg/ \int_{x_{\min}}^{x_{\max}} P(x', y_0)\,dx' \Rightarrow x = x_0$$

Distribution of particles in the laboratory system

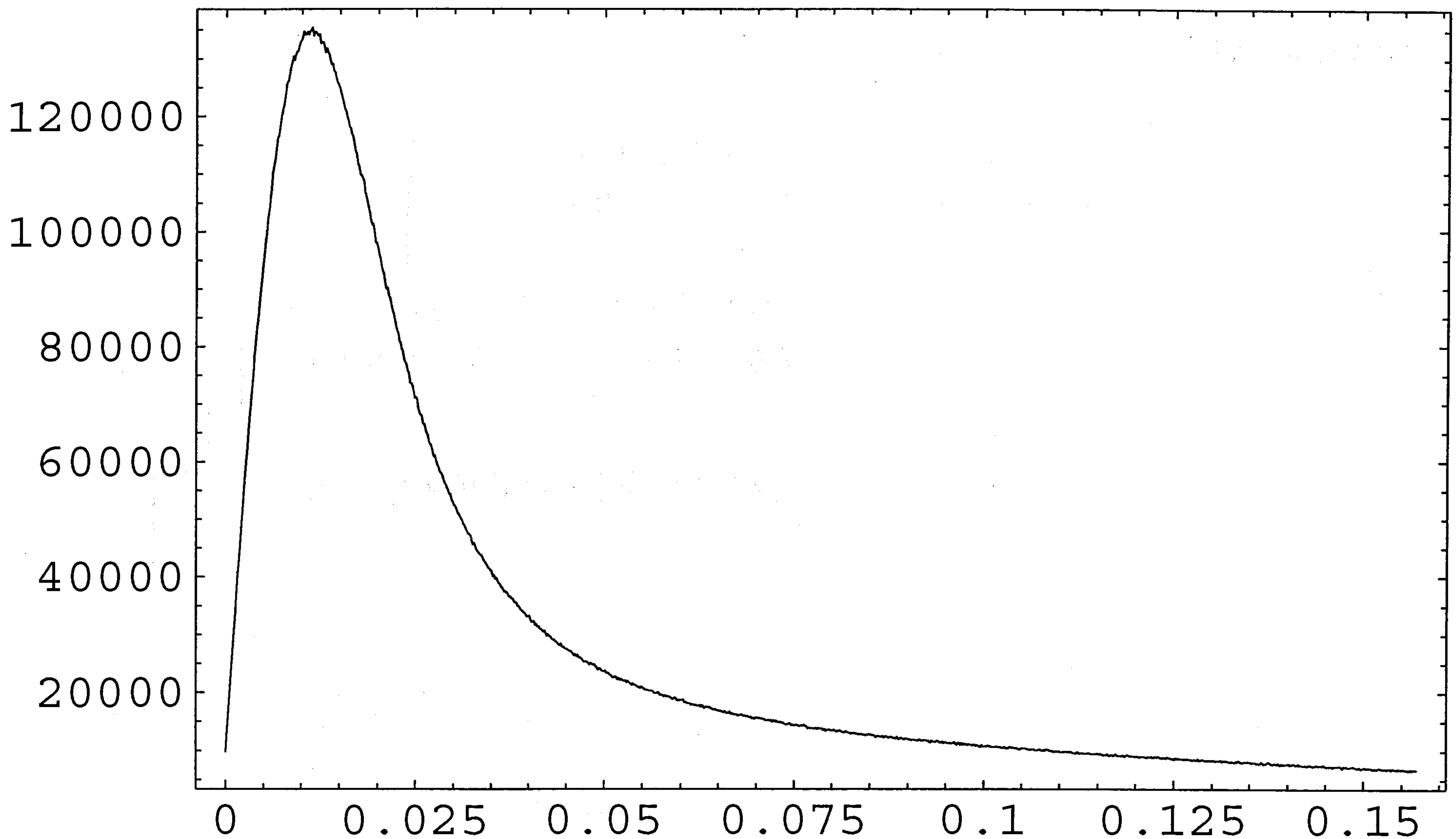

Scheme of events generator

Select number of charged $\pi^{\pm}$

$\sim Z_8 \sim Z_6 \sim Z_4 \qquad \sim Z_2$

0 1

$T(10^6\ events)$ □ $112\ second$

Select number of neutral π^0

Choose $N-1$ moments & θ , φ_i - select randomly

From moments conservation low calculate p_N & θ_N

From energy conservation low

$$E - \sum_{i=1}^{N} \sqrt{p_i^2 + m_i^2} = 0$$

correct lengths of moments

Behavior of part of transverse momenta as function of pion number

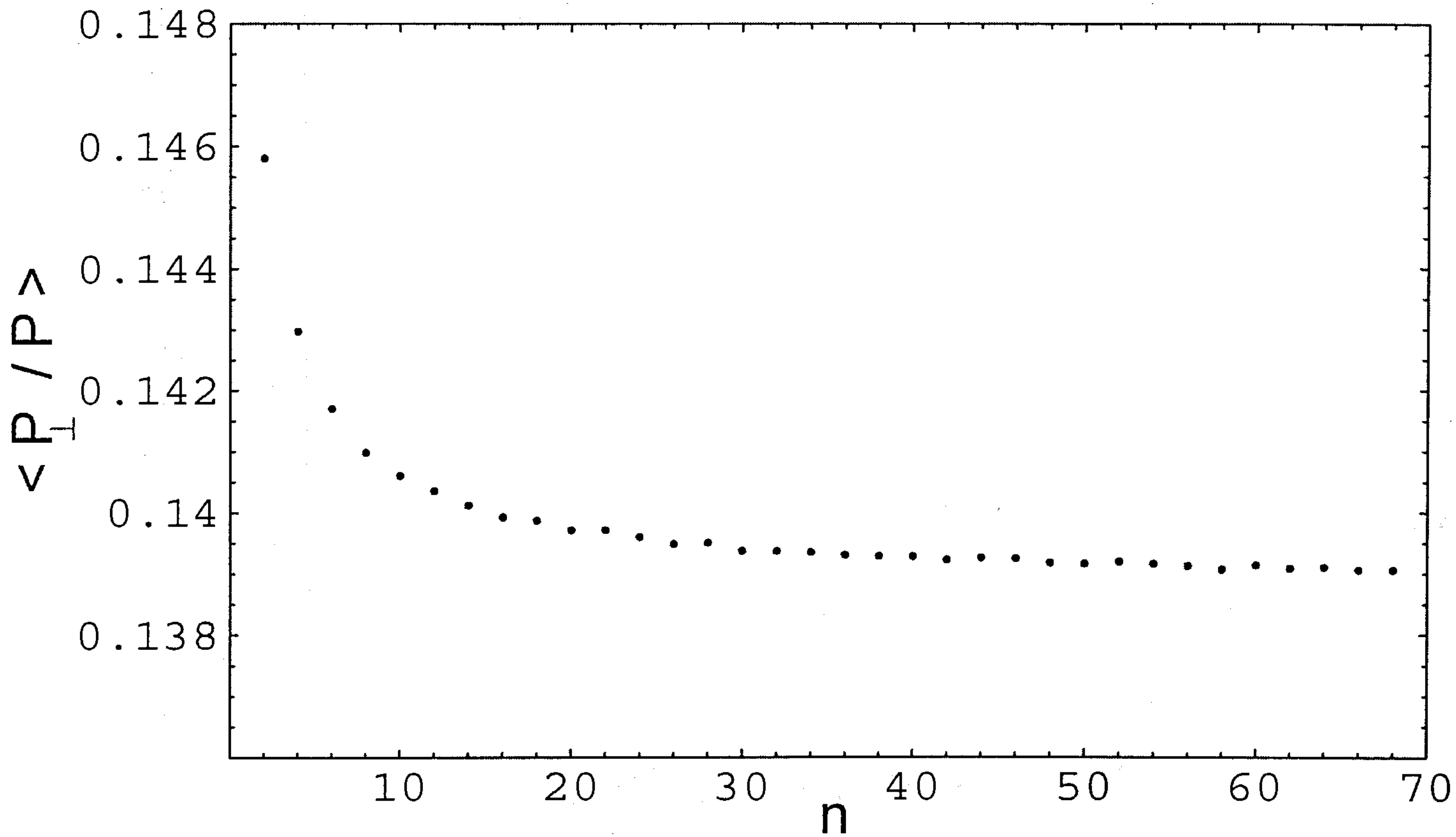

Behavior of transverse and longitudinal momenta as function of pion number

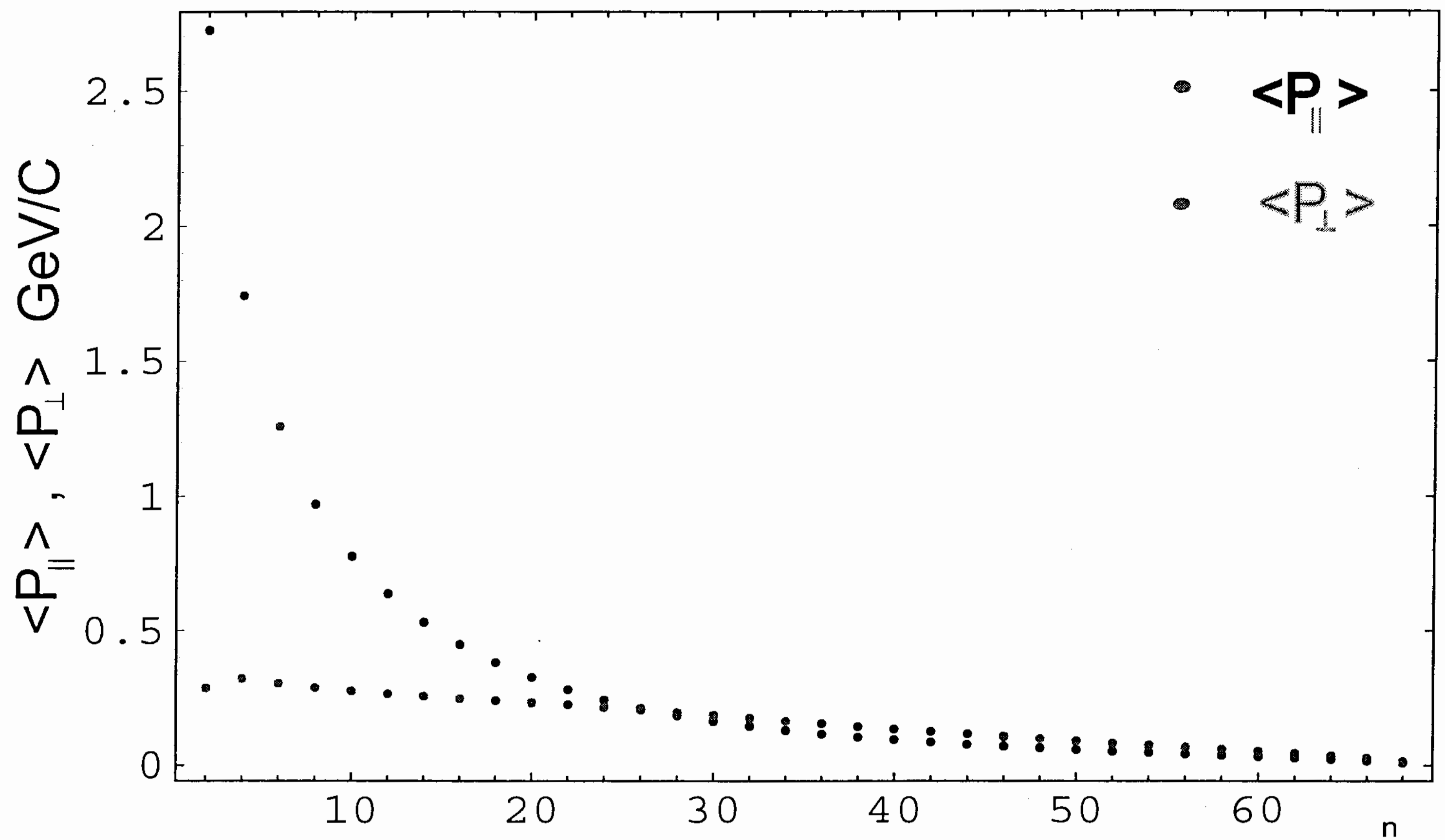

Typical behavior of cross sections as function of pion number

$$p + p \rightarrow p + p + \pi^+ + \pi^- + \pi^+ + \pi^- + \underbrace{\pi^0 + \ldots + \pi^0}_{\lambda}$$

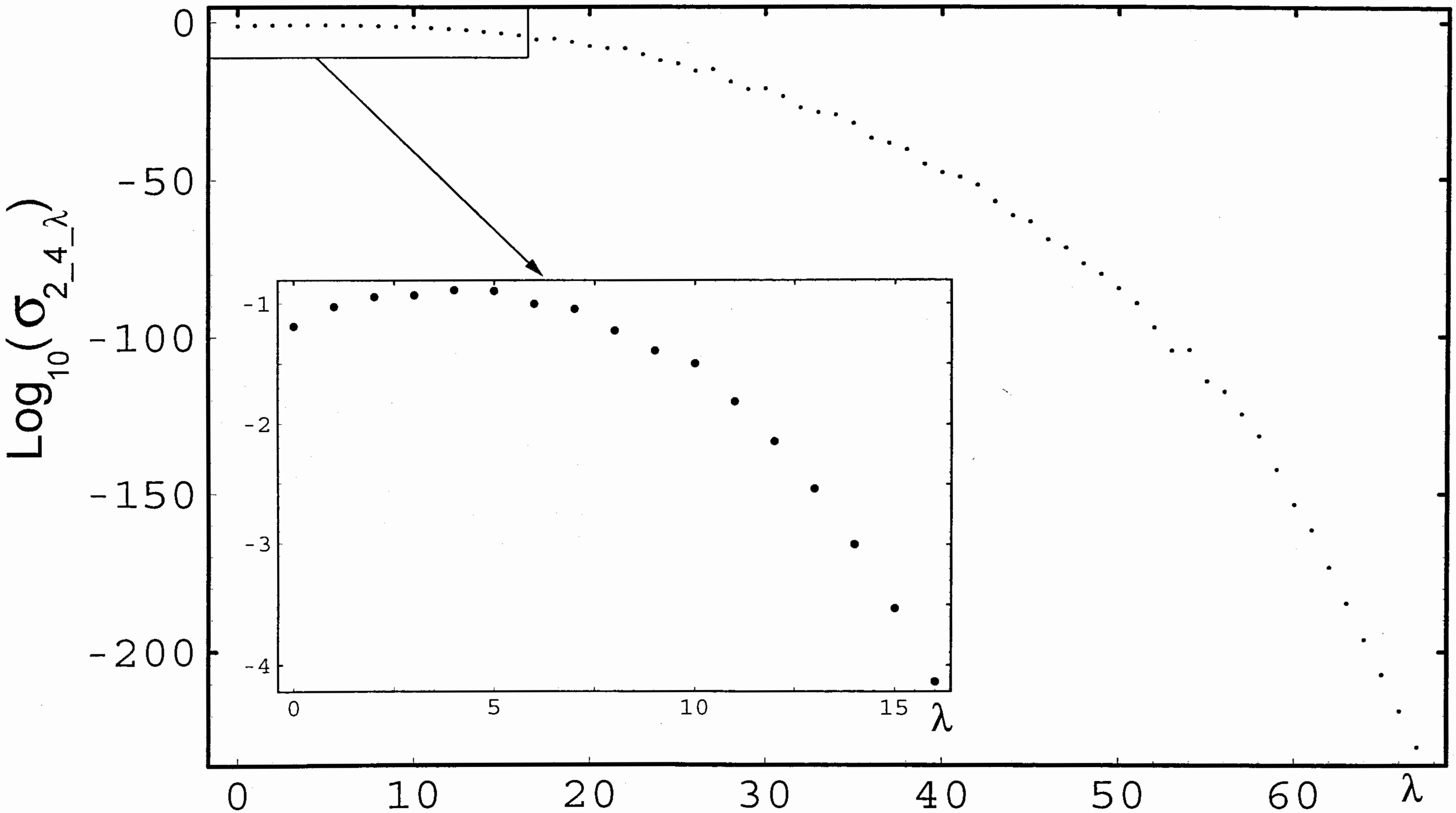

Behavior of cross sections as function of neutral and charged mezons number

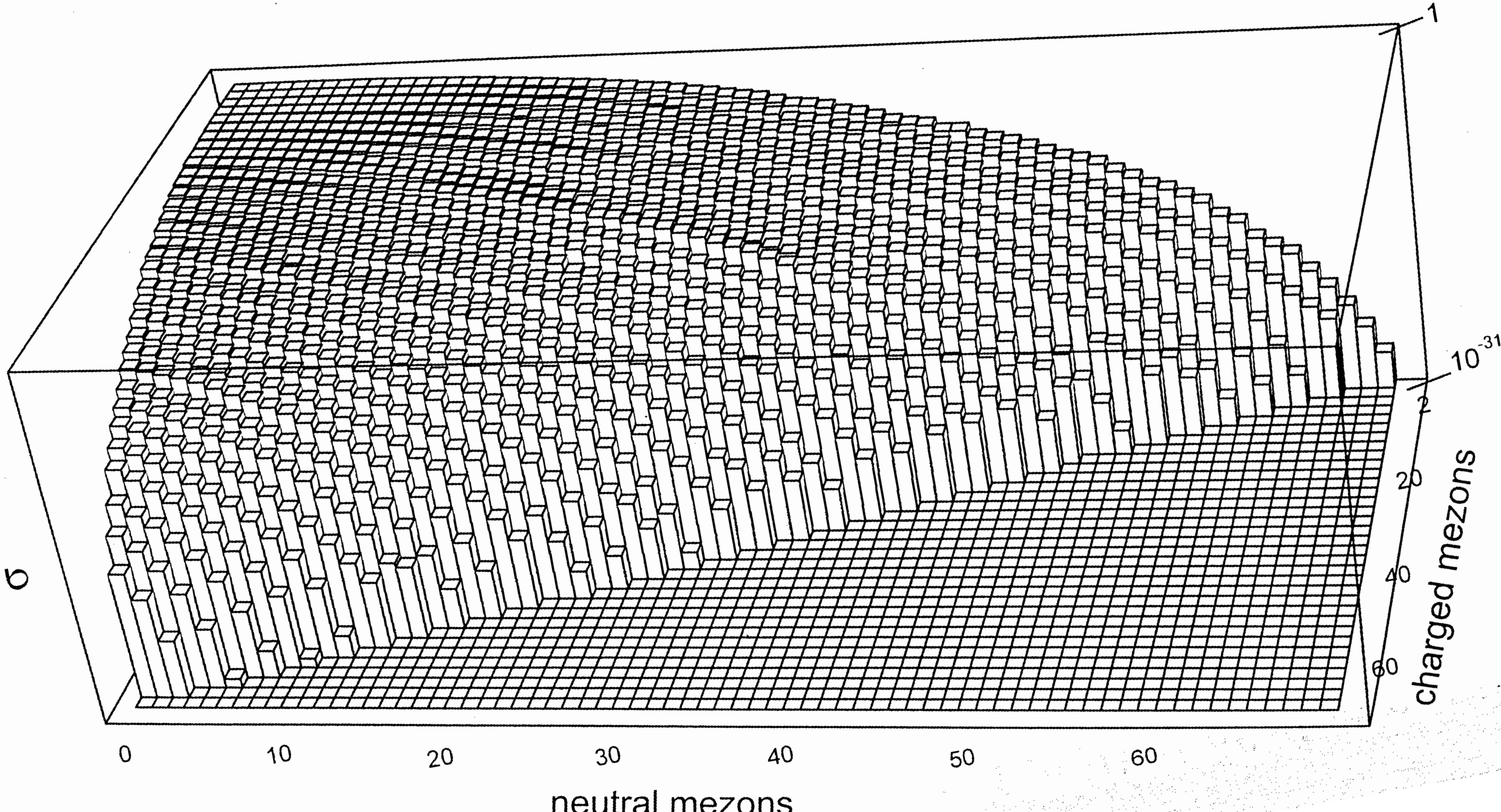

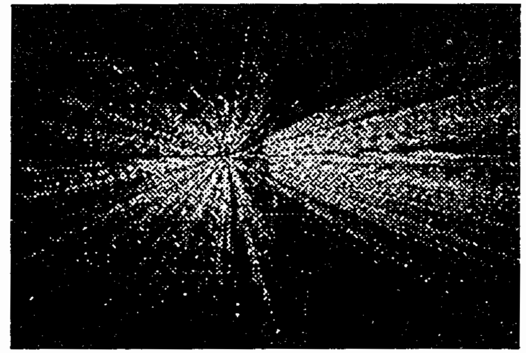

Bose-Einstein correlations in Pythia

Ľubomír Lovás

Faculty of Mathematics, Physics and Informatics,
Comenius University

Involved people: S. Tokár (CU), G. Kozlov, A.N. Sissakian (JINR)

Content:

- **Introduction**
- **BEC effect in Pythia**
- **Pythia simulations**
  - Reproducing of input BEC parameters
  - The case when correlations are not included
- **Detector CDF**
  - More realistic simulation: Momentum blurring
  - More realistic simulation: Energy cut
- **Conclusion of 1st part**
- **Analysis of ALEPH data in frame of Kozlov model**
- **Conclusion of 2nd part.**

Introduction

Bose-Einstein Correlations: Enhanced probability for the emission of identical bosons with similar momenta.

Provides information about space-time characteristics of the particle emission region

The two-particles correlation function is given by : $C_2(p_1,p_2)=\dfrac{P(p_1,p_2)}{P(p_1)P(p_2)}$

$P(p_1,p_2)$ - two-particles probability density function
$P(p_1)$, $P(p_2)$ - single particle probability

$$C_2(Q)=N(1+\lambda\times e^{-R^2Q^2})$$

The construction of correlation function is given by:

is the two-particles four-momentum difference distribution
is the corresponding reference sample.

Bose-Einstein effect in Pythia 6.205

There is a possibility to include Bose-Einstein correlations, but it is only a first approximation to BE effect.

First of all the Q_{ij} value is evaluated: $Q_{ij} = \sqrt{(p_i + p_j)^2 - 4m^2}$

And then the shifted Q'_{ij} is found as the solution to the equation:

$$\int_0^{Q_{ij}} \frac{Q^2 dQ}{\sqrt{Q^2 + 4m^2}} = \int_0^{Q'_{ij}} C_2(Q) \frac{Q^2 dQ}{\sqrt{Q^2 + 4m^2}}$$

$$C_2(Q) = 1 + \lambda \times e^{-\left(\frac{Q}{d}\right)^r}$$

And finally after evaluation of all Q'_{ij} the original momenta are really shifted.

Pythia simulations

In Pythia collisions at 1.96 TeV (Tevatron CDF) are simulated .

Correlation spectrum $N(Q)$ for π^+:

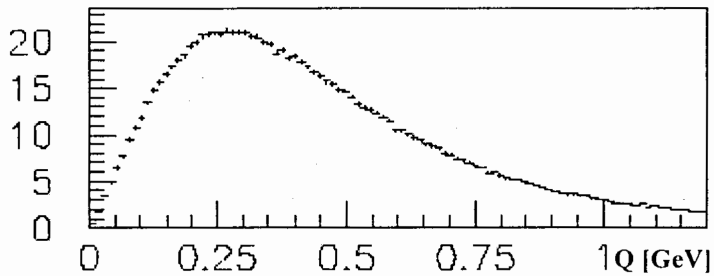

Similar spectrum for $N^{ref}(Q)$

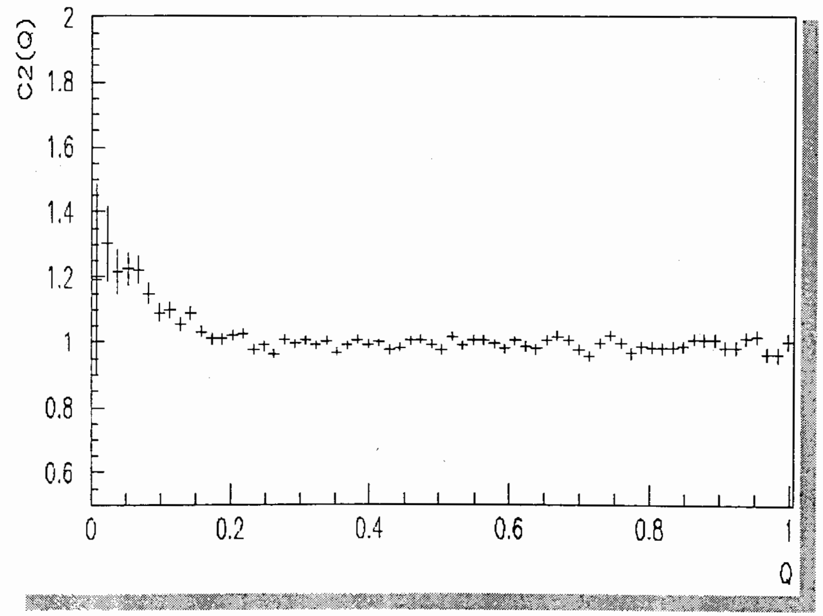

And C_2 is obtained as:

Shape of C_2 function used to fit our simulated data:

Reproduction of input parameters

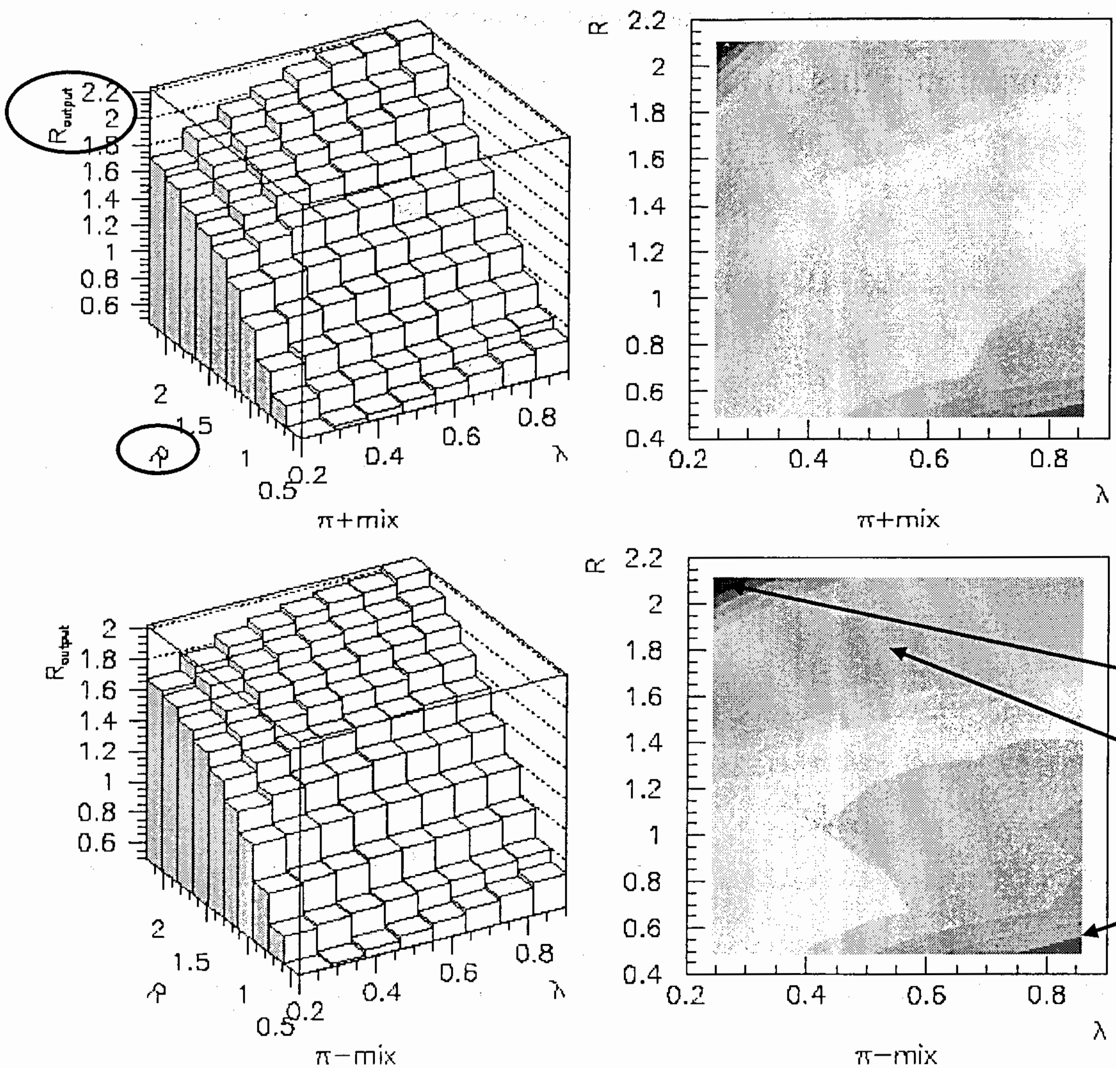

Dependence of the output parameter R on the input parameters λ and R

Used formula:

$$C_2 = N\left(1 + \lambda e^{-R^2 x^2}\right)$$

Color spectrum:

- 0.5

0 good area

+ 0.2

Reproduction of input parameters

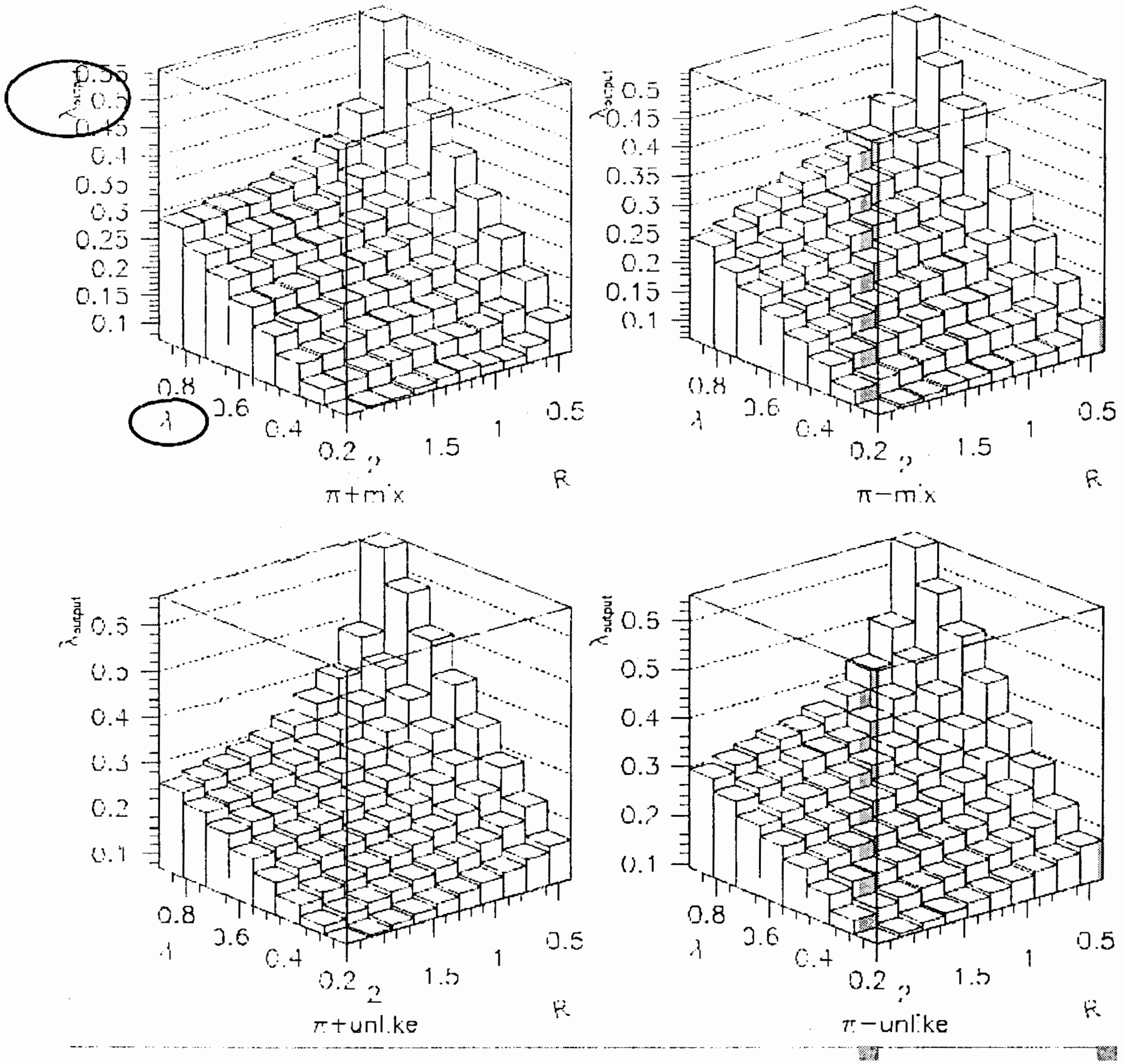

Dependence of the output parameter λ on the input parameters λ and R

Used formula:

$$C_2 = N\left(1 + \lambda e^{-R^2 x^2}\right)$$

There is no green area!

The case when correlations are not included.

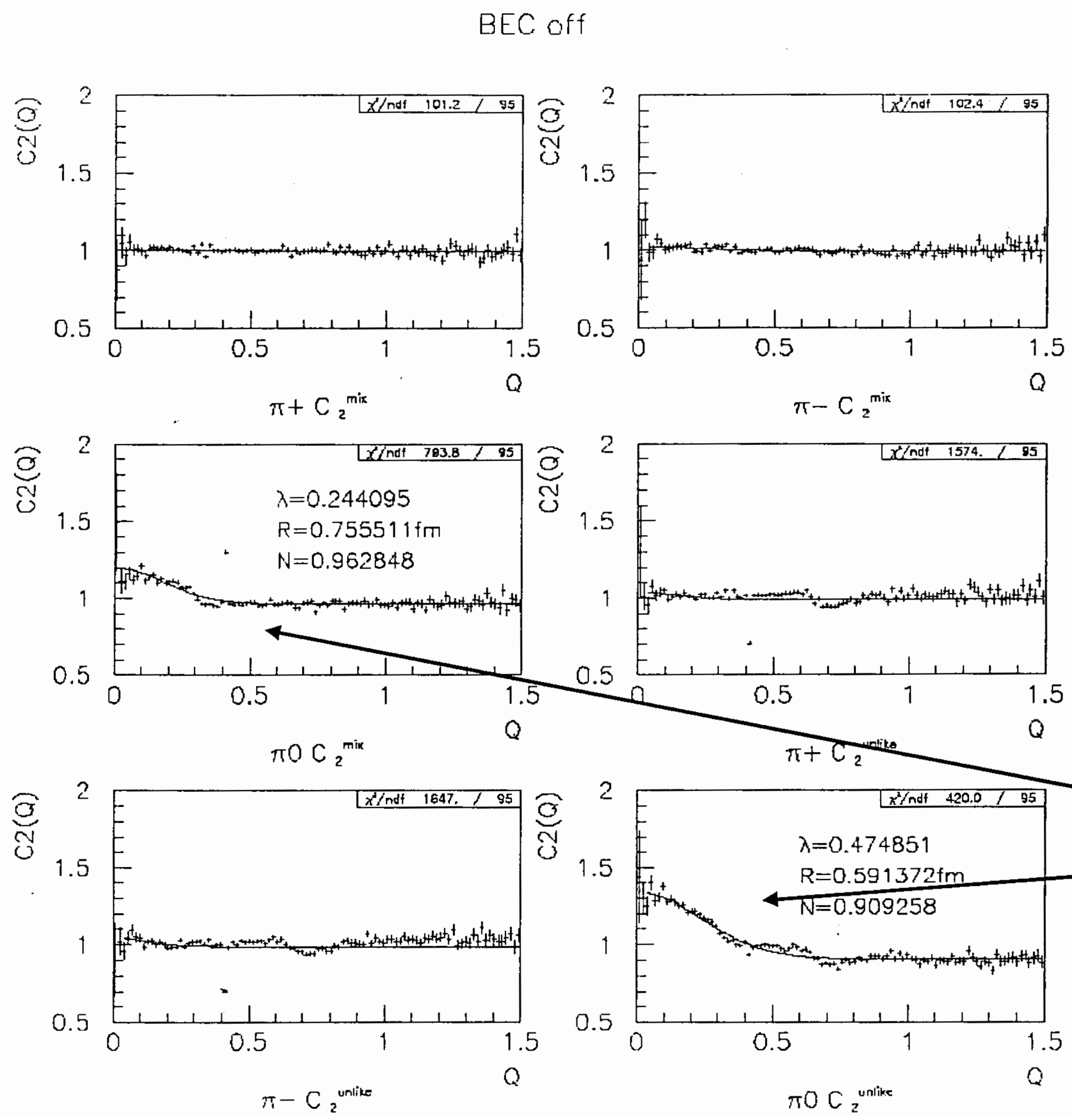

It is expected that correlations disappear when they are not included in Pythia

There is a problem with π^0

Detector CDF

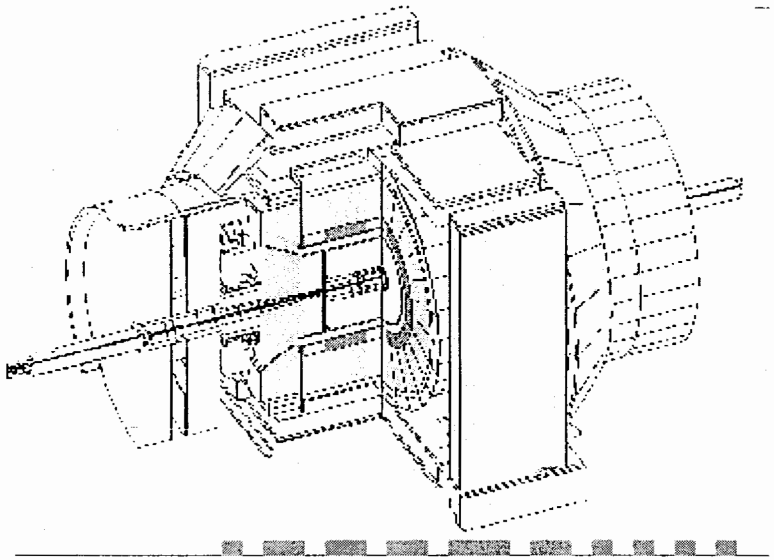

<u>Central Outer Tracker</u>

Momentum Resolution: $\frac{\delta p_t}{p_t} \approx 0.15\% p_t [GeV^{-1}]$

<u>Central Calorimeter</u> Hadron Calorimeter

Energy Resolution: $\frac{\delta E}{E} \quad 0.5/\sqrt{E}[GeV]$

But the energy is too small for some pions to reach hadron calorimeter.

To blur all momenta we used the formulas: $p'_{x,y} = p_{x,y} + r p_t^2 \frac{0.15\%}{\sqrt{2}}$, $p'_z = p_z + r p_z^2 \frac{0.15\%}{tan(\theta)}$

Then using this momenta the new energy for all pions was calculated:

Random number from Gaussian distribution

$$E_{new} = \sqrt{p_x^2 + p_y^2 + p_z^2 + m_\pi^2}$$

More realistic simulation: Momentum blurring

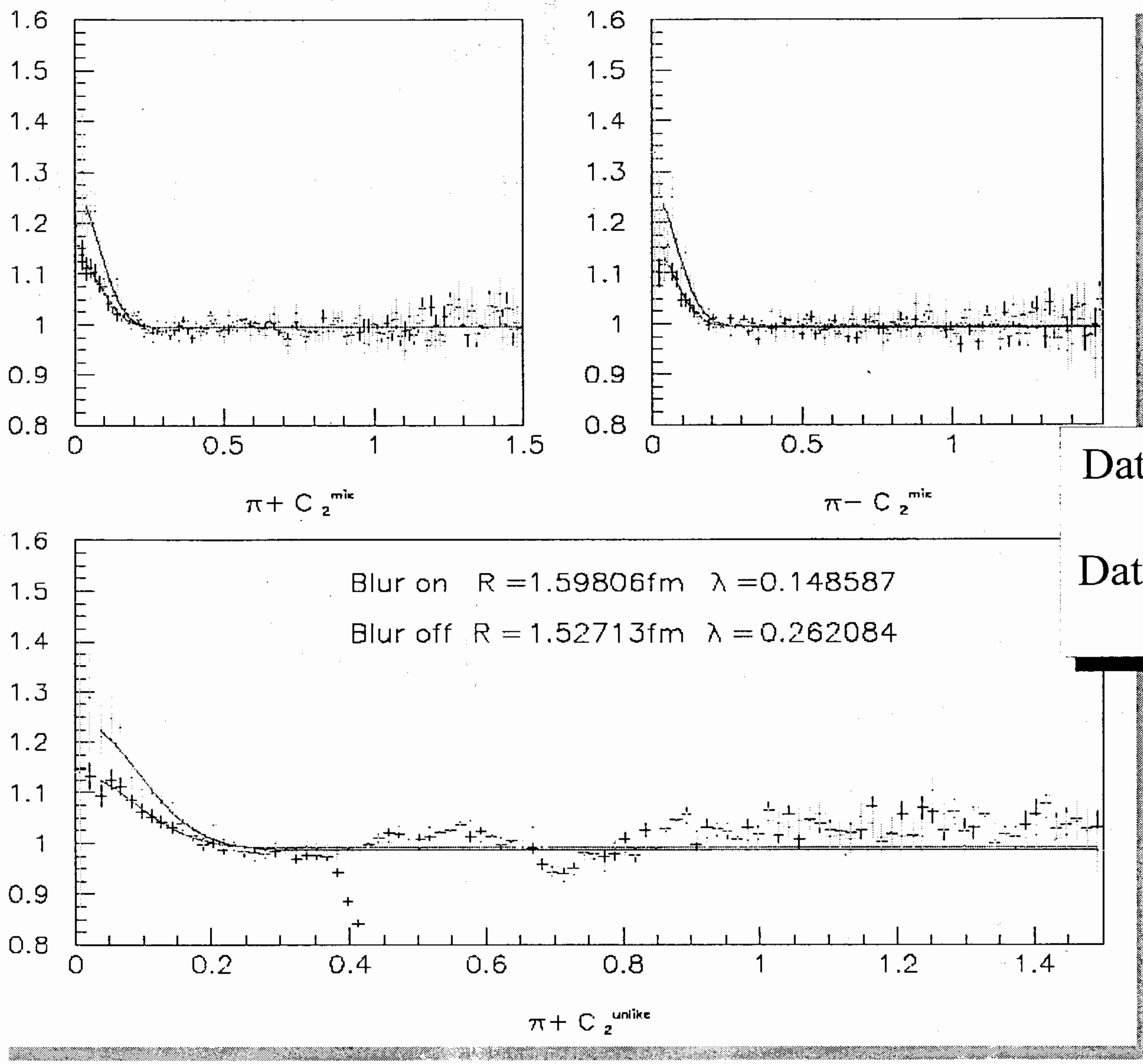

Input parameters:
R = 1.6fm
λ = 0.8

Data simulated with blurring on:
The blue ones
Data simulated with blurring off:
The green ones

The red curves are fitting lines

More realistic simulation: Energy cut

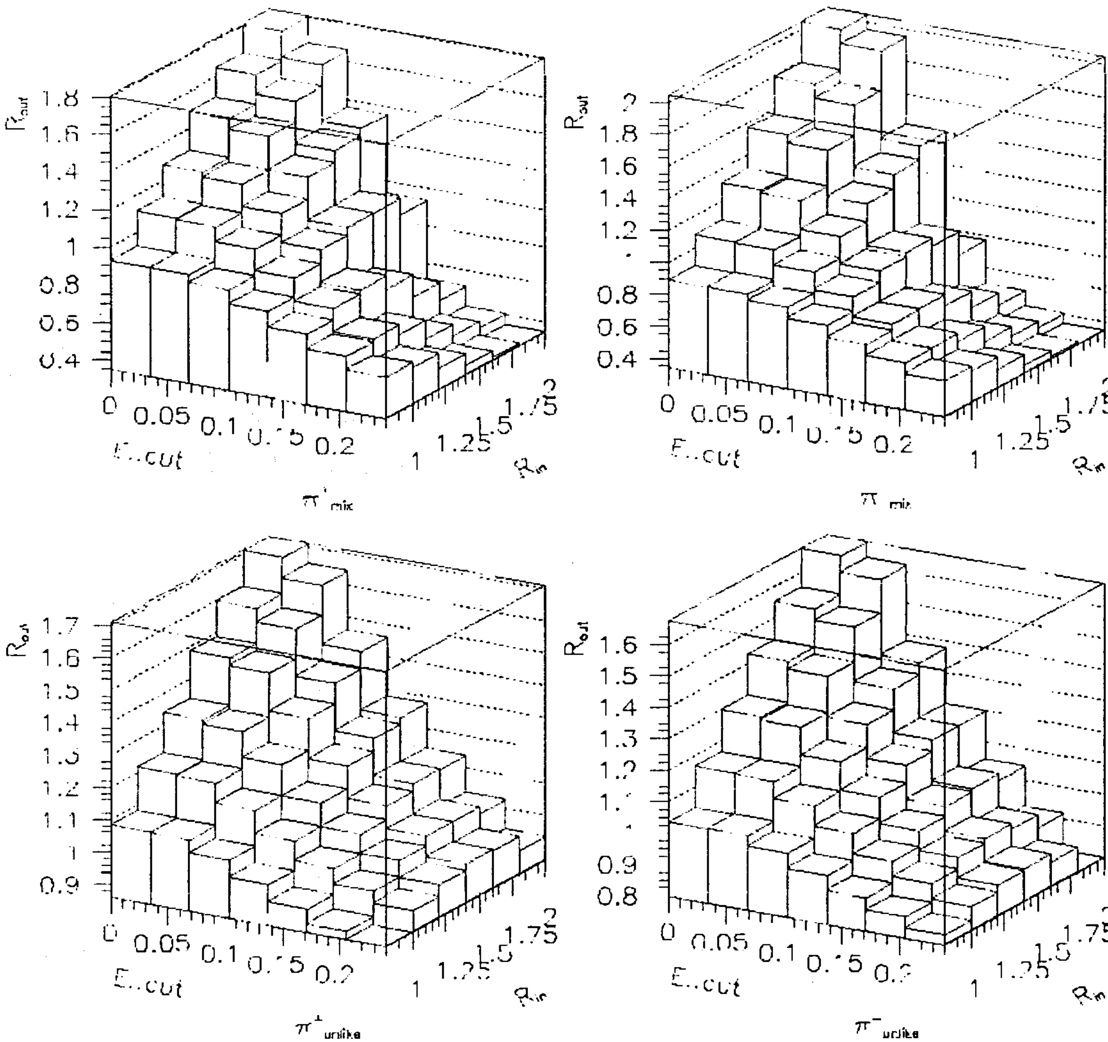

λ set to 0.8

Dependence of the output parameter R on energy cut and on the input parameter R

We can see the importance to register low energy particles

Conclusion of 1st part

- Pythia:
  - Parameter R has bounded area of good reproduction
  - Parameter λ has no area of good reproduction
  - There are non vanishing correlations for π^0 mesons.

- **It is important to register low energy particles.**

Experinent ALEPH

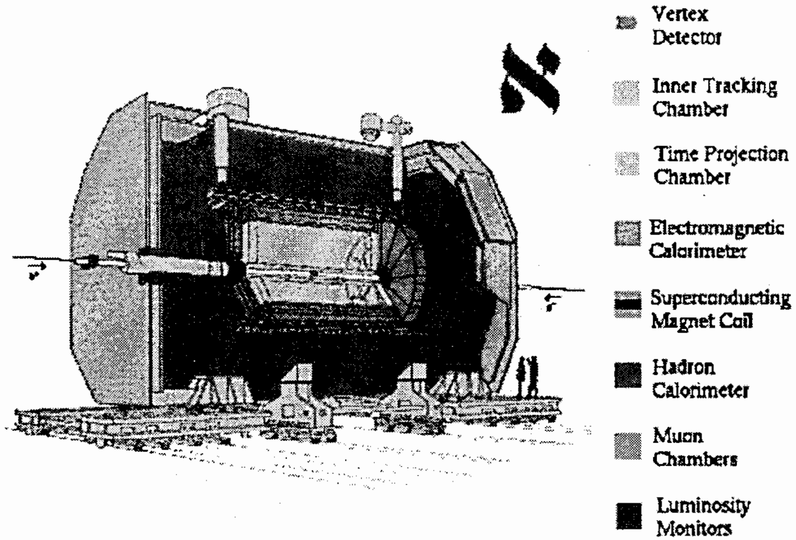

The ALEPH Detector

Standard parameterization:

$$C_2(Q) = N[1 + \lambda \exp(-(RQ)^2)](1 + \varepsilon Q + ...)$$

- λ coherence strength factor.
- R is related to the size of the boson emission region.

$$R_2(Q) = \frac{\rho_2(p_1, p_2)}{\rho_0(p_1, p_2)}$$ **- Two-particle correlation function**

$\rho_2(p_1, p_2)$ **- Two-particle density distribution**

Detector inadequacies, effects introduced by the reference sample are obtained from MC without BEC: $R_2^{\mathrm{MC}} = N_{\pm\pm}^{\mathrm{MC}} / N_{\mathrm{ref}}^{\mathrm{MC}}$

The measured correlation function is given by:

More informations in:
Eur. Phys. J. C36: 2004, 147

ALEPH fit

C_2 function for ALEPH data and different reference samples fitted with $C_2(Q) = N\left(1+\lambda e^{-(QR)^2}\right)[1+\varepsilon Q]$

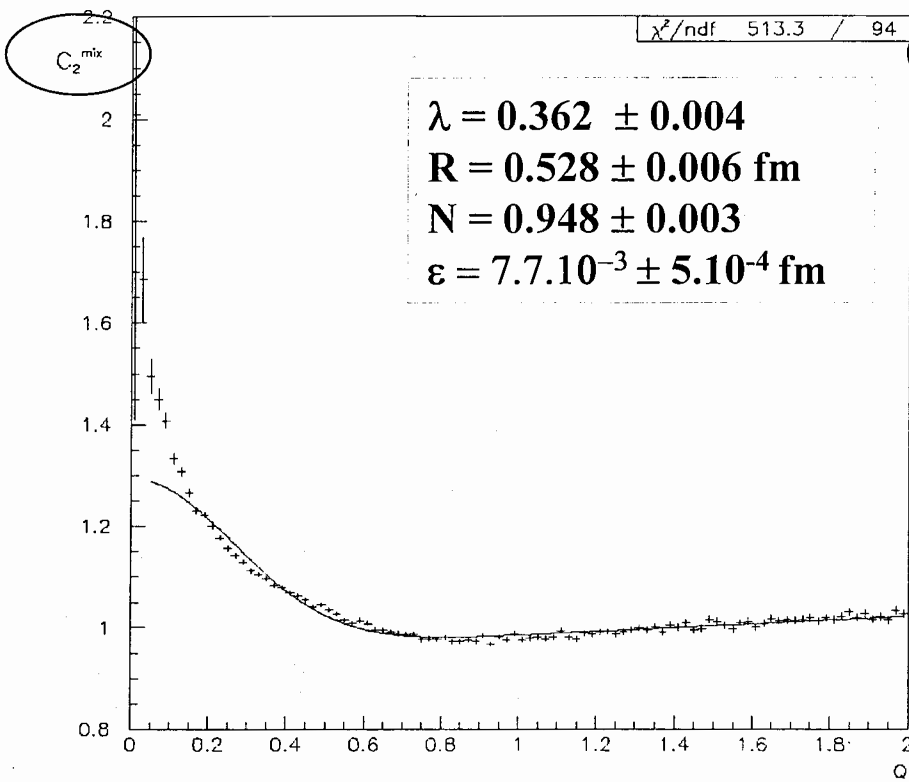

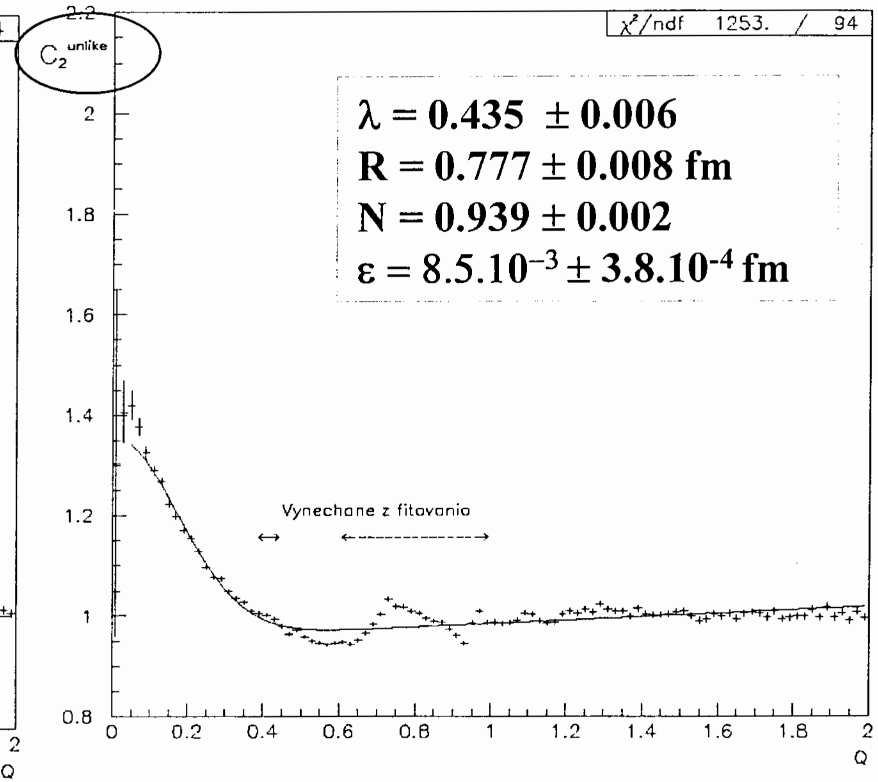

We reproduce their results.

Kozlov fit

The same C_2 functions versus Kozlov theory

QFT based, Langevin evolution equation used.
Ref: arXiv:hep-ph/0304091 v3

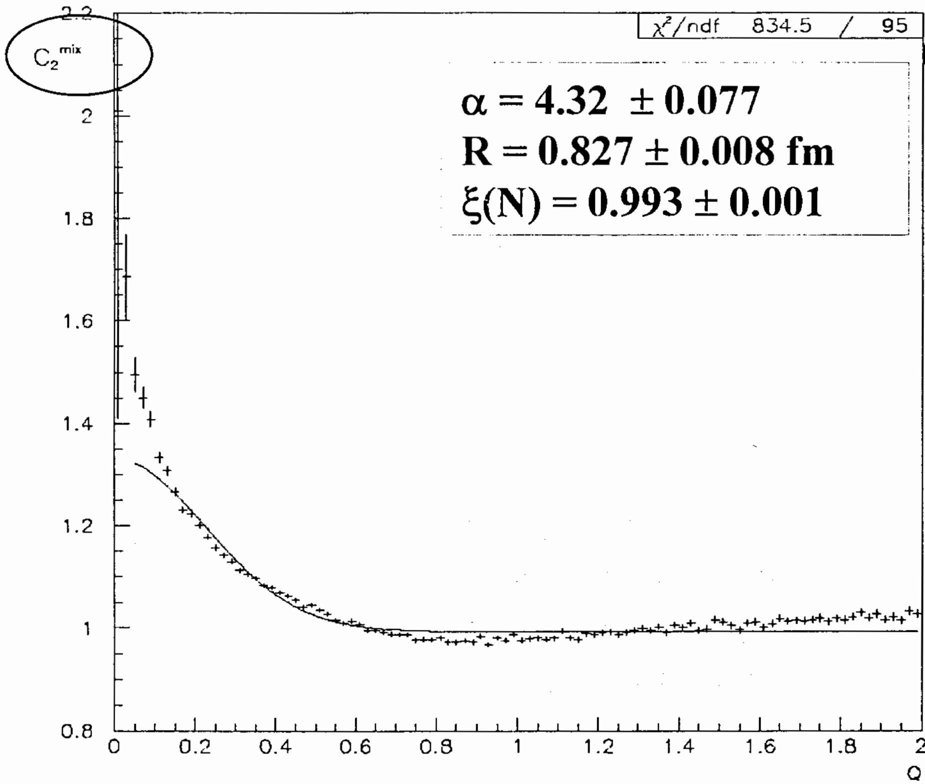

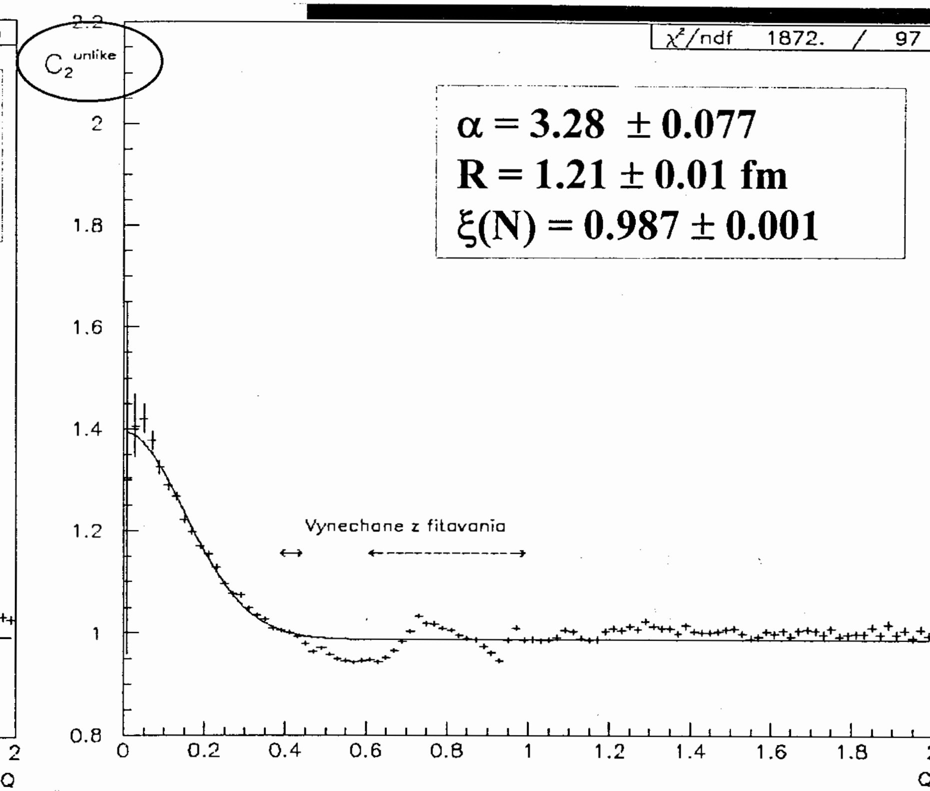

The function used to fit ALEPH data:

$$C_2(Q) = \xi(N)\left(1 + \frac{2\alpha}{(1+\alpha)^2} e^{-\frac{(QR)^2}{2}} + \frac{1}{(1+\alpha)^2} e^{-(QR)^2}\right)$$

Modified Kozlov fit

The same C_2 function versus modified Kozlov C_2 function.

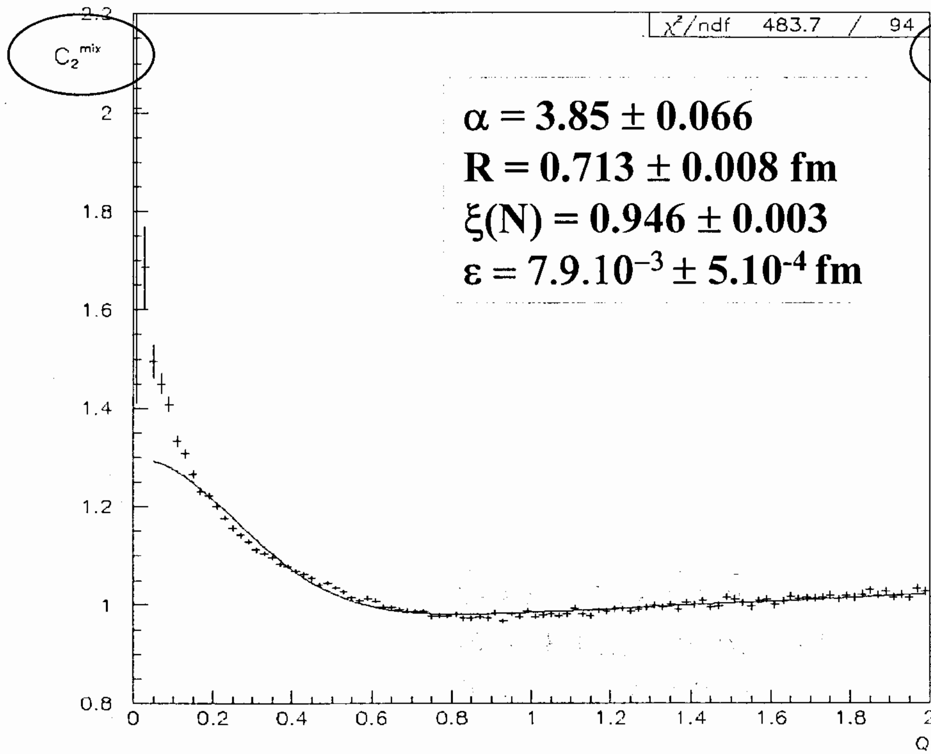

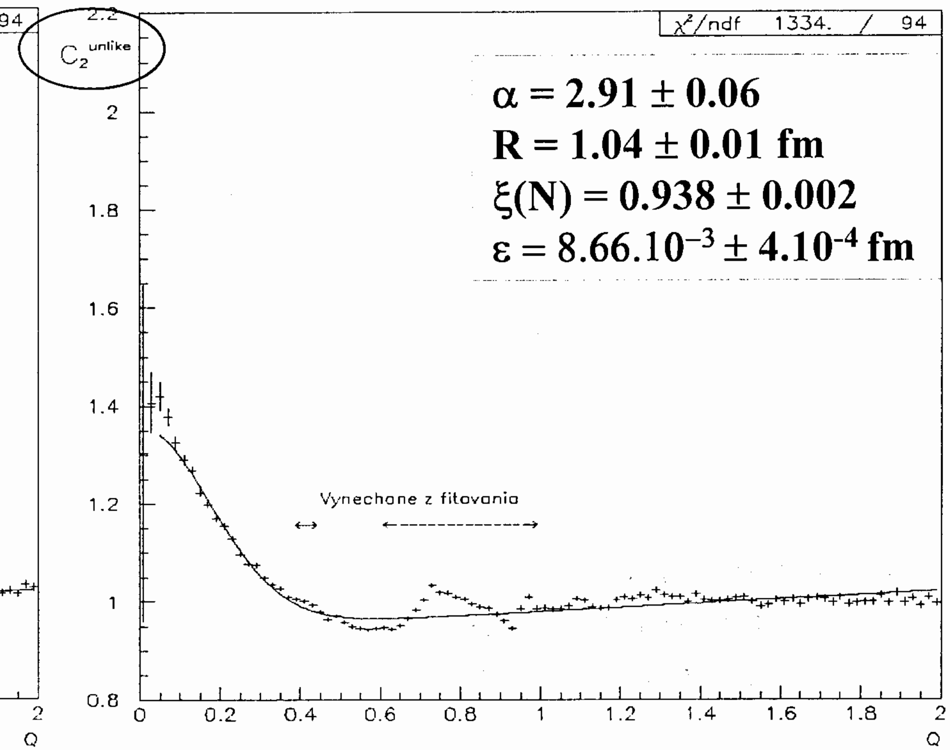

Modified function of Kozlov approach:

$$C_2(Q) = \xi(N)\left(1 + \frac{2\alpha}{(1+\alpha)^2} e^{-\frac{(QR)^2}{2}} + \frac{1}{(1+\alpha)^2} e^{-(QR)^2}\right)(1 + \varepsilon Q)$$

Summary table of our results:

	Aleph C_2			Kozlov C_2	
	$C_2^{mix}(Q)$	$C_2^{+-}(Q)$		$C_2^{mix}(Q)$	$C_2^{+-}(Q)$
N	**0.948**	**0.939**	$\xi(N)$	**0.946**	**0.938**
λ	**0.362**	**0.435**	α	**3.848**	**2.918**
R (fm)	**0.5287**	**0.7777**	R (fm)	**0.713**	**1.043**
ε (fm)	**0.769e-2**	**0.852e-2**	ε (fm)	**0.793e-2**	**0.867e-2**
χ^2 / ndf	**513 / 94**	**1253 / 94**	χ^2 / ndf	**483.7 / 94**	**1334 / 94**

Conclusions of 2nd part.

- Correlation analysis of ALEPH data was done in frame of Kozlov model
- To explain the increase of $C_2(Q)$, modification factor $(1+\varepsilon Q)$ should be edit to the theoretical C_2 function
- This factor can be explained by the presence of the non equilibrium processes (?) – In Kozlov approach stationary (equilibrium) state is assumed.

УДК 539.126.4; 539.17.015

STRANGENESS CONSERVATION AND PAIR CORRELATIONS OF NEUTRAL KAONS WITH CLOSE MOMENTA PRODUCED IN INCLUSIVE MULTIPARTICLE PROCESSES

V.L. Lyuboshitz [1] and V.V. Lyuboshitz [2]

Joint Institute for Nuclear Research,
141980, Dubna, Moscow Region, Russia

E-mail: [1] *lyubosh@sunhe.jinr.ru* [2] *Valery.Lyuboshitz@jinr.ru*

Abstract

The phenomenological structure of inclusive cross-sections of the production of two neutral K-mesons in collisions of hadrons and nuclei is investigated taking into account the strangeness conservation in strong and electromagnetic interactions. The relations describing the dependence of the correlations of two short-lived and two long-lived neutral kaons $K^0_S K^0_S$, $K^0_L K^0_L$ and the correlations of "mixed" pairs $K^0_S K^0_L$ at small relative momenta upon the space-time parameters of the generation region of K^0 and $\bar{K}^0$- mesons, which involve the contributions of Bose-statistics and S-wave strong final-state interaction, have been obtained. It is shown that under the strangeness conservation the correlation functions of the pairs $K^0_S K^0_S$ and $K^0_L K^0_L$, produced in the same inclusive process, coincide, and the difference between the correlation functions of the pairs $K^0_S K^0_S$ and $K^0_S K^0_L$ is conditioned by the production of the pairs of non-identical neutral kaons $K^0 \bar{K}^0$.

1 Consequences of the strangeness conservation

In the work [1] the properties of the density matrix of two neutral K-mesons, following from the strangeness conservation in strong and electromagnetic interactions, have been investigated. By definition, the diagonal elements of the non-normalized two-particle density matrix coincide with the two-particle structure functions, which are proportional to the double inclusive cross-sections.

Strangeness is the additive quantum number. Taking into account the strangeness conservation, the pairs of neutral kaons K^0K^0 (strangeness $S=+2$), $\bar{K}^0\bar{K}^0$ (strangeness $S=-2$) and $K^0\bar{K}^0$ (strangeness $S=0$) are produced incoherently. This means that in the K^0-$\bar{K}^0$- representation the non-diagonal elements of the density matrix between the states K^0K^0 and $\bar{K}^0\bar{K}^0$, K^0K^0 and $K^0\bar{K}^0$, $\bar{K}^0\bar{K}^0$ and $K^0\bar{K}^0$ are equal to zero. However, the non-diagonal elements of the two-kaon density matrix between the two states $|K^0\rangle^{(\mathbf{p}_1)}|\bar{K}^0\rangle^{(\mathbf{p}_2)}$ and $|\bar{K}^0\rangle^{(\mathbf{p}_1)}|K^0\rangle^{(\mathbf{p}_2)}$ with the zero strangeness are not equal to zero, in general. Here $\mathbf{p}_1$ and $\mathbf{p}_2$ are the momenta of the first and second kaons.

The internal states of K^0 -meson ($S=1$) and $\bar{K}^0$ -meson ($S=-1$) are the superpositions of the states $|K^0_S\rangle$ and $|K^0_L\rangle$, where K^0_S is the short-lived neutral kaon and K^0_L is the long-lived one. Neglecting the small effect of CP non-invariance, the CP-parity of the state K^0_S is equal to $(+1)$, and the CP-parity of the state K^0_L is equal to (-1); in doing so,

$$|K^0\rangle = \frac{1}{\sqrt{2}}(|K_S^0\rangle + |K_L^0\rangle), \quad |\bar{K}^0\rangle = \frac{1}{\sqrt{2}}(|K_S^0\rangle - |K_L^0\rangle).$$

It is clear that both the quasistationary states of the neutral kaon have no definite strangeness.

It is easy to show that

$$|K^0\rangle^{(\mathbf{p}_1)} \otimes |K^0\rangle^{(\mathbf{p}_2)} = \frac{1}{2}(|K_S^0\rangle^{(\mathbf{p}_1)} \otimes |K_S^0\rangle^{(\mathbf{p}_2)} + |K_L^0\rangle^{(\mathbf{p}_1)} \otimes |K_L^0\rangle^{(\mathbf{p}_2)} +$$

$$+|K_S^0\rangle^{(\mathbf{p}_1)} \otimes |K_L^0\rangle^{(\mathbf{p}_2)} + |K_L^0\rangle^{(\mathbf{p}_1)} \otimes |K_S^0\rangle^{(\mathbf{p}_2)}), \tag{1}$$

$$|\bar{K}^0\rangle^{(\mathbf{p}_1)} \otimes |\bar{K}^0\rangle^{(\mathbf{p}_2)} = \frac{1}{2}(|K_S^0\rangle^{(\mathbf{p}_1)} \otimes |K_S^0\rangle^{(\mathbf{p}_2)} + |K_L^0\rangle^{(\mathbf{p}_1)} \otimes |K_L^0\rangle^{(\mathbf{p}_2)} -$$

$$-|K_S^0\rangle^{(\mathbf{p}_1)} \otimes |K_L^0\rangle^{(\mathbf{p}_2)} - |K_L^0\rangle^{(\mathbf{p}_1)} \otimes |K_S^0\rangle^{(\mathbf{p}_2)}). \tag{2}$$

It follows from the Bose-symmetry of the wave function of two neutral kaons with respect to the total permutation of internal states and momenta that the CP-parity of the system $K^0\bar{K}^0$ is always positive [2] (the C-parity is $(-1)^L$, the space parity is $P = (-1)^L$, where L is the orbital momentum).

The system of two non-identical neutral kaons $K^0\bar{K}^0$ in the symmetric internal state, corresponding to even orbital momenta, is decomposed into the schemes $|K_S^0\rangle|K_S^0\rangle$ and $|K_L^0\rangle|K_L^0\rangle$ [2]:

$$|\psi^+\rangle = \frac{1}{\sqrt{2}}(|K^0\rangle^{(\mathbf{p}_1)} \otimes |\bar{K}^0\rangle^{(\mathbf{p}_2)} + |\bar{K}^0\rangle^{(\mathbf{p}_1)} \otimes |K^0\rangle^{(\mathbf{p}_2)}) =$$

$$= \frac{1}{\sqrt{2}}(|K_S^0\rangle^{(\mathbf{p}_1)} \otimes |K_S^0\rangle^{(\mathbf{p}_2)} - |K_L^0\rangle^{(\mathbf{p}_1)} \otimes |K_L^0\rangle^{(\mathbf{p}_2)}); \tag{3}$$

meantime, the system $K^0\bar{K}^0$ in the antisymmetric internal state, corresponding to odd orbital momenta, is decomposed into the scheme $|K_S^0\rangle|K_L^0\rangle$ [2]:

$$|\psi^-\rangle = \frac{1}{\sqrt{2}}(|K^0\rangle^{(\mathbf{p}_1)} \otimes |\bar{K}^0\rangle^{(\mathbf{p}_2)} - |\bar{K}^0\rangle^{(\mathbf{p}_1)} \otimes |K^0\rangle^{(\mathbf{p}_2)}) =$$

$$= \frac{1}{\sqrt{2}}(|K_S^0\rangle^{(\mathbf{p}_1)} \otimes |K_L^0\rangle^{(\mathbf{p}_2)} - |K_L^0\rangle^{(\mathbf{p}_1)} \otimes |K_S^0\rangle^{(\mathbf{p}_2)}). \tag{4}$$

The strangeness conservation leads to the fact that all the double inclusive cross-sections of production of pairs $K_S^0K_S^0$, $K_L^0K_L^0$ and $K_S^0K_L^0$ (two-particle structure functions) prove to be symmetric with respect to the permutation of momenta $\mathbf{p}_1$ and $\mathbf{p}_2$:

$$f_{SS}(\mathbf{p}_1, \mathbf{p}_2) = f_{SS}(\mathbf{p}_2, \mathbf{p}_1); \quad f_{LL}(\mathbf{p}_1, \mathbf{p}_2) = f_{LL}(\mathbf{p}_2, \mathbf{p}_1);$$

$$f_{SL}(\mathbf{p}_1, \mathbf{p}_2) = f_{SL}(\mathbf{p}_2, \mathbf{p}_1). \tag{5}$$

Besides, due to the strangeness conservation, the structure functions of neutral K-mesons produced in inclusive processes are invariant with respect to the replacement of the short-lived state K_S^0 by the long-lived state K_L^0, and *vice versa* [1]:

$$f_{SS}(\mathbf{p}_1, \mathbf{p}_2) = f_{LL}(\mathbf{p}_1, \mathbf{p}_2) = \frac{1}{4}[f_{K^0K^0}(\mathbf{p}_1, \mathbf{p}_2) + f_{\bar{K}^0\bar{K}^0}(\mathbf{p}_1, \mathbf{p}_2) +$$

$$+f_{K^0\bar{K}^0}(\mathbf{p}_1,\mathbf{p}_2)+f_{\bar{K}^0K^0}(\mathbf{p}_1,\mathbf{p}_2)]+\frac{1}{2}\,\mathrm{Re}\,\rho_{K^0\bar{K}^0\to\bar{K}^0K^0}(\mathbf{p}_1,\mathbf{p}_2), \quad (6)$$

$$f_{SL}(\mathbf{p}_1,\mathbf{p}_2)=f_{LS}(\mathbf{p}_1,\mathbf{p}_2)=\frac{1}{4}\,[f_{K^0K^0}(\mathbf{p}_1,\mathbf{p}_2)+f_{\bar{K}^0\bar{K}^0}(\mathbf{p}_1,\mathbf{p}_2)+$$

$$+f_{K^0\bar{K}^0}(\mathbf{p}_1,\mathbf{p}_2)+f_{\bar{K}^0K^0}(\mathbf{p}_1,\mathbf{p}_2)]-\frac{1}{2}\,\mathrm{Re}\,\rho_{K^0\bar{K}^0\to\bar{K}^0K^0}(\mathbf{p}_1,\mathbf{p}_2), \quad (7)$$

where $\rho_{K^0\bar{K}^0\to\bar{K}^0K^0}(\mathbf{p}_1,\mathbf{p}_2)=(\rho_{\bar{K}^0K^0\to K^0\bar{K}^0}(\mathbf{p}_1,\mathbf{p}_2))^*$ are the non-diagonal elements of the two-kaon density matrix. The difference between the two-particle structure functions f_{SS} and f_{SL} is connected just with the contribution of these non-diagonal elements.

It is evident that the one-particle structure functions for the production of K_S^0 and K_L^0 are equal to each other. After integrating the relations (6) over the momentum distribution of neutral kaons one can obtain the mutual equality of the average multiplicities of the K_S^0 and K_L^0-states, as well as the mutual equality of the average squares of multiplicities:

$$\langle n_S\rangle=\langle n_L\rangle, \qquad \langle n_S^2\rangle=\langle n_L^2\rangle. \quad (8)$$

2 Structure of pair correlations of identical and non-identical neutral kaons with close momenta

Now let us consider the correlations of pairs of neutral K-mesons with close momenta within the model of one-particle sources [2-7]. In the case of the identical states $K_S^0K_S^0$ and $K_L^0K_L^0$ we obtain the following expressions for the correlation functions R_{SS}, R_{LL} (proportional to the structure functions), normalized to unity at large relative momenta:

$$R_{SS}(\mathbf{k})=R_{LL}(\mathbf{k})=\lambda_{K^0K^0}\,[1+F_{K^0}(2\mathbf{k})+2\,b_{\mathrm{int}}(\mathbf{k})]+$$

$$+\lambda_{\bar{K}^0\bar{K}^0}\left[1+F_{\bar{K}^0}(2\mathbf{k})+2\,\tilde{b}_{\mathrm{int}}(\mathbf{k})\right]+$$

$$+\lambda_{K^0\bar{K}^0}\,[1+F_{K^0\bar{K}^0}(2\mathbf{k})+2\,B_{\mathrm{int}}(\mathbf{k})]\,. \quad (9)$$

Here $\mathbf{k}$ is the momentum of one of the kaons in the c.m. frame of the pair, and the quantities $\lambda_{K^0K^0}$, $\lambda_{\bar{K}^0\bar{K}^0}$ and $\lambda_{K^0\bar{K}^0}$ are the relative fractions of the average numbers of produced pairs K^0K^0, $\bar{K}^0\bar{K}^0$ and $K^0\bar{K}^0$, respectively ($\lambda_{K^0K^0}+\lambda_{\bar{K}^0\bar{K}^0}+\lambda_{K^0\bar{K}^0}=1$) . The "formfactors" $F_{K^0}(2\mathbf{k})$, $F_{\bar{K}^0}(2\mathbf{k})$ and $F_{K^0\bar{K}^0}(2\mathbf{k})$ appear due to the contribution of Bose-statistics:

$$F_{K^0}(2\mathbf{k})=\int W_{K^0}(\mathbf{r})\,\cos(2\mathbf{kr})\,d^3\mathbf{r}, \qquad F_{\bar{K}^0}(2\mathbf{k})=\int W_{\bar{K}^0}(\mathbf{r})\,\cos(2\mathbf{kr})\,d^3\mathbf{r},$$

$$F_{K^0\bar{K}^0}(2\mathbf{k})=\int W_{K^0\bar{K}^0}(\mathbf{r})\,\cos(2\mathbf{kr})\,d^3\mathbf{r}. \quad (10)$$

where $W_{K^0}(\mathbf{r})$, $W_{\bar{K}^0}(\mathbf{r})$ and $W_{K^0\bar{K}^0}(\mathbf{r})$ are the probability distributions of distances between the sources of emission of two K^0-mesons, between the sources of emission of two $\bar{K}^0$-mesons and between the sources of emission of the K^0-meson and $\bar{K}^0$-meson, respectively, in the c.m. frame of the kaon pair. Meantime, the quantity $b_{\mathrm{int}}(\mathbf{k})$ describes the contribution of the S-wave interaction of two K^0-mesons, the quantity $\tilde{b}_{\mathrm{int}}(\mathbf{k})$ describes the contribution of the S-wave interaction of two $\bar{K}^0$-mesons and the quantity $B_{\mathrm{int}}(\mathbf{k})$

describes the contribution of the S-wave interaction of the K^0-meson with the $\bar{K}^0$-meson. Due to the CP-invariance, the quantities $b_{\text{int}}(\mathbf{k})$ and $\tilde{b}_{\text{int}}(\mathbf{k})$ can be expressed by means of averaging the same function $b(\mathbf{k},\mathbf{r})$ over the different distributions:

$$b_{\text{int}}(\mathbf{k}) = \int W_{K^0}(\mathbf{r}) b(\mathbf{k},\mathbf{r}) d^3\mathbf{r}, \quad \tilde{b}_{\text{int}}(\mathbf{k}) = \int W_{\bar{K}^0}(\mathbf{r}) b(\mathbf{k},\mathbf{r}) d^3\mathbf{r}.$$

The quantity $B_{\text{int}}(\mathbf{k})$ has the structure

$$B_{\text{int}}(\mathbf{k}) = \int W_{K^0\bar{K}^0}(\mathbf{r}) B(\mathbf{k},\mathbf{r}) d^3\mathbf{r},$$

where $B(\mathbf{k},\mathbf{r}) \neq b(\mathbf{k},\mathbf{r})$.

Let us emphasize that when the pair of non-identical neutral kaons $K^0\bar{K}^0$ is produced but the pair of identical quasistationary states $K_S^0K_S^0$ (or $K_L^0K_L^0$) is registered over decays, the two-particle correlations at small relative momenta have the same character as in the case of usual identical bosons with zero spin [2].

For the pairs of non-identical kaon states $K_S^0K_L^0$ the correlation functions at small relative momenta have the form:

$$\begin{aligned} R_{SL}(\mathbf{k}) = R_{LS}(\mathbf{k}) &= \lambda_{K^0K^0}\left[1 + F_{K^0}(2\mathbf{k}) + 2\,b_{\text{int}}(\mathbf{k})\right] + \\ &+ \lambda_{\bar{K}^0\bar{K}^0}\left[1 + F_{\bar{K}^0}(2\mathbf{k}) + 2\,\tilde{b}_{\text{int}}(\mathbf{k})\right] + \\ &+ \lambda_{K^0\bar{K}^0}\left[1 - F_{K^0\bar{K}^0}(2\mathbf{k})\right]. \end{aligned} \tag{11}$$

In accordance with Eq.(11), at the production of the pair of non-identical neutral kaons $K^0\bar{K}^0$ and the registration of the two-particle state $K_S^0K_L^0$ over decays the pair correlations are analogous to the correlations of two identical fermions with the same spin projections. This is connected with the fact that in the considered case the pair $K_S^0K_L^0$ has odd orbital momenta [2].

It follows from Eqs.(9) and (11) that the correlation functions of pairs of neutral K-mesons with close momenta, which are created in inclusive processes, satisfy the relation

$$\begin{aligned} R_{SS}(\mathbf{k}) + R_{LL}(\mathbf{k}) - R_{SL}(\mathbf{k}) - R_{LS}(\mathbf{k}) &= 2\left[R_{SS}(\mathbf{k}) - R_{SL}(\mathbf{k})\right] = \\ &= 4\lambda_{K^0\bar{K}^0}\left[F_{K^0\bar{K}^0}(2\mathbf{k}) + B_{\text{int}}(\mathbf{k})\right]. \end{aligned} \tag{12}$$

We see that the difference between the correlation functions of the pairs of identical neutral kaons $K_S^0K_S^0$ and pairs of non-identical neutral kaons $K_S^0K_L^0$ is conditioned exclusively by the generation of $K^0\bar{K}^0$-pairs.

The relations connecting the contribution of the S-wave strong interaction into the pair correlations of particles at small relative momenta with the parameters of low-energy scattering were obtained earlier in the papers [4-7]. It is essential that the "formfactors" (10) and the functions $b_{\text{int}}(\mathbf{k})$, $\tilde{b}_{\text{int}}(\mathbf{k})$ and $B_{\text{int}}(\mathbf{k})$ depend on the space-time parameters of the generation region of neutral kaons and tend to zero at high values of the relative momentum $q = 2|\mathbf{k}|$ of two neutral kaons. [1)]

[1)] Let us note that, in principle, the P-wave resonance (ϕ-meson, $M = 1021$ MeV/c^2, $\Gamma = 4$ MeV) may influence the $K_S^0K_L^0$ - correlations. But this influence manifests itself only in the narrow region of comparatively large relative momenta $2k \approx 220$ MeV/c, and it is strongly suppressed at small relative momenta which are discussed here.

3 Contribution of the S-wave $K^0\bar{K}^0$ -interaction

The function $B(\mathbf{k},\mathbf{r})$, describing the contribution of the final-state interaction between K^0 and $\bar{K}^0$ mesons into the $K_S^0K_S^0$- correlations and into the difference of the correlation functions $(R_{SS}(\mathbf{k}) - R_{SL}(\mathbf{k}))$, may be calculated analytically using the approximation of the superposition of the plane and spherical waves, if characteristic distances r_0 between sources of K^0- and $\bar{K}^0$-mesons are: $r_0 \gg d_0$, where d_0 is the radius of action of short-range forces between the K^0-meson and $\bar{K}^0$- meson (really, already at $r_0 > d_0$) [4]. In so doing

$$B(\mathbf{k},\mathbf{r}) = |A_{K^0\bar{K}^0}(k)|^2\frac{1}{r^2} + 2\,\mathrm{Re}\left(A_{K_0\bar{K}_0}(k)\frac{\exp(ikr)\cos\mathbf{kr}}{r}\right), \tag{13}$$

where $A_{K^0\bar{K}^0}(k) \equiv A_{K^0\bar{K}^0\to K^0\bar{K}^0}(k)$ is the amplitude of the S-wave $K^0\bar{K}^0$-scattering, $k = |\mathbf{k}|$, $r = |\mathbf{r}|$.

Now let us take into account the effect of the possible transition $K^+K^- \to K^0\bar{K}^0$ between the pairs of oppositely charged and neutral kaons on the pair correlations of two identical kaons with small relative momenta. We can use here the theory of the S-wave multichannel scattering [7]. Assuming that pairs K^+K^- and $K^0\bar{K}^0$ are emitted with equal probabilities by the same pairs of isotopically unpolarized sources, the function $B(\mathbf{k},\mathbf{r})$ should be replaced by $\widetilde{B}(\mathbf{k},\mathbf{r}) = B(\mathbf{k},\mathbf{r}) + \Delta B(\mathbf{k},\mathbf{r})$, where [7]

$$\Delta B(\mathbf{k},\mathbf{r}) = \left|A^{(c)}_{K^+K^-\to K^0\bar{K}^0}(k)\right|^2 \frac{\cos^2\widetilde{k}r + C(\widetilde{k}a_c)\sin^2\widetilde{k}r}{r^2}. \tag{14}$$

Here $\widetilde{k} = \sqrt{k^2 + 2M_K\Delta M_K}$ and k are the moduli of the momentum of each of the charged kaons and of each of the neutral kaons, respectively, in the c.m. frame of the pair $K^0\bar{K}^0$,
$M_K = (M_{K^0} + M_{K^+})/2 \approx 495.6$ MeV/c^2,
$\Delta M_K = M_{K^0} - M_{K^+} \approx 4$ MeV/c^2,
$a_c = 2\hbar^2/(M_{K^+}e^2) \approx 108.5$ Fm is the Bohr radius of the K^+K^--system,

$$C(\widetilde{k}a_c) = \frac{2\pi/\widetilde{k}a_c}{1-\exp(-2\pi/\widetilde{k}a_c)}$$

is the Coulomb factor corresponding to the attraction of the oppositely charged kaons, $A^{(c)}_{K^+K^-\to K^0\bar{K}^0}(k)$ is the effective amplitude of the reaction $K^+K^- \to K^0\bar{K}^0$, renormalized by the Coulomb interaction. [2)]

At $k = 0$ the modulus of the momentum of the K^+ (K^-)-meson in the c.m. frame of the pair $K^0\bar{K}^0$ is equal to $\widetilde{k}_0 = \sqrt{2M_K\Delta M_K} \approx 62.8$ MeV/c. As a result, the Coulomb factor incorporated in Eq.(14) is close to unity:

$$1 < C(\widetilde{k}a_c) \leq C(\widetilde{k}_0a_c) \approx 1.0934.$$

[2)] The S-wave amplitude, determining directly the effective cross-section of the process $K^+K^- \to K^0\bar{K}^0$ according to the standard formula

$$\sigma_{K^+K^-\to K^0\bar{K}^0}(k) = 4\pi\,|A_{K^+K^-\to K^0\bar{K}^0}(k)|^2\,\frac{k}{\widetilde{k}},$$

is $A_{K^+K^-\to K^0\bar{K}^0}(k) = \sqrt{C(\widetilde{k}a_c)}A^{(c)}_{K^+K^-\to K^0\bar{K}^0}(k)$.

Thus, with the precision of the order of 10% we obtain

$$\Delta B(\mathbf{k},\mathbf{r}) = \left|A^{(c)}_{K^+K^-\to K^0\bar{K}^0}(k)\right|^2 \frac{1}{r^2}\,. \tag{15}$$

It is known that the amplitudes $A_{K^0\bar{K}^0\to K^0\bar{K}^0}(k)$ and $A_{K^+K^-\to K^0\bar{K}^0}(k)$ are determined by the contribution of the sub-threshold S-wave resonances $f_0(980)$ (isotopic spin $T=0$) and $a_0(980)$ (isotopic spin $T=1$) [4,7]:

$$A_{K^0\bar{K}^0\to K^0\bar{K}^0}(k) = \frac{1}{2}\,[A^{(T=0)}(k) + A^{(T=1)}(k)],$$

$$A_{K^+K^-\to K^0\bar{K}^0}(k) = \frac{1}{2}\,[A^{(T=0)}(k) - A^{(T=1)}](k). \tag{16}$$

According to Eqs. (13), (15) and (16), we come to the following approximate relation:

$$\widetilde{B}(\mathbf{k},\mathbf{r}) = B(\mathbf{k},\mathbf{r}) + \Delta B(\mathbf{k},\mathbf{r}) = [\,|A^{(T=0)}(k)|^2 + |A^{(T=1)}(k)|^2\,]\,\frac{1}{2r^2} +$$

$$+\,\mathrm{Re}\left(\,[A^{(T=0)}(k) + A^{(T=1)}(k)]\,\frac{\exp(ikr)\cos(\mathbf{kr})}{r}\right). \tag{17}$$

4 Summary

1. It is shown that, taking into account the strangeness conservation, the double inclusive cross-sections of the production of two short-lived neutral K-mesons and two long-lived neutral K-mesons are equal to each other. This result is the direct consequence of the strangeness conservation.

2. Within the model of one-particle sources the formulas for the correlation functions $R_{SS} = R_{LL}$ and $R_{SL} = R_{LS}$ are obtained, which involve the contributions of Bose-statistics, of the S-wave final-state interaction of two K^0 ($\bar{K}^0$)-mesons as well as of a K^0-meson with a $\bar{K}^0$-meson, and also the contribution of transitions $K^+K^- \to K^0\bar{K}^0$, and depend upon the relative fractions of produced pairs K^0K^0, $\bar{K}^0\bar{K}^0$ and $K^0\bar{K}^0$.

3. It is shown that the production of $K^0\bar{K}^0$-pairs with the zero strangeness leads to the difference between the correlation functions R_{SS} and R_{SL} of two neutral kaons.

This work is supported by Russian Foundation for Basic Research (Grant No. 05-02-16674).

References

1. *Lyuboshitz V.L.* // Yad. Fiz. 1976. V.23. P. 1266-1271 [Sov. J. Nucl. Phys. 1976. V.23. P.673].
2. *Lyuboshitz V.L., Podgoretsky M.I.*// Yad. Fiz. 1979. V.30. P. 789-797 [Sov. J. Nucl. Phys. 1979. V.30. P.407]
3. *Podgoretsky M.I.*// EChAYa. 1989. V.20. P. 628-668 [Sov. J. Part. Nucl. 1989. V.20. P.266].
4. *Lednicky R., Lyuboshitz V.L.*// Yad. Fiz. 1982. V.35. P. 1316-1330 [Sov. J. Nucl. Phys. 1982. V.35. P.770].
5. *Lyuboshitz V.L.*// Yad. Fiz. 1985. V.41. P. 820-827 [Sov. J. Nucl. Phys. 1985. V.41. P.523].
6. *Lyuboshitz V.L.*// Yad. Fiz. 1988. V.48. P. 1501-1512 [Sov. J. Nucl. Phys. 1988. V.48. P.956].
7. *Lednicky R., Lyuboshitz V.V., Lyuboshitz V.L.*// Yad. Fiz. 1998. V.61. P. 2161-2174 [Phys. At. Nucl. 1998. V.61. P.2050].

Научное издание

Very High Multiplicity Physics

Proceedings of the Sixth International Workshop

Физика очень больших множественностей

Труды VI Международного рабочего совещания

Д1,2-2007-67

Сборник отпечатан методом прямого репродуцирования
с оригиналов, предоставленных оргкомитетом.

Ответственный за подготовку сборника к печати *Н. И. Шубитидзе.*

Подписано в печать 27.06.2007.
Формат 60 × 84/8. Бумага офсетная. Печать офсетная.
Усл. печ. л. 64,62. Уч.-изд. л. 57,63. Тираж 100 экз. Заказ № 55800.

Издательский отдел Объединенного института ядерных исследований
141980, г. Дубна, Московская обл., ул. Жолио-Кюри, 6.
E-mail: publish@pds.jinr.ru
www.jinr.ru/publish/